

(2)

FTD-ID(RS)T-0459-85

AD-A167 844

FOREIGN TECHNOLOGY DIVISION



DTIC
SELECTED
MAY 19 1986
S D
P

AVIATION AMMUNITION
(Selected Chapters)

by

A.N. Dorofeyev, V.A. Kuznetsov and R.S. Sarkisyan



JMC FILE COPY

Approved for public release;
Distribution unlimited.



86 5 16 119

HUMAN TRANSLATION

FTD-ID(RS)T-0459-85

25 April 1985

MICROFICHE NR: FTD-86-C-001769

AVIATION AMMUNITION (Selected Chapters)

By: A.N. Dorofeyev, V.A. Kuznetsov and R.S. Sarkisyan

English pages: 603

Source: Aviatsionnyye Boyepripasy, 1960, 1-58; 136-510

Country of origin: USSR

Translated by: FLS, INC.

F33657-85-D-2079

Requester: FTD/SDNW

Approved for public release; Distribution unlimited.

THIS TRANSLATION IS A RENDITION OF THE ORIGINAL FOREIGN TEXT WITHOUT ANY ANALYTICAL OR EDITORIAL COMMENT. STATEMENTS OR THEORIES ADVOCATED OR IMPLIED ARE THOSE OF THE SOURCE AND DO NOT NECESSARILY REFLECT THE POSITION OR OPINION OF THE FOREIGN TECHNOLOGY DIVISION.

PREPARED BY:

TRANSLATION DIVISION
FOREIGN TECHNOLOGY DIVISION
WPAFB, OHIO.
45433-6553

Partial

Table of Contents:

U.S. Board on Geographic Names Transliteration System	ii
Introduction	iii
Section One. ➤ Physicotechnical Bases of the Design and Damaging Effect of Aircraft Ammunition	1
Chapter 1. ➤ Explosives,.....	6
Chapter 3. The Blast Effect of Ammunition,.....	70
Chapter 4. The Percussion Effect of Ammunition,.....	175
Chapter 5. The Shaped-Charge Effect of Ammunition,.....	234
Chapter 6. The Fragmentation Effect of Aviation Ammunition,.....	274
Section Two. Aviation Fuses,.....	385
Chapter 7. General Information on Fuses	385
Chapter 8. Mechanical Impact Fuses,.....	394
Chapter 9. Electrical Impact Fuses,.....	444
Chapter 10. Time Fuses,.....	462
Chapter 11. General Information on Proximity Fuses. Electrostatic, Magnetic and Acoustic Proximity Fuses,.....	482
Chapter 12. Radio Fuses,.....	504
Chapter 13. Optical Fuses,.....	588

Distribution /	
Availability Codes	
Dist	Avail and/or Special
A-1	

Transliteration, USSR Russia

U. S. BOARD ON GEOGRAPHIC NAMES TRANSLITERATION SYSTEM

Block	Italic	Transliteration	Block	Italic	Transliteration
А а	А ё	A, a	Р р	Р ё	R, r
Б б	Б ё	B, b	С с	С ё	S, s
В в	В ё	V, v	Т т	Т ё	T, t
Г г	Г ё	G, g	Ү ү	Ү ё	U, u
Д д	Д ё	D, d	Ф ф	Ф ё	F, f
Е е	Е ё	Ye, ye; E, e*	Х х	Х ё	Kh, kh
Ж ж	Ж ё	Zh, zh	Ц ц	Ц ё	Ts, ts
З з	З ё	Z, z	Ч ч	Ч ё	Ch, ch
И и	И ё	I, i	Ш ш	Ш ё	Sh, sh
Й й	Й ё	Y, y	Щ щ	Щ ё	Shch, shch
К к	К ё	K, k	Ь ѿ	Ь ё	"
Л л	Л ё	L, l	Ҥ ҥ	Ҥ ё	Y, y
М м	М ё	M, m	Ծ Ծ	Ծ ё	'
Н н	Н ё	N, n	Э э	Э ё	E, e
О о	О ё	O, o	Ӯ ѿ	Ӯ ё	Yu, yu
П п	П ё	P, p	Я я	Я ё	Ya, ya

*ye initially, after vowels, and after ѿ, ѿ; e elsewhere.
When written as ё in Russian, transliterate as yё or ё.

RUSSIAN AND ENGLISH TRIGONOMETRIC FUNCTIONS

Russian	English	Russian	English	Russian	English
sin	sin	sh	sinh	arc sh	sinh ⁻¹
cos	cos	ch	cosh	arc ch	cosh ⁻¹
tg	tan	th	tanh	arc th	tanh ⁻¹
ctg	cot	cth	coth	arc cth	coth ⁻¹
sec	sec	sch	sech	arc sch	sech ⁻¹
cosec	csc	csch	csch	arc csch	csch ⁻¹

Russian English

rot curl

lg log

GRAPHICS DISCLAIMER

All figures, graphics, tables, equations, etc. merged into this translation were extracted from the best quality copy available.

INTRODUCTION

The "Aviation Ammunition" course is part of a set of courses dealing with the study of the aircraft armament system and lying at the foundation of training for the engineer-specialist in the use of aircraft armaments.

By aircraft armament system is meant the collection of various types of armament that provide for the execution of all missions facing aviation.

Within the total system of military aircraft equipment, aircraft armaments occupy a special and prominent place, since it is the availability of aircraft armament that allows aircraft to perform all the missions facing them.

The current system of aircraft armaments includes the following types of armaments:

-- artillery (aircraft cannons, installations for weapon mounting and fire control, sights for airborne firing, and cartridges with shells and fuses);

-- bombing (bombing installations for carrying and releasing bombs, bombing sights, aerial bombs and fuses for them);

-- guided and free-flight rocket armaments (rocket-missile implements for mounting and launching rocket missiles, aiming devices and systems for homing guided missiles to target, rocket missiles with various types of warheads and fuses for them).

All of the elements of which any armament system consists can be subdivided into two groups.

Comprising the first group are elements directly intended for damaging and destroying various enemy targets. Belonging to this group are projectiles and bombs of various types and the warheads of rocket missiles and their fuses. The elements comprising the first group (means of destruction) are usually called ammunition.

The second group is made up of elements that are means of employing bombs and shells (cannons, mountings, sights, etc.).

Consequently, the aircraft armament system consists essentially of ammunition and means of employing it.

The effectiveness of aviation combat operations is determined to a considerable extent by the effectiveness of the ammunition's action on the target. All of the other elements of the armament system are merely means of delivering ammunition to the target. It can be said that, no matter how perfect the cannons, bombing devices, sights, etc., they do not provide the necessary result if the employed ammunition is not effective enough. It would be incorrect, however, to consider that the effectiveness of aircraft armament is determined only by the degree of ammunition perfection. It also depends in a substantial way on the quality of all the other elements of the armament system and on the tactics of combat use of aircraft weapons.

The above considerations fairly clearly define the place occupied by aircraft ammunition within the aircraft armament system, and attest to the fact that the maximum combat effectiveness of

aircraft armament can be achieved only by improving the entire assembly of aircraft armament elements.

The modern aircraft armament system is a complex set of radio, electronic, optical, and mechanical apparatuses and devices. Serving as an example is the construction of the radio fuse, which includes a miniature electric power set, a radio transmitter, a receiver, and an actuator that provides explosion of the bomb or projectile at some distance from the target at which reliable target destruction occurs.

A number of special courses deal with study of the aircraft armament system. The "Aviation Ammunition" course is one of them. Its subjects are: foundations of devices, the effects and projection of bombs, aircraft artillery shells, warheads of free-flight and guided aircraft rockets, and the fuses for all of these weapons; the foundations of the destructive action of aircraft ammunition, evaluations of the effectiveness of the action, and the combat application and use of all types of aircraft ammunition.

SECTION ONE

PHYSICOTECHNICAL BASES OF THE DESIGN AND DAMAGING EFFECT OF AIRCRAFT AMMUNITION

A. N. Dorofeyev, V. A. Kuznetsov and R. S. Sarkisyan

By destructive or damaging effect of ammunition is usually meant the destruction or damage of different types of structures and objects, as well as the annihilation, neutralization, or blockading of enemy troops.

The damaging and destructive factors upon explosion of conventional ammunition are: 1) gaseous products of the explosion; 2) shock wave; 3) shell fragments; 4) kinetic energy of the moving ammunition.

Depending on the properties of the medium in which the explosion occurred, and on the relative positions of the ammunition and the targets, destruction (damage) of any objects may occur as a result of:

-- the brisance upon explosion of ammunition in contact with the destroyed object. The destroyed object may be both in the air and on the surface of an obstacle, in water or on the ground;

-- the blast effect upon explosion of ammunition in the air, in water, or in the soil;

-- the fragmentation effect upon explosion of ammunition in the air or on the surface of an obstacle;

-- the fragmentation-blast effect upon explosion of ammunition in the air or on the surface of an obstacle;

-- the cumulative effect upon direct hit on the object;

-- the percussive effect upon direct hit of ammunition on an object or upon penetration of water or soil by ammunition;

-- the seismic effect upon explosion of ammunition in the soil.

It should be noted that brisance is a particular case of the blast effect of an explosion, and in classification can be included in the concept of "blast effect of an explosion."

Depending on the properties of the ammunition, the properties of the target, and the properties of the medium in which the explosion occurred, the distance to the target, and the time of action of the explosive charge, all destructions caused by the effect of ammunition on the target can be subdivided into local and general destructions.

Local destructions of an object are accompanied by destruction or deformation of individual elements of its construction, without disturbance of the general structural outline of the object. Local destructions are usually the following:

-- blast effect (brisance) of ammunition upon explosion in the air or in water;

-- blast effect (brisance) of ammunition upon explosion in the soil or in other dense media;

-- cumulative effect of ammunition;

-- fragmentation effect of ammunition;

-- blast effect of ammunition.

For example, when ammunition explodes at a sufficiently great distance from objects, such local destructions or damages may occur as damage to the skin, controls, or other assemblies of an aircraft (airplane); destruction of windows and crumbling of plaster, damage to the roofs of buildings, the appearance of surface cracks in walls, bending of beams or displacement of structures not producing disturbance of the integrity of the object or building, etc.

General destruction of an object is characterized by such effects on the supporting members of its construction that lead to deformation of the structural outline of the object and in many cases to complete or partial destruction of the object. Examples of such general destructions could be cases of aircraft (airplane) structural destruction, destructions and collapses of building walls, breakage of beams and load-bearing columns, destruction of ceilings, destruction of the foundation, piercing of holes in cast-in-place constructions (ship, pill-box), overturning and hurling back of objects of fighting equipment, accompanied by destruction of their structures, etc. General destructions are usually observed upon explosion of conventional ammunition within buildings as the result of the combined effect of the gaseous products of the explosion, shock wave, and fragments. They also occur upon explosion of heavy high-explosive bombs at some distance from the object. General destructions usually lead to complete or partial destruction or annihilation of the object. In many cases, however, local destructions also lead to putting the target out of action, for example: fragment damage to objects of fighting equipment (aircraft), transport vehicles, and the machinery of factories,

penetration by fragments of the supporting members of a bridge's construction, etc.

Thus when studying the destructive effect of ammunition both general and local destructions have to be borne in mind, the more so as they usually occur in combination when an explosion takes place. From the standpoint of intensity, all destructions occurring with the effect of ammunition are usually classified as severe, moderate, and slight destructions.

As applied to industrial- and urban-type buildings, these types of destructions are associated:

- severe -- with destruction of stone or brick masonry;
- moderate -- with destruction of wooden parts and thick windows;
- slight -- with breaks in the continuity of roofs and destruction of normal glass of buildings.

Thus it can be concluded that the damaging effect of aircraft ammunition depends on the combined effect of a large number of different factors, the basic ones being:

- the properties of the ammunition (type, caliber, type of filling, capacity, etc.);
- the properties of the target (size and shape, strength characteristics, etc.);
- the properties of the medium in which the explosion occurred;
- the distance between the explosion site and the object.

Certain elements of the target's construction may ignite upon the explosion of conventional ammunition as the result of the

basic damaging factors listed above. When the target ignites, of course, damages may be inflicted that exceed many times the damaging energy capabilities of the ammunition acting on the target.

The high effectiveness of the incendiary effect of ammunition on a large group of targets with different purposes has led to the arming of aircraft with an extensive class of incendiary and combined (fragmentation - high-explosive - incendiary, armor-piercing - incendiary, etc.) ammunition. Experience in the massive use of incendiaries by the American aggressors in the criminal military operations in both Korea and Viet-Nam has confirmed the severe damaging effect of aircraft incendiary ammunition loaded with, for example, incendiary materials of the napalm type.

A detailed examination of the theoretical foundations of the damaging effect of ammunition and special methods of evaluating the effectiveness of incendiaries is beyond the scope of this textbook. Chapter 1 provides the necessary information about the properties of incendiary compositions used in aircraft ammunition.

Methods of calculating the incendiary effect accompanying the manifestation of the basic damaging factors of conventional ammunition (especially with damage of airborne targets by fragments) are fairly thoroughly examined in the textbook.

The last chapters of this section will provide basic information about explosives, and the theory of the genesis and propagation of explosive processes, and will examine the physical essence and methods of evaluating the damaging effect of ammunition loaded with conventional explosives.

CHAPTER 1

EXPLOSIVES

§ 1. THE CONCEPT OF EXPLOSIVE PROCESSES AND EXPLOSIVES

The phenomenon consisting of an extremely rapid change in the condition of a material, accompanied by conversion of its potential energy into mechanical work, is called an explosion.

A characteristic feature of an explosion is an abrupt, rapid change of pressure in the medium surrounding the explosion site. This rapid change serves as the immediate cause of the destructive effect of the explosion, which is produced by rapid expansion of gases or vapors either existing before the explosion or formed during it.

Explosions can be caused by various physical or chemical phenomena. Examples of them could be:

- explosions of steam boilers or compressed-air tanks;
- powerful spark discharges (lightning);
- collision of bodies moving at high speeds;
- volcanic phenomena, earthquakes, etc.

A steam boiler explosion is caused by rapid conversion of heated water into a vapor state, where the steam pressure exceeds

the ultimate strength of the boiler's walls.

With powerful spark discharges the difference in potentials equalizes in a time interval on the order of 10^{-6} - 10^{-7} sec, because of which extremely high temperatures (on the order of tens of thousands of degrees) arise in the discharge zone, and this, in turn, leads to a severe air pressure increase at the discharge site and propagation of a shock wave in the medium.

The greatest application in technology is found by explosions associated with transformations of special materials called explosives (VV). Under the influence of external effects, explosives are capable of very rapid chemical or physical transformations with release of a large amount of heat and the formation of strongly heated gases.

Two types of explosives are known: chemical and nuclear. The explosion of chemical VV represents a rapidly occurring chemical reaction, as a result of which the original material is converted into other materials -- the explosion products. The energy released in this is a part of the internal energy of the material, released as a result of rearrangement of the VV molecule's atoms.

Explosion of nuclear VV is caused either by a uranium- or plutonium-nucleus splitting reaction or by synthesis of nuclei of light elements such as hydrogen isotopes. The energy contained within the atomic nuclei is released in nuclear explosions. Nuclear explosions differ from chemical in releasing significantly greater energy, since the basic portion of an atom's energy is concentrated in its nucleus. Considerably smaller energy content belongs to the electron shell. For example, explosion of 1 kg of trinitrotoluene [TNT] (a chemical VV) releases an energy of $4 \cdot 10^5$ kg-m, while explosion of 1 kg of uranium releases $9 \cdot 10^{12}$ kg-m.

Only chemical explosions and VV now used extensively in aircraft ammunition are examined later in this book. Nuclear VV comprise the subject of independent examination.

The possibility of chemical explosion is determined by three conditions: the exothermicity of the reaction (heat release), high speed of its spread, and the presence of gaseous products of the reaction.

We shall briefly examine the significance of each of these conditions.

Reaction exothermicity (heat release) is the first necessary condition, without which the explosion process is altogether impossible. An explosive reaction usually develops under the influence of an external impulse on a limited area of the material. Conversion of a reaction into a process of decomposition of the entire material can occur only if it spreads throughout the material spontaneously, which is possible only with a constant influx of heat. The amount of heat released in an explosive reaction also determines the energy of the explosion, and thus also the work that can be performed by the explosion products upon expansion. The greater the heat of the reaction and the rate of its spread, the greater the destructive effect of the explosion. The heat of reaction is the criterion of the strength of an explosive and a most important characteristic of it. For modern VV used to the greatest extent in technology, the heat of explosive transformation lies between 900 and 1800 kcal/kg.

High speed of the process is the most characteristic feature of an explosion, one which distinguishes it from other chemical reactions. Often the incorrect statement can be heard that the destructive effect of an explosion supposedly is caused by the extremely high potential energy contained in explosives. These incorrect statements about VV sometimes serve as the grounds for various kinds of suggestions about replacing common fuels in internal combustion engines (kerosene, gasoline) with explosives.

Table 1.1 gives a comparison of common combustibles with explosives as to heat content.

Table 1.1. Heat content of some combustibles and explosives.

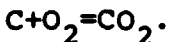
(1) Название вещества	(2) Температура теплосвободы при разложении, ккал/кг
3) Дерево	4200-4500
4) Антрацит	5000
5) Газин	10000
6) Керосин	12000
7) Тротил	10000
8) Чёрный порох	7000
9) Гидратная ртуть	10000

Key: (1) Designation of materials; (2) Heat released upon decomposition, kcal/kg; (3) Wood; (4) Anthracite; (5) Gasoline; (6) Kerosene; (7) TNT; (8) Black powder; (9) Mercury fulminate.

It follows from the table that the decomposition of a VV is explosive in nature (has a destructive effect) in no case because VV contain large energy stores, since explosives are significantly inferior to common fuels (kerosene, gasoline, etc.) in energy stores per 1 kg of weight. The explosive nature of the VV decomposition reaction is explained by the fact that this reaction is accomplished extremely rapidly. While 1 kg of gasoline burns in an automobile engine in 5-6 min, a mere 1-2 hundred thousandths of a second are needed for the explosive decomposition of 1 kg of TNT. Consequently, energy is released tens of millions of times faster during an explosion than during combustion of common fuels. This produces the high power of an explosion and the capability of destructive effect. Explosive reactions significantly exceed the combustion reactions of common fuels in power.

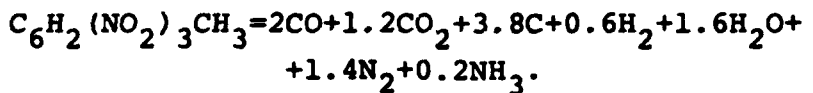
Thus VV, inferior to common fuels in heat content, significantly exceed them in rate of chemical decomposition. The rate of chemical decomposition of VV is usually judged on the basis of the value of the linear speed of propagation of an explosion per charge of VV. The maximum speed of propagation of an explosion for modern VV used in technology lies between 2000 and 9000 m/sec. The capability of VV for extremely rapid chemical decomposition is produced by peculiarities of their chemical nature. To explain the special nature of VV, we shall compare two reactions: the combustion reaction of a common fuel and the decomposition reaction of a VV.

As the first reaction, we shall examine the combustion of coal:



The essence of the combustion reaction of coal consists in the fact that the carbon atoms of which coal consists combine with oxygen atoms of the air to form a molecule of carbon dioxide gas. The rate of this reaction is comparatively small, since not all of the carbon atoms in the lump of coal combine simultaneously with oxygen atoms, but only those that are on its surface and in contact with the air. Thus the combustion of a lump of coal proceeds by parallel layers, spreading gradually inward from the outer surface.

We shall now examine the explosive decomposition reaction of TNT:

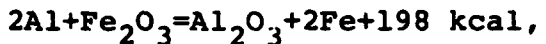


By nature, this reaction is also a combustion reaction. It can be seen from the chemical formula of TNT, $C_6H_2(NO_2)_3CH_3$, that its molecule contains all the chemical elements needed for a reaction. Therefore it has no need for extraneous oxygen and is accomplished because of the elements comprising the TNT molecule. Originating under the influence of an external effect, it rapidly spreads throughout the entire volume of the explosive charge.

Thus the capability of most VV for rapid decomposition is explained by the presence in their molecules of all the chemical elements needed for the reaction to occur.

Gaseous explosion products play the role of the working medium that converts heat into mechanical work. The heated explosion products, under high pressure, when expanding strike the surrounding medium and thereby perform work in destroying or jarring the medium. About 1000 l of gaseous products per 1 l of explosive forms during

the explosion of chemical VV. If there is no gas formation, even when the first two conditions are fulfilled, the decomposition reaction is not explosive in nature. The simplest reaction of this type is the combustion reaction of thermite,



which generally proceeds without explosion, despite the fact that the thermal effect of the reaction is sufficient to heat the end products (Fe , Al_2O_3) to a temperature of 3000° , at which they are in a liquid state.

Thus, based on what has been stated, we can conclude that an explosion is a combination of three factors: exothermicity, speed of the process, and gas formation.

§ 2. CLASSIFICATION OF EXPLOSION PROCESSES

The nature of the propagation and effect of an explosion on the surrounding medium depends to a severe extent on the rate of explosive transformation of the VV. Depending on the rate of explosive transformation, three types of explosive processes are distinguished: combustion, explosion, and detonation.

Combustion is what is called the process of explosive transformation that proceeds comparatively slowly and at a varying speed -- usually from fractions of a centimeter to several meters a second. The combustion speed depends substantially on external pressure. When the pressure rises, the speed increases. In open air this process is not accompanied by a significant sound effect or marked mechanical action. In a restricted space, however, the process proceeds more intensively and is characterized by a more or less rapid pressure rise and capability of the gaseous combustion products to produce the work of propulsion. An example of such a process could be the combustion of powder in the chamber of a gun. Combustion is a characteristic type of explosive transformation of powders.

An explosion is what is called the process of transformation that also occurs at a varying speed, but still measured in thousands of meters a second, and depends comparatively little on external conditions. The process is characterized by an abrupt and rapid pressure rise at the explosion site and an impact of gases on the surrounding medium, producing shattering and severe deformations of objects at relatively small distances.

Detonation is an explosion propagating at a constant velocity, one that is the maximum possible for a given VV and the given conditions.

The detonation velocity is some constant for the given conditions for each VV and is one of its most important characteristics. By nature the detonation phenomenon is no different from the explosion process, but is merely its steady form. The maximum destructive effect of an explosion is achieved with detonation.

Explosion and detonation processes differ from the combustion process in the nature of propagation. Self-propagation of combustion through the mass of a VV occurs through the phenomena of heat conduction, diffusion, and radiation -- via energy transfer, in the form of heat, from the hot decomposition products to the nearest layers of the explosive. The temperature of the material in these layers increases and a reaction originates in them.

Explosion and detonation self-propagation proceeds through transfer of energy from layer to layer by a compression wave (shock wave). The speed of the process's propagation exceeds the speed of sound in a given material.

§ 3. CLASSIFICATION OF EXPLOSIVES

An extremely large number of explosives is now known, differing one from the other both by composition and by physico-chemical and explosive properties.

The most prevalent classification of VV is their classification by application. Explosives are divided into four groups, depending on application:

- initiating VV;
- high-explosive VV;
- propellant VV or powder;
- pyrotechnic compounds.

Initiating VV are used to fill various means of initiation -- devices designed to initiate the explosive decomposition of other VV.

The characteristic feature of initiating VV consists in the fact that a minor external action is needed to initiate their explosion in the form of detonation, but the explosion process itself is distinguished by a very small period of rise in rate to its maximum value -- incomparably smaller than for other VV types. Because of the latter property, only an extremely small charge of initiator is usually needed to initiate the explosion of high-explosive VV.

The most important representatives of initiating VV are: mercury fulminate, lead azide, lead styphynate (TRNS), and tetrazene.

High-explosive VV are used as bursting charges in ammunition and in blasting explosives. The basic type of explosive decomposition of high-explosive VV is detonation. In distinction to initiating VV, they have a lower susceptibility to external actions and a larger period of rise in decomposition rate to a maximum value. Their detonation is usually produced by the explosion of initiating VV. By chemical nature, high-explosive VV are subdivided into homogeneous and inhomogeneous (mixtures and alloys). The most important representatives of homogeneous high-explosive VV are: TNT, picric acid, tetryl, hexogen, pentaerythritol tetranitrate (t.e.n.), pyroxylin, and nitroglycerin. Representatives of inhomogeneous VV are: ammonite, dynamite, alloys of TNT with hexogen, etc.

Powders are used chiefly to propel projectiles in a firearm and create reaction force in rockets. The basic type of explosive decomposition for powders is combustion, which does not transform into detonation even at high pressures. Powders are divided into two groups by physical structure: mixed and nitrocellulose or smokeless powders.

Mixed powders are mechanical mixtures of oxidants, combustibles, and binders. The simplest mixed powder is gunpowder or black powder, which consists of potassium nitrate, charcoal, and sulfur.

Solid mixed powders have come into extensive use in recent years. In these powders the oxidants are nitrates and perchlorates, and the combustible-binders are high molecular weight compounds: rubbers, plastics, resins, etc.

The base for powders of the second group is nitrocellulose. Until recently nitrocellulose powders were called colloids. In light of recent ideas about the structure of polymers and their solutions, this designation has proven inaccurate. Nitrocellulose powders represent homogeneous systems that are plasticized and consolidated with cellulose nitrates. Production of powders from cellulose nitrates is based on the formation of plastics when cellulose nitrates are acted upon by various solvents (plasticizers). Depending on the nature of the solvent, nitrocellulose powders are divided into:

- volatile-solvent powders or single-base powders;
- low-volatility-solvent and non-volatile-solvent powders;
- mixed-solvent powders.

Pyrotechnic compositions are used to charge various pyrotechnic devices: incendiary weapons, illumination devices, signal devices, etc. They are generally mechanical mixtures of inorganic oxidants with organic or metal combustibles. The basic type of explosive transformation of pyrotechnic compositions is combustion.

§ 4. SENSITIVITY OF EXPLOSIVES

To initiate an explosive transformation, an external action has to be exerted on the explosive -- some amount of energy has to be imparted to it. This external action is termed the initial impulse, and the process of initiating an explosion is called the initiation process. Experience has shown that a weak action is sufficient for initiating the explosion of some VV, while others require stronger actions. For example, hydrogen iodide explodes when touched by the tuft of a bird feather, but TNT does not explode even when a machine-gun bullet is shot through it. In other words, different VV have varying sensitivities to external actions.

An explosive's capability for explosive transformation under the influence of an initial impulse is called its sensitivity. The numerical measure of a VV's sensitivity is the minimum amount of energy sufficient to initiate an explosive transformation. Depending on the form of energy, the following types of initial impulses are differentiated:

- mechanical (impact, pinholes, friction);
- thermal (heating, a ray of flame);
- electrical (spark discharge);
- chemical (action of a chemical substance);
- detonation (explosion energy of an initiating VV).

The first four types are simple forms of initial impulse, the last is a complex form, since the action of a detonation impulse is reduced to the combined action of impulse and heating of the VV. No strict equivalence is observed among the various types of initial impulse with regard to results of the action on the same VV. For example, lead azide is more sensitive to mechanical actions than to thermal impulse, while for TRNS the opposite pattern is seen. The selective ability of VV to perceive an external impulse is determined by collective manifestation of their chemical and physical properties, which have a substantial effect on the energy-absorption conditions of explosives. Sensitivity is one of the

most important characteristics of VV determining the possibility of their practical use. Sensitivity that is too high makes an explosive dangerous to handle and use. Sensitivity that is too low necessitates a very large initial impulse to initiate the explosion of a VV and may make it difficult to use in practice. The sensitivity of VV depends on a large number of factors: VV temperature, aggregate state, physical structure and density of charge, size of crystals, presence of impurities, etc.

Temperature of VV. The sensitivity of a VV rises with increasing initial temperature, which is explained by weakening of molecular bonds upon heating and corresponding reduction in the energy needed to initiate explosive transformation. Characteristic in this regard is celluloid, which at normal temperature is insensitive to impact, but at a temperature of 100-180° is capable of exploding upon impact. The sensitivity of VV drops when there is a significant reduction of temperature. For example, when mercury fulminate is cooled to the temperature of liquid air it often fails to ignite.

Aggregate state. Sensitivity generally increases when a VV changes from the solid to the liquid state, a fact explained by increase in the charge temperature, and thus in the internal energy of the material. The effect of charge temperature and aggregate state on the sensitivity of TNT is illustrated in Table 1.2. Adopted in the table as a measure of sensitivity is the height H of dropping a 2-kg weight at which, under the defined conditions of the experiment, even one explosion is obtained out of ten experiments.

Physical structure and density of charge. Increase in the charge density of a VV and changing from a porous to a solid structure leads to decrease in VV sensitivity. Some initiating VV, such as mercury fulminate, completely lose the ability to detonate under the action of a thermal impulse when the density is increased above a certain limit. In compressed form, explosives (TNT, picric acid, etc.) have a significantly better susceptibility to detonation than when in cast form, even with the same density. This effect can

Table 1.2. Sensitivity of TNT to impact at various temperatures.

Температура (1) тротила, °C	(2) Агрегатное состояние	(3) H, см
- 40	Твердый (4)	46
20	,	36
80	Жидкий (5)	18
90	,	8
105—110	,	5

Key: (1) TNT temperature, °C;
 (2) Aggregate state; (3) H, cm;
 (4) Solid; (5) Liquid.

be explained by the fact that when the density is increased the same amount of initial impulse energy is distributed on a larger mass of material, and thus the energy exerted per unit mass decreases. Furthermore, when the density increases and when the structure changes to solid there is a smaller possibility of relative displacement of crystals and it is more difficult for hot combustion products to penetrate between VV particles.

Crystal size. For most VV, sensitivity to mechanical actions rises when crystal size is increased. The sensitivity of initiating VV depends also upon crystal shape. Lead azide, for instance, can be obtained in two crystal shapes: short columnar and acicular. Lead azide crystals of short columnar shape are less sensitive to impact than crystals of acicular shape. The formation of large acicular-shaped crystals is sometimes accompanied by spontaneous explosions.

Impurities. Inert impurities have different effects on the sensitivity of explosives: in some cases increasing sensitivity and in others reducing it. Impurities promoting higher VV sensitivity are called sensitizers, and impurities reducing sensitivity are called desensitizers. Good sensitizers are materials whose particles have sharp edges, which have great hardness, and which have a high melting point (such as fine glass, sand, metal powder, etc.). These materials promote concentration of the impact energy at the sharp

edges of crystals, are foci of intensive friction, and lead to the formation in the charge of numerous local hot spots, which help the explosion to penetrate it.

Desensitizing properties are possessed by such materials as paraffin, wax, vaseline, camphor, etc. Desensitizers coat the surface of the VV crystals with a soft, elastic film and thereby promote more even distribution of stresses in the charge and reduce friction between individual particles.

The numerical characteristics of VV sensitivity are determined experimentally in special devices with certain experimental conditions. Thus they are of a conditional nature and are used only for comparative evaluation of the sensitivity of different explosives.

Flash point serves as a measure of VV sensitivity to thermal impulse. Used to determine flash point is a metal vessel (bath) filled with a low-melting metal or oil, and these are heated to a temperature of 100°C. At the point when this temperature is reached, a test tube filled with a suspension of the VV undergoing testing (0.1-0.5 g) is placed in the vessel and further heating is performed at a rate of 20° per minute. The moment the VV ignites, note is made of the bath temperature, which is taken as the characteristic sensitivity of the VV to thermal impulse. The flash point values for various VV are given in Table 1.3.

The sensitivity of explosives to impact is determined in devices called impact testing machines, which are apparatuses allowing a load of a certain weight to be dropped on a suspension of the VV undergoing testing.

Serving as characteristics of the sensitivity of initiating VV to impact are the minimum drop height of a weight at which 100% explosions are obtained in a certain number of tests (usually five) and the maximum drop height of a weight at which 100% failures are obtained in the same number of tests. The first height is called the upper and the second the lower sensitivity limit. The

Table 1.3. Flash point of explosives.

(1)	(2)	(1)	(2)
{(3) Tetrazene	140	{(10) Hexogen	215-230
{(4) Mercury fulminate	170-180	{(11) TRNS	270-280
{(5) Smokeless powder	180-200	{(12) TNT	295-300
{(6) Tetryl	195-200	{(13) Picric acid	300-310
{(7) Guncotton	195-200		
{(8) Nitroglycerin	210-220	{(14) Black powder	
{(9) Lead azide	210-220	{(15) Lead azide	

Key: (1) VV; (2) Flash point, °C;
 (3) Tetrazene; (4) Mercury fulminate;
 (5) Smokeless powder; (6) Tetryl;
 (7) Guncotton; (8) Nitroglycerin;
 (9) T.e.n.; (10) Hexogen; (11) TRNS;
 (12) TNT; (13) Picric acid; (14) Black
 powder; (15) Lead azide.

characteristics of the sensitivity of initiating VV to impact are given in Table 1.4.

Table 1.4. Sensitivity of initiating VV to impact.

(1) VV	(2) Вес груза, кг	(3) Верхний предел чувствительности, см	(4) Нижний предел чувствительности, см
Гремучая ртуть (5)	0.09	8.5	5.5
Тетразен (6)	0.69	12.5	7
Азид свинца (7)	0.98	23	7
TNRS (8)	1.43	25	14

Key: (1) VV; (2) Load weight, kg; (3) Upper sensitivity limit, cm; (4) Lower sensitivity limit, cm; (5) Mercury fulminate; (6) Tetrazene; (7) Lead azide; (8) TNRS.

The sensitivity of high explosives to impact is usually characterized by the percentage of explosions occurring when a weight is dropped from a certain height.

Data on the sensitivity of high explosives to impact, obtained when a 10-kg weight is dropped from a height of 25 cm, are given in Table 1.5.

Table 1.5. Sensitivity
of high explosives to
impact.

(1) VV	(2) Frequency of explosions, %
(3) TNT	4-8
(4) Ammatols	18-30
(5) Picric acid	21-32
(6) Tetryl	50-60
(7) Hexogen	70-80
(8) Smokeless powder	70-80
(9) T.e.n.	No

Key: (1) VV; (2) Frequency
of explosions, %; (3) TNT;
(4) Ammatols; (5) Picric acid;
(6) Tetryl; (7) Hexogen;
(8) Smokeless powder; (9) T.e.n.

Explosives used for military purposes are usually tested by shooting a bullet through them. In such tests the VV are placed in a cast iron pipe 5 cm long and 5 cm in diameter, covered on both sides with screwed-on lids, and fired at from a rifle 9 m away. The test results for some high explosives fired at with a bullet are given in Table 1.6.

Table 1.6. Results of bullet-penetration
tests of VV.

(1)	(2)	(3)	(4)	(5)	(6)	(7)
(8)	0	0	5	7	10	10

Key: (1) VV; (2) Ammonium nitrate; (3) TNT;
(4) Picric acid; (5) Tetryl; (6) Hexogen;
(7) T.e.n.; (8) Number of explosions per 10
tests.

The sensitivity of high explosives to detonation impulse is characterized by the value of the extreme (minimum) charge of initiating VV capable of causing complete detonation of a certain amount of high explosive. To determine this minimum charge, 1 gram of high explosive is pressed into a metal casing at a pressure of

1000 kg/cm², and above it at a pressure of about 500 kg/cm² is a charge of initiating VV. During the tests the sample of initiating VV is sequentially increased in weight until complete detonation of the VV undergoing testing is achieved. The completeness of detonation is judged either by the nature of the explosion's effect on a lead plate or by the amount of expansion of the cylindrical channel of the lead bomblet into which the casing and charge are placed. The values of the minimum charges of initiating VV are given in Table 1.7.

Table 1.7. Minimum charges of initiating VV in grams.

(1)	(2)	(3)	(4)	(5)	(6)
Initiating VV	High explosives	TNT	Tetryl	Hexogen	T.e.n.
{(7) Lead azide	0.09			0.05	0.03
{(8) Mercury fulminate	0.36		0.49	0.19	0.17
{(9) Tetrazenes		=	>1.0	=	=
(10) TNRS		=	>1.7	=	=

Key: (1) Initiating VV; (2) High explosives;
 (3) TNT; (4) Tetryl; (5) Hexogen; (6) T.e.n.;
 (7) Lead azide; (8) Mercury fulminate; (9) Tetrazenes; (10) TNRS.

The value of the minimum charge can be treated the same as a characteristic of the initiating power of initiating VV.

§ 5. STABILITY OF EXPLOSIVES

By the stability of explosives is meant their ability to maintain their properties unchanged during prolonged storage. Explosives may alter their properties when affected by moisture, temperature variations, and chemical transformations, and some of them even self-ignite. For example, because of the hygroscopicity of ammonium nitrate, ammotol is capable of absorbing moisture when stored. Because of repeated processes of moisture absorption and desiccation occurring during storage, ammotol hardens (cakes) and its density, thus its susceptibility to detonation, changes. With charge

densities exceeding 1.2-1.4 g/cm³ ammotol has a low sensitivity to detonation. Like sensitivity, stability is a very important characteristic of explosives that determines the possibility of their practical use. Unstable VV obviously cannot be used in practice.

Two types of stability are distinguished for explosives -- physical and chemical. Physical stability is the term for a VV's ability to maintain its physical properties under the practical conditions of storage. The physical stability of VV is determined by such physical properties as volatility, hygroscopicity (ability to absorb moisture), and mechanical strength. Chemical stability is the term for the ability of VV not to undergo chemical transformations under normal storage conditions. By nature, explosives are chemical compounds that are relatively low in stability. Thus, unavoidably, they decompose during prolonged storage. But the various VV differ from one another as to different rates of decomposition. Explosives are divided into unstable and stable, depending on the rate of decomposition. Those in the first category decompose markedly during prolonged storage. This refers chiefly to powders and pyrotechnic compositions. Those in the second category do not decompose markedly under normal storage conditions. Change can be found in their chemical structure only after several years of storage. Most high explosives are stable. The chemical stability of VV depends on a number of factors: the chemical structure of the VV, the presence of impurities, etc.

Chemical structure determines the strength of the VV's molecules and thus its ability to decompose. Least stable of the VV used in practice are nitric acid esters (guncotton, nitroglycerin), in which the NO₂ group is bonded with a carbon atom through oxygen. Nitro compounds (TNT, tetryl, hexogen), in which the nitro group is bonded directly to a carbon atom, are extremely stable.

Impurities can have different effects on the stability of explosives. Impurities that accelerate the process of VV decomposition are called catalysts, and those that slow down decomposition are called stabilizers.

Among the catalysts are traces of free acids (hydrogen ions) left in the VV from the manufacturing process and the decomposition products themselves -- nitric oxides. Together with the moisture contained in the VV and released during decomposition, nitric oxides form nitrous and nitric acids, which accelerate the decomposition process. The phenomenon of decomposition by the products of decomposition themselves is called autocatalysis.

Stabilizers are such materials as diphenylamine, centralite, acetone, etc. Stabilizers interact easily with the products of VV decomposition -- nitric oxides -- to form with them chemically stable compounds that have no effect on accelerating VV decomposition. The process of introducing stabilizers into VV is called stabilization.

The chemical stability of VV is determined experimentally. The methods of determining VV stability used in practice are based on artificial acceleration of the decomposition process by subjecting the VV undergoing testing to increased temperatures. Serving as the characteristic of stability is the duration of heating at a certain temperature until the appearance of the corresponding signs of decomposition.

§ 6. HEAT AND TEMPERATURE OF EXPLOSION, VOLUME AND COMPOSITION OF GASEOUS PRODUCTS OF EXPLOSION

The heat and temperature of explosion, specific volume and composition of explosion products are most important characteristics of explosives.

Heat of explosion is the term for the amount of heat, Q_V , given off in the explosion of 1 kg of explosive. As we know, the thermal effect of a process occurring with the participation of gases or vapors may be different, depending on whether or not it goes on in a constant volume. In calculations of the thermal effect of explosion processes it is considered that the reaction of VV transformation can occur before the explosion products begin to expand. Thus the thermal effect of an explosion is computed at

a constant volume. There are two methods of determining the heat of explosion -- theoretical and experimental. Heat of explosion is determined theoretically by the method of the thermochemistry of explosives. Heat of explosion is determined experimentally using a special calorimetric device in which a certain amount of the VV undergoing testing is burned. The heat given off is transmitted to water, the temperature change of which is observed by thermometer. The value of Q_V is found by the change in water temperature. Values of Q_V for some VV are given in Table 1.8.

Table 1.8. Explosion heat of VV.

(1)	(2)
(3)	1480
(4)	1480
(5)	1390
(6)	1070
(7)	1070
(8)	1010
(9)	690
(10)	665
(11)	550
(12)	417
(13)	370
(14)	367
(15)	371

Key: (1) VV; (2) kcal/kg;
 (3) Nitroglycerin; (4) T.e.n.;
 (5) Hexogen; (6) Tetryl; (7) Gun-
 cotton; (8) TNT; (9) Dinitro-
 naphthalene; (10) Black powder;
 (11) Tetrazene; (12) Mercury ful-
 minate; (13) TNRS; (14) Lead azide;
 (15) Ammonium nitrate.

Temperature of explosion is the term for the maximum temperature to which the products of VV transformation are heated. Direct experimental determination of explosion temperature has thus far proven difficult. The difficulty of measurement is produced by the fact that the time interval during which the maximum temperature is reached is extremely short, and the temperature of the explosion products begins to drop sharply upon reaching maximum. In view of this, explosion temperature is usually determined by calculations. The calculations are based on the assumption that an explosion is an

adiabatic process occurring in a constant volume, and thus that the heat given off during an explosion is expended on heating the products of the transformation. Used to calculate the explosion temperature T_B is the formula

$$Q_V = \bar{c}_V T_B, \quad (1.1)$$

where \bar{c}_V is the mean heat capacity, at a constant volume, of all the explosion products in the temperature interval from 0° to T_B .

The dependence of heat capacity on temperature is usually accepted as

$$\bar{c}_V = a + bT.$$

Coefficients a and b are determined from special tables.

The values of explosion temperature, T_B , for some VV are given in Table 1.9.

Table 1.9. Explosion temperature of VV.

(1)	T_B °C
(2)	4350
(3)	4250
(4)	4010
(5)	3530
(6)	3450
(7)	3370
(8)	3260
(9)	2830

Key: (1) VV; (2) Mercury fulminate; (3) Nitroglycerin; (4) T.e.n.; (5) Tetryl; (6) Lead azide; (7) Hexogen; (8) TNT; (9) Black powder.

Composition of explosion products can be determined theoretically or by experiment. Experimental determination of the composition of explosion products is performed using the method of gas analysis, based on sequential absorption of gases by various

absorbents. It should be noted that precise determination of the composition of explosion products is a very complicated task. This is because the composition of the cooled products of an explosion depends substantially on external conditions (surrounding medium, cooling time) and may differ from the original composition that corresponds to the explosion temperature. In addition, the nature of the explosive reactions, and thus also the composition of the explosion products, change depending on the means of initiating the explosion (heating, impact, initiation by detonator), the density of the charge, and other factors.

Volume of explosion products is determined in two ways: by calculation -- according to the VV decomposition reaction -- and by experimental means -- measuring the volume of gases formed when a certain amount of explosive is exploded. The value of the V_0 of gaseous explosion products for some VV is given in Table 1.10.

Table 1.10. Volume of gaseous explosion products.

(1)	(2)	(3)
{(4)	1.5	890
{(5)	1.65	790
{(6)	1.5	750
{(7)	1.55	710
{(8)	1.6	690
{(9)	3.77	300

Key: (1) VV; (2) Charge density, g/cm³; (3) V_0 , l/kg; (4) Hexogen; (5) T.e.n.; (6) TNT; (7) Tetryl; (8) Nitroglycerin; (9) Mercury fulminate.

§ 7. BRISANCE AND BLAST EFFECT OF EXPLOSION

The destructive effect of an explosion is produced by the work performed by gaseous explosion products in expansion. Two basic forms of explosion are distinguished: brisance and blast effect.

Brisance is the term for the capability of explosives for local destructive effect, which is the result of the sudden impact of the explosion products on the objects surrounding the VV. Brisance is manifested only at close distances from the explosion site, where the pressure and energy density of the explosion products are still fairly high. Brisance produces pulverization, perforation, or breakup of the medium adjacent to the explosive charge. Experience has shown that brisance depends chiefly on charge density and the detonation velocity of the VV. Usually brisance is assessed theoretically by the power of the VV, referred either to a unit of weight or unit of volume of the charge. There are several formulas for assessing brisance, the formula of K. K. Snitko, for example:

$$B = \frac{Q_V \rho_0 D}{l} [\text{kcal/l-sec}], \quad (1.2)$$

where ρ_0 is the density of the VV;
 D is the detonation velocity;
 l is the length of the charge;
 Q_V is the heat of explosion.

According the K. K. Snitko's formula, brisance, B , is assessed by the VV power referred to a unit volume of the charge. Table 1.11 gives the values of B for some VV, calculated using formula (1.2).

Table 1.11. Value of brisance of VV

(1) VV	(2) ρ_0 , g/cm ³	(3) l , m	(4) Q_V , kcal/kg	(5) D , m/sec	(6) B , kcal/l-sec
(7) Ammotol 80/20	1.5	0.108	1016	5300	74·10 ⁶
(8) TNT	1.52	0.108	1010	6600	93·10 ⁶
(9) Tetryl	1.55	0.108	1090	7500	117·10 ⁶
(10) T.e.n.	1.55	0.103	111	7800	156·10 ⁶

Key: (1) VV; (2) ρ_0 , g/cm³; (3) l , m;
(4) Q_V , kcal/kg; (5) D , m/sec; (6) B ,
kcal/l-sec; (7) Ammotol 80/20; (8) TNT;
(9) Tetryl; (10) T.e.n.

All of the theoretical formulas for calculating brisance are conditional in nature and used only for comparative assessment of

the brisance of different explosives. Brisance is assessed experimentally by the amount of compression of a lead cylinder of a certain size when a certain amount of explosive undergoing testing is exploded on it. The lead cylinder is compressed in the explosion and becomes mushroom-shaped. The difference in the heights of the cylinder before and after the explosion serves as a measure of the VV's brisance. Brisance can also be assessed by the amount of breakup of the metal casing surrounding the charge or of the metal slab on which it is mounted. The criterion of brisance in this case is the number of fragments weighing over 1 g, referred to a unit weight of the charge.

Fugacity is the term for the capability of explosives for a destructive effect through expansion of the explosion products to comparatively low pressures and passage of a shock wave through the medium. This blast effect is manifested as splitting and expulsion of the medium in which the explosion occurs. Fugacity is very often called the efficiency of an explosive.

Usually adopted as a measure of an explosive's efficiency is the amount of work that could be performed by the explosion products of 1 kg of VV during expansion up to a temperature of absolute zero. Under conditions of adiabatic expansion of gases, this work equals:

$$A = EQ_V, \quad (1.3)$$

where $E=427 \text{ kg-m/kcal}$ is the mechanical equivalent of heat.

In explosives theory, the value A is called the potential energy, or the potential of the VV. For most VV the potential, A , lies between $4 \cdot 10^5 \text{ kg-m/kg}$ and $6 \cdot 10^5 \text{ kg-m/kg}$. A different characteristic, called the force of a VV (force of a powder, when applied to powders), is used when assessing the efficiency of powders.

The force of an explosive, F , is the term for the work performed by the gaseous explosion products of 1 kg of VV, expanding at atmospheric pressure, when heated from 0° to the explosion temperature, T :

$$F = nRT_B, \quad (1.4)$$

where n is the number of moles of products from explosion of 1 kg VV; R is the gas constant, numerically equal to the work of expansion upon the heating of 1 mole of gas under atmospheric pressure by 1°.

The numerical value of the universal gas constant equals:

$$R = 0.08204 \frac{\text{J} \cdot \text{atm}}{\text{mole} \cdot \text{deg}}.$$

For nitrocellulose powders the force $F = (9400-10,200) \frac{\text{J} \cdot \text{atm}}{\text{kg}}$, and for nitroglycerin powders $F = (11,100-11,700) \frac{\text{J} \cdot \text{atm}}{\text{kg}}$. The energy capabilities of solid propellants are usually assessed by the value of the unit impulse of the propellant, I_{I} . The unit impulse of a propellant is the term for the amount of movement (impulse) imparted to a rocket's engine by each kilogram of gas (propellant) emitted from the nozzle. For modern rocket propellants the value of the specific impulse is $(180-250) \frac{\text{kg} \cdot \text{sec}}{\text{kg}}$.

The amount of useful work of the explosion is significantly less than the potential of the VV, which is explained by the presence of solid and liquid materials in the composition of the explosion products. Experiment shows that the efficiency of a VV depends not only on the heat of explosion, but also on the specific volume and composition of the explosion products. Usually used for practical assessment of VV efficiency is the so-called lead-bomb expansion test. A charge of the VV being tested, of a certain weight, is exploded in the cylindrical channel of a lead bomb. The channel expands during the explosion and becomes mushroom-shaped. The difference between the volumes of the channel before and after the explosion is a practical measure of VV efficiency. This value characterizes the relative efficiency of VV and is used only for comparative assessment of explosives.

§ 8. INITIATING EXPLOSIVES

Mercury fulminate, $\text{Hg}(\text{ONC})_2$, is a crystalline material, white or grey in color, with a density of 4.31 g/cm^3 . It is obtained by dissolving metallic mercury in nitric acid and subsequently combining the solution with ethyl alcohol. The stability of mercury fulminate is comparatively low, but sufficient for practical use. In the presence of moisture it reacts easily with aluminum. Explosion may occur because of the heat given off in this reaction. Thus compositions with mercury fulminate are kept away from aluminum. It is used in casings made of copper or brass, covered with tin. Mercury fulminate is the most sensitive initiating VV. It is easily exploded from a minor shock. The sensitivity of mercury fulminate depends heavily on humidity and the pressure of compression. At a compression pressure above 500 kg/cm^2 it does not detonate because of a beam of flame, but only burns. At a humidity of 10% it only burns, without detonating. The explosive properties of mercury fulminate are characterized by the following data: $Q_v = 415 \text{ kcal/kg}$, detonation speed $D = 4500-5000 \text{ m/sec}$. Mercury fulminate is used to manufacture the percussion and cap compositions of igniter set caps and igniters.

Lead azide, $\text{Pb}(\text{N}_3)_2$ is a crystalline material, white in color, with a density of 4.8 g/cm^3 . The initial products for producing lead azide are sodium azide and lead nitrate. Lead azide is close to mercury fulminate in explosive properties ($Q_v = 370 \text{ kcal/kg}$, $D = 4500-5000 \text{ m/sec}$), is chemically stable, and its sensitivity to mechanical effects is 2-3 times lower than mercury fulminate. Lead azide is insufficiently sensitive to a beam of flame and pinholes. Pressure of compression and humidity have little effect on the sensitivity of lead azide. Lead azide interacts readily with copper to form copper salts that are very sensitive to mechanical influences. It does not interact with aluminum, so it is used in aluminum casings. A valuable property of lead azide is its high initiating power (5-10 times higher than mercury fulminate). Lead azide is used in igniters and in detonating cords in a mixture with high explosives.

TNRS (trinitroresorcinate or lead styphynate), $C_6H(O_2Pb)(NO_2)_3H_2O$, is obtained through the interaction of sodium styphynate with lead nitrate. TNRS is a crystalline substance, yellow in color, with a density of 3.12 g/cm^3 , and chemically stable. It is second to mercury fulminate in sensitivity to flame. Its sensitivity to impact is half that of lead azide. A feature of TNRS is its great capacity for electrization and high sensitivity to electric discharges. Its initiating power is lower than other initiating VV. At a charge density of 2.9 g/cm^3 the detonation velocity of TNRS is 5200 m/sec, the heat of explosion 370 kcal/kg. TNRS is used in combined igniters to transmit detonation from flame to lead azide, in firing compositions, and in igniter set caps.

Tetrazene, $C_2H_8ON_{10}'$ is a crystalline substance with a yellow tinge and a density of 1.65 g/cm^3 . In sensitivity to impact it is close to mercury fulminate, and its initiating power is low. The heat of explosion of tetrazene is 550 kcal/kg, the detonation velocity 5000 m/sec at a charge density of 1.47 g/cm^3 . Tetrazene is used in the pin compositions of igniters as a supplement to lead azide, in igniter set caps instead of mercury fulminate, and in cap compositions of igniters in a mixture with TNRS.

§ 9. HIGH EXPLOSIVES

Homogeneous VV

Trotyl (trinitrotoluene, TNT), $C_6H_2(NO_2)_3CH_3$, is a crystalline substance, yellow in color. The initial material for obtaining TNT is toluene -- a product of coal carbonization or petroleum hydrolysis and a mixture of sulfuric and nitric acids. TNT compresses and melts easily (melting point about 81°C). The density of compressed TNT reaches 1.6 g/cm^3 , of cast TNT $1.55-1.59 \text{ g/cm}^3$. TNT practically does not interact with metals and is chemically stable (can be stored for decades). The sensitivity to impact is comparatively low. It does not detonate when shot with a bullet. In open air it burns smoothly and with a smoking flame. The susceptibility to detonation of compressed TNT is significantly greater than cast TNT. A relay detonator is needed to detonate cast TNT, while one igniter is sufficient to explode compressed TNT. The explosive properties of TNT

are characterized by the following data: $Q_V=1000$ kcal/kg, $D=6900$ m/sec at a density of 1.59 g/cm 3 . TNT is one of the basic high explosives used in practice. In its pure form it is used to fill ammunition and manufacture cartridges and blocks for blasting operations. In modern ammunition TNT is usually used in mixtures and alloys with other high explosives (hexogen, ammonium nitrate, etc.).

A valuable auxiliary explosive is an intermediate product of TNT production -- dinitrotoluene. Dinitrotoluene belongs to the group of weak VV that have low sensitivity to detonation. Its detonation velocity $D=5900$ m/sec at a charge density of 1.52, its explosion heat is 900 kcal/kg. Dinitrotoluene is not used as an independent VV. It is used in the production of some industrial VV and nitrocellulose powders.

Picric acid, $C_6H_2(NO_2)_3OH$, is a hard crystalline substance of light yellow color. It is close to TNT in explosive properties. The great shortcoming of picric acid is its ability, in the presence of small amounts of moisture, to form salts when in contact with metals. Some of these salts are highly sensitive to impact, which makes the use of picric acid dangerous in the metal casings of ammunition. In connection with this shortcoming, the use of picric acid has virtually ceased in recent years.

The ammonium salt of picric acid -- ammonium picrate ("explosive D"), which is less sensitive to impact than picric acid and TNT -- has found use in the U.S.A. to fill aerial bombs. The detonation velocity of ammonium picrate at a density of 1.6 g/cm 3 equals 7400 m/sec, the heat of explosion 845 kcal/kg.

Tetryl, $C_6H_2(NO_2)_3N\cdot NO_2CH_3$, is a crystalline substance, pale yellow in color, with a density of 1.78 g/cm 3 , is easily compressed and decomposes upon melting, so charges of tetryl cannot be manufactured by pouring. Its stability of somewhat lower than TNT. Its sensitivity to mechanical influences and susceptibility to detonation are much higher than TNT. Tetryl is a more powerful VV than TNT ($Q_V=1090$ kcal/kg, $D=7740$ m/sec at a density of 1.61 g/cm 3). Because

of its high sensitivity to mechanical influences, tetryl is not suitable in its pure form for filling ammunition. It is used as auxiliary detonators, in primer mixtures, and in alloys with TNT or hexogen.

Hexogen, $C_3H_6O_6N_6$, is a crystalline substance, white in color, with a density of 1.82 g/cm^3 , decomposes upon melting, and is easily compressed and chemically stable. Its sensitivity to mechanical influences and susceptibility to detonation are higher than tetryl. Thus, in its pure form hexogen is used only for manufacturing igniters. The power of hexogen is higher than TNT or tetryl ($Q_V = 1390 \text{ kcal/kg}$, $D=8400 \text{ m/sec}$ at a density of 1.70 g/cm^3). Hexogen is now widely used to fill ammunition in alloys with TNT.

T.e.n. (pentaerythritol tetranitrate), $C(CH_2ONO_2)_4$, is a white crystalline substance with a density of 1.77 g/cm^3 , easily compressed, chemically stable, and decomposes upon melting. Its sensitivity to mechanical influences and susceptibility to detonation are higher than hexogen. T.e.n. and hexogen are the most powerful high explosives used today. In pure form, t.e.n. is used in igniters and detonating cords, and in its desensitized form it is used as auxiliary detonators.

Guncotton, $C_{24}H_{29}O_9(ONO_2)_{11}$, is a white-colored, hard substance with a density of 1.66 g/cm^3 . It is now used only to produce nitrocellulose powders.

Nitroglycerin, $C_3H_5(ONO_2)_3$, is a thick, oily liquid, white or yellow in color, with a density of 1.6 g/cm^3 , and is distinguished by high sensitivity to mechanical influences. Nitroglycerin is used to manufacture nitrocellulose powders and in blasting explosives in a mixture with inert substances.

Dinitronaphthalene, trinitroxylene, and dinitrobenzene are high explosives distinguished by low cost, inadequately high explosive properties, and low sensitivity to detonation. In practice they are used in alloys with TNT and other high explosives.

VV Alloys

Composite VV formed from several melted and interdissolved homogeneous VV are called alloys of explosives. Alloys make it possible to use in ammunition filling the most powerful VV (hexogen, t.e.n., etc.), use of which in the pure form is limited because of high sensitivity and the impossibility of charging using simple methods (pouring). Alloys of TNT with hexogen and TNT with dinitro-naphthalene are the VV alloys finding the greatest use in filling ammunition.

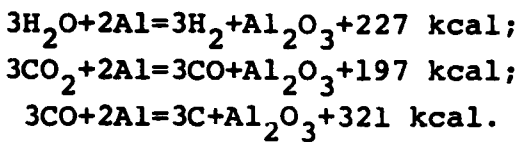
Alloys of TNT with hexogen (TG) are manufactured by introducing into melted TNT a powdered hexogen, which after mixing is in liquid TNT in the form of a suspension. This mixture is poured into a casing of ammunition and cooled. The density of poured charges or charges compressed in a hot state varies from 1.63 to 1.7 g/cm³. The relationship of the components in TG may be different: from 20 to 60% hexogen and 80 to 40% TNT, respectively. With a lower TNT content the castings are insufficiently homogeneous or strong. But mixtures of TG containing less than 40% TNT are plastic in the hot state and can be additionally compacted by vibration, tamping, or compression. TG alloys are more powerful than TNT, significantly less sensitive than pure hexogen, and have a higher susceptibility to detonation, which is explained by the sensitizing effect of hexogen. TG alloys are now among the most prevalent VV in both military and peaceful technology. The explosive properties of TG are given in Table 1.12.

Alloys of TNT with hexogen and aluminum (TGA) differ from TG alloys in higher fugacity of effect, by have somewhat lower detonation velocities and brisance. The higher fugacity of effect is produced by introduction into the alloy of powdered aluminum, which after charge detonation reacts with the explosion products: water vapor, carbon dioxide, and carbon monoxide.

Table 1.12. Basic characteristics of alloys and mixtures with hexogen.

(1)	(2)	(3)	(4)	(5)	(6)	(7)	(8)	(9)	(10)	(11)
(13)										
(14)										
(15)										
(16)										
(17)										
(18)										
(19)										
(20)										

Key: (1) Designation of VV; (2) Composition of alloy or mixture; (3) Specific weight g/cm³; (4) Density, g/cm³; (5) Compressed charge; (6) Poured charge; (7) Detonation velocity, m/sec; (8) Heat of explosion, kcal/kg; (9) Temperature of explosion, °C; (10) Specific volume of gases, l/kg; (11) Flash point, °C; (12) A-IX-1; (13) Hexogen -- 95%, desensitizer -- 5%; (14) A-IX-2; (15) A-IX-1 -- 80%, aluminum powder -- 20%; (16) TG 50/50; (17) TNT -- 50%, hexogen -- 50%; (18) TGA; (19) TNT -- 60%, hexogen -- 24%. aluminum powder and dust; (20) TNT -- 60%, hexogen -- 24%, aluminum powder -- 5%, aluminum dust -- 11%, and holowax -- 5% over 100%.



These reactions are accompanied by the release of a large amount of heat, which not only compensates for, but even exceeds energy losses because of the introduction into the VV of aluminum, which plays the role of inert additive in the first stage of the explosion. Thanks to the additional heat, the adiabatic work of the explosion products increases and their time of action lengthens. Since the oxidation reaction of aluminum proceeds outside the detonation zone, the excess heat that is released is transformed into mechanical work in the scattering of the explosion products, i.e., in the period of the explosion's blast effect.

Formed in the oxidation of aluminum are red-hot solid slags of aluminum, Al_2O_3 , which increase the blaze of the explosion and its incendiary effect. TGA alloys are differentiated as to the percent content of its components. The optimal aluminum content in the alloy is 16-20%. The hexogen content can be varied between 18 and 70%. The power of the alloy increases with increasing hexogen content. The hexogen content is limited, however, by the technical capabilities of manufacturing the charges. With a hexogen content above 30% the alloy does not have satisfactory flowability, which is needed for filling ammunition by pouring, and can be packed only by vibration. The shortcoming of TGA alloys is their high sensitivity to impact and friction. This shortcoming is eliminated by introducing into the alloy desensitizers, which reduce the sensitivity of the alloy to the sensitivity level of TNT without thereby having a substantial effect on the alloy's power. Holowax (a mixture of tetra- and trichloronaphthalenes), an alloy of stearin and ceresin, etc., are used to desensitize TGA alloys. All types of TGA alloys have high chemical stability, are practically non-hygroscopic, and withstand prolonged storage. Their explosive properties are given in Table 1.12. In the U.S.A., TGA alloys are known by the following names:

-- HBX (contains 38% TNT, 40% hexogen, 17% aluminum, and 5% desensitizer);

-- HBX-1 -- (contains 40% TNT, 42% hexogen, 18% aluminum, and 0.7% desensitizer);

-- torpex (contains 41% TNT, 41% hexogen, and 18% aluminum).

Alloys of TNT with dinitronaphthalene are used to charge fragmentation and fragmentation-demolition bombs when the construction of the bomb does not provide any measures ensuring breakup of the casing into fragments of a certain weight. When TNT or other more powerful VV are used in these bombs there is excessively intensive breakup of the housing into fragments. Then a significant portion of the housing's metal is not expended productively, being broken into very small fragments that have a small damaging effect. The alloy of TNT with dinitronaphthalene (DNN) is less powerful than pure TNT. The dinitronaphthalene content in the alloy varies from 10 to 50%. Used to fill aerial bombs are alloys known by the numbers:

-- K-2 (contains 70% TNT and 30% DNN or 90% TNT and 10% DNN);

-- K-3 (contains 84% TNT and 16% DNN).

Alloys with DNN detonate only from powerful detonators and belong to the medium-power VV. The detonation velocity of alloy 50/50 at a charge density of 1.3 g/cm^3 equals 4435 m/sec.

Besides alloys of TNT with hexogen and dinitronaphthalene, alloys of TNT with t.e.n., tetryl, and other explosives find use in practice. Of the alloys of TNT with t.e.n., alloy 50/50 has found extensive use in the U.S.A., having been termed pentolite-50. Used in the past were alloys with dinitronaphthalene based on picric acid, known by the terms Russian mixture and French mixture.

Desensitized VV

Desensitized hexogen and t.e.n. are the most-used desensitized VV. Hexogen is desensitized with paraffin and paraffin-ceresin alloy. Desensitization of VV is conducted using the emulsion method in a aqueous medium. An aqueous emulsion of the desensitizer is mixed with a hot aqueous suspension of the VV, as a result of which the desensitizer is fairly evenly distributed among the VV particles. Upon subsequent cooling the desensitizer solidifies to form a film around the VV particles. The desensitized particles are separated from the water by filtration and desiccated. Hexogen that contains 5-6% desensitizer is known by the number A-IX-1. It is used to fill the warheads of missiles, artillery shells, mines, and other devices. Its explosive properties are characterized by the following data: $Q_v=1250$ kcal/kg, $D=7500-8000$ m/sec at a density of $1.6-1.68$ g/cm³.

The mechanical mixture of desensitized hexogen with aluminum dust, in a relationship of 80% A-IX-1 and 20% aluminum, has been designated A-IX-2. This mixture has powerful blast and incendiary effects. The heat of explosion of the mixture $Q_v=1500-1650$ kcal/kg and the detonation velocity $D=6700-7800$ m/sec at a charge density of $1.6-1.68$ g/cm³. A-IX-2 is used mainly to fill aircraft artillery shells, naval mines, and torpedoes.

T.e.n. desensitized with 5% paraffin is used in detonating cords and for the manufacture of detonators. It is distinguished by high sensitivity, even with up to 15-20% paraffin content, so it is not used to manufacture ammunition charges. Desensitized hexogen and t.e.n. are used in powdered form.

Plastic VV

Plastic VV is the term for explosives that are easily deformed under the influence of slight external forces and that retain the residual deformation after the external loads have ceased operation. They are very soft and elastic, thanks to which they are easily formed into any geometric shape. This property of plastic VV is

extremely valuable for explosives work, since it allows making charges of complicated and varied forms directly at the explosion site. Plastic VV may find use in ammunition having a charge which, in order to increase the area of contact with an object, has to be plastically deformed (flattened). During the Second World War plastic VV were used in Germany to place caseless mines in ice.

Plastic VV are produced either by mechanically mixing free-flowing VV in plastic materials or by gelatinizing VV. Used as the plastic materials are high-viscosity hydrocarbons: vaseline, thickened mineral oils, thickened castor oil, etc. These substances are introduced into the composition of the VV either in a melted state or in the form of a solvent in 5-20% amounts.

The second method of plasticizing VV is based on the ability of VV to form plastic systems (gels) when interacting with certain substances. Here either all the VV becomes plastic or only a part of it does, and this part, evenly distributed among the particles of the remaining mass of the VV, provides plasticity of the entire charge. Partial plasticization is performed when manufacturing plastic VV. Complete plasticization is used in the production of nitrocellulose powders. Plastic VV can be made based on solid VV (hexogen, t.e.n., and TNT), based on nitroglycerin, and based on a mixed type. Serving as plasticizers of solid VV are colloxylin and gelatinized TNT or dinitrotoluene. The amount of plasticizer varies between 25 and 50%. A possible example of plastic VV is a composition containing 50% hexogen, 40% TNT, and 10% colloxylin. Plastic VV based on nitroglycerin are called gelatin dynamites, and if there is a nitroglycerin content above 90% they are called blasting gelatin.

Oxidant-Based Composite VV

Oxidant-based composite VV is the term for mixtures of combustibles and oxidants, capable of explosive transformation with the release of gaseous products of complete oxidation. These VV are the cheapest and most accessible, because of which they have become most prevalent

in industrial explosives technology. A serious shortcoming of oxidant-based composite VV is the hygroscopicity and water-solubility of many oxidants, which limits the storage time for charges manufactured from these VV. In a comparatively short storage period the charges become damp and deteriorate, losing their original physical-chemical properties and ability to detonate. The storage period for charges made of composite VV is restricted to 3-12 months. Creation of mobilization stores of charges made of oxidant-based VV with prolonged storage times is precluded. Thus, in peacetime these VV are not used to fill ammunition. Experience in the two world wars indicates, however, that in wartime they are used in vast quantities to fill all types of ammunition.

Composite VV contain, besides combustibles and oxidants, sensitizers and explosive-effect controllers. Usually used as the desensitizers are powerful high explosives: TNT, nitroglycerin, t.e.n., etc. The sensitizing effect of high explosives consists in the fact that they provide reliability of initiation and occurrence of detonation through the entire mass of the charge. Explosive-effect controllers are introduced into VV to intensify the fugacity of the explosion, reduce its flash, and for other purposes. Of the large number of oxidant-based composite VV, ammonium nitrate VV, oxyliquits, and liquid explosive mixtures find the greatest use.

Ammonium nitrate VV is the term for explosive mixtures in which the role of oxidant is played by ammonium nitrate (NH_4NO_3). Ammonium nitrate is produced by industry in large quantities, as an extremely valuable fertilizer, from nitric acid and ammonium -- products of the synthesis of atmospheric air and water. The raw materials base of ammonium nitrate is virtually unlimited.

Ammonium nitrate has slight explosive properties: heat of explosion $Q_v=379$ kcal/kg, detonation velocity $D=1000-3000$ m/sec. Its sensitivity to all types of initial impulses is very low. Besides an igniter, a powerful detonator weighing up to 250 g is needed to initiate the detonation of ammonium nitrate. Ammonium nitrate is highly hygroscopic and very easily dissolved in water. The

susceptibility to detonation diminishes severely with moistening and deterioration. With a moisture content above 5% it completely loses its ability to detonate. Explosion of ammonium nitrate results in the formation of only gaseous products containing up to 20% free oxygen by weight. This property of ammonium nitrate, in combination with its low cost, serves as the basis for its use as an oxidant in explosive mixtures. Serving as combustibles in ammonium nitrate VV are high explosives (TNT, dinitronaphthalene, dinitrobenzene, etc.) and non-explosive materials: pine-bark meal, peat meal, cake meal, cotton-seed meal, etc. The following compositions of ammonium nitrate VV are used to fill ammunition:

- amatols (contain NH_4NO_3 and TNT);
- ammonals (contain NH_4NO_3 , TNT, and aluminum);
- ammoxyl (contains 82% NH_4NO_3 and 18% xylyl);
- schneiderite (contains 88% NH_4NO_3 and 12% dinitronaphthalene);
- bellite (contains 80% NH_4NO_3 and 20% dinitrobenzene);
- maysite (contains 72% NH_4NO_3 and 28% ammonium picrate);
- dynammons (contain NH_4NO_3 and non-explosive combustibles).

The content of ammonium nitrate in amatols varies between 40 and 90%. Amatols are designated by the numbers A-40, A-50, etc., in which the number indicates the percent content of ammonium nitrate, or the fractions 40/60, 50/50, etc. In the second instance the percent content of ammonium nitrate is indicated in the numerator of the fraction. Amatols containing over 20% TNT are filled in ammunition by pouring. The filling compound is prepared by mixing heated aluminum nitrate with melted TNT. It is dangerous to melt amatols with a large (80-90%) ammonium nitrate content. The explosive properties of ammonium nitrate VV are given in Table 1.13.

Ammonium nitrate VV used in industry are usually termed ammonites. They are distinguished by a low content of high explosives (no more than 30%). Depending on purpose, ammonites are divided into two groups: impermissible and permissible. Permissible ammonites, sometimes called safety VV, are designed for blasting in mines and pits. Because of the danger of coal-dust or gas

Table 1.13. Basic characteristics of mixtures with ammonium nitrate.

(1)	(2)	(3)	(4)	(5)
{ 6 Amatol	5300-5500	970	2890	200
{ 7 Ammonoxyl	5000	980	2890	200
{ 8 Ammonal	5100	1180	3320	200
{ 9 Bellite	5000	968	2850	200
{ 10 Schneiderite	5100	921	2250	200
{ 11 Maysite	5000	955	2870	200
{ 12 Dynammon	4000	970	1900	200

Key: (1) VV designation; (2) Detonation velocity, m/sec; (3) Explosion heat, kcal/kg; (4) Explosion temperature, °C; (5) Flash point, °C; (6) Amatol; (7) Ammonoxyl; (8) Ammonal; (9) Bellite; (10) Schneiderite; (11) Maysite; (12) Dynammon.

explosion during blasting, special demands are placed on VV used in the mining industry. Combustible gases, the chief component of which is methane, are released into the atmosphere of a mine during the extraction of coal. In combination with air, methane forms explosive and easily combustible mixtures. Furthermore, coal dust is formed during coal blasting, loading, and transportation. This dust, too, may explode when suspended in the air. Permissible VV are distinguished by reduced temperature and heat of explosion and the absence of combustible gases and free oxygen among the explosion products. The specific properties of permissible ammonites are achieved by including in them inert additives (halogen salts of alkaline metals) that reduce the temperature of the explosion products, facilitate completeness of the explosive reaction, and hinder ignition of the methane-air mixture.

Oxyliquits is the term for explosive mixtures of combustibles with liquid oxygen. Used as combustibles in oxyliquits are solids that have absorptive power: charcoal, wood flour, sawdust, peat, moss, etc. Oxyliquits are distinguished by high fugacity of effect (Q_v up to 2000 kcal/kg) and low physical stability. They rapidly lose explosive effect because of oxygen evaporation.

Oxyliquits are used chiefly for demolition work in industry. In wartime, however, they can be used to fill large high-explosive aerial bombs.

Liquid explosive mixtures are solutions of liquid or solid combustibles in liquid oxidants. Nitric acid, hydrogen peroxide, tetranitromethane, etc., can be used as oxidants. Benzene, toluene, nitrobenzene, alcohols, and many other organic substances can act as combustibles. Liquid explosive mixtures have high power, are very sensitive to external influences, but have low physical stability. The low cost of liquid explosive mixtures and the broad raw-materials base for their manufacture make them promising for use in wartime. They can be used to fill large high-explosive bombs. Used during the Great Patriotic War for filling aerial bombs was mixture KD, composed of 60% nitric acid and 40% dichloroethane. To reduce the corrosive effect of the mixture on metal, a small amount of oleum was added to it. With a specific weight of about 1.4 g/cm^3 , the KD mixture had a heat of explosion $Q_V = 1080 \text{ kcal/kg}$ and a detonation velocity $D = 6180 \text{ m/sec.}$

§ 10. INITIATION EQUIPMENT

Initiation equipment is the term for devices designed for initiating the explosive transformation of VV charges. The effect of initiating equipment is produced by simple initial impulses: impact, incandescence, flame. Initiating equipment is divided into two groups, depending on the type of explosive transformation produced: ignition devices and detonation devices.

Ignition Devices

Ignition devices serve to create a flame. Among these are percussion caps and detonators, primer cups, flash tubes, electric detonators, pyrotechnic cartridges, electric primer caps, and safety (Bickford) fuses.

Percussion caps are used in the cartridges of firearms for igniting the powder charge and normally operate from the impact of a firing pin. A percussion cap (Fig. 1.1) consists of a metal cap 1, into which is compressed a percussion composition 2, covered on top with a foil disk 3. The most prevalent percussion composition is a mixture of mercury fulminate, potassium chlorate, and antimony trisulfide. In this composition, mercury fulminate is the initiator (provides ignition of the composition upon firing-pin impact), potassium chlorate is the oxidant, and antimony is the combustible. The weight of the percussion cap's percussion composition lies between 0.02 and 0.03 g. The shortcoming of mercury fulminate percussion caps is the damaging effect of the percussion composition's combustion products on the barrel and shell case. When burning, the percussion composition releases, in addition to gaseous products, solid particles of potassium chloride and metallic mercury. The potassium chloride, deposited on the surface of the bore, absorbs moisture from the air and becomes an aqueous solution. The chlorine ions in the solution cause intensive corrosion of the barrel. Metallic mercury amalgamates copper and tin shell cases, causing them to crack, and thereby reducing their service life. Therefore, in addition to mercury fulminate compositions, so-called non-corroding percussion compositions find use in percussion caps; in these compositions mercury fulminate is replaced by a mixture of tetrazene with TNRS and the potassium chloride is replaced by barium nitrate.

Fig. 1.1.

Detonators are used in fuses to ignite fuse compositions, delay elements, and flash caps. A detonator (Fig. 1.2) consists of a copper cap 1, percussion composition 2, and cup 3. The detonator usually operates by being pierced by a striker needle. The percussion composition of detonators is the same as for percussion caps. They differ, however, in having a higher content of



Fig. 1.2.

mercury fulminate (up to 50%) and high weight (0.13-0.20 g). The increased mercury fulminate content provides the detonator's high sensitivity to piercing, and the high weight of the composition intensifies the combustibility of the detonator.

The important characteristics of detonators are sensitivity to piercing by the striker needle and actuation time, which limits the rapidity of fuse action. The sensitivity of detonators is determined by the amount of kinetic energy of the striker needle at the moment of piercing, E_0 , which is needed for failure-proof actuation. Experience shows that the value of E_0 depends on the velocity of piercing, v_H . This dependence is adopted in the form

$$E_0 = 900e^{-0.1v_H},$$

where E_0 is measured in g-cm, and v_H in m/sec.

The actuation time of the detonator is counted from the moment the striker pin comes in contact with the cup to the beginning of the efflux of explosion products from the detonator's casing. This time depends on the formula of the detonator composition, its density, the material and strength of the cap and cup, the piercing velocity, and other factors. Data on the dependence of actuation time on the piercing velocity for a detonator used in aviation fuses are given in Table 1.14.

Primer cups and flash tubes are a combination of percussion caps with an additional black powder fuse. The percussion cap and black-powder suspension are structurally joined in a single device that is

Table 1.14. Igniter set cap actuation time.

(1)	1.2	1.5	2.5	5.0	10.0	20.0	30	40	120	140
(2)	601	320	141	86	64	60	40	27	22	20

Key: (1) Piercing speed, m/sec; (2) Actuation time, μ sec.

either twisted into the case or embedded in it. A device of the first type (Fig. 1.3) is called a primer cup, of the second type (Fig. 1.4) a flash tube. Primer cups and flash tubes are used in the cartridges of large-caliber weapons (over 20 mm) instead of a common igniter set cap. An additional igniter made of black powder intensifies the effect of the percussion cap and provides more reliable ignition of the charge.



Fig. 1.3.

Electric detonators are used to create a flash using an electric current. Structurally an electric detonator (Fig. 1.5) consists of two conductors, to the ends of which is soldered a bridge made of a thin Nichrome, constantan, or platinum-iridium wire. A drop of firing composition (TNRS or a mixture of lead thiocyanate with potassium chlorate) is applied to the bridge. The fuse is enclosed in a metal or cardboard sleeve and fastened in it using a mastic, rubber, or plastic plug. The actuation time of an electric detonator depends on the current strength and varies between 70 and

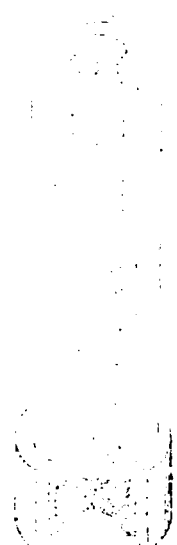


Fig. 1.4.



Mastic *Firing composition*

Fig. 1.5.

200 μ sec. Electric detonators are used in fuses to create a flash and in electric detonators employed in blasting.

Pyrotechnic cartridges are used to ignite the fuses of the propellant charges of rocket missiles. The construction of a pyrotechnic cartridge (Fig. 1.6) consists of a case 1, an electric detonator 2, a contact device 3, and a firing composition 4. The contact device serves as a connection between the electric detonator and the aircraft's on-board source. This connection is accomplished through a contact core 5 and the case of the pyrotechnic cartridge, and these are insulated from each other. The bridge of the fuse is attached to them using foil plates 6. The pyrotechnic cartridge is mounted in the wall of the rocket-motor tube so that, after the missile is installed on the aircraft, it touches the contact device

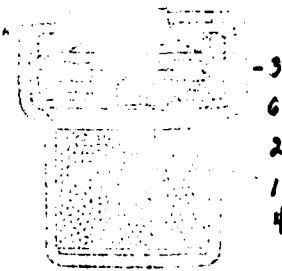


Fig. 1.6.

of the launcher through the contact core. To launch the missile, a current pulse is fed from the on-board source to the electric detonator of the pyrotechnic cartridge. The PP-9RS pyrotechnic cartridge for rocket missiles weighs 10 g, the length of the pyrotechnic cartridge is about 20 mm, the minimum actuation-current strength is 0.9 A, and the average actuation time is on the order of 0.001 sec.

Electric primers have the same purpose as igniter set caps. As opposed to the latter, they are actuated by an electric current pulse. An electric primer (Fig. 1.7) consists of a case 1, a firing composition 2, an electric detonator 4, a contact rod 5, and insulating sleeves 3. The thread on the case serves for screwing the primer cap into the cartridge base. The electric detonator 4 is attached to a power source through the contact rod and primer cap case, and these are insulated from each other by plastic sleeves 3.



Fig. 1.7.

To produce a shot, a current pulse is fed through the contact rod to the bridge. The electric detonator actuates and ignites the

firing composition, which in turn ignites the cartridge case powder charge.

Safety fuses serve to transmit a thermal energy pulse (flash) for a distance. A fuse consists of a core and a wrapping (Fig. 1.8). The core of the fuse is filled with densely compacted grains of black powder, and the wrapping is made of linen or cotton threads and a waterproofing composition. The burning speed of a fuse is on the order of 1 cm/sec.

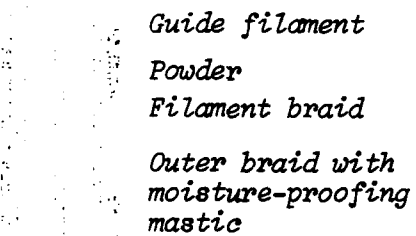


Fig. 1.8.

Detonation Devices

Detonation devices are used to create an explosive impulse. Belonging to this group are igniters, electric detonators, safety fuse detonator sets, and detonating cords.

Igniters are used to ignite the detonation of high-explosive charges of assorted ammunition and demolition charges. Depending on the type of initial impulse producing their action, they are divided into pierced or flash types. Figure 1.9 shows a TAT-type flash-action igniter device. The filling of the igniter consists of three explosives -- TNRS 1, lead azide 2, and tetryl 3. In this composition lead azide is the basic initiator, as it has the greatest initiating power. TNRS is used to increase the reliability of explosion of the lead azide, which has low sensitivity to thermal impulse. Tetryl increases the power of the igniter. The tetryl charge is compressed into the igniter in three layers with sequentially increasing compression pressure, on which, of course, the susceptibility of the VV to detonation depends. The igniter charge is covered on top by a



Fig. 1.9.

cup 4, which protects it from external effects and improves the initiating power (the cup decreases somewhat the dispersion of the gases of the top layer of the charge). The cup has an opening for passage of the flash which is covered by a silk gauze 5. The actuation time for flash igniters is determined basically by the power of the initiating impulse and lies between 20 and 100 μ sec. Figure 1.10 shows a piercing-action igniter. The filling of the igniter is made of a piercing composition, lead azide, and tetryl. Used as the piercing composition is a mixture of tetrazene, TNRS, barium nitrate, and antimony. As with igniter set caps, the actuation time for igniters depends on the speed of the cap's piercing by a striker needle. When the piercing speed varies between 30 and 180 m/sec it lies in the 20-100- μ sec range.



Fig. 1.10.

Electric detonators serve to create an explosive impulse initiated by an electric current. They are used in blasting

and demolition work with an electric blasting device. An electric detonator used in blasting work (Fig. 1.11) is a combination of an electric detonator with an igniter in a common sleeve. The electric detonators of fuses (Fig. 1.12) have a construction like flash-action igniters, differing from them by the presence of a fuse head soldered to two conductors.

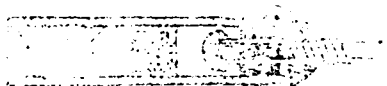


Fig. 1.11.

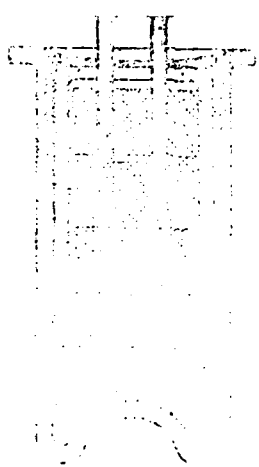


Fig. 1.12.

Safety fuse detonator sets are a combination of a safety fuse with a flash-action igniter, and they are used with the flash method of blasting.

Detonating cords (DSh) are used for rapid transmission of detonation with simultaneous explosion of a series of charges. In construction, detonating cords resemble fuses, differing from them in the core, which consists of a high explosive. There are several brands of detonating cords. For example, the DSh-34 is made of hexogen (transmits detonation at a speed of 7600 m/sec) and the DSh-39 is made of a mixture of hexogen with tetryl ($D=6500$ m/sec).

§ 11. GENERAL REQUIREMENTS FOR V.V. AND METHODS OF FILLING AMMUNITION WITH EXPLOSIVES

A large number of explosives is now known. Only comparatively few of them, however, have found use in ammunition and blasting explosives. This is because most known VV do not meet the basic requirements placed on them by practice. The basic requirements determining the suitability of explosives for practical use are the following:

-- enough efficiency (energy, power) to provide the necessary projectile or destructive effect;

-- certain limits of sensitivity to external influences, providing, on one hand, safety in service use and, on the other, ease of initiating explosion;

-- enough stability to allow storage for a prolonged period;

-- accessibility of raw materials, simplicity and safety of factory production;

-- a number of special requirements associated with the specific conditions of use for the explosives, such as ability to melt without breaking down -- for explosives placed into the shells of ammunition by pouring, flamelessness -- for powders, etc.

In their initial state, high explosives used to fill ammunition are solid, powdered materials. The task of the technology of filling ammunition consists in converting the explosive from a powdered state to a solid-body state. An ammunition charge should meet the following basic requirements:

-- it should have the greatest possible density, which is evenly distributed through the mass of the charge;

-- it should have no structural defects (air bubbles, large crystals, flaws, etc.);

-- it should not have gaps between it and the inner space of the shell.

The greater the density of the charge, the greater the amount of VV that can be placed in the same volume of the warhead's inner space. In addition, as the density of the charge increases, the detonation velocity rises, because of which the power of the explosion increases. Air bubbles between the VV crystals may cause premature action of the ammunition through adiabatic compression of them when shot or at the moment of impacting an obstacle. The same effect is exerted by air bubbles between the charge and the walls of the shell. When the charge settles as it is fired or upon impact on an obstacle, there is adiabatic compression of the air space, in which the temperature of the air may increase to a value several times above the flash point of the VV.

Three methods of filling ammunition are used in practice:

- mechanical packing;
- thermoplastic packing;
- pouring.

Mechanical packing can be performed by screw filling or compression. Screw filling consists of continuously feeding the VV into the space of the shell and compacting it using a worm screw. VV having low sensitivity to mechanical effects, especially friction, can be charged by screw filling. This filling method is used for filling TNT and amatols into medium- and large-caliber artillery and mortar shells.

Packing of VV by compression is used with the separate-charging method of filling. The VV charge is packed not directly in the ammunition, but in special molds. The compressed blocks are encased in binding paste and placed in the ammunition shell. The separate-charging method of filling allows using for filling ammunition desensitized powerful VV (A-IX-1, A-IX-2, t.e.n.) whose high sensitivity does not permit screw filling. The separate-charging method is used

to fill aircraft artillery shells, the warheads of small rockets, and the shells of land and naval artillery.

The thermoplastic packing method is used to fill large-caliber ammunition (high-explosive bombs, the warheads of rockets, etc.) with VV alloys (TG, TGA) containing over 50% hexogen. The alloy is prepared in the form of a plastic mass by heating the VV mixture in a vacuum to the melting point of TNT. The mass prepared in a vacuum does not contain air bubbles and thus requires a lower pressure for its packing. When the ammunition shell is filled, the mass is packed using vibration and then cooled.

With filling by pouring, the VV is melted and put in the ammunition in liquid form. Two methods of pouring are distinguished: continuous and lump. Continuous pouring is used when the charge must have a fine-crystalline structure and high, uniform density. To obtain a fine-crystalline structure and uniform density, the charge is subjected to shimoization in the pouring process. The shimoization operation consists in energetic mixing of the VV alloy, as a result of which the VV crystals are broken down, and there is thereby an increase in the number of crystallization centers that promote obtaining a fine-crystalline casting. Continuous pouring is distinguished by the complexity and duration of the production process. With the lump method of pouring, previously cast lumps of explosive are added to the melted VV. This method of pouring permits obtaining charges of somewhat reduced quality, as compared to continuous pouring, but because of the simpler technology it has found extensive use in filling aerial bombs. The pouring method is used to fill ammunition with TNT, alloys of TNT with hexogen (TG, TGA), dintronaphthalene, and ammonium nitrate. Cast charges are, as a rule, denser than charges obtained by screw filling or thermoplastic packing with vibration.

§ 12. POWDERS

Mixed Powders

Gunpowder or black powder is a mechanical mixture of potassium nitrate, charcoal, and sulfur. In the powder composition the charcoal is the combustible, the nitrate the oxidant, and the sulfur the cementing agent binding the nitrate and the charcoal. Having a lower ignition temperature than charcoal, sulfur also facilitates ignition of the powder. There are several varieties of black powder -- military, hunting, fuse, and others -- that differ as to the percent content of components. Military powder consists of 75% nitrate, 15% charcoal, and 10% sulfur. Black powder is made in the form of individual grains of slate-grey color with a matte gloss. Large grains are often of blue-black to grey-black color with a metallic sheen. The density of the grains varies from 1.5 to 1.93 g/cm^3 . The powder is easily ignited by flame and spark. Small amounts of powder merely flash when ignited, but large amounts explode. When burning, black powder gives off a large number of glowing solid particles together with gaseous products. Black powder is highly sensitive to humidity. It is hard to ignite at a humidity of 2%, and completely loses the ability to ignite at a humidity of 15%. It exceeds some high explosives in sensitivity to impact. The impact of a bullet with a velocity over 500 m/sec produces explosion of the powder. The burning rate of a powder depends on its composition, grain density, and the pressure of the surrounding medium. This dependence is expressed as

$$u=u_1 p^v,$$

where p is the pressure in kg/cm^2 ;

u_1 is the burning rate in mm/sec at pressure $p=1 \text{ kg/cm}^2$.

For military powders, $u_1 = 8-10 \text{ mm/sec}$, $v=0.45-0.55$ at a grain density of 1.7 g/cm^3 . Experiments have shown that at a pressure of 450 mmHg partial extinguishment of the burning powder begins, and at pressures below 350 mmHg the burning is completely extinguished.

The heat of explosion of black powder $Q_V = 665$ kcal/kg and the temperature of explosion $T_B = 2500-2600^\circ\text{K}$.

Black powder is used in military technology only for auxiliary purposes -- in igniters for charges made of nitrocellulose powders in the bursting charges of aerial bombs and shells, in fuses (flash delays and boosters, etc.), in safety fuses, etc. Black powder is used as a means of projection in cartridges for hunting rifles. Close to black powder in properties are ammonium powders, which are a mixture of 90% ammonium nitrate and 10% carbon. Ammonium powders are distinguished by low cost (4-5 times cheaper than black powder) and low physical stability (because of the hygroscopicity of ammonium nitrate). Ammonium powders are used as additives to normal black powder.

Mixed solid propellants are new types of solid fuels for rockets. They are distinguished from nitrocellulose solid propellants by increased unit impulse ($I_1 = 240-250$ kg-sec/kg). Used as oxidants in mixed solid propellants are ammonium perchlorate, ammonium nitrate, potassium chlorate, etc. Serving as fuel-binding agents of mixed solid propellants are polysulfides (substances employed in the manufacture of synthetic rubber), polyurethane rubbers, and polyhydrocarbons. Typical mixed solid propellants are the American Halsite and Thikol propellants, the compositions of which are given in Table 1.15.

Nitrocellulose powders

The following basic components make up nitrocellulose powders: cellulose nitrate, solvents, stabilizers, desensitizers, flash-inhibiting additives, etc.

Cellulose nitrates are the base for all nitrocellulose powders. They determine the power of the powder to a significant extent. Cellulose nitrates are a product of the nitration of cellulose with nitric acid. Cellulose is contained in cotton, wood, flax, straw, etc., in amounts from 92-93% (cotton) to 50-60% (wood). Cellulose

Table 1.15. Mixed powders.

	(1) Components	(2) Composition of powder, %	(3) Halsite	(4) Thiokol
(5) Потасиевая соль	—	60		
(6) Аммонийная соль	75	—		
(7) Битум с небольшим контентом нефти	25	—		
(8) Тиокол (полисульфид резина)	—	20		
(9) Толуен	—	20		

Key: (1) Components; (2) Composition of powder, %; (3) Halsite; (4) Thiokol; (5) Ammonium perchlorate; (6) Potassium perchlorate; (7) Bitumen with a small petroleum content; (8) Thiokol (polysulfide rubber); (9) Toluene.

nitrates are differentiated by percent content of nitrogen. Nitrates with a nitrogen content above 12% are called pyroxylins, those with a nitrogen content below 12% are called colloxylins. All cellulose nitrates are explosives whose power increases with increasing nitrogen content.

A characteristic feature of nitrates is their ability to form plastic masses when affected by assorted solvents. Both pyroxylins and colloxylins are used in the production of powders. Cellulose nitrates play the role of energy source in the powder composition, through which the combustion products perform mechanical work.

Solvents of cellulose nitrates are substances that convert them into a plastic state. Used as solvents in powder production are:

-- volatile solvents: an alcohol-ether mixture (ethyl alcohol and ethyl ether in a 1:1.5 ratio) and acetone;

-- low-volatility solvents: nitroglycerin, nitrodiglycol, etc.;

-- non-volatile solvents: TNT, dinitrotoluene, etc.

After the powder is manufactured the volatile solvents are removed from it almost completely by drying the powders or soaking them in cold and hot water.

Non-volatile and low-volatility solvents are not removed but, remaining in the powder, act as an energy source in addition to the cellulose nitrates.

Stabilizers serve to increase the powder's chemical stability. The action of stabilizers consists in the fact that they chemically bind the nitric oxides or acids released by the powder during storage and thereby slow the powder's decomposition process. Used as stabilizers are diphenylamine and centralite.

Desensitizers are introduced into powder to reduce the combustion rate. Camphor is usually used to desensitize powders.

Flash-inhibiting additives are introduced into the powder composition to obtain a flashless discharge. Rosin and potassium sulfite are used as flash-inhibiting additives.

In some cases such substances as dibutyl phthalate, petroleum jelly, and graphite are introduced into the powder. Dibutyl phthalate is introduced either to reduce the powder's hygroscopicity or to decrease the heat and temperature of combustion. Petroleum jelly is introduced in an amount of about 1% as a technological additive that facilitates the powder-formation process. Graphite is used to cover the surface of fine grades of grain or square cross-section grain powders in order to increase the gravimetric density of the powder and preclude its electrification.

Nitrocellulose powders are divided into several types, depending on the nature of the solvent:

1) Powders based on a volatile solvent, or pyroxylin powders. They are produced by exposing pyroxylin to a volatile solvent -- an alcohol-ether solution. About 40-50% solvent is contained in

plastic mass going to formation. Later the solvent is removed from the formed powder elements by soaking and drying. In the molding process, powder elements made of pyroxylin powder can be given the shape of a ribbon, plate, tube, or grain with one, seven, and more channels. Pyroxylin powders are used to fill the cartridges of firearms (rifles, pistols, aircraft cannons, etc.). The composition of a pyroxylin powder for rifles contains: pyroxylin (91-95%), solvent (1%), diphenylamine (1%), desensitizer (2-6%), graphite (0.2-0.3%), and moisture (1.3-1.5%).

2) Powders based on a low-volatility and non-volatile solvent, or ballistites. The basic component in obtaining ballistites is colloxylin, which is plasticized either by low-volatility solvents -- nitroglycerin, nitrodiglycol, and others, or by non-volatile solvents -- TNT, dinitrotoluene, etc. The designations of ballistites correspond to the designation of the solvent, for example, nitroglycerin powder, nitrodiglycol powder, etc. Ballistite powders are widely used as mortar, gun, and rocket powders. A typical representative of ballistite rocket propellants could be the American IPN powder, the composition of which includes: colloxylin (51.5%), nitroglycerin (43%), centralite (1%), diethyl phthalate (3.25%), carbon black (0.2%), potassium sulfate (1.25%), vaseline (0.08%), and moisture (0.6% above 100%). Ballistite powders can be made in the form of plates, ribbons, rings, tubes, and complex shapes.

3) Powders based on a mixed solvent contain, as basic components, pyroxylin and nitroglycerin. In connection with the fact that pyroxylin is difficult to dissolve in nitroglycerin, used in addition to the low-volatility solvent -- nitroglycerin -- are volatile solvents -- alcohol-acetone or alcohol-ether solutions, which are later removed as in the production of pyroxylin powders. Nitroglycerin powders based on a mixed solvent are called cordites. They are used as powder for rifles, mortars, and guns. An example of cordite composition is the following: pyroxylin -- 64%, nitroglycerin -- 28%, centralite or diphenylamine -- 3%, vaseline -- 2%, alcohol-acetone solution -- 2%, moisture -- 0.7%.

4) Emulsion powders are obtained by treating cellulose nitrates with an emulsion of mixed solvents in water. When the powder masses are mixed in special apparatuses, spherical powder elements are formed, as a consequence of which these powders are called spherical powders. The obtained spherical elements are removed from the emulsion, dried, and desensitized. Emulsion powders are used only in charges for rifles.

5) Powders without solvents are used in mortars and rifles. They are obtained through nitration of ground parchment or viscose filament.

In external appearance, nitrocellulose powders are a corniculate, jelly-like material with greater or lesser transparency. The powders may vary in color: light yellow, dark yellow, grey-green, brown, black, etc. The color depends on the composition, and to some extent on the technology of powder manufacture. The powder's density depends chiefly on the composition, and for various types of pyroxylin powders lies between 1.56 and 1.65 g/cm³. Nitroglycerin powders have a density from 1.54 to 1.62 g/cm³. Existing nitrocellulose powders are less chemically and physically stable than high explosives and initiating explosives. During the storage process a change occurs in the content of volatile materials in the powder and its basic components -- cellulose nitrates and nitroglycerin -- undergo chemical breakdown. The change in the content of volatile materials in pyroxylin powders is the result of evaporation of the residual volatile solvent and change in the powder's moisture content. Also possible in nitroglycerin powders, besides evaporation of the solvent -- nitroglycerin -- is its "sweating out" (exudation) in a liquid state to the surface of the powder elements. Exudation of nitroglycerin increases the danger when handling nitroglycerin powders, because of nitroglycerin's high sensitivity to mechanical influences. Change in the composition of the powder and its gradual breakdown under storage conditions lead to change in the ballistic quality of the powder -- efficiency, combustion rate, etc. The stability of nitroglycerin powders depends on the composition of the powder and the storage conditions (humidity, temperature).

Increasing the temperature of the surrounding medium by 5° accelerates the powder's chemical breakdown process 1.5 to 2 times. To ensure constancy of ballistic qualities, nitrocellulose powders have to be stored in air-tight packaging and at moderate temperature.

The basic type of explosive transformation of powders is combustion. Under certain conditions, however, nitrocellulose powders are capable of detonation. The powder from a common igniter does not detonate, but when a booster charge, such as 50 g of picric acid, is used all types of nitrocellulose powders detonate.¹ Their rate of detonation is around 6000 m/s. According to some data, the powders may detonate when shot with a bullet or struck by fragments at high speed (over 1000 m/sec). Nitrocellulose powders are considerably less sensitive to mechanical influences than initiating VV, but more sensitive than many high explosives. For nitrocellulose powders the sensitivity rises with increasing content of nitroglycerin, but for pyroxylin powders it rises with increasing nitrogen content in the pyroxylin. The burning of most nitrocellulose powders is subject to a certain regularity: the powder burns in parallel layers from the surface of the grain inward. The combustion rate depends on its composition and external conditions, primarily on external pressure and the initial temperature of the powder elements. The combustion rate increases with increasing calorific value of the powder (Q_V), external pressure, and initial temperature and with decreasing density. The dependence of a powder's combustion rate on pressure is termed the combustion rate law. A number of expressions for this law have been proposed by different researchers on powder combustion. The latest studies indicate that each of the proposed formulas is valid only in a certain range of pressures. For example, at pressures on the order of 1000 kg/cm² the formula

$$u = Ap$$

is usable, where A is a constant factor depending on the composition of the powder.

The combustion rate of various powders is usually characterized by the value of factor A in the law $u=Ap$, numerically equal to the combustion rate of the powder u_1 at pressure $p=1$.

Burning of nitrocellulose powders forms chiefly gaseous products, and only in some cases a small amount of solid substances. The basic products of the explosive transformation of powders are CO_2 , CO , H_2 , N_2 , and water vapors.

The calorific value (heat of explosion, C_V) depends on the composition of the powder. For nitroglycerin powders it lies between 650 and 1300 kcal/kg, and for pyroxylin powders between 700 and 1000 kcal/kg. The temperature of explosive transformation of nitroglycerin powder equals 3000°C , of pyroxylin powder 2500°C .

Of all the types of nitrocellulose powders, pyroxylin and nitroglycerin powders find the greatest use in practice. When comparing these two types of powders it must be borne in mind that nitroglycerin powders are distinguished by high power, and are more stable and cheaper than pyroxylin powders. The manufacturing process for pyroxylin powders is longer: 6-10 days for grain powders and over a month for some forms of powder elements. As opposed to pyroxylin powders, ballistite powders are manufactured significantly more quickly (6-8 hours). Nitroglycerin powders made of ballistites are 20-30% cheaper than pyroxylin powder. An essential shortcoming of nitroglycerin powders is the increased scoring of the weapon's bore, which is explained by the high temperature of their explosive transformation and the intense burning of the powder. Also shortcomings of nitroglycerin powders are greater danger in production, compared with pyroxylin powders, and the ability of nitroglycerin to sweat out of the powder (the exudation phenomenon). In aircraft ammunition pyroxylin powders are used to fill the cartridges of aircraft cannons and nitroglycerin powders are used to manufacture the charges of the rocket motors in guided and free-flight missiles.

A certain shape (plate, tube, cylinder, etc.) is given to nitrocellulose powders in the production process. A particle of powder with an established shape and size is called a powder element. Important characteristics of a powder element (Fig. 1.13) are: web thickness, $2e_1$, and geometric dimensions, such as, for single-perforate tube powders, channel diameter, outer diameter, and length of the powder element. Web thickness, $2e_1$, is the term for the least wall thickness of the powder element. This powder-element dimension determines the burning time of the powder. For single-perforated tube powders the web thickness equals the wall thickness, for square cross-section grain powders it equals the thickness of the plate, for grains with seven channels it equals the distance along the diameter between the outer cylindrical surface of the grain (Fig. 1.14) and the circumference of the channel, and also the circumferences of the channels along the diameter and along a straight line joining the channel centers.

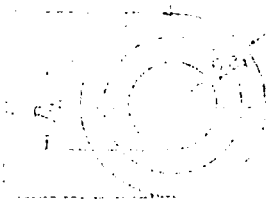


Fig. 1.13.



Fig. 1.14.

The thickness of rocket-propellant powders significantly exceeds that of common gun powders. For this reason the powder elements of rocket propellants have been termed powder grains.

Depending on the shape of a powder element, its burning may be progressive or degressive. Progressive burning is that with which the rate of gas formation increases as the powder burns. Conversely, degressive burning is that with which the rate of gas formation diminishes as the powder burns. The rate of gas formation depends on the nature of change in the powder-element surface during burning. The rate of gas formation increases with increase in the surface of the hot powder. Accordingly, the shape of powder elements with an increasing burning surface is called a progressive shape, and with a decreasing burning surface a degressive shape. Among the degressive shapes are the sphere, cube, prism, etc. Progressive shapes are the cylindrical grain with seven channels, the shaped grain with seven or more channels, etc. When strip and single-perforated tube powders burn, the burning surface remains roughly constant. These powder shapes stand at the boundary between progressive and degressive. Single-perforated tube powders covered on the outer surface with a non-burning composition (inhibitor) belong to the powders with progressive shape. These powders are termed inhibited. The inhibitor prevents the powder from burning inward -- from the lateral surface and from the ends. Progressive burning of a powder provides the best conditions for using the energy of the powder in a firearm, making it possible to achieve a given projectile muzzle velocity at lower pressure of powder gases in the barrel than with degressive burning.

To differentiate the various types of nitrocellulose powders, each of them has been given a certain arbitrary designation (make). The labeling of a powder reflects: the nature of the powder, the shape and geometric characteristics of the powder elements, peculiarities of the technological process of manufacture, information about the manufacturing plant, the powder batch and times of manufacture, etc. Square cross-section powders are designated with the index P1 and two numbers: the first indicates the web thickness in hundredths of a millimeter, the second the plate width in tenths of a millimeter. For example, the make P1-12-10 means that the square cross-section grain powder has a web thickness of 0.12 mm, and a width of 1 mm. Strip powders are designated by the

letter L and a number indicating the strip thickness in hundredths of a millimeter, for example, L-35. Grain and single-perforated tube powders are designated in the form of a fraction: the numerator designates the web thickness in tenths of a millimeter and the denominator designates the number of channels in the grain. The letters Tr are added to the label for single-perforated tube powders. For example, 9/7 means a seven-channel grain with a web thickness of 0.9 mm; 22/1 Tr means a single-perforated tube powder with a web thickness of 2.2 mm. Rifle powders are designated by the letter V, rifle powders for a heavy bullet by the letters VT.

The nature and composition of a powder are designated as follows:

N -- nitroglycerin powder;
NTs and NF -- nitroglycerin powder with increased content of centralite and dibutyl phthalate;
Sv -- powder made of fresh pyroxylin;
Per. -- powder obtained by reprocessing old powders, etc.

Peculiarities of the technological process of the powder's manufacture are designated by the letters:

v/v -- powder manufactured under wartime technological conditions;
uf -- powder from accelerated manufacture (production), etc.

The number of the batch and the year of manufacture are designated in the form of a fraction: the numerator designates the batch number, the denominator the last two numbers of the year of manufacture. The manufacturing plant is designated by a code -- one or several letters.

Given below are several examples of arbitrary designations of powders.

$\frac{12}{7} \text{Sv} \frac{5}{41} \text{TUF}$ -- pyroxylin grain powder with seven channels, with a web thickness of 1.2 mm, made of fresh pyroxylin,

5th batch, 1941, factory "T," accelerated manufacture.

$\frac{13}{1}$ NF $\frac{2}{41}$ P -- nitroglycerin powder with increased content of dibutyl phthalate, single-perforated tube shape (nitroglycerin powders are not made in grains, so the designation Tr is not used), web thickness 1.3 mm, with one channel, 2d batch, 1941, factory "P."

§ 13. PYROTECHNIC COMPOSITIONS

Pyrotechnic compositions is the term for substances and mixtures producing light, heat, smoke, and sound effects upon burning. In military technology pyrotechnic compositions are used to fill illuminants, photo-illuminants, signals, tracers, incendiaries, and concealment and simulation devices. They are also used in rocket propellants and powder cartridges, as igniters of powder charges, and in fuses -- for transmitting flash (delay elements, time fuse compositions). Pyrotechnic compositions are mechanical mixtures consisting of a combustible, an oxidant, and materials giving the composition special properties: coloring flames, forming a colored smoke, reducing the composition's sensitivity (desensitizers), increasing the mechanical stability of a compressed composition (cementers), etc. Used as combustibles in pyrotechnic compositions are high calorific-value metals (aluminum, magnesium, alloys of aluminum with magnesium, etc.) and organic substances (gasoline, kerosene, petroleum, fuel oil, benzene, starch, etc.). Used as oxidants are nitrates (barium, potassium, sodium, and strontium nitrates), hypochlorites (potassium and barium), perchlorates (potassium perchlorate), etc. Production of a colored flame in the burning of pyrotechnic compositions is based on the ability of some chemical elements (such as sodium, barium, strontium, and copper) to give a flame of a certain color at high temperature. Strontium compounds make a red-colored flame, barium compounds a green flame, and copper compounds a blue flame. Normally used to obtain colored smokes are intermediate products and dyes that are colored organic compounds converting to the vapor state upon burning. Used as desensitizers are resins, paraffin, and oils.

Used as cementers are drying oil, natural resins (rosin, shellac), and synthetic resins (iditol, bakelite, etc.). The basic form of chemical transformation of pyrotechnic compositions is combustion.

Illuminants are used in flare cartridges, grenades, shells, mines, etc. In aircraft ammunition they are used chiefly to fill illuminating (glowing) aerial bombs, which serve to illuminate the terrain during nighttime bombing. The illuminants of bombs are mixtures of barium, aluminum, and magnesium nitrates and other substances. Molded of these compositions are illumination charges -- flares that burn for several minutes, creating luminous intensity up to several million candlepower.

Photo-illuminants (photomixtures) are used to fill photo-flash bombs (FOTAB) that illuminate the terrain during aerial photography at night. Used as photomixtures are illuminants in powdered form, which are usually ignited by an explosive impulse. When a photo-flash bomb is actuated the photomixture detonates at a velocity on the order of 1000-3000 m/sec, as a result of which an "instantaneous" (0.1-0.05 sec) flash occurs with a luminous intensity up to several million candlepower.

Signal compositions are used in cartridges, grenades, mines, rockets, etc., for communication (signalling) within military sub-units and between different arms of service. In aviation, signal compositions are used to fill position-indication bombs: TsOSAB (colored), NOSAB [night-position markers], and DOSAB (night and day). These bombs are designed to designate targets, check-and-identification points, route of flight for a formation of aircraft under nighttime conditions, and for other purposes. Daylight signal compositions produce white smoke when burning, and nighttime compositions give off a colored flame.

Tracer compositions serve to mark the flight trajectory of a shell or rocket by creating a colored trail (trace). In artillery shells the tracer composition is placed in the rear of the shell body and is usually ignited by powder gases. Tracer compositions

are no different, in principle, from illuminants and signal compositions as to components.

Smoke-concealment compositions are used in aerial smoke-bombs (DAB), shells, charges, etc., to set up a non-toxic smoke screen in an area in order to conceal the attack and maneuvering of a side's troops, and also to blind an enemy's fire plan, his observation and command posts, etc. Most often used as smoke compositions are substances that form a white smoke (white phosphorus, sulfur trioxide, etc.). Varieties of concealment compositions are those used to set up interference against infrared instruments.

Simulation compositions are used in aerial simulation-bombs (IAB) cartridges, grenades, etc., to simulate the effect of the corresponding ammunition, such as nuclear explosions.

Incendiaries are used to fill aerial incendiary bombs, shells, mines, etc. Used as incendiary compositions in aerial bombs are thermite, electron, organic combustibles, self-igniting compounds, etc.

Thermite is a mechanical mixture of a combustible metal, such as aluminum, and an oxidant -- a metal oxide (iron, manganese, barium, etc.). When a thermite composition burns, free metal oxidizes because of the oxide's oxygen, so thermite can burn even under water. The thermite composition of 25% aluminum and 75% iron oxides has become most prevalent. Thermite ignites at high temperature, so special igniters and intermediate compositions are used to ignite it. When burning, thermite forms poorly spreading red-hot cinders that are capable of not only igniting the combustible material, but also melting the metal. Thermite is not sensitive to mechanical influences and is safe to handle. The combustion temperature of thermite is about 2500°C. Thermite is used to fill small incendiary bombs and in the manufacture of the incendiary charges filling large-sized bombs.

Electron is a combustible alloy of aluminum (10%) with magnesium (90%). Electron burns because of the oxygen in the air, and a temperature of about 2800°C then develops. Electron is used to manufacture the shells of small incendiary bombs filled with thermite.

Liquid organic combustibles -- petroleum, kerosene, gasoline, etc. -- burn because of the oxygen in the air. They are distinguished by easy ignition, prolonged burning, and large flame. They have a number of shortcomings when compared with thermite compositions, however -- low combustion temperature (about 800°), low density, ease of extinguishing, etc. The incendiary power of liquid combustibles is considerably lower than that of thermite compositions, so they are used for effect on easily ignited objects. Organic combustibles are now used in thickened form to fill aerial bombs. Liquid-combustible thickener has been termed napalm. Normally the term "napalm" is used in a broader sense and refers to the entire burning mixture. Napalm is aluminum salts (soaps) in a mixture of organic acids. Used in the standard method of obtaining napalm is a mixture containing 25% naphthenic acid, 25% oleic acid, and 50% a mixture of palmitic, lauric, and other acids given off in the saponification of coconut oil. The designation "napalm" is derived from the beginning of the words "naphthenic" and "palmitic" acids. Viscous burning mixtures are manufactured by adding 4-8% powdered napalm to gasoline and kerosene. Different napalm formulas, having different compositions and ratios of the initial acids, are used in practice. A viscous burning mixture is a gelatinous mass. Special additives to this mass give it the ability to adhere to the surfaces of various objects and stay on them. Metal powders, such as magnesium, are added to napalm to increase the combustion temperature.

White phosphorus, which ignites easily in air, is the self-igniting substance most used in military technology. A temperature of about 1000°C is developed when phosphorus burns.

CHAPTER 3

THE BLAST EFFECT OF AMMUNITION

The destructive effect of the explosion of the bursting charge of ammunition in different media is sometimes called the blast effect of the ammunition. The blast effect of ammunition at short relative distances is conditioned by the effect of gaseous explosion products. With an increase in the distance, it is caused by the joint action of gaseous explosion products and the shock wave formed in the medium. At sufficiently great distances, the blast effect is conditioned by the action of the shock wave propagated in the medium.

In certain published sources, one can encounter the idea of the blast effect of an explosion as no more than the destruction and blow-out of some dense medium (most often the ground) in which the explosion occurred.

As already noted, the destructive effect of a bursting charge in direct contact with the surface of the object being destroyed is manifested in the form of an effect of breaking up and is called the brisance of the explosion.

In the case of the blast effect of an explosion, one of the most important factors of the destructive effect is the shock wave formed in a medium in the explosion of an explosive charge

in it.

Since the relative dimensions of the zone of the action of gaseous explosion products are comparatively small, consideration of the destructive effect of a shock wave propagated in the medium as a result of an explosion is of the greatest interest.

We shall consider the blase effect of ammunition in explosion in air, water and the ground.

§ 1. EXPLOSION OF A CHARGE IN AIR

The size of the zone of the direct effect of explosion products in an explosion in air is comparatively small and is equal to 2000-4000 times the volume of the explosive charge; i.e., the effect is manifested at distances of 12-16 times the charge radius from the center of the explosion. The joint effect of explosion products and the shock wave is exhibited up to distances of approximately 20 times the charge radius.

In further expansion, the pressure in the explosion products drops to a level at which their mechanical effect on destruction objects practically ceases.

The destructive effect of an explosion in the case in question, however, is not limited to the zone directly surrounding the charge, within which the action of the gaseous explosion products themselves occurs, but spreads far beyond this zone. This feature of the blast effect of an explosion is involved with the emergence of a shock wave in the medium surrounding the charge and is determined by the following physical phenomena. Gases formed as a result of the explosion which are heated up sharply and are compressed to an extremely high pressure (of the order of hundreds of thousands of atmospheres) in their expansion produce a sharp

shock on the surrounding medium. As a result of this shock, the layer of the medium, such as air, adjacent to the explosive charge undergoes strong compression and, in trying to expand, intensely compresses the next layer of the medium. The latter, being compressed and trying to expand, compresses still another new layer, the next layer of the medium. Thus compression is transmitted from the layers adjacent to the charge to the next layers of the medium, from them to the next layers, etc. Simultaneously with compression of the respective layers, a sharp increase in pressure - a pressure shock - occurs in them. The temperature of the respective layers of the medium also increases as a result of the sharp compression, as does the density.

As a result, a disturbance of a special kind - a shock wave, in the form of a jump in the pressure (density, temperature) propagated over the medium at supersonic speed - emerges in the medium in which the explosion occurred. The shock wave belongs to a special type of waves characterized by the fact that the change in the state of the medium through which the wave is propagated which is typical of all wave processes does not occur smoothly and gradually (as in the case of propagation of an acoustic wave, for example) but sharply, with a sudden change. Such a sharp, abrupt change in the state of the medium is explained, in particular, by the circumstance that the shock wave is propagated through the medium at a speed which always exceeds the velocity of sound in the medium in question.

Of all the parameters characterizing the state of a medium, the most important from the point of view of a mechanical effect is the pressure. In connection with this, an abrupt change in pressure spreading in the medium at a supersonic speed (for the medium in question) is often called a shock wave.

Shock waves, as we know, can arise in any compressible medium

under the condition of the appearance of a sufficiently sharp initial pressure shock (increase) in the medium (under the action of some factor). The boundary dividing the undisturbed medium from the medium with characteristics which have increased as a result of the action of the shock wave is called the shock wave front. It is assumed practically that the parameters of the medium change abruptly on the surface of the shock wave front. The actual structure of a shock wave front was considered in Chapter 2.

Three types of shock waves are normally considered:

- the plane shock wave - the shock wave front has the form of a plane situated perpendicular to the direction of propagation of the wave;
- the cylindric shock wave - the shock wave front has the form of a cylindric surface;
- the spherical shock wave - the shock wave front has the form of a spherical surface.

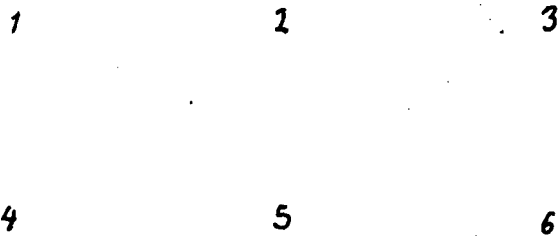


Fig. 3.1.

In the initial stage of formation, the shock wave moves together with the source of its initiation - the explosion products - ahead of them. The pressure in the explosion products and the velocity of their movement decrease in proportion to expansion of the "gas bubble" - the space occupied by the explosion products. The velocity of movement of the explosion products drops to zero, and the pressure in them, as a result of the fact that the explosion products have continued to move for some time by inertia, becomes less than the pressure in the surrounding medium. The explosion products change their direction of movement and begin to move in the opposite direction - toward the explosion center. Such a stage in the development of the process sets in when the shock wave separates, as it were, from the explosion products which have caused its appearance and continues to spread, but independently. The process of separation of the shock wave from the explosion products can be traced in photographs (Fig. 3.1) of the explosion of a charge in air taken with an FP-22 high-speed movie camera with a frequency of 100,000 frames per second.

It is customary to call the distance at which the shock wave separates from the explosion products the critical distance R_K .

The change in pressure at a point of the medium at some distance from the explosion center is shown in Fig. 3.2.

Fig. 3.2.

The designations made in the figure have the following meanings:

p_0 represents atmospheric pressure;

p_1 is the maximum pressure in the shock wave;

τ is the time of action of the excess pressure of the shock wave;

τ_p is the time of action of the rarefaction wave.

As one can see from the graph (Fig. 3.2), the pressure at each point reached by a shock wave propagated through the medium reaches the maximum value with a jump. Then, as a result of the pressure differential between the shock wave and the medium, the pressure begins to decrease and falls to atmospheric pressure (the pressure in the undisturbed medium surrounding the explosive charge) in a definite time interval τ . Particles of the medium which make up the flow of the medium behind the shock wave front pass through an equilibrium position (a pressure equal to atmospheric pressure) by inertia; the pressure at the point in question becomes lower than atmospheric pressure - a rarefaction zone is formed. Movement of the flow of the medium in the direction of wave propagation is a characteristic feature of a shock wave arising, in particular, as a result of the explosion of a charge in air.

The velocity of movement of an air flow can reach a considerable value and will be greater the greater the pressure and the velocity of propagation of the shock wave front.

Chapter 2 considered in detail the basic physical patterns and quantitative correlations describing the character of the emergence

and propagation and also the structure of detonation and shock waves. These correlations give the possibility of determining, in particular, the basic parameters of a shock wave emerging in air. For example, the following relationships can be used for evaluating the parameters of strong air shock waves [see expressions (2.54), (2.55) and (2.56)]:

$$\begin{aligned}\rho_m &= \frac{k+1}{k-1} \rho_0 \\ u_1 &= \frac{2}{k+1} D_B \\ p_1 &= \frac{2}{k+1} \rho_0 D_B\end{aligned}\quad (3.1)$$

Here ρ_0 is the density of air before approach of the shock wave; ρ_m is the density of air at the shock wave front; u_1 is the velocity of the air flow behind the shock wave front; D_B is the velocity of propagation of the shock wave front; p_1 is the pressure on the shock wave front; k is the ratio of the heat capacity of the air at a constant pressure (c_p) to the heat capacity at a constant volume (c_v).

For evaluating the destructive effect of an explosion in cases where the shock wave is the main damaging factor, it is necessary to know the form of the dependence $p(t)$ (Fig. 3.2) for any point of the medium surrounding the explosive charge.

As a result of the fact that establishing the analytical form of the dependence $p(t)$ for different distances from the location of the explosion is a comparatively difficult problem, for practical calculations of the effect of the shock wave of an explosion, we limit ourselves to obtaining calculation relationships for determining the maximum pressure (p_1) on the shock wave front and the time (τ) of the action of excess pressure of the shock wave (Fig. 3.2). These relationships make it

possible to compute the values of p_1 and τ at the point under examination in the space surrounding the charge for the range of variation of the distance (R) from the explosion center which is of practical interest and the basic characteristics of the bursting charge used in the type of aviation ammunition in question.

Determining the Pressure on a Shock Wave Front

The maximum pressure in an air shock wave or the pressure on the shock wave front p_1 (often designated p_m) is one of the basic characteristics of the destructive effect of an explosion in air. The value of the excess pressure $\Delta p_1 = p_1 - p_0$, where p_0 is atmospheric pressure, is determined instead of the maximum pressure in an air shock wave for practical calculations. In order to have the possibility of calculating the value of p_1 (or Δp_1), it is necessary to know the dependence of p_1 on both the characteristics of the bursting charge and the distance to the focus (center) of the explosion. Among the characteristics of the bursting charge, the most important are the weight of the charge w and the specific heat of explosive decomposition Q_v , since it is just these variables which determine the energy possibilities of the charge and, consequently, are decisive in an explosion in the medium in question for the parameters of the shock wave which emerges in the explosion.

The problem thus can be reduced to determining the form of the dependence $\Delta p_1 = f(R, w, Q_v)$, where R is the distance from the center of the explosion to the point at which the excess pressure is determined. The formulas for calculating Δp_1 were obtained by various authors. The most thoroughly substantiated formula, which has found extensive practical application, is the formula proposed by M. A. Sadovskiy. This formula was derived based on the theory of similarity of explosive processes, and the numerical coefficients included in it were obtained by processing extensive

experimental data.

As already noted previously (see Chapter 2), if energy losses which occur in an explosion are not taken into consideration, and geometrically similar charges are selected under identical initiation conditions, theoretical analysis of the effect of explosion of these charges and extensive experimental research make it possible to formulate a law of geometric similarity which occurs in an explosion: the distances at which parameters of shock waves formed in the explosion of charges of a given explosive which differ in regard to absolute dimensions are equal are proportionate to the linear dimensions of the explosive charge. For example, in explosion of n spherical charges of the same explosive with radii r_1, r_2, \dots, r_n , identical values of the shock wave parameters, the maximum pressure, in particular, will occur at distances from the charges of R_1, R_2, \dots, R_n , respectively, under the following condition:

$$\frac{R_1}{r_1} = \frac{R_2}{r_2} = \dots = \frac{R_n}{r_n}.$$

Using the law of geometric similarity, one can write the following expression:

$$p_1 = k_1 f_1 \left(\frac{R}{r} \right) \quad \text{or} \quad p_1 = k_2 f_2 \left(\frac{r}{R} \right),$$

where k_1 and k_2 are coefficients whose values are determined from an experiment.

The form of the function f_1 or f_2 is also determined by analysis of experimental data.

It proves more convenient to represent p_1 in the form of a function not of the charge radius r but of the charge weight w for solving practical problems. Since $r = \sqrt[3]{\frac{3}{4\pi\gamma} w}$:

(where γ is the specific gravity of the explosive); one can write:

$$p_1 = k\varphi \left(\frac{\sqrt[3]{\omega}}{R} \right).$$

Based on processing of data of extensive experimental research, M. A. Sadovskiy obtained a formula for calculation of $\Delta p_1 = p_1 - p_0$ in the following form:

$$\Delta p_1 = 0.84 \frac{\sqrt[3]{\omega}}{R} + 2.7 \left(\frac{\sqrt[3]{\omega}}{R} \right)^2 + 7.0 \frac{\omega}{R^3} \quad (3.2)$$

In this formula, Δp_1 is expressed in kg/cm^2 , ω is in kilograms, and R is in meters.

The formula (3.2) is applicable for the following conditions:

- the explosive is tetryl;
- the charge has no metallic shell;
- $\omega > 100 \text{ kg}$;
- explosion of the charge occurs in air at a height sufficient for excluding a noticeable effect of reflecting action of the ground surface on values of parameters of the air shock wave.

Practically, the altitude of the explosion should be no less than the distance at which the shock wave passes into a sound wave for fulfilling the latter condition.

In the case of an explosion on the ground, as a result of reflection of the explosion products from the ground surface, one can assume approximately that the energy of the explosion is distributed not in a sphere, as occurs in an explosion in air, but in a hemisphere. Consequently, a ground explosion is approximately equivalent in regard to the shock wave parameters to an air

explosion with a doubled charge. It follows from this that in the application of formula (3.2) for a case of a ground explosion, the value 2ω must be substituted into the formula for the value ω ; then the formula has the following form:

$$\Delta p_1 = 1.07 \frac{\sqrt[3]{\omega}}{R} + 4.2 \left(\frac{\sqrt[3]{\omega}}{R} \right)^2 + 14 \frac{\omega}{R^3} \quad (3.3)$$

In the use of formula (3.2) for calculation of the pressure in explosion of small charges (with a weight less than 100 kg), it is necessary to substitute the so-called active quantity of the explosive ω_a for ω ; i.e., it is necessary to take into consideration only that part of the explosive whose energy is expended for formation of the shock wave. In this case, the energy of the rest of the charge ($\omega - \omega_a$) is spent on various losses, the magnitude of which cannot be neglected in view of the relatively small weight of the charge.

The greatest part of the lost energy proves to be concentrated in the surface layer of the charge, which is scattered in an explosive transformation of the deeper layers and does not participate in the formation of gaseous explosion products. The thickness (Δ) of this surface, scattered layer (sometimes called the Yu. B. Khariton layer) does not depend on the absolute dimensions of the charge but remains constant for charges produced from an explosive of a given type under identical initiation conditions and with the same shape of the charges.

M. A. Sadovskiy suggests using the following formula for computing ω_a :

$$\frac{\omega_a}{\omega} = \left(1 - \frac{\delta}{r} \right)^3,$$

where δ is the thickness of the VV [explosive] layer which is scattered, and r is the VV charge radius.

The presence of a shell of the charge, on the one hand, reduces the value of ω_a , since some part of the energy of the

explosive is spent for breaking up the shell and imparting the initial velocity to the fragments; i.e., it results in some decrease in ω_a . On the other hand, a charge shell promotes a decrease in energy losses and, consequently, leads to an increase in ω_a . With a degree of accuracy sufficient for practical work, one can assume the pressure values for typical explosives to be proportionate to $\sqrt[3]{Q_v}$, where Q_v is the specific heat of the explosion, with identical values of the dimensionless ratio $\frac{\sqrt[3]{Q_v}}{R}$. Therefore, in order to use formula (3.2) for determining the pressure in explosions of explosives other than trotyl, it is sufficient to multiply the coefficients in this formula by

$$\sqrt[3]{\frac{Q_{BB}}{Q_{TNT}}},$$

where Q_{BB} is the explosion heat of the VV in question, and Q_{TNT} is the explosion heat of trotyl.

Formula (3.2) thus can be used in this case in the following form:

$$\Delta p_{1,00} = \Delta p_{1,TNT} \sqrt[3]{\frac{Q_{BB}}{Q_{TNT}}} \quad (3.4)$$

The method which has been presented for determining the pressure on an air shock wave front possesses accuracy which is quite sufficient for practical calculations and makes it possible to compute Δp_1 in an extremely broad range of conditions of the effect of an explosion in air.

Determining the Time of Action of a Shock Wave

As has already been mentioned, it is customary to consider the time τ of the action of excess pressure as the time of action of a shock wave (Fig. 3.3). In considering a method for determining the value of this time, it is necessary to take into consideration the following features of movement of the shock wave. Since the

pressure is greater in the shock wave front (1-1) than in all other layers of the wave, while the velocity of movement of compressed gas, as we know, increases with an increase in the pressure, the wave front propagates more rapidly than all other layers of the wave. Different layers of the shock wave propagate at different velocities, and the closer the layer is located to the rear section - the "tail" - of the wave, the more the velocity decreases. The tail of the wave itself, in which the excess pressure $\Delta p_1 = 0$, moves at a velocity somewhat greater than the velocity of sound in undisturbed air c_0 . As a result of the velocity gradient, the shock wave stretches out in proportion to the distance from the location of the explosion; the wave front gradually moves away from the "tail" in time, and the time τ increases. In this case, as M. A. Sadovskiy points out, the wave, while stretching out in time, preserves a practically constant depth, since not only does the time τ increase in proportion to the distance from the explosion location, but the velocity of movement of the front itself, like that of the other layers of the shock wave, also drops at the same time.

Fig. 3.3.

The value of τ thus depends on the distance R between the point at which the time of action of the shock wave is determined and the center of the explosion,

$$\tau = \tau_1(R). \quad (3.5)$$

M. A. Sadovskiy established based on processing of data of experimental research that with a predetermined weight (ω) of the explosive, the dependence (3.5) has the form $\tau = k/\sqrt{R}$.

On the other hand, it is obvious that the value of τ , like other parameters of the shock wave, is determined at any distance by the weight ω of the charge: $\tau = \tau_2(\omega)$.

Thus, for predetermined explosion conditions,

$$\tau = \tau(\omega, R).$$

Analysis of extensive experimental data made it possible to obtain a formula for determining the value of τ in the following form:

$$\tau = 1.3 \cdot 10^{-3} \sqrt[6]{\omega} \cdot \sqrt{R}. \quad (3.6)$$

In this formula, τ is expressed in seconds, ω is in kilograms, and R is in meters. Formula (3.6) produces the most precise calculation data in ranges of variation of distances from 2 to 500 m and charge sizes from 0.04 to 1000 kg. These limits of variation of R and ω cover most of the cases of practical importance in evaluation of the destructive effect of an explosion in air.

Reflection of a Shock Wave from an Obstacle

Cases of determination of the parameters of air shock waves when the wave is freely propagated at a given point in space, i.e., there is no obstacle in the path of propagation of the wave at this point, were considered above. We shall consider how the pressure in a shock wave changes if there proves to be an obstacle in its path.

First we shall consider a case in which the surface of the obstacle which absorbs the pressure is situated perpendicular to the direction of propagation of the shock wave (Fig. 3.4). In considering the character of variation of the pressure in reflection of the shock wave, we shall start with two assumptions:

1) The partition is undeformable. For charges of normal explosives, when the time τ of action of excess pressure of the shock wave is substantially less than the period T of natural oscillations of obstacles actually encountered, this assumption actually reflects the true picture of the phenomenon, and one can neglect deformation of the obstacle which occurs in the course of the time of action of the excess pressure.

2) The dimensions of the obstacle are unlimited. This assumption essentially means that the phenomenon of flow of the shock wave around the obstacle is not taken into consideration. Methods for accounting for the effect of the flow will be considered somewhat later.

Fig. 3.4.

As the shock wave front approaches the surface of the obstacle, the pressure essentially begins suddenly to act on the obstacle; the pressure actually is made up of two parts: the pressure p_1 of the air on the shock wave front and the pressure conditioned by sharp stopping of compressed air layers moving behind the shock wave front.

The first component normally is called the static pressure, while the second - which essentially is the pressure of the velocity head of moving compressed layers of air - is called the dynamic pressure. The dynamic component of the total pressure is caused by

the fact that with sharp slowing down of moving masses of air at the obstacle, the energy of their movement is transformed into pressure energy. The dynamic pressure, especially in the action of shock waves of great intensity on an obstacle, can substantially exceed the static pressure p_1 , and the total pressure on the obstacle (p_2) accordingly can prove to be significantly greater than the pressure p_1 .

The circumstances which have been considered result in the fact that a new, stronger pressure differential (shock) develops at the surface of the obstacle when a shock wave hits.

It has been established in examination of the process of formation of shock waves that the appearance of a pressure shock in air leads to propagation of this shock in the surrounding medium, i.e., to the formation of a shock wave. In a similar way, in a case where a shock wave encounters an obstacle, in the zone of the appearance of a new, stronger pressure differential, a new shock wave develops; the new wave is propagated from the obstacle toward the original shock wave.

The newly formed shock wave is called a reflected shock wave, while the original wave approaching the obstacle is called the incident shock wave.

The process of reflection of an air shock wave from an undeformable obstacle can be traced in photographs (Fig. 3.5) taken with an FP-22 high-speed movie camera with a frequency of 100,000 frames per second.

A characteristic feature of the process of propagation of a reflected shock wave is the fact that it propagates in the mass of air compressed by the incident wave, while the incident shock wave propagates in an undisturbed air medium. As a result, the pressure on the front of the reflected wave p_2 is greater than the pressure

on the front of the incident wave p_1 .

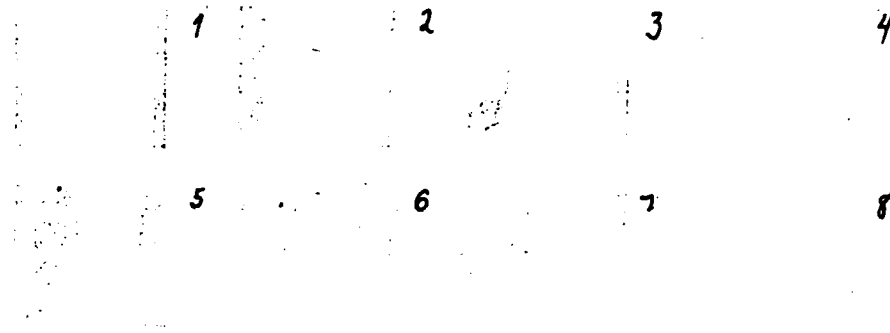


Fig. 3.5.

We shall determine the value of the maximum pressure on an obstacle in reflection of an air shock wave. The maximum pressure on the obstacle emerges at the moment when the incident shock wave encounters the obstacle. At this initial moment of development of the reflection process, the static pressure is the greatest, and the dynamic component of the total pressure is also the greatest. For determining the value of the maximum pressure, we shall use a relationship obtained in calculation of the parameters of shock waves for a velocity u_1 of movement of air particles behind a shock wave front [see expression (2.43)].

Transforming expression (2.43) to the form

$$u_1 = \sqrt{\frac{(p_1 - p_0)v_0}{(k + 1)p_1 + (k - 1)p_0}} \left(1 - \frac{v_1}{v_0}\right)$$

and substituting the value of v_1/v_0 from expression (2.51), we obtain

$$u_1 = (p_1 - p_0) \sqrt{\frac{2}{p_0[(k + 1)p_1 + (k - 1)p_0]}} \quad (3.7)$$

where p_1 is the pressure on the front of an incident shock wave; p_0 is the pressure in an undisturbed air medium - atmospheric pressure; ρ_0 is the density of the undisturbed air medium; k is the ratio c_p/c_v of the heat capacity at a constant pressure to the heat

capacity at a constant volume for the air.

It was assumed in deriving this formula that the velocity of movement of particles of the undisturbed medium $u_0=0$, since the shock wave propagates in undisturbed air. But in a general case, with $u_0 \neq 0$, the formula (3.7) has the following form:

$$u_1 = (p_1 - p_0) \sqrt{\frac{2}{p_0 [(k+1)p_1 + (k-1)p_0]}} - u_0 \quad (3.8)$$

Similarly, for determining the velocity of air on the front of a reflected shock wave, by cyclical substitution of the appropriate parameters, we obtain the following expression:

$$u_2 = (p_2 - p_1) \sqrt{\frac{2}{p_1 [(k+1)p_2 + (k-1)p_1]}} - u_0 \quad (3.9)$$

The parameters of a reflected shock wave in formula (3.9) have the index "2" while parameters of the medium through which the reflected wave propagates, in this case the parameters of air compressed by the incident shock wave, have the index "1." As already noted, the maximum pressure p_2 on an obstacle arises at the moment when the incident wave meets the surface of the obstacle. At this moment, the front of the reflected shock wave coincides with the surface of the obstacle, and the mass velocity of air particles behind the reflected wave front is equal to zero ($u_2=0$). Comparing formulas (3.7) and (3.9) under this condition, we obtain the following equation:

$$\begin{aligned} & (p_2 - p_1) \sqrt{\frac{2}{p_1 [(k+1)p_2 + (k-1)p_1]}} = \\ & = (p_1 - p_0) \sqrt{\frac{2}{p_0 [(k+1)p_1 + (k-1)p_0]}} \end{aligned} \quad (3.10)$$

Transforming this equation, we obtain

$$\frac{(p_2 - p_1)^2}{[(k+1)p_2 + (k-1)p_1]p_1} = \frac{(p_1 - p_0)^2}{[(k+1)p_1 + (k-1)p_0]p_0}$$

or

$$\frac{(p_2 + p_1)^2}{(p_1 - p_0)^2} = \frac{(k+1)p_2 + (k-1)p_1}{(k-1)p_1 + (k+1)p_0} \quad (3.11)$$

We shall represent the ratio p_1/p_0 with a Gyugonio [as transliterated] adiabatic curve expression (see Chapter 2) in the following form:

$$\frac{p_1}{p_0} = \frac{(k+1)p_1 + (k-1)p_0}{(k-1)p_1 + (k+1)p_0}$$

Substituting this relationship into expression (3.11), we obtain

$$\frac{(p_2 - p_1)^2}{(p_1 - p_0)^2} = \frac{(k+1)p_2 + (k-1)p_1}{(k-1)p_1 + (k+1)p_0} \quad (3.12)$$

After the appropriate transformations, from equation (3.12) we obtain the formula for determining the value of the maximum pressure p_2 in reflection of an air shock wave from an obstacle:

$$p_2 = \frac{(3k-1)p_1 - (k-1)p_1}{(k-1)p_1 + (k+1)p_0} - p_1 \quad (3.13)$$

This formula is called the S. V. Izmaylov formula.

As already noted previously, it is convenient for practical calculations to have a formula for the excess maximum pressure rather than the maximum pressure, for $\Delta p_2 = p_2 - p_0$ rather than for p_2 , in this case; the formula accordingly is expressed through the value of the excess pressure on the incident shock wave front $\Delta p_1 = p_1 - p_0$. It is not difficult to transform formula (3.13) to the following form:

$$\Delta p_2 = 2\Delta p_1 + \frac{\frac{k+1}{k-1} \Delta p_1^2}{4p_1 + \frac{2k}{k-1} p_0} \quad (3.14)$$

Substituting the values $k=1.4$ and $p_0=1 \text{ kg/cm}^2$ into this expression, we obtain

$$\Delta p_2 = 24p_1 + \frac{6\Delta p_1^2}{\Delta p_1 + 7} \quad (3.15)$$

This formula normally is used for practical calculations in computing the excess pressure in a reflected shock wave.

We shall evaluate the maximum possible values of the variables p_2 and Δp_2 or, more precisely, establish the greatest values of the following ratios:

$$\frac{p_2}{p_1} \quad \text{and} \quad \frac{\Delta p_2}{\Delta p_1}$$

One can see from formula (3.14) that the values of the ratios p_2/p_1 and $\Delta p_2/\Delta p_1$, as well as the absolute value of p_2 (Δp_2), increases with an increase in p_1 (Δp_1).

From the relationship (3.13), with $k=1.4$ and $p_1 \gg p_0$, we obtain

$$\left(\frac{p_2}{p_1}\right)_{\max} = \frac{3k-1}{k-1} = 8$$

Accordingly, from formula (3.14) under the same conditions ($k=1.4$ and $p_1 \gg p_0$), we obtain

$$\left(\frac{\Delta p_2}{\Delta p_1}\right)_{\max} = 2 + \frac{k+1}{k-1} = 8.$$

The maximum pressure increase on a reflected shock wave front thus is an eightfold increase as compared to the pressure on the incident wave front. For very intense, strong shock waves (with high values of p_1), the value of k can prove to be less than 1.4; the maximum values of the ratios p_2/p_1 and $\Delta p_2/\Delta p_1$ increase accordingly.

An increase in the pressure in reflection by a factor of 10-11, which corresponds to a value of k of approximately 1.2, is obtained in experiments for strong waves. This increase in pressure as compared with the calculated value is explained by the fact that phenomena of ionization and dissociation of molecules develop at very great pressures, and the value of k decreases.

Evaluating the value of the ratio $\Delta p_2/\Delta p_1$ in a case of reflection of weak shock waves, where $\Delta p_1 \ll \Delta p_0$, and the value of Δp_1 as compared

to p_0 can be neglected, is also of interest.

Under this condition, from formula (3.14) we obtain $\Delta p_2/\Delta p_1 = 2$; i.e., the excess pressure doubles in reflection of weak shock waves. This result coincides with data in reflection of sound (acoustical) waves.

Irregular Reflection of a Shock Wave from an Obstacle

The consideration of the process of reflection of a shock wave from an obstacle which has been presented above was performed for a case in which the direction of propagation of the incident shock wave is perpendicular to the surface of the obstacle (the angle α between the vector of the wave propagation velocity and a normal to the obstacle is equal to zero).

Fig. 3.6.

This angle α actually can vary (Fig. 3.6), changing in absolute value from 0 to 90° . In these cases, both the conditions of contact of the shock wave with the obstacle and the conditions of reflection change, which leads to a change in values of the parameters of the reflected shock wave as compared to the corresponding values of parameters in a "direct" reflected shock wave. In contact of shock waves with obstacles at different angles, other complex physical processes of interaction of the wave with the obstacle occur in addition to the phenomenon of reflection itself; one of these processes is the process of so-called irregular reflection.

The phenomenon of reflection considered previously (with $\alpha=0$) is called regular reflection. In this case, from each elementary area (point) on the surface of the obstacle approached by a definite section of the incident shock wave, a corresponding section of the reflected shock wave propagates as if in a mirror image, in a directly opposite direction. Although some spreading of compressed air over the surface of the obstacle occurs in this case in addition to reflection, this circumstance is neglected for purposes of schematizing the phenomenon, since it does not introduce substantial changes into the reflection picture and practically does not influence the direction of propagation of the reflected shock wave.

The situation is different in a case where the incident shock wave front forms some angle α with the obstacle (Fig. 3.7). In this case, the phenomenon of spreading of particles of compressed air over the obstacle surface cannot be neglected. As a result of such "oblique" contact of the wave with the obstacle, a qualitatively new phenomenon involved with the formation of a "leading edge" shock wave which influences the variation in parameters of the reflected shock wave substantially develops under certain conditions.

(1) (2)

Fig. 3.7.
Key: (1) reflected wave front;
(2) incident shock wave front.

Assume (Fig. 3.7) that the front of an incident shock wave propagating at a velocity D_1 encounters the surface of an obstacle at an angle α . Particles of compressed air are moving at a velocity u_1 directly behind the wave front in the same direction.

Point A is the first point at which the incident shock wave front has reached the obstacle surface at the moment in time under consideration. The velocity of air particles u_1 can be divided into two components: u_{1H} , at a perpendicular to the surface of the obstacle, and u_{1N} , parallel to the surface of the obstacle. At point A where contact of the shock wave with the obstacle occurred, the movement of air particles in the direction of a perpendicular to the obstacle surface is slowed down sharply as a result of slowing of the particles by the partition. A shock wave is formed as a result in a manner similar to the shock considered previously, and an ordinary, regular reflected shock wave develops.

However, the movement of air carried along by the incident shock wave front stops at point A only in the direction of a perpendicular to the obstacle, while the movement of air along the surface of the obstacle continues at the velocity u_{1N} , on the strength of which the conditions are created for the development of a new shock wave moving in the same direction. Point A also moves in this same direction. We shall designate the velocity of movement of point A as v_A . One can see from the diagram (Fig. 3.7) that

$$v_A = \frac{D_1}{\sin \alpha} \quad (3.16)$$

The pressure on the front of the new reflected wave at point A, as we already know from the foregoing, is greater than the pressure on the incident shock wave front (p_1), and since the velocity of movement of a shock wave increases with an increase in the pressure, the velocity of the reflected shock wave front D_2 , α will be greater than D_1 .

We shall specify the following:

$$D_{1n} = k D_{1i}$$

(3.17)

where $k > 1$.

Up to some value of the angle α , so long as the condition $1/\sin \alpha > k$ is adhered to, the velocity of movement of point A is greater than the velocity of movement of the shock wave which has emerged at point A ($v_A > D_2, \alpha$). The value of v_A will decrease in proportion to the increase in the angle α and, beginning at some value α_k which depends on the intensity of the incident shock wave, will become less than D_2, α . The velocity of the wave (generated) at point A grows greater than the velocity of movement of point A itself, the wave separates from this point, and regular reflection breaks down; the reflected shock wave no longer originates from the point of contact with the obstacle surface where the incident wave arrived. Air sharply compressed in reflection, creating a unique air "cushion," forces back the incident wave, as it were, and, in overtaking this wave, moves forward along the line of "least resistance." A new, so-called leading edge shock wave (line a-b, Fig. 3.8) is formed as a result. The front of this wave is perpendicular to the surface of the obstacle, since the wave has been caused by movement of particles of the medium directed along the obstacle surface. Point a, at which the fronts of the three waves - incident, reflected and leading edge - intersect is called the triple point. Up to certain values of the angle α which depend on the pressure in the incident wave, the intensity (the excess pressure on the front) of the leading edge wave increases, after which the leading edge shock wave increases in height in proportion to the increase in the angle α , while its intensity drops.

As a result of the causes indicated, the total reflection pressure on an obstacle first drops up to certain values of the angle α (until the effect of irregular reflection begins to show up), after which it begins to increase and when a maximum depending on the intensity of the incident shock wave is reached, it decreases

again, reaching the value of the pressure p_1 in the incident shock wave at $\alpha=90^\circ$.



Fig. 3.8.

Key: (1) reflected wave front;
(2) incident wave front; (3) leading edge wave front.

We shall consider briefly a method for calculating the value of the maximum pressure on obstacles in reflection of a shock wave in its contact with an obstacle at some angle α . This pressure, as already noted, is made up of a "static" component and a "dynamic" component. The static component, as we know, is equal to p_1 . The dynamic component is determined from the following considerations. This component is essentially the pressure of the velocity head of air particles moving directly behind the shock wave front, as a result of which it is often called the "wind pressure." Keeping in mind the diagram shown in Fig. 3.6, one can write an expression for determining the maximum excess pressure Δp_2 , α on an obstacle in reflection of a shock wave striking the obstacle at an angle α :

$$\Delta p_2 = \rho_1 u_1^2 \frac{\rho_1 u_1^2}{2} \cos^2 \alpha \quad (3.18)$$

where Δp_2 is the excess pressure on the incident shock wave front; ρ_1 is the air density on the incident shock wave front; u_1 is the velocity of air particles behind the shock wave front.

It is extremely difficult to perform calculations according to this formula, since the value of ρ_1 increases in reflection, and it

is difficult to determine it due to the effect of flowing around the obstacle. Therefore, formula (3.18) is written in a somewhat different form:

$$\Delta p_{2\alpha} = \Delta p_1 + x \cos^2 \alpha \quad (3.19)$$

with $\alpha=0$, and $\Delta p_2 = \Delta p_1 + x$ or $x = \Delta p_2 - \Delta p_1$.

Having determined the value of Δp_2 according to the Izmaylov formula (3.14), one can determine the value of x :

$$x = \Delta p_1 + \frac{\frac{k+1}{k-1} (\Delta p_1)^2}{\Delta p_1 + \frac{2kp_0}{k-1}}$$

For the air medium, $k=1.4$, and $x = \Delta p_1 + \frac{6(\Delta p_1)^2}{\Delta p_1 + 7}$.

Substituting this value of x into formula (3.19), we obtain

$$\Delta p_{2\alpha} = \Delta p_1 + \left[\Delta p_1 + \frac{6(\Delta p_1)^2}{\Delta p_1 + 7} \right] \cos^2 \alpha \quad (3.20)$$

where Δp_2 , α is the maximum excess pressure in reflection from an obstacle of a shock wave striking the obstacle at an angle;

Δp_1 is the excess pressure on the incident shock wave front;

α is the angle between the vector of the velocity of propagation of the incident shock wave and a normal to the obstacle.

Formula (3.20) is suitable for determining the maximum excess pressure on the front of a reflected shock wave only in a case of regular reflection. As a result, it is valid for comparatively small angles of impact of an incident shock wave with an obstacle. Depending on the intensity of the incident shock wave and the properties of the obstacle, the practical application of formula (3.20) for evaluating the effect of an explosion in air is permissible up to values of the angles of the order of $30-40^\circ$. With larger values of the angle α , as a rule, the phenomenon of irregular reflection emerges, and the actual reflection pressure can increase

considerably; the pressure reaches some maximum, after which it decreases, coinciding at $\alpha=90^\circ$ with the value computed according to formula (3.20). The physical nature of the phenomenon of irregular reflection was examined above.

Fig. 3.9.

Figure 3.9 shows schematically the character of the change in the value of the ratio $\Delta p_2, \alpha/\Delta p_1$ as a result of the development of irregular reflection.

Curve a corresponds to the change in the ratio $\Delta p_2, \alpha/\Delta p_1$ for a case where irregular reflection is absent, and $\Delta p_2, \alpha$ is determined solely by formula (3.20); curve b corresponds to the actual change in the ratio $\Delta p_2, \alpha/\Delta p_1$ with the development of an irregular reflection process. The value of the angle $\alpha_{\text{пред}}$ corresponds to some maximum value at which the phenomenon of irregular reflection of an incident shock wave arises.

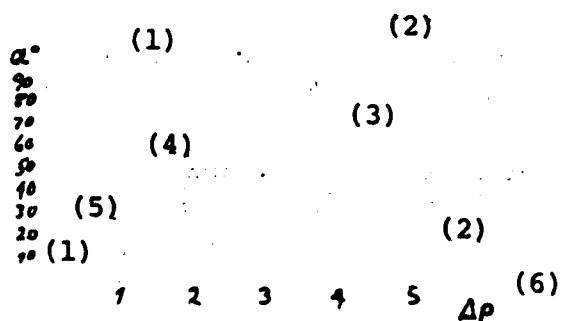


Fig. 3.10.

Key: (1) reflected wave; (2) direct wave; (3) leading edge wave; (4) region of irregular reflection (5) region of regular reflection; (6) kg/cm^2 .

Corresponding graphs (Fig. 3.10) can be used for practical evaluation of the effect of the reflection phenomenon; these graphs make it possible to determine the boundary of variation of the angle α dividing regions of regular and irregular reflection.

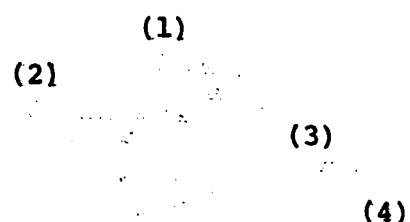


Fig. 3.11.

Key: (1) incident wave; (2) reflected wave;
(3) triple point; (4) leading edge wave.

The phenomenon of irregular reflection which has been considered occurs not only in contact of a plane shock wave with an obstacle at some angle but also develops in explosion of practically any concentrated charge located at some distance from an obstacle. In this case (Fig. 3.11), strictly speaking, only at a point A_0 under the charge (at the epicenter of the explosion) is the incident spherical shock wave front directed along a perpendicular to a plane obstacle. At all other A_1, A_2, A_3, \dots , the shock wave front encounters the obstacle at angles $\alpha_1, \alpha_2, \alpha_3, \dots$, which increase in proportion to the increase in the distance of the point in question from the epicenter of the explosion. As follows from what has been presented previously, irregular reflection unavoidably begins at some distance corresponding to the limit value of the angle $\alpha_{\text{пред}}$.

The development of conditions of irregular reflection and the formation of a leading edge shock wave have great significance in the propagation of shock waves of a nuclear explosion. In the process of propagation of a shock wave and its reflection from an obstacle, the angle of impact α varies within considerable limits, and the

moment of development of a leading edge shock waves comes, which leads, under the conditions of a powerful explosion, to substantial strengthening of the destructive effect of the explosion at considerable distances from the epicenter of the explosion.

Flowing of a Shock Wave Around Obstacles

The phenomenon of reflection of a shock wave from an obstacle which has been considered above occurs only in a case where the dimensions of the obstacle which absorbs the effect of the incident shock wave are infinitely great. In the case of a real obstacle with finite dimensions, on the other hand, another phenomenon emerges in addition to reflection of the shock wave from the obstacle; this other phenomenon - the phenomenon of flowing of the shock wave around the obstacle - influences the character of the change in pressure in reflection.

In contact with an obstacle, only that part of the wave is reflected which comes into contact with the obstacle and directly exerts pressure on it. The rest of the wave goes past the obstacle. In contact of a wave with an obstacle, a pressure shock - reflected shock wave with a pressure on the front equal to p_2 - develops at the surface of the obstacle, as has already been considered. As a result of the extremely rapid and abrupt increase in pressure on the obstacle, the value of the pressure on the reflected shock wave front remains practically unchanged, regardless of the dimensions of the obstacle. In other respects, however, the character of interaction of the wave with the obstacle with the passage of time and the character of variation of the pressure in time in the presence of an obstacle of finite dimensions differ from what occurs in contact of a wave with an obstacle of infinite dimensions. At the edges of the obstacle, particles of air from the zone of increased pressure (reflection pressure) began to spread to the sides, into regions where the pressure proves to be lower. As a result of this, zones in which the pressure is less than the reflection pressure

are formed in the vicinity of the edges of the obstacle. Particles of the air medium which are carried along by the incident wave and strike the obstacle encounter zones at the edges of the obstacle with a lower pressure than in the central part of the obstacle, as a result of which they are deflected from the direction of their initial movement in the direction of these zones of reduced pressure - a process of flowing around the obstacle develops. After some time interval from the beginning of flowing around, the process becomes a steady-state, stationary process. The velocity of the air flow around the obstacle comes to be equal to the mass velocity u_1 in the shock wave. Figure 3.12 schematically shows the phenomena of reflection and flowing around which occur in contact of a shock wave with an obstacle of finite dimensions.

a b c d

Fig. 3.12.

The vertical broken line indicates the incident shock wave front; the crosshatching indicates the region with increased pressure (reflection pressure); ordinary shading indicates zones with the pressure of flowing around ($p_{\text{обт}}$), and the dotted shading behind the obstacle indicates a region where reduced pressure (less than p_1) is established - a rarefaction zone. Four sequential stages (a, b, c and d) of the development of the process of flowing around are shown in this diagram. In considering features of the propagation of shock waves in a case of flowing around obstacles, one must keep in mind the following extremely interesting circumstance.

Fig. 3.13.

As was established in analysis of the phenomenon of flowing around an obstacle, a rarefaction zone with reduced pressure is established behind the obstacle with the flow around it. However, as a result of the fact that waves rounding the obstacle from different sides are directed into this region of reduced pressure, they collide within the region. As a result, a region with increased pressure and with an effect which is strengthened as a result of the increased pressure develops at some distance from the obstacle. The nature of this phenomenon and the individual stages of its development are shown schematically in Fig. 3.13. The pressure in the zone of the strengthened shock wave effect behind an obstacle with a flow around it, according to data of M. A. Sadovskiy obtained based on experimental determination of pressures, not only can reach a value corresponding to the pressure at the same distance from the explosion location occurring in the absence of an obstacle but can even exceed it. According to available data, the zone of increased pressure behind an obstacle is located in the range from a distance equal to half the width of the obstacle to a distance beyond the obstacle equal to the width of the obstacle. And the boundary of this zone proved to be extremely sharply defined: under real conditions, at a distance of one-two meters, the pressure value essentially can vary from a level which is safe for life to a level which causes fatal injuries.

This circumstance should be kept in mind in the construction and use of various structures intended for protection against the effect

of an explosion shock wave. Reflection and flowing around will be in different ratios depending on the dimensions of the obstacle. The process of flowing around, propagated from the edges of the obstacle toward its center, conditions a pressure drop - development of an unusual rarefaction wave (but with a pressure exceeding the value of p_1), which also propagates from the edges of the obstacle toward its center.

At the moment when the flowing around process under consideration (the rarefaction wave from the edge of the obstacle), propagating the velocity of sound in the air medium compressed by the wave, reaches any point on the surface of the obstacle, the pressure at this point drops.

The character of the change in the pressure p_{06T} at a point located at the center of the obstacle is shown in Fig. 3.14.

Fig. 3.14.

A point at the center of the obstacle does not "sense" that the process of flowing around has begun until the moment when the rarefaction wave approaches it. Curves reflecting the character of variation of the pressure p_{06T} for a case of reflection from an obstacle of infinite dimensions and the pressure p_1 in the incident wave are presented on the same graph for comparison. The time τ_{06T} is the time from the moment of contact of the shock wave with the obstacle in the course of which the effect of the process of flowing around on the value of the pressure in the reflection wave begins to show up at the point located at the center of the

obstacle; i.e., during this time, a rarefaction wave propagating from the edges of the obstacle reaches the center of the obstacle.

The picture of the pressure variation in time looks somewhat different if one determines the average pressure on the obstacle rather than measuring the pressure at a point. In this case, the curve of pressure variation in time differs immediately, the moment the process of flowing around begins, from a curve characterizing the variation in the reflection pressure for an obstacle of infinite dimensions (Fig. 3.15).

Fig. 3.15.

The phenomenon of flowing around must be taken into consideration both in the use of different instruments for pressure measurement and in evaluation of the destructive effect of an explosion. For example, an instrument which measures the pressure and is placed with its surface which absorbs the pressure parallel to the direction of propagation of the shock wave front will record the pressure in a passing, (free-running) shock wave without reflection (p_1 or Δp_1 , Figs. 3.14 and 3.15).

The same instrument (normally of relatively small dimensions) placed perpendicular to the direction of propagation of the shock wave front will record the pressure of flowing around (p_{06T} . Figs. 3.14 and 3.15). Finally, the same instrument built into an obstacle of sufficiently large dimensions (it is calculated so that the time τ of the action of excess pressure proves less than the time needed for approach of the rarefaction wave from the nearest edge of the

obstacle to the instrument) placed perpendicular to the direction of propagation of the shock wave will record the total reflection pressure. These cases are shown schematically in Fig. 3.16. The effect of the process of flowing around on the pressure value also explains the fact that elements of the structure of equal mechanical strength, differing only in shape and relative dimensions (different streamlining), possess different levels of resistance to the effect of the shock wave. By the influence of the effect of flowing around, one can explain a phenomenon observed in practice, when such structures as factory chimneys, cylindric towers and other structures with a good streamlined form at identical distances from the location of an explosion proved to be more resistant to the explosion than structures (buildings) which are mechanically stronger but have an inferior "aerodynamic" shape. Buildings which are taller but are relatively small in regard to horizontal dimensions are also more resistant to the effects of an air shock wave than buildings which are lower but longer and wider.

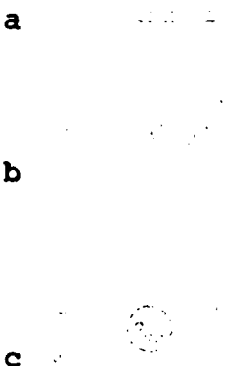


Fig. 3.16.

In view of the considerable complexity of the process of the flow of a shock wave around an obstacle, the theory and methods for

evaluating the effect of this phenomenon have not yet been worked out adequately. For a case of waves of relatively low intensity, where $\Delta p_1 \leq 3 \text{ kg/cm}^2$, one can adopt a linear law of the variation in pressure as a function of time with a level of precision sufficient for practical work. Yu. B. Khariton and T. V. Zakharova have developed an approximate theory. According to this theory, the pressure of flowing around can be calculated by the following formula:

(3.21)

If we substitute $k=1.4$ and $p_0=1 \text{ kg/cm}^2$ into this formula, we obtain

(3.22)

P

Fig. 3.17.

The authors of this theory also demonstrated that the excess pressure comes to be equal to half the excess pressure on the reflected wave front from the moment of establishment of conditions of flowing around (the moment of approach of the rarefaction wave from the edge of the obstacle to the point at which the pressure is being determined) (Fig. 3.17).

Explosion of an Explosive Charge in an Enclosed Space

In the practical use of aviation ammunition, cases of its explosion in an enclosed space are encountered: explosion of a projectile inside one of the compartments of an aircraft after piercing its skin, explosion of an aerial bomb inside a structure, building, ship, etc.

Explosion of a charge in an enclosed space has features which must be taken into consideration in evaluating the destructive effect of an explosion in an air medium. For discovering the physical nature of the phenomenon in question, we shall assume that explosion of the charge occurs in a completely enclosed space bounded by sufficiently strong walls, which are not destroyed during the time for occurrence of the process of the effect of the explosion under these conditions; the charge is located at the center of the enclosed space. After explosion of the charge, the explosion products and shock waves, in spreading from the point of the explosion, reach the walls. As a result of impact against a wall, as has already been considered previously, reflection of the shock wave (and of the detonation products at short distances) occurs, with a corresponding increase in the intensity of the reflected wave. Waves reflected from opposite walls, in propagation toward each other, collide and are reflected mutually from each other. As research has demonstrated, in such a collision of waves, reflection of the waves similar in principle to reflection of each of the shock waves from a rigid, undeformable obstacle occurs. Having been reflected from each other, the shock waves reverse the direction of their propagation and, approaching the walls again, are reflected from them.

A hydraulic model of such a process is shown in Fig. 3.18. The photographs show several sequential stages of development of a process of repeated reflection of a surface wave in a liquid, which has developed as a result of impact of a liquid drop against

the surface of the liquid, from the walls of a container.

Fig. 3.18.

With completely undeformable walls and a total absence of energy losses, the process of repeated reflection of shock waves from walls and mutual reflection of the waves from each other would continue indefinitely. In reality, energy losses are unavoidable in propagation and reflection of shock waves. A considerable part of the energy is spent on deformation of the walls of a real enclosed space, on the formation of shock waves in the walls themselves, and on heating up of the walls and the surrounding space; part of the energy is carried outward by explosion products escaping through the opening in the walls pierced by the projectile or bomb. As a result of all these unavoidable losses, the intensity of shock waves gradually decreases, and even if the structure inside which the explosion occurred has not been destroyed, the action of

shock waves stops after some time. Nevertheless, the effect of an explosion on elements of the structure proves substantially greater than in explosion of the same charge outside the enclosed space at the same distance as a result of repeated reflection of the waves.

Fig. 3.19.

Figure 31.9 shows a graph of the variation in pressure as a function of the time for a case of an explosion in an enclosed space. If we compare this graph to a similar graph for the case of an explosion outside an enclosed space (the graph shown in Fig. 3.2, for example), one can observe two characteristic features:

- there is not one pressure maximum but several corresponding to reflections of the shock waves;
- the total time of the action of excess pressure is considerably greater than in an explosion outside an enclosed space.

As a result of the indicated features, the total impulse of a shock wave in an explosion in an enclosed space increases by a factor of 5-6 as compared to the impulse of the same charge in an explosion outside the enclosed space, and this, in turn, results in the fact that the destructive effect of the explosion in an enclosed space substantially exceeds the effect of an explosion in an open medium in a number of cases.

The Specific Impulse of a Shock Wave

In many cases, it is not the maximum pressure value but the value of the impulse of an air shock wave which is of basic interest for evaluating the destructive effect of an explosion. This is explained by the fact that the time τ of the action of excess pressure in a considerable number of cases proves much smaller in practice than a time equal to a fourth of the period of natural oscillations of the object hit by the wave.

For example, the period of natural oscillations T for various brick and reinforced concrete building varies within limits of 0.25-0.70 s, while the time τ for charges with a weight of 100 to 10,000 kg in an explosion at distances of 500-1000 m from the explosion point is within limits of 0.07-0.15 s. The relationship $\tau \ll T$ is more accurate the smaller the distance from the center of the explosion, since the intensity and, consequently, the velocity of propagation of a shock wave are higher at short distances.

The maximum possible deflection of a system (a mechanical structure) under the action of a blast wave will occur in a case where the total deflection of the system in the direction of the effect of the wave takes place in the time τ . Then in reverse movement of the system (in the process of free oscillations), a load will act on it and increase the deflection, since a section of reduced pressure or rarefaction follows the section of excess pressure in the shock wave (Fig. 3.2). The presence of a zone of reduced pressure, moreover, will cause the appearance of an additional load, which increases the amplitude of oscillations of the system, in the course of a time not exceeding τ_1 (Fig. 3.2). As a result of summation of the effect of pressures of compression and rarefaction, a resonance effect of the load will develop; this effect is capable of causing destruction, even in a case where the "direct" effect of the excess pressure does not lead to destruction of the object of the damage.

In most cases, however, the period T of natural oscillations and one fourth of this period are significantly greater than the time τ of the action of excess pressure in an air shock wave in explosion of aviation ammunition filled with normal explosives.

In these cases, the system (structure) essentially does not manage to change its position in the time τ , although it takes on a definite initial velocity in this case and takes on some amount of movement corresponding to the impulse of the air shock wave. The amount of movement which has been taken on it the source of further movement, deformation and failure of the structure. It should be noted that the development of stresses and strains of a structure under the action of the amount of movement which has been taken on will occur even only after stopping of the effect of the shock wave. As a result, calculation of the destructive effect must be performed for the impulse load, and, consequently, the need arises for determining the impulse of the air shock wave. A characteristic of the effect of a shock wave called the specific impulse I_1 is normally used in practical calculations. The specific impulse is equal to the impulse per unit of surface area absorbing the effect of the explosion. The specific impulse I_1 is numerically equal in value to the area under the curve of the excess pressure $\Delta p(t)$; i.e., it can be determined from the following formula (Fig. 3.20):

$$I_1 = \int \Delta p(t) dt.$$

Computing I_1 with this formula involves great difficulties, mainly the difficulty of determining an analytical expression for the function $\Delta p(t)$ which is suitable for practical calculations and reflects the dependence of the value of Δp on the distance to the explosion center (R) and the charge weight (w). Therefore, formulas for engineering calculations involved with determination of I_1 are derived in a somewhat different way.

Fig. 3.20.

A bursting charge in the form of a spherical charge with initiation from the center of the sphere is assumed for determining the specific impulse. In calculations of the effect of an explosion, practically any charge which does not possess a clearly pronounced directivity of its effect is replaced with the so-called adjusted charge, i.e., a charge of a spherical shape equivalent in weight to the charge in question. The radius of the spherical charge selected in this way is called the adjusted radius of the given charge.

Since the value of the specific impulse is determined by the pressure of the air shock wave and the time of its action on the obstacle, and the values of these parameters with a given type of explosive depend on the charge weight ω and the distance from the explosion center R , the value of the specific impulse depends on the size of the charge and the distance from the charge to the target. Consequently, it is necessary to determine the form of the dependence $I_1 = I_1(\omega, R)$. The total amount of movement (the

impulse flow) possessed by a body of a mass M is defined as $I = \int_0^{\infty} v dM$, where v is the value of the velocity of an elementary particle of a mass dM .

If we assume that all particles of a mass M move at the same velocity $v = \text{const}$,

$$I = v \int_0^M dM = vM \quad (3.23)$$

Suppose the total energy possessed by a moving mass M is equal to

u ; then $\frac{Mv^2}{2}$, from which $v = \sqrt{\frac{2u}{M}}$. Thus,

$$I = vM = M \sqrt{\frac{2u}{M}} \sqrt{2uM} \quad (3.24)$$

With respect to calculation of the impulse of a shock wave, formula (3.24) in a general case takes on the following form:

$$I = \sqrt{2u(M_B + M_{\text{exp}})}, \quad (3.25)$$

where M_B is the mass of air compressed by the shock wave; M_{exp} is the mass of the explosion products.

As has already been established, at relatively small distances, a shock wave is propagated together with expanding explosion products, after which the shock wave separates from the explosion products and propagates independently in the air medium. As a result, the conditions which influence the value of the specific impulse of an air shock wave vary with variation in the distance from the explosion point, and the value of I_1 is calculated for two cases:

- a) for short distances from the explosion center, $R < R_K$;
- b) for long distances from the explosion center, $R > R_K$, where R_K is the distance at which the air shock wave separates from the explosion products - the critical distance.

Determining the Specific Impulse for Short Distances ($R < R_K$)

The mass of the explosive (the mass of explosion products) is greater in this case than the mass of air drawn into motion by the explosion and possesses substantially more energy; therefore, one can neglect the mass of the air in formula (3.25).

The energy of a bursting charge with a mass M can be expressed in terms of the specific energy of the explosive charge u_1 (u_1 is the amount of energy released in decomposition of a unit of mass of the explosive): $u=u_1 M$.

Expression (3.25) thus will take on the following form:

$$I = \sqrt{2M u} / M = M \sqrt{2u_1}. \quad (3.26)$$

This formula determines the value of the impulse possessed by explosion products under the assumption made previously - that all the particles have the same velocity.

In reality, however, the particles of explosion products move at different velocities and, as research demonstrates, a smaller impulse than is given by calculation by formula (3.26) is obtained. In addition, the formula fails to take into consideration chemical losses.

The decrease in the total impulse value is taken into account by introducing some coefficient κ_1 into the calculation, and formula (3.26) takes on the form

$$I = \kappa_1 M \sqrt{2u_1}. \quad (3.27)$$

The coefficient κ_1 takes into account the distribution of velocities within the mass of explosion products and also the chemical losses of energy.

At a distance R from the explosion center, the specific impulse on the surface of a sphere with a radius R will be expressed by the following formula:

$$\begin{aligned} I_s &= \frac{I}{4\pi R^2} = \kappa_1 \sqrt{2u_1} \frac{M}{4\pi R^2} = A \frac{M}{R^2}; \\ I_s &= A \frac{M}{R^2} \end{aligned} \quad (3.28)$$

The coefficient A depends on the specific energy of the explosive, which varies only slightly - within limits of 400-450 kg-m/g - in the explosives normally used.

Such a variation in the energy of the explosive has a small effect on the value of the coefficient A, and the coefficient varies only slightly in the transition from one explosive to another. If the weight of the charge w in kilograms is substituted into formula (3.28) in place of the charge mass M, the formula will take on the following form:

(3.29)

The coefficient A_1 is expressed in dimensions of time.

Based on experimental data, one can assume $A_1 = 24$ s; then

(3.30)

Formula (3.29) is used for practical calculations of the value of the specific impulse of an explosion for distances $R < R_K$.

Determining the Specific Impulse for Long Distances ($R > R_K$)

One cannot neglect the mass of the air drawn into motion by the explosion in this case, but one can neglect the mass of the explosion products, and formula (3.25) takes on the following form:

$$I = \sqrt{2\gamma M_g} \quad (3.31)$$

The value of u in this formula will be $u = v u_1 M$, where v is a coefficient which takes into consideration the part of the energy of explosion products which is transmitted to the shock wave. The values of v are within limits of 0.3 to 0.7.

We shall rewrite expression (3.31) in the form

$$I = \chi \sqrt{2\gamma} M M_w$$

where κ_2 is a coefficient which has the same physical meaning as the coefficient κ_1 ; i.e., it takes into account the distribution of velocities among particles of the air medium drawn into motion by the explosion.

Passing on to the specific impulse, we obtain

$$I_I = \frac{\kappa_2 \sqrt{2v_{u_1} M M_b}}{4\pi R^2} \quad (3.32)$$

The mass of the air drawn into motion can be computed approximately by the following formula:

$$M_b = 4\pi R^2 \lambda \rho_b \quad (3.33)$$

where λ is the thickness of the disturbed air layer (Fig. 3.21); ρ_b is the air density.

Fig. 3.21. Zone of air compressed (condensed) by a shock wave.

Then, recalling the law of geometric similarity in an explosion which was formulated previously, we can write the following:

$$\lambda = \alpha R_0 \quad (3.34)$$

where α is a proportionality coefficient; R_0 is the charge radius (or adjusted radius).

It is obvious that

$$R = \sqrt[3]{\frac{3}{4\pi\rho} \cdot \sqrt{M}} \quad$$

where ρ_{BB} is the density of the explosive. Substituting this value of R_0 into formula (3.34), we obtain

$$\lambda = a \sqrt[3]{\frac{3}{4\pi\rho_{BB}}} \sqrt[3]{M}$$

or

$$\lambda = \beta \sqrt[3]{M} \quad (3.35)$$

where

$$\beta = a \sqrt[3]{\frac{3}{4\pi\rho_{BB}}}$$

Inserting the value obtained for λ into (3.33), we obtain $M_g = 4\pi R^2 p_0 \beta^3 \sqrt[3]{M}$. Thus, with consideration for the expression obtained for M_B , we obtain

$$\text{or } I_1 = \frac{\pi_2 \sqrt{24} \sqrt{M} M^{2/3} 4\pi R^2 p_0 \beta^3 v}{4\pi R^2} = \frac{\pi_2 \sqrt{24} p_0 \beta^3 v}{\sqrt{4\pi}} \frac{M^{2/3}}{R}$$

$$I_1 = B \frac{M^{2/3}}{R}$$

where

$$B = \frac{\pi_2 \sqrt{24} p_0 \beta^3 v}{\sqrt{4\pi}}$$

Having substituted the weight of the charge w for its mass M , we obtain

$$I_1 = B_1 \frac{w^{2/3}}{R} \quad (3.36)$$

Processing of extensive experimental data for charges of trotyl produces a value

$$B_1 \approx 58 \text{ [kgf}^{1/3} \text{ s/m]}$$

with

$$\rho_B = 0.125 \text{ [}\frac{\text{kgf}}{\text{m}^4}\text{].}$$

Thus we finally obtain a formula for practical calculations of the specific impulse of an explosion for distances $R > R_K$:

$$I_1 = 58 \frac{w^{2/3}}{R} \text{ [}\frac{\text{kgf s}}{\text{m}^2}\text{].} \quad (3.37)$$

The coefficient B_1 depends on the value of the density of the

air ρ_B and decreases with a decrease in ρ_B ; i.e., the specific impulse of the shock wave of an explosion decreases with a decrease in the density of the air. This circumstance is extremely important in evaluating the effect of the shock wave of an explosion under different conditions, especially under conditions of the use of aviation ammunition from high altitudes.

(1)

Fig. 3.22.
Key: (1) experimental curve.

The dependence $I_1(R)$ can be represented by the graph shown in Fig. 3.22. Using this graph, one can determine approximately the value of R_K - the distance at which separation of an air shock wave from explosion products occurs. With $R=R_K$, the value of I_1 computed by the two formulas (3.29) and (3.36) should be equal:

$$A_1 = \frac{\omega}{R_K^2} = B_1 \frac{\omega^{1/3}}{R}$$

Hence

$$R_K = \frac{A_1}{B_1} \omega^{1/3}. \quad (3.38)$$

For a charge of a spherical shape, $\omega = \frac{4}{3}\pi R_0^3 \gamma_{BB}$, from which

$\omega^{1/3} = \sqrt[3]{\frac{4}{3}\pi \gamma_{BB} R_0}$, where γ_{BB} is the specific gravity of the explosive. If we substitute the value obtained for $\omega^{1/3}$ into formula (3.38) and assume $\gamma_{BB} = 1600 \text{ kg/m}^3$ for trotyl, we obtain

$$R_K = \frac{24}{58} \left(\frac{4}{3} \times 1600 \right)^{1/3} R_0 \quad \text{or} \quad R_K \approx 8R. \quad (3.39)$$

We know from experimental data that the value of R_K is within limits of 8 to 15 R_0 . Formula (3.39) thus gives the bottom limit of variation of the values of R_K in explosion of an explosive charge in an air medium.

Calculation of the Destructive Effect of an Explosion in Air

In the explosion of aviation ammunition in an air medium, the destructive effect in regard to various objects, as has already been observed, is accomplished by the blast wave - explosion products and an air shock wave. In this case, at distances less than the "critical" distance (with $R < R_K$), the basic destructive effect is inflicted by rapidly expanding explosion products; at distances greater than the "critical" distance (with $R > R_K$), the destructive effect is inflicted by the air shock wave. If the bursting charge is enclosed in a metal shell, or housing, the destructive effect is also accomplished by fragments formed in fragmentation of the housing as a result of the explosion. In a case of explosion of ammunition with a high volumetric efficiency (such as high-explosive aerial bombs), the destructive effect of the fragments has relatively smaller importance, and the destructive effect is calculated with consideration for the action of fragments, after which the necessary corrections are introduced into the calculation formulas based on experimental study of the destructive effect of ammunition in regard to various targets.

In this way, in deriving of formulas for evaluating the destructive effect of an explosion, one normally takes into consideration only the effect of the air shock wave or the blast wave (in the joint action of explosion products and the shock wave).

The statement of the problem in calculation of the destructive effect of an explosion in air can be formulated in two ways, depending on the purpose of the calculation.

The problem can be stated as follows: there is some object which must be destroyed by explosion of an explosive charge.

However, the problem can also be stated differently: there is an object which must be protected against the effect of an explosion. The principle of the calculation remains the same in both the first and second cases.

The degree of destruction of the target in explosion of a charge in an air medium is determined by three factors:

- the properties of the target: its shape and dimensions, the strength of the material, the strength of the target as a structure and the level of its resistance to the destructive effect of an explosive load;

- the properties of the charge which determine its destructive capability: the power and specific energy of the explosive, the charge weight and, in certain cases, the shape of the charge and its location in relation to the target;

- the distance between the charge and the target.

The problem in calculating the destructive effect is to establish the relationship among these three factors. The problem of calculating the destructive effect of an explosion in relation to different objects is very complex and difficult. In an explosion effect, a load which is extremely powerful, short-lived and variable in time acts on the object. The behavior of materials under the action of such a load has not yet been studied adequately; therefore, calculation of the destructive effect of an explosion even on an individual element of a construction (structure) is an extremely difficult problem. Moreover, a real structure includes a large number of different elements possessing different properties, and destruction of different elements shows up differently in destruction.

of the structure as a whole. We shall become acquainted briefly with an approach to solving this complex problem and shall consider the nature of different methods used for practical evaluation of the destructive effect of an explosion in air.

We shall examine the problem under the following assumptions:

1) The structure of the destruction target will be considered as a combination of simple elements - beams, plates, rods, etc. - similar to what is done in statics and dynamics of structures. The effect of the explosion will be considered for any one element. As an example of such an element, we shall select a beam on two supports and shall assume that the character of the dependences obtained will be valid for the structure as a whole; the difference can be only in values of the coefficients, which are subject to experimental determination.

a

b

Fig. 3.23.

We shall designate the distance at which destruction of the element of the structure occurs under the action of the explosion as R_p . The value of R_p for the structure as a whole obviously will be some average value of R_p for the individual elements. This value of R_p will require experimental refinement.

2) We shall replace the real beam which has been selected, with an arbitrary law of the distribution of mass M along its length and with an infinitely large number of degrees of freedom (Fig. 3.23, a), with a dynamically equivalent theoretical beam with one degree of freedom and with a concentrated mass M_0 (Fig. 3.23, b).

In this case, $M_0 = \alpha M$, where $\alpha < 1$. As we know, two systems are referred to as dynamically equivalent if the kinetic energies of these systems at any moments in time are equal.

Fig. 3.24.

3) In an explosion, an explosive load which varies through time $p(t)$ acts on the beam; the load is distributed over the entire surface of the beam facing in the direction of the bursting charge (Fig. 3.24, a). We shall replace this load with a concentrated load $P_0(t)$ applied at the same point as M_0 (Fig. 3.24, b). In this case, $P_0(t) = \beta S_0 p(t)$, where $\beta < 1$, and S_0 is the area of the beam surface facing in the direction of the explosive charge.

We shall consider some features of the effect of the explosive load.

- The action of the load on any system can be realized in two ways: in the form of either a static load or a dynamic load.

With static loading, constant external forces, before the beginning of plastic deformation, are balanced at each moment in time by internal forces of elasticity of the system.

With dynamic loading, external forces which are variable in time are not balanced by forces of elasticity: accelerations are imparted to elements of the system, and the external forces are

balanced jointly by both internal forces of elasticity and forces of inertia of moving masses of the system.

It follows from analysis of the character of an explosive load that it can be classified as a dynamic load.

- In explosion of charges of ordinary explosives, the time of action of the explosive load, as we know, is substantially less than the period of natural oscillations (T) of structures and constructions encountered most often: $\tau \ll T$. Under this condition, the explosive load acting on the object should be considered as an impulsive load. Under the action of an impulsive load, the mass M_0 is drawn out of a state of rest and takes on some initial velocity v_0 , after which the action of the load stops, and the mass continues movement as a result of the impulse received.

- We shall perform the calculation assuming that destruction of a structure sets in when deformations exceed some limit characteristic of the material in question - y_p ; i.e., we write the condition of destruction in the following form: $y_{\max} > y_p$.

Fig. 3.25.

We shall pass on now to examination of the deformation (deflection) of the theoretical beam with a concentrated mass M_0 and a concentrated load $P_0(t)$ (Fig. 3.25).

We shall write the equation of motion of the beam in the following form:

$$ky \quad (3.40)$$

where k is the rigidity of the beam, and y is the deflection of the beam. We shall transform equation (3.40) to the following form:

$$+ \quad (3.41)$$

As a result of the impulsive character of the load, we can represent equation (3.41) in the following form:

$$+ \pi^2 y = 0 \quad (3.42)$$

where

$$\sqrt{\frac{k}{M_0}}$$

Equation (3.42) is an equation of free oscillations of the beam with an oscillation frequency π .

The solution of this equation is obtained, as we know, in the following form:

$$y = A \sin \pi t + B \cos \pi t \quad (3.43)$$

We shall determine the value of B from the following initial conditions:

$$t=0; y=0; B=0.$$

Then, in differentiating expression (3.43), we obtain

$$\frac{dy}{dt} \quad (3.44)$$

under the initial conditions $t=0, \frac{dy}{dt} = v_0$, we find

$$A = \frac{v_0}{\pi}.$$

The value of v_0 is found from the condition $M_0 v_0 = I_0$, where

$I_0 = \int p_0(t) dt$. However, since $p_0(t) = \rho S_0 p(t)$, then $I_0 = \rho S_0 \int p(t) dt = \rho S_0 I_1$, where I_1 is the specific impulse of the explosion effect, and expressions for v_0 and A are obtained in the form

and

$$A = \frac{v_0}{n} = \frac{\beta S_c}{\sqrt{RM_0}}$$

Equation (3.43) thus can be written in the following form

$$y = \frac{\beta S_c}{\sqrt{RM_0}} I_1 \sin \pi t \quad (3.45)$$

The value of y_{\max} is of interest from the point of view of evaluating the destructive effect. From (3.45) we obtain

$$y_{\max} = \frac{\beta S_c}{\sqrt{RM_0}} I_1 \quad (3.46)$$

The value of I_1 is determined by formulas (3.29) and (3.36). We shall determine the value of y_{\max} for a section $R < R_k$. Substituting the value of I_1 according to formula (3.29) into expression (3.46), we obtain

$$y_{\max} = \frac{\beta S_c}{\sqrt{RM_0}} A_1 \frac{\omega}{R^2} \quad (3.47)$$

The distance from the center of an explosion R_p at which destruction will occur is determined from formula (3.47) under the condition

$y_{\max} = y_p$:

$$R_p = \sqrt{\frac{\beta S_c}{\sqrt{RM_0}} \frac{A_1}{y_p}} \sqrt{\omega}$$

or

$$R_p = R_1 \sqrt{\omega}, \quad (3.48)$$

where

$$k_1 = \sqrt{\frac{\beta S_c}{\sqrt{RM_0}} \frac{A_1}{y_p}}$$

The value of k_1 depends on the properties of the explosive and the type and properties of the structure being destroyed.

We shall determine the value of y_{\max} for a case with $R > R_k$. Substituting the value of I_1 according to formula (3.36) into expression (3.46), we obtain

$$y_{\max} = \frac{\beta S_c}{\sqrt{RM_0}} \frac{B_1}{y_p} \omega^{2/3}$$

Assuming the $y_{\max} = y_p$, we obtain a formula for calculating R_p :

or

$$R_p = \frac{BS_6}{\sqrt{RM_o}} \frac{B_1}{y_p} \omega^{2/3}$$

$$R_p = k_2 \omega^{2/3}$$

(3.49)

where

$$k_2 = \frac{BS_6}{\sqrt{RM}} \frac{B_1}{y_p}$$

The value of k_2 , like k_1 , depends on the properties of the explosive and the type and properties of the structure being destroyed.

Formulas (3.48) and (3.49) are calculation formulas for evaluating the destructive effect of an explosion in relation to different targets; in this case, the values of k_1 and k_2 for typical targets are determined experimentally. As a result, quantitative corrections are introduced for assumptions made for schematization of the phenomenon for obtaining comparatively simple calculation formulas which are convenient for practical use.

Values of the coefficient k_1 for certain targets are presented in Table 3.1.

Table 3.1. Values of the coefficient k_1 .

	k_1
(1)	
(2)	$\frac{0.4}{\sqrt{b}}$
(3)	$\frac{0.1}{\sqrt{b}}$
(4)	$\frac{0.16}{\sqrt{b}}$
(5)	0.50
(6)	0.20
(7)	0.15
(8)	0.50
(9)	2.8
(10)	10

*b - wall thickness in meters.

Table 3.1.

Key: (1) name of target; (2) brick walls (breach); (3) concrete walls; (4) reinforced concrete walls; (5) light tank; (6) medium tank; (7) heavy tank; (8) trains; (9) window frames, doors, wooden partitions (destruction); (10) windows of buildings (destruction).

It follows from formula (3.49) that the radius of the destructive effect for distances $R > R_k$ is proportionate to $\omega^{2/3}$. However, for many years, while accumulation of experimental data was going on, and while calculation methods for evaluation of the destructive effect of an explosion still have not been adequately developed, processing of the results of experiments was performed on the assumption that the dependence $R_p = k\sqrt{\omega}$ is valid for any distance. As a result, the values of the coefficient k_1 contained in most tables are given for a formula of the type of (3.48).

Transmission of Detonation for a Distance

One of the important types of the destructive effect of an explosion is the transmission of detonation for a distance.

It has been established in study of processes of the emergence and development of an explosion that the explosion of a charge of one explosive (the initiating charge) in direct proximity to a charge of another explosive is capable of causing detonation of this charge. Appropriate research has demonstrated that the initiation of explosive decomposition of one explosive in explosion of another can also be accomplished in a case where such charges are at a distance apart and are separated by any inert medium.

The phenomenon of transmission of detonation from one explosive charge to another through an inert medium is called "detonation at a distance" or "sympathetic detonation." The initiator charge which initiates detonation normally is called the active charge,

while the charge which receives detonation is called the passive charge. Initiation of detonation of the passive charge at short distances can be accomplished directly by products of explosion of the active charge in sharp impact on the passive charge. Initiation of detonation of the passive charge at great distances is accomplished by products of explosion of the active charge together with the shock wave. At distances where explosion products are no longer capable of causing detonation of the passive charge, detonation can be caused by a shock wave, if the intensity of the wave still proves sufficient. In a case where active and passive charges are separated by a dense inert medium (a barrier), the shock wave alone is the initiator of detonation of the passive charge. In explosion of an active charge in an inert barrier, a shock wave develops and, in propagation through this barrier and in reaching the surface of the passive charge, it initiates a shock wave in the explosive. With sufficient intensity of this shock wave, detonation of the passive charge will occur.

The range of transmission of detonation depends on many factors, of which the main factors are as follows: the weight and properties of the active charge, the properties of the passive charge, the mutual positioning of the charges, and the properties of the medium separating the charges. We shall consider briefly the effects of some of these factors. The dependence of the range of transmission of detonation on the weight of the active charge is expressed by a formula obtained based on extensive research:

$$R = k\sqrt{\omega} \quad (3.50)$$

where R is the distance between charges (the range of transmission of detonation) in meters; ω is the weight of the active charge in kilograms; k is a coefficient which depends on the properties of the charges and the medium separating the charges.

Special tables have been composed for values of k determined experimentally.

It should be noted that formula (3.5Q) provides essentially satisfactory coincidence with experimental data with an active charge weight up to 1000 kg. In a case of charges of greater weight, the exponent in this formula should not be 1/2 any longer; it decreases, and its value is within limits of 1/2 to 1/3.

With an increase in the rate of detonation and an increase in the density of the explosive of the active charge, the range of transmission of detonation (R) increases.

With an increase in the density and, consequently, a decrease in the sensitivity of the explosive of the passive charge to the effect of an explosion, the range of transmission of detonation decreases.

Features of the mutual positioning of the charges have a substantial effect on the value of R , mainly in the use of active charges of a comparatively small weight (up to a few kilograms); the location of the detonator in the active charge in relation to the passive charge is of basic importance in this case (Fig. 3.26).

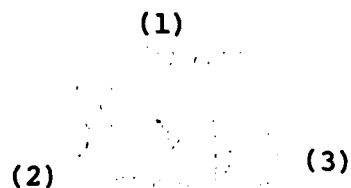


Fig. 3.26.
Key: (1) detonator; (2) active charge;
(3) passive charge.

The casing of charges also has an effect on the range of transmission of detonation. The presence of a sufficiently strong casing for the active charge increases the value of R, since fragments formed in fragmentation of the casing in explosion of the active charge in this case are capable of causing detonation of the passive charge at considerable distances. At the same time, the presence of a strong casing for the passive charge reduces the range of transmission of detonation.

When both charges have casings, combustion of the passive charge often develops. As a result of the fact that the combustion occurs essentially in an enclosed space bounded by a strong casing, an increase in pressure can result in transformation of combustion to explosion and detonation.

The range of transmission of detonation also depends essentially on the properties of the medium separating the active and passive charges. For example, in explosion of an active charge of picric acid (with a density of 1.25 g/cm³) in a paper casing, the range of transmission of detonation to a passive charge also of picric acid (with a density of 1.0 g/cm³) in a paper casing is as follows: 28 cm through air; 4.0 cm through water; 2.5 cm through clay; 1.5 cm through sand; 1.5 cm through steel. The capacity of explosives for transmitting and receiving sympathetic detonation must be taken into consideration in their use, especially in organization of the storage of explosives and ammunition.

A storehouse with explosives and ammunition racks and stacks must be placed at distances from each other such that explosion of one of the objects does not cause explosion of others.

Safe distances are determined according to a formula similar in form to formula (3.50):

$$R = k \sqrt{w},$$

where R is the safe distance, at which there is no effect of

detonation transmission, in meters; ω is the explosive charge weight, in kilograms.

Reference tables of values of the coefficient k depending on the properties of dangerously explosive objects are presented in the special instructions on determining safe distances. For example, the value of k is approximately 5.0 for objects without special protection (banking) in the absence of an intensive fragmentation effect.

§ 2. EXPLOSION OF A CHARGE IN WATER

General Information on an Explosion in Water

An explosion of a charge in water or an underwater explosion is one of the basic types of the harmful effect in combat use of aviation ammunition. As in the examination of explosion of an explosive charge in air, we shall become acquainted with the overall physical picture of the development of explosion of a charge in a liquid (in water), we shall learn the basic patterns characteristic of this phenomenon, and we shall establish the basic relationships for calculating the destructive effect of an underwater explosion.

It is natural that the overall physical picture of an explosion in water should have many features in common with the explosion in air considered previously. At the same time, the underwater explosion has essential features which distinguish it from an explosion in air. These features are determined by the difference between properties of a gaseous (air) medium and a liquid medium in which explosions of explosive charges occur. For identifying features of explosion of a charge in a liquid, we shall consider an explosion in a limitless liquid medium; i.e., we shall consider an explosion at a point of a liquid which is sufficiently far from the surface, the bottom and the side walls of the container.

Assume that a spherical explosive charge with a weight ω and a radius R_0 explodes in a liquid medium (R_0 will be the adjusted charge radius for a charge whose shape is not spherical). In the process of the explosion (detonation) of the explosive charge, sharply compressed gaseous explosion products are formed. Since we know that the time for occurrence of the charge detonation process is approximately three orders less than the time for development of subsequent processes accompanying the explosion phenomenon, one can assume essentially that the explosive charge is instantaneously transformed into gaseous detonation products, which occupy a space equal to the volume of a sphere with the radius R_0 at the initial moment. A sharp pressure differential at the boundary separating the charge and the surrounding medium is created as a result of detonation, as in an explosion in air.

The pressure on the surface of the detonated charge depends on the properties of the explosive and amounts to a value of the order of $200,000 \text{ kg/cm}^2$, while the pressure in the surrounding liquid is equal to the hydrostatic pressure, which depends on the depth of immersion of the charge.

This sharp pressure differential leads to rapid expansion of the explosion products. The explosion products in expansion create a sharp impact on adjacent layers of the liquid and compress these layers and force them back. With sharp compression of the liquid layers, a shock wave is formed with an initial propagation velocity considerably exceeding the velocity of sound in the liquid and reaching a value of the order of 6000-7000 m/s.

The formation of the shock wave and its "separation" from the detonation products in an explosion in a liquid, in contrast to an explosion in air, occur directly at the surface of the charge, in view of the low compressibility and greater density of the liquid (water).

The shock wave front propagating in the liquid rapidly moves away from the boundary separating the detonation products and the liquid. We know that movement of particles of the medium in the direction of propagation of the shock wave front occurs in a shock wave. In addition, in the case of underwater explosion under consideration, intensive movement of water in radial directions will occur under the action of expanding explosion products. The radial movement of the liquid which develops as a result of this creates a so-called hydroflow in an underwater explosion.

The expanding explosion products form a gas bubble. After completion of the detonation process, the volume of the gas bubble is equal to the volume of the original explosive charge. Then the radius of the gas bubble begins to increase rapidly. The rate of expansion of the gas bubble decreases in proportion to its expansion, and the pressure inside the bubble drops and at some moment reaches the value of the hydrostatic pressure. However, as a result of inertia of the liquid particles which are being pushed back, an additional increase in the dimensions of the gas bubble occurs, and the pressure of the gaseous explosion products comes to be less than the hydrostatic pressure. The gas bubble begins to contract under the action of the hydrostatic pressure, and compression of the gaseous explosion product occurs. As a result of inertia of the liquid particles moving toward the center of the explosion and striving to close the cavity of the gas bubble, the boundary of the gas bubble jumps through the equilibrium position (corresponding to the moment when the pressure inside the bubble is equal to the hydrostatic pressure), the pressure inside the gas bubble again increases sharply, and a new pressure differential between the gaseous explosion products and the surrounding medium is created as a result. This new pressure differential naturally proves considerably less intense than the initial pressure differential. However, by an experiment one can detect the development of a secondary shock wave even in this case and repeated expansion of the gas bubble, accompanied by the appearance of a hydroflow. Periodic expansion and compression of the

gas bubble can occur repeatedly; this process is called pulsation of the gas bubble. The amplitude of variation of the dimensions of the gas bubble decreases with each successive pulsation period, the pressure in the secondary waves drops, the energy of the gaseous explosion products runs low, and the gas bubble collapses and disappears: the explosion products scatter and are dissolved in the liquid medium. In the process of pulsation, the gas bubble floats up toward the free surface, and partial solution of the explosion products in the liquid also occurs. Under certain conditions, the gas bubble which is floating up reaches the free surface of the liquid and gets into a zone of an emulsion in the liquid formed by a rarefaction wave which develops in reflection of the shock wave from the free surface. In breaking of the gas bubble which has reached the free surface, the gaseous explosion products burst out into the air medium. The cavity (depression) of the gas bubble on the surface of the water in this case closes up actively, and a splash in the form of a column of liquid is formed.

Such is the physical picture of the development of the underwater explosion phenomenon in its general features.

The initial stage of an underwater explosion is shown in a diagram (Fig. 3.27) and a photograph (Fig. 3.28). The photograph was taken with a high-speed camera of the SFR [high-speed photorecorder] type.

In this way, the following emerge in an explosion in a liquid (in water):

- a shock wave (the first, most intense wave);
- a hydroflow - masses of water moving in radial directions from the explosion center;
- a pulsing gas bubble containing gaseous explosion products.

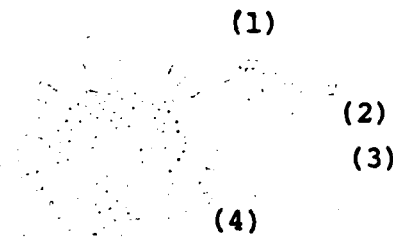


Fig. 3.27.

Key: (1) shock wave front; (2) gas bubble; (3) hydroflow zone; (4) undisturbed water.

Fig. 3.28.

The Destructive Effect of an Underwater Explosion

Many researchers have worked on studying the underwater explosion and its effect, and by now there is sufficient detailed information about the basic quantitative relationships characteristic of this physical phenomenon.

The destructive effect of an underwater explosion is conditioned by the action of: the shock wave, the hydroflow and the gaseous explosion products located in the gas bubble. We shall consider each of these factors which determine the effect of an explosion in water in greater detail. The field of a shock wave in water will differ from the field of an air shock wave. The reason for this lies

in the fact that the initial pressures on the shock wave front are different in these media: pressures do not exceed $1500-2000 \text{ kg/cm}^2$ for powerful explosives in air, while pressures reach values of the order of $150,000 \text{ kg/cm}^2$ for typical explosives in water.

In addition, in view of the comparatively low compressibility of water, its temperature will increase extremely little, the increase in entropy will be small, and the energy passing into the shock wave will go for mechanical work (propagation of the wave) to a comparatively great degree rather than for heating the water.

The low compressibility of water under the action of external pressure is explained by the fact that water is strongly compressed by internal pressure. The molecular pressure for a liquid is of an order of $1000-10,000 \text{ kg/cm}^2$; it reaches a value of $10,000 \text{ kg/cm}^2$ for natural water.

The overall effect of a shock wave in water will be somewhat stronger than the effect of a shock wave in air, since the pressure in the shock wave in water is many times greater than in air.

Water can be considered practically incompressible in certain cases, such as in examination of the hydroflow. However, in examination of the shock wave, the concept of the compressibility of the liquid is of fundamental importance, because a shock wave in any medium is a density, pressure and temperature shock.

The change in density on the front of a strong shock wave in water can be significant. For example, with a pressure of the order of $10,000 \text{ kg/cm}^2$, the density of water reaches a value of 1.5 g/cm^3 .

The form of a shock wave in water will differ sharply from the form of an air shock wave. A very sharp pressure drop behind the wave front is characteristic of a shock wave in water even at the first moment of its formation. Therefore, one can assume in this

case that the greatest energy density in the shock wave will be concentrated in an extremely narrow zone.

- Attenuation of shock waves in water occurs more slowly than in air; therefore, at identical relative distances, the pressure in a shock wave in water is considerably higher than in air. An especially strong destructive effect of an explosion is exhibited in the space occupied by explosion products. The effect of the explosion is relatively small at distances exceeding the radius of the gas bubble, despite the high value of initial pressures, on the strength of the fact that the pressure in the shock wave drops extremely sharply. The basic problem of the theory of an underwater explosion is to study the unsteady movement of liquid between boundary surfaces - the shock wave front and the surface of the gas bubble - and to establish patterns determining the character of the movement of these surfaces on the assumption that water is a nonviscous compressible liquid, and the movement of water behind a shock wave front can be considered by application of basic laws of the mechanics of continuous media: the law of the conservation of mass, the law of the conservation of momentum, the law of the conservation of energy and the equation of state of the medium (see Chapter 2). For a case of spherical symmetry, these relationships lead to the following system of equations describing the process in question:

$$\frac{dp}{dt} + p \left(\frac{\partial v}{\partial R} + 2 \frac{v}{R} \right) = 0$$

- continuity equation;

$$\frac{dv}{dt} = - \frac{1}{\rho} \frac{\partial p}{\partial R}$$

- equation of conservation of momentum;

$$\rho \frac{d}{dt} \left(E + \frac{v^2}{2} \right) = - \rho \left(\frac{\partial v}{\partial R} + 2 \frac{v}{R} \right) - \frac{\partial p}{\partial R}$$

- equation of conservation of energy;

$$p = B \left(\frac{v}{v_0} \right)^n - 1 \quad (3.51)$$

- equation of state of water in Tate form.

Here v is the velocity of radial movement of the liquid; R is the current radius; p is the pressure; t is the time; ρ is the current value of the density of the medium; ρ_0 is the initial density of water; B and n are constants whose values in a general case depend on the pressure value. It is assumed for practical calculations that $B=3070 \text{ kg/cm}^2$ and $n=7$.

Solution of this system of equations with partial derivatives produces dependences which define the process in question:

$$p = p(R, t); \quad v = v(R, t) \quad \text{and} \quad \rho = \rho(R, t).$$

The system of differential equations (3.51) in general can be solved by one of the well-known methods. However, the diversity of the facts, a significant portion of which practically cannot be taken into consideration, forces researchers to look for approximate solutions, resting mainly on the results of experimental investigation of an underwater explosion.

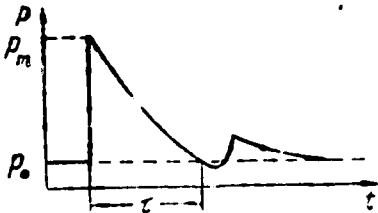


Fig. 3.29.

Figure 3.29 shows the character of variation of the pressure through time in a shock wave in an underwater explosion.

The form represented for the dependence $p(t)$ is typical of an underwater explosion. The second pressure maximum corresponds to

the second wave which develops in pulsation of the gas bubble.

The basic characteristics of a shock wave which determine its destructive effect, as we know, are the maximum pressure p_m , the time of action of excess pressure τ and the pressure impulse I.

The method for determining the characteristics of a shock wave is based on the same idea as in an explosion in air - the theory of similarity of explosion processes.

With the use of principles of similarity in an explosion, values characterizing processes which occur in a model and in an actual explosion at identical relative distances (R) measured in adjusted charge radii (R_0) under otherwise identical conditions are compared. The adjusted charge radius, as we know, is proportionate to the value of $\omega^{1/3}$, since the linear dimensions of the charge are proportionate to the cube root of the size (the weight ω) of the charge. Under these conditions, as in consideration of an explosion in air, we obtain a dependence for determining the value of the maximum pressure p_m in the following form:

$$p_m = f\left(\frac{\omega^{1/3}}{R}\right).$$

The following formula was obtained based on analysis of extensive experimental data for determination of p_m :

$$p_m = A_0 \left(\frac{\omega^{1/3}}{R}\right)^a.$$

The value of A and a are determined from an experiment. For charges of an explosive of the trotyl (TNT) type, processing of experimental data produces a dependence of the form

$$p_m = 540 \left(\frac{\omega^{1/3}}{R}\right)^{1.19} \quad (3.52)$$

where ω is the charge weight, in kilograms; R is the distance, in meters.

For more powerful explosives, such as explosives of the TGA [alloys of TNT with hexogen and aluminum] type, the values are $A_0 = 555$ and $a = 1.13$.

Formulas of the type of (3.52) are used for practical calculations of the maximum pressure in an underwater explosion. The expression for determining p_m can also be presented in a somewhat different form:

$$p_m = 3070 \left(e^{\frac{3R_0}{R}} - 1 \right)$$

or

$$p_m = 9210 \frac{R_0}{R}.$$

The character of the pressure variation through time in a shock wave in underwater explosion is described well by the following dependence (without consideration for the secondary pressure peak):

$$p(t) = \frac{p_m}{2} \left(e^{-\alpha \frac{t}{R_0}} + e^{-\beta \frac{t}{R_0}} \right), \quad (3.53)$$

where c_0 is the velocity of sound in undisturbed water; α and β are constants determined from an experiment.

The values of p_m obtained experimentally for basic elements of a structure of typical underwater targets have been assembled in special reference tables.

One feature of a shock wave in an underwater explosion should be mentioned. Corresponding research indicates that the value of the time of action of the excess pressure in the shock wave for a given charge does not depend on the distance. Consequently, in contrast to an air shock wave, the shock wave in an explosion in water practically does not stretch out in propagation. This is explained by the fact that the pressure drops very steeply behind the shock wave front, and an overwhelming portion of the wave energy as a result is concentrated in an extremely narrow zone adjoining the leading part of the wave. The tail section which stretches out in the process of propagation of the wave practically does not influence the value of the impulse of a shock wave in water, since

it creates a total of only 1-2% of the overall pulse. In addition, elongation of the shock wave due to the fact that the velocity of its leading section is greater than that of the tail section will be insignificant, since these velocities differ only slightly, already beginning at a distance equal to five times the charge radius.

The following formula thus essentially is valid for a charge of a given weight:

$$P_m = k I_1 \quad (3.54)$$

where I_1 is the specific impulse of the shock wave; k is a constant.

Using the formula (3.54), one can solve the problem of what to select as the measure of the destructive effect of an underwater explosion - pressure or impulse.

The underwater explosion is normally used for action in relation to targets for which, as a rule, the condition $\tau \ll T$ is valid, where τ is the time of action of the excess pressure of the shock wave, and T is the period of natural oscillations of the destruction object. Under these conditions, the impulse should be selected as the measure of the destructive effect. However, keeping in mind formula (3.54), the maximum pressure p_m can also be adopted as the measure of the destructive effect. The need for computing the value of the specific impulse in an underwater explosion can arise in a number of cases. The following dependence has been obtained for determining the specific impulse I_1 in an underwater explosion based on the principle of similarity of explosion processes:

$$I_1 = B \frac{\omega^{1/3}}{R} \quad (3.55)$$

where ω is the charge weight, in kilograms; R is the distance, in meters; B is a coefficient determined by processing experimental data. The value of this coefficient is within limits of 500-520. However, the value of coefficient B can also be determined in another way. The following relationship is valid for an explosion in water and in air:

$$\frac{I_{\text{возд}}}{I_{\text{газы}}} = \sqrt[3]{\frac{P_{\text{возд}}}{P_{\text{газ}}}} = \frac{B_{\text{возд}}}{B_{\text{газ}}}$$

The ratio $\frac{P_{\text{возд}}}{P_{\text{газ}}}$ is approximately equal to 800, and $B_{\text{возд}}=58$. Then $B_{\text{газ}}=540$, and formula (3.55) will take on the form

$$I_1 = 540 \frac{\omega^{2/3}}{R} \quad (3.56)$$

The character of variation of the velocity of movement of water in the hydroflow can be established on the assumption that water is incompressible. Having distinguished two concentric spheres in the hydroflow (Fig. 3.30), we compose a condition of incompressibility in the form

$$4\pi R_1^2 v_1 dt = 4\pi R_2^2 v_2 dt$$

or

$$v_2 = \frac{R_1^2}{R_2^2} v_1$$

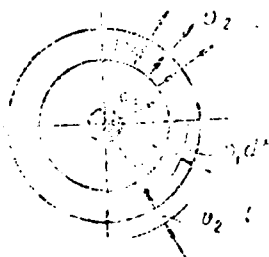


Fig. 3.30.

The conclusion that the velocity of movement of water in the hydroflow is inversely proportionate to the square of the distance from the explosion center follows from this formula:

$$v = k R^{-2}$$

The character of variation of the dimensions of the gas bubble in its pulsation is established by processing frames of a photographic

record of an underwater explosion (Fig. 3.31).

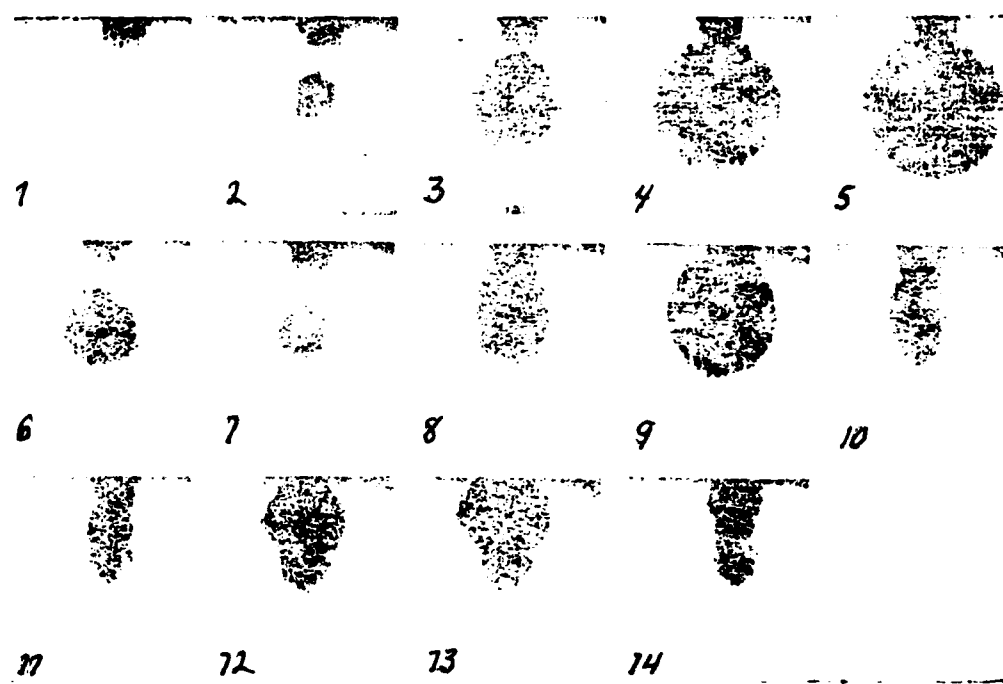


Fig. 3.31.

The photography was done with an SKS-1 camera.

Figure 3.32 shows the time dependence of the radius of the gas bubble. The maximum value of the radius (R_{\max}) of the gas bubble can be established by calculation according to the following formula

$$\left(\frac{R_{\max}}{R_0} \right)^n = \frac{8.13 \cdot 10^4}{p_0},$$

where R_0 is the adjusted explosive charge radius; n is the polytropic curve index for explosion products in the final stage of their expansion; p_0 is the hydrostatic pressure at the depth of immersion of the charge in the explosion.

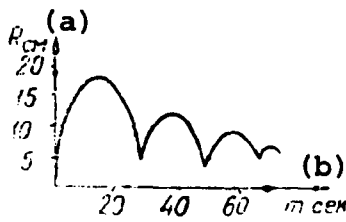


Fig. 3.32.
Key: (a) cm; (b) ms.

Floating up of the gas bubble is extremely slight up to the moment of its expansion; therefore, one can select a pressure value corresponding to the depth of immersion at the moment of the explosion as p_0 .

We shall consider briefly the features of the effect of an underwater explosion in blasting under conditions of real reservoirs, where an effect of the bottom and the side walls of the reservoir and also of the free surface of the water is possible. The effect of the bottom of the reservoir depends to a considerable degree on the condition and strength of the bottom and results in some increase in the impulse. This impulse increment occurs under the condition $H_{\Delta} < R$ (Fig. 3.33), when the shock wave reflected from the bottom manages to show up in the impulse value.



Fig. 3.33.
Key: (1) increased
impulse.

The effect of the side walls is similar to that of the bottom. At the same time, as we know, an increase in the pressure, reaching a twofold value in an underwater explosion, occurs at an obstacle.

The effect of the free surface is determined by the fact that a rarefaction wave is formed in reflection of the shock wave from the free surface (the wave crosses the boundary with a less dense medium) and propagates from the surface to the bottom of the water; the rarefaction wave is capable of cutting off part of the impulse acting on the volume. This effect of the rarefaction wave is possible under the condition $H_{\Pi} < R$ (Fig. 3.34).

It has been established in the practice of use of underwater explosions that an air cavity in water absorbs a considerable part of the energy of the explosion, since part of the energy is directed along the line of least resistance and is spent on

compression and heating of the air located in the cavity.

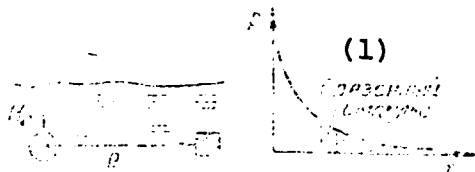


Fig. 3.34.
Key: (1) cut impulse.

An air cavity can reduce the destructive effect of an explosion; for example, a cavitation cavity formed behind an aerial bomb penetrating into water reduces the destructive effect of the underwater explosion.

This property of air cavities can be used for protecting underwater structures against the effect of an underwater explosion. An air cavity can also be used in certain other cases of control of the effect of an underwater explosion. For example, in destruction of an underwater structure by an explosion, in a case where there is an air cavity behind an obstacle at the level where the explosive charge is situated, a charge with a weight 5-6 times smaller is needed for destroying the obstacle than in a case of destruction of an obstacle without the cavity.

§ 3. EXPLOSION OF A CHARGE IN THE GROUND

General Information on an Explosion in Solid Media

Explosion of a charge in the ground or an underground explosion is one of the basic types of the effect of an explosion in combat use of aviation ammunition. A considerable number of important targets are located at a significant depth for protection against powerful and superpower explosions. In addition, strong explosive loads can develop in adjacent volumes of the ground in both air and

underwater explosions and, as a result, conditions can develop for damage or destruction of ground or underground structures.

In examining an explosion in the ground, we shall consider an explosion in a solid medium in general, including any solid and any soil (rocky, sandy, clay, loose, water saturated, etc.) in this concept.

We shall consider the physical picture of the effect of explosion of an explosive charge in the ground, in a manner similar to what was done in examination of explosions in air and in water, and we shall establish the basic principles and relationships for calculating the effect of an underground explosion.

The overall physical picture of an explosion in a solid medium naturally has many features in common with explosions in air and water.

However, an explosion in a solid medium possesses essential features which distinguish this type of explosion from explosions in air and water. These features are determined by the differences in properties of gaseous, liquid and solid media. For identifying these features, we shall consider the explosion of a charge in an unbounded solid medium (the ground). Assume that a VV [explosive] charge of a spherical shape explodes in a solid medium: w is the weight of the charge, and R_0 is the radius (R_0 is the adjusted charge radius for a charge which is not of spherical shape).

The explosion products in expansion create a sharp impact on adjacent layers of the solid medium and compress these layers and force them back. Sharp compression of the layers of the medium leads to the formation of a shock wave in the solid medium. The initial velocity of propagation of the shock wave in solid media depends on the compressibility of the medium and the velocity of sound in it and, depending on the values of these parameters, the

velocity of the shock wave can exceed the velocity of the detonation wave. In this case, the density can increase by 10-20% for metals.

The formation of a shock wave and its "separation" from detonation products in an explosion in a solid medium occur directly at the charge surface, which is conditioned by the low compressibility and great density of the medium. The coefficient of volumetric compression is $5 \cdot 10^{-5}$ for water, while this coefficient is approximately $5 \cdot 10^{-7}$ for a material of the type of steel; i.e., it has a value two orders less.

The resistance of solids to deformations is considerably greater than that of liquids. For a material of the steel type, the pressure which creates noticeable plastic deformations is approximately 20,000 kg/cm². In addition, a solid medium, as a rule, is capable of retaining the shape obtained as a result of deformation after the active load produces stresses less than some critical stress at which residual deformations occur.

It is obvious in consideration of final deformations of a solid medium under the action of an explosive load that it is efficient to exclude small elastic components of these deformations from consideration. Now, as a result of sharp compression of layers of the medium in an explosion, a shock wave will propagate in radial directions from the point of the explosion. The shock wave front, propagating in the solid medium, will move away rapidly from the boundary separating the detonation products and the medium. We know that movement of particles in the direction of propagation of the shock wave front occurs in a shock wave. In propagation of a shock wave in a solid medium, displacement of particles in the direction of movement of the wave front occurs. Intense movement of the medium in radial directions under the action of expanding detonation products will also occur.

The development of a so-called hydroflow was pointed out in consideration of an underwater explosion. In the case of an explosion in a solid medium, this "hydroflow" proves to be "frozen" the moment the stresses in the medium created by expanding explosion products and the developing wave process become less than the stresses necessary for producing residual deformations of the solid medium. Forces of internal cohesion in the solid medium "catch" the emerging movement of particles of the medium in some initial section of their radial movement from the explosion center.

As with an explosion in water, expanding detonation products, in forcing back adjacent layers of the medium, form a "gas bubble," i.e., a cavity occupied by detonation products. While periodic oscillating movement of the cloud of explosion products (air) and the gas bubble (water) accompanied by the emergence of secondary pressure waves was pointed out in consideration of explosions in air and water, in considering an explosion in a solid medium, one can speak only of the aperiodic movement of the "gas bubble." Expansion of the space occupied by detonation products will occur up to the moment when the pressure in the detonation products is balanced by forces of internal cohesion of particles of the medium. It is obvious that the dimensions of the gas cavity will also depend on the density of the medium.

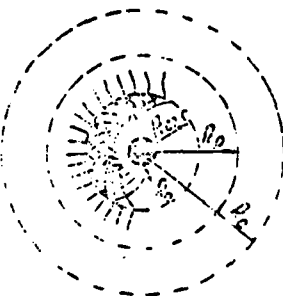


Fig. 3.35.

The physical picture of the development of the phenomenon of an explosion in a solid medium thus is extremely similar in its general features to the picture of the beginning of development of an explosion in air and in water and is a kind of initial stage of the effect of an explosion in less dense and less rigid media "frozen" by enormous internal forces. Figure 3.35 shows a picture of the effect of an explosion in an unbounded solid deformable medium in the form of a diagram. The designations adopted have the following meanings: R_0 is the VV charge radius; R_{cx} is the radius of the internal zone of deformation of the solid medium (the compression zone), R_p is the radius of the second zone of deformation of the solid medium (the destruction zone), and R_c is the radius of the zone of vibration of the medium. In the first zone - the compression zone - deformation of the medium is so intense that the medium, in a state of all-round compression, is severely compacted, undergoes plastic deformation, and "flows" and is displaced from this zone. In the second zone - the destruction zone - deformation of the medium is less intense, but the medium also is broken up completely. Destruction occurs in this case mainly as a result of the development of fracture cracks under the action of large normal stresses. In the third zone - the vibration zone - deformation of the medium remains elastic, there is no destruction of the medium, and vibration and oscillation of the medium occur - a so-called seismic effect. The dimensions of this zone in an unbounded solid medium theoretically are extremely great. The dimensions of the vibration zone are limited in practice by the value of the critical amplitude of shifting of the medium in analysis of the destruction of some object. The volume of each of the zones listed will be different for different media and is determined by the density and strength properties of the medium.

It is convenient to represent the deformation of a solid medium under the action of an explosive load in the form of a system of waves propagating into the mass of the medium from the interface with the charge. Figure 3.36 shows the propagation of

these waves. Line 1 ($\delta=v_0 t$) corresponds to a shock wave front in a solid medium. The velocity of propagation of the shock wave front is always greater than the velocity of sound in the medium in question, although the velocity of the shock wave differs only slightly from the velocity of propagation of elastic oscillations - the velocity of sound v_c - in the case of an explosion in metals even at comparatively small distances from the charge. Line 2 ($\delta=v_{pl} t$) corresponds to a wave of small elastoplastic deformations. This wave, generally speaking, propagates at a variable velocity. Some average value has been adopted as the value shown in the graph for v_{pl} , the velocity of propagation of this wave. Line 3 ($\delta=v_p t$) corresponds to the boundary of propagation of a state of intense plastic deformation of the medium. This state propagates at a velocity v_p determined by the modulus of plastic deformation or of strengthening of the material of the medium.



Fig. 3.36.

The value of v_{pl} considered above varies within limits from v_c to v_p . The values of the velocities v_e , v_{pl} and v_p are normally in such a relationship ($v_e > v_{pl} > v_p$) and are determined based on analysis of the diagram of dynamic deformation of the material of the medium $\sigma=\sigma(e)$, where σ is the stress, and e is the relative deformation. However, since the form of the diagram of $\sigma(e)$ in dynamic tests differs only slightly from the form of this diagram for static tests (for most materials), one can use the static diagram of $\sigma(e)$ for approximate determination of v_{pl} and v_p . The value of the modulus of elasticity practically does not change in

dynamic tests; therefore, determination of v_e in this way will be extremely precise. The values of v_e , v_{pl} and v_p can be computed by the following formulas:

$$v_e = \sqrt{\frac{E}{\rho}}; \quad v_{pl} = \sqrt{\frac{E'}{\rho}} \quad \text{and} \quad v_p = \sqrt{\frac{E''}{\rho}},$$

where E , E' and E'' are shown in Fig. 3.37 and represent the modulus of elasticity, the modulus of small elastoplastic deformations (the "tangent" module) and the module of strengthening (the module of large plastic deformations), respectively, and ρ is the density of the material (metal).

For a material of the type of ordinary steel, one can assume $v_e = 5 \cdot 10^3$ m/s; $v_{pl} = 3 \cdot 10^3$ m/s; $v_p = 1 \cdot 10^3$ m/s. It should be noted that some characteristics of the mechanical properties of materials (metals) under dynamic loading can be determined by explosive tests of appropriate specimens of the material under investigation, in addition to the generally known standard testing methods.

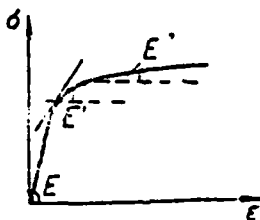


Fig. 3.37.

The ground as a medium in which it is of practical importance to investigate the effect of an explosion has peculiarities as compared to other solid media. The ground is an inhomogeneous medium with sharply pronounced stratification and, consequently, anisotropy of its properties. The density of typical soils is considerably less than the density of metals and is approximately twice as great as the density of liquids:

$$\rho_g = (1.8 - 2.4)\rho_{steel}. \quad (3.57)$$

An essential feature of the ground is its porosity (macro-discreteness of the structure). This feature of the ground results in the fact that the conditions of the effect of an explosion in the ground differ from the conditions in liquids and metals. Convergence of separate particles occurs at first in compression of the soil, leading to an increase in the density of the medium. Then compression of the particles which make up the ground occurs at high pressures. Compacting in the ground (even water-saturated ground) as a result of convergence of the particles thus can be more significant than in the case of normal adiabatic compression. Compacting of the ground which occurs due to elimination of its porosity emerges even at pressure which are not high, of the order of hundreds of atmospheres for typical soils.

In the action of an explosion in the ground, a considerable part of the energy is expended for breaking up soil particles and for irreversible deformation of the ground. The magnitude of these irreversible energy losses depends on the pressure and drops with a decrease in the pressure. The energy losses become insignificant at low pressures, and weak compression waves emerge, creating a seismic effect of the explosion even at comparatively great distances from the explosion point.

Thus, in an explosion in solid media, a shock wave and three zones of deformation of the medium emerge: a compression zone, a disintegration zone and a vibration zone.

The explosion in the ground is of the greatest interest from the point of view of practical application of aviation ammunition. We shall consider the destructive effect of an explosion in the ground in greater detail.

The Destructive Effect of an Explosion in the Ground

The study of the phenomenon of an explosion in the ground has attracted the attention of many researchers, and basic relationships which make it possible to evaluate and calculate the effect of an explosion in the ground have been obtained by now.

The destructive effect of an explosion in the ground is conditioned by the effect of the shock wave and expanding products of the explosion, which create the three zones of deformation of the ground considered above.

The character of propagation of a shock wave in the ground will differ from the character of propagation of the shock wave in a liquid or in a gas medium. This difference is involved primarily with the porosity of the ground, which leads to considerable compacting of the ground due to the convergence of its particles. The latter circumstance has given rise to a hypothesis concerning representing the properties of the ground in its dynamic deformations under the action of a shock or an explosion in the form of properties of some medium called a "plastic gas," i.e., a gas which preserves the density obtained in the shock wave front. After passage of the shock wave front, such a gas can be considered as an incompressible fluid.

The propagation of a shock wave in the ground can be represented in the form of a process of propagation of the zone of compacting of the soil. For establishing basic patterns of which define the process of propagation of a shock wave in the ground, one should start from basic, fundamental relationships of continuum mechanics and an equation of state of the soil relating the values of pressure and density in the compressible soil, as in the case of an explosion in air and in water. This connection can be expressed by the following relationships:

with $p < p_{kp}$ $\rho_0 \leq \rho \leq \rho_0^*$; } (3.58)

with $p > p_{kp}$ $\rho = \rho_0^* - \frac{p-p_0}{\alpha}$.

where ρ_0 is the initial density of the ground; ρ_0^* is the density at a pressure p_{kp} ; p_{kp} is the critical value of the pressure at which the ground ceases to be porous.

If we neglect the value of adiabatic compression of soil particles as compared to the value of compression which occurs due to the elimination of porosity of the ground, the process of emergence and propagation of the shock wave can be described by the following basic equations:

$$\left. \begin{aligned} \frac{\partial v}{\partial t} + v \frac{\partial v}{\partial R} + \frac{1}{\rho} \frac{\partial p}{\partial R} &= 0 \\ \frac{\partial p}{\partial t} + v \frac{\partial p}{\partial R} + \rho \frac{\partial v}{\partial R} + \frac{2\rho v}{R} &= 0 \end{aligned} \right\} \quad (3.59)$$

These equations should be integrated both with respect to expanding explosion products and for the ground under the following boundary conditions:

$$p_2 = p_1; \quad v_2 = v_1 = \frac{dR}{dt},$$

where R is the distance; p_2 is the pressure in the explosion products; p_1 is the pressure in the ground; v_2 is the velocity of the explosion products; v_1 is the velocity of soil particles.

Solution of the equations (3.59) with consideration for (3.58) produces the following dependences:

$$p = p(R, t), \quad v = v(R, t) \quad \text{and} \quad \rho = \rho(R, t).$$

However, phenomena of deformation of the ground and propagation of the shock wave in the ground are such complex phenomena that they cannot be considered purely theoretically. For further development of a theory of the effect of an explosion in the ground, research on the amount of energy spent on deformation of soil particles and establishment of a law of compressibility of the ground with consideration for its basic properties and structure

Table 3.2. Initial parameters of shock waves in metals.

(1)	(2) Сталь				(3) Медь				(4) дуралюминий			
	Название ВВ (5)	Ро (6) г/см ³	(7) kg/cm ³	(6) m/s m/сек	(7) m/сек m/сек	Ро м (8) г/см ³	Ро м kg/cm ³	(7) m/s m/сек	(8) kg/cm ²	(7) m/s m/сек	(8) kg/cm ²	(7) m/s m/сек
(9) Тротил	1.30	115000	6030	207000	565	5150	1,099	176000	310	40700	115	17100
(10) То же	1.55	174000	6740	--	--	--	--	264000	725	1650	1.23	--
(11) Стабилизиро- ванный гексоген	1.00	248000	8060	403000	555	5750	1,174	278000	36	4550	11.3	25700
(10) То же	1.40	162000	7320	--	--	--	--	270000	730	4260	1.21	--

Key: (1) name of VV explosive; (2) steel; (3) copper; (4) duralumin; (5) g/cm³; (6) kg/cm³; (7) m/s; (8) kg/cm²; (9) trotyl; (10) the same; (11) stabilized hexogen.

are necessary. The complexity of the phenomenon and the impossibility of taking into consideration basic factors in theoretical description of the process of an explosion in the ground lead to the necessity of seeking approximate solutions resting mainly on experimental research.

It has been established experimentally that the initial pressure of a shock wave in the ground (clay) in explosion of a hexogen charge reaches $2 \cdot 10^5$ kg/cm². The initial velocity of movement of soil particles behind the wave front proves to be 1700 m/s. In this case, the density shock is approximately 1.40, and the soil density proves to be 3.0 g/cm³. The initial density of the soil is 2.8 g/cm³. It follows from this that even at $R=R_0$, an increase in density occurs mainly due to the elimination of the porosity of the ground.

In practical calculations of the destructive effect of an explosion in solid media, data on the initial parameters of shock waves in metals obtained by B. I. Shekhter (Table 3.2) can be of interest.

The following designations have been used in the table:
 ρ_0 - initial density of VV [explosive]; p_H - the pressure on the detonation wave front; D_H - the detonation speed; ρ_{0M} - the initial density of the metal; ρ_1 - the density of metal on the shock wave front in the metal; p_1 - the initial pressure on the shock wave front in the metal; D_1 - the velocity of the shock wave front in the metal; u_1 - the velocity of movement of metal particles behind the shock wave front.

One can see from the data presented that the initial pressure on the shock wave front in a solid medium (metal) exceeds the pressure on the detonation wave front. And this pressure is less in all cases than the pressure in reflection of an absolutely undeformable wall, where $p_1/p_H=2.4$ (in right-angle incidence of

the wave). The initial velocity of a shock wave in metal exceeds the velocity of sound in it. In the emergence of strong shock waves in metals, a considerable increase in the density in the metal occurs.

Practical engineering calculations for determining the dimensions of the three zones indicated above for deformation of the ground in an explosion are performed based on empirical formulas, whose form is established by means of principles of the theory of similarity of physical phenomena in an explosion.

The first zone - the zone of compression of the soil - has a volume approximately 200-300 times the charge volume; the volume of the second zone - the disintegration zone - is approximately 2000-6000 times the charge volume. The radii of the zones of deformation of the ground are determined according to the following formulas:

$$R_c = R_{c0} \cdot v^{\frac{2}{3}} \quad - \text{radius of compression zone};$$

$$R_p = R_{p0} \cdot v^{\frac{1}{3}} \quad - \text{radius of disintegration zone}; \quad (3.60)$$

$$R_v = R_{v0} \cdot v^{\frac{1}{3}} \quad - \text{radius of vibration zone}.$$

Here $k_{cx} = 0.36k_p$, and $k_c = 1.83k_p$. The value of k_p is determined based on experimental data. Values of k_p for certain media are presented in Table 3.3.

Table 3.3. Values of coefficient.

Medium of object	k_p
Freshly saturated earth	1.4
Ordinary soil	1.07
Dense sand	1.04
Rocky ground	0.96
Clay	0.94
Limestone	0.92
Masonry	0.84
Concrete	0.77
Reinforced concrete	0.65
Destruction of underground depots, underground wire communications and highway and VPP [runway] beds	0.5-0.9

Destruction of weapon pits, trenches and DZOT [earth-and-timber emplacements]	0.14
Destruction of the walls of assembled DOT [permanent pillboxes] with a thickness of up to 0.4 m	0.40.

For the case of explosion of a charge in unbounded ground which is under consideration, the value of the maximum shock wave pressure is determined according to a general formula obtained based on the theory of similarity:

$$p_m = \sum^n A_i \left(\frac{\omega^{1/3}}{R} \right)^{4/3}$$

The coefficients A_i and a_i are determined by processing experimental data, and their values depend on the properties of the soil. The maximum pressures in explosions of VV charges in ordinary soil preliminarily compacted by explosions can be determined by the following formula:

$$p_m = 15 \left(\frac{\omega^{1/3}}{R} \right)^{4/3} \quad (3.61)$$

For sandy soil which is not water saturated, one can use the following formula:

$$p_m = 9 \frac{\omega}{R^2}$$

The pressures in freshly poured soil can be calculated according to the following formula:

$$p_m = 6 \left(\frac{\omega^{1/3}}{R} \right)^{4/3} + 1.32 \frac{\omega^{1/3}}{R} \quad (3.62)$$

In these formulas, p_m is expressed in kg/cm^2 , ω is the charge weight in kg, and R is the distance in m.

Research of G. M. Lyakhov to determine the maximum pressure of a blast wave in water-saturated sand and sand with a low moisture content of a natural structure has led to the following correlation for determining p_m :

$$p_m = A \left(\frac{\omega^{1/3}}{R} \right)^a . \quad (3.63)$$

The values of the coefficient A and the exponent a, as experiments demonstrate, depend on the physical and mechanical properties of the sand, primarily its compressibility.

Table 3.4 presents values of A and a which correspond to different concentrations of air in sandy soil.

Table 3.4. Values of coefficients A and a.

Среда (1)	(5) Примерное значение Δ	A	a
Водонасыщенный (2) песок	0	600	1
То же (3)	$5 \cdot 10^{-4}$	450	1.5
То же	10^{-2}	250	2
То же	$3 \cdot 10^{-2}$	50	2.5
Неводонасыщенный (4) песок	0.35	7	3

Key: (1) medium; (2) water-saturated sand; (3) the same; (4) sand not saturated with water; (5) approximate value of Δ .

The value of Δ is equal to the concentration (proportion) of air in the soil by volume. In a case of sand not saturated with water ($\Delta=0.35$), the values of A and a depend essentially on the compressibility of the sand skeleton; therefore, they can have different values in different sands. The impulse of the shock wave of an explosion in the ground can be determined according to formulas, the form of which is also determined based on the requirements of the theory of similarity:

$$I = B \omega^{1/3} \left(\frac{\omega^{1/3}}{R} \right)^a . \quad (3.64)$$

The values of the coefficient B and the exponent b are determined by physical and mechanical properties of the soil - primarily by the trapped air concentration (Δ) in water-saturated sands.

Table 3.5 presents values of B and b corresponding to different concentrations (Δ) of air in sandy soil. The impulse in sandy water-saturated soil depends on the compressibility of the sand skeleton; therefore, values of B and b can prove to be different in other sands not saturated with water. Possible deviations of B and b, however, should be substantially less than the deviations of values of A and b in the expression for p_m .

Table 3.5. Values of coefficients B and b.

(1)	(2)	A	B	b
(1) medium				
(2) water-saturated sand	0-5·10 ⁻⁴	as	1.1	
(3) the same	0.01	as	1.2	
(4) sand not saturated with water	0.35	a1	1.5	

Key: (1) medium; (2) water-saturated sand; (3) the same; (4) sand not saturated with water.

Possible deviations of B and b in sands of a natural texture with a porosity within limits of 0.35-0.45 should not exceed 30-50% of the values presented in the table. The information presented is applicable mainly to a case of explosion of a VV charge in unbounded ground, i.e., in a soil mass such that one can disregard the influence of a free surface area or other interfaces of the soil with media possessing different physical and mechanical properties on the effect of the explosion.

An explosion in the ground essentially can be of two types:

1. An explosion in the vicinity of the free (day) surface of the ground. Such an explosion, as a rule, leads to the formation

of the three soil deformation zones described above and to blowing out of soil - the formation of a crater. This form of explosion is sometimes called an explosion for blowing out of ground. Figure 3.38 shows several photographs of the initial stage of an explosion for blowing out of ground obtained under laboratory conditions with an FP-22 high-speed movie camera.

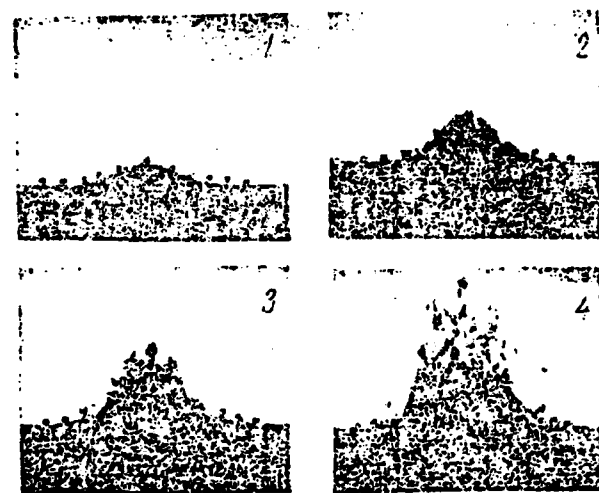


Fig. 3.38.

2. An explosion at a sufficiently great depth from the free surface. Such an explosion is not accompanied by blowing out of soil and results only in the formation of the three zones of deformation of the ground described above. This form of explosion is called a camouflet.

Thus it is necessary to consider two types of destructive effects of an explosion in the ground:

1. An explosion for blowing out of ground - the formation of a crater. Such explosions are used for both military and peaceful

purposes.

2. Destruction of underground structures with an explosion.

Before going on to a consideration of methods for evaluating the indicated types of destructive effect of an explosion in the ground, we shall establish the degree of the effect of the free surface of the ground on the characteristics of the destructive effect of an explosion - on the value of the maximum pressure of the shock wave of an explosion in the ground, for example. For taking into consideration the effect of the free surface on the pressure level in an explosion in the ground, one can use the familiar hypothetical charge system.

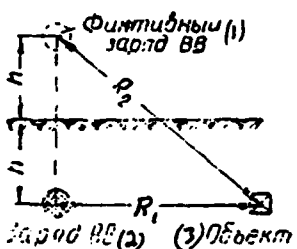


Fig. 3.39.

Key: (1) hypothetical VV charge;
(2) VV charge; (3) object.

Assume that the VV charge is located in the ground at a depth h (Fig. 3.39). A shock wave will propagate in explosion of the charge in the ground. The excess pressure at the ground surface can be assumed to be equal to zero. The latter condition is satisfied if we assume that an explosion in unbounded ground is being considered, and that a hypothetical charge which creates the same field of pressures as the actual charge, but with an inverse sign, is located at a distance from the VV charge from the side of the free surface.

Based on these ideas, we can put down that the maximum pressure

in a case of an effect of the free surface can be calculated by a formula of the following type:

$$P_m = A \left[\left(\frac{w_1}{R_1} \right)^4 + \left(\frac{w_2}{R_2} \right)^4 \right] \quad (3.65)$$

while the pressure in unbounded ground is computed by formula (3.61). If the pressure in unbounded ground is determined by formula (3.62), the maximum pressure with consideration for the effect of the free surface is determined by a formula of the following form:

$$P_m = A_2 \left[\left(\frac{w_1}{R_1} \right)^4 - \left(\frac{w_1}{R_1} \right)^4 + A_3 \left(\frac{w_2}{R_2} \right)^4 - \left(\frac{w_2}{R_2} \right)^4 \right] \quad (3.66)$$

The coefficients A_1 , A_2 and A_3 are determined by processing experimental data.

The state of the free surface has a substantial effect on the magnitude of the maximum pressure in a case of an effect of this surface. For example, appropriate experiments indicate that values of A_1 , A_2 and A_3 prove to be different for experiments which are similar but are conducted under summer conditions and winter conditions (with freezing of the top layer of the ground).

Average values of the coefficients A_1 , A_2 and A_3 obtained from an experiment are as follows:

under conditions of summer tests, $A_1=12$; $A_2=9$; $A_3=2.1$;

under conditions of winter tests, $A_1=70$; $A_2=54$; $A_3=9$.

It must be noted that empirical formulas which have been considered, like other formulas of this kind, can produce familiar deviations for conditions differing from the conditions of the experiments which served as the basis for determination of coefficients A_1 , A_2 and A_3 . However, these relationships are applicable for approximate evaluation of the influence of a free

surface on the effect of the action of an explosion in the ground.



Fig. 3.40.

In evaluation of the explosion effect in the case of an explosion for blowing out of soil, calculation of the crater is performed. Calculation of craters formed in an explosion is performed depending on the predetermined depth (h) of the position of the charge and the radius (r) of the crater formed in the plane of the free surface of the ground (Fig. 3.40). The calculation relationships are expressed through the blow-out index n :

$$n = \frac{r}{h} \quad (3.67)$$

The basic parameters of the crater are indicated in Fig. 3.40. It is customary to assume that the depth of the crater formed is approximately equal to the depth at which the charge is placed. The minimum distance from the charge to the free surface is called the line of least resistance (LNS).

Three types of craters are distinguished:

a normal blow-out crater, $n=1$ ($\alpha=90^\circ$);

a reduced blow-out crater, $n < 1$ ($\alpha < 90^\circ$);

an intensified blow-out crater, $n > 1$ ($\alpha > 90^\circ$).

Formation of a crater obviously is possible only under the condition $h < R_p$, where R_p is the radius of the zone of destruction

of the ground. It should be noted in passing that formula (3.63), with which one can determine the value of the maximum pressure in an explosion in the ground, proves valid both in the case of a camouflet and in the case of explosions for blowing out with a blow-out index $n < 2$.

The relationship between the size of the VV charge and the crater parameters is established for practical calculations.

The physical picture of the effect of an explosion in the ground considered above leads to the conclusion that theoretical calculation of craters is very complex and practically impossible. Therefore, in solving this problem we proceed mainly from results of analysis of extensive experimental data. The problem for calculating craters is posed as follows: find the weight (ω) of a VV charge which, with a given depth (h) for burying in soil with given properties, forms a crater of given dimensions (n). The expression for calculating the effect of an explosion for blowing out of soil has the form

$$\omega = k_1 f(n) h^3, \quad (3.68)$$

where k_1 is a coefficient which depends on the properties of the VV and the soil; h is the crater depth; $f(n)$ is a function of the blow-out index.

Many researchers have worked on determination of the form of the function $f(n)$, and various expressions for $f(n)$ have been obtained based on analysis of extensive experimental data. The following expression, obtained by M. M. Boreskov, is used most often:

$$f(n) = 0.4 + 0.6n^3, \quad (3.69)$$

with $n=1$, $f(n)=1$.

Table 3.6 presents values of the coefficient k_1 with the use of the function $f(n)$ in the form of equation (3.69).

Table 3.6. Values of coefficient k_1 .

(1) - среда	(10) Среди взрывчатых веществ	(11) Аммониты
(2) свежессыпаный грунт	0.43	0.50
(3) обычессыпаный грунт	0.95	1.10
(4) глина	1.18	1.37
(5) песок	1.34	1.44
(6) известник	1.57	2.15
(7) мраморная кладка	1.57	2.15
(8) гранитная скала	2.25	2.58
(9) бетон	2.16	3.89

Key: (1) medium; (2) freshly poured soil; (3) ordinary soil; (4) clay; (5) sand; (6) limestone; (7) masonry; (8) granite rock; (9) concrete; (10) normal high explosives; (11) ammonites.

The shape of a crater formed in blowing out of soil is extremely similar to the shape of a truncated cone, since the crater is partially filled with soil which falls into the crater after the explosion (Fig. 3.41). It is assumed in calculations that the radius of the smaller base r_1 is equal to $r/2$.



Fig. 3.41.

Then the crater volume is determined by the formula

$$\text{or } W = \frac{1}{3} \pi h (r^2 + rr_1 + r_1^2) = 1.83 h r^3$$

$$W = 1.83 h r^3. \quad (3.70)$$

In destroying such targets as highways, railroads, airstrips (VPP), airfields, etc., it is necessary to achieve formation of craters with a maximum volume. A blow-out index of the order $n=1.5-2.2$ is most advantageous in this case. Figure 3.42 shows the form of the dependence of the volume of the crater formed on the relative depth of burying of the aerial bomb. A crater of maximum size is produced in penetration of the aerial bomb to a depth equal to two-three times the length (L) of the shell of the aerial bomb.

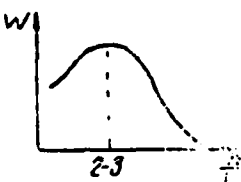


Fig. 3.42.

A value of n of the order of 0.75-1 will be most advantageous for most effective destruction of underground structures, where a maximum depth of penetration is needed.

Using formula (3.68), one can solve two problems:

1. Determining the necessary weight (ω) of a charge of an explosive of the type in question with given values of the depth (h) for location of the charge and the blow-out index (n).
2. Determining the necessary value of the depth for burying (h) of the charge with given values of the explosive charge weight (ω) and the blow-out index (n).

A need for solving the latter problem can arise, for example, in determining the necessary depth of penetration of an aerial bomb of a given caliber with a given value of the soil blow-out index. If the bombing conditions are known, the necessary fuse delay time can be established according to the value of the optimum

penetration depth.

Table 3.7 presents experimental data for dimensions of craters formed in bombing from altitudes of 1200-3500 m with aerial bombs of different calibers on limestone with establishment of a fuse delay of 0.2 s.

Table 3.7. Data on dimensions of craters.

(1) Калибр авиабомбы	(3) Размеры воронки	
	(4) диаметр, м	(5) глубина, м
ФАБ-100(2)	1.5-2.0	0.7-1.0
ФАБ-250	4.5-5.5	1.2-1.5
ФАБ-500	6.0-8.0	1.5-2.0
ФАБ-1000	11.0-12.0*	4.1-4.5*
ФАБ-2000	16.0-18.0	5.0-6.0
	21.0-21.5	6.0-6.5

*Bombing on loam.

Key: (1) aerial bomb caliber; (2) FAB; (3) crater dimensions; (4) diameter, in m; (5) depth, in m.

Table 3.8 presents data on volumes in m^3 of craters formed in bombing from a TU-4 airplane on normal soil with demolition bombs with a fuse of the APUV [aviation pneumatic universal fuse] type with a delay of 0.2 s.

Table 3.8. Crater volume.

(1) Калибр авиабомбы	(3) Высота бомбометания, м		
	2000	6000	8000
ФАБ-250 М-46 (2)	47,6	53,0	54,4
ФАБ-500 М-46	71,1	85,2	98,4

Key: (1) aerial bomb caliber; (2) FAB; (3) bombing altitude, in m.

Evaluation of the destructive effect of an explosion in regard to underground structures is performed based on the condition that destruction of underground structures (targets) sets in when the target is located within the destruction zone $R_p = k_p \omega^{1/3}$. The purpose of calculation of the destruction of underground structures can be represented in the form of two problems:

1. The properties of the soil (k_p) and the material (k_{pl}) of the destruction object are given; the charge weight (ω) and the wall thickness (b) of the object are also given (Fig. 3.43). The problem is to determine the distance (R_p) at which destruction of the underground object will occur.

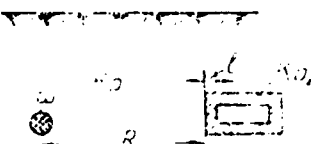


Fig. 3.43.

2. The properties of the soil (k_p) and the material (k_{pl}) of the destruction object are given; the object wall thickness (b) and the distance (R_p) at which destruction should occur are also given. The problem is to determine the charge weight (ω) necessary for destroying the object. The method of equivalent layers is used in solving these problems. The first problem is solved as follows: a layer of material with a thickness b and properties determined by the parameter k_{pl} is replaced with a soil layer equivalent in regard to strength with properties determined by the parameter k_p . The thickness b_e of the equivalent layer obviously will be determined from the following relationships:

$$\frac{b_e}{k_p} = \frac{b}{k_{pl}} ; \quad b_e = b \frac{k_p}{k_{pl}} . \quad (3.71)$$

Then, proceeding from the condition that destruction of the object sets in in a case where it is located within the destruction zone, we can write

$$R_p = R_p + b - k_p \omega^{1/3}. \quad (3.72)$$

Hence the actual distance (R_p) at which destruction of the underground object will occur is as follows:

$$R_p = k_p \left(\omega^{1/3} - \frac{b}{k_{p1}} \right). \quad (3.73)$$

In solving the second problem also, using expressions of (3.71), we can write equation (3.72) in the form

$$R_p + \frac{b k_p}{k_{p1}} \omega^{1/3}.$$

Hence

$$\omega = \left(\frac{R_p}{k_p} + \frac{b}{k_{p1}} \right)^3. \quad (3.74)$$

Based on analysis of the physical picture of the development of the process of an explosion in solid media, especially in soils, one can establish the principles of accomplishment of a directed effect of an explosion in the ground. The same principle is used in controlling the effect of an explosion in the ground as in controlling the effect of an underwater explosion. If there is a cavity containing a substance of lower density in the vicinity of the VV charge located in a dense medium (soil), the greatest part of the energy of the explosion is directed along the shortest path between the VV charge and this cavity; i.e., it is directed along the line of least resistance (LNS).

The information presented is also valid in a case where the explosion of a charge in the vicinity of the free surface area of a dense medium (the ground) is being considered. For example, applying this principle to controlling the effect of an explosion in blowing out of soil, one can build earth dams and other structures, conduct stripping in mining of minerals, etc. Directed blowing out

of soil in explosions can be accomplished by sequential explosion of several charges in such a way that the LNS in explosion of each of the charges is oriented in the direction of desired movement of the soil (Fig. 3.44). A directed explosion in the ground has been investigated in extremely great detail by now, especially by G. I. Pokrovskiy and his students, and is being used widely for peaceful purposes in the USSR and other socialist countries. The use of directed and mass explosions for blowing out and disposal of soil is proving an extremely effective means for solving important problems of the national economy. Calculations of mass and directed explosions intended for blowing out or moving a large amount of soil have their own features, and a more detailed consideration of these features is beyond the scope of this textbook.

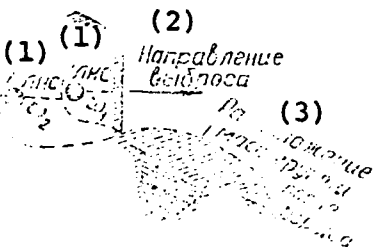


Fig. 3.44.

Key: (1) LNS; (2) direction of blowing out; (3) location of masses of soil after explosion.

The seismic effect of an explosion is manifested in the fact that soil particles take on accelerations and displacements far beyond the zone of destruction of the ground. The destructive effect of an explosion on structures is determined in this case by oscillating shifts of soil particles. The phenomenon of the seismic effect of an explosion was investigated by M. A. Sadovskiy. The calculation formula for determining the maximum velocity (v_m) of the oscillation of soil particles has the following form:

$$v_m = 200 \left(\frac{13.45}{R} \right) [m/s] \quad (3.75)$$

where ω is the VV charge weight in kg; R is the distance from the explosion point in m.

However, the value of the velocity v_m also depends on the blow-out index n , and formula (3.75) is applicable only for a case with $n=1$, i.e., for an explosion which forms a normal blow-out crater.

The value of the maximum velocity of oscillation of soil particles for a random blow-out index can be determined by the following formula:

$$v_n = \frac{200}{f(n)} \left(\frac{\omega R}{R} \right)^{1.5} \quad (3.76)$$

Here $f(n)$ is a function of the blow-out index determined according to formula (3.69).

The total oscillation period of soil particles in the main phase can be evaluated by the formula

$$T = \tau \lg R, \quad (3.77)$$

where R is the distance from the VV charge in m; τ is a coefficient depending on the properties of the soil.

The values of the coefficient τ are as follows:

- 0.11-0.13 for water-saturated soil (peat bogs, quicksand);
- 0.06-0.09 for alluvial soil of average strength;
- 0.01-0.03 for rocky soil.

Assuming that the oscillations of soil particles are sinusoidal, with a knowledge of v_m and T , one can determine the amplitude and acceleration of the oscillations. The amplitude a of the oscillations is determined according to the formula

$$a = \frac{v_m T}{2\pi}.$$

Inserting values of v_m and T , we obtain

$$a = \frac{200 \pi \lg R}{2\pi f(n)} \cdot \frac{\omega^2}{R} \quad (3.78)$$

The maximum acceleration in oscillations will be as follows:

$$j_m = \frac{\omega^2}{a} = \sqrt{\frac{2\pi \cdot 200}{f(n) \cdot \lg R}} \left(\frac{\omega^2}{R} \right)^{1/2} \quad (3.79)$$

Knowing the values of v_m , a , j_m and T , one can evaluate the degree of danger of a seismic effect of an explosion by comparing these values to the dynamic characteristics of the structure or object under consideration.

* * *

It follows from the consideration of the phenomenon of an explosion in various media performed above that the overall picture of the development of the explosion process in different media (from gaseous to solid media) is the same in its general features.

Substantial differences observed are explained by different physicochemical properties of the media and primarily by their different compressibility and different density and strength. In explosion of an explosive charge in any medium, a sharp impact of expanding explosion products against adjacent layers of the medium occurs. Sharp compression, intensive deformation and forcing back of these layers of the medium from the explosion point occur as a result. A shock wave develops in this process in practically any medium, and the energy of the explosion in propagation of the shock wave is transported for distances which are not within the reach of expanding detonation products.

For proper understanding of the process of development of a

shock wave in an explosion or shock, the idea of the compressibility of the medium is of fundamental importance - development of a shock wave is impossible in an absolutely incompressible medium. In passage of a shock wave from a medium of one density into a medium of another density, the parameters of the shock wave change. If a shock wave propagating in any medium encounters a medium of greater density in its path, reflection of the shock wave occurs, with an increase in all its parameters.

If a shock wave propagating in a medium encounters a medium of lesser density in its path, the shock wave in the initial medium is transformed from a compression wave into a rarefaction wave propagating from the boundary of the medium.

Principles for evaluating the destructive effect of an explosion in different media are also similar and at present are based on principles of the theory of similarity and the introduction of coefficients determined experimentally.

For example, the general dependence for determining the maximum pressure of a shock wave in an explosion has the following form:

$$p_m = \sum_{i=1}^n A_i \left(\frac{\omega^{1/3}}{R} \right)^{a_i}$$

The values of A_i and a_i are determined or refined based on analysis of experimental data. The general dependence for determining the destruction distances in an explosion has the following form:

$$R_p = k_p \omega^\alpha.$$

The value of the exponent α for an explosion in air is as follows: $\alpha=1/3$ with $R < R_K$, and $\alpha=2/3$ with $R > R_K$. For an explosion in solid media, $\alpha=1/3$. The value of k_p is taken from an experiment depending on the degree of destruction required.

Further study of the effect of an explosion in different

media is an important task, because possibilities for deep theoretical and experimental investigation and practical use of extremely interesting physical and mechanical processes which accompany the phenomenon of an explosion and its effect have not yet been nearly exhausted.

CHAPTER 4

THE PERCUSSION EFFECT OF AMMUNITION

§ 1. THE NATURE OF THE PERCUSSION EFFECT IN AMMUNITION

The problem of theoretical and experimental study of the process of the percussion effect of ammunition arises in connection with the necessity of evaluating the destructive effect of ammunition in impact against an obstacle or in penetration into the ground.

The destructive effect of ammunition in a given case is determined by the magnitude of the kinetic energy which it possesses as it encounters the obstacle.

A knowledge of the laws of motion of ammunition as it penetrates uniform solid media makes it possible to solve most effectively one of the important problems - the problem of hitting targets deeply sheltered in the ground. This problem takes on special urgency in connection with training forces for conducting combat actions under conditions of the use of nuclear weapons, since the most reliable protection for forces and combat equipment is underground shelters and cover of different kinds. Solution of the problem of penetration of ammunition in its percussion effect also provides initial grounds for selecting proper methods for calculation and rational design of aviation fuses for providing optimum delay in action for obtaining the maximum destructive effect.

The problem of calculating the strength and reliability of ammunition in hitting an obstacle can arise in a considerable number of cases at present in connection with the increase in bombing velocities and altitudes and in connection with the use of such powerful weapons as ballistic missiles. The latter problems naturally can be solved only in a case where sufficiently reliable engineering relationships describing the process of the percussion effect of ammunition are known.

The basic physical process which occurs in the percussion effect is the movement of ammunition in some resisting medium. This movement is accompanied by deformation of the medium, and the penetrating body also undergoes loading, which leads to the appearance of corresponding stresses and strains in the body itself.

The movement of any penetrating body in a uniform medium is possible only in disruption of the uniformity of this medium and displacement of part of the medium to the sides and forward in the direction of movement of the body. The kinetic energy of the penetrating body is spent on deformation of the medium and imparting accelerating to particles of the medium - on deformation of the penetrating body itself, on heating the medium and the body in the process of their interaction, and on shaking the medium. Deformation of the medium in impact and penetration can spread for a considerable distance from the point of contact of the body with the surface of the medium. Features of the process of impact and penetration of a body into some medium are determined primarily by the degree to which this process is a dynamic one and depend on the relationship between the velocity at which the body encounters the surface of the medium and the velocity of the propagation of sound in this medium.

The density and strength of the medium are also of substantial importance. If the velocity (v) of the penetrating body is low as compared to the velocity of sound (v_{SB}) in the medium, deformation

of the medium covers an extremely large volume as compared to the dimensions of the penetrating body. The magnitude of deformation gradually fades in proportion to the distance from the penetrating body. The two following limit cases are possible, depending on the elastic properties and strength of the medium.

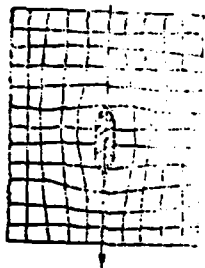


Fig. 4.1.

The medium is elastic and in an undisturbed state is under the influence of some pressure (its own weight or an external load). The medium is mobile to the extent that the indicated pressure is sufficient for deformation of the medium. Water under the influence of gravity and rubber under the influence of internal elastic forces can serve as examples of such a medium. In this case, in movement of the penetrating body, the medium separates and closes behind the body (Fig. 4.1).

The medium is inelastic and sufficiently strong so that its own weight for the external pressure cannot deform it. In this case, some cavity is preserved in the medium after passage of the body. Residual deformations of the medium occur in some space near the penetrating body (Fig. 4.2).

If the velocity (v) of the penetrating body is near the velocity of sound (v_{SB}) in the medium but is somewhat less than the velocity of sound, the zone of deformation of the medium is restricted by the deformation wave front. Depending on the elastic properties and strength of the medium, two cases are also possible in this case.

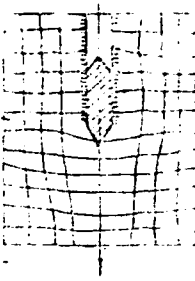


Fig. 4.2.



Fig. 4.3.

The medium is elastic or mobile and is under the influence of its own weight or external pressure. A deformation wave is formed in front of the penetrating body. Due to the compressibility of the medium, a cavity is formed behind the penetrating body and closes at some distance from the body (Fig. 4.3).

The medium is inelastic and sufficiently strong so that residual deformations produced in penetration are preserved. The deformation wave propagates in front of the moving body. A cavity which does not close is formed behind the moving body (Fig. 4.4).

If the velocity (v) of the penetrating body is greater than the velocity of sound (v_{SB}) in the medium, a conical deformation wave front separating the deformed zone from the undeformed zone develops in front of the penetrating body. The emerging wave is similar to the well-known ballistic wave which arises in movement

of bodies in air at supersonic velocities. Depending on the elastic properties and strength of the medium, two cases are also possible here.



Fig. 4.4.

The medium is elastic or mobile and is under the influence of its own weight or external pressure. A conical deformation wave front is formed in front of the penetrating body. A cavity of significant volume is formed behind the penetrating body and closes at some distance from the body (Fig. 4.5).



Fig. 4.5.

The medium is inelastic and sufficiently strong. A conical deformation wave front is formed in front of the penetrating body. A cavity which does not close is formed behind the penetrating body, and the volume of the cavity is significantly greater than the volumes of cavities formed in the cases considered previously (Fig. 4.6).

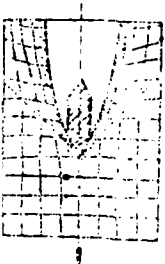


Fig. 4.6.

The phenomenon of formation of cavities in a medium in movement (or penetration) of bodies is normally called cavitation. Cavitation cavities can reach extremely large sizes - their diameter can exceed the diameter of the penetration body substantially - at high penetration velocities in sufficiently pliable media. The picture of penetration into elastic media is more similar to the picture of penetration into inelastic and strong media at supersonic velocities than at subsonic velocities.

The cases of penetration of bodies which have been considered can occur practically in a percussion effect of ammunition under modern conditions of combat use of ammunition. The character of the penetration process is determined by the ratio of the velocity of the penetrating body and the velocity of sound in the medium. To make it possible to evaluate the character of the process of penetration of some specific type of ammunition into various media, Table 4.1 presents values of the velocity of sound for certain media.

Table 4.1. Values of the velocity of sound.

Medium	Velocity of sound, in m/s
Concrete	3000
Granite	3000
Limestone	2000

Water	1500
Water-saturated soils (clays)	1500
Sand	200-500
Humus	100-300
Peat, freshly poured earth, loose sand	30-50

The concluding part of this chapter will consider features of the process of penetration at supersonic impact velocities, where the concentrations of energy in the zone of interaction of the body and the obstacle are so great that a hydrodynamic analogy can be used for analysis of the process, in a manner similar to what is done in describing the phenomenon of accumulation and evaluating the casualty effect of shaped charges (see Chapter 5).

In the most general statement, the problem of the penetration of ammunition into uniform media belongs to an extremely broad class of problems of the movement of bodies in resisting media. The physical picture of the movement of a body has many common features in a gas or liquid medium and in a solid uniform medium. The distinguishing features observed and the differences are conditioned by differences in physical and mechanical properties of the media (different compressibility, density and strength). The problem of the penetration of bodies into media is posed as follows: assume that the characteristics of the body (mass, shape, etc.) are known; the physical and mechanical characteristics of the medium and initial and boundary conditions are also known. It is necessary to find the law of movement of the body in the medium and the distribution of forces of pressure from the resisting medium on the body at each moment of movement. Questions involved with the movement of bodies in air are studies in aerodynamic and in external ballistics. The movement of bodies in water is studies in hydrodynamics. However, it has not been possible to solve the problem in the complete statement formulated above even for such media as air and water, for which the physical and mechanical characteristics have been studied sufficiently thoroughly.

The appropriate coefficients, which have a definite physical meaning and are determined experimentally, are introduced in solving the problem of movement of bodies in air or water. Solution of problems of this kind, as a rule, is performed by numerical methods. Investigating processes of impact and penetration of bodies into solid uniform media is an incomparably more complex problem which cannot be solved in a complete statement. The process of impact and penetration of bodies into solid media is a typical unsteady, nonstationary dynamic process. The medium in this case is anisotropic, as a rule, and its physical and mechanical properties are extremely varies and have received little study. We shall consider general physical and mechanical grounds for solving the problem of the penetration of a body into any continuous medium (gas, liquid, solid, etc.).

In penetration of a body into a medium, the particles of the medium take on an acceleration \bar{a} , which is determined by the acceleration (without consideration for the effect of gravitational forces)

$$\rho \bar{a} = \frac{\partial \bar{\tau}_x}{\partial x} + \frac{\partial \bar{\tau}_y}{\partial y} + \frac{\partial \bar{\tau}_z}{\partial z} \quad (4.1)$$

where ρ is the density of the medium; $\bar{\tau}_x$, $\bar{\tau}_y$ and $\bar{\tau}_z$ are vectors of stresses on faces perpendicular to x , y and z axes.

The value of \bar{a} can also be expressed in terms of the rate of deformation \bar{v} :

$$\bar{a} = \frac{\partial \bar{v}}{\partial t} + v_x \frac{\partial \bar{v}}{\partial x} + v_y \frac{\partial \bar{v}}{\partial y} + v_z \frac{\partial \bar{v}}{\partial z}$$

If the deformation rates are very low, one can express the acceleration in terms of the vector of displacement of a particle:

$$\bar{a} = \frac{\partial^2 \bar{u}}{\partial t^2}$$

The vector equation (4.1) can be represented in the form of three scalar equations in partial derivatives relating the values of u_x , u_y and u_z or v_x , v_y and v_z to stress components τ_{xx} , τ_{yy} ,

τ_{zz} , τ_{xy} , τ_{yz} and τ_{zx} . All the indicated variables should be determined as functions of coordinates x , y and z and the time t , if the initial and boundary conditions are given. Having represented the stress components in the form of a function of the values x , y , z and t , one can compute the main vector and the main moment of forces acting on the body and, consequently, one can find the law of movement of the body in the medium.

In order to determine the stress components from the system of equations (4.1), however, one must know the so-called equation of state of the medium in question; i.e., one must know the dependence between the stress components and the components of deformations and the rates of deformations. This dependence will be different for media with different physical and mechanical properties and even for the same medium under different deformation conditions - different diagrams of the stressed state. As already noted, in consideration of the effect of an explosion in different media (see Chapter 3), the equation of state of some medium under deformation at high pressures or under some other conditions can be selected in a form sufficiently simple and convenient for practical calculations.

For metals, for example, just as for water, the equation of state can be adopted in a comparatively simple form:

$$p = A \left[\left(\frac{\rho}{\rho_0} \right)^n - 1 \right], \quad (4.2)$$

where p is the pressure; ρ_0 is the initial density of the metal; ρ is the density of the metal at the pressure p ; n is the exponent for most metals, which essentially is equal to 4; A is a coefficient determined by the formula

$$A = \frac{\rho_0 c_0^2}{n},$$

where c_0 is the velocity of propagation of sound in the metal.

Attempts at theoretical consideration of the process of penetration of ammunition into the ground until recently did not

lead to practically acceptable results. The most substantial difficulty in solving this problem is the lack of a diagram of deformation of the ground in the penetration of bodies sufficiently similar to the corresponding reality. Well-known successes in the field of theoretical investigation of the phenomenon of penetration of bodies into solid media, especially soils, have appeared recently. The hypothesis first introduced by Kh. A. Rakhmatulin concerning representation of soil properties in the form of properties of some ideal medium - "plastic gas" - has proven extremely fruitful. Properties of the "plastic gas" were considered in the chapter devoted to the effect of an explosion in soils (see Chapter 3). Basically all studies on theoretical investigation of the phenomenon of penetration which have been conducted up to now have been based on the use of a "plastic gas" system with some modifications. For example, a more or less complete solution of the problem of penetration of a body into the ground can be obtained under the following basic assumptions.

The soil is considered as an ideal uniform medium, i.e., a medium in which there are no tangential stresses. This assumption is applicable in deformations of the soil under the influence of high pressures.

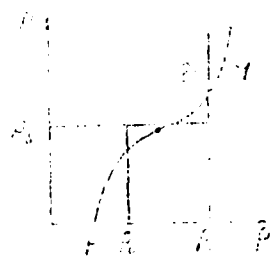


Fig. 4.7.

The soil deformation diagram is represented as a special type of dependence between pressure and density for the "plastic gas." The essence of this diagram lies in the fact that the actual dependence between the pressure and density of the soil (Fig. 4.7,

curve 1) is replaced with the broken line (Fig. 4.7, line 2).

Thus it is assumed that at pressures which do not exceed some value p_s characteristic of the soil in question, the soil undergoes deformation according to the law of ideal incompressibility of a fluid of the density in question ρ_0 . At a pressure equal to p_s , compaction of the soil occurs to a density ρ_1 , after which the soil again undergoes deformation as an ideal fluid, but now at a constant density ρ_1 .

The movement of soil particles is assumed to occur in planes perpendicular to the axis of symmetry of the body. Furthermore, the axis of symmetry is considered to coincide with a perpendicular to the free surface of the ground. In other words, it is assumed that there is no movement of the soil in the direction of movement of the body. This hypothesis, called the hypothesis of plane sections, was proposed by A. A. Il'yushin and has been used in considering various problems. In particular, this hypothesis was used in considering penetration of armor at supersonic velocities. One can establish the boundaries of applicability of this hypothesis finally only by conducting additional research.

Based on the basic suppositions which have been formulated, next one can compose motion and continuity equations for soil particles. With a knowledge of the shape of the penetrating body, one can carry the solution of the problem to the end.

However, despite the fact that theoretical results are in satisfactory agreement with experimental data in a number of cases, theoretical analysis of the phenomenon of penetration of bodies into the ground at present cannot provide the results necessary for practical calculations involved with the process of penetration of bodies into the ground. The theory of dynamic deformation of the soil has only begun to develop, and it is natural that the first results which provide an answer to extremely important practical

problems are being obtained with the simplest idealized premises, which do not reflect all the features of the phenomenon in question.

Solution of the problem of the penetration of bodies into uniform solid media (especially soils) thus is involved with overcoming very great difficulties, which result in the fact that this problem cannot be solved in a complete statement, despite the important successes which have been achieved by now in the field of the theory of elasticity and plasticity, mechanics of continuous and dispersion media, and statics and dynamics of soils.

On the strength of the circumstances indicated, study of the phenomenon of the penetration of ammunition into solid media, especially soils, begun in the first half of the nineteenth century - during a period of intense development of artillery - is based mainly on establishment of empirical and semiempirical relationships defining the effects of basic factors on the penetration process. The form of these relationships is selected based on deep analysis of the physical picture of the penetration process.

The basic factors (of the entire spectrum of factors which define the process in question) whose effect is taken into consideration in practice up to now in describing the process of penetration of bodies are as follows: the physical and mechanical characteristics and properties of the medium, the weight and shape of the penetrating body, and the velocity at which the body encounters the obstacle.

In studying the phenomenon of penetration of bodies into various media, it is necessary to keep in mind the fact that this phenomenon, as a rule, is made up of three stages:

- impact against the surface of the medium;
- penetration of the medium by the body;

- movement of the body in the medium.

The character of the interaction of the body with the medium has its own features in these three stages. In examination of the penetration of ammunition, taking into consideration all three stages is not always obligatory and depends on the conditions of combat use of the ammunition. For example, in studying the movement of ammunition in an air medium, as a rule, one considers only the third stage - the stage of steady-state movement. Cases where it is necessary to investigate the character of movement of the ammunition in passage into an air flow which possesses different parameters (the initial stage of releasing of aerial bombs from internal bomb racks) or a case where it is necessary to study the character of movement of ammunition in "impact" and "penetration" into the air medium from a medium of greater density (such as launching of missiles from submarines while submerged) can constitute exceptions.

Study of the phenomenon of penetration of ammunition into water, soil and other stronger media normally involves analyzing all three of the stages indicated or of only the first two stages. Two characteristic types of the penetration phenomenon can be distinguished in practical use of ammunition:

- penetration of ammunition into a uniform medium occupying a large volume (a solid mass), where one can consider penetration into a half space occupied by the medium in question. The medium can either be homogeneous or can have a complex structure. In this case, it is customary to call the phenomenon in question penetration;

- encountering of comparatively thin obstacles by the ammunition, where the kinetic energy of the ammunition proves sufficient for breaking through the entire thickness of the obstacle, and the phenomenon of penetration, as a rule, can consist of only two stages - impact and penetration. In this case, it is customary

to speak of piercing obstacles.

§ 2. THE FORCE OF RESISTANCE OF THE OBSTACLE IN PENETRATION

In the penetration of bodies into uniform media, especially soil, as already noted, one should distinguish three stages of development of the process.

The initial stage is impact of the body against the surface of the medium (obstacle). This stage is characterized by the development of conditions at the point of impact under which a compression shock wave emerges both in the ground and in the body striking it. At this initial moment of contact of the body with the obstacle, as a result of sharp slowing down of the body, large overloads emerge, plastic flow phenomena can occur, etc. Due to the difficulties involved in experimental study of this stage of penetration, it has been studied least thoroughly.

The second extremely important stage is penetration of the body into the obstacle. This stage of the penetration process can develop in different ways, depending on the angle at which the body approaches the surface of the obstacle. It has been established that with given properties of the obstacle and a definite form and a predetermined velocity of contact, there is some critical angle θ_{np} which defines the boundary between two qualitatively different types of development of this stage of the penetration process (Fig. 4.8). If the angle θ_c of contact of the body with the surface of the obstacle is greater than the critical (limit) angle of impact ($\theta_c > \theta_{np}$), the body penetrates into the obstacle (the ground) and will continue movement in the obstacle. If the angle of impact of the body with the surface of the obstacle is less than the critical angle of impact ($\theta_c < \theta_{np}$), the body rebounds from the ground surface and will continue movement in the air medium. This phenomenon is called ricocheting or ricochet of the body in impact against the obstacle.

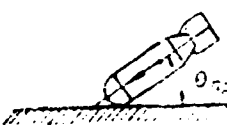


Fig. 4.8.

In a case where the body begins to penetrate into the obstacle, the area of interaction of the nose section of the penetrating body with the obstacle will increase, and the force of resistance (the reaction of the obstacle) will increase (Fig. 4.9). The shock disturbance which emerges at the point of penetration

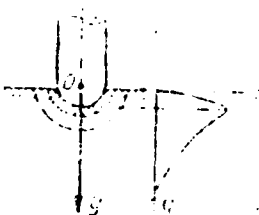


Fig. 4.9.

of the body (the compression shock wave) propagates into the mass of the obstacle. The compression shock wave, as we know, is reflected from the free surface of the obstacle in the form of a stretching wave. The stretching wave, propagating from the free surface of the medium, leads to displacement of particles of the medium located at the surface, and a ridge is formed under the action of the penetrating body near the point of its penetration. Beginning from this moment, the force of resistance of the medium, as a rule, gradually decreases, although the contact area of the body with the medium can still increase. The third stage of the penetration process - movement of the body in the medium - sets in. The penetrating body, in continuing its movement, separates the particles of the medium to the sides; the medium is compacted - the formation of a penetration cavity occurs - and part of the medium

moves in front of the body, forming a kind of additional attached mass which moves together with the penetrating body. Under real conditions of penetration of a body, the reaction of the medium (such as soil) proves to be different at different points of the area of contact with the body. This circumstance results in the fact that the vector of the resultant force of resistance does not coincide with the axis of symmetry of the body, and the trajectory of movement of the body in the medium is distorted (Fig. 4.10) and can have the form of a curve with a double curvature. The deviation of the trajectory of movement of the body, on the one hand, leads to a decrease in the depth of penetration and can sometimes cause deformation of the penetrating body due to the appearance of unbalances local loads which exceed the calculated loads, which are assumed to be symmetrical and uniform in calculations of a penetrating body for strength. On the other hand, the deviation of the trajectory of the penetrating body severely complicates studies for finding the position of ammunition after penetration, in the ground, for example. Great difficulties often arise in connection with this in test studies with ammunition or in detection and neutralization of unexploded ammunition.

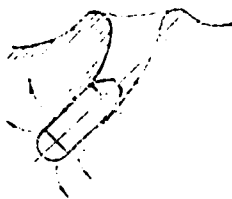


Fig. 4.10.

In piercing of comparatively thin obstacles, the third stage has features involved with the appearance of splitting off of material from the rear side of the obstacle (Fig. 4.11). The compression wave, in reflection from the back side of the obstacle, forms a breaking away under certain conditions which increases the

depth of penetration (piercing).

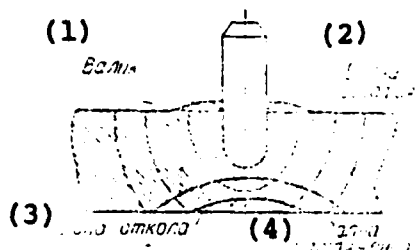


Fig. 4.11.

Key: (1) ridge; (2) compression wave; (3) splitting-off zone; (4) stretching wave.

Figure 4.12 shows the position of a body (aviation bomb, shell, etc.) moving in a solid mass of the medium. The resultant (\bar{F}_{Σ}) of forces of resistance of the medium to movement of the body is applied at the center of resistance (ts. s.), which is located in front of the center of gravity (ts. t.). We shall assume that the angle of attack δ (the angle between the axis of the body and the direction of the velocity vector \bar{v}) lies in the plane of the angle of impact (θ_c) of the body with the surface of the obstacle. Then the resultant (F_{Σ}) of forces of resistance of the medium can be replaced with a force F_{Σ} applied at the center of gravity of the body and the momentum M (Fig. 4.12). We shall divide the force F_{Σ} applied at the center of gravity of the body into two components:

- The force F_v directed at a tangent to the trajectory of movement of the body - the frontal resistance of the medium (obstacle);

- the force F_N directed at a perpendicular to the trajectory of movement of the body - the lateral resistance of the medium (obstacle).

The lateral resistance of the medium causes distortion of the trajectory in movement of the body in the medium. We shall refer

to the force of frontal resistance, which tries to stop the body, as the force (F) of resistance of the medium to penetration.

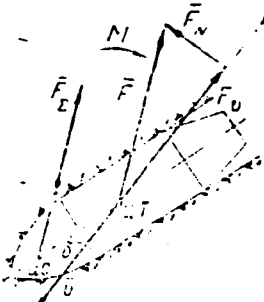


Fig. 4.12.

The force of resistance of the medium to penetration in general is a combination of three components:

$$F = F_1 + F_2 + F_3 \quad (4.3)$$

The force F_1 is the force of dynamic resistance of the medium. The appearance of this component is conditioned by inertia of particles of the medium driven into motion in penetration of the body. The value of F_1 is determined by the formula

$$F_1 = c_1 S \frac{\rho v^2}{2} \quad (4.4)$$

where $S = \frac{\pi d^2}{4}$ is the cross section area of the body; d is the

diameter of the penetrating body; c_1 is a coefficient which depends on the shape of the body and the angle of attack.

The force F_2 is the force necessary for overcoming friction between particles of the medium - the toughness of the medium. The value of this force is conditioned by toughness properties of the medium and can be calculated by the formula

$$F_2 = c_2 \mu v d, \quad (4.5)$$

where μ is the viscosity factor of the medium; v is the velocity of movement of the body; d is the diameter of the penetrating body;

c_2 is a coefficient which depends on the shape of the body.

The force F_3 characterizes the resistance of the medium in static loading. The value of this force, conditioned by strength connections between particles of the medium, does not depend on the velocity of movement of the body and can be determined from the formula

$$F_3 = c_3 S p_0 \quad (4.6)$$

where p_0 is the crushing strength of the medium; c_3 is a coefficient which depends on the shape of the penetrating body.

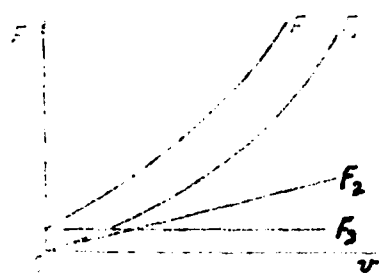


Fig. 4.13.

The relationship among components of the force of resistance of the medium depends on the velocity of movement of the penetrating body (Fig. 4.13). At a low velocity of movement of the body, static resistance F_3 makes up the main part of the force of resistance of the obstacle, since toughness F_2 and dynamic resistance F_1 are relatively low. At high velocities, the components F_1 and F_2 considerably exceed F_3 , and one can neglect the static component. At very high velocities, dynamic resistance involved with a sharp increase in the inertial resistance of particles of the medium with an increase in the velocity of the penetrating body will be the basic component.

§ 3. PENETRATION INTO DENSE SOLID MEDIA

As a result of consideration of the penetration of ammunition into solid obstacles, it is necessary to obtain expressions for determining the law of movement of the body in the medium and formulas for determining the total depth of penetration, i.e., the time of movement of the body to the total depth of penetration. The process of penetration of ammunition into solid obstacles will be considered under the following assumptions:

- contact of the body with the obstacle occurs at a perpendicular;
- the trajectory of movement of the body in the obstacle is rectilinear;
- the penetrating body in the process of impact and movement in the obstacle does not undergo deformation.

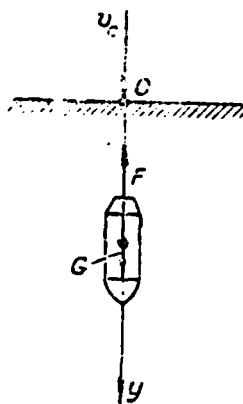


Fig. 4.14.

Under the assumptions which have been made, having adopted the appropriate designations (Fig. 4.14) - G is the weight of the

body, v_c is the velocity of impact of the body with the obstacle, and F is the force of resistance of the obstacle to movement of the body - we obtain an equation of motion of the body in the obstacle in the following form:

$$\frac{G}{g} \frac{d^2y}{dt^2} = G - F.$$

In penetration of ammunition into various media, the value of the force of resistance of the medium normally significantly exceeds the weight of the penetrating body ($F \gg G$).

Then

$$\frac{d^2y}{dt^2} = -\frac{g}{G} F. \quad (4.7)$$

We shall take an expression for the force of resistance in the form of a so-called two-member law of resistance, first proposed by the well-known Russian scientist N. A. Zabudskiy:

$$F = F_1 + F_2,$$

i.e., we do not take into consideration the component F_2 of the force of resistance of the medium, which is determined by the toughness properties of the medium.

Keeping in mind expressions (4.4) and (4.6), and designating

$$\frac{c_1 p}{2c_3 p_0} = b \text{ and } c_3 p_0 = A,$$

we obtain

$$F = SA(1 + bv^2). \quad (4.8)$$

Expression (4.8) is familiar under the name of the Zabudskiy formula for the force of resistance of a medium. A formula similar in structure for determining the force of resistance of soil was proposed somewhat earlier by N. V. Mayevskiy, a well-known researcher in the field of ballistics.

Thus equation (4.7) will be written in the form

$$\frac{d^2y}{dt^2} = -\frac{gS}{G} A(1+bv^2). \quad (4.9)$$

The initial conditions are as follows:

$$t=0; y=0; \frac{dv}{dt}=v_0$$

We shall seek a law of movement of the body in the medium in parametric form,

$$\begin{aligned} y &= y(v) \\ t &= t(v) \end{aligned}$$

We shall determine the dependence $y=y(v)$. We shall rewrite equation (4.9) in a somewhat transformed aspect:

$$v \frac{dy}{dv} = -\frac{gS}{G} A(1+bv^2).$$

Integrating this equation under the initial conditions indicated above, we obtain

$$y = L_0 \ln \frac{1+bv_0^2}{1+bv^2}. \quad (4.10)$$

where the following is designated:

$$L_0 = \frac{G}{2 \cdot g b A S}$$

We shall determine the dependence $t=t(v)$. We shall write equation (4.9) in the following form:

$$\frac{dv}{dt} = -\frac{gS}{G} A(1+bv^2).$$

Integrating this equation under the initial conditions which have been selected, we obtain

$$t = 2\sqrt{b} L_0 [\operatorname{arctg}(\sqrt{b} v_0) - \operatorname{arctg}(\sqrt{b} v)]. \quad (4.11)$$

Expressions (4.10) and (4.11) represent a law of movement of the body written in parametric form. Using the expressions of (4.10) and (4.11), one can establish the dependence $y=y(t)$ (in the form of a graph or a table); i.e., one can solve the first of the problems which have been stated, which is involved with determining the law of movement of the body in the obstacle.

Assuming that $v=0$ in formulas (4.10) and (4.11), we shall obtain expressions for determining the total depth of penetration

L and the limit time of penetration t_{pp} of the body to this depth:

$$L = L_0 \ln(1 + b v_c^2) \quad (4.12)$$

$$t_{\text{pp}} = 2\sqrt{b} L_0 \arctg(\sqrt{b} v_c). \quad (4.13)$$

Formula (4.12) is called the Zubudskiy formula.

The coefficients A and b necessary for calculations by these formulas are determined experimentally; their values for certain media for penetration of ammunition of the normal form are presented in Table 4.2.

Table 4.2. Values of coefficients A , b and k_{Π} .

(1)	(2)	(3)	(4)	(5)	(6)	A	b	k_{Π}
	свежесыпанная					$0.461 \cdot 10^6$	$60 \cdot 10^{-6}$	$17 \cdot 10^{-6}$
	земля					$0.435 \cdot 10^6$	$20 \cdot 10^{-6}$	$4.5 \cdot 10^{-6}$
	песок (сырой)					$0.445 \cdot 10^6$	$35 \cdot 10^{-6}$	$10 \cdot 10^{-6}$
	песок					$0.460 \cdot 10^6$	$10 \cdot 10^{-6}$	$6 \cdot 10^{-6}$
	дерево (сосна, ель)					$3.16 \cdot 10^6$	$15 \cdot 10^{-6}$	$2.5 \cdot 10^{-6}$
	кирпичная кладка							

Key: (1) medium; (2) freshly poured earth; (3) sand (soil); (4) clay; (5) wood (pine, spruce); (6) brickwork.

In a number of cases of practical importance, the dependence of the velocity of penetration of the body on the depth of penetration can be of interest. This dependence can be obtained by joint examination of expressions (4.10) and (4.12):

$$v = \frac{1}{\sqrt{b}} \sqrt{\frac{L-y_0}{e^{\frac{L-y_0}{b}} - 1}}. \quad (4.14)$$

It follows from the Zubudskiy formula for the force of resistance of the medium (4.8) that at $v = \frac{1}{\sqrt{b}} = 4^*$ the dynamic component of resistance of the medium is equal to the static component (Fig. 4.15). Consequently, the expressions obtained above for determining the law of movement of the body in the medium, as already noted, were derived based on a so-called

two-member law of resistance (4.8). However, calculation formulas obtained based on another law of resistance are quite widely known in practical work. This law of resistance is based on the assumption that the dependence of the force of resistance of the medium on the velocity of movement of the body is exponential,

$$F = k S v^m, \quad (4.15)$$

where k is a coefficient which takes into consideration the properties of the medium and the shape of the penetrating body; S is the cross section area of the body; v is the velocity of movement of the body.

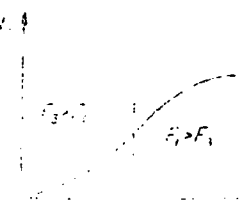


Fig. 4.15.

The following dependence between the total depth of penetration L and the impact velocity v_c and the characteristics of the medium and the penetrating body was obtained based on this law of resistance by extensive experimental research conducted in Russia on Berezan' Island (1908-1912):

$$L = \lambda \frac{G}{d^2} v_c \quad (4.16)$$

where G is the weight of the penetration body, d is the diameter of the body, λ is the penetration coefficient characterizing the properties of the medium, and λ is a coefficient which depends on the shape of the nose section of the penetrating body.

Formula (4.16) is familiar under the name Berezan' formula or Engineering formula. In further research, this formula was subjected to refinement with respect to conditions of bombing

on soils, values of the coefficient k_{II} were refined, and the effect of the impact angle θ_c of an aerial bomb with the ground surface was investigated.

This formula is used at present in the following form:

$$L = \lambda k_{II} \frac{G}{d^2} v_i \sin \theta_c. \quad (4.17)$$

The value of L in this case is the total depth of penetration of the body at a perpendicular to the surface of the obstacle (the ground), since it is just this characteristic which is of the greatest practical interest. Values of the coefficient k_{II} for certain media are presented in Table 4.2; values of the coefficient λ depending on the relative dimensions of the nose section of the penetrating body are presented in Table 4.3.

Table 4.3.

$\frac{l_r}{d}$	λ
0 - 0.5	4.0
0.5 - 1.0	1.1
1.0 - 1.5	1.25
1.5 - 2.0	1.4

The following designations are used in the table; l_r is the length of the nose section; d is the diameter of the penetrating body.

Attempts have been made in some research to determine the values of the penetration coefficient k_{II} by calculation.

The following expressions were obtained as a result:

$$\lambda_n = \frac{2.15}{g \sqrt{E \rho}}, \quad (4.18)$$

where g is the acceleration of gravity; E is the modulus of elasticity of the medium; ρ is the density of the medium;

$$k_{II} = \frac{2.55}{\gamma \rho}, \quad (4.19)$$

where γ is the specific gravity of the medium; c_0 is the velocity of propagation of sound in the medium.

The Berezan' formula (4.16) can be obtained if we assume that the force of resistance of the medium is proportionate to the penetration path,

$$F = ky, \quad (4.20)$$

where y is the penetration path of the body.

The relationships derived above (4.10) and (4.11), obtained based on a two-member law of resistance, are normally used for determining the characteristics of movement of a penetrating body. Therefore, we shall limit ourselves in this case to establishing only the dependence of the velocity v of penetration of the body on the penetration path y . The equation of motion of the body in the soil for a law of resistance taken in the form of (4.20) will be written in the following form:

$$\frac{G}{g} v \frac{dv}{dy} = -ky$$

or

$$v \frac{dv}{dy} = -By$$

where

$$B = \frac{kg}{G}$$

Integrating this equation under the initial conditions $y=0$ and $v=v_c$, we obtain

$$v^2 - v_c^2 = -By^2$$

The value of the coefficient B is determined from the conditions $v=0$, $y=L$.

$$B = \frac{v_c^2}{L^2}$$

Thus, after simple transformations, we obtain

$$v = v_c \sqrt{1 - \left(\frac{y}{L}\right)^2}. \quad (4.21)$$

The value of the total depth of penetration is determined in this case by the Berezan' formula (4.16). Comparison of calculation and experimental data indicates that the Berezan' formula produces the best results at high velocities of impact of the body with an obstacle, while the Zabudskiy formula gives better results at low velocities.

The formulas obtained naturally provide an approximate description of the penetration process, since they do not take into consideration the entire spectrum of factors which determine the course of this process and are based on the use of certain averaged coefficients characterizing the properties of the medium. In addition, these formulas were obtained for a case of penetration of a body into an isotropic solid mass.

§ 4. PENETRATION INTO LAYERED OBSTACLES

Special problems arise in a number of cases in regard to calculation of the penetration of ammunition into overhead covers or other protective devices with a layered structure; the layers can differ substantially in their physical and mechanical properties.

We shall consider the features of calculation of the penetration of bodies into heterogeneous (layered) obstacles. There are two methods for calculating the penetration of bodies into a layered solid mass:

- the method of velocities;
- the method of equivalent layers.

The essence of the method of velocities is as follows. Assume that a body (an aerial bomb) encounters a layered obstacle in its path (Fig. 4.16) and penetrates this obstacle to some depth $L = l_1 + l_2$; as a result of preliminary calculation, we know that $L > l_1$.

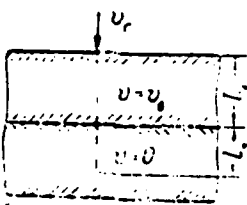


Fig. 4.16.

The properties of the material of the first layer are characterized by a penetration coefficient k_{n1} , and the properties of the second layer by k_{n2} . We shall determine the velocity v_1 which the body will possess after piercing the first layer. It is obvious that $v_1 < v_c$. Using the formulas (4.14) or (4.21), we shall find the value of v_1 . Then, assuming that the process of penetration of the body into the second layer in this case will be the same as in a case where the surface of this layer is a free surface, we can calculate the total depth of penetration of the body into this layer, but under the condition that the impact velocity is equal to v_1 :

$$l_2 = \lambda R_{n2} \frac{G}{d^2} v_1$$

For verifying the condition $L > l_1$, we can also use the Berezan' formula,

$$l_2 = \lambda R_{n1} \frac{G}{d^2} v_c$$

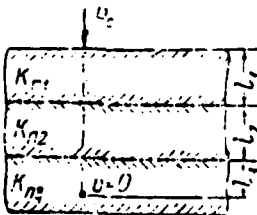


Fig. 4.17.

If the number of layers is greater than two, one must use the indicated calculation system repeatedly, for each layer in turn. It is obvious that calculation by the method of velocities in the latter case leads to awkward computations, and the second method - the method of equivalent layers - is used in practice. The essence of this method is as follows. Assume that the obstacle into which penetration of the body (the aerial bomb) occurs has the structure shown in Fig. 4.17. The properties of the layers are characterized by the penetration coefficients k_{n1} , k_{n2} and k_{n3} , respectively. We must determine $L = l_1 + l_2 + l_3$. Since the values of l_1 and l_2 are determined by the structure of the obstacle, the problem actually can be reduced to determining the total depth of penetration of the body into the bottom layer - l_3 .

For solving the problem, we make use of the idea of equivalent layers. Equivalent layers is also used to mean layers for piercing of which the same impact velocity is necessary. It is obvious that if the physical and mechanical properties of materials of the layers are different, the thicknesses of the equivalent layers will be different. Normally the very bottom layer is adopted as the equivalent. All the other layers of the obstacle are set equal to this layer. This adjustment is accomplished with the Berezan' formula.

The equivalent thicknesses of the layers accordingly will be as follows:

$$l'_1 = l_1 \frac{k_{n3}}{k_{n1}}, \quad l'_2 = l_2 \frac{k_{n3}}{k_{n2}}, \quad l'_3 = l_3,$$

where l'_1 , l'_2 and l'_3 are the thicknesses of equivalent layers adjusted to the material of the bottom layer k_{n3} . The the total depth of penetration L' , but of penetration into a homogeneous solid mass now, will be as follows:

$$L' = l'_1 + l'_2 + l'_3 \quad \lambda k_m \frac{G}{d_i} v_c$$

Hence

$$l_3 = k_{n3} \frac{G}{d^2} v_c - l_1' - l_2'$$

or

$$l_3 = k_{n3} \frac{G}{d^2} v_c - l_1 \frac{k_{n1}}{k_{n2}} - l_2 \frac{k_{n2}}{k_{n1}}.$$

and the total depth of penetration of the body into the layered obstacle finally is determined by the following formula:

$$L = l_1 + l_2, \quad l_3 = k_{n3} \frac{G}{d^2} v_c + l_1 \left(1 - \frac{k_{n3}}{k_{n1}} \right) + l_2 \left(1 - \frac{k_{n3}}{k_{n2}} \right).$$

In a general case, if the obstacle is made up of m different layers, the total depth of penetration can be calculated by the formula

$$L = k_{n3} \frac{G}{d^2} v_c + \sum_{i=1}^{m-1} l_i \left(1 - \frac{k_{ni}}{k_{ni+1}} \right), \quad (4.22)$$

where k_{n3} is the penetration coefficient of the layer selected as the equivalent; k_{ni} is the penetration coefficient of the i layer; l_i is the thickness of the i layer.

§ 5. PENETRATION INTO WATER

The entire process of penetration of a body (aerial bomb, shell, rocket, missile) into water can be divided into three stages:

- impact with the water and penetration of the body into the water;
- cavitation conditions of movement (movement of the body in an air cavity);
- conditions of movement of the body in the water without cavitation.

If the splashdown velocity (the velocity of impact of the body with the surface of the water) is low, i.e., has a value of

the order of 5-10 m/s, the conditions of penetration of the body will be without cavitation from the very beginning, the flow of liquid around the body will be a jet flow, and no air cavity (pocket) is formed. The conditions for a process of penetration into water of this type are created, for example, in dropping of depth charges.

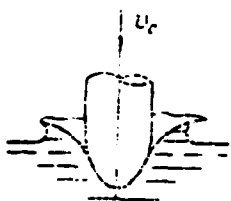


Fig. 4.18.

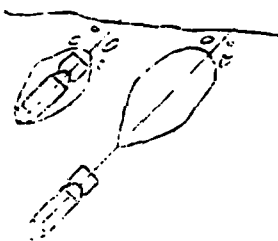


Fig. 4.19.

If the splashdown velocity is sufficiently great and reaches a value of the order of 70-200 m/s or more, a crater is formed in contact of the body with the surface of the water, and an intense liquid splash occurs (Fig. 4.18). Then a gradually closing air cavity is formed; the cavity can accompany the body moving in the water to an extremely great depth (Fig. 4.19). For example, at a splashdown velocity of approximately 150 m/s, the air cavitation cavity accompanies the body to a depth of the order of 50-60 m. The cavitation cavity formed in this stage of movement of the body in water complicates the operation of stabilizing devices and is harmful from the point of view of efficiency of the

destructive effect of an underwater explosion (see Chapter 3).

An air cavity also impedes normal operation of hydrostatic fuses; therefore, hydrostatic fuses are not installed on aviation bombs which have a high splashdown velocity.

In further movement of the body in the water, the velocity of its movement becomes practically constant, and the movement steadies. The value of the velocity of this movement depends on the shape of the body and the density of the water. The initial velocity v_0 of movement of the body in the water will not be equal to the velocity v_c of impact of the body with the surface of the water.

The initial velocity of movement of the body can be determined in a comparatively simple way. This way of determining the initial velocity v_0 of movement of the body in the liquid was pointed out by N. Ye. Zhukovskiy. In impact on the water, the body imparts some velocity to water particles adjacent to its surface (Fig. 4.20). The velocity of the water particles, generally speaking, will not be the same, and the overall impulse obtained by the volume W of liquid will be as follows:

$$I = \iiint_W v_x(x, y, z) dx dy dz$$

and the problem is reduced to extremely complex and awkward computations.

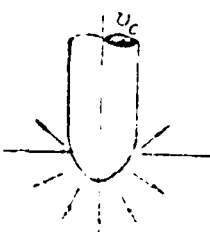


Fig. 4.20.

For approximate determination of the value of v_0 , we shall assume that the velocity taken on by water particles is constant: $v_x = \text{const} = v$; and we shall write an expression for the impulse I in the form

$$I = mv,$$

where m is the so-called attached mass of water.

The hypothetical mass of water whose particles move at a constant velocity thus is called the attached mass; this mass possesses the same amount of movement as the radial mass of water driven into movement in impact and penetration of the body.

The value of the driven mass depends on the volume of the body and can be determined by the formula

$$m \approx \mu W_0 \rho_w \quad (4.23)$$

where μ is the coefficient of the attached mass; W_0 is the volume of the body (the bomb); ρ_w is the density of the water.

The values of the coefficient μ have been determined depending on the relative dimensions of the body for bodies with an ellipsoid shape (Fig. 4.21) and are presented in Table 4.4.

Table 4.4.

a/b	1	1.5	2	3	4	5	6
μ	0.5	0.305	0.209	0.122	0.082	0.06	0.045

In practical determination of the coefficient μ , for an aviation bomb, for example, an ellipsoid is substituted for the latter under the conditions $d=b$ and $L=a$ (Fig. 4.22).

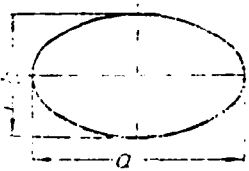


Fig. 4.21.

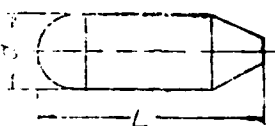


Fig. 4.22.

Then, using a theorem of the amount of movement, we obtain

$$M_0 v_c = (M_0 + m) v_0$$

where M_0 is the mass of the body (the bomb); the other designations have been explained previously. After the appropriate transformations, we obtain

$$v_0 = \frac{1}{1 + \frac{m}{M_0}} v_c$$

or, using the equality $M_0 \approx W_0 \rho_0$, and expressions (4.23), we reduce this formula to the following form:

$$v_0 = \frac{1}{1 + \frac{\rho_0}{\rho_0} \mu} v_c. \quad (4.24)$$

A calculation performed for a PLAB-100 aerial bomb with $\rho_0 \approx 2 \rho_0$, produces $\mu = 0.12$, and $v_0 = 0.94 v_c$.

We shall pass on to establishing the relationships which determine the law of movement of a body in water. The resistance of water to the movement of the body should be adopted in the form $F = F_1$ in accordance with expression (4.4), since the static component

F_2 and the toughness component F_3 are negligibly slight in this case as compared to the dynamic component of the force of resistance. Thus we have

$$F = c_1 S \frac{\rho v^2}{2}. \quad (4.25)$$

Assume that the penetrating body has a weight G ; then the force of the weight of the body in movement in water, as we know, will be

$$G^* = G - W_s \rho_0 g,$$

where g is the acceleration of gravity.

With a knowledge of the values of F and G^* and having established the magnitude of the attached mass m and having oriented the axis of coordinates Oy along the axis of symmetry of the body (Fig. 4.23), we compose an equation of motion of the body (the bomb) in the following form:

$$\left(\frac{G}{g} + m\right) \frac{d^2y}{dt^2} = G^* - c_1 S \frac{\rho v^2}{2}. \quad (4.26)$$

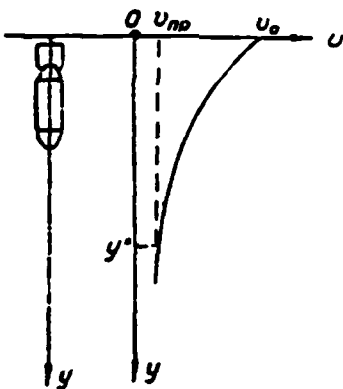


Fig. 4.23.

Before solving this equation, we shall consider another feature of the movement of a body in water. In movement of a body in water (similar to what happens in dropping a body from a great height in air), the dependence of the penetration velocity v on the penetration path y has the form shown in Fig. 4.23. Beginning at some value y^* , the penetration velocity comes to be equal to the limit velocity of movement (immersion) v_{np} , and $dv/dt=0$.

The value of the limit velocity of movement v_{np} is determined from equation (4.26) under the condition $dv/dt=0$:

$$v_{np} = \sqrt{\frac{2G^*}{c_1 S_p}} . \quad (4.27)$$

We shall go on to solve equation (4.26). We shall seek the solution, as in the case of consideration of penetration into dense media, in parametric form.

Designating

$$\frac{G}{g} + m = A$$

and keeping in mind (4.27), we shall rewrite equation (4.26) in the following form:

$$A \frac{dv}{dt} = 1 - \left(\frac{v}{v_{np}} \right)^2 . \quad (4.28)$$

We shall introduce the parameter $u=v/v_{np}$ and shall bring this equation to the following form:

$$Av_{np} \frac{du}{dt} = 1 - u^2 .$$

Integrating this equation with the initial conditions $t=0$, $v=v_0$ and $u=u_0$, we obtain an expression for determining the time for penetration of the body into water:

$$t = \frac{Av_{np}}{2} \ln \left(\frac{1+u_0}{u_0-1} \frac{1-u_0}{u_0+u_0} \right) . \quad (4.29)$$

For determining the depth of penetration y , we present the equation (4.28) in somewhat different form:

$$Av \frac{dv}{dt} = 1 - \left(\frac{v}{v_{np}} \right)^2.$$

or, after introduction of the parameter u ,

$$\frac{Av_{np}^2}{2} \frac{d(u^2)}{dy} = 1 - u^2.$$

Integrating this equation under the initial conditions $y=0$, $v=v_0$ and $u=u_0$, we obtain an expression for determining the depth of penetration of the body into the water:

$$y = \frac{Av_{np}^2}{2} \ln \frac{1+u_0^2}{1-u^2}. \quad (4.30)$$

The formulas (4.30) and (4.29) have the form of a law of movement of a body in water written in parametric form:

$$\begin{aligned} y &= y(u); \\ t &= t(u). \end{aligned}$$

Values obtained for y and t are represented in the form of a table or a graph. The dependence $y=y(t)$ determined in this way in a case of penetration of aviation ammunition into water can be used for establishing the necessary delay in the action of fuses.

For evaluating the character of resistance of water to the movement of a penetrating body in the initial penetration section (impact and the initial period of penetration), a value of the resistance coefficient c_1 exceeding the value obtained in steady movement by a factor of approximately three is normally adopted for the calculation.

§ 6. OVERLOADS EMERGING IN PENETRATION

The concept of the overload coefficient, which is widely familiar in practical calculation work and in the design of the widest variety of engineering structures and objects, is often introduced for practical calculations of the process of penetration and especially in calculation of the penetrating bodies themselves (the ammunition) for strength.

To define the overload coefficient (n) - it is the ratio of the resistance force F acting on the body in penetration to the weight G of the penetrating body:

$$n = \frac{F}{G}$$

or

$$n = \frac{j}{g},$$

where j is the acceleration which the body undergoes in the process of penetration; g is the acceleration of gravity.

The overload coefficient n obviously depends in general on the time of movement of the body in the ground. However, in order to establish the character of this dependence, one must know the law of variation of the force of resistance in regard to time, $F=F(t)$.

Experimental determination of the dependence $F(t)$ presents considerable difficulties. The method of determination of the dependence $F(t)$ by double differentiation of the law of movement of the body $y=y(t)$ obtained experimentally results in substantial errors, as a rule. The use of the calculation relationships considered above for obtaining the dependence $F(t)$ is also extremely rough and awkward. Due to the indicated circumstances, certain fixed values of the overload coefficient - the average overload coefficient n_{cp} and the maximum overload coefficient n_{max} - are used in practical calculations.

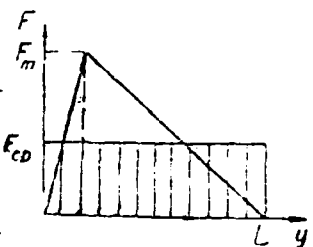


Fig. 4.24.

In determining the average overload coefficient, we proceed from the assumption that the force of resistance of the ground is constant throughout the penetration path and is equal to some average value F_{cp} (Fig. 4.24). It is assumed further that the kinetic energy of the penetrating body is spent completely on the work of this average force of resistance on the total penetration path:

$$F_{cp} L = \frac{G v_e^2}{2g},$$

hence

$$F_{cp} = \frac{G v_e^2}{2g L},$$

where L is the total penetration depth, determined by the Berezan' formula, for example.

With a knowledge of F_{cp} , it is easy to determine the value of the average overload coefficient:

$$n_{cp} = \frac{v_e^2}{2g L}. \quad (4.31)$$

In determining the maximum overload coefficient, we assume that the force of resistance of the medium varies depending on the penetration path according to a triangle law (Fig. 4.24). It is obvious then that $F_m = 2F_{cp}$ and $n_m = 2n_{cp}$; i.e., the maximum overload coefficient is as follows:

$$n_m = \frac{v_e^2}{gL}. \quad (4.32)$$

Calculation of ammunition for strength in penetration is normally performed in regard to the maximum overload coefficient.

As a result of special experimental and theoretical research, an approximate dependence of n_m on certain penetration characteristics of aerial bombs has been established:

$$n_m = \frac{608 \cdot 10^{-4}}{k_n} \frac{\pi d^3}{4hG} v_c^2, \quad (4.33)$$

where k_n is the penetration coefficient; d is the diameter of the aerial bomb; h is the height of the nose section of the aerial bomb; G is the weight of the aerial bomb; v_c is the velocity of impact of the aerial bomb against the surface of the obstacle.

Features of determination of the overload coefficient in piercing of armor are considered in an examination of the phenomenon of the armor-piercing effect of ammunition.

§ 7. THE ARMOR-PIERCING EFFECT

Piercing of armor or the armor-piercing effect is a special case of the phenomenon of penetration. Setting apart of this case is explained by the specific properties of armor, primarily its strength. The high strength of armor prompts the need for providing a high velocity and special strength of ammunition intended for action against armor and also for envisaging measures for combatting ricochet phenomenon.

The armor-piercing effect of ammunition has been studied for a comparatively long time, and many studies of both domestic and foreign researchers are well known.

Due to the great complexity of the phenomenon, mainly empirical and semiempirical formulas are used for practical calculations, as in the case of penetration into the ground. These formulas were obtained either based on the two-member law of resistance considered

above or based on a law expressing the exponential dependence of the force of resistance on the velocity of movement of the body.

For example, the empirical formula which is most popular in calculation of the armor-piercing effect was obtained based on a resistance law of the type of (4.15), which can also be presented in the form

$$F = k_1 \frac{\pi d^2}{4} \left(\frac{b}{d}\right)^n . \quad (4.34)$$

where d is the diameter of the piercing body, and b is the thickness of the armor being pierced.

The initial relationship for obtaining the necessary calculation dependences for the armor-piercing process has the following form:

$$a \frac{G v_c^2}{2g} = \int_0^y F(y) dy. \quad (4.35)$$

In its physical nature, this relationship expresses a law of the preservation of energy: the kinetic energy of the piercing body is spent for accomplishing work against forces of resistance of the armor in the piercing path. The coefficient $a < 1$ takes into consideration energy losses for processes which accompany the piercing phenomenon.

Assume that the thickness of the armor being pierced is equal to b ; then, assuming that the force of resistance F determined by expression (4.34) remains constant throughout the piercing path, the relationship (4.35) can be written in the form

$$\begin{aligned} a \frac{G v_c^2}{2g} &= k_1 \frac{\pi d^2}{4} \left(\frac{b}{d}\right)^n b \\ \text{or} \\ v_c &= K \frac{b^{\frac{1+n}{2}} d^{\frac{2-n}{2}}}{G^{1/2}}, \end{aligned} \quad (4.36)$$

where

$$K = \sqrt{\frac{\pi g k_1}{2a}}.$$

Extensive experimental data indicates that the best coincidence of calculation and experimental data occurs with $n=1/2$ and a decrease in the exponent at b from 0.75 to 0.70. In this case, the formula takes on the following form:

$$v_c = K \frac{d^{0.75} b^{0.7}}{G^{0.5}}$$

If the axis of symmetry of the piercing body at the moment of impact with the armor surface forms some angle θ_c with this surface, the formula for determining the necessary impact velocity v_c at which the body in question is capable of piercing armor with a thickness b will be written in the form

$$v_c = K \frac{d^{0.75} b^{0.7}}{G^{0.5} \sin \theta_c} \quad (4.37)$$

or

$$b = \frac{G^{0.75}}{\pi} \left(\frac{v_c \sin \theta_c}{K} \right)^{1.43}$$

where v_c is the impact velocity in m/s; d is the diameter of the body in decimeters; b is the thickness of the armor being pierced in decimeters; G is the weight of the body in kg; K is a coefficient characterizing the properties of the armor.

Formula (4.37) is known as the Zhakov-DeMarr [as transliterated] formula. Some calculation formulas obtained based on the two-member law of resistance, adopted in the following form, are also well known:

$$F = S(a_0 + b_0 v^2). \quad (4.38)$$

The physical significance of the coefficients in expression

(4.38) has been refined based on appropriate research with the use of modern experimental equipment (x-ray pulse devices and high-speed photography). It was established in this way that for steel armor, a_0 can be equal to the dynamic hardness, the dynamic yield limit or the conditional yield limit multiplied by some expression obtained from solution of the problem of pressing of an absolutely hard body into a plastic medium. It is recommended that a value of a_0 equal to the cubic strength of reinforced concrete be selected for reinforced concrete.

A value of the coefficient b_0 equal to the product of the density of the material of the obstacle being pierced and a coefficient of the shape of the nose section of the piercing body is adopted.

For determining the maximum overload coefficient n_m in piercing of armor, the force of resistance of the armor is assumed to be a constant value F_m .

In this case, $\frac{Gv_e^2}{2g} = F_m(b+h)$, where h is the length of the nose section of the body (bomb), and the armor is considered to be pierced if the nose section of the body emerges beyond the back side of the armor plate, and the value of n_m is as follows:

$$n_m = \frac{v_e^2}{2g(b+h)} . \quad (4.39)$$

In calculation of the overload coefficient by this formula, it is necessary to select the velocity necessary for piercing of the armor, determined according to formula (4.37), as the velocity v_c .

Therefore, based on analysis of the physical nature of the phenomenon and corresponding experimental data, one can conclude that the effect of armor piercing depends on the following: the

properties of the armor; the strength and shape of the nose section of the piercing body; the angle of impact and the impact velocity at the moment of impact. Special armor steel appeared only at the end of the last century (1886). Iron plates were used as protection up to that time, since ordinary steel did not possess sufficient toughness, was too brittle and split easily. Special steels came into use for armor protection beginning in 1890.

Modern armor can be divided into two types:

- homogeneous armor;
- heterogeneous armor.

Homogeneous armor, or uniform armor, is armor whose strength properties are the same over the entire thickness. Armor of this type is normally used for protecting ships and tanks.

Heterogeneous armor, or nonuniform armor, has a layered structure. The face layer (cemented) makes up from 15 to 40% of the overall thickness of the armor and is very strong, but brittle. The second layer possesses increased toughness. The combination of these two layers gives the armor special stability and requires increased strength from the nose section of the piercing body. Armor of this type is used for protecting the most vulnerable points of aircraft and especially important objects on tanks, ships and submarines.

The strength of heterogeneous armor is higher than that of homogeneous armor. The value of the coefficient K in formula (4.37) is 1600-2000 for homogeneous armor (low hardness); K=2000-3000 for heterogeneous armor (medium and high hardness).

The deformation of armor of low and high hardness in piercing is different.

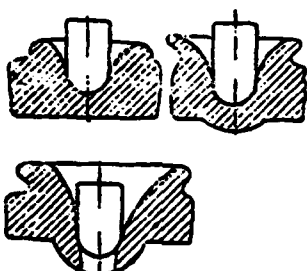


Fig. 4.25.

Armor of low hardness (the diameter of the indentation in testing for hardness $d_B = 3.7-4.1$) undergoes deformation by a unique puncture (Fig. 4.25). A swelling is formed on the face surface of the armor and then grows larger. A bulge emerges on the back side which bursts in further movement of the body. The main form of deformation is radial compression and bending. Deformation of armor of medium hardness ($d_B = 3.3-3.6$) occurs by shearing and ends in formation of a plug which is driven out by the penetrating body (Fig. 4.26).

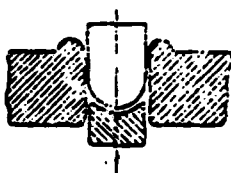


Fig. 4.26.

Deformation of armor of high hardness is normally accompanied by splitting off from both the face and rear surfaces, and a plug is formed by shearing (Fig. 4.27).

The nose section of the body plays a special role in the matter of piercing of armor (especially in piercing of homogeneous armor). Designs of armor-piercing ammunition with both sharp and blunted

nose sections are familiar. Ammunition with a sharpened nose section pierces homogeneous armor well, while ammunition with a blunted nose section pierces heterogeneous armor better.

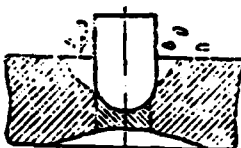


Fig. 4.27.

In impact against armor, enormous stresses emerge reaching values of the order of $25,000\text{-}30,000 \text{ kg/cm}^2$; therefore, special measures are taken for protecting the shells of armor-piercing ammunition against damage. Armor-piercing caps (first proposed by Admiral S. O. Makarov) are used for this purpose. The caps are manufactured from a material stronger than the shell of the ammunition. The purpose of the cap is to pierce the cemented face layer of the armor and to break up in the process, thus protecting the shell against damage.

Another method for protection of the ammunition shell against destruction is also familiar. Special cuts are made on the nose section of the shell. In impact against armor, stresses are concentrated on these cuts, and local compression and partial destruction of the nose section occur, but the integrity and strength of the shell are preserved.

Table 4.5 presents some data on tests of armor plates with a thickness of 200 mm by firing with shells with a caliber of 191 mm. The minimum velocity v_{\min} which is necessary for piercing armor of the thickness in question with a shell of the caliber in question was adopted as the measure of the strength of the armor.

Table 4.5. Values of the minimum velocity necessary for piercing armor.

(1) Род брони	(2) v_{\min} , м/сек
(3) Железная плита (техническое железо)	365
(4) Гомогенная броня (обыкновенная углеродистая сталь)	471
(5) Гетерогенная броня (без специальной термообработки)	612
(6) То же, с термообработкой	700

Key: (1) type of armor; (2) m/s; (3) iron plate (technical grade iron); (4) homogeneous armor (ordinary carbon steel); (5) heterogeneous armor (without special heat treatment); (6) the same, with heat treatment.

The angle of impact of the piercing body with the armor surface has a substantial influence on the armor-piercing effect: the smaller the impact angle (θ_c), the lower the thickness of the armor which can be pierced.

In connection with this, one must dwell on certain features of the armor-piercing effect in regard to the structure of an airplane. Armor, or another sufficiently strong obstacle, located on an airplane is normally shielded by the skin of the airplane. As special research demonstrates, a thin screen located in front of the main obstacle (the armor) can result in sharp worsening of the armor-piercing effect of ammunition. The physical nature of the indicated effect of a screen lies in the following. As we know, a projectile in flight undergoes nutational oscillations and has some nutation angle in contact with the screen. Due to the presence of the nutation angle, asymmetry of the impulses of forces of resistance of the screen develops. Before the moment of passage of the center of gravity of the projectile through the screen, a destabilizing moment will emerge which strives to increase the nutation angle. After passage of the center of gravity of the

projectile through the screen, a moment of an opposite sign will appear. A thin but sufficiently strong screen thus causes a peculiar "rolling" of the projectile, which leads to an increase in the angular velocity of nutation. As a result, the probability that the projectile will approach the main obstacle with a large nutation angle increases. The latter circumstance leads both to a decrease in the thickness of armor which can be pierced and to the emergence of the ricochet phenomenon.

§ 8. PENETRATION AT HIGH IMPACT VELOCITIES

The formulas considered above for calculating the depth of penetration into solid media and for calculating the thickness of armor which can be pierced make it possible to calculate corresponding characteristics of the percussion effect of ammunition at velocities of impact of the ammunition with the surface of an obstacle of the order of 1000-1200 m/s, i.e., at so-called artillery impact velocities. This is related to the fact that it is assumed in derivation of these calculation formulas that the penetrating body does not undergo deformation.

With an increase in the impact velocity, deformation occurs not only in the obstacle but in the penetrating body, and the formulas presented above produce an overstated result.

Therefore, with a collision at high velocities, one must take into consideration both the deformation of the obstacle and the deformation of the penetrating body itself. The generally accepted theory of penetration and piercing at high velocities at present is the hydrodynamic theory of penetration. This theory, as demonstrated in Chapter 5, was developed with respect to the armor-piercing effect of shaped charges. The bases of this theory are considered in detail in analysis of the shaped-charge effect of ammunition. According to the hydrodynamic theory of penetration,

the basic formula for calculating the depth of penetration (L) has the form

$$L = L_c \sqrt{\frac{\rho_c}{\rho_n}}, \quad (4.40)$$

where L_c is the length of the penetrating body; ρ_c is the density of the penetrating body; ρ_n is the density of the obstacle being pierced.

It is assumed in derivation of formula (4.40) that the process of penetration ends at the moment of complete consumption of the penetrating body (the hollow-charge jet), the material of which spreads over the surface of the cavity formed in the medium being pierced.

In reality, however, the process of deepening of the hole does not end after complete consumption (wearing away) of the penetrating body. This circumstance has particular importance in a case of penetration at a high velocity of a body possessing a sufficiently large mass as compared to the mass of the metallic hollow-charge jet.

After complete (wearing away) of the penetrating body, the material of the medium (the obstacle), possessing a definite flow velocity, continues movement by inertia. This leads to an increase in the dimensions of the hole in both axial and radial directions. This stage, essentially the second stage of penetration at high velocities, is called the aftereffect or afterflow of material of the medium (the obstacle). The strength of the obstacle plays an essential role in this stage.

M. A. Lavrent'yev has proposed the following correction to the basic formula for calculating the depth of penetration (L) for accounting for the aftereffect phenomenon in penetration at high impact velocities:

$$\Delta L = a \left(\frac{\rho_n v_c^2}{\sigma_{yII}} \right)^{1/3},$$

where a is a constant coefficient, the value of which is near one; σ_{yII} is the yield limit of the obstacle material ($\sigma_{yII} = 20-30$ kg/mm² for normal steel).

It is obvious that the hydrodynamic theory of penetration at high impact velocities has well-known limits of applicability in regard to its physical nature. It should be noted first of all, that the hydrodynamic theory of penetration is applicable for penetrating bodies with a comparatively great relative elongation. This is explained by the fact that the process of penetration is identified with the penetration of a metallic liquid stream into a liquid medium. This analogy is valid only beginning from the moment when the penetrating body has gone into the obstacle by a distance of twice its diameter (two calibers), when the mass of the obstacle drawn into motion is sufficiently great, i.e., when the process of penetration becomes stationary. The bottom limit of velocities at which the hydrodynamic theory of penetration is applicable can be evaluated from the condition that the dynamic resistance of the material of the medium (the obstacle) significantly exceeds the static resistance.

The value of the pressure (p_n) at the interface between the penetrating body and the obstacle is as follows:

$$p_n = \frac{\rho_n v_n^2}{2},$$

where ρ_n is the density of the obstacle material, and v_n is the velocity of movement of the "penetrating body-obstacle" boundary.

The value of the velocity v_n is determined by the formula (see Chapter 5)

$$v_n = \frac{v_c}{1 + \sqrt{\frac{\rho_n}{\rho_c}}}.$$

where v_c is the velocity of impact of the penetrating body with the surface of the obstacle; ρ_{II} is the density of the obstacle material; ρ_c is the density of the penetrating body.

If the yield limit of the obstacle material (σ_{II}) is adopted as the measure of static resistance of the obstacle, the condition for determining the bottom velocity limit at which the hydrodynamic theory of penetration is applicable will be written in the following form:

$$\frac{\rho_n v_c^2}{2 \left(1 + \sqrt{\frac{\rho_n}{\rho_c}} \right)^2} = A \sigma_{II}$$

Assuming that the realization of this condition will be complete (with consideration for the assumptions which have been made) in a case where the dynamic resistance of the medium is two orders higher than the static resistance, i.e., $A=100$, and assuming, for an example, that $\rho_{II}=\rho_c$ for steel of medium strength ($\sigma_{II}=20 \text{ kg/mm}^2$), we obtain

$$v_c \approx 4000 \text{ m/s.}$$

Experience indicates that the hydrodynamic theory of penetration is applicable beginning at impact velocities at 3000-4000 m/s. Figure 4.28 shows holes (craters) formed by a duralumin projectile with a weight of 8 grams in massive obstacles: lead (Fig. 4.28, a), duralumin (Fig. 4.28, b) and titanium (Fig. 4.28, c) obstacles, at an impact velocity of the order of 4000 m/s. The velocity was imparted to the projectile by means of a light gas unit (a helium gun); the relative dimensions of the projectile are shown schematically in Fig. 4.28. The top velocity limit at which the hydrodynamic theory of penetration is valid is determined by the fact that adiabatic compression of the material of the penetrating body and the obstacle occurs at superhigh impact velocities, and considerable heating up of the material, rapid evaporation and, as a result, an explosion emerge in adiabatic compression.

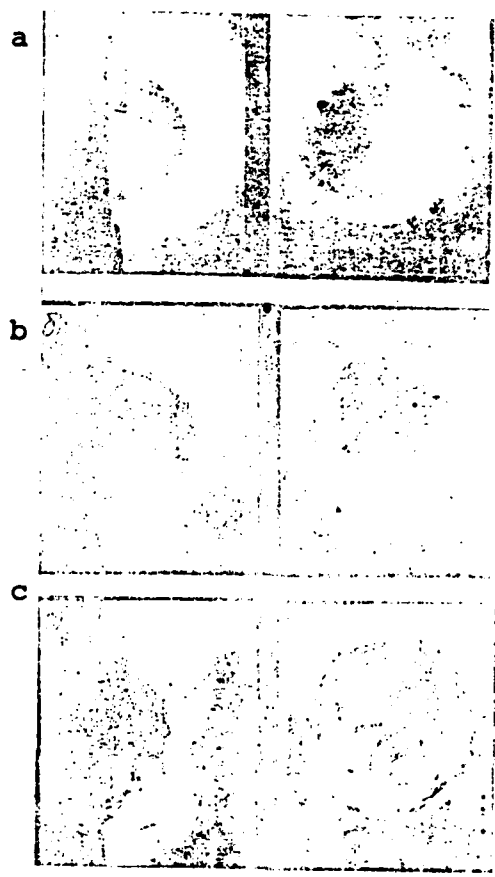


Fig. 4.28.

The depth of the hole formed in this case is determined by calculation of the effect of an explosion on the surface of the obstacle. The top velocity limit for penetrating body and obstacle materials normally used is estimated as a value of the order of 8-10 km/s.

Therefore, one can assume that the hydrodynamic theory of piercing is valid in a range of velocities from 3 to 10 km/s. This range of velocities naturally is provisional to a certain degree and can be refined for specific combinations of properties

of the colliding body and the medium (the obstacle). However, it is quite obvious that it is necessary to take into consideration the strength properties of the materials of the penetrating body and the obstacle in the vicinity of the bottom velocity boundary. Accounting for the compressibility (consideration of the process of emergence and propagation of shock waves) of the materials of the penetrating body and the medium (the obstacle) is essential in the vicinity of the top boundary. Study of the percussion effect at velocities of the order of 5000 m/s or higher recently has aroused special interest in connection with the problem of defense against missiles and space weapons and also in connection with solution of urgent problems of destruction and protection of hypersonic, orbital and space flying vehicles.

Investigation of the phenomenon of high-speed impact under laboratory and range conditions is taking on great importance.

Various methods for obtaining high launching velocities of compact solid bodies or definite amounts of matter in the form of plasma formations and streams under these conditions are well known. High velocities for projecting matter can be obtained by explosive methods (special shaped charges and accelerators); by so-called light gas devices (helium and hydrogen guns); by means of electrical and electromagnetic accelerators; and, finally, by means of specially designed installations with lasers.

§ 9. RICOCHETING OF AMMUNITION

Accounting for the effect of the phenomenon of ricochetting emerging in impact of ammunition against the surface of a medium (an obstacle) is extremely important in evaluating the efficiency of the percussion effect of ammunition. During the initial period of penetration of the body (bomb, projectile) into the obstacle, forces of resistance of the obstacle act on it; the resultant of these forces is applied in front of the center of

gravity (Fig. 4.29). The following designations are used in Fig. 4.29: \bar{F} is the resultant of forces of resistance of the obstacle; \bar{F}_{tp} is the force of friction of the body against the surface of the obstacle; \bar{v} is the direction of the vector of the velocity of the body at the moment of impact with the obstacle; δ is the angle of attack; θ_c is the impact angle of the body with the obstacle.

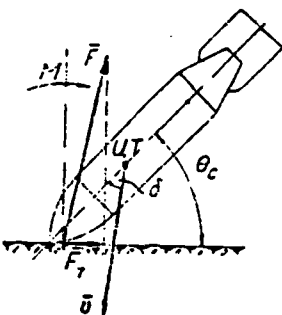


Fig. 4.29.

The resultant of forces of resistance of the obstacle does not coincide with a perpendicular to the surface of the obstacle. It is rotated by some angle, the value of which is determined by the action of the force of friction of the body against the surface of the obstacle. Since the line of the effect \bar{F} passes to the left of the center of gravity, a moment M emerges which strives to turn the body in the direction of an increase in the angle of attack (a decrease in the impact angle) - the phenomenon of denormalization develops. The magnitude and direction of the moment M depend on the values of the impact angle, the angle attack, the shape of the nose section of the body and the magnitude of the friction force at the initial moment of impact.

For example, if the penetrating body has a blunted nose section, and the value of the friction force reaches comparatively large values (Fig. 4.30), the resultant of forces of resistance of the obstacle can be turned in such a way that the moment which develops will tend to increase the angle of impact of the body with the

surface of the obstacle. The so-called normalization phenomenon develops.

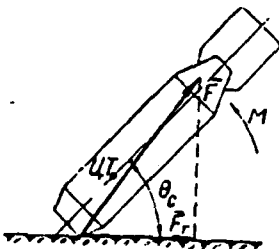


Fig. 4.30.

The denormalizing moment which emerges at low impact angles can be so great that a positive angle of attack will always be created in penetration of the nose section of the body into the obstacle (the vector of the velocity of movement of the projectile will be located under the axis of the body). As a result, the body will turn and tend to go away from the obstacle. If the body (aerial bomb, projectile) possesses sufficient kinetic energy, the ricochet phenomenon sets in - the body rebounds from the surface of the obstacle with some loss in velocity.

It is obvious that for the conditions in question for collision of a body with an obstacle, there is some limit value of the impact angle $\theta_i = \theta_{np}$, at which the ricochet phenomenon sets in. The possibility of the development of a ricochet is judged according to the magnitude of this limit angle. Table 4.6 presents values of θ_{np} for some obstacles and ammunition of a normal shape.

In a case of transition of the body into ricochetting conditions, the ricochet process can be a repeated process. For example, cases of repeated ricochetting have been established in bombing with high-explosive aviation bombs, where the bomb rebounded several

times at a distance of 300 meters or more in 8-10 s.

654

Table 4.6. Value of the limit angle
for ricochetting

(1) Elongated	α_{lim}
(2) water surface	4-10
(4) (3) hard ground	10-12
deport's report	12-15
(5) armor-concrete	10-15

Key: (1) obstacle; (2) water surface;
(3) soft ground; (4) hard ground; (5)
armor-concrete.

We shall consider the theoretical grounds for quantitative description of the ricochet phenomenon.

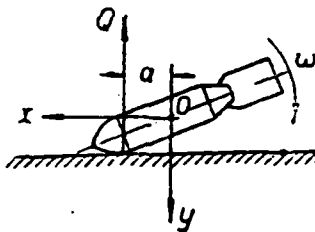


Fig. 4.31.

Assume that some body (aerial bomb, projectile) strikes an obstacle at a low impact angle (Fig. 4.31). The velocity of the center of gravity of the body at the moment of impact is v_c . The system of coordinates is shown in Fig. 4.31. In impact of the body against the surface of the obstacle, some force $F(t)$ which varies in time acts on the body for a very short time interval Δt and imparts considerable acceleration to the body. Since the force and the acceleration are variables, the intensity of interaction of the body with the obstacle can be characterized more

conveniently not by the force but by its impulse for the time Δt . This impulse is sometimes called the "impact force" and is determined by the formula

$$Q = \int F(t) dt.$$

It is normally assumed that the direction of impact is perpendicular to the general collision plane. Then the "impact force" Q will also be directed along a perpendicular to the obstacle surface, and some impulse moment will be created in impact as follows:

$$M = aQ,$$

where a is the arm of the "impact force" in relation to the center of gravity of the body.

The angular velocity of rotation of the body caused by this moment will be as follows:

$$\omega = \frac{M}{A} = \frac{aQ}{A}, \quad (4.41)$$

where A is the equatorial moment of inertia of the colliding body.

We shall designate components of the velocity of the center of gravity of the body as follows: before impact, v_x and v_y ; after impact, v'_x and v'_y . Based on the law of the preservation of momentum, we can write the following:

$$\left. \begin{aligned} \frac{G}{g} (v_x - v'_x) &= 0 \\ \frac{G}{g} (v_y - v'_y) &= Q \end{aligned} \right\} \quad (4.42)$$

where G is the weight of the body, and g is the acceleration of gravity.

From expressions (4.41) and (4.42), we find an expression for determining the angular velocity ω of rotation of the body around the center of gravity caused by impact against the obstacle:

$$\epsilon = \frac{aG}{gA} (v_y - v_y'). \quad (4.43)$$

Experimental determination of all the necessary characteristics of the process of impact of a body on the surface of an obstacle - the restitution coefficient, the "impact force" and the angular velocity of movement of the body in relation to the center of gravity - can be accomplished based on this relationship. Therefore, the development of a ricochet depends on many factors: the shape of the nose section and the position of the center of gravity of the body, the impact angle and the relative velocity at the moment of impact, the properties of the obstacle, etc. The ricochet phenomenon either can be harmful or can be used for enhancing the efficiency of destruction of targets, depending on the character of the combat use of the ammunition.

Ricochet of ammunition is harmful, for example, when firing or bombing is being conducted on armored or concrete targets and in firing on modern airplanes with percussion shells. The strength of the ammunition shells often is impaired in "glancing" impact of the ammunition, normal operation of the fuses is disrupted, and breaking off of the fuses occurs.

Methods for using the ricochet phenomenon for enhancing the efficiency of disruption of targets are well known: for example, firing on personnel sheltered in trenches with artillery shells, so-called "ricochet fire." A fuse delay such that explosion of the shell occurs above the shelter after rebound of the shell from the surface of the ground is selected. The so-called masthead method for bombing ships of a naval fleet was used during the Second World War. The attacking airplane flew over the target at the height of the "masthead lamp" of the ship and released the bomb so as to effect a ricochet from the surface of the water. The bomb hit the target after skipping off the water.

Various measures are used for combatting the ricochet

phenomenon:

- the center of gravity of the ammunition is shifted forward;
- special pins, prongs or projections are made on the nose section of the ammunition;
- the nose section of the ammunition is made flat;
- parachutes are used in some cases for forced normalization of the ammunition just before the moment of impact.

However, the measures presented, as a rule, involve a decrease in the depth of penetration of the ammunition.

In conclusion of the consideration of the percussion effect of ammunition, one should mention some prospects for increasing the depth of penetration. A noticeable increase in the depth of penetration into the ground can be achieved by using ammunition with a special auxiliary jet engine. The distinguishing feature of the use of the jet engine in this case is the fact that the engine is put into operation after impact on the obstacle and operates in movement of the ammunition in the ground, imparting additional energy to the penetrating body.

CHAPTER 5

THE SHAPED-CHARGE EFFECT OF AMMUNITION

Strengthening of the destructive effect in a definite direction conditioned by a special shape of the charge - the presence of a recess in it, the so-called hollow-charge recess - is called the shaped-charge effect, or accumulation, in explosion of an explosive charge. Of the different methods for controlling the effect of an explosion, accumulation occupies a special place as one of the basic forms of directed action of an explosion, which has received the most extensive practical use in designs of aviation ammunition.

The phenomenon of accumulation in the effect of an explosion was discovered as early as 1864 by the Russian artilleryman Boreskov, who discovered in working with mines that charges of nitroglycerin with a recess possess a significantly higher destructive effect than ordinary charges in the direction of this recess.

In 1865, Captain Andriyevskiy, in working together with N. N. Zinin, proved the possibility of a significant strengthening of the effect of a nitroglycerin detonator in the presence of a hollow in it in the form of a conical recess.

The shaped-charge effect was observed by Foerster in 1883,

and Monroe worked on studying the effect of hollow charges in 1888.

The first systematic research on the phenomenon of accumulation with the creation of the first series of sapper shaped charges was conducted in 1923-1926 under the direction of M. A. Sukharevskiy at the NII KA [Red Army Scientific Research Institute]. Based on experimental research, he established the dependence of the piercing effect of shaped charges on the geometric parameters of the charge and the recess. Despite the fact that the phenomenon of accumulation was well known for many years, it did not receive extensive practical use for a long time mainly as a result of the absence of strong (armored) targets in massive numbers.

Shaped-charged ammunition received extensive use for the first time as a combat resource during the Second World War. The use of such strong, low-vulnerability targets as tanks, armored vehicles, etc., in mass numbers on battlefields prompted the development and adoption of mass means for effective destruction of these targets. Ammunition with a shaped-charge effect - antitank aviation bombs, antitank grenades, shaped-charge artillery shells and other shaped-charge weapons - prove to be one of the most effective weapons for destroying the indicated targets. For example, antitank aviation bombs (PTAB) developed in 1943 by designer I. A. Larionov played an extremely large role in destruction of the fascist tank hordes in a historic battle near Belgorod and Kursk during the Great Patriotic War. From this moment until the end of the war, Soviet aviation, as the sole possessor of shaped-charge antitank aerial bombs, used more than 9 million of them.

Shaped-charge ammunition (charges) are finding more and more extensive use in the national economy, such as in oil production.

Serious theoretical and experimental research on accumulation also began to be conducted during the Second World War. The

most important research is that of M. A. Lavrent'yev, G. I. Pokrovskiy, F. A. Baum and their co-workers. Research was also being carried on at the same time by foreign researchers, especially Taylor.

§ 1. THE NATURE OF THE SHAPED-CHARGE EFFECT OF AN EXPLOSION

Chapter 2 pointed out that the effect of an explosion near the charge depends on the shape of the charge. Figure 5.1 shows a diagram of the effect of charges with different shapes of the face section adjoining the obstacle in relation to a steel obstacle. Figure 5.1, a, shows the effect of the action of a charge which has no recess on the steel obstacle - the effect was exhibited in the form of a comparatively shallow depression. The effect on the obstacle of a charge equipped with a recess in the face section adjoining the obstacle is shown in Fig. 5.1, b.

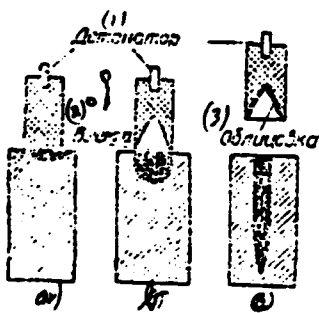


Fig. 5.1.
Key: (1) detonator; (2) recess;
(3) lining.

The effect of the charge in this case proves to be stronger, despite the fact that the charge weight is reduced (due to removal of explosive from the recess cavity), and the greater part of the explosive mass adjoining the obstacle is withdrawn from the surface of the obstacle.

Figure 5.1, c, shows the result of the action of a charge whose recess has a thin metal lining on a steel obstacle for comparison. The effect of directed action of such a charge is exhibited even more clearly, and a deep hollow with a somewhat smaller diameter than the diameter of the depressions in the first two cases but with a significantly greater depth is formed in the obstacle. The increase in the directed nature of the effect of such a charge proves all the more paradoxical as the explosive of the fact section of the charge is separated from the obstacle by a metallic lining (although the lining is comparatively thin), and the charge itself, as shown in the diagram, is withdrawn for some distance from the obstacle.

We shall consider the physical nature of the processes which determine the features noted for the effects of charges with shaped-charge recesses in greater detail.

As one can see from the diagram shown in Fig. 5.1, shaped charges can be of two types: charges which have no lining of the shaped-charge recess, and charges with a lining of the shaped-charge recess. First of all, we shall consider the phenomenon of accumulation in explosion of a charge which has no lining of the shaped-charge recess.

Accumulation in Explosion of a Charge with No Lining of the Shaped-Charge Recess

Chapter 2 (§6) demonstrated that the scattering of detonation products from the surface of the charge occurs in directions near a perpendicular to the surface of the charge in the scattering zone. Figure 5.2 shows the direction of scattering of detonation products from the surface of a charge (at point A). The following designations are used in the diagram: u_1 is the velocity of movement of particles behind the detonation wave front; c_1 is the velocity of sound behind the detonation wave front; U is the velocity of scattering of detonation products from the charge surface. It is

obvious that flows of detonation products scattered from the surface of the shaped-charge recess after detonation of the charge will be directed toward the axis of the charge (in the case of a recess of a conical shape) or toward some center (in the case of a spherical recess), as shown schematically in Fig. 5.3. Converging streams of gaseous detonation products collide and form a very powerful gas flow directed along the charge axis. The density of the detonation products increases sharply in proportion to the convergence of the flow of detonation products, and the pressure and temperature in the gaseous stream which has been formed simultaneously increase sharply; the stream is called the hollow-charge jet. As a result of compression of the detonation products around the axis of the hollow-charge jet and the creation of a zone of very high pressure, part of the mass of the gaseous detonation products is pushed out (displaced) forward at an extremely high velocity. The pressure in the jet reaches a million atmospheres, the temperature reaches 6-7 thousand degrees, and the velocity can reach values of the order of 20 thousand meters per second.

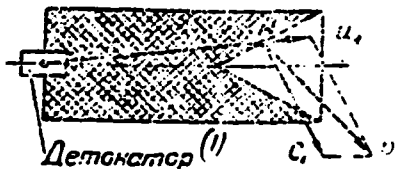


Fig. 5.2.
Key: (1) detonator.

The main parameters characterizing the state of the gases (pressure, density, velocity and temperature) thus reach increased values in the hollow-charge jet. And this explains the efficiency of the effect of the hollow-charge jet which is higher than a normal flow of explosion products.

A sharp pressure differential between the jet and the surrounding

medium develops after formation of the hollow-charge jet. This pressure differential leads to expansion of the jet in directions perpendicular to the direction of its movement. Consequently, the cross sections of the jet at different distances will be different in the process of formation and movement of the jet. It is obvious that a section in which the thickness (diameter) of the jet is minimal will be located at some distance from the charge, and the values of all the parameters of the flow of detonation products will be maximal. This minimum cross section of the jet, in which the greatest flow density and, consequently, the greatest concentration of energy in the jet will be located, is called the focus of the hollow-charge jet (the hollow-charge focus).

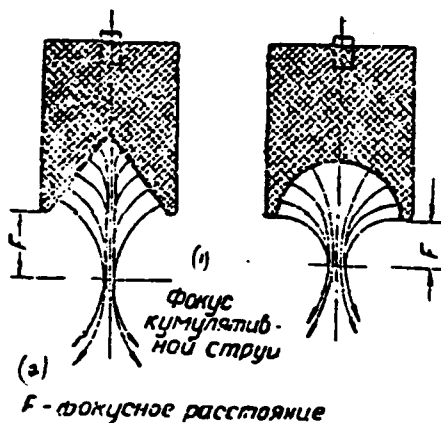


Fig. 5.3.
Key: (1) focus of hollow-charge jet;
(2) F - focal length.

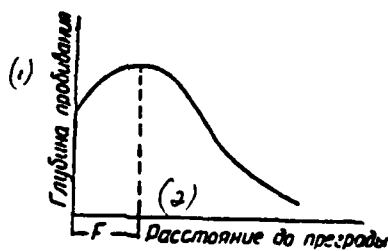


Fig. 5.4.
Key: (1) piercing depth; (2) distance to obstacle.

The distance from the base of the shaped-charge recess to the focus is called the focal length F (Fig. 5.3). In withdrawal of the shaped-charge recess from the base by a distance greater than the focal length, the hollow-charge jet disperses (degenerates) rapidly, since detonation products compressed in the jet undergo intense scattering to the sides as a result of the sharp pressure differential mentioned above.

The greatest effect of the hollow-charge jet (the piercing effect, for example) thus will occur when the shaped charge is located at the distance of the focal length from the obstacle (Fig. 5.4). The magnitude of the focal length with a given charge depends on the shape and dimensions of the shaped-charge recess. The deeper the shaped-charge recess and the greater the curvature of its surface, the more sharply the direction of movement of detonation products changes in formation of the hollow-charge jet, and the smaller the focal length of the charge. A shallower recess with less curvature of the surface is characteristic of longer-focus shaped charges. The shape of the shaped-charge recess can be conical, spherical, horn-shaped, etc. (Fig. 5.5).

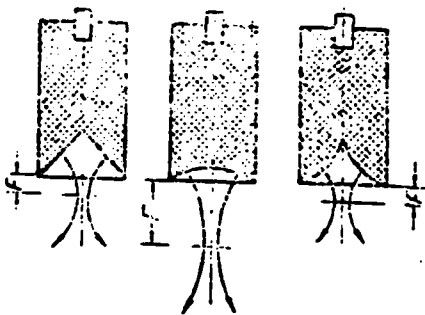


Fig. 5.5.

Since dispersion of the explosion products in explosion of a shaped charge, as in explosion of an ordinary charge, occurs over the entire charge surface, only part of the explosive which scatters

in the direction of the shaped-charge recess participates in formation of the hollow-charge jet. This part of the charge is called the active part of the charge or the directly accumulating part of the charge.

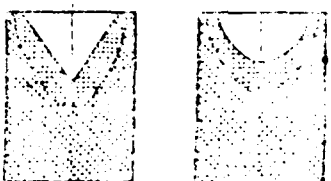


Fig. 5.6.

The shape and size of the active part of the charge with a given charge depend mainly on the shape and dimensions of the shaped-charge recess (Fig. 5.6). The size and shape of the active part of a shaped charge can be calculated approximately if one proceeds from a hypothesis of instantaneous detonation of the charge. The essence of this calculation, proposed by F. A. Baum, is reduced to the following. In a case of instantaneous detonation, rarefaction waves emerge simultaneously and proceed from all surfaces of the charge at the same velocity. This makes it possible to determine the shape of the contact surface of two rarefaction waves moving from two given surfaces of the charge, i.e., to define the boundary between parts of the charge which scatter after detonation in the direction of each of the charge surfaces under consideration, quite simply (Fig. 5.7).

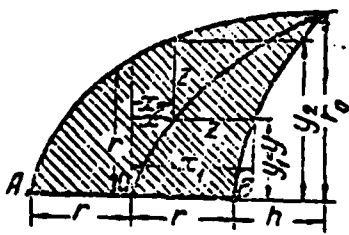


Fig. 5.7.

Assume that the equation of surface 1 has the form

$$y_1 = f_1(x_1).$$

The equation of surface 2 -

$$y_2 = f_2(x_2).$$

The desired equation of the boundary between parts of the charge scattering is different directions is written in the form

$$y = f(x).$$

It is easy to establish from plotting that

$$x = x_1 - z; \quad y = y_1; \quad x = x_2; \quad y = y_2 - z. \quad (5.1)$$

Eliminating z from these equations, we obtain

$$y - y_2 = x - x_1. \quad (5.2)$$

since

$$x = \varphi_1(y_1) \text{ and } y_1 = y.$$

and

$$y_2 = f_2(x_2) \text{ and } x = x_2.$$

the relationship (5.2) will take on the form

$$y + \varphi_1(y) = x + f_2(x). \quad (5.3)$$

This equation defines the desired contact surface of two rarefaction waves. It is obvious that the line $y=f(x)$ should be equidistant from lines $y_1=f_1(x_1)$ and $y_2=f_2(x_2)$. Theoretically it is easy to find the equation of this line. However, since the flow of detonation products disperses more slowly inside the recess than on the outside, a relatively large part of the detonation products accordingly will flow out from the outside. Therefore, the line $y=f(x)$ shifts closer to line $y_2=f_2(x_2)$. If the distance from the rear surface of the charge (Fig. 5.7) to point O is not less than the distance from point O to the peak of the recess ($AO > OB$), the line of contact of the rarefaction waves will be approximately the line of the interface of masses of explosion products scattering in different directions.

It is obvious that the volume of the active part of the charge w_a , i.e., the part moving in the direction of the shaped-charge recess, if one does not take into account shifts of the line $y=f(x)$

due to somewhat different conditions of flow of the detonation products from the outer and inner surfaces, will be determined from the relationship

$$w_s = \pi \int_0^{r_0} y^2 dx - \pi \int_0^{r_0} y_1^2 dx. \quad (5.4)$$

In this case, $y=y_1$ and $dx=dx_1+dy_1-dy_2$, as follows from formula (5.2).

Knowing that $x_1=\phi_1(y_1)$, we obtain

$$dx_1 = \frac{d\phi_1}{dy_1} dy_1,$$

then

$$w_s = \pi \int_0^{r_0} y_1^2 \left(dy_1 + \frac{d\phi_1}{dy_1} dy_1 + dy_2 \right) - \pi \int_0^{r_0} y_1^2 \frac{d\phi_1}{dy_1} dy_1,$$

or, after transformations

$$w_s = \frac{\pi r_0^3}{3} - \pi \int_0^{r_0} y_1^2 dy_2. \quad (5.5)$$

Then it is not difficult to find the dependence of y_2 on y_1 , since
 $y_1 = f_1(x_1)$ and $y_2 = f_2(x_2)$.

At the boundary of the active part, we have

$$x = \varphi_1(y_1) = \varphi_2(y_2),$$

from which

$$y_2 = \Phi(y_1).$$

Substituting this dependence into the formula (5.5), we obtain

$$w_s = \frac{\pi r_0^3}{3} - \pi \int_0^{r_0} y_1^2 \frac{d\Phi}{dy_1} dy_1. \quad (5.6)$$

For a special case of the cylindric charge, expression (5.3) takes on the form

$$y + z_1(y) = x + r_0$$

and the volume of the active part is determined by the formula

$$w_s = \frac{\pi r_0^3}{3}. \quad (5.7)$$

i.e., the volume of the active part in this case depends only on the diameter (caliber) of the charge. It is assumed in this case that the radius of the base of the recess is equal to the charge radius. A conclusion to the effect that the active part of the charge is reduced with a change in the diameter of the base of the recess follows from this. For obtaining a larger volume of the active part in a charge of a given diameter, one must make the diameter of the base of the recess as large as possible.

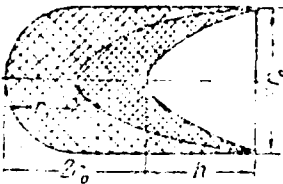


Fig. 5.8.

As an example, we shall consider a cylindric charge with a hemispherical rear section and a recess of arbitrary form (Fig. 5.8). The height of the charge is equal to $2r_0 + h$. The volume of such a charge is as follows:

$$\begin{aligned} w_0 &= \pi r_0^2 (r_0 + h) + \frac{2}{3} \pi r_0^3 - \pi \int_{y_1'}^{y_0} \frac{y_1^2 dy}{y_1'} = \\ &= \frac{5}{3} \pi r_0^3 + \pi r_0^2 h - \int_{y_1'}^{y_0} \frac{y_1^2 dy}{y_1'} . \end{aligned}$$

We shall determine the ratio of the charge volume to the volume of the active part as follows:

$$\frac{w_0}{w_a} = 5 + 3 \frac{h}{r_0} - \frac{3}{r_0^2} \int_0^{y_0} \frac{y_1^2 dy}{y_1'} ,$$

where

$$y_1' = \frac{dy_1}{dx} .$$

For a recess of conical form,

$$\pi \int_0^h \frac{y_1^2 dy}{y} = \pi r_0^3 h, w_0 = \frac{5}{3} \pi r_0^3 + \frac{2}{3} \pi r_0^3 h,$$

$$\frac{w_0}{w_a} = 5 + 2 \frac{h}{r_0}. \quad (5.8)$$

One can see from this that for real charges ($h=2r_0$),

$$\frac{w_0}{w_a} \approx 9$$

In other words, the mass of the active part of the charge in this case will amount to 11% of the mass of the entire charge. The charge shown in Fig. 5.8 has the minimum possible volume at which all of its computed active part is used.

In the case of a cylindric charge without a shaped-charge recess, but with a hemispherical rear section, the active part also will be as follows:

$$w_a = \frac{\pi}{3} r_0^3$$

The minimum volume of such a charge is as follows:

$$w_0 = \pi r_0^3 + \frac{2}{3} \pi r_0^3 = \frac{5}{3} \pi r_0^3.$$

The value $w_0/w_a = 5$, which can be obtained from formula (5.8), with the assumption $h=0$.

Accordingly, for a cylindric charge without curvature, we obtain

$$w_0 = 2\pi r_0^3 \quad \text{and} \quad \frac{w_0}{w_a} = 6.$$

As already noted, calculation of the volume of the active part of a charge was performed with the assumption of instantaneous detonation of the charge. K. P. Stanyukovich has investigated in detail the picture of propagation of rarefaction waves with consideration for a finite rate of detonation and has demonstrated that the relationships obtained with the assumption of instantaneous detonation can be used with an accuracy of less than 5% for calculations of the dimensions of the active parts of various charges in real detonation.

The calculations which have been performed make it possible to draw the following conclusions. The minimum charge height at which the active part of the charge reaches the maximum possible volume is as follows, in the case of a charge of a cylindric shape: $H_{np} = 2r_0 + h$. With a decrease in the charge length, the weight of the active part decreases more slowly than the weight of the entire charge. With an increase in the diameter of the base of the shaped-charge recess, the shaped-charge effect increases, since the volume of the active part increases in proportion to the cube of the charge radius.

By increasing the height of the charge H_3 and the diameter of the charge d_3 , with unchanged parameters of the shaped-charge recess, one can increase the volume w_a of the active part of the charge up to a definite limit (Fig. 5.9).

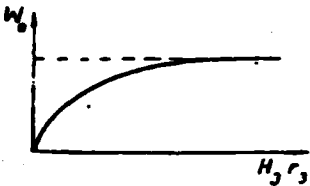


Fig. 5.9.

By more complex calculations, one can also determine approximately the active part of a charge in the presence of a side shell and metallic lining of the shaped-charge recess. One must keep in mind in this case that in the presence of a metallic lining of the recess, the active part of the charge can be larger than the directly accumulating part. We shall pass on to a consideration of the phenomenon of accumulation in explosion of a charge with lining of the shaped-charge recess.

Accumulation in Explosion of a Charge with Lining of the Shaped-Charge Recess

Extensive research indicates that the efficiency of the effect of a shaped charge increases to a very high degree if there is a metallic shell - a lining of the shaped-charge recess (Fig. 5.10) - inside the shaped-charge recess.



Fig. 5.10.

Key: (1) lining of shaped-charge recess.

Experimental and theoretical study of this phenomenon indicates that strengthening of the shaped-charge effect in the presence of lining of the shaped-charge recess is involved with a redistribution of energy between the explosion products and the metal of the lining and a transition of part of the lining metal into the hollow-charge jet.

The physical process of formation of the hollow-charge jet in the presence of a metallic lining differs substantially from the process of formation of the jet in explosion of a charge without a lining of the shaped-charge recess.

Modern experimental methods (pulsed x-ray photography, spark photography, etc.) and theoretical research have made it possible to obtain a sufficiently clear picture of the mechanism of formation of a hollow-charge jet in the presence of a metallic lining of the shaped-charge recess.

As a result of explosion of the charge, the detonation products

effect sharp compression of the metallic lining; the pressure of the detonation products in this process reaches a value of the order of 10^6 kg/cm². As a result of such sharp compression, where the pressure forces are immeasurably greater than the forces of toughness and internal friction and greatly exceed the ultimate strength of the lining material, the lining undergoes intense deformation, individual parts of the lining start to "flake" sharply, and a metallic hollow-charge jet possessing a high velocity, a high concentration of energy and a great piercing capability is "extracted" from them. Some intermediate stage of compression of the metallic lining of the shaped-charge recess and formation of the metallic hollow-charge jet is shown in Fig. 5.11.



Fig. 5.11.

Individual sequential stages of the process of formation of the hollow-charge jet are shown in Fig. 5.12, which was composed as a result of analysis of photographs obtained by means of pulsed x-ray photography. Figure 5.12, a, shows the beginning of compression of the peak of the lining of a conical shaped-charged recess by the detonation wave and detonation products. The detonation wave has reached the face section of the charge in Fig. 5.12, c and d. Under the effect of the pressure of the explosion, the lining begins to move toward the axis of the charge, and intensive compression and closing of the lining occur. In the process of this compression and closing, it is as if the lining is divided into two parts, which play quite different roles in the further development of the shaped-charge effect. A "rammer" (or "rod") is formed from the outer layers of the lining, and the greater part of the lining material passes into it. A metallic hollow-charge jet, possessing a significantly lower mass than the

"rammer," is formed from the inner layers of the lining. This metallic jet, moving at a very high velocity, determines the high efficiency of the effect (the piercing effect, for example) of a shaped charge with a lining of the shaped-charge recess.

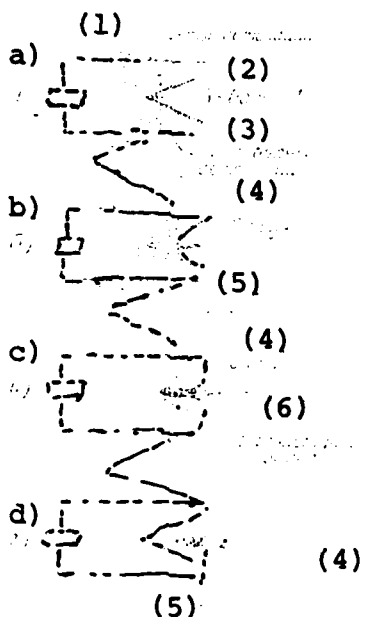


Fig. 5.12.

Key: (1) detonation products; (2) lining;
(3) detonation wave front; (4) jet; (5)
rammer; (6) ballistic wave.

As a result of the fact that the volumetric expansion coefficient of the metal is incomparably less than that of the gases, the metallic hollow-charge jet does not expand to the sides, does not become unbalanced and, consequently, is more stable than a gas hollow-charge jet formed in explosion of a charge which has no lining of the shaped-charge recess.

Since the concentration of energy in a metallic hollow-charge jet is substantially greater than in the hollow-charge jet of a charge without a lining, the efficiency of the effect of charges increases significantly in the presence of a metallic lining of

the shaped-charge recess. For example, the efficiency of the effect of a shaped charge with a lining of the shaped-charge recess exceeds the efficiency of the effect of a similar "charge" by a factor of 3-4 or more in explosion directly at the obstacle; this difference is still greater in a case of explosion at a distance from the obstacle. This explains the fact that all shaped-charge ammunition - shell, mines, bombs, etc. - contain a lining of the shaped-charge recess in their design.

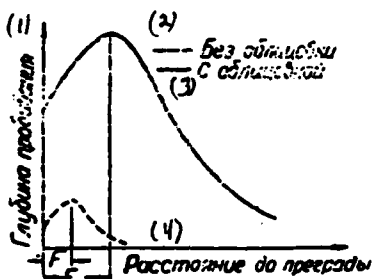


Fig. 5.13.

Key: (1) piercing depth; (2) without lining; (3) with lining; (4) distance to obstacle.

The piercing effect of a shaped charge with a lining increases to some limit in proportion to the distance from the obstacle, after which it drops (Fig. 5.13), similar to what occurred in explosion of a charge without a lining of the shaped-charge recess.

The optimum distance between the charge and the obstacle, at which the piercing effect reaches a maximum value, is called the focal length in this case as well.

However, the indicated analogy does not characterize similarity of the phenomena under consideration in regard to their physical nature. The difference in the mechanism of formation of the hollow-charge jet for the two types of charges also conditions a difference

of the causes which determine the character of variation of the shaped-charge effect in proportion to the distance of the charge from the obstacle which has been described above. For the case of a charge without a lining of the shaped-charge recess, such a character of the variation of the shaped-charge effect is explained, as was already demonstrated previously, by the fact that greater and greater compression of the hollow-charge jet, an increase in the energy concentration and an increase in the efficiency of the effect of the charge occur in proportion to the distance of the charge from the obstacle up to a certain distance (the focal length). With a further increase in the distance, a sharp expansion of the gas jet and a decrease in the efficiency of the effect of the charge set in.

In the case of a charge with a lining of the shaped-charge recess, the dependence of the piercing effect on the distance between the charge and the obstacle is explained in a different way.

It will be shown in greater detail later that the piercing effect of a metallic hollow-charge jet is proportionate to its length. And the length of the hollow-charge jet formed in compression of a metallic lining does not remain constant. There is a velocity gradient in regard to the length of the jet. Normally the leading section of the jet possesses a relatively great velocity, due to which the jet stretches out and becomes elongated in the process of formation in the first section of movement. The presence of the velocity gradient is conditioned by the structure of the shaped charge (Fig. 5.11) and the character of the effect of the explosive load on the lining of the shaped-charge recess.

Parts of the lining located nearer to the peak are not only involved in the process of deformation earlier than the peripheral parts of the lining (since the detonation wave reaches the peak of the lining earlier than its periphery); they also take on a

higher velocity as a result of the fact that a thicker layer of the explosive adjoins the peak of the lining. The effect of detonation products on elements of the lining located at the peak proves stronger, and these elements receive a larger specific impulse and undergo more intense compression. In closing of elements of the lining near the peak of the lining, the leading section of the hollow-charge jet is formed; in closing (flaking) of the peripheral parts (lying near the base of the lining), the tail section of the hollow-charge jet is formed. The leading section of the hollow-charge jet takes on a higher velocity than its tail section. Since the rate of stretching of the hollow-charge jet is very high, the material of the jet, rather than breaking up into individual parts, can take on an extremely great relative elongation. For example, steel, which has a relative elongation of the order of 25% at low stretching rates, can stretch by a factor of more than three in a hollow-charge jet. Features of the formation and movement of a hollow-charge jet which have been presented also determine the character of variation of the shaped-charge effect in proportion to the distance of the charge from the obstacle. At first, when the distances between the charge and the obstacle are small, the jet manages to stretch out more and become elongated in proportion to the increase in this distance before the moment of contact with the obstacle, and this, as already mentioned, increases the efficiency of its effect. However, when some critical elongation corresponding to the dynamic ultimate strength of the jet material is reached, further stretching leads to breaking up of the jet into separate parts and to dispersion of the jet, as a result of which the efficiency of the effect of the jet decreases substantially.

The distance corresponding to maximum efficiency of the effect of the jet is the focal length. As in the case of a charge without a lining of the recess, both the shape and the relative dimensions of the lining of the shaped-charge recess influence the size of the

focal length. Deep shaped-charge recesses with a lining possess a short focal length, while shallow recesses possess a longer focal length. The efficiency of the effect also depends on the size of the active part of the charge.

§ 2. THE HYDRODYNAMIC THEORY OF ACCUMULATION

The character of formation of a hollow-charge jet in the presence of a lining of the shaped-charge recess is described well by the hydrodynamic theory of accumulation.

The hydrodynamic theory of accumulation is based on the assumption that at the high pressure which develop in explosion of a shaped charge, one can neglect the strength forces within the metal, consider the metal as an ideal incompressible fluid and, consequently, use the basic relationships of the hydrodynamics of an incompressible fluid in considering the process of deformation of the lining of the shaped-charge recess. We shall consider the following hydrodynamic problem.

Assume that two cylindric fluid streams with identical diameters and identical absolute values of the velocity v_a of movement are directed opposite to each other (Fig. 5.14). In colliding, these streams spread out in directions which turn perpendicular to the direction of their initial movement at some distance, forming a disc with a gradually decreasing thickness. The velocity of movement of the fluid in this disc at a sufficiently great distance from the axis will also be equal to v_a , if we neglect the losses of energy to viscous resistance of the fluid in a change in the direction of movement. If the colliding streams have different diameters, the picture changes noticeably: the spreading fluid is deflected in the direction of movement of the stream with the larger diameter, forming a conical shroud (Fig. 5.15) instead of a disc.

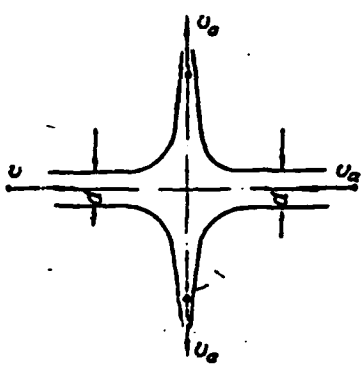


Fig. 5.14.

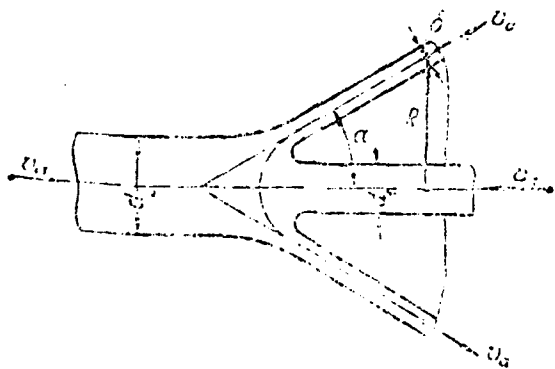


Fig. 5.15.

We shall consider the relationships between the values of the diameters d_1 and d_2 and the value of the angle α .

The momentum of a fluid which has passed through the cross sections of colliding streams in a time t is as follows:

$$\frac{\pi d_2^2}{4} \rho v_3 t v_3 - \frac{\pi d_1^2}{4} \rho v_1 t v_1 = \frac{\pi}{4} \rho v_3^2 t (d_2^2 - d_1^2), \quad (5.9)$$

where ρ is the density of the fluid.

A component (parallel to the axis of the streams) of the

overall momentum of the fluid which has passed through the cross section of the conical shroud in the same time t will be as follows:

$$\left(\frac{\pi d_2^2}{4} \rho v_s t + \frac{\pi d_1^2}{4} \rho v_s t \right) v_s \cos \alpha. \quad (5.10)$$

Setting equal the relationships (5.9) and (5.10) based on the law of the preservation of momentum, we obtain

$$d_2^2 - d_1^2 = (d_2^2 + d_1^2) \cos \alpha. \quad (5.11)$$

Hence, with a knowledge of the values of d_1 and d_2 , one can determine the value of the angle α :

$$\cos \alpha = \frac{d_2^2 - d_1^2}{d_2^2 + d_1^2}. \quad (5.12)$$

Next we shall establish the relationship between the values of d_1 , d_2 and α and the dimensions of the conical shroud of the fluid (R and δ , Fig. 5.15).

On the strength of the assumption of incompressibility of the fluid, one can assume that the volume of the fluid passing through the section of both streams in the time t is equal to the volume of fluid passing through the conical shroud in the same time:

$$\frac{\pi}{4} (d_1^2 + d_2^2) v_s t = 2\pi R \delta v_s t,$$

from which

$$8R\delta = d_1^2 + d_2^2. \quad (5.13)$$

Solving equations (5.12) and (5.13) jointly, we obtain

$$\left. \begin{aligned} d_1 &= 2\sqrt{R\delta} \sqrt{1 - \cos \alpha} \\ d_2 &= 2\sqrt{R\delta} \sqrt{1 + \cos \alpha} \end{aligned} \right\}. \quad (5.14)$$

The relationships which have been obtained define the phenomenon in question, if we exclude the complex picture which occurs directly in the stream collision zone.

Under ideal hydrodynamic conditions, when an incompressible fluid moving without internal friction is being considered, no energy losses occur; processes proceed without a change in entropy and, consequently, are completely reversible.

If we reverse all the directions of the velocities in the picture of a collision of streams which has been considered, we shall obtain the following pattern of the phenomenon.

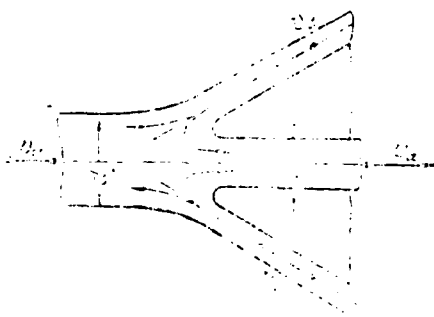


Fig. 5.16.

Fluid moving in a converging flow toward the peak of a conical shroud, in spreading along the axis of symmetry of this shroud, forms two streams moving in opposite directions in relation to the peak of the conical shroud (Fig. 5.16). The values of the diameters of these streams (d_1 and d_2) can be evaluated depending on the characteristics of the fluid shroud by means of the relationships of (5.14).

This problem from the field of hydrodynamics of an incompressible fluid is applicable in principle for describing the phenomenon of accumulation in explosion of a charge with a metallic lining of the shaped-charge recess.

The detonation products (as already considered previously) scatter from the charge surface in directions near a perpendicular to the charge surface. As a result, one can assume approximately that in explosion of a charge with a conical shaped-charge recess, the lining of this recess will undergo compression under the influence of the detonation products and will move in directions perpendicular to the surface of the shaped-charge recess. The value of the

velocity (v_0) of movement of the lining in the indicated direction can be determined with a special formula available in the appropriate reference literature.

This velocity can be broken down into two components: the velocity (v_a) of movement of a converging flow of the lining material along the generatrix of the conical recess (shroud) and the velocity (v_M) of throwing ("drift") of the lining as a unified whole in the direction of the axis of symmetry of the shaped charge (Fig. 5.17).

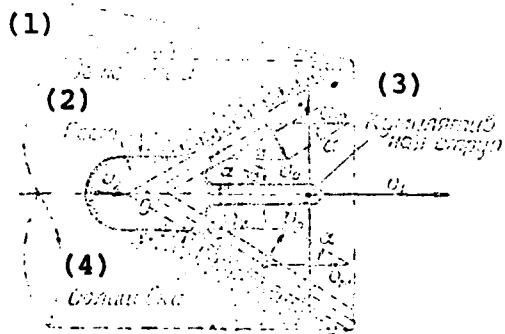


Fig. 5.17.

Key: (1) detonation products; (2) rammer;
(3) hollow-charge jet; (4) lining.

The value of the velocity v_a , the velocity of movement of the converging flow of the lining material in a moving system of coordinates, the origin of which is tied to the peak of the conical lining (point O), and, consequently, the value of the velocity of movement of the strains formed will be as follows:

$$v_a = \frac{v_0}{\operatorname{tg} \alpha}$$

The velocity of throwing of the lining along the charge axis to the right (the velocity of "drift" of the mobile system of coordinates)

will be as follows:

$$v_u = \frac{v_0}{\sin \alpha}$$

The absolute velocities of the streams (in a stationary system of coordinates) are determined from the following relationships:

$$v_1 = v_u + v_s = v_0 \left(\frac{1 + \cos \alpha}{\sin \alpha} \right); \quad (5.15)$$

$$v_2 = v_u - v_s = v_0 \left(\frac{1 - \cos \alpha}{\sin \alpha} \right). \quad (5.16)$$

The relationships obtained give accurate qualitative dependences but are approximate in a quantitative regard. For clarifying the nature of the phenomenon of accumulation, we have considered its simplest theoretical pattern. More complex, refined versions of the theoretical description of the phenomenon of accumulation in explosion of a charge with a lining of the shaped-charge recess have been created by now.

The stream moving at a velocity v_1 and with the diameter d_1 is called the hollow-charge jet. It corresponds in weight to approximately 10% of the lining weight and has a velocity of the order of 8-12 km/s.

The stream moving at a velocity v_2 and with the diameter d_2 forms the so-called rammer and takes on a velocity of the order of 500-1000 m/s.

The hollow-charge jet is formed from the lining material adjoining the inner surface of the lining (Fig. 5.18). The rammer is formed from the larger part of the lining adjoining its outer surface.

The hollow-charge jet, which possesses a high velocity, provides high efficiency of all types of damaging effect of shaped

charges. The rammer, which has a considerably lower velocity, as a rule, is preserved after the explosion and often gets stuck at the beginning of the hole created in the obstacle by the hollow-charge jet. Thus, from the consideration of the process of formation of the hollow-charge jet which has been presented, one can conclude that the parameters of this jet (primarily its velocity) depend on the angle α at the peak of the conical lining. In other words, by changing the height, (h_k) and the diameter (d_k) of the lining of the shaped-charge recess, one can change the relationship between axial (v_z) and radial (v_r) components of the velocity of movement of elements of the lining (Fig. 5.19), one can obtain different types of deformation of the lining and, consequently, one can control the process of deformation of the lining in explosion of a shaped charge. From the diagram presented in Fig. 5.19, one can see that the deeper the shaped-charge recess (the larger the ratio h_k/d_k), the larger the ratio v_r/v_z and, on the other hand, the smaller h_k/d_k , the smaller v_r/v_z . As a result, with relatively tall cones, where the radial component of the velocity of movement of elements of the lining significantly exceeds the axial component, intensive compression of the lining occurs with the formation of the hollow-charge jet. For obtaining sharper compression of the lining, one must enlarge the layer of the explosive adjoining the peripheral sections of the lining. For this purpose, the charge diameter (d_g) must be made greater than the diameter of the shaped-charge recess (Fig. 5.19).

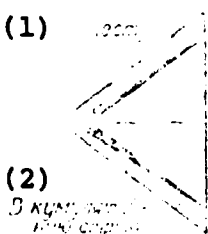


Fig. 5.18.

Key: (1) to rammer; (2) to hollow-charge jet.

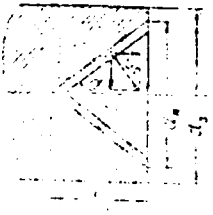


Fig. 5.19.

With relatively shallow conical recesses, essentially where $h_K/d_K < 0.25$, the axial velocity components exceed the radial components, and reversal of the lining and breaking up of the lining into separate elements - fragments which move at a high velocity in some sector in directions near the axis of the charge and are capable of effecting quite a strong damaging effect at sufficiently great distances (of the order of tens of meters) - occur together with some compression of the lining. A further (fragmentation) directed effect of shaped charges is exhibited in this case.

Everything which has been said also pertains to charges with linings of a spherical shape. With a deep lining (a small curvature radius), sharp compression of the lining occurs as a result of the explosion with the formation of a classical hollow-charge jet. With a relatively shallow lining (a large curvature radius), reversal of the lining and breaking up of the lining into fragments which fly at high velocities - a directed fragmentation effect - occur along with some compression of the lining, as in the case of a shallow shaped-charge recess of a conical shape.

We shall consider an interesting extreme case of control of the process of formation of the hollow-charge jet. One can see from formula (5.15) that with a decrease in the angle α , the value of the velocity of the hollow-charge jet (v_1) can increase without limit.

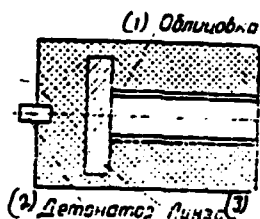


Fig. 5.20.

Key: (1) lining; (2) detonator;
 (3) lens.

Appropriate experiments conducted, in particular, by American researchers have demonstrated that if one uses cylindric ($\alpha=0$) tubes of light metals as the lining, very high velocities of movement of the hollow-charge jet formed can be obtained in explosion of shaped charges of a special structure; i.e., one can observe the phenomenon of so-called superhigh-speed accumulation. The structure of such a charge is shown schematically in Fig. 5.20. By means of a massive lens, it is possible to create optimum compression conditions in regard to the length of the cylindric shaped-charge lining. Experiments with charges of this kind have demonstrated that the velocity of the leading section of the hollow-charge jet in this case can reach values of the order of several tens of kilometers per second; the pressure on the axis of the cylindric lining can reach several million atmospheres. And the value of this velocity proves greater for linings manufactured from materials with a lower density. For example, a maximum jet velocity of 90 km/s was obtained for a lining of beryllium (density, 1.5). Since the velocity was obtained for a jet propagating in a vacuum, the mass and density of the jet were very small; consequently, the destructive capability of the jet was extremely slight. The method described for obtaining superhigh velocities of movement of material by means of the phenomenon of explosive accumulation, along with methods for obtaining such velocities by means of powerful magnetic fields and strong electrical discharges, is of great

interest for modern physics, especially plasma physics.

§ 3. THE DAMAGING EFFECT OF SHAPED-CHARGE AMMUNITION

The Armor-Piercing Effect

The armor-destroying or armor-piercing effect of shaped-charged ammunition is the basic type of the damaging effect of such ammunition. Shaped-charge ammunition was created specifically as ammunition for an armor-piercing effect.

Concepts of the hydrodynamic theory of armor piercing are used for describing the process of piercing of an obstacle (armor) by a metallic hollow-charge jet. The hydrodynamic theory of armor piercing is a special development of the hydrodynamic theory of accumulation and proceeds from the same basic assumption; i.e., it is assumed that in collision of a metallic hollow-charge jet with armor, such high pressures develop that one can neglect the strength forces of the metal in comparison to these pressures and can consider the armor as an ideal incompressible fluid.

The penetration of armor by a hollow-charge jet thus can be considered as a process similar to the process of collision of streams, the picture of which was considered at the beginning of the examination of the nature of the hydrodynamic theory of accumulation. One can assume that the process of piercing of armor consists of the creation of a corresponding cavity - a hole - in the armor by the hollow-charge jet and entering the solid mass of the armor; in this case, the jet itself, as a whole, disappears (the jet is worn away) as a result of its spreading over the surface of the hole which has been formed.

By analogy with the process of collision of streams considered previously, we shall have the following picture of the process of piercing of armor by a hollow-charge jet.

If the hollow-charge jet encounters armor material in its path in the form of a column with a diameter equal to the jet diameter, spreading of the metal occurs in directions perpendicular to the axes of the streams as a result of the collision (Fig. 5.21, shown by broken line). However, since the area of the armor, as a rule, is much greater than the dimensions of the jet cross section, spreading of the colliding masses will occur in directions deflected from perpendicularly to the axes in the direction of the stream of the smaller diameter, i.e., in the direction of the hollow-charge jet, and the latter, as already noted, will spread over the surface of the hole (Fig. 5.21).

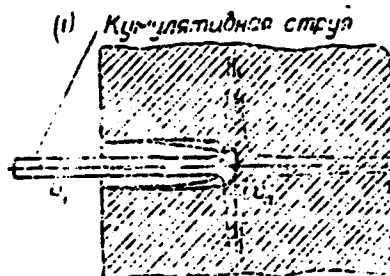


Fig. 5.21.
Key: (1) hollow-charge jet.

Assume that the jet moves in a direction toward the armor at a velocity v_1 , and the boundary of the hole formed advances into the solid mass of the armor at a velocity v_{II} . We shall also consider the density of the hollow-charge jet (ρ_c) and the density of the armor material (ρ_g) as known. We shall determine the value of v_{II} . We shall consider the movement of the jet and the hole boundary in a mobile system of coordinates with the origin of the coordinates at point A (the ultimate point of the hole). The hollow-charge jet will move in relation to point A at a velocity $v_1 - v_{II}$. The pressure (p_c) exerted by the hollow-charge jet on the armor is determined from the Bernoulli equation and will be as follows:

$$p_c = p_c \frac{(v_i - v_n)^2}{2}$$

The armor "hits" the hollow-charge jet at the velocity v_n and creates a pressure p_6 - the resistance of the armor to the effect of the hollow-charge jet - as follows

$$p_6 = p_6 \frac{v_n^2}{2}$$

Equality of the effect to the opposing effect occurs at the "jet-armor" interface; i.e.,

$$p_c = p_6,$$

or

$$p_c(v_i - v_n)^2 = p_6 v_n^2,$$

from which

$$\frac{v_i}{v_n} = \sqrt{\frac{p_6}{p_c} + 1}. \quad (5.17)$$

If we assume that the lining and the armor are made of steel ($\rho_c = \rho_6$), we obtain

$$v_n = \frac{1}{2} v_i. \quad (5.18)$$

Thus, in the presence of a steel lining of the shaped-charge recess, the rate of formation of a hole in steel armor is two times less than the velocity of the hollow-charge jet. Experimental research provides adequate confirmation for the result obtained.

We shall determine the maximum thickness L of armor which can be pierced. The time (t) in which the jet penetrates the armor and is completely "worn away" in the process is determined from the following expression:

$$t = \frac{L}{v_n} \quad (5.19)$$

On the other hand, this time t can be determined from the following formula:

$$t = \frac{L_c}{v_1 - v_n}, \quad (5.20)$$

where L_c is the length of the hollow-charge jet. Comparing expressions (5.19) and (5.20), we obtain

$$L = \frac{L_c}{v_1 - v_n} v_n = \frac{L_c}{\frac{v_1}{v_n} - 1}$$

Inserting the value of v_1/v_n from formula (5.17), we obtain

$$L = L_c \sqrt{\frac{\rho_e}{\rho_n}} \quad (5.21)$$

It follows from this formula, in particular, that the thickness of armor which can be pierced depends only on the length of the hollow-charge jet (at given densities of the lining and armor materials) and does not depend on the velocity of the hollow-charge jet; i.e., for improving the efficiency of the armor-piercing effect, one must strive to increase the length of the hollow-charge jet.

The hydrodynamic theory of armor piercing, like the hydrodynamic theory of accumulation, reveals only basic patterns and makes it possible to establish the character of the effect of basic factors on the efficiency of the armor-piercing effect of shaped charges and to take note of theoretical possibilities and ways of enhancing the efficiency of the effect of shaped-charge ammunition. This is the large role which has been played by the hydrodynamic theory of armor piercing, like the hydrodynamic theory of accumulation. It must be noted, however, that a number of questions of serious importance for the study of the shaped-charge effect are not taken into consideration and are not explained by these theories.

For example, the hydrodynamic theory of armor piercing does not take into account the physical and mechanical properties of

the lining material or the material of the obstacle (the armor) except for one property - density.

At the same time, as theoretical and experimental research demonstrates, such properties as strength and compressibility of the material of the lining and the obstacle, for example, can have a substantial influence on the efficiency of the piercing effect of the hollow-charge jet. Theoretical research in which attempts have been made to take into account most of the factors which influence the character of the development of the process of formation of a hollow-charge jet and the efficiency of the armor-piercing effect of shaped charges to some degree is well known.

However, in connection with the great complexity of the phenomenon, it is extremely difficult to establish theoretically a calculation formula which would take into consideration the influence of the entire spectrum of various factors on the efficiency of the effect of shaped charges fully and accurately and could be used directly for calculating the effect of shaped-charge ammunition. Even in a case of quite strict theoretical derivation of the formula, the need arises for additional experimental determination or refinement of individual variables included in the formula. This circumstance explains the fact the most of the calculation formulas used for calculating the armor-piercing effect of shaped charges are essentially semiempirical formulas. The shortcoming of many of the formulas is the fact that they fail to take into consideration the structural parameters of the charges.

For example, formula (5.21), which is known as the M. A. Lavrent'yev formula, can be used for calculating the depth of the hole in the action of a shaped charge.

F. A. Baum, K. P. Stanyukovich and B. I. Shekhter have proposed a formula of the form

$$L = \bar{l}_0 \sqrt{\frac{a_0 p_c}{a_c \epsilon_0}},$$

where \bar{l}_0 is the length of the hollow-charge jet at the moment of contact with the armor; a_c is the coefficient of compressibility of the jet material; ϵ_0 is the coefficient of compressibility of the armor material.

The other designations have been explained previously.

One of the formulas proposed by G. I. Pokrovskiy for calculating the armor-piercing effect of well-designed shaped charges has the following form:

$$L = 20 \sqrt{\frac{w}{\omega}}$$

where L is the thickness of the armor being pierced, in cm; w is the weight of the explosive charge, in kg.

These formulas are presented as an example; one could mention several more formulas of this type.

Considering the shortcomings of available calculation formulas and the circumstance that practically all formulas of a semiempirical and empirical type produce good coincidence of calculation and actual data, basically within the scope of the specific conditions under which the experimental coefficients were determined and the corresponding refinements were performed, it is necessary in a significant number of cases to supplement the calculations by the formulas with experimental research.

The Incendiary Effect

In impact of a hollow-charge jet moving at a high velocity against an obstacle, a high pressure emerges, and a very high temperature develops, as a result of which a strong incendiary effect is provided when a hollow-charge jet hits a medium capable of ignition.

The incendiary effect is especially effective when the hollow-charge jet gets into fuel or fuel vapors after piercing armor. For example, in hitting such targets as tanks with shaped-charge ammunition, fire and explosion inside the tank after the hollow-charge jet pierces the protective armor are among the basic damaging factors. For evaluating the incendiary effect of shaped-charge ammunition, data available in the appropriate reference literature can be used.

The Initiating Effect

The combination of the mechanical and thermal effect of a hollow-charge jet, in action on ammunition of different types filled with explosives, provides the creation of quite a powerful initial impulse capable of causing initiation of the explosives and charges. The high initiating capacity of shaped-charge ammunition was used successfully during the Great Patriotic War, when shaped-charge aviation bombs proved the most effective means for hitting such targets as open ammunition depots. As a rule, when a shaped-charge aerial bomb gets into the shell of a projectile of bomb filled with an explosive, it causes detonation.

Appropriate calculation and experimental data have been obtained for quantitative evaluation of the initiation capacity of shaped-charge ammunition and are available in the appropriate reference literature.

Factors which Influence the Damaging Effect of Shaped-Charge Ammunition

As already noted, the main type of damaging effect of shaped-charge ammunition is the armor-piercing effect of the hollow-charge jet. Therefore, we shall limit ourselves to consideration of the effects of certain factors mainly on the piercing effect of shaped-charge ammunition.

The influence of the diameter and height of the shaped charge was considered in evaluation of the dependence of the accumulation effect on the size of the active part of the charge. Increasing the diameter and height of a shaped charge of a cylindric shape, with given parameters of the lining of the shaped-charge recess, results in an increase in the efficiency of the effect (the depth of piercing) up to a definite limit. The optimum ratio of the height of the charge to its diameter in the case in question amounts to a value of the order of three.

The effect of the shape and dimensions of the shaped-charge recess on the armor-piercing effect of shaped charges proves extremely significant. The optimum ratio of the height of the shaped-charge recess to its diameter for a case of a recess of a conical shape is approximately 1.5. With an increase in the ratio of the height to the diameter of a conical shaped-charge recess up to the indicated optimum value, an increase occurs in the depth of armor which can be pierced. This occurs because a stable hollow-charge jet with a good gradient of velocities along the jet axis is obtained with these parameters; the jet stretches well and, as a result, the piercing depth increases. With an increase in the ratio of the height of the shaped-charge recess to its diameter above the optimum value, a less stable jet is obtained, the jet rapidly breaks into parts and, as a result, the depth of armor piercing begins to drop.

Shaped-charge recesses of different shapes produce approximately the same results in piercing of armor. Therefore, recesses of a conical or hemispherical shape are selected for practical use as the most technologically effective. The best result in piercing of concrete is obtained in explosion of a charge with a hemispherical shaped-charge recess. An investigation of the effect of the thickness and the material of the lining of the shaped-charge recess on the efficiency of the effect of shaped charges indicated that there is an optimum ratio of the lining thickness to the diameter of the shaped-charge recess amounting to a value within limits of 3-4% for a case

of a lining of a conical shape. This can be explained as follows. If we take two extreme cases, a very thin lining and a very thick lining, the shaped-charge effect will not be sufficiently sharply pronounced in either case. In the former case, this is the result of the fact that the amount of material can prove insufficient for forming a full-fledged hollow-charge jet. In the latter case, it is due to the fact that the impulse absorbed by the lining can prove to be insufficient for intensive compression of the lining and formation of a hollow-charge jet with a large wall thickness. Experiments confirm that the curve of the dependence of the depth of piercing on the thickness of the lining of the shaped-charge recess actually has quite a clearly pronounced maximum. In addition to the geometric parameters of the lining, the physical and mechanical properties of the lining material have a noticeable influence on the efficiency of the shaped-charge effect. Appropriate research indicates that materials with high strength together with good plasticity should be considered most suitable for manufacture of the lining of shaped-charge recesses. Shaped charges whose shaped-charge recess linings are manufactured from low-carbon steel, copper and certain alloys possess the greatest piercing effect. The use of cadmium for production of linings of shaped-charge recesses produces an especially good effect.

The presence of a side jacket of the shaped charge creates a fragmentation effect in lateral directions, which enhances the lethality of shaped-charge ammunition. In addition, the use of a side jacket for the charge results in an increase in the volume of the active part of the charge and thereby causes improvement of the efficiency of the effect of the hollow-charge jet. Using a side jacket for the charge can improve the efficiency of the casualty effect of shaped-charge ammunition by 15-20%.

The effect of properties of the explosive on the efficiency of the shaped-charge effect is determined by the power of the explosive and its rate of detonation. These two indicators determine

the character and intensity of compression of the lining of the shaped-charge recess. Explosives which possess a relatively low detonation rate (such as ammonites) produce a reduced shaped-charge effect. The use of more powerful explosives (such as alloys of the TG [trotyl-hexogen] type) results in improvement of the shaped-charge effect by 15-20% as compared to the use of ordinary trotyl. In evaluating the effect of the properties of the explosive on the shaped-charge effect, it is also necessary to consider the fact that cases are possible in which the use of an explosive which is too powerful with a comparatively thin lining of the shaped-charge recess can cause a reduction of the shaped-charge effect. This is explained by the extremely intense breaking up of the thin lining in compression.

One of the factors which sharply reduce the shaped-charge effect and, in particular, the armor-piercing effect of a shaped charge is rotation of the shaped charge around the longitudinal axis.

For example, in firing of rotating shaped-charge projectiles, their armor-piercing effect decreases to 50% as compared to nonrotating projectiles, and other types of damaging effect of shaped-charge projectiles are also weakened.

The influence of rotating movement on the shaped-charge effect is conditioned by the joint action of several factors which are interrelated.

Based on the law of the preservation of momentum, in compression of a charge lining which possesses some initial angular velocity as a result of rotation, the angular velocities of elements of the lining will increase in inverse proportion to the square of the distance of these elements from the rotation axis,

$$\omega_K = \omega_H \left(\frac{r_H}{r_K} \right)^2,$$

where ω_H and ω_K are the initial and final angular velocities, respectively, of rotation of the lining element; r_H and r_K are the initial and final distances of the lining element from the axis of the projectile.

It is obvious that a metallic hollow-charge jet will have an angular velocity of rotation which exceeds the initial angular velocity of rotation of the projectile by many times. As a result of the effect of the centrifugal forces which develop, this results in an increase in the diameter of the hollow-charge jet and to disturbance of the jet and, consequently, weakening of the shaped-charge effect. The circumstance which has been mentioned is aggravated even more by the fact that the angular velocity of rotation of the hollow-charge jet is not constant - it increases in proportion to movement away from the peak of the lining toward its base. As a result, twisting of the jet will occur in addition to stretching.

It is also necessary in evaluating the effect of rotation of a projectile on the efficiency of the shaped-charge effect to consider the fact that the specific structure of the shaped charge does not possess strict symmetry as a result of such causes as:

- inaccuracy of manufacture of the lining;
- inaccuracy of placement of the lining in the shaped-charge recess of the charge;
- inaccuracy of manufacture of the outer (side) jacket of the charge;
- heterogeneity of the properties of the material of the lining and the outer jacket of the charge;

- inaccuracy of placement of the detonator in relation to the charge axis.

With significant asymmetry in the structure of the charge, even under stationary testing conditions, forking and splitting of the hollow-charge jet and a sharp decrease in its armor-piercing effect are observed. Moreover, in a case of rotation, in the presence of significant centrifugal forces, a slight initial asymmetry causes premature disturbance of the hollow-charge jet and a decrease in the efficiency of its damaging effect.

Appropriate research on this question indicates that conical linings are more sensitive to rotation than spherical linings; deep linings are more sensitive to rotation than shallow ones; an increase in the lining diameter also leads to an increase in the sensitivity of the shaped charge to rotation (as one can see from the formula presented above).

Theoretical and experimental research indicates that a reduction of losses in the armor-piercing effect in rotation of a shaped charge can be achieved primarily by reducing the angular velocity of rotation of the lining itself. Such a method in practice involves introducing a device which provides the possibility of turning of the lining in relation to the shaped charge into the projectile design.

CHAPTER 6

THE FRAGMENTATION EFFECT OF AVIATION AMMUNITION

§ 1. GENERAL INFORMATION ON THE FRAGMENTATION EFFECT

The fragmentation effect is one of the basic forms of the damaging effect of ammunition. It is conditioned by the fact that breaking up of the shell of the bomb or projectile occurs in explosion of a bursting charge. The fragments formed in this process, possessing a high initial velocity, scatter in all directions from the point of the explosion and, in hitting a target, are capable of inflicting damage of different kinds on it.

Ammunition which destroys a target mainly due to the effect of fragments is called fragmentation effect ammunition. This ammunition occupies a special place in the system of aviation ammunition (fragmentation aerial bombs, most of the projectiles for aircraft guns, warheads of free-flight and guided missiles, etc.).

The efficiency of the fragmentation effect depends primarily on such structural parameters of the ammunition as the overall weight of the warhead, the filling coefficient, the shell shape and the method of initiation, the properties of the shell metal and the properties of the VV [explosive], features of the design, etc. All these structural parameters determine the character of

breaking up of the shell into fragments (the weights of fragments formed in the explosion and the total number of fragments), the initial velocity of the fragments and the character of their dispersion in space.

For evaluating the efficiency of the fragmentation effect, it is also necessary to know the properties of the target on which firing or bombing is being conducted, namely: the total area of the target, the area of different vulnerable parts and assemblies, and their resistance in relation to the damaging effect of the fragments.

Finally, the efficiency of the fragmentation effect depends in an essential way on the distance to the target and the orientation of the axis of the bomb or missile in relation to the target, i.e., on the angle of impact of the bomb with the plane of the ground (or the angle of approach at which firing is conducted) and the angle formed at the moment of bursting by the axis of the warhead with the direction to the target. All these coordinates characterizing the mutual positioning of the bomb (missile) and the target obviously are determined by the conditions of bombing (the conditions of firing) and the parameters of the fuses used to make up the fragmentation ammunition.

The main problem involved with evaluating the effect of fragmentation ammunition is to determine the probability of destroying a given target under the condition that the warhead, all structural parameters of which are known, bursts at some point with coordinates x , y and z in relation to the target. This probability is designated as $G(x, y, z)$ and is called the coordinate law of target kill. It is obvious that the form of the function $G(x, y, z)$, i.e., the numerical value of the probability of target kill with given coordinates of the explosion point, depends on the structural parameters of the warhead, the type of target and the conditions of bombing (firing).

For determining the probability of target kill, it is necessary to know how structural data of the warhead influence the characteristics of breaking up of the shell into fragments (the weights of the fragments and the total number of fragments) and the character of the dispersion of the fragments in space, how to determine the initial velocity of the fragments and to take into account the decrease in the velocity of a fragment on its trajectory in view of the presence of the force of resistance of air, how to evaluate the efficiency of the effect of a fragment which has hit the target if its weight and velocity at the moment of impact are known and, finally, how to determine the number of fragments which hit the target with given coordinates of the explosion point and given conditions of bombing or firing.

Subsequent sections of this chapter are devoted to considering all these questions.

§ 2. DESTRUCTION OF THE CASING UNDER THE EFFECT OF AN EXPLOSION

We shall consider the physical picture of the process of explosion of a charge in a case and phenomena of deformation of the case, its destruction and the formation of fragments related to the explosion process. We shall assume that the bursting charge is enclosed in a cylindric casing, and initiation of the charge is accomplished from the direction of one end of the casing (Fig. 6.1). As we know, in this case a detonation wave will begin propagating over the VV charge; the pressure on the detonation wave front reaches several hundred thousand atmospheres. The pressure drops sharply behind the detonation wave front; therefore, if we consider any cross section of the charge, the character of the change in the internal pressure acting on the charge case can be represented in the form of the graph of Fig. 6.2. Such a sharp drop in the pressure behind the detonation wave front is conditioned by the fact that the process of propagation of the detonation wave over the charge is accompanied by outflow of explosion products from the end of the

charge at which the detonator was located.

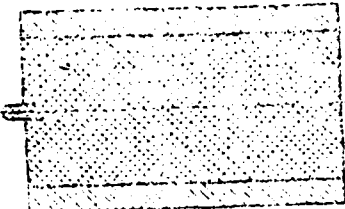


Fig. 6.1.

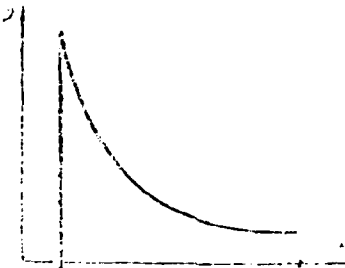


Fig. 6.2.

However, the graph of the pressure $p(t)$ acting on the charge case shown in Fig. 6.2 will characterize the actual explosive load only in a case where the opposite end (the right end in Fig. 6.1) of the charge is located at an infinite distance from the initiation point. In real ammunition designs, the two ends of the charge are located at a finite distance apart. If the end of the charge opposite the detonator is open in this case, intensive free outflow of the detonation products from this end of the charge also will begin after approach of the detonation wave to it. In other words, a rarefaction wave which reduces the pressure of the detonation products in this case will begin to move from the right end of the charge into the depths of the detonation products. Therefore, the change in the internal pressure in some cross section of the case in a charge in a case with open ends will have the form shown in Fig. 6.3. Point A in the graph of Fig. 6.3 corresponds to the moment

of arrival of the detonation wave at the cross section in question, while point B corresponds to the moment of approach of the rarefaction wave from the right end of the charge.

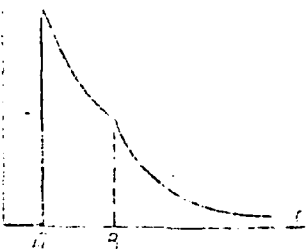


Fig. 6.3.

On the other hand, if the case shown in Fig. 6.1 has a solid bottom on the side of the end opposite the detonator, a sharp increase in the pressure on the detonation wave front will occur at the moment of impact of the detonation wave on the end (bottom) part of the case, and a reflected wave will begin propagating from this end into the depths of the detonation products. After reflection of the detonation wave from the end, the bottom part breaks away from the case, and more or less free outflow of the detonation products from this end of the charge begins, which leads to the formation of a rarefaction wave, which also will move into the depths of the detonation products after the reflected wave. The character of the change in internal pressure in some cross section of the case will be represented in this case in the form of the graph 6.4, in which point A corresponds to the moment of arrival of the detonation wave at the given cross section, while point B corresponds to the moment of arrival of the reflected wave from the bottom part of the case, and point C corresponds to the moment of arrival of the rarefaction wave from the already separated bottom part of the charge.

The internal pressure acting on the charge case thus will vary along the length of the charge; the character of the variation of

this pressure depends essentially on the time. For example, Fig. 6.5 shows the character of the pressure distribution along the length of a cylindric case with open ends at different moments in time. The solid curve corresponds to a moment when the detonation wave has not yet reached the opposite end of the charge; the dotted curve corresponds to a moment when outflow from the open right end of the charge has begun, and a rarefaction wave is already moving along the charge.

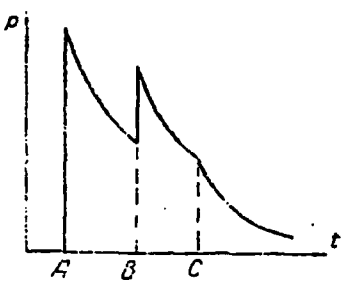


Fig. 6.4.

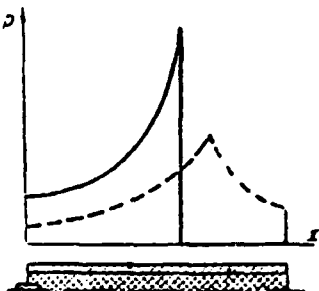


Fig. 6.5.

The basic patterns which determine the distribution of internal pressure along the length of a charge case and the dependence of this distribution on the time can be obtained proceeding from general conditions of the hydrodynamic theory of detonation as applied to a case of detonation of a cylindric charge.

The character of variation of the internal pressure acting on the charge case considered above produces a representation of the explosive load under the action of which deformation of the case, its destruction and the formation of fragments occur. It is obvious that different cross sections of the case will begin to undergo deformation and will be involved in movement not simultaneously but sequentially, in proportion to the passage of the detonation wave over the charge. In addition, the sizes of deformations and movements of different sections of the case will differ as a result of differences in the forces of pressure of the detonation products acting in each section. Specifically, increased pressure will be preserved longer in the sections of the charge in which contact of rarefaction waves moving in opposition to each other from the ends of the charge occurs. As we know, in charges with open ends, contact of the rarefaction waves occurs in sections located near the end of the charge opposite the detonator (2.154). If this end of the charge is closed, the outflow of detonation products from this end will begin somewhat later and, consequently, contact of the rarefaction waves will recur still further from the detonator. The zone of increased explosive loads thus will be shifted more in the direction away from the detonator the stronger and heavier the bottom part of the charge case is made.

The character of variation of the explosive load described above results in the fact that the sizes of deformations of the case metal will be different in different sections of the case. It is natural that the most intense deformations of the metal will occur in a zone of increased explosive loads. Each section of the deformed case is drawn into motion by detonation products expanding in a radial direction. As a result of this, the entire case as a whole in its movement takes on a barrel shape which changes continuously in time. In this process, the thickness of the walls of the case decrease substantially (relative deformations reach 30-50%). With a certain degree of expansion, destruction of the case occurs, and the case breaks up into separate fragments, which

scatter at certain velocities in the corresponding directions in space. By the moment of destruction of the case, the maximum outer diameter of the case in certain cases can exceed its diameter before the explosion significantly (by a factor of 1.5). It is obvious that the velocity of the fragments will be determined by the velocity of movement of the expanding case at the moment of its destruction, and the directions in which the fragments fly depend entirely on the shape of the case at the moment of formation of the fragments.

Research on the stressed state of a case in an explosion and on the process of destruction of the case was conducted by Professor V. A. Kuznetsov. The results of this theoretical research made it possible to determine the dimensions and weights of fragments formed in explosion of a charge in a case by calculation. We shall consider how the process of formation of fragments occurs in accordance with this theory in destruction of relatively short and thick-walled cases typical of the design of fragmentation ammunition, keeping in mind that the time of the effect of the explosive load for such cases is substantially less than the time of deformation and destruction of the case. Therefore, the process of expansion and deformation of such thick-walled cases will begin to develop by the moment of completion of the effect of the explosive load. In considering the effect of internal pressure of detonation products on such a heavy case in the form of an impulse load which varies along the length of the charge, we shall determine the stressed state in which the case metal will be found in the action of this explosive load on it and the character of wave phenomena which emerge and develop in the case in explosion of the charge.

As we know, with a sharp impact on the surface of any medium, a shock wave (a compression wave) emerges in the medium and propagates into the depths of the medium at a velocity near the velocity of propagation of elastic deformations in the medium in

question (the velocity of propagation of elastic deformations, in turn, is equal to the velocity of sound in the medium).

It has already been noted above that the pressure acting on the inner surface of the case is applied not simultaneously over the entire length of the case but sequentially, in proportion to advancing of the detonation wave along the charge. Therefore, in movement of the detonation wave along the charge, a compression shock wave, whose front is shown in Fig. 6.6 by line OA, will propagate in the case metal.

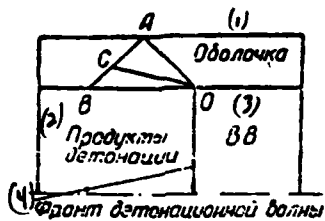


Fig. 6.6.

Key: (1) case; (2) detonation products;
(3) VV; (4) detonation wave front.

We know also that if a compression shock wave propagating in a medium approaches a free surface of the medium, it is transformed into a stretching wave propagating at the velocity of sound in the medium in question from the free surface into the depths of the medium. Since the compression shock wave front approaches the outer surface of the case at some angle, the position of the reflected wave front is shown in Fig. 6.6 in the form of a line AB (one can assume that the reflection of shock waves in this case occurs in accordance with the laws of geometric optics). The case material behind the stretching wave front will undergo tensile stresses.

The pressure of detonation products acting on the inner surface

of a section of the case which has been reached by the detonation wave exceeds the ultimate strength of the case material by hundreds of times; therefore, the inner part of the case which directly absorbs the effect of the pressure of the detonation products will begin to undergo plastic deformation, in addition to the stressed state which has been described. The inner zone of the case will be covered by plastic deformations not immediately but gradually. Since the velocity of propagation of the plastic deformations is several times less than the velocity of propagation of elastic deformations, the wave front of plastic deformations is shown in Fig. 6.6 in the form of line OC. It is obvious that the maximum depth of the zone of plastic deformations is determined by the position of point C, because a further increase in the depth of the zone of plastic deformations becomes impossible in the zone of the effect of the stretching wave, where the case material has been subjected to strong tensile stresses.

An overall picture of the momentary stressed state of the case material is shown in Fig. 6.7. At the moment when the detonation wave moving along the charge reaches point O, the case material which has not yet been reached by the compression wave front will be in an unstresses state (the part of the case located to the right of line OA in Fig. 6.7). The part of the case material enclosed between the elastic deformation wave front, the stretching wave front and the plastic deformation wave front (the triangle OAC) will undergo elastic compression deformations. The formation of two characteristic deformation zones occurs behind the stretching wave front: an inner zone, in which intensive plastic flows of the material occur (the boundary of the inner zone - OCD), and an outer zone, in which the case metal undergoes strong tensile stresses (the boundary of the outer zone - ACD). We shall note that wave phenomena in each section of the case end by the moment of the end of the process of formation of the two indicated deformation zones.

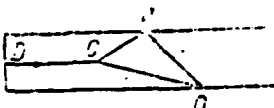


Fig. 6.7.

In considering the diagram of the stressed state of the case material presented in Fig. 6.7., it is necessary to keep in mind that in reality, as a result of the irregularity of the distribution of the explosive load which occurs over the length of the case, the depth of the zone of plastic deformations does not remain constant over the entire length of the case; rather it varies, repeating the law of variation of the load in some way.

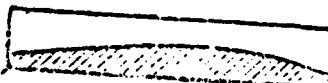


Fig. 6.8.

Figure 6.8 shows schematically the charge case at the moment of completion of wave processes in the case metal and formation of the zone of plastic deformations over the entire length of the case (the zone of plastic deformations is shaded). By the moment of completion of wave processes in a given section of the case, the stresses which emerge in the case material reach their maximum values over the entire case section. In this process, as research on the stressed state of the case indicates, the maximum stresses at this moment reach their greatest values in the layers of the outer deformation zone. The character of the distribution of maximum stresses over the thickness of a case cross section is shown in Fig. 6.9. The greatest stresses thus emerge in the middle layers of the outer zone by the moment of the end of the process of formation of the two deformation zones. The case material located in this layer will be stretched by tangential and axial stresses.

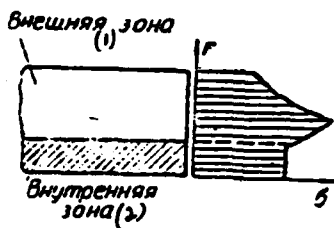


Fig. 6.9.

Key: (1) outer zone; (2) inner zone.

However, in connection with the fact that the explosive load is applied instantaneously to each section of the case, three-dimensional damped oscillations of different frequencies emerge very rapidly throughout the case and, consequently, in the layers of the case in which the stresses reach their maximum values. As a result, the stresses which emerge in the case layer under consideration will be distributed unevenly along the length and circumference of this layer. In certain elements of the longitudinal section of the layer in question, the axial tensile stresses, which are the result of oscillations of the case in an axial direction, will reach maximum values. A similar picture is also observed for elements of the layer in a cross section, where elements which undergo more intensive stretching by tangential stresses active in the cross sections of the layer can be distinguished. Therefore, in the case layer in question, one can distinguish individual longitudinal and transverse sections in which the tensile stresses in the process of oscillation of a case under deformation will be maximal by the moment of the beginning of radial expansion of the entire case. The appearance of such dynamic irregularities in the distribution of stresses (i.e., localization of maximum destructive stresses in individual sections of the case, which is the result of the dynamic nature of the process and of oscillations of the case which emerge in connection with this) results in the formation of cracks arranged in a definite way along the length and the circumference of the case (Fig. 6.10). These cracks in further radial expansion of the

case determine the process of subsequent disintegration of the case and formation of fragments.*

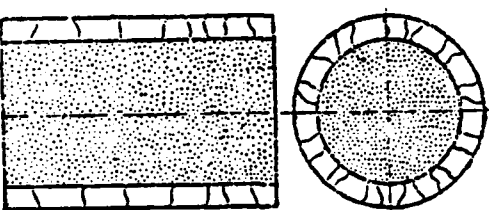


Fig. 6.10.

The distances between cracks in longitudinal and transverse directions are determined by the frequencies of the oscillations which develop. Since oscillations of different frequencies emerge simultaneously in the case in an explosion under the action of the impact of detonation products, the distances between emerging cracks which determine their dimensions and, consequently, the weights of the fragments formed, will also be different. It is obvious that these cracks will emerge only in sections of the case in which the peaks of stresses exceed the limits of dynamic strength of the case material. Therefore, the number of transverse and longitudinal sections in which cracks emerge will be greater the more intense the explosive load. Consequently, a case will be subject to the most intensive breaking up in the zone of the effect of maximum explosive loads.

*Along with these cracks, which are the result of dynamic irregularities which emerge in the process of three-dimensional oscillations of the case which have been considered, cracks are also formed in the case metal due to different kinds of structural defects and statistical heterogeneity of the strength properties of the metal. The influence of these factors on the process of breaking up of the case will be considered in the next section.

Such, briefly, is the picture of the complex phenomena which develop in explosion of a charge in thick-walled cases of fragmentation ammunition. The process of deformation and disintegration of thin-walled cases occurs somewhat differently. Such cases, possessing low inertia, are drawn into movement immediately by expanding detonation products, the internal pressure of which will act on the case throughout the time of expansion of the case. Therefore, the wave phenomena considered above and the three-dimensional oscillations of the case related to them, as a result of which dynamic irregularities are exhibited in the case metal, do not manage to develop fully in thin-walled cases. Such cases break up into fragments mainly due to structural defects and heterogeneity of the strength properties of the case metal.

§ 3. THE TOTAL NUMBER OF FRAGMENTS. THE LAW OF THE DISTRIBUTION OF FRAGMENTS BY WEIGHT.

The efficiency of the effect of fragmentation ammunition depends essentially on the characteristics of breaking up of the case of the charge into fragments, i.e., on the total number of fragments formed in the explosion, and on the character of distribution of fragments by different weight groups. The efficiency of the fragmentation effect is also determined to some degree by the shape of the fragments and the relationships of their geometric dimensions.

All these characteristics of breaking up of the shells of fragmentation ammunition can be determined experimentally. For example, one can conduct special explosions of fragmentation ammunition in an armored chamber filled with sand or sawdust for this purpose. After the explosion, all the fragments collected must be sorted by weight groups, the number of fragments belonging to each weight group must be counted, and the total number of all fragments must be counted.

In addition, after conducting the experiment, one can produce

a conclusion concerning characteristic shapes of the fragments and their relationships of their geometric dimensions (one can determine the length, width and thickness of a typical fragment). Since the total number of fragments and the numbers of fragments of different weight groups vary from one explosion to another in explosions of the same ammunition, it is necessary to conduct several explosions and to determine the average numbers of fragments.

Experimental data obtained in this way are the basis for construction of the so-called law of the distribution of fragments by weight, which is performed as follows. We shall assume that all the fragments whose weight exceeds some minimum weight q_0 have been collected in the explosion. Normally q_0 is equal to 0.5 g or 1.0 g, because fragments of a smaller weight as a rule are not included in the calculation in evaluating the efficiency of the effect. In addition, in processing the results of experiments on explosion in armored pits, it is technically very difficult to collect fragments with a weight less than the indicated weight and to separate them from the medium with which the armored pit has been filled. Assume in this case that the weight of the maximum fragment formed in the explosion is equal to q_m . We shall divide the range of possible values of weights of the fragments collected $q_0 - q_m$ into individual intervals:

$$q_0, q_1, q_2, \dots, q_i, \dots, q_r, \dots, q_m.$$

We shall designate the size of an interval as Δq_i :

$$\Delta q_i = q_i - q_{i-1}.$$

We shall note that the intervals Δq_i need not be equal; as a rule, with an increase in the fragment weight q_i , the size of the interval increases.*

*The fragments are normally divided into the following weight groups: 1-2 g; 2-4 g; 4-6 g; 6-10 g; 10-15 g; 15-20 g; 20-30 g; 30-40 g; 40-50 g; 50-60 g; 60-75 g; 75-100 g, and more than 100 g.

We shall designate the total number of fragments collected whose weight is greater than q_0 as N and the number of fragments belonging to the weight group $q_{i-1} - q_i$ as ΔN_i .

Then the ratio $\Delta N_i/N$ represents the statistical probability that a fragment selected at random will belong to a particular weight group and is equal to the relative number of fragments whose weight is within the interval $q_{i-1} - q_i$.

It is customary to represent the law of the distribution of fragments by weight in the form of a histogram of the distribution $t^*(q)$. As we know, for plotting a histogram of the distribution $t^*(q)$, it is necessary to divide the statistical probability $\Delta N_i/N$ by the size of the weight interval Δq_i :

$$t^*(q) = \frac{\Delta N_i}{N \Delta q_i} \quad (6.1)$$

An illustration of a distribution histogram is shown in Fig. 6.11. It is obvious that the area of each rectangle of the histogram is equal to the statistical probability of the distribution of fragments by weight (i.e., to the relative number of fragments of the weight group in question), because

$$t^*(q) \Delta q_i = \frac{\Delta N_i}{N}$$

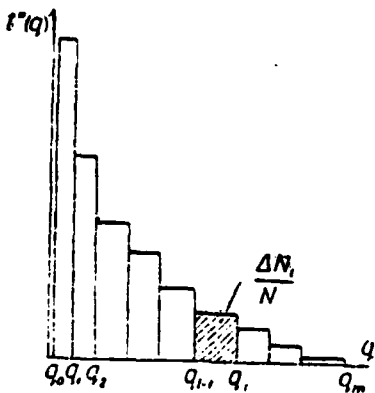


Fig. 6.11.

The total area of all the rectangles of the histogram is equal to one:

$$\sum_{i=1}^n t^*(q) \Delta q_i = \sum_{i=1}^n \frac{\Delta N_i}{N} = 1.$$

With the law of the distribution of fragments by weight, one can also determine the mathematical expectation of the weight of a fragment (i.e., the average fragment weight) by a well-known formula of probability theory:

$$\bar{q} = \sum_{i=1}^n q_i t^*(q) \Delta q_i = \sum_{i=1}^n q_i \frac{\Delta N_i}{N}. \quad (6.2)$$

The value of \bar{q} is one of the indicators of breaking up of the charge case; obviously the greater \bar{q} under otherwise equal conditions, the larger the fragments into which the case breaks up in an explosion.

The histogram of the distribution $t^*(q)$ obtained in this way fully characterizes the law of the distribution of fragments by weight. In certain cases in performance of calculations for evaluating the efficiency of the fragmentation effect, it proves more efficient to represent experimental data not in the form of a histogram of the distribution $t^*(q)$, which has the sense of a statistical differential distribution law, but in the form of a statistical integral law of the distribution $T^*(q)$.

According to the definition of the statistical integral law of the distribution,

$$T^*(q) = \frac{N(q)}{N}, \quad (6.3)$$

where $N(q)$ is the number of fragments whose weight is less than q .

It is obvious that

$$N(q) = \sum \Delta N_i. \quad (6.4)$$

where the summation is extended to all values of the index i for which $q_i < q$.

Thus, the statistical integral distribution law in this case essentially is the relative number of fragments whose weight is less than the given weight q . An illustration of a statistical integral law is shown in Fig. 6.12.

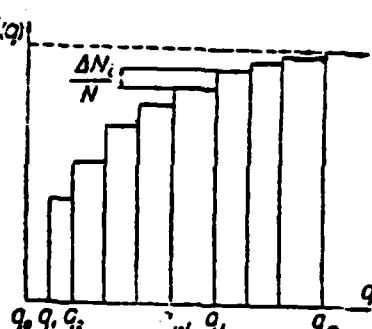


Fig. 6.12.

Keeping in mind formulas (6.3) and (6.4), one can write the following:

$$T^*(q) = \frac{\sum \Delta N_i}{N} = \sum t^*(q) \Delta q_i,$$

where the summation has been extended as before to values of i for which $q_i < q$.

Consequently, each ordinate of the integral law is the sum of areas of rectangles of the distribution histogram located to the left of point q . It proves more convenient in certain cases to use differential and integral laws of the distribution of fragments by weight $t(q)$ and $T(q)$, respectively, rather than the histogram of the distribution of fragments by weight $t^*(q)$ or the statistical integral law of the distribution $T^*(q)$. The indicated differential and integral laws are obtained with the use of normal methods of smoothing of exponential functions. In other words, the distributions $t^*(q)$ and $T^*(q)$ obtained experimentally are replaced with

corresponding analytical expressions $t(q)$ and $T(q)$, which coincide best with the experimental distribution laws $t^*(q)$ and $T^*(q)$. Graphs of the functions $t(q)$ and $T(q)$ have the form shown in Figs. 6.13 and 6.14.

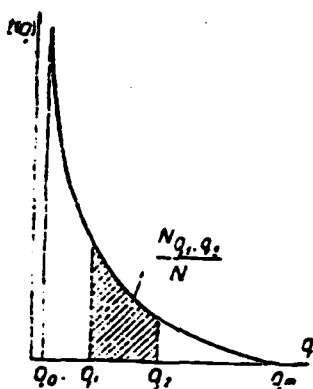


Fig. 6.13.

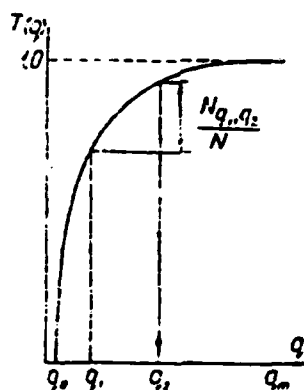


Fig. 6.14.

It is obvious that if one could replace the distribution histogram in some way with the continuous function $t(q)$, one could express the number of fragments whose weight is within any range q_1-q_2 with the area under the curve of the differential distribution law on the range q_1-q_2 according to the formula

$$N_{q_1 \dots q_m} = N \int_{q_1}^{q_m} t(q) dq. \quad (6.5)$$

Keeping in mind the well-known relationship between integral and differential distribution laws, we obtain

$$T(q) = \int_{q_1}^q t(q) dq.$$

Consequently, the number of fragments whose weight is within the range $q_1 \dots q_2$ can also be expressed by means of an integral distribution law $T(q)$ as the difference of ordinates of the integral distribution law at corresponding points:

$$N_{q_1 \dots q_2} = N[T(q_2) - T(q_1)]. \quad (6.6)$$

In conclusion, we shall recall the general properties which are familiar from probability theory which are also satisfied by the laws in question for the distribution of fragments by weight $t(q)$ and $T(q)$:

$$\int_{q_1}^{q_m} t(q) dq = 1; \quad T(q_1) = 0; \quad T(q_m) = 1.$$

Therefore, with experimental data on the results of explosions of fragmentation ammunition in armored chambers, one can plot a histogram of the distribution of fragments by weight $t^*(q)$ and a statistical integral law $T^*(q)$ and, when necessary, one can replace the experimental distributions obtained with corresponding continuous functions $t(q)$ and $T(q)$.

It should be noted that the method described for determining the characteristics of breaking up by explosion of ammunition in armored chambers is distinguished by exceptional awkwardness and is applicable only for fragmentation ammunition of comparatively small calibers. With a large weight of the ammunition, determining the necessary characteristics of breaking up by explosion in armored

chambers becomes practically impossible. The explosions of fragmentation ammunition can be conducted in these cases in a special target arrangement, in open air (a description of the target installation is presented in the next section). The total number of holes left by fragments in the screens of the target installation and the areas of all the holes formed are determined in this case. In addition, the number of holes whose areas are within certain ranges (such as the number of holes whose area is in the range of $0.5-1.0 \text{ cm}^2$, $1.0-1.5 \text{ cm}^2$, etc.) is counted. Since the area of a hole is related in a specific way to the weight of the fragment which has left the hole in the screen, using the experimental data obtained on the character of the distribution of areas of the holes, one can determine the law of the distribution of fragments among different weight groups by special calculations.

Theoretical methods which make it possible to determine all the necessary characteristics of breaking up by calculation are also finding use at present in addition to the experimental methods described above for determining the characteristics of breaking up of the shells of fragmentation ammunition. Calculation methods for computing the characteristics of breaking up are based on the physical representations of the process of deformation and disintegration of a charge case in an explosion which have been presented above. In performing such calculations, one determines the number of rings into which a case breaks up in an explosion and computes the width of each ring, which is equal to the length of the fragment formed; then one determines the number of fragments into which each of the rings which has been formed breaks up and computes the width of each fragment. In other words, the procedure for conducting such calculations makes it possible to determine the total number of fragments formed in breaking up of the case and the geometric dimensions and, consequently, the weight of each of the fragments. Using the results of these calculations, one can group the fragments by different weight categories and can calculate the number of fragments of each weight group.

However, it must be mentioned that the calculation procedure for determining the characteristics of breaking up of a charge case provides the possibility of determining only the number of so-called regular fragments, i.e., fragments obtained as a result of breaking up of the case strictly according to the network of lengthwise and radial cracks described above. In reality, due to the presence of structural defects and irregularities of different kinds in the case metal (microcracks, blisters, impurities, etc.) distributed randomly over the entire metal volume, the process of formation of fragments can differ substantially from the idealized pattern considered previously, which forms the basis of the procedure for determining the characteristics of breaking up by calculation.

In particular, cases are possible in which part of the cracks which appear in the case in accordance with the calculated pattern and which predetermine the formation of fragments of a certain weight are not able to develop through the entire thickness of the case wall due to the presence of structural irregularities. Such a deviation from the calculation pattern will lead to the formation of a smaller number of fragments of a larger weight at this point of the case. On the other hand, cases can occur very often in which the presence of any defect in the process of deformation of the case under the influence of an explosion will lead to the appearance of additional cracks, as a result of which a larger number of fragments whose weight will be smaller than the calculated weights will be formed in breaking up of this elementary volume. In addition, it is not possible to determine the number of fragments of comparatively small weight groups which are formed at the boundaries of surfaces of formation of the regular fragments by calculation. In large-caliber fragmentation ammunition, the weights of such fragments which do not fit into the calculation pattern can even be sufficient for inflicting noticeable damage on the target which is being hit, and the number of such fragments can exceed the number of so-called regular fragments by several times.

All this gives the process of breaking up of the case into fragments a random character and does not provide the possibility of direct use of calculation results for determining the real characteristics of fragmentation of the case in evaluating the efficiency of the effect of fragmentation ammunition. Nevertheless, using basic conditions of the theory of deformation and disintegration of charge cases and the results of calculations conducted in accordance with this theory, one can obtain a number of general quantitative patterns which define the process of fragmentation of a case. In addition, based on available calculation methods for determining the characteristics of breaking up of a case, one can also establish how structural data of the warhead influence the total number of fragments formed in an explosion and the character of their distribution among different weight groups. Conclusions obtained based on analysis of the results of appropriate calculations are in good qualitative agreement with experimental data and basically boil down to the following.

The character of fragmentation of a charge case depends essentially on the physical and mechanical properties of the case metal and primarily on its toughness. With an increase in the toughness of the case metal, the relative amount of the metal transformed into dust or breaking up into extremely fine ("not useful") fragments decreases; i.e., losses of metal which are useless from the point of view of the fragmentation effect decrease with an increase in the toughness of the metal. The total number of fragments also decreases in this case, although tougher case metal under otherwise equal conditions produces a relatively greater number of large fragments; i.e., the average weight of a fragment increases with an increase in the toughness of the metal; the weight of the maximum fragment formed in an explosion also increases.

As an illustration, Table 6.1 presents some data characterizing breaking up of cases of steel, wrought iron and semisteel cast iron.

Table 6.1. The effect of mechanical properties of the metal on the character of fragmentation of a shell.

(1) Металл корпуса Характеристики проблечия	(2)	(3) Сталь	(4) Ковкий чугун	(5) Стальстый чугун
(6) Общее количество осколков весом более 1 г		572	1032	1301
(7) Вес металла (в процентах), используемого при образовании осколков весом менее 1 г (потери металла)		10.0	36.6	48.3
(8) Средний вес осколка (г)		5.5	2.5	2.0

Key: (1) shell metal; (2) characteristics of breaking up; (3) steel; (4) wrought iron; (5) semisteel cast iron; (6) total number of fragments with a weight greater than 1 g; (7) weight of metal (in percent) used for formation of fragments with a weight less than 1 g (metal losses); (8) average fragment weight (in g).

The total number of fragments and the character of their distribution by weight groups also depend on the properties of the explosive used and, in particular, on its brisant properties. The more brisant the explosive, the larger the number of fragments formed in breaking up of the case and the more fragments of a low weight which are produced, while the number of large fragments, on the other hand, decreases. The weight of the maximum fragment formed in breaking up of a case will be smaller the more brisant the charge explosive. For example, in breaking up of cases filled with trotyl, the total number of fragments with a weight greater than 1 g is 578; in a case of filling of the same cases with ammonal, the number of such fragments is 490.

The character of breaking up of the shell into fragments depends on the total weight of the shell metal, i.e., on the caliber of the bomb or projectile with a constant filling

coefficient. With an increase in the caliber, the total number of fragments increases, the percentage of shell metal losses going for formation of very fine fragments decreases, the number of large fragments increases, and the maximum and average weights of the fragments increase.

The intensity of fragmentation of a shell depends to a considerable extent on the relative quantity of explosive, i.e., on the filling coefficient of the charge case. With an increase in the filling coefficient, the total number of fragments increases, and this increase occurs due to an increase in the number of small fragments. In other words, the process of breaking up becomes more intense with an increase in the filling coefficient; i.e., the average weight of a fragment and the weight of the maximum fragment decreases.

An extremely significant parameter of breaking up which defines the dependence of all the other characteristics of breaking up on the basic properties of the case metal, the explosive charge and the geometric dimensions of the charge and the case to a great extent is the weight of the maximum fragment formed in breaking up of the case. The smaller the weight of the maximum fragment, under otherwise equal conditions, the more intense the fragmentation of the case will be. However, this characteristic to a great degree is subject to the influence of all the random factors which determine the process of breaking up and are involved with structural defects of the material. It is well known that the weight of the maximum fragment can vary substantially from one explosion to another in the same ammunition. Therefore, the weight of the maximum fragment is normally understood to mean some provisional average weight of the heaviest fragments formed in several explosions of the same warheads. Calculations by formulas for determining such an average maximum fragment weight obtained based on consideration of the idealized system of the

process of breaking up of a case under the effect of an explosion considered above coincide with the results of corresponding experiments not only qualitatively but quantitatively as well.

After some simplifications, one can write the formula obtained by B. A. Kuznetsov for determining the average weight of the maximum fragment formed in breaking up of a cylindric case in the following form:

$$q_m = \chi \frac{\gamma_M}{k_p^2} \left(\frac{1 + \frac{a}{216 \cdot b}}{1 + \frac{a}{4}} \right)^2 \delta_0, \quad (6.7)$$

where q_m is the average weight of the maximum fragment; γ_M is the density of the case metal; δ_0 is the thickness of the case;

$$k_p = \sqrt{\frac{2(1-\mu)}{3-\mu}};$$

$$a = \frac{\gamma_{BB}}{\gamma_M} \frac{D^2}{c_e c_p};$$

$$b = \frac{\delta_0}{l_0} \frac{D}{c_e},$$

where μ is the Poisson coefficient of the case metal; γ_{BB} is the density of the VV; D is the detonation rate of the VV; c_e is the velocity of propagation of elastic deformations in the case metal; c_p is the velocity of propagation of plastic deformations in the case metal; l_0 is the case length.

The coefficient χ included in formula (6.7) depends on certain structural features of the case, on the properties of the case metal and on the filling coefficient and can vary within extremely broad limits. For example, with other conditions equal, the coefficient χ in shells with open ends is five times greater than the coefficient χ for shells with closed ends.

The formula presented makes it possible to determine the weight of the maximum fragment in regard to given geometric parameters of

the case with known properties of the case metal and the explosive and can be recommended for calculations in a case of a lack of experimental data on breaking up of the case.

However, for evaluating the efficiency of the effect of fragmentation ammunition, it is necessary to know fully the character of the distribution of fragments by weight, i.e., to know the histogram of $t^*(q)$ and the total number of fragments formed in the explosion N . In the absence of experimental data, the indicated characteristics of breaking up can be determined in a first approximation in the following way.

As theoretical and experimental research pertaining to study of the characteristics of breaking up of charge cases demonstrates, with variation in the structural data of the case and the charge (geometric dimensions, properties of the metal and properties of the VV), the weights of the fragments formed in an explosion q vary in approximately the same relationship as the weight of the maximum fragment q_m , and the numbers of fragments in different weight groups ΔN vary in approximately the same relationship as the total number of fragments N .

In other words, if the weight of the maximum fragment proves to be 100 g ($q_{m1}=100$) in bursting of one case, and the relative number of fragments with a weight less than 10 g is 0.6

$$(q_1 = 10 \text{ g}, \frac{q_1}{q_{m1}} = 0.1, \frac{1}{N_1} \sum_{q_1}^{q_{m1}} \Delta N_i = 0.6), \text{ for example, and the weight of}$$

the maximum fragment is 200 g ($q_{m2}=200$) in explosion of another case differing from the first in its structural data, the relative number of fragments with a weight less than 20 g will also be 0.6 for the second case:*

*Here N_1 and N_2 are the total numbers of fragments formed in breaking up of the first and second cases, respectively.

$$\left(q_2 = 20 \text{ t}; \frac{q_2}{q_m} = 0.1; \frac{1}{N_2} \sum_{q_i < q_2} \Delta N_i = 0.6 \right)$$

It has been mentioned above that the relative number of fragments whose weight is less than some given weight q represents an integral law of the distribution of fragments by weight. Consequently, one can confirm that the integral law of the distribution of fragments in regard to their relative weights does not depend on the structural parameters of the shell or the charge.

We shall designate the relative weight of a fragment as λ :

$$\lambda = \frac{q}{q_m} . \quad (6.8)$$

then, in accordance with the conclusion formulated above, one can assume that the form of the integral law of the distribution $T(\lambda)$ and, consequently, of the differential law $t(\lambda)$ does not depend in the first approximation on such parameters of the case and the charge as the properties of the case metal, the properties of the VV, the weight of the case metal, the filling coefficient, etc.

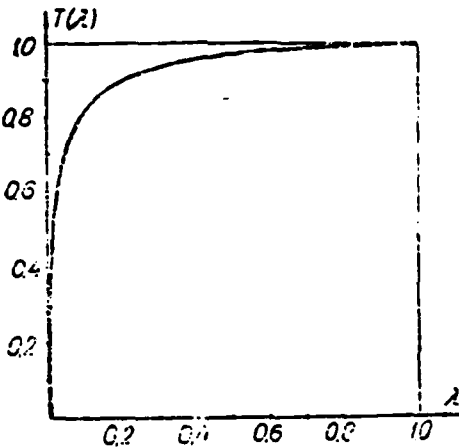


Fig. 6.15.

Laws of the distribution of fragments by relative weights $t(\lambda)$ and $T(\lambda)$ can be obtained based on processing of experimental data pertaining to research on the process of breaking up of fragmentation ammunition shells. An illustration of an integral distribution law $T(\lambda)$ is shown in Fig. 6.15. An analytical expression for the corresponding differential distribution law can be written in the following form:

$$t(\lambda) = A_1 \lambda^{-\alpha_1} (1 - \lambda)^{\beta_1}, \quad (6.9)$$

where α_1 and β_1 are constant coefficients characterizing the process of breaking up of fragmentation ammunition shells; A_1 is a norming factor of the distribution law.

The norming factor A_1 is determined from the following condition:

$$\int_0^1 t(\lambda) d\lambda = 1.$$

Integrating the distribution law (6.9), we obtain:

$$A_1 \int_0^1 \lambda^{-\alpha_1} (1 - \lambda)^{\beta_1} d\lambda = 1.$$

This integral is expressed in terms of familiar gamma functions:

$$\int_0^1 \lambda^{-\alpha_1} (1 - \lambda)^{\beta_1} d\lambda = \frac{\Gamma(1 - \alpha_1) \Gamma(1 + \beta_1)}{\Gamma(2 - \alpha_1 + \beta_1)}, \quad (6.10)$$

where

$$\Gamma(x) = (x - 1)!$$

One can find the values of the gamma function (factorial) in any mathematical handbook. The norming factor A_1 thus can be determined if the constant coefficients α_1 and β_1 characterizing the process of breaking up of shells in an explosion are known:

$$A_1 = \frac{\Gamma(2 - \alpha_1 + \beta_1)}{\Gamma(1 - \alpha_1) \Gamma(1 + \beta_1)}. \quad (6.11)$$

Using formulas (6.7), (6.8) and (6.9), and with a knowledge of the coefficients α_1 and β_1 , one can determine the law of the

distribution of fragments by weight for any warhead extremely simply in the first approximation, if it is not possible to conduct appropriate experiments in an armored chamber. The weight of the maximum fragment q_m is determined for this purpose by formula (6.7). The law of the distribution $t(q)$ is easily found with the use of familiar rules of probability theory:

$$t(q) = t(\lambda(q)) \frac{d\lambda}{dq}.$$

Keeping in mind formulas (6.8) and (6.9), we obtain

$$t(q) = A_1 q_m^{1+\alpha-3} q^{-\alpha} (q_m - q)^{\beta}. \quad (6.12)$$

It is more convenient to determine the integral law of the distribution of fragments by weight $T(q)$ graphically in such cases. It is obvious that replottedting of the distribution law $T(\lambda)$ shown in Fig. 6.15 as a law of the distribution of fragments by weight $T(q)$ can be reduced to increasing the scale of the λ axis by a factor q_m , because the relative weight of a fragment $\lambda=1$ corresponds to a fragment weight $q=q_m$.

Thus, having computed the weight of the maximum fragment q_m by formula (6.8) and having substituted its value into formula (6.12), we obtain an expression for the law of the distribution of fragments by weight $t(q)$. If it is necessary to obtain a law of the distribution of fragments in integral form $T(q)$, one must replot the graph of the function $T(\lambda)$ (Fig. 6.15) by the method indicated above, having computed the weight of the maximum fragment q_m preliminarily.

For evaluating the efficiency of the effect of fragmentation ammunition, it is also necessary to know the total number of fragments formed in an explosion. In a case of a lack of

experimental data, the total number of fragments can be determined by the formula

$$N = \frac{G_M}{\bar{q}},$$

where G_M is the weight of the case metal; \bar{q} is the average fragment weight.

The average fragment weight is expressed in terms of the relative average fragment weight $\bar{\lambda}$ and the maximum fragment weight q_m :

$$\bar{q} = \bar{\lambda} q_m$$

The relative average fragment weight (the mathematical expectation of the relative average fragment weight) $\bar{\lambda}$ can be determined by using the well-known formula

$$\bar{\lambda} = \int_0^1 \lambda t(\lambda) d\lambda$$

Substituting the value of $t(\lambda)$ from (6.9) into this formula and integrating, we obtain the following by analogy with formula (6.10):

$$\bar{\lambda} = A_1 \int_0^1 \lambda^{1-\alpha_1} (1-\lambda)^{\beta_1} d\lambda = A_1 \frac{\Gamma(2-\alpha_1) \Gamma(1-\beta_1)}{\Gamma(3-\alpha_1+\beta_1)}.$$

Keeping in mind formula (6.11), one can write the following expression for $\bar{\lambda}$:

$$\bar{\lambda} = \frac{\Gamma(2-\alpha_1)}{\Gamma(1-\alpha_1)} \frac{\Gamma(2-\alpha_1+\beta_1)}{\Gamma(3-\alpha_1+\beta_1)}.$$

However, according to determination of the gamma function,

$$\Gamma(x) = (x-1)! = (x-1)(x-2)! = (x-1)\Gamma(x-1).$$

Consequently,

$$\Gamma(2-\alpha_1) = (1-\alpha_1)\Gamma(1-\alpha_1);$$

$$\Gamma(3-\alpha_1+\beta_1) = (2-\alpha_1+\beta_1)\Gamma(2-\alpha_1+\beta_1).$$

Using these formulas, one can rewrite the final expression for the average relative fragment weight in the following form:

$$\bar{\lambda} = \frac{1-\alpha_1}{2-\alpha_1+\beta_1} = \text{const.}$$

The average fragment weight \bar{q} thus always amounts to a constant fraction of the maximum fragment weight q_m :

$$\bar{q} = \frac{1 - z_1}{2 - z_1 + \beta_1} q_m.$$

Then the formula for determining the total number of fragments formed in accordance with the pattern of breaking up considered above will have the following form:

$$N = \frac{2 - z_1 + \beta_1}{1 - z_1} \frac{G_u}{q_m}. \quad (6.13)$$

The weight of the maximum fragment included in expression (6.13) is determined by formula (6.7).

We shall note that there are several more empirical formulas for determining the total number of fragments. For example, the Yustrov formula for determining the number of fragments with a weight greater than 1 gram is well known:

$$N = c_{BB} \frac{\omega}{d} \frac{\sigma_e}{\delta \sigma_s} \frac{z_1^2 + 0.5}{z_1^2 - 1}, \quad (6.14)$$

where c_{BB} is a coefficient characterizing the properties of the VV [explosive]; ω is the weight of the VV charge; d is the case diameter; σ_e and σ_s are the elastic limit and the ultimate strength, respectively, of the case material; δ is the relative elongation of the shell material in breaking; z_1 is some coefficient which depends on the geometric dimensions of the case.

A similar formula of the following form also enjoyed extensive use at one time:

$$N = \beta_0 \frac{\omega}{d} \frac{z_1 R}{B}, \quad (6.15)$$

where β_0 is a coefficient which depends on the properties of the VV; $B=f(z_1, \psi)$ is a coefficient characterizing the properties of the metal and structural data of the case; ψ is the relative narrowing of a neck of the shell material; all the other variables

included in formula (6.15) have the same meaning as in formula (6.14).

The characteristics of breaking up necessary for evaluating the efficiency of the fragmentation effect - the total number of fragments N and the law of the distribution of fragments by weight $t(q)$ or $T(q)$ - thus can be determined either by processing the results of experiments on explosion of ammunition in armored chambers or, in the first approximation, by corresponding calculations by formulas (6.7), (6.12) and (6.13).

We shall note in conclusion that the characteristics of breaking up presented above and the methods for their determination by calculation pertain to a case in which no structural measures were taken in design of the ammunition for providing breaking up of the case into fragments of a given weight. In bursting of a charge case, as follows from consideration of the character of the distribution of fragments by weight, in addition to a large number of fragments of a low weight, which possess extremely low efficiency of the effect, extremely large fragments are also formed, and the efficiency of their effect, as a rule, proves excessive, and a considerable weight of the shell metal is spent on their formation. In connection with this, the need has arisen for providing breaking up of a case into identical fragments of a predetermined weight in some way.*

One can control the process of breaking up of a charge case for obtaining fragments of a predetermined weight by various

*The weight of such a fragment obviously can be determined after appropriate calculations from the condition of providing maximum efficiency of the effect. The optimum fragment weight depends primarily on the vulnerability of the target in relation to the fragmentation effect, on the velocity of impact of a fragment with the target, etc.

design methods. The basic idea of all these methods lies either in altering the characteristics of the effect of the explosive load on the charge case by giving the outer surface of the charge a special shape or in changing the picture of the stressed state of the case in explosion by preconceived weakening of the strength of the shell walls in the appropriate sections.



Fig. 6.16.

One can obtain the assigned fragmentation, for example, if one applies circular and lengthwise shaped-charge recesses on the outer surface of the VV charge (Fig. 6.16). In detonation of such a charge, the pressure of the explosion products will be distributed unevenly over the inner surface of the case. Pressure "surges" (the shaped-charge effect) will occur directly opposite the shaped-charge recesses; the arrangement of these surges is determined by the pattern of the arrangement of shaped-charge recesses on the charge. As a result, failure of the case will occur predominantly along sections located in the zone of the effect of increased explosive loads; i.e., in explosion of such a charge, the case will break up into fragments whose dimensions and, consequently, whose weight are determined by the distances between shaped-charge recesses on the charge.

Predetermined fragmentation of a charge case can be provided only by means of special grooves on the outer and inner surface of the case (Fig. 6.17). The indicated grooves, which weaken the strength of the case walls, can be applied by appropriate machining

of the case (turning, milling, cold rolling, etc.). The grooves can be arranged on the case surface in different ways: a system of circular and lengthwise grooves (Fig. 6.18), a system of spiral grooves with right and left threading (Fig. 6.19), etc. It is obvious that with a given thickness of the case walls, the number and arrangement of such grooves determine the dimensions and weights of the fragments formed.

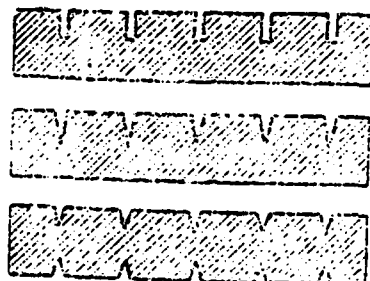


Fig. 6.17.



Fig. 6.18.



Fig. 6.19.

In accomplishment of predetermined breaking up by means of grooves of different kinds, breaking up of a case normally occurs in a less regular way in cross sections; i.e., not all of the transverse grooves result in breaking up of the case into the predetermined number of rings. In connection with this, obtaining fragments of a given weight can be ensured due to manufacture of the case either from separate rings placed on an additional thin-walled charge case (Fig. 6.20) or from a bar of the appropriate cross section coiled in the form of a spring (Fig. 6.21). Such structural methods for production of fragments of the assigned weight can be combined with the methods described previously for providing regular breaking up of rings or spring coils in lengthwise directions (lengthwise grooves which weaken the sections of the rings, lengthwise shaped-charge recesses on the charge surface, etc.).

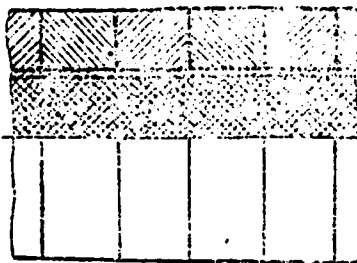


Fig. 6.20.

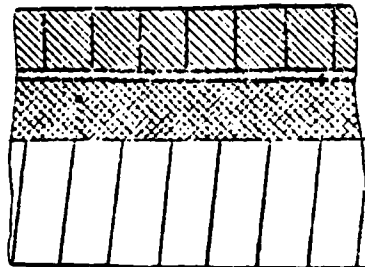


Fig. 6.21.

We shall note that the limit for structural changes of a charge case made for producing fragments of a predetermined weight is a case produced from finished fragments. In this case, fragments of the assigned weight are fitted in a definite order between a thin-walled charge case and the outer shell case. The fragments should be packed in such a way as to prevent, insofar as possible, the breaking through of detonation products before the moment of complete separation of the fragments from each other. Otherwise great losses of energy of the gases will occur in radial expansion of the detonation products, which will lead to a noticeable decrease in the initial velocity of the fragments. All the methods described above for providing regular breaking up of a charge case into fragments of a predetermined weight thus require appropriate modification of the design of the charge and the case (shaped-charge recesses on the charge, grooves and notches of different kinds on the inner or outer surface of the case, etc.). The specific structural parameters of all these changes are normally selected experimentally. The number of fragments of the assigned weight formed in fragmentation of such cases is determined by the pattern of preliminary division of the case with weakening sections. One must keep in mind that the process of breaking up of a case into fragments of a predetermined weight is accompanied by the formation of a large number of very fine fragments from metal adjoining the zone of the weakened sections (the result of different kinds of additional failures and fragments); therefore, the actual weight of a regular fragment formed in fragmentation proves to be somewhat less than the calculated fragment weight.

§ 4. THE LAW OF THE DISTRIBUTION OF FRAGMENTS BY DIRECTIONS OF SCATTERING

In calculations of the efficiency of the fragmentation effect, it is necessary to know the number of fragments which have hit the target with given mutual positions of the warhead and the target.

It is obvious that with other conditions the same, the number of fragments which have hit the target in the final analysis depends on the character of the distribution of fragments in space.

In consideration of the physics of the phenomenon of explosion of a charge in a cylindric case, it was established that the character of scattering of fragments in space, i.e., the character of the distribution of directions in which the fragments scatter, is determined by the shape taken on by the case expanding under the influence of detonation products by the moment of its failure and the formation of fragments.

After failure of the case, each fragment, having taken on its respective initial velocity, will fly in the direction of movement of the component of the expanding case from which the fragment in question was formed. The direction of movement of each component of the case before bursting, in turn, approximately coincides at each given moment with the direction of a perpendicular to the case surface. Therefore, one can assume that the direction in which a fragment will fly practically coincides with a perpendicular to the case surface at the moment of failure of the case (Fig. 6.22).

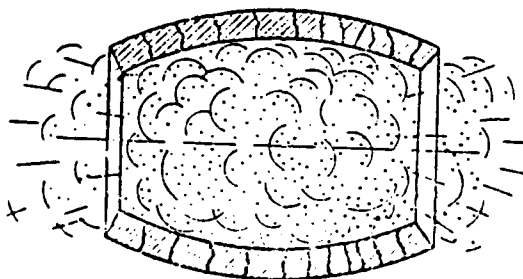


Fig. 6.22.

In a system of coordinates related to the warhead, it is customary to define the direction of further flight of a fragment

by two angles: the angle ϕ in the meridian plane and the angle θ in the equatorial plane (Fig. 6.23). In consideration of the character of the distribution of scattering directions of fragments in space, all the fragments are assumed to take off from a single point O - the center of mass of the warhead; i.e., the dimensions of the warhead as compared to the dimensions of the region of scattering of the fragments are neglected. Since all ammunition possesses axial symmetry, one can also assume that all the fragments are evenly distributed in the equatorial plane.

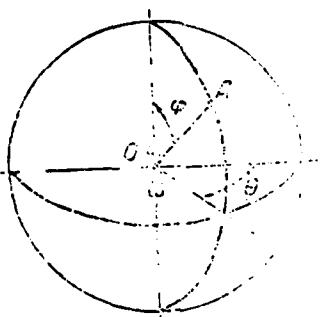


Fig. 6.23.

In reality, some irregularity occurs in the distribution of the fragments in regard to the angle θ , which is explained by the effect of such statistical factors as deviations of the structural parameters of the case and the charge from their nominal values (the presence of eccentricity, in particular), possible asymmetry in placement of the detonator, a random character of breaking away of a fragment at the moment of its formation, a random character of further flowing of detonation products around the fragments, etc., on the fragmentation process. However, when one keeps in mind that the distribution of fragments in regard to the angle θ differs only slightly from a uniform distribution, and that taking into account the effects of the statistical factors indicated above is impossible at present, the picture of the distribution of fragments in the equatorial plane is assumed to be symmetrical in all calculations.

Thus, in order to characterize the distribution of fragments in space, one must know only the distribution of fragments in the meridian plane, i.e., in regard to the angle ϕ .

Fig. 6.24.

The character of the distribution of fragments in the meridian plane can be determined experimentally. It is necessary for this purpose to explode a warhead in a special target installation, which is a vertical wall constructed in the shape of a half cylinder; the test model is placed at the center of the half cylinder in a horizontal position (Fig. 6.24). The wall is covered with plywood, cardbord, ruberoid or any other utility material in which a clear hole is formed in piercing by a fragment.* Contours of a projection of part of a sphere enclosed between two meridian sections, the angular distance between which $\Delta\theta$ determines the relative number of fragments intercepted by the target installation and recorded in the experiment, are applied to the wall (for example, if $\Delta\theta$ is 9° , 1/40 of the sphere of scattering of the fragments is used in conducting the experiments; i.e., 1/40 of the total number of fragments formed in the explosion are intercepted).

Vertical lines corresponding to boundaries of angle sectors with some spacing $\Delta\phi$ are also applied to the wall. The target installation

*Such a target installation, as already mentioned, is also used in determining the law of the distribution of areas of holes of fragments necessary for plotting the law of the distribution of fragments by weight by a calculation method.

is shown in unfolded form in Fig. 6.25. The warhead is situated at the height of the middle line AB in the explosion.

A target installation thus makes it possible to record holes from fragments flying in each of the angular intervals $\Delta\phi$ whose boundaries are defined by angles ϕ_j :

$$\phi_0, \phi_1, \phi_2, \dots, \phi_{j-1}, \phi_j, \dots, \phi_{n-1}, \phi_n.$$

It is obvious that $\phi_0=0^\circ$, $\phi_n=180^\circ$ and

$$\Delta\phi = \phi_j - \phi_{j-1}.$$

For example, if $\Delta\phi=5^\circ$, one can record fragments flying in the following angular intervals in conducting the experiments:

$$0-5^\circ; 5-10^\circ; 10-15^\circ \dots 170-175^\circ; 175-180^\circ.$$

After accomplishment of the explosion, the numbers of fragments ΔN_j , which have hit each angle sector and the total number of fragments intercepted by the target installation N are determined. Since the statistical factors indicated above give the distribution of fragments a random character, the numbers of fragments in each angle sector ΔN_j and the total number of fragments N will vary from one explosion to another in explosion of the same ammunition. In connection with this, several explosions are normally conducted, and the average values of ΔN_j and N are determined.

The ratio $\Delta N_j/N$ is the statistical probability that a fragment will fly in a given angle sector; i.e., this ratio is equal to the relative number of fragments which fly in an angular interval $\phi_{j-1}-\phi_j$.

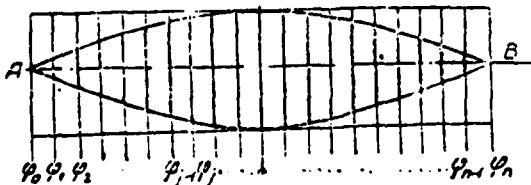


Fig. 6.25.

The law of the distribution of fragments in regard to the direction of scattering is represented in the form of a histogram of the distribution $f^*(\phi)$:

$$f^*(\phi) = \frac{\Delta N_j}{\Delta \phi N} \quad (6.16)$$

An illustration of a histogram of the distribution for most fragmentation ammunition has the form shown in Fig. 6.26.

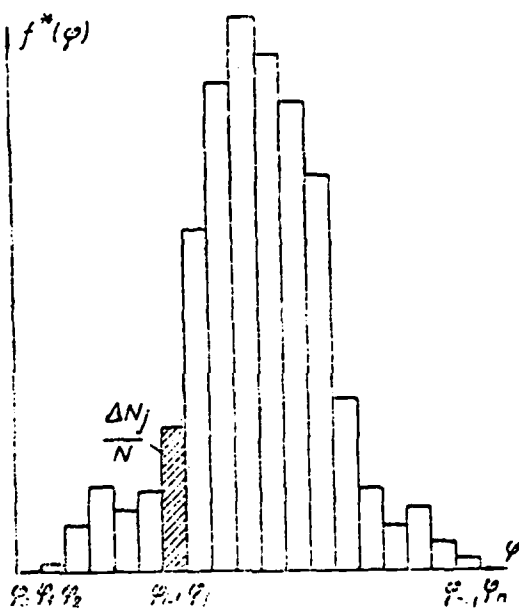


Fig. 6.26.

It follows from formula (6.16) that the area of each rectangle of the histogram is equal to the relative number of fragments $\Delta N_j/N$. It is also obvious that the total area of all the rectangles is equal to one.

It should be noted that the histogram of the distribution $f^*(\phi)$ is plotted according to experimental data pertaining to some angle sector $\Delta\theta$ in the equatorial plane. As a result of the assumed

regularity of the distribution of fragments in the equatorial plane, the relative number of fragments flying between two conical surfaces with aperture angles $2\phi_j$ and $2\phi_{j-1}$, respectively, is as follows:

$$\Delta N_j \frac{360}{\Delta\theta}$$

and the total number of fragments formed in the explosion is as follows:

$$N \frac{360}{\Delta\theta}$$

Due to the circumstances which have been mentioned, one can assume that the distribution histogram, whose ordinates are determined by formula (6.16), characterizes the law of the distribution of all fragments in regard to scattering directions, because the statistical probabilities of the appearance of fragments in a given angle sector and between corresponding conical surfaces are equal:

$$\frac{\Delta N_j \frac{360}{\Delta\theta}}{N \frac{360}{\Delta\theta}} = \frac{\Delta N_j}{N}$$

Therefore, we shall assume hereinafter that the numbers of fragments ΔN_j and N pertain to the entire fragment scattering sphere.

It follows from consideration of the distribution histogram shown in Fig. 6.26 that in explosion of real ammunition, the main mass of fragments flies in directions near a perpendicular to the cylindric part of the cases. Some part of the fragments from the ogival part of the case fly forward, and an insignificant part of the fragments formed in fragmentation of the tail section fly backward.

An extremely characteristic indicator of the law of scattering of fragments is the average direction of scattering of the fragments in space (the mathematical expectation of the direction of scattering), which is determined according to the well-known formula

$$\bar{\varphi} = \sum_{j=0}^N \varphi_j f^*(\varphi) \Delta \varphi.$$

The average direction of scattering for all ammunition normally practically coincides with the direction of a normal to the cylindric part of the charge case ($\bar{\phi} \approx 90^\circ$).

For convenience of subsequent calculations, it is more efficient to represent the distribution of fragments by scattering directions in the form of a statistical integral law of the distribution $F^*(\phi)$:

$$F^*(\phi) = \frac{N(\phi)}{N}, \quad (6.17)$$

where N is the total number of fragments; $N(\phi)$ is the number of fragments flying in a cone with an aperture angle 2ϕ .

It is obvious that

$$N(\phi) = \sum \Delta N_j, \quad (6.18)$$

where the summation is extended to values of the index j for which $\phi_j < \phi$.

Consequently, the integral law of the distribution of fragments by scattering directions is the relative number of fragments flying in a cone with an aperture angle 2ϕ . Figure 6.27 shows a graph of a statistical integral law of $F^*(\phi)$ corresponding to the distribution histogram shown in Fig. 6.26. The ordinates of the integral law are in the form of the sum of areas of rectangles of the histogram located to the left of the point ϕ , because based on formulas (6.18) and (6.16), one can write

$$F^*(\phi) := \frac{1}{N} \sum \Delta N_j = \sum f^*(\varphi) \Delta \varphi.$$

where the summation is extended as before to values of the index j for which $\phi_j < \phi$.

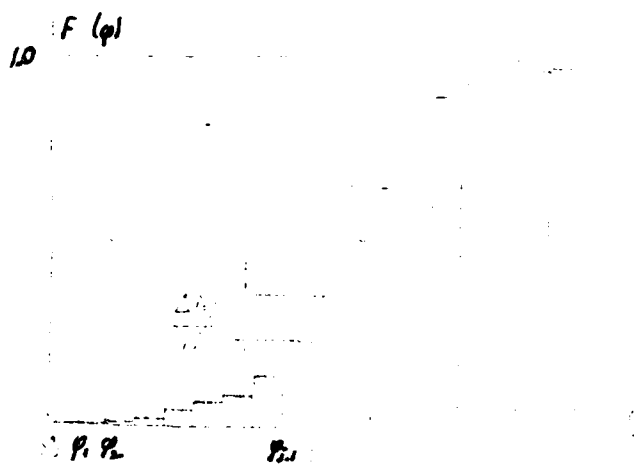


Fig. 6.27.

Using familiar methods of smoothing of step functions, one can replace the histogram of the distribution $f^*(\phi)$ with some continuous function $f(\phi)$, which would have its own analytical expression. The function $f(\phi)$ obtained in this way is simply the differential law of the distribution of fragments by directions of scattering.

The corresponding integral distribution law can be found by a well-known formula of probability theory:

$$F(\phi) = \int_0^\phi f(\varphi) d\varphi$$

Graphs of functions $f(\phi)$ and $F(\phi)$ corresponding to the histogram of $f^*(\phi)$ and the integral statistical law $F^*(\phi)$ are shown in Figs. 6.28 and 6.29.

However, there is no need to have an analytical expression for the function $F(\phi)$ in solving practical problems; therefore, the functions $F^*(\phi)$ are normally smoothed by an extremely

approximate method (Fig. 6.30).

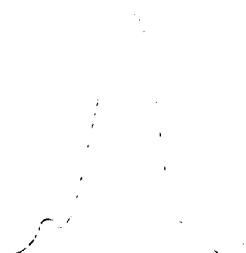


Fig. 6.28.



Fig. 6.29.

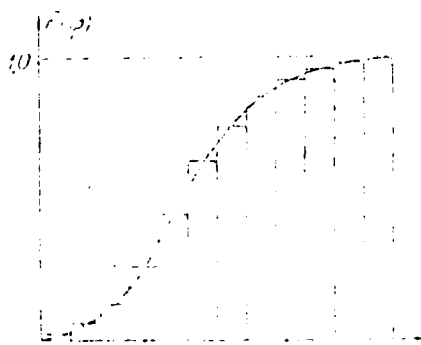


Fig. 6.30.

Using available analytical expression or graphs of the distribution laws in differential and integral form, one can determine the numbers of fragments flying between two conical surfaces with aperture angles $2\phi_1$ and $2\phi_2$, respectively:

$$N_{\phi_1.. \phi_2} = N \int_{\phi_1}^{\phi_2} f(\phi) d\phi \quad (6.19)$$

or

$$N_{\phi_1.. \phi_2} = N |F(\phi_2) - F(\phi_1)|. \quad (6.20)$$

Thus, with experimental data on the results of explosion of ammunition in the target installation described above, one can plot a histogram of the distribution of $f^*(\phi)$ and the statistical integral law of the distribution of $F^*(\phi)$ and then, smoothing the graph of $F^*(\phi)$ by an approximate method, one can determine the graph of the function $F(\phi)$ necessary for further calculations.

It should be noted that the law of the distribution of fragments by scattering directions can also be obtained by calculation. The basic content of such calculations boils down to determining the shape of the charge case at the moment of its breaking up into fragments, because, as already noted, the direction in which the fragments formed from a given case section fly approximately coincides with the direction of a perpendicular to the case surface at the moment of bursting of the case. Consequently, having determined the shape of the charge case at the moment of its breaking up, one can find the direction of flight of the fragments formed from the case section in question.

The number of fragments ΔN_j scattering in a given direction $\phi_{j-1} - \phi_j$, i.e., the number of fragments formed in breaking up of a section of the case under consideration, can be determined by appropriate calculations, which were referred to in the previous section (we shall recall that the intensity of fragmentation of the charge case depends on the character of the distribution of

the explosive load along the length of the case; therefore, the numbers of fragments formed in breaking up of different sections of the case will be different).

However, calculation methods for determining the law of scattering of fragments can be applicable only to cylindric charge cases, because determination of the shape of the case at the moment of its breaking up and of the number of fragments formed from any section of the case for real ammunition with an ogival-cylindric shape is involved with solution of an exceptionally complex problem of the dynamic expansion of axially symmetric cases.

In addition, calculation methods do not make it possible to take into consideration the effects of a number of random factors which determine the process of breaking up of the case, the formation of fragments, possible changing of the initial direction of flight of a fragment as a result of flowing of detonation products around the fragment, etc., to a considerable extent on the character of fragment scattering. Therefore, only the method for experimental determination of the laws of scattering of fragments described above is finding use at present. Nevertheless, one can establish the qualitative effects of different structural parameters of the case and the charge on the character of the distribution of fragments by directions based on the results of calculations to determine the laws of scattering of fragments.

Basic conclusions obtained in such a consideration coincide with the results of corresponding experiments to determine the laws of scattering of fragments and amount to the following.

The character of the distribution of fragments by scattering directions is determined primarily by the shape of the case and the charge. In cases of a cylindric shape, the basic mass of the fragments scatters in a comparatively narrow angle sector in a

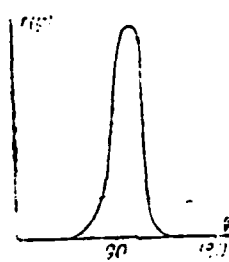


Fig. 6.31.



Fig. 6.32.

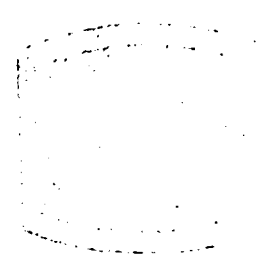


Fig. 6.33.

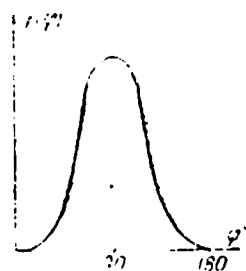


Fig. 6.34.

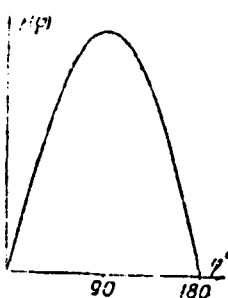


Fig. 6.35.

direction which approximately coincides with a perpendicular to the case surface (Fig. 6.31). An even narrower scattering cone can be obtained by giving the case the shape shown in Fig. 6.32 (cases of a spool shape). In cases whose generatrix has a convex form (cases of a barrel shape) (Fig. 6.33), the angle sector of scattering of the fragments increases to a greater degree the greater the curvature of the generatrix. Figure 6.34 as an illustration shows a sample view of the law of the distribution of fragments $f(\phi)$ for a case with a generatrix of a convex form, while Fig. 6.35 shows the law of the distribution of fragments $f(\phi)$ of a case of spherical form (the limit form of cases with a convex form of the generatrix). Such an effect of the charge shape on the character of scattering of fragments is quite explicable if one keeps in mind that the fragments scatter in directions near a perpendicular to the case surface at the moment of its breaking up, and the shape of the case at the moment of bursting depends to a great extent on the initial shape of the case.

The position of the detonator in the charge also influences the law of the distribution of fragments by scattering directions, because the position of the point of initiation, with other conditions the same, influences the character of the distribution of the explosive load along the length of the case and, consequently, the shape of the case at the moment of its bursting. If the point of initiation is located at one end of the charge, the effect of

the position of the initiation point on the law of the distribution of fragments by scattering directions boils down to a shift of the distribution maximum in a direction opposite from the position of the initiation point by $5-15^\circ$.



Fig. 6.36.

In particular, the distribution law shown in Fig. 6.31 corresponds to explosion of a cylindric charge from the end from which the angle ϕ is measured; the average scattering direction and the maximum of the distribution law, as follows from a consideration of Fig. 6.31, are deflected from the perpendicular by approximately 10° .



Fig. 6.37.

In a case of the use of bilateral initiation (initiation of the charge is effected simultaneously from both ends of the charge), the average scattering direction coincides with a perpendicular to the charge surface; the aperture angle of the sector in which the fragments fly in this case will be substantially less than in a case of unilateral initiation.

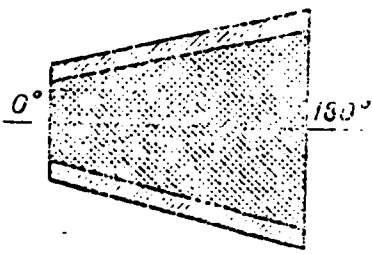


Fig. 6.38.

The joint effect of the shape of the charge and the method of initiation can be illustrated by distribution laws shown in Figs. 6.36 and 6.37 and pertaining to a case of explosion of a charge case manufactured in the form of a truncated cone (Fig. 6.38).

In this case, the distribution shown in the figures corresponds to a case of initiation from the larger end of the charge for Figs. 6.36 and the smaller end for 6.37.

To the extent that such structural parameters of the case and the charge as the filling coefficient, the properties of the case metal, the properties of the VV [explosive], the presence or absence of closed ends of the charge, etc., influence the shape of the case by the moment of its bursting, an effect of these factors on the law of scattering of fragments in regard to directions is also exhibited. In particular, the average direction of scattering of the fragments shifts somewhat in the direction of larger angles ϕ with an increase in the filling coefficient; the aperture angle of the sector of scattering of the fragments increases slightly in this case. Charge cases manufactured from brittle metal produce scattering of fragments characterized by somewhat smaller angles of the scattering sector than cases manufactured from a tougher metal. The effects of other structural factors on the law of scattering of fragments are so insignificant that considering them makes no

practical sense.

The data presented above on laws of scattering of fragments pertain to a case of explosion of ammunition in a stationary state. In reality, however, all ammunition has some inherent velocity at the moment of bursting.

In the presence of an inherent velocity of the warhead, the picture of scattering of fragments and the character of their distribution in space can change significantly. While a fragment had an initial velocity oriented at an angle ϕ in relation to the warhead axis under conditions of stationary explosion, in the presence of an inherent velocity of the projectile, the angle formed by this fragment with the axis of the warhead will decrease and become equal to the angle ϕ' (Fig. 6.39).

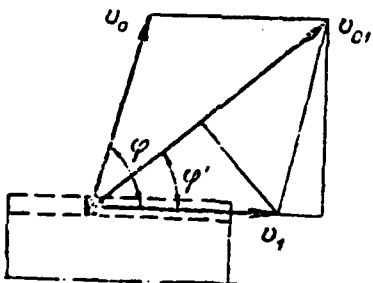


Fig. 6.39.

The presence of an inherent velocity at the moment of bursting thus leads to a change in the direction of scattering of the fragments, i.e., to contraction of the flow of fragments (a decrease in the angle sector in which the basic mass of fragments is scattered) and a shift in the average direction of scattering of fragments toward the direction of movement of the bomb or projectile (a decrease in the angle ϕ). In addition, the presence of an inherent velocity at the moment of bursting leads to some

increase in the initial velocity of a fragment in the trajectory.

It follows from consideration of Fig. 6.39 that the angles ϕ and ϕ' are related by the following relationship:

$$\tan \phi' = \frac{v_0 \sin \phi}{v_1 + v_0 \cos \phi}$$

where v_0 is the initial velocity of the fragment; v_1 is the inherent velocity of the warhead at the moment of bursting.

The initial velocity of the fragment on the trajectory, with consideration for the inherent velocity of the bomb at the moment of bursting, can also be determined based on the diagram of Fig. 6.39:

$$v_{01} = \sqrt{v_0^2 + v_1^2 + 2v_0 v_1 \cos \phi}$$

In addition, the velocity v_{01} can be expressed in terms of the angle ϕ' - the angle formed by the fragment with the axis of the warhead in a case where the latter has a velocity v_1 at the moment of bursting:

$$v_{01} = v_1 \cos \phi' + \sqrt{v_0^2 - v_1^2 \sin^2 \phi'}. \quad (6.21)$$

If we introduce the relative velocity of the bomb w_1 into the consideration,

$$w_1 = \frac{v_1}{v_0},$$

the formula for determining the angle ϕ' will be written in the following form:

$$\phi' = \arctan \frac{\sin \phi}{w_1 + \cos \phi}. \quad (6.22)$$

Graphs of the dependence of the angle ϕ' on the angle ϕ for different relative velocities w_1 are shown in Fig. 6.40.

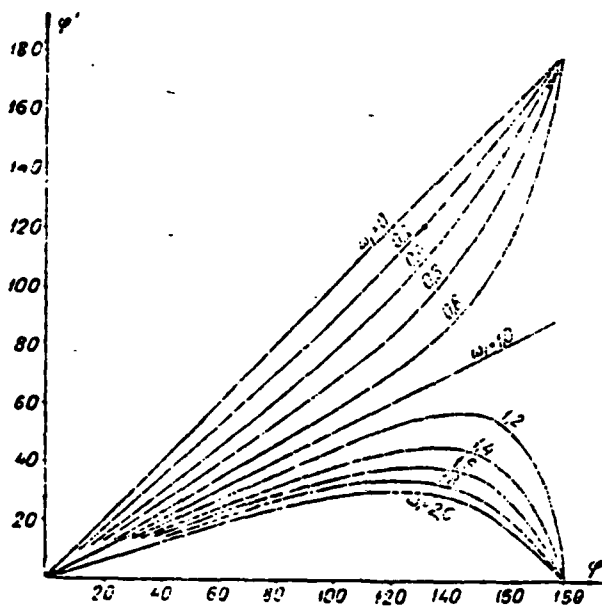


Fig. 6.40.

With a knowledge of the law of the distribution of fragments under conditions of a stationary explosion, using formula (6.22) or this graph, one can obtain the distribution law corresponding to some velocity of the warhead at the moment of bursting.

Such a problem can be solved most simply in a case where the law of the distribution of fragments of a stationary bomb is given in integral form. We shall assume that the integral law of the distribution of fragments by directions $F(\phi)$, plotted according to explosion results and smoothed by a graphic method, is known. The ordinate of the law of the distribution $F(\phi)$ is the relative number of fragments flying within a cone with an aperture angle 2ϕ .

In the case of bursting of a moving bomb, the angle ϕ' will correspond to the angle ϕ , and the value of the angle ϕ' is determined by formula (6.22). The number of fragments flying within a cone with an angle at the peak equal to 2ϕ in a case of

a stationary explosion obviously will be equal to the number of fragments flying within a cone with an aperture angle $2\phi'$ in a case of bursting of a moving warhead.

If we designate the law of the distribution of fragments of a moving warhead as $f_v(\phi')$, it follows from the considerations which have been presented above that

$$F(\phi) = F_v(\phi'). \quad (6.23)$$

Thus, for determining the desired law $F_v(\phi')$, it is necessary to replot the curve of $F(\phi)$ so that the condition (6.23) is fulfilled; i.e., the replotting can be reduced to replotting the graph of $F(\phi)$ only in regard to the abscissa axis with preservation of the same ordinates. Such a replotting is shown in Fig. 6.41 for one point ϕ_j . Having computed the angle ϕ'_j corresponding to a given angle ϕ_j by formula (6.22), we enter it on the ϕ axis. Then, due to the condition (6.23), the point M' of the curve of $f_v(\phi')$ has the same ordinate as the point M of the curve of $F(\phi)$, because the relative number of fragments flying within a cone with an angle at the peak $2\phi'$ is equal to the relative number of fragments flying in a cone with 2ϕ for a stationary warhead. By performing similar replotting for a number of selected values of ϕ and connecting the points obtained with a smooth curve, one can plot a graph of the desired law $F_v(\phi')$.

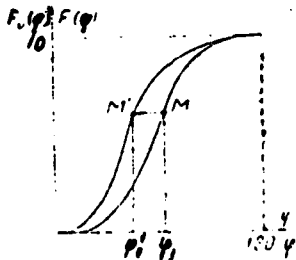


Fig. 6.41.

The law of the distribution of fragments by scattering directions obtained in this manner is included in further calculations to evaluate the efficiency of the effect of fragmentation ammunition. The differential distribution law corresponding to this integral law is normally designated as $f_v(\phi')$.

§ 5. THE INITIAL VELOCITY OF FRAGMENTS

It has been demonstrated above that for replotting the law of the distribution of fragments by scattering directions, it is necessary to know the initial velocity of the fragments v_0 . In addition, the initial velocity of a fragment determines its velocity on the trajectory at the moment of impact with the target and, consequently, determines the efficiency, in the final analysis, of the effect of a fragment which has hit the target.

It was established in consideration of the physical picture of the phenomenon of explosion of a charge in a case that the initial velocity of the fragments is determined by the maximum velocity of radial expansion of the case, i.e., the velocity of movement of individual elements of the case at the moment of its breaking up. Since the velocity of escape of detonation products from cracks formed in breaking up of the case exceeds the velocity of expansion of the bursting case, the detonation products, in continuing to expand after formation of the fragments, will blow the fragments out, imparting some additional velocity to them.

The value of the initial velocity of scattering of the fragments can be determined either experimentally or by calculations according to the appropriate formulas. The basic idea of experimental methods for determining the initial velocity lies in determining the time of flight by a fragment for a distance from the point of explosion to some screen (the moment when the fragment pierces the screen can be recorded with a high-speed movie camera). If one knows this time,

he can compute the initial velocity of the fragments by formulas which will be obtained in the next section.

The initial velocity of scattering of fragments can be determined directly by calculations according to special formulas which make it possible to compute the initial velocity of fragments if structural data of the warhead are known. Most of the formulas of this kind were obtained based on processing of results of appropriate experiments. The simplest of them has the following form:

$$v_0 = a_0 \sqrt{\gamma_1} \quad (6.24)$$

where v_0 is the initial velocity of the fragments; γ is the filling coefficient; a_0 is some coefficient which depends on the properties of the VV (for example, $a_0 = 2500$ for trotyl).

This class of formulas also includes another formula in which the properties of the case metal are taken into consideration in some way:

$$v_0 = a_0 \frac{\frac{1}{\psi^{50}}}{\frac{1}{\sigma^{27}}} \sqrt{\gamma_1} \quad (6.25)$$

where v_0 is the initial velocity of the fragments; γ is the filling coefficient; a_0 is some coefficient which depends on the properties of the VV (for example, $a_0 = 3000$ for trotyl); ψ is the relative narrowing of the cross section of the case metal ($\psi = 0.4$ for steel; $\psi = 0.03$ for semisteel cast iron); σ is the breaking point of the case metal ($\sigma = 70 \text{ kg/mm}^2$ for steel; $\sigma = 20 \text{ kg/mm}^2$ for semisteel cast iron).

Formulas obtained as a result of more or less detailed theoretic theoretical study of the process of expansion of the charge case under the influence of detonation products are also well known.

The derivation of such formulas is based on integration of the

equation of motion of a case expanding under the influence of internal pressure of the detonation products and determination of the velocity of movement of case elements at the moment of breaking up of the case.

Since the explosive load is unevenly distributed along the length of the case, calculation formulas obtained based on such a consideration make it possible to determine the initial velocity of fragments formed from any section of the case. In particular, in bursting of a case with open ends, as corresponding calculations demonstrate, fragments formed from sections of the case in which the greatest explosive loads are active have the maximum initial velocity; fragments formed from sections of the case near the ends have a velocity which differs noticeably from the maximum value. The distribution of velocities of fragments along the length of the case generatrix is shown as an illustration in Fig. 6.42. Such a character of the distribution of initial velocities of the fragments also finds experimental confirmation. It should be noted that the irregularity of the distribution of initial velocities of fragments which has been mentioned is exhibited to only a slight degree for cases with closed ends (the real pattern of fragmentation ammunition).

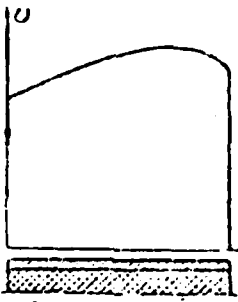


Fig. 6.42.

Therefore, the average velocity of all the fragments, regardless of the point of their formation, is introduced into the calculation in evaluating the efficiency of the effect of

fragmentation ammunition. It is just these average initial velocities of the fragments which are determined by the formulas (6.42) and (6.43) presented above. However, as a result of the fact that these formulas produce large discrepancies with the results of experiments, and the use of more accurate formulas which make it possible to take into consideration the irregularity of the distribution of initial velocities of the fragments along the length of the case leads to considerable complication of the calculations, formulas for determining the average velocity of scattering of fragments whose derivation is based on the use of general energy patterns of the phenomenon of explosion of a charge in a case have come into extensive use in practical work of calculations involved with evaluating the efficiency of the fragmentation effect.

The derivation of the formula of Professor G. I. Pokrovskiy will be given below as an illustration of methods and procedures on which the derivation of such formulas is based.

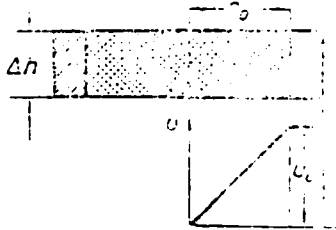


Fig. 6.43.

We shall consider a cylindric charge case of infinite length and shall cut from it some element with a length Δh (Fig. 6.43) by two equatorial cuts. We shall designate the mass of the case element at m_0 and the mass of the charge element as m_{BB} . We shall assume that the process of detonation of the charge element in question has been completed, and radial expansion of the detonation products is beginning, as a result of which some initial velocity

v_0 will be imparted to the fragments formed in breaking up of the case. It is obvious that at this moment (i.e., at the moment of breaking up of the case and the beginning of escape of detonation products through cracks of the case), the velocity of radial expansion of the detonation products directly adjacent to the inner surface of the charge case will also be equal to v_0 .

The velocity of radial movement of internal layers of expanding detonation products at the moment in time which is under consideration naturally will be less than v_0 , and the closer to the charge axis a given layer is located, the lower its velocity will be (in particular, detonation products located at the charge axis will have a velocity equal to zero). Corresponding gas dynamic calculations indicate that an approximately constant velocity gradient is established within the expanding detonation products at the moment of breaking up of the charge case; i.e., the velocity of the detonation products varies according to a linear law (Fig. 6.43):

$$v = v_0 \frac{r}{r_0}, \quad (6.26)$$

where r_0 is the inner radius of the case.

(We shall note that a similar picture occurs in the bore in firing a round, when the velocity of powder gases moving in the wake of the projectile is assumed to vary at each given moment in time according to a linear law.)

We shall determine the kinetic energy of expanding detonation products contained in an elementary circular layer with a thickness dr , the radius of which is r :

$$dE_{\text{kin}} = \frac{v^2}{2} dm_{\text{BB}}. \quad (6.27)$$

here dE_{kin} is the kinetic energy of the elementary circular layer; dm_{BB} is the mass of detonation products of the elementary layer

(the mass of the VV located in the layer in question before detonation).

- It is obvious that -

$$dm_{BB} = \rho_{BB} (2\pi r) \Delta h dr, \quad (6.28)$$

where ρ_{BB} is the density of the VV.

Substituting the value of the velocity v from (6.26) and the value of the mass dm_{BB} from (6.28) into (6.27), we have

$$dE_{DD} = \frac{\pi \rho_{BB} \Delta h v_0^2}{r_0^2} r^3 dr.$$

By integrating the expression obtained, one can determine the total kinetic energy of expanding detonation products:

$$E_{DD} = \frac{\pi \rho_{BB} \Delta h v_0^2}{r_0^2} \int_0^{r_0} r^3 dr = \frac{\pi}{4} \rho_{BB} r_0^2 \Delta h v_0^2.$$

We shall note that

$$\pi r_0^2 \Delta h \rho_{BB} = m_{BB}.$$

Consequently,

$$E_{DD} = \frac{1}{4} m_{BB} v_0^2. \quad (6.29)$$

However, the charge case will also be drawn into motion by expanding detonation products after detonation of the charge. The kinetic energy absorbed by the charge case (the energy of case fragments) can be determined by the formula

$$E_0 = \frac{m_0 v_0^2}{2}. \quad (6.30)$$

Movement of the detonation products and the fragments will occur due to potential energy released in detonation of the VV charge.

We shall designate the specific energy of the VV as u_1 (u_1

is the energy released in explosion of a unit of mass of the VV in the case in question; u_1 is expressed in $\text{kgf}\cdot\text{m}/\text{t.e.m.}$ [technical unit of mass], or, expressing the t.e.m. as $\text{kgf}\cdot\text{s}^2/\text{m}$, we obtain the units m^2/s^2 for u_1 ; for example, $u_1 = 4.1 \cdot 10^6 \text{ m}^2/\text{s}^2$ for trotyl). It is obvious, then, that the total energy released in detonation of the part of the charge in question will be as follows:

$$E = u_1 m_{BB}. \quad (6.31)$$

If one assumes in the first approximation that all the energy of the VV is spent on imparting velocity to the expanding detonation products and on throwing the fragments, one can write the following based on the law of the conservation of energy:

$$E = E_{kin} + E_0. \quad (6.32)$$

Or, keeping in mind (6.29), (6.30) and (6.31):

$$u_1 m_{BB} = \frac{m_{BB} v_0^2}{4} + \frac{m_0 v_0^2}{2}.$$

Solving the equation obtained for v_0 , we have the following:

$$v_0 = \sqrt{\frac{2u_1}{\frac{m_0}{m_{BB}} + \frac{1}{2}}}. \quad (6.33)$$

We shall express the ratio m_0/m_{BB} in terms of the filling coefficient η :

$$\frac{m_{BB}}{m_0 + m_{BB}} = \eta.$$

from which we have

$$\frac{m_0}{m_{BB}} = \frac{1}{\eta} - 1. \quad (6.34)$$

Substituting (6.34) into (6.33), we finally obtain the following formula for determining the average initial velocity of scattering of fragments:

$$v_0 = \sqrt{\frac{2u_1}{\frac{1}{\eta} - \frac{1}{2}}}. \quad (6.35)$$

Formula (6.35), as follows from (6.32), was obtained on the assumption that all the energy of the VV is spent only on radial expansion of the detonation products and imparting of initial velocity to the fragments. In reality, on the other hand, some part of the energy of the VV in explosion of a charge is spent on breaking up of the case and on imparting velocity in an axial direction to detonation products escaping from the ends of the charge.

The appropriate calculations indicate that for real filling coefficients, the energy spent on fragmentation of the charge case amounts to an insignificant fraction of the energy of the bursting charge; therefore, one can neglect energy losses for breaking up of the case.

Losses of energy due to escape ("blowing out") of detonation products from the ends of the charge depend on the relative dimensions of the charge and on its weight. Obviously the shorter the charge, the greater the relative part of the energy which will be "blown out" from the ends of the charge, and the more sharply the velocities of fragments formed from parts of the case near the ends will differ from the maximum velocity of the fragments and, consequently, the lower the average velocity of the fragments will be. The losses of energy to "blowing out" thus depend on the relative length of the charge. In addition, the magnitude of these losses also depends on the absolute dimensions of the charge (i.e., on the weight of the charge). The relative losses of energy will be higher the lower the weight of the charge, because rarefaction waves propagating from the end surfaces into the depths of the charge move at constant velocities which do not depend on the dimensions of the charge. Consequently, at a given relative length of the charge, the smaller the absolute length of the charge or (with a given relative length) the smaller the charge weight, the larger the relative part of the case adjoining the ends of the charge which

will be subject to the effect of explosive loads weakened by the rarefaction wave.

One can take into consideration the indicated losses by reducing the specific energy of the VV in the appropriate way:

$$u_{1e} = k_1 k_2 u_1$$

here u_{1e} is the specific energy of the VV which is effective from the point of view of the fragmentation effect; k_1 is a coefficient which takes into consideration the energy losses depending on the relative length of the charge b/d ; k_2 is a coefficient which takes into account the energy losses depending on the weight of the charge w .

The numerical values of the coefficients k_1 and k_2 are determined experimentally.

Thus one can recommend the following formula for computing the initial velocity of scattering of fragments:

$$v_0 = \sqrt{\frac{2u_{1e} k_1 k_2}{\eta - \frac{1}{2}}} \quad (6.36)$$

It follows from consideration of formulas (6.24), (6.25) and (6.36) that the initial velocity of the fragments is determined primarily by the filling coefficient. The greater the filling coefficient, the greater the initial velocity of the fragments. The character of the dependence $v_0(\eta)$ is shown in the graph of Fig. 6.44. The initial velocity of the fragments also depends on the properties of the VV. For example, the initial velocity of fragments in filling of the case with a charge of hexogen ($u_1 = 5.6 \cdot 10^6 \text{ m}^2/\text{s}^2$) with the other conditions the same will be approximately 20% higher than in filling with trotyl ($u_1 = 4.1 \cdot 10^6 \text{ m}^2/\text{s}^2$). The effect of geometric parameters of the charge on the value of the average initial velocity of the fragments is taken into consideration by the coefficients k_1 and k_2 . All the other structural data of the

case and the charge and the properties of the case metal influence the initial velocity of scattering of the fragments so slightly that their effect is ignored in practical calculations. The character of the influence of the indicated structural parameters on the initial velocity of the fragments is determined by the effect of these parameters on the magnitude of the explosive load. In particular, a case with closed ends breaks up into fragments with a somewhat greater velocity than a case with open ends; increasing the strength of the case metal somewhat reduces the initial velocity of the fragments, etc.

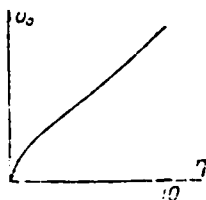


Fig. 6.44.

In conclusion, we shall make one remark pertaining equally to the question of initial velocities of the fragments and to the laws of scattering of the fragments and their distribution by weight.

It was pointed out in the consideration of the process of explosion of a charge in a case that the velocity of radial expansion of each section of the case depends on the intensity of the explosive load active in the section in question. The irregularity of the distribution of the explosive load along the length of a case results in differences in the initial velocities of the fragments formed from different sections of the case; i.e., fragments formed from sections of the case located in the zone of the effect of the maximum explosive loads will have a greater initial velocity. The intensity of fragmentation of the case section in question and the directions of scattering of fragments formed in breaking up of the section in question, as already mentioned more than once, are

also determined, in turn, by the character of the distribution of the explosive load along the length of the case. Specifically, the case breaks up more intensively in the zone of the effect of the maximum explosive loads; sections of the case located near the ends of the charge break up less intensively. In addition, the fragments formed from the sections of the case which break up most intensively scatter in directions near the average direction of scattering of the fragments; fragments formed from sections of the case near the ends of the charge will have the greatest deviations from the average scattering direction.

Therefore, in considering all the phenomena in combination, one can affirm that there are fully defined mutual relationships and dependences among the weights of the fragments, the directions of their scattering and the initial velocities of the fragments; i.e., the law of the distribution of fragments by weight, strictly speaking, depends on the direction of scattering of the fragments, and each direction has its own law of the distribution of fragments by weight. In addition, a fully defined initial velocity of scattering of the fragments corresponds to each direction of scattering. It is also obvious that fragments of a smaller weight will have the greatest velocity in the overall mass of fragments, because it is just these weights of the fragments which will be most typical of scattering directions corresponding to the greatest initial velocities, i.e., to more intensive fragmentation.

The considerations presented above are also finding experimental confirmation. However, experiments attest to the comparatively weak dependence between the law of breaking up of fragments, the law of their distribution by directions and the initial velocities of the fragments. Therefore, it is normally assumed that the characteristics of fragmentation obtained for the entire case are valid for any direction of scattering, that the initial velocity of the fragments does not depend on the direction of scattering and, finally, that the initial velocity of a fragment also does not depend on the weight

of the fragment.

§ 6. BALLISTICS OF FRAGMENTS

The character and degree of damage inflicted by fragments are determined to a considerable extent by the velocity of the fragment at the moment of impact on the target.

If a fragment has taken on some initial velocity v_0 (or an initial velocity v_{01} with consideration for the inherent velocity of the warhead) in bursting of the warhead, the velocity of the fragment will constantly decrease in proportion to further movement on the trajectory due to the presence of the force of air resistance. It is obvious that for evaluating the efficiency of the effect of fragmentation ammunition bursting at some distance from a target, one must know the way in which the velocity of a fragment on the trajectory depends on the distance to the bursting point, the weight of the fragment and its dimensions and shape.

Since a fragment formed in an explosion has an extremely arbitrary and irregular shape, in movement on the trajectory it will rotate around its center of mass in a most disordered way. In connection with this, the configuration of the part of the fragment around which the flow moves and the area which it presents to the flow will also vary with the passage of time in the most random way. One should also keep in mind that the character of such disordered motion of the fragment is individual for each specific fragment, because the fragments formed in an explosion possess an extreme variety of shapes and, strictly speaking, there are no two fragments which are completely identical in their shape and configuration.

The features of movement of a fragment in air mentioned above do not provide a possibility for solving the problem of determining the velocity of a fragment on the trajectory by normal methods of

external ballistics.

A study of the ballistics of a fragment by methods of mathematical statistics was performed by Professor Ye. S. Venttsel' [as transliterated]. Statistical ballistics of a fragment takes into account all the contingencies involved with the variety and irregularity of the shapes of fragments and the lack of any patterns of their rotating movement in relation to the center of mass. In this case, it is necessary first to define the random value of the force of air resistance acting on a fragment in flight. The general expression for the force of resistance R has the following form:

$$R = c_x S \frac{\rho v^2}{2}, \quad (6.37)$$

where c_x is the drag coefficient of the fragment; S is the area of a projection of the fragment on a plane perpendicular to the direction of flight (the maximum midsection of the fragment); ρ is the density of the air; v is the velocity of flight of the fragment.

Both the drag coefficient c_x and the transverse area of the fragment S obviously are certain random functions of the time.

The character of variation of the area of the maximum mid-section of the fragment along the flight trajectory can be determined by firing real fragments at lacquered paper screens located on the trajectory of the fragments and measuring the areas of the holes formed. The results of such experiments attest to the fact that the value of the area of the maximum midsection of a fragment in flight S fluctuates around some average value \bar{S} (Fig. 6.45).

In this case, the area of the maximum midsection of the fragment varies comparatively rapidly on the trajectory: the average period of fluctuations expressed in meters amounts to

1.5-2.0 m. Since the actual ranges of a fragment substantially exceed the indicated value of the period, such a character of variation of the fragment area (intensive rotation of the fragment on the trajectory) makes it possible to determine the value of the force of air resistance R in regard to an area of the maximum mid-section averaged along the trajectory \bar{S} . The value of the average transverse area of the fragment (the average area of the maximum midsection of the fragment) S depends on the weight and configuration of the fragment and can be determined based on the following considerations. It is obvious that a relationship of the following type always occurs for similar fragments:

$$\bar{S} = \Phi q^{2/3}, \quad (6.38)$$

where q is the weight of the fragment, and Φ is a parameter characterizing the shape of the fragment.

$\bar{S} = \Phi q^{2/3}$

Fig. 6.45.

For example, if the fragments had the shape of a sphere with a diameter d ,

$$\Phi = \frac{\bar{S}}{q^{2/3}} = \left(\frac{\pi d^2}{4} \right) : \left(\frac{\pi d^3}{6} \gamma \right)^{2/3} = \sqrt[3]{\frac{9\pi}{16\gamma^2}},$$

here γ is the density of the fragment.

All real fragments can be represented schematically in the first approximation in the form of rectangular parallelepipeds. We shall determine the shape parameter of a rectangular parallelepiped with sides a , b and c ($a \geq b \geq c$).

We shall project the parallelepiped on an arbitrarily oriented plane whose position is determined by a unit vector \vec{n} of a perpendicular to this plane (Fig. 6.46).

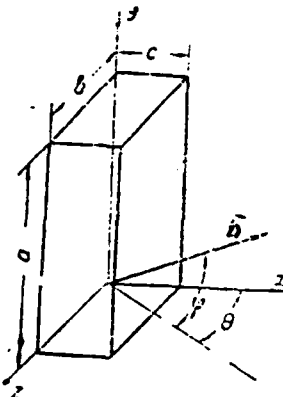


Fig. 6.46.

Assume that the orientation of the vector \vec{n} is defined by angles ϕ and θ of a spherical system of coordinates. Then the area of the projection of the parallelepiped on the plane in question will be as follows:

$$S(\phi, \theta) = bc \sin \varphi + ab \cos \varphi \cos \theta + ac \cos \varphi \sin \theta. \quad (6.39)$$

Since orientations of the unit vector are equally probable (the parallelepiped is oriented in space in an arbitrary way), the differential law of the distribution of random angles ϕ and θ has the following form:

$$f(\phi, \theta) = \frac{2}{\pi} \cos \varphi \begin{cases} (0 < \varphi < \frac{\pi}{2}); \\ (0 < \theta < \frac{\pi}{2}). \end{cases} \quad (6.40)$$

The average area of the projection of the parallelepiped (the mathematical expectation of the random variable S) can be

determined by the following formula:

$$\bar{S} = \int_0^{\frac{\pi}{2}} \int_0^{\frac{\pi}{2}} S(\varphi, \theta) f(\varphi, \theta) d\varphi d\theta. \quad (6.41)$$

Substituting the values of the integrands of (6.39) and (6.40) into formula (6.41) and integrating, we obtain

$$\bar{S} = \frac{1}{2} (ab + bc + ac).$$

Consequently, the shape parameter of a rectangular parallelepiped will be as follows:

$$\Phi = \frac{\bar{S}}{q^{3/2}} = \frac{ab + bc + ac}{2\gamma^{3/2} (abc)^{1/2}}. \quad (6.42)$$

If we introduce dimensionless relationships into the consideration,

$$\alpha = \frac{a}{c}, \beta = \frac{b}{c}, \quad (6.43)$$

formula (6.42) will take on the following form:

$$\Phi(z, \beta) = \frac{\alpha\beta + \alpha + \beta}{2\gamma^{3/2} (z\beta)^{1/2}}, \quad (6.44)$$

here γ is the metal density in kg/m^3 .

Since α and β are dimensionless quantities, the shape parameter has the dimensionality $\text{m}^2/\text{kg}^{2/3}$.

If we characterize the shape of a real fragment with three of its basic dimensions:

a - the greatest dimension of the fragment (length);

b - the greatest typical dimension perpendicular to the length of the fragment (width);

c - the least dimension of the fragment (thickness),

the shape parameter of such a fragment Φ^* is extremely similar to the shape parameter of a parallelepiped with the same relationship of the basic dimensions:

$$\Phi^*(x, \theta) = 1.08 \Phi(x, \beta).$$

Thus one can assume that for real fragments, the average area of their maximum midsection is defined by the formula

$$\bar{S} = \Psi^* (\alpha, \beta) g^{23}, \quad (6.45)$$

where q is the fragment weight in kg; \bar{S} is the average area of the maximum midsection of the fragment in m^2 .

The shape parameter of an actual fragment can be determined either by formula (6.44) or by the graph of Fig. 6.47.

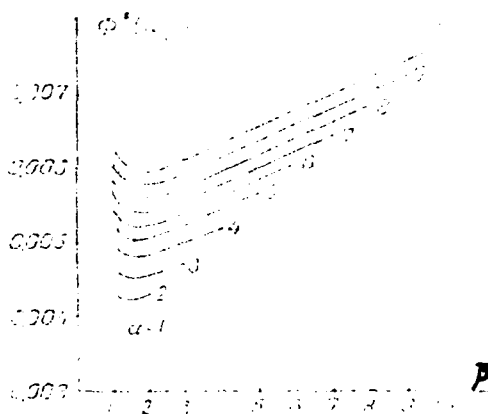


Fig. 6.47.

It follows from consideration of the graph of Fig. 6.47 that the shape parameter of a fragment is a comparatively slowly changing function of its arguments α and β , in connection with which some indeterminacy involved with computation of the relative dimensions of the fragments α and β and conditioned by irregularity of the shape of actual fragments is not of substantial importance in determining the average area of the maximum midsection of a fragment \bar{S} .

Expression (6.37) for the force of air resistance thus can be written in the following form:

$$R = c_x \bar{S} \frac{\rho v^3}{2} \quad (6.46)$$

The value of the drag coefficient of the fragment c_x included in formula (6.46) is determined experimentally by well-known methods of external ballistics relating to research on ballistic characteristics of projectiles (tests in a wind tunnel and parallel firing on target frames). The results of such experiments attest to the lack of a clearly pronounced dependence of the drag coefficient on the velocity. If one also takes into consideration in this case the fact that the variation in the coefficient c_x also has a fluctuating character as a result of intensive rotation on the trajectory, one can replace the coefficient c_x with some average value \bar{c}_x , as was done for the area of the maximum midsection of the fragment. The drag coefficient \bar{c}_x determined along the trajectory of the fragment obviously should be selected from conditions of equality of the velocities of the actual fragment and a hypothetical fragment with a constant average area of the maximum midsection \bar{S} and a constant drag coefficient \bar{c}_x . The specific value of the average value of the coefficient \bar{c}_x obtained in this way unquestionably will depend on the features of the configuration of the fragment and, strictly speaking, will not be constant for all fragments. However, introducing individual ballistic characteristics of each fragment into the calculation would excessively complicate all calculations involved with determining the impact velocity of a fragment on the target. Therefore, such calculations can be performed for some fragment which is typical in its configuration. The drag coefficient of such a fragment c_x^* can be determined based on processing of available experimental data in regard to coefficients \bar{c}_x for fragments with the widest variety of shapes.

Consequently, the expression for the force of resistance will take on the final form

$$R = c_x^* \bar{S} \frac{\rho v^3}{2} \quad (6.47)$$

It must be mentioned here that the force of gravity (the weight of the fragment) also acts on a fragment in flight and causes curvature of the trajectory of the fragment. However, at high velocities of the fragment, the numerical value of the force of air resistance R exceeds the weight of the fragment by a factor of tens. Only the initial section of the trajectory, in which the fragment has the very highest velocities, is of practical interest for evaluating the efficiency of the fragmentation effect. In connection with this, one can neglect the force of gravity of the fragment and consider rectilinear movement of the fragment in the action of only the force of air resistance on it with a degree of precision sufficient for practical work.

In this case, the equation of motion of the fragment will have the form

$$m \frac{d^2x}{dt^2} = -R$$

where m is the mass of the fragment.

Substituting values of the force of air resistance R into this equation, we obtain

$$m \frac{d^2x}{dt^2} = -c_x * \bar{S} \frac{\rho v^2}{2}$$

We shall express the mass of the fragment by its weight and replace the average area \bar{S} with its expression from (6.45):

$$\frac{d^2x}{dt^2} = -\frac{c_x * \rho g \Phi^*}{2q^{1/3}} v^2. \quad (6.48)$$

We shall introduce the following designations:

$$\left. \begin{aligned} k_H &= \frac{1}{2} c_x * \rho g \Phi^* \\ c_H &= \frac{k_H}{\sqrt[3]{q}} \end{aligned} \right\} \quad (6.49)$$

Here

$$\rho \sim \text{kg} \cdot \text{s}^2 / \text{m}^4, \quad \Phi^* \sim \text{m}^2 / \text{kg}^{2/3}, \quad q - \text{kg} \text{ and } g = 9.81 \text{ m/s}^2.$$

We shall note that the coefficient c_H depends on the altitude at which bursting of the warhead occurred, because

$$\rho = \rho_0 H(y),$$

where ρ_0 is the density of the air at the ground ($\rho_0 = 0.125 \text{ kg} \cdot \text{s}^2 / \text{m}^4$); $H(y)$ is a function of the variation of the density of air with the altitude.

One can write equation (6.48) in the new designations in the following form:

$$\frac{d^2x}{dt^2} = -c_H v^2. \quad (6.50)$$

Keeping in mind that

$$\frac{d^2x}{dt^2} = \frac{dv}{dt} = v \frac{dv}{dx}, \quad (6.51)$$

we finally obtain

$$\frac{dv}{dx} = -c_H v.$$

Integrating the latter equation, we have

$$v = v_{01} e^{-c_H x}, \quad (6.52)$$

where v_{01} is the initial velocity of the fragment, determined with consideration for the inherent velocity of the warhead (6.21).

Formula (6.52) makes it possible to determine the velocity of a fragment at a given distance x , if the initial velocity of the fragment v_{01} and its ballistic coefficient c_H are known.

It follows from consideration of formulas (6.50) and (6.52) that the larger the ballistic coefficient c_H , i.e., the smaller the weight of the fragment q , the worse the shape of the fragment (the greater the coefficient c_x^* and the shape parameter of the fragment

*) and the lower the altitude of bursting of the bomb or projectile (the greater the air density ρ), the more rapidly the velocity of the fragment will decrease.

In solving certain special problems involved with evaluating the efficiency of the fragmentation effect, and in conducting experimental studies, it is necessary to have dependences which make it possible to determine the distance which a fragment has covered along the trajectory and its velocity in regard to a given flight time. Both these dependences can also be obtained by integrating the original equation of motion of the fragment (6.50). Keeping in mind (6.51), equation (6.50) can be written in the following form:

$$\frac{dv}{dt} = -c_H v^2$$

Integrating this equation under the initial conditions

$$t=0, \quad v=v_{01},$$

we obtain

$$v = \frac{v_{01}}{1 + c_H v_{01} t} \quad (6.53)$$

Expression (6.53) makes it possible to determine the velocity of a fragment if its flight time is given.

Expression (6.53) can be written in the following form:

$$\frac{dx}{dt} = \frac{v_{01}}{1 + c_H v_{01} t}$$

Integrating the latter equation under the initial conditions

$$t=0, \quad x=0,$$

we have

$$t = \frac{1}{v_{01} c_H} (e^{c_H x} - 1). \quad (6.54)$$

The latter formula makes it possible to determine the flight time of a fragment for a given range x and is finding use in processing of experimental data for determining the initial velocities of fragments, when the time for a fragment to fly a given distance is known.

§ 7. CHARACTERISTICS OF THE VULNERABILITY OF A TARGET IN RELATION TO THE FRAGMENTATION EFFECT. THE TARGET VULNERABILITY FUNCTION $S^*(g, v)$

In determining the probability of damage to a target by fragmentation ammunition, one must establish preliminarily in what way specifically the damaging effect of a fragment which has hit the target is manifested. One can assume based on available data that there are three basic types of damaging effect of a fragment:

- the piercing effect (mechanical damage of individual vulnerable assemblies of the target);
- the incendiary effect (the emergence of a fire when a fragment hits tanks with fuel or pipelines of the fuel system of engines of aerial targets or ground transport vehicles);
- the initiating effect (detonation of the filling of ammunition when fragments hit it).

We shall consider each of the types of damaging effect listed in greater detail.

The piercing effect. The piercing effect is the most characteristic and also the most varied type of damaging effect and includes such types of damage as mechanical damage of different kinds to individual components of the structure of vital assemblies of the target, resulting in their destruction and breakdown.

For example, if the engine of an airplane is considered as such a vital assembly, the piercing effect of fragments is exhibited in the form of mechanical damage to the turbine, compressor, fuel pumps and filters and drives of different kinds; breaking up of pipelines of the fuel and oil systems of the engine and pull rods and cables for control of the engine, etc. For such a target as a ground artillery gun, for example, the piercing effect of the fragments conditions mechanical damage to drives for control of the gun, destruction of sights and fire control instruments, etc. Injuries to personnel are also a manifestation of this type of effect of fragments.

The character and degree of mechanical damage inflicted by a fragment on different damaged components of the target are determined primarily by the thickness of the obstacle which must be pierced by a fragment with a given impact velocity and weight. In a number of cases, it is also necessary to know the area of the hole left in the obstacle by the fragment for evaluating the degree of damage.

One should keep in mind in evaluating the efficiency of the piercing effect of a fragment that the shape of the fragment and its orientation at the moment of impact on the obstacle are random variables. In connection with this, the area of the hole left by the fragment in the obstacle and the thickness of the obstacle pierced by a fragment of a given weight with a given impact velocity will also be random, because the thickness of the obstacle which a fragment is capable of piercing, with other conditions the same, obviously depends essentially on the cross section area of the fragment at the moment of impact on the obstacle.

Thus, if we know that it is necessary to pierce some element of the target structure with a thickness h and to leave a hole with an area not less than S_0 in it for destroying some assembly of the target, a fragment with a weight q with a given velocity at the moment of impact v can destroy this target assembly only with a

certain probability.

The qualitative relationships necessary for evaluating the efficiency of the piercing effect of fragments, which make it possible to determine the desired probability, can be obtained based on theoretical research involved with study of the phenomenon of interaction of fragments with an obstacle.

We know from the theory of plastic deformations that in piercing of obstacles, the energy spent on deformation of the obstacle related to the unity of the deformed volume of the obstacle is a constant value, which does not depend on either the mass or shape of the body striking the obstacle or on the thickness of the obstacle:

$$\frac{E}{V} = \text{const}, \quad (6.55)$$

where E is the energy spent on piercing the obstacle; V is the volume of the hole formed in the obstacle.

The numerical value of the indicated ratio depends only on the strength characteristics of the obstacle and is proportionate to the magnitude of ultimate tangential stresses of the obstacle material τ . It should be noted that at high impact velocities corresponding to actual conditions of impact of a fragment on an obstacle, the resistance of the obstacle increases noticeably. The increase in the strength properties of the obstacle can be characterized by some dynamic response factor k.

Keeping in mind all these circumstances, one can write expression (6.55) in the following form:

$$\frac{E}{V} = a k \tau, \quad (6.56)$$

where a is a constant coefficient.

Assuming that in impact on an obstacle, all the energy of the body striking the obstacle is spent on piercing the obstacle, using

formula (6.56), one can obtain a basic relationship for determining the maximum thickness of the obstacle h which a fragment with a weight q , a velocity v and a collision area S is capable of piercing:

$$\frac{qv^2}{2gSh} = ak\tau.$$

Since the area of the collision of a fragment with the obstacle (the hole area) is a random variable, the fragment obviously is capable of piercing the obstacle only in a case where

$$\frac{qv^2}{2gSh} \geq ak\tau.$$

Or, dividing both members of the inequality by the average area of a projection of the fragment on the obstacle \bar{S} , we obtain

$$\frac{qv^2}{2g\bar{S}h} \geq ak \cdot \frac{S}{\bar{S}}. \quad (6.57)$$

The left member of the inequality represents the energy of the fragment in relation to the average area of its maximum mid-section and the thickness of the obstacle which can be pierced:

$$E_h = \frac{qv^2}{2g\bar{S}h}.$$

If we express the average area of the average midsection of the fragment \bar{S} in terms of the weight of the fragment (6.45), the formula for determining E_h will have the following form:

$$E_h = \frac{q^{1/3} v^2}{2gh^{1/4} \Phi^*(\alpha, \beta)}. \quad (6.58)$$

The parameter E_h can be adopted as the basic characteristic defining the piercing effect of a fragment.

The ratio S/\bar{S} included in the right member of the inequality is a random variable which depends on the orientation of the fragment at the moment of impact on the obstacle.

We shall designate the relative area of the maximum midsection of the fragment as σ ,

$$\sigma = \frac{S}{\bar{S}} \quad (6.59)$$

and we shall rewrite inequality (6.57) in the following form

$$\sigma < \frac{E_h}{ak\tau} \quad (6.60)$$

The fragment thus is capable of piercing the obstacle only in a case where the random value of the relative area of the maximum midsection of the fragment satisfies inequality (6.60). It is obvious for given collision conditions (fragment weight, fragment velocity at the moment of impact, obstacle thickness and material), the probability of piercing of the obstacle is numerically equal to the probability of fulfillment of inequality (6.60). The probability that the random variable σ will take on a value less than some given value σ_1 ,

$$\sigma_1 = \frac{E_h}{ak\tau}, \quad (6.61)$$

in turn, can be found if the integral law of the distribution of relative areas of holes left by a fragment in the obstacle $F(\sigma)$ is known:

$$P(\sigma \leq \sigma_1) = F(\sigma_1).$$

Consequently, the probability of piercing of an obstacle by a fragment p_{II} will be determined by the numerical value of the variable σ_1 and the form of the integral law of the distribution of relative areas of holes,

$$p_{II} = P(\sigma \leq \sigma_1) = F(\sigma_1) = F\left(\frac{E_h}{ak\tau}\right) \quad (6.62)$$

The theoretical considerations presented above can form the basis for experimental methods for determining the probability of piercing of an obstacle.

If fragments of any definite weight are used for firing, with maintaining of a constant value of their impact velocity on an obstacle of a given thickness, the probability of piercing p_{II} can be determined directly as the ratio of the number of cases of piercing of the obstacle to the total number of shots. By conducting such firing for different combinations of weights of fragments, velocities of fragments and thicknesses of obstacles and computing the value of the parameter E_h (6.58) for each combination, one can plot a graph of the dependence $p_{II}(E_h)$.

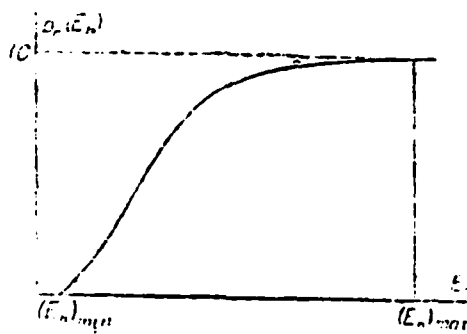


Fig. 6.48.

The character of such a dependence is shown in Fig. 6.48. It follows from consideration of Fig. 6.48 that the probability of piercing of obstacles, which is equal to zero with $E_h = (E_h)_{min}$, increases continuously with an increase in the parameter E_h and reaches unity with $E_h = (E_h)_{max}$.

On the other hand, the dependence of the probability of a piercing effect of fragments on the parameter E_h can also be determined by conducting indirect experiments which are less awkward in size for determining the law of the distribution of areas of the holes (the area of the maximum midsection of the fragment) in firing fragments at lacquered paper screens. An illustration of the integral law of the distribution of relative areas of holes $F(\sigma)$ is shown in the graph of Fig. 6.49.

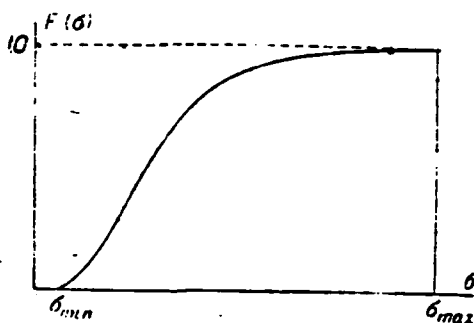


Fig. 6.49.

It follows from formulas (6.61) and (6.62) that if the scale of the dependence $p_{II}(E_h)$ is reduced by a factor $ak\tau$ in regard to the abscissa axis, the two dependences will coincide, because

$$p_{II}(E_h) = F\left(\frac{E_h}{ak\tau}\right). \quad (6.63)$$

It is natural that with such a change in the scale, the numerical values of the parameters k and τ should correspond to the obstacle material for which the dependence $p_{II}(E_h)$ was determined by direct firing.

For determining the probability of a piercing effect, it is most convenient to use the dependence $p_{II}(E_h)$ pertaining to duralumin obstacles. In determining the probability of piercing of obstacles of another material, it is necessary to replace the obstacle in question in the calculations preliminarily with a duralumin obstacle equivalent to it from the point of view of the probability of piercing; the thickness of the duralumin obstacle can be determined based on the following considerations: one can conclude from consideration of formulas (6.58) and (6.62) that with a given weight and velocity of the fragment, the probabilities of piercing of two different obstacles will be the same if the same value of the product $hk\tau$ for the obstacles is provided. Assuming for a given obstacle its thickness h' and the material (k' and τ') are known, and with a

knowledge of similar characteristics of the duralumin obstacle (k and τ), we obtain the following formula for determining the equivalent thickness of the duralumin obstacle:

$$h = h' \frac{k' \tau}{k \tau} \quad (6.64)$$

However, as already mentioned above, it is insufficient in some cases for destroying some assembly merely to pierce any of its vulnerable components, because breakdown on the assembly can be achieved only in a case where the area of the hole left by the fragment is sufficiently great.

Assume that a hole of an area not less than S_0 is required for destroying an assembly. Then the relative area of this hole (the area of the hole in relation to the average area of the maximum midsection of the fragment) will be as follows:

$$\sigma_0 = \frac{S_0}{S}$$

For destroying the assembly in this case, it is obviously necessary that the relative area of the hole left by the fragment in the obstacle be greater than σ_0 :

$$\sigma > \sigma_0$$

Therefore, for the fragment to destroy the assembly (pierce the obstacle and leave in it a hole with an area greater than S_0), fulfillment of the following conditions is necessary:

$$\sigma < \sigma_1; \quad \sigma \geq \sigma_0$$

Or, combining the two conditions, we obtain

$$\sigma_0 < \sigma < \sigma_1 \quad (6.65)$$

The probability of destroying an assembly will be equal to the probability of fulfillment of inequality (6.65), which, in turn, can be determined easily if the integral law of the

distribution of the random variable σ is known:

$$p_n' = p(c_0 < \sigma \leq c_1) = F(c_1) - F(c_0).$$

Since $F(\sigma_1)$ represents the probability of piercing of the obstacle $p_n(E_h)$, it is necessary for determining the probability of destruction of the assembly with consideration for the area of the hole left by the fragment in the obstacle p_n' only to determine in addition the value of $F(\sigma_0)$.

The value of $F(\sigma_0)$ can be found easily by a graph of $F(\sigma)$ (Fig. 6.49), although it is more convenient, keeping in mind the fact that the graph of the integral law $F(\sigma)$ differs from the graph of the dependence $p_n(F_h)$ only in the scale in regard to the abscissa axis, to use a curve of $p_n(E_h)$ of the type shown in Fig. 6.48 and pertaining to piercing of duralumin obstacles for determining $F(\sigma_0)$. The formula for determining the probability of destruction of an assembly in this case will have the following form:

$$P_n = p_n(E_h) - p_n(E_h'). \quad (6.66)$$

where

$$E_h' = ak\tau \frac{S_0}{\bar{S}}.$$

Expressing the average hole area \bar{S} in terms of the fragment weight q (6.45), we obtain

$$E_h' = \frac{ak\tau}{\phi^*(\alpha, \beta)} \frac{S_0}{q^{2/\beta}}. \quad (6.67)$$

It is natural in this case that the values of the parameters k and τ included in formula (6.67) should correspond to a duralumin obstacle, since a curve of $p_n(E_h)$ pertaining to duralumin is the source curve for conducting such calculations.

In the process of calculations, it can sometimes turn out that $E_h' > E_h$. This means that it is impossible to satisfy both members of

inequality (6.65) at the same time under the given conditions. In other words, it is necessary for piercing the obstacle in this case for the hole area to be less than the area S_0 which is necessary for destroying the assembly. One obviously must assume in such cases that the probability of destruction p_n' is equal to zero.

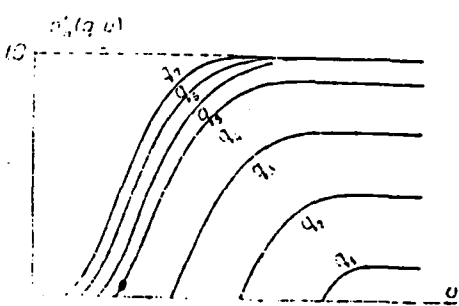


Fig. 6.5Q.

Thus, if the thickness of the obstacle h and the necessary hole area S_0 are given, using the formulas and the graph of $p_{II}(E_h)$ which have been obtained, one can determine the dependence of the probability of destruction of an assembly on the fragment weight q and the fragment velocity at the moment of impact v . As an illustration, Fig. 6.50 presents a sample view of a family of curves of $p_{II}'(q, v)$ characterizing variation in the probability of destruction of an assembly due to the piercing effect of fragments with some equivalent thickness of the duralumin obstacle and with a definite value of the minimum necessary hole area S_0 . Such graphs of the variation of the probability of destruction of an assembly depending on the weight and velocity of the fragment hitting the target fully characterize the vulnerability of some vulnerable element of the target in relation to the fragmentation effect.

We shall note in conclusion that the values of the thickness of the duralumin equivalent of the vulnerable assembly and the minimum necessary hole area included in the calculation can be obtained only based on careful analysis of the structure of the

assembly, from the point of view of evaluating the possibility of its normal functioning in the presence of some mechanical damage in it.

In evaluating the efficiency of the effect of fragmentation ammunition in regard to live targets, the latter are also provisionally replaced in the calculations with a duralumin obstacle of a certain thickness, the probability of piercing of which is equivalent to the probability of destruction of live targets. Minimum necessary hole area S_0 in this case is assumed to be equal to the area of a hole from a bullet of a normal caliber.

The incendiary effect. Accounting for the incendiary effect of fragments is of substantial importance in evaluating the efficiency of fragmentation ammunition used for hitting targets whose structure includes tanks of different kinds filled with fuel. Such targets primarily include aircraft. The basic cause leading to ignition of fuel in fuel tanks is the presence of the duralumin skin of the airplane. Just before piercing the tank, the fragment pierces the duralumin skin, which plays the role of a screen standing in the path of the fragment. In piercing of this duralumin screen, a colossal number of fine red hot particles are formed - an unusual "torch" of red hot dispersed metal. If the fragment has formed a hole in the adjacent fuel tank in the process, direct contact of the "torch" of red hot particles and vapors of the fuel running out of the hole becomes possible, which can lead with a certain probability to ignition and subsequent combustion of the fuel.

The probability character of the process of ignition of the fuel is conditioned by such random factors as the intensity of the torch of red hot particles and its fluctuations, which are determined by the random value of the collision area of the fragment and the random nature of its shape, the combinations of the space occupied

by the torch and the space in which vapors of fuel flowing out of the tank are located, the particular degree of concentration of the fuel vapors, etc.

The complexity of physical phenomena involved with the incendiary effect of fragments does not permit creating theoretical grounds on the basis of which one could obtain any satisfactory theoretical solution of the problem of determining the probability of ignition of fuel when a fragment with a given velocity v and a given weight q hits a fuel tank of a given structure. Therefore, the probability of the incendiary effect of fragments can be determined only experimentally, by firing fragments of different weights with different impact velocities at fuel tanks located in the structure of an airplane.

The basic quantitative characteristic of a fragment which determines its incendiary effect in regard to fuel tanks is the specific impulse,

$$i = \frac{mv}{s}$$

Expressing the mass of the fragment by its weight q and replacing the average area of the cross section of the fragment with its value from (6.45), we have

$$i = \frac{q^{1/3}v}{g\Phi(x, \beta)} \quad (6.68)$$

An illustration of the dependence of the probability of the incendiary effect on the specific impulse of the fragment is shown in Fig. 6.51. The character of the dependence $p_3(i)$ obviously will depend on the type of fuel tank and the conditions of its position in the structure of the target, the type of fuel being used, the degree of fire protection of the target, etc.

It follows from consideration of the graph of Fig. 6.51 that values of the parameter i less than i_{\min} , the probability of

ignition of the fuel will be equal to zero. With an increase in the parameter i , the probability of the incendiary effect of fragments increases, and at $i=i_{\max}$, it essentially reaches one.

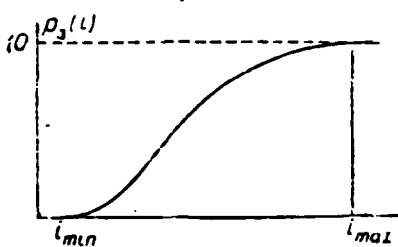


Fig. 6.51.

Using formula (6.68) and the graph of the dependence $p_3(i)$ (Fig. 6.51) pertaining to a given tank design, one can determine the dependence of the probability of ignition of fuel tanks on the weight of the fragment q and its velocity at the moment of impact v . Figure 6.52 presents the approximate character of a family of curves of $p_3(q, v)$, which will characterize the vulnerability of fuel tanks under consideration in relation to the incendiary effect of fragments, as an illustration.

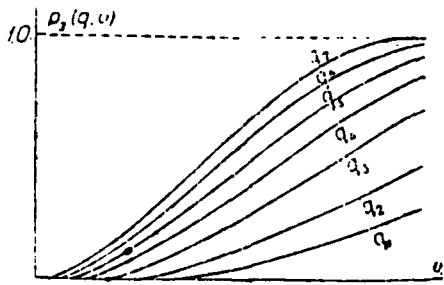


Fig. 6.52.

However, probabilities obtained in this way will pertain to a case of fragments hitting fuel tanks located at the ground. In

evaluating the efficiency of the effect of fragmentation ammunition in relation to airplanes in the air, it is necessary to take into consideration in some way the effect of the flight altitude of the aircraft target on the probability of ignition of the fuel. With an increase in the flight altitude of the aircraft target, the temperature decreases, and the pressure of the surrounding medium decreases, which leads to a change in all the physicochemical properties of the mixture of air and fuel flowing out of the hole which determine the probability of ignition. In particular, the partial pressure of fuel vapors decreases, the concentration of the mixture decreases, and the amount of oxygen in the mixture and in the surrounding air decreases, which sharply reduces the possibility of normal ignition and combustion of the fuel, the ignition temperature of the mixture increases, the necessary conditions for heat conduction and heat transfer deteriorate, etc. As a result of such a change in the properties of the mixture, the probability of an incendiary effect of fragments decreases with an increase in altitude. There is a maximum altitude H^* at which ignition and combustion of fuel can no longer occur at all ("the ignition ceiling").

In view of the extreme difficulties involved with theoretical solution of this problem and conditioned by the exceptional complexity of the phenomenon under consideration, one can take into consideration the effect of the flight altitude on the probability of an incendiary effect of fragments at present only based on experimental data. Such experiments normally are performed in an altitude chamber, in which conditions simulate the flight of an airplane at some altitude are created. Thus, with consideration for the flight altitude of the target, the probability of ignition and combustion of the fuel can be represented in the first approximation as follows:

$$p'_s = p_s F(H), \quad (6.69)$$

where p'_s is the probability of ignition of fuel at some altitude H ; p_s is the probability of ignition of the fuel at the ground;

$F(H)$ is some experimentally determined function characterizing the decrease in the probability of ignition of the fuel at the altitude.

The initiating effect. In a number of cases, in evaluating the efficiency of the fragmentation effect, it is necessary to deal with targets containing fighting sections (the bomb section of an airplane, the warhead of a missile, etc.). If a fragment which has hit such a section has a sufficient weight and a high initial velocity, it is capable in penetrating the casing of ammunition located in the section of causing detonation of the explosive, which leads to unconditional destruction of the target.

The initiating effect of fragments thus develops in the capacity of the VV for explosive transformations under the effect of a sharp shock. As we know, in impact of any body (the fragment) flying at a high velocity, a shock wave emerges in the VV charge, and a sharp pressure, temperature and density differential occurs on the shock wave front. Under the effect of the increased pressure on the shock wave front, stresses develop in the VV charge and, as a result of heterogeneities of the physical structure of the VV, these stresses are distributed in an irregular way in the layer of compressed VV on the shock wave front. Therefore, "peaks" of increased stresses emerge at certain points of the VV; these peaks will be the points of the most intense strains and, consequently, the centers of maximum local heating up. These centers ("hot spots") are the most probable local centers of initiation. In this case, such a "microexplosion" is possible if the temperature of a "hot spot" is higher than the temperature of thermal decomposition of the VV.

It is obvious that the more intensive the formation of "hot spots" (the greater the number of hot spots formed per unit of time in the passage of the compression shock wave front over the charge), the greater the amount of energy released in thermal decomposition

of the VV and, consequently, the greater the probability that the energy of the VV released in direct proximity to the impact point will be sufficient for exciting detonation of the entire charge.

The total number of "hot spots" formed in the VV charge, in turn, is proportionate to the energy of the body striking the charge, which is absorbed by the VV mass. And the number of "hot spots" formed at the point of impact per unit of time is proportionate to the energy absorbed by the VV charge deformed at the point of impact per unit of time, i.e., the power transmitted to the VV charge by the body striking it at the moment of impact, because further development of the detonation process will not occur any more due to the formation of new "hot spots" from the compression shock wave; it will proceed due to the energy released in explosion of part of the charge adjoining the impact point.

The basic characteristic determining the initiating capacity of a body striking a target thus is the power transmitted by the body to the VV charge at the moment of impact W_0 . We shall note that even at the same values of the parameter W_0 , the process of detonation of the entire charge can begin only with some probability. The probability character of the phenomenon in question is conditioned primarily by heterogeneities of the crystalline structure and other physical properties of the same VV charge.

The dependence of the probability of initiation of the VV charge p_H on the parameter W_0 can be determined experimentally, by firing cylindric fragment models at a VV charge. The use of cylindric models which are stabilized in flight provides constancy of the collision area (the area of the base of the cylinder) and makes it possible to exclude contingencies conditioned by variation of cross section areas of actual fragments from the experiment, i.e., to establish the basic patterns of the phenomenon of initiation of a VV by impact in pure form. The approximate character of the dependence $p_H(W_0)$ for certain VV is shown in

Fig. 6.53. Dependences $p_u(W_0)$ essentially repeat in some way the well-known results pertaining to standard tests of the sensitivity of VV by means of impact machines (so-called curves of the impact sensitivity of VV, which produce a dependence of the frequency of an explosion on the height of the falling weight). In particular, it follows from a comparison of the curves shown in Fig. 6.53 that pressed trotyl is most sensitive to impact by such bodies; a mixture of trotyl with hexogen (TG) is somewhat inferior to it in sensitivity; cast trotyl possesses the lowest sensitivity.

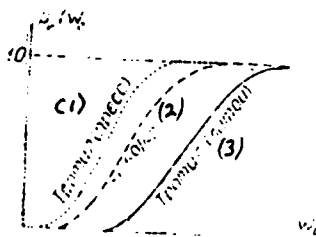


Fig. 6.53.

Key: (1) trotyl (pressed); (2) TG 50/50;
(3) trotyl (cast).

The data presented above characterize the capability of fragments of accomplishing full detonation of a VV charge. For evaluating the efficiency of the effect of fragmentation ammunition, cases of combustion of VV and cases of incomplete detonation of VV accompanied by more or less intense destruction of the ammunition shells are also of interest. Such cases obviously can also be the cause of unconditional destruction of the target. As an illustration, Fig. 6.54 presents dependences $p_u(W_0)$ pertaining to trotyl and plotted with consideration for all the cases of incomplete detonation and intense combustion which have occurred (top curve) and without consideration for these cases (bottom curve).

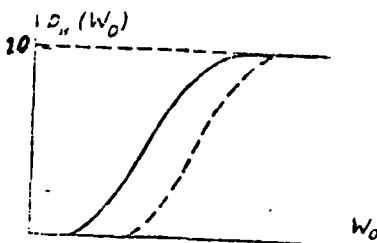


Fig. 6.54.

In order to have the possibility of determining the probability of an initiating effect of actual fragments in regard to actual ammunition (a VV charge situated in a charge case) by means of experimental dependences $p_H(W_0)$ obtained for cylindric models, it is necessary to establish the way in which different parameters of the colliding body (velocity, weight, collision area) and the VV (density, sensitivity and other properties) and the collision conditions (the presence of a case, the thickness of the case) influence the value of the parameter W_0 .

Assume that a fragment with a weight q , whose velocity at the moment of impact is v , strikes a charge case with a cross section area S at this moment. If the thickness of the case is h , one can assume that an element whose area is S and whose thickness is h will be stamped out of the case. We shall assume that after piercing of the case, the velocity of movement of the fragment and the element which has been stamped out are equal to v_1 ; then it is obvious that a pressure emerges on the surface of contact of the element with the VV at the moment of impact with a value which is determined according to the well-known formula (2.41), which can be written for strong shock waves ($p_1 \gg p_0$) in the following form:

$$p = \rho_0 v_1 D,$$

where ρ_0 is the initial density of the VV; v_1 is the velocity of the element [this velocity, which is equal to the piston velocity,

is designated as u_1 in formula (2.41)]; D is the velocity of propagation of the shock wave in the VV.

In advancing of the element into the VV to a depth dx , the VV takes on the energy lost by the element in penetration:

$$dE = (\rho_0 v_i D) S dx.$$

The power absorbed by this layer of VV compressed by the wave at the moment of impact obviously will be as follows:

$$W_0 = \frac{dE}{dt} \Big|_{t=0} = \rho_0 v_i D S \frac{dx}{dt} \Big|_{t=0}.$$

Keeping in mind that $\frac{dx}{dt} \Big|_{t=0} = v_i$, we obtain

$$W_0 = \rho_0 S v_i^2 D.$$

It follows from (2.42), however, that the following relationship between the velocity of propagation of a shock wave and the velocity of movement of the medium occurs for shock waves:

$$v_i = \left(1 - \frac{\rho_0}{\rho_1} \right) D,$$

where ρ_1 is the density of the VV on the compression shock wave front.

For strong shock waves, as we know, the ratio ρ_1/ρ_0 is a constant value; consequently,

$$D = \mu_0 v_i,$$

where μ_0 is a constant coefficient.

The final formula for W_0 thus can be written in the following form:

$$W_0 = \mu_0 \rho_0 S v_i^2 \quad (6.70)$$

It follows from consideration of the formula (6.70) that the initiating capacity of a fragment is determined by the magnitude

of the random collision area and depends to a high degree on the velocity of the fragment after piercing of the charge case. The latter, in turn, depends on the velocity of the fragment at the moment of impact on the case, the thickness of the case and the random value of the collision area which the fragment possessed in impact on the case. We shall note that if there is some screen (the skin of an airplane or other screening elements of the structure) in the path of the fragment, the velocity v_1 will also depend on the thickness and material of this additional obstacle.

The circumstance that the numerical value of the parameter W_0 depends essentially on the value of the random collision area of the fragment intensifies the probability character of the problem of evaluating the initiating capacity of fragments to a still greater degree, because while it was established previously that some detonation probability $p_u(W_0)$ corresponds to a given value of W_0 , it turns out that with other conditions the same, the value of W_0 itself is also random for an actual fragment and is determined by the random value of the fragment cross section area at the moment of impact.

The indicated circumstance can be taken into account if we express the velocity of the fragment v_1 after piercing of the additional screen and the shell case in terms of the value of the fragment velocity at the moment of impact on the target v and the fragment cross section area S : we substitute the value obtained for the velocity v_1 into formula (6.70) and then express the value of W_0 as a function of the random collision area S . Using this dependence, with other conditions the same, one can find the dependence $p_u(S)$ with the curve of $p_u(W_0)$. Now if we determine the dependence $p_u(S)$, with consideration for the law of the distribution of random collision areas $F(S)$ (the graph of $F(s)$ in Fig. 6.49), we can find the value of the probability p_u averaged in regard to the collision area:

$$P_H = \int_{S_{\min}}^{S_{\max}} p_H(S) dF(S).$$

The results of such computations, which are extremely awkward in size, can be represented in the form of a family of curves of $p_H(A, a)$, an illustration of which is shown in Fig. 6.55.

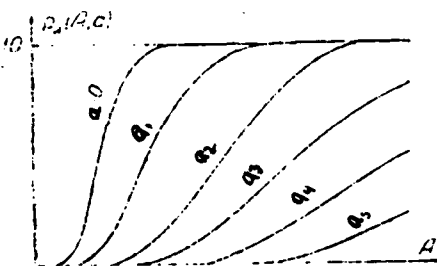


Fig. 6.55.

In this case, the parameters A and a are expressed as follows:

$$A = \mu \rho_0 \Phi^*(\alpha, \beta) q^{2/3} v^2$$

$$a = \Phi^*(\alpha, \beta) \frac{\gamma_M h_A + \gamma_s h_s}{\sqrt{q}} \quad (6.71)$$

where μ is a constant coefficient; ρ_0 is the density of the VV charge; q is the fragment weight; v is the impact velocity of the fragment on the target; γ_M is the density of the charge case metal; h_A is the thickness of the case; γ_s is the density of the screening metal; h_s is the screening thickness; $\Phi^*(\alpha, \beta)$ is the shape coefficient of the fragment.

The physical meaning of the parameter A is the power transmitted by the fragment to the VV charge at the moment of impact with an average collision area \bar{S} .

Using graphs of the type of Fig. 6.55 and the formulas (6.71), one can determine the dependence of the probability of an initiating

effect $p_u(q, v)$ of fragments on the weight and velocity of the fragment which has hit the target under given impact conditions (Fig. 6.56). Calculations for computing the probability $p_u(q, v)$ attest to the fact that the initiating effect of the fragments should be taken into account in a case where fragments of a large weight are formed in an explosion, and the impact velocity of the fragments on the target is comparatively great.

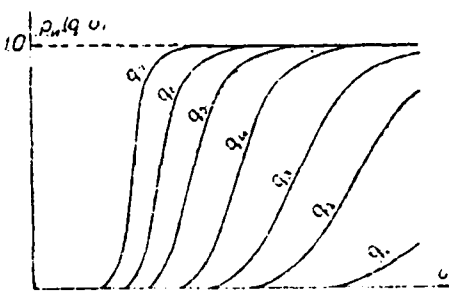


Fig. 6.56.

Briefly stated, this is the basic information on the piercing, incendiary and initiating effects of fragments. Using the methods which have been presented above, one can determine the dependence of the probability of destruction of any assembly on the weight and velocity of the fragment which has hit the assembly $p(q, v)$ comparatively simply with given bombing or firing conditions. The family of curves of $p(q, v)$ fully characterizes the vulnerability of the assembly in question in relation to the fragmentation effect.

However, any target, as a rule, is made up of not one but several assemblies, destruction of each of which can result in breakdown on the entire target. For example, if we consider an airplane in air as the target, destruction of the airplane can be ensured due to a total loss of fuel, a fire, explosion of ammunition, death of the pilot, loss of control, engine failure, etc. It is obvious that destruction of any of the assemblies listed will lead to destruction of the entire airplane as a whole. We shall call

such assemblies of the target the vulnerable elements. With characteristics of vulnerability of each vulnerable element, one can determine the characteristics of vulnerability of the entire target.

Assume that the total number of vulnerable assemblies of the target is equal to k , and that the vulnerability of each of them is characterized by the familiar dependence $p_i(q, v)$ ($i=1, 2, \dots, k$). We shall assume also that the average vulnerable areas S_i , i.e., the areas of the elements averaged in regard to all possible directions of approach of a fragment for which the vulnerable element can be put out of operation if the areas are hit, are known for each element.

Since the target can be put out of action with destruction of even one of the elements, the average probability of destruction of the target by one fragment of a weight q with a velocity of impact on the target v obviously can be determined by the following formula:

$$P(q, v) = \sum_{i=1}^k p_i(q, v) \frac{S_i}{S_t} \quad (6.72)$$

where S_i/S_t is the relative vulnerable area of the element; $S_t =$

$\sum_{i=1}^k S_i$ is the total vulnerable area of the entire target.

The probability of destruction of a target by one fragment obtained in this way is one of the characteristics determining the vulnerability of the entire target in relation to the fragmentation effect. However, normally it proves more efficient in practice to compute not the average probability of destruction of the target $P(q, v)$ but the mathematical expectation of the total vulnerable area of the target $S^*(q, v)$:

$$S^*(q, v) = S_t P(q, v) = \sum_{i=1}^k p_i(q, v) S_i \quad (6.73)$$

The numerical value of the variable $S^*(q, v)$ obviously is the area of the target for which, when it is hit by one fragment of a weight q with a velocity of impact on the target v , the target is taken out of action with a probability of one.

The dependence $S^*(q, v)$ computed by formula (6.73) is called the target vulnerability function.

In performing practical calculations involved with computing the vulnerability function $S^*(q, v)$, it is necessary first of all to study carefully and to analyze the structure of the entire target and the character of operation of each of its assemblies, to distinguish those elements in the target structure whose destruction can result in breakdown of the entire target, and to determine the average vulnerable areas of each of the vulnerable elements. Then it is necessary to designate the required degree of damage for each of the vulnerable elements (the thickness of the duralumin equivalent, the minimum necessary hole area which must be left by the fragment in the assembly) and to compute the probability of destruction of each element $p_i(q, v)$ for all real values of weights and velocities of fragments. With all these data, one can compute the values of the vulnerability function $S^*(q, v)$ for all the values of q and v which have been selected.

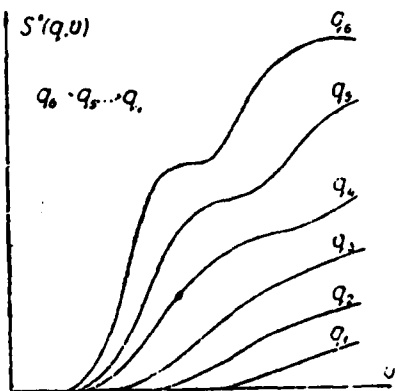


Fig. 6.57.

The results of such computations are normally represented in the form of graphs. As an illustration, Fig. 6.57 presents graphs of the vulnerability function of a target which has elements in its structure which are vulnerable due to piercing, incendiary and initiating effects of the fragments. Breaks and bend points of the curves attest to the fact that the probability of destruction of certain less vulnerable elements comes to be different from zero with an increase in the velocity of impact of the fragment on the target, and they begin to play a significant role in the overall target vulnerability balance. It is obvious that the form of the function $S^*(q, v)$ is determined only by the characteristics of vulnerability of the vulnerable elements and the ratio of their areas and does not depend at all on the structural data of the warhead or the conditions of firing or bombing (with the exception of the flight altitude of the target in consideration of the incendiary effect).

§ 8. THE MATHEMATICAL EXPECTATION OF THE NUMBER OF FRAGMENTS DAMAGING A TARGET

All the characteristics of ammunition considered above which determine their fragmentation effect (the total number of fragments formed in breaking up of a shell, the law of the distribution of fragments by weight and directions of scattering, the initial velocity of the fragments) and the characteristics of vulnerability of the target (the average target kill probability for a single fragment or the target vulnerability function) are necessary for computing the target kill probability with known conditions for use of the ammunition and with given coordinates of the point of burst in relation to the target.

This probability can be computed extremely simply by normal formulas of the theory of probabilities, if the mathematical expectation of the number of fragments damaging the target is known for the given coordinates of the point of burst and

conditions for use of the ammunition. The mathematical expectation of the number of fragments damaging the target \bar{m} is the average number of fragments which strike the target with a probability equal to unity and is equal to the product of the average target kill probability for a single fragment $P(q, v)$ and the mathematical expectation of the number of fragments \bar{n} hitting the vulnerable area of the target:

$$\bar{m} = \bar{n} P(q, v). \quad (6.74)$$

The probability $P(q, v)$ characterizes the damaging effect of fragments hitting the target and is determined by formula (6.73). It is more convenient to perform calculations for computing the average number of fragments hitting the vulnerable area of the target \bar{n} in a polar system of coordinates related to a moving warhead, with subsequent transition to a system of coordinates x, y and z related to the target.

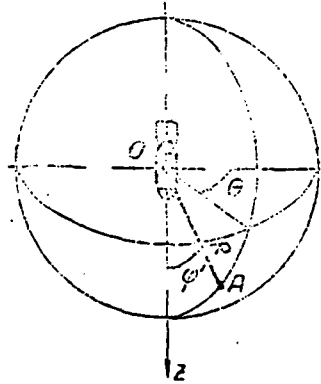


Fig. 6.58.

We shall determine the position of this polar system of coordinates in the following manner (Fig. 6.58). We shall place point O at the point of burst, and we shall orient the polar axis on the warhead axis. It is obvious that the average number of fragments hitting the target in this system of coordinates will be a function of the distance R from the point in space in question

A to the point of burst of the warhead O and the angles ϕ' and θ which determine the position of point A on a sphere with the radius R.

Here and throughout further calculations, the angle ϕ' defines the direction of flight of the fragments with consideration for the inherent velocity of the warhead at the moment of bursting. Assuming that the dimensions of the target are small as compared to the distance R to the point of burst of the bomb, one can determine the average number of fragments hitting the vulnerable area of the target by the formula

$$\bar{n}(R, \phi', \theta) = \pi(R, \phi', \theta) S_{\Sigma} \quad (6.75)$$

where $n(R, \phi', \theta)$ is the mathematical expectation of the total number of fragments hitting the vulnerable area of the target with a given position of the target in relation to the point of burst; $\pi(R, \phi', \theta)$ is the fragment flow density at a given point in space (the number of fragments for each m^2 of area of the sphere); S_{Σ} is the total vulnerable area of all vulnerable elements of the target (the vulnerable area of the target).

In a case where the dimensions of the vulnerable area of the target are comparable to the distance to the point of burst, it is necessary in computing the average number of fragments hitting the target \bar{n} to take into consideration the heterogeneous fragment flow density over the surface of the target. The latter significantly complicates solution of the problem of determining the number of fragments.

However, cases of explosion of a warhead at small distances from the target will always correspond to a very large number of fragments hitting the vulnerable area of the target, i.e., a target kill probability near unity. Therefore, errors involved with the use of formula (6.75) for computing the target kill probability will be slight in these cases, and one can use formula (6.75) in the first approximation for determining the number of

fragments hitting the vulnerable area of the target at any distance from the target to the point of burst.

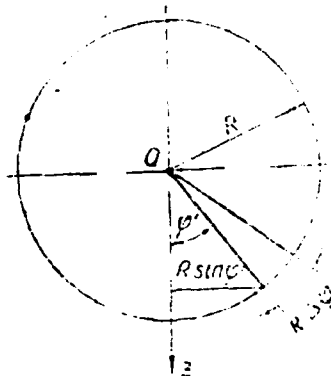


Fig. 6.59.

Now we shall determine the fragment flow density $\pi(R, \phi', \theta)$. As already mentioned, on the strength of the axial symmetry of ammunition, one can assume that the distribution of fragments in the equatorial plane is uniform. In other words, the distribution of fragments in space is characterized only by their distribution in the equatorial plane, i.e., by the law of the distribution $f_v(\phi')$ or $F_v(\phi')$. Consequently, the fragment flow density depends only on two coordinates: the distance R and the angle ϕ' . We shall consider a section of the sphere (Fig. 6.58) as the plane of a large circle (Fig. 6.59) and shall determine the number of fragments $\Delta N_{\phi'}$ flying between two conical surfaces with aperture angles $2\phi'$ and $2(\phi' + \Delta\phi')$ in accordance with formula (6.19):

$$\Delta N_{\phi'} = N f_v(\phi') \Delta\phi'. \quad (6.76)$$

where N is the total number of fragments formed in bursting of the shell; $f_v(\phi')$ is the differential law of the distribution of fragments by directions of scattering with consideration for the inherent velocity of the warhead; $\Delta\phi'$ is the aperture angle of the elementary scattering sector.

If we express the number of fragments $\Delta N_{\phi'}$ in terms of the integral law of the distribution of fragments by directions of scattering $F_v(\phi')$, in accordance with (6.20), we obtain:

$$\Delta N_{\phi'} = N [F_v(\phi' + \Delta \phi') - F_v(\phi')]$$

or

$$\Delta N_{\phi'} = N \Delta F_v(\phi'), \quad (6.77)$$

where $\Delta F_v(\phi')$ is the increment of the ordinate of the integral law.

The area of the elementary area (ring) reached by these fragments can be determined from consideration of the diagram of Fig. 6.59:

$$\Delta S = 2\pi(R \sin \phi')(R \Delta \phi') \quad (6.78)$$

It is obvious that the fragment flow density $\pi(R, \phi')$ is determined by the following formula:

$$\pi(R, \phi') = \frac{\Delta N_{\phi'}}{\Delta S}$$

Inserting values of the variables included from (6.77) and (6.78) into this formula, we obtain:

$$\pi(R, \phi') = \frac{N}{2\pi R^2} \frac{\Delta F_v(\phi')}{\sin \phi' \Delta \phi'} \quad (6.79)$$

Then, in accordance with (6.75), the average number of fragments hitting the vulnerable area of the target, which is located at a distance R from the point of burst in positions for which the direction to the point of burst forms an angle ϕ' with the axis of the warhead, is determined by the formula

$$\bar{n}(R, \phi') = \frac{N}{2\pi R^2} \frac{\Delta F_v(\phi')}{\sin \phi' \Delta \phi'} S_1. \quad (6.80)$$

We shall introduce the following designations:

$$\Pi(R) = \frac{N}{2\pi R^2}; \quad \Phi(\phi') = \frac{\Delta F_v(\phi')}{\sin \phi' \Delta \phi'} . \quad (6.81)$$

The function $\Pi(R)$ characterizes the dependence of the fragment flow density on the distance to the target R .

The function $\Phi(\phi')$ is proportionate to a derivative of the integral law of the distribution of fragments by directions of scattering plotted with consideration for the inherent velocity of the warhead. The value of this derivative is determined in regard to the tangent of the incline angle of a tangential law of the distribution $F_v(\phi')$. The function $\Phi(\phi')$ takes into account the heterogeneity of the fragment flow density in different scattering directions.

The formula for determining the maximum mathematical expectation of the number of fragments hitting the vulnerable area of the target thus has the following form:

$$\bar{n}(R, \phi') = \Pi(R)\Phi(\phi')S_z . \quad (6.82)$$

For determining the mathematical expectation of the number of fragments damaging the target \bar{m} , the value obtained for $\bar{n}(R, \phi')$ in accordance with formula (6.74) must be multiplied by the average target kill probability for a single fragment $P(q, v)$.

Using the target vulnerability function $S^*(q, v)$ introduced above, we obtain (6.73):

$$\bar{m}(R, \phi') = \bar{n}(R, \phi')P(q, v) = \Pi(R)\Phi(\phi')S^*(q, v) . \quad (6.83)$$

The numerical value of the target vulnerability function depends on the velocity of the fragment hitting the target \bar{v} , which is determined for the given explosion conditions, in turn, by the

distance to the target R and the angle ϕ' .

The dependence of the velocity of impact of a fragment against the target on the coordinates R and ϕ' determining the position of the target can be found by formulas (6.52) and (6.21):

$$v = v(R, \phi') = v_0 e^{-c_H R} \cdot (v_0 \cos \phi' + \sqrt{v_0^2 - v_1^2 \sin^2 \phi'}) e^{-c_H R}.$$

Using the formula for the ballistic coefficient of a fragment c_H (6.49), we finally obtain

$$v(R, \phi') = (v_0 \cos \phi' + \sqrt{v_0^2 - v_1^2 \sin^2 \phi'}) e^{-\frac{c_H R}{\sqrt{1 - q}}} \quad (6.84)$$

Thus, for given explosion conditions, the velocity of impact of a fragment on the target depends only on the coordinates R and ϕ' determining the position of the target in relation to the point of explosion of the warhead.

Using formula (6.84), one can compute the velocity of impact of a fragment on the target and then, by means of graphs of the vulnerability function $S^*(q, v)$, one can determine the value of the vulnerable area of the target. Substituting the value obtained for the vulnerability function into (6.83), one can find the mathematical expectation of the number of fragments damaging the target. Since the velocity of impact of a fragment on the target depends on the target coordinates R and ϕ' , the value of the vulnerability function included in (6.83) finally is determined as the function of these same coordinates R and ϕ' .

It should be noted here that both the velocity of impact of the fragment on the target $v(R, \phi')$ (6.84) and the value of the vulnerability function $S^*(q, v)$ (6.73) depend on the weight of the fragment hitting the target. Consequently, the mathematical expectation of the number of fragments damaging the target $\bar{m}(R, \phi')$ will depend on the characteristics of fragmentation of the warhead shell. If the warhead breaks up into fragments of the same weight,

the given fragment weight value is substituted into formula (6.84) in computing the impact velocity v , and the value of the vulnerable area of the target S^* is determined according to the dependence $S^*(q, v)$ corresponding to this fragment weight.

Thus, in this case the mathematical expectation of the number of fragments hitting the target $\bar{m}(R, \phi')$ computed by formula (6.83) will characterize the damaging effect of fragments of the given weight.

If the warhead breaks up into fragments of different weights, and the law of the distribution of fragments by weight is known, it is necessary to compute the dependence of the mathematical expectation of the number of fragments damaging the target on the weight of a fragment hitting the target $\bar{m}(R, \phi', q)$ preliminarily for each set of reported coordinates of the target R and ϕ' . With this dependence one can find the average value of the mathematical expectation of the number of fragments damaging the target by the well-known formula

$$\bar{\bar{m}}(R, \phi') = \int_{q_0}^{q_m} \bar{m}(R, \phi', q) t(q) dq, \quad (6.85)$$

where $t(q)$ is the law of the distribution of fragments by weight; q_0 and q_m are the weights of minimum and maximum fragments, respectively, formed in breaking up of the shell.

In performing such calculations, one normally computes the values of $\bar{m}(R, \phi', q)$ corresponding to the average value of the fragment weight of each weight group, and one uses the following formula instead of formula (6.85):

$$\bar{\bar{m}}(R, \phi') = \sum_{i=1}^n \bar{m}(R, \phi', q_i) \frac{\Delta N_i}{N}, \quad (6.86)$$

where $\Delta N_i/N$ is the relative number of fragments of the i weight group; n is the number of weight groups of fragments.

Values of the mathematical expectation of the number of fragments damaging a target $\bar{m}(R, \phi')$ obtained in this way (6.83) or the average value of this number $\bar{M}(R, \phi')$ (6.86) fully characterizes the damaging effect of fragments of a warhead with given coordinates of the target R and ϕ' and forms the basis for all formulas for computing the target kill probability.

SECTION II

AVIATION FUSES

CHAPTER 7

GENERAL INFORMATION ON FUSES

§ 1. THE PURPOSE OF FUSES

Devices intended for putting the filling of ammunition into action at a predetermined moment in time are called fuses. The use of fuses is prompted by the fact that a powerful initial impulse is required for exciting action of the ammunition. As we know, high explosive VV [explosives] and pyrotechnic compositions used as ammunition charges possess a comparatively low sensitivity to external effects (shock, heating, etc.). This feature of the VV makes the process of filling and use of explosives practically safe. For example, with adherence to the rules for safety procedures, one can drill or melt the most widely used VV - trotyl (it does not explode in the process). Lighted trotyl burns in open air without an explosion. Trotyl normally does not explode in firing of an ordinary bullet through the charge.

The sensitivity of the VV used in practical work is such that one cannot even guarantee their explosion which artillery projectiles hit such strong obstacles as armor or concrete. For initiating

explosion of high explosive VV, igniters easily capable of detonation from the effect of simple types of initial impulses - shock, splitting, a beam of fire - are used. Igniter set caps which create a powerful beam of fire are used for igniting pyrotechnic compositions of ammunition for special and auxiliary purposes.

In addition to solving the basic problem - explosion or ignition of the filling of ammunition - the following basic requirements are placed on modern fuses:

- safety in storage, transporting, service handling and combat use;
- determination of the optimum moment of functioning;
- reliability in functioning under any climatic or meteorological conditions which can be encountered under combat conditions.

The safety requirement is conditioned by the use in fuses of capsules distinguished by high sensitivity to simple types of initial impulses. If protection measures are not included in the fuse design, the detonators can be the cause of premature functioning of the fuses in the process of service or in combat use of the ammunition. Premature response of the fuses can occur from shaking of the detonators in careless handling of the fuses, from the effect of inertial forces during flight of an airplane, in firing and on the trajectory of the missile or bomb on parts of the fuse, including the detonators.

Fuses have the task of determining the optimum moment for functioning in connection with the fact that the efficiency of the damaging effect of an explosion on many targets depends on their position at the moment of explosion in relation to the

ammunition. For example, the damage inflicted on a building by an aerial bomb which has struck it takes on a maximum value if the explosion of the bomb occurs at the level of the foundation of the building. The greatest effect of the moment of the explosion on the degree of damage to the target is exhibited in firing of antiaircraft missiles with remote-action warheads possessing directed scattering of the fragments. Target kill becomes possible in this case only with explosion of the warhead in a definite, extremely limited part of the space associated with the target. The fragments will fly past the target with an early or late explosion (Fig. 7.1).

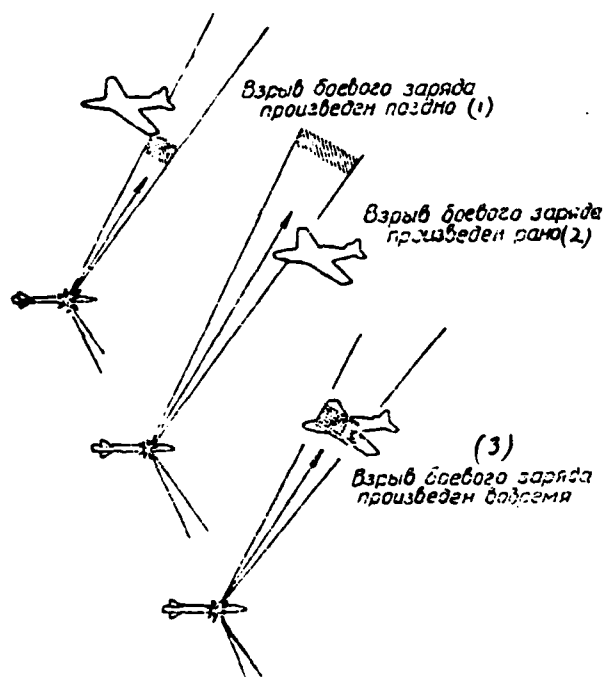


Fig. 7.1.

Key: (1) explosion of the warhead has been effected late; (2) explosion of the warhead has been effected early; (3) explosion of the warhead has been effected on time.

The requirement of high functional reliability from fuses is explained by the fact that the success of combat use of ammunition, in the final analysis, depends on whether the fuse works or fails. In malfunctions of fuses, no explosion of the ammunition occurs; consequently, there is no damage to enemy targets. Fuses which do not operate reliably can be the cause of low efficiency of the entire system of aviation armaments.

Aviation fuses have a great deal in common with the fuses used in other service arms in regard to their principle of operation and their structure. They can vary extremely widely in regard to the complexity of their structure, beginning with the simplest impact fuses of aerial bombs and ending with proximity fuses of antiaircraft missiles, which determine the location and velocity of the target and solve the problem of the most advantageous moment for explosion of the warhead. The simplest fuses are independent devices not structurally connected to the ammunition. They are attached to the ammunition either at the factory or in the process of preparing the aircraft for an operational flight. In the most complex fuses, called detonating devices or destruct systems, the individual units are not joined in a unified structure; on the contrary, they are distributed over different parts of the ammunition. Some of these units can perform other tasks in addition to fuse functions. Fuses involved with missile guidance systems which use data of the guidance systems for determining the moment of detonation can serve as an example of detonating devices.

§ 2. FUNCTIONAL DIAGRAM OF A FUSE

A generalized functional diagram of a fuse is shown in Fig. 7.2.

The common units of fuses are as follows:

- the working command transmitter;
- the command transmission unit;
- safety devices;
- the remote arming mechanism.

The command transmitter is a device which forms the command for functioning of the fuse. This command is formed either as a result of interaction of the transmitter with the target or independently of the target, by means of special time mechanisms which count off the time from the moment of firing or dropping of the bomb. Depending on the type of transmitter, the command created by it can have the character of an explosive impulse, a beam of fire or an electrical signal. A device (Fig. 7.3) consisting of a prong 1, an igniter set cap 2 and a spring 3 holding the prong at a definite distance from the cap can serve as an example of the simplest transmitter. The transmitter responds at the moment of impact on an obstacle, with piercing of the cap by the prong, and a command in the form of a beam of fire is formed.

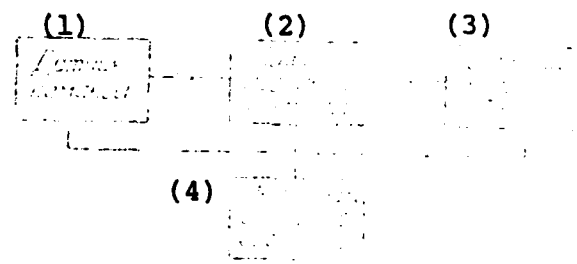


Fig. 7.2.

Key: (1) command transmitter; (2) command transmission unit; (3) actuating unit; (4) remote arming mechanism.

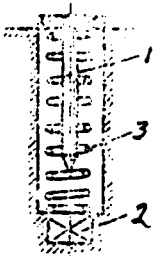


Fig. 7.3.

The command transmission unit is intended for transmitting the functioning command from the transmitter to the actuating unit with a definite time delay. The delay in transmission of the command provides the optimum moment of explosion or ignition of the ammunition filling. The projectile or bomb moves by a definite distance in relation to the target during the delay and by the moment of the explosion occupies a position at which the damage inflicted on the target is maximal. In a case where the optimum moment of the explosion coincides with the moment of creation of the command, there is no need for a delay. In fuses of antiaircraft missiles, an additional device which determines the necessary time delay depending on the conditions of closing of the missile on the target and other factors can control the operation of the command transmission unit.

The actuating unit serves for creating a powerful explosive or heat impulse which causes action of the ammunition filling.

Safety devices ensure safety of the fuse in all stages of service: in storage, transporting, service handling and in combat use. The safety devices structurally are normally components of the sensors and units through which the command for functioning passes. They do not permit functioning of the sensors or passage of a command through subsequent units. Functioning of the fuse

becomes possible only after removal of all safety devices. The process of removal of the safety devices, which is called arming of the fuse, normally begins at the moment of firing (dropping of the bomb) and is completed by the moment when the missile or bomb has gone a safe distance from the carrier airplane. The magnitude of this distance is called the arming range and is selected from the condition of firing safety. The arming range should be a distance such that explosion of the ammunition in accidental (premature) functioning of the fuses after removal of all safety devices is safe for the carrier aircraft. Devices called remote arming mechanisms perform the operation of arming of the fuse.

In addition to safety devices involved with remote arming mechanisms, fuses can have temporary safety devices which are removed in the process of preparation for combat use. Such factors as releasing of the ammunition from the aircraft, achievement of a definite velocity or acceleration by the ammunition, the beginning of operation of the motor, etc., for example, are used for putting the remote arming mechanisms into operation.

§ 3. CLASSIFICATION OF FUSES

Depending on their purpose, aviation fuses are divided into the following:

- fuses for guided and free-flight missiles;
- fuses for aerial gun shells;
- fuses for aerial bombs;
- fuses for aircraft-laid mines and glide-bombs.

Depending on the principle of operation of the command

transmitter, fuses are divided into the following:

- percussion (impact) fuses;
- time fuses;
- proximity fuses.

Fuses whose command transmitter responds to impact on an obstacle are called percussion fuses. As a result of impact, movement of the mobile parts of the transmitter occurs and is used either for piercing set caps or for closing contacts of an electrical circuit. Fuses for impact action are most widely used at present in aerial bombs, free-flight missiles and gun shells.

Fuses with a time monitor, which function after a time established in advance on the trajectory of the ammunition, are called time fuses. The time monitor measures the time from the moment of its engagement to the moment of creation of the command for functioning. This time is established either on the ground just before the operational flight, or immediately before firing, or after firing. Time fuses are used in ammunition for special and auxiliary purposes: illuminating ammunition, signal ammunition, smoke ammunition, etc.

Fuses whose command transmitter forms a command for functioning under the effect of energy emitted or reflected by the target are called proximity fuses. Radio fuses, optical fuses, acoustical and magnetic fuses, etc., can serve as examples of proximity fuses. Fuses with barometric and hydrostatic sensors which react to the pressure level of air and water are also proximity fuses. Proximity fuses are used most extensively in antiaircraft guided missiles. In addition to impact, time and proximity fuses, one can encounter fuses in practical work which do not have their own command transmitter and which accomplish explosion of the ammunition by a

command transmitted from the ground or from the airplane. Fuse devices of this type are used in "Nike-Hercules" antiaircraft guided missiles and the "Nike-Zeus" antimissile missile of the USA. Launching and flight of missiles of the "Nike" system are controlled by a special computer located at the ground launch site, to which data are transmitted concerning the coordinates of the missile and the target from radar target and missile tracking stations. The computer generates appropriate control commands by comparing the coordinates, and the commands are transmitted to the missile. At the moment when the coordinates of the target and the missile coincide, the computer forms a command for explosion of the warhead. The fuses (detonating devices) which function on a command from the ground or from an airplane are called command fuses.

Fuses are divided into mechanical and electrical fuses depending on the principle of construction of the command transmitter. In mechanical fuses, the command for functioning is formed as a result of piercing of the set cap by a prong, while in electrical fuses, the command is formed as a result of closing of an electrical circuit containing a power source and an electric igniter. Fuses which have two types of command transmitters - mechanical and electric - are called electromechanical fuses.

In addition to principles of operation and construction of the command transmitters, fuses are also classified according to the principles of operation and construction of other units, their location (nose and base fuses) and a number of other features which reflect their design peculiarities and characteristics. Classification of fuses according to these features will be considered below.

CHAPTER 8

MECHANICAL IMPACT FUSES

§ 1. FORCES USED FOR OPERATION OF FUSES

Forces of elasticity of springs, the pressure force of powder gases and external forces acting on parts during the period of time beginning with the moment of firing (dropping of the bomb) and ending with the moment of impact on the obstacle are used for operation of individual units of mechanical fuses. The basic forces which can be used by fuses are as follows.

The Force of Inertia from Linear Acceleration of the Projectile

Under the effect of linear acceleration on a projectile,* inertial forces will act on all its elements, including the parts of the fuse; these forces are oriented in a direction opposite to the acceleration. The level of the force of inertia from linear acceleration of a projectile acting on a part of a fuse with a weight q (Fig. 8.1) is defined by the following expression:

*The term "projectile" will be used hereinafter in a generalized sense, indicating both an artillery shell and a missile.

$$s = \frac{g}{2} \frac{dv}{dt}, \quad (8.1)$$

where v is the velocity of the projectile.

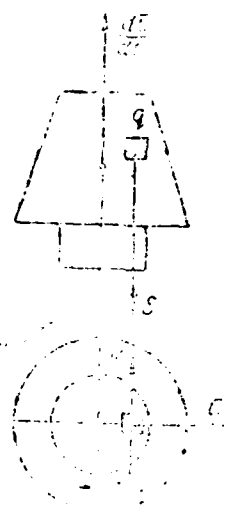


Fig. 8.1.

The acceleration dv/dt can be determined from the equation of motion of the center of mass of the projectile, which has the following form in a general case:

$$\frac{G}{g} \frac{dv}{dt} = |\sum \bar{F}_i(t)|, \quad (8.2)$$

where G is the weight of the projectile.

The right member of equation (8.2) represents the modulus of the resultant of all external forces F_i acting on the projectile. Such forces include the force of pressure of outer gases, the force of friction of the shell against the walls of the bore, the force of gravity and the aerodynamic force of air resistance for artillery shells. The first force is active during movement of the shell along the bore and in a small section of the air trajectory of the shell adjacent to the muzzle of the gun (the period of the after-effect of the gases). The second force is active only during movement

of the shell in the barrel. The last two forces are active throughout the time of movement of the shell both in the barrel and in the air. Similar forces act on missiles as well. The only fundamental difference in these forces lies in the fact that the force of pressure of the powder gases on the missile caused by the jet power or thrust of the engine is active longer - until the end of operation of the missile engine. The active section of the trajectory in which this force is active exceeds the length of an artillery gun barrel by many times.

First we shall find the value of the force of inertia from linear acceleration for a case of firing from an artillery gun. For the period of movement of the shell in the barrel, one can ignore the effect of all forces as compared to the force of the pressure of powder gases.

With such an assumption, the equation of motion of the projectile will take on the following form:

$$\frac{G}{g} \frac{dv}{dt} = \frac{\pi d^2}{4} p(t), \quad (8.3)$$

where d is the caliber of the shell; $p(t)$ is the pressure of powder gases in the barrel.

It follows from equation (8.3) that

$$\frac{dv}{dt} = p(t) \frac{\pi d^2}{4 G}. \quad (8.4)$$

Inserting the value of dv/dt from expression (8.4) into formula (8.1), we obtain

$$S = p(t) \frac{\pi d^2}{4} \frac{q}{G}. \quad (8.5)$$

Formula (8.5) indicates that the force of inertia from linear acceleration of a projectile depends on the time of movement of the shell in the barrel, while the character of variation of this force is determined by the law of variation of the pressure in the barrel (Fig. 8.2). The force S reaches a maximum value S_m at

$t=t_m$ ($p=p_m$), after which it decreases, taking on a value S_0 at the moment of escape of the shell from the bore t_0 . At the end of the period of the aftereffect of the gases t_K , the force S drops to zero. With a curve of the pressure $p(t)$, one can determine the value of the force S at any moment in time. The curve of $p(t)$ can be plotted by well-known methods of internal ballistics. The force of inertia from linear acceleration of a projectile is used in artillery fuses for moving the parts in firing and for removal of safety devices - arming of the fuses - as a result. The effect of the force S must also be taken into consideration in strength calculation of a fuse. It is sufficient in most cases in practice to know only the maximum value of the inertial force $S=S_m$.

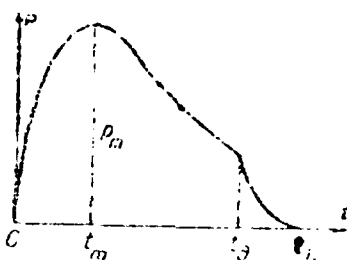


Fig. 8.2.

It follows from formula (8.5) that

$$S_m = p_m \frac{\pi d^2}{4} \frac{q}{G}, \quad (8.6)$$

where p_m is the maximum pressure in the bore.

Having specified $p_m = \frac{\pi d^2}{4G} = k_1$, we obtain

$$S_m = k_1 q. \quad (8.7)$$

The coefficient k_1 indicating the factor by which the inertial weight of a part exceeds its true weight is called the linear arming coefficient. The linear arming coefficient for a particular gun, shell and charge is a constant value and is the maximum

coefficient of the overload acting along the axis of the shell. For aviation artillery systems, the values of the coefficient k_1 are within limits of 40,000 to 100,000.

In movement in air, the basic force acting on a projectile is drag, which reduces the velocity of the projectile. Parts of the fuse located inside the housing are not subject to the effect of air resistance; therefore, they tend to move by inertia in relation to the fuse housing in the direction of movement of the projectile. The inertial force which effects such a movement of the parts is called the drag force. The value of the drag force F_H (Fig. 8.3) is equal to the product of the coefficient of acceleration of the projectile in the direction of its axis and the weight of the fuse part under consideration:

$$F_H = nq, \quad (8.8)$$

where $n=R/G$ - in the projectile acceleration coefficient; R - the force of air resistance.

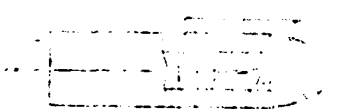


Fig. 8.3.

The value of the force of air resistance is determined by a well-known formula of external ballistics:

$$R = \frac{G}{g} c H(y) F(v), \quad (8.9)$$

where c is the ballistic coefficient of the projectile; $H(y)$ is a function of variation of the density of the air with the altitude y ; $F(v)$ is a function of the air resistance.

Since the function $F(v)$ decreases with a decrease in the

velocity of the projectile, the maximum drag force is active immediately after the end of the period of the aftereffect of the gases, when the projectile takes on its maximum velocity. The drag force increases with a decrease in the flight altitude of the projectile. We shall find the maximum possible value of the drag force, assuming the velocity of the projectile v to be equal to its initial velocity v_0 , and the function $H(y)=1$.

It follows from expression (8.8) and (8.9) that

$$F_{\text{drag}} = \frac{cF(v_0)}{g} q = k_2 g. \quad (8.10)$$

where k_2 is the drag coefficient.

For aviation artillery shells, the value of the coefficient k_2 is within limits of 10-100. The drag force acting on mobile parts of the fuse and causing their movement can result in premature piercing of the set cap by the prong. For preventing premature functioning of fuses under the action of the drag force, their designs should include special safety devices.

We shall go on to consider inertial forces for a case of firing of missiles. The equation of motion of a missile in the active section of its trajectory can be written approximately without consideration for the effect of air resistance and the force of gravity:

$$\frac{G(t) \frac{dv}{dt}}{g} = P(t) \quad (8.11)$$

where $G(t)$ is the weight of the missile, which varies in time due to fuel consumption; $P(t)$ is the engine thrust.

It follows from equation (8.11) that

$$\frac{dv}{dt} = \frac{g}{G(t)} P(t). \quad (8.12)$$

The dependence of the acceleration on time for rocket missiles of the M-8, M-13 and M-31 type is shown in Fig. 8.4. At the beginning of operation of the engine, the acceleration of the projectile rapidly reaches the maximum value and then varies only slightly up to the end of the active section of the trajectory, where it drops to zero.

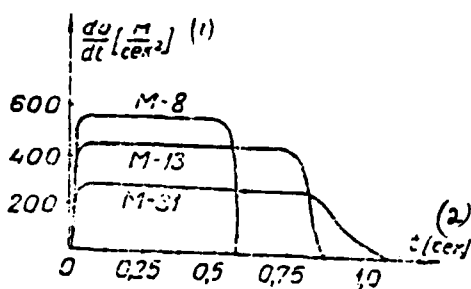


Fig. 8.4.
Key: (1) m/s^2 ; (2) s.

In contrast to artillery shells, missiles experience significantly smaller positive accelerations and, consequently, smaller inertial stresses. The linear arming coefficient has an order of 5-10 for missiles with liquid-fuel engines and 20-100 for missiles with a solid-propellant engine. Another feature of missiles lies in the fact that they move with a positive acceleration for a comparatively long time. In artillery guns, the time interval in which the powder charge undergoes combustion and the shell moves with a positive acceleration is very small - of the order of 0.002-0.05 s. In solid-propellant missiles, the time for operation of the engine and for accelerated movement ranges from tenths of a second to several seconds. In some liquid-fuel rockets, the time for operation of the engine reaches several tens of seconds. For example, the engine of the FAU-2 missile operated for about 65 s. This feature of missiles makes it possible to use safety devices in the fuses which are armed under the effect of slight but

prolonged inertial stresses and, at the same time, are not armed with brief, although significant, stresses, which can be active under handling conditions - in movements, in accidental dropping, etc.

The drag force in missile fuses operates from the beginning of the passive section of the trajectory. Its magnitude is determined by expression (8.10), which was obtained for artillery shells.

Inertial Force from Tangential Acceleration of a Projectile

In cases where an angular acceleration $d\omega/dt$ is imparted to a projectile, a tangential acceleration will act on fuse parts which are offset in relation to the rotation axis. The magnitude of the tangential acceleration is determined by the expression

$$\omega = r \frac{d\omega}{dt},$$

where r is the distance of the fuse part (Fig. 8.1) from the rotation axis of the projectile.

The inertial force K conditioned by the effect of this acceleration is as follows:

$$K = \frac{q}{g} r \frac{d\omega}{dt}. \quad (8.13)$$

It is oriented at a tangent to a circle with the radius r in a direction which is opposite to the vector $\bar{\omega}$. In accelerated rotation of the projectile, the force K acts in a direction opposite to the direction of rotation of the projectile. We shall find the value of the angular acceleration and the force K for an artillery shell. In firing from an artillery gun, one can assume that the angular acceleration acts on the shell only during its movement along the bore. During movement of the shell in air, its angular velocity drops slightly, which makes it possible to neglect the effect of a negative angular acceleration

on the shell.

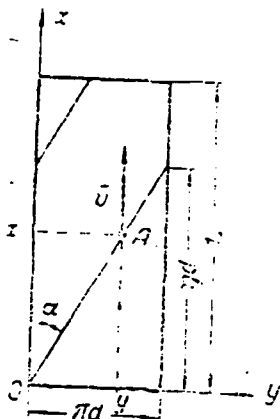


Fig. 8.5.

We shall assume that the shell moves along a bore with rifling of a constant curvature. We shall open the inner surface of the barrel on the plane of a diagram (Fig. 8.5). Rifling of the barrel is shown in the presentation by the line which forms the angle α with the generatrix, while the barrel surface is shown by the rectangle with the base πd and a height equal to the barrel length L . We shall relate the rectangular coordinate system Oxy to the position of the shell before firing; we shall direct the x axis along the axis of the bore and the y axis perpendicular to the x axis. We shall consider the movement of some point A located on the surface of the shell and moving along the riflings together with it in this system of coordinates. The point A will move along the riflings with a velocity v in the direction of the x axis equal to the linear velocity of the shell.

It follows from Fig. 8.5 that

$$\frac{x}{y} = \frac{\eta d}{\pi d} = \frac{\eta}{\pi}, \quad (8.14)$$

where η is the length of the course of the riflings in calibers;

y is the path traversed by point A around the circumference.

From expression (8.14), we find

$$y = \frac{\pi}{\eta} x. \quad (8.15)$$

Differentiating both members of equation (8.15), we find the annular velocity of the shell:

$$\frac{dy}{dt} = \frac{\pi}{\eta} \frac{dx}{dt} = \frac{\pi}{\eta} v. \quad (8.16)$$

The annular velocity of the shell is related to its angular velocity ω by an obvious relationship:

$$\frac{dy}{dt} = \frac{d}{2} \omega. \quad (8.17)$$

Setting equal the right members of expressions (8.16) and (8.17), we obtain

$$\omega = \frac{2\pi}{\eta d} v. \quad (8.18)$$

Substituting the value obtained for ω into formula (8.13), we find

$$K = \frac{2\pi r}{\eta d} \frac{q}{g} \frac{dv}{dt}.$$

Taking into consideration formula (8.4), we finally obtain

$$K = p(t) \frac{\pi^2 d}{2\eta} \frac{q}{G} r. \quad (8.19)$$

As one can see, the inertial force from tangential acceleration, like the force S , varies in proportion to variation in the pressure in the barrel. During the period of the aftereffect of the gases, this force, in contrast to the force S , is equal to zero. The greater the distance from the center of mass of the part to the rotation axis of the projectile, the greater the value of the force K .

The inertial force from tangential acceleration tends to turn the fuse parts in relation to the rotation axis and can be used for removing safety devices and arming the fuse. The numerical value

of the force K is substantially less than the value of the force S . It follows from formulas (8.5) and (8.19) that

$$\frac{K}{S} = \frac{2\pi}{\eta d} r.$$

Assuming that $\eta=20$ and $r=d/2$, we find that $K=0.15S$. The force K reaches the maximum value at $p=p_m$:

$$K_m = p_m \frac{\pi^2 d}{2\eta G} q r.$$

Having specified $p_m \frac{\pi^2 d}{2\eta G} = k_3$, we shall reduce the formula for K_m to the following form:

$$K_m = k_3 qr. \quad (8.20)$$

The coefficient k_3 , which is constant for a given gun, shell and charge, is called the coefficient of the tangential acceleration force. The numerical value of this coefficient characterizes the maximum tangential force acting on a part with a unit of weight located at a distance of a unit of length from the rotation axis of the shell. For aviation artillery systems, the values of the coefficient k_3 are within limits of 2000-10,000.

Centrifugal Force

Centrifugal force is conditioned by rotation of the projectile. Like the inertial force from tangential acceleration which has just been considered, it acts on parts of fuses which are offset from the rotation axis. The value of centrifugal force is expressed by the following formula:

$$C = \frac{q}{g} r \omega^2. \quad (8.21)$$

The centrifugal force is directed along the radius (Fig. 8.1) in a direction away from the rotation axis. Centrifugal force acts on parts of artillery fuses both during movement of the shell along the bore and on the trajectory in air. Replacing the value of ω in formula (8.21) with its value from (8.18), we obtain an expression for the force C in movement of the shell along the bore:

$$C = \frac{q}{g} r \left(\frac{2\pi}{\eta d} \right)^2 v^2. \quad (8.22)$$

As one can see, the centrifugal force during movement of the shell in the bore varies in proportion to the square of the linear velocity of the shell. The centrifugal force reaches its maximum value at the moment of escape of the shell from the barrel.

Consequently,

$$C_m = \frac{q}{g} r \left(\frac{2\pi}{\eta d} \right)^2 v_0^2, \quad (8.23)$$

where v_0 is the initial velocity of the shell.

The maximum value of the centrifugal force is comparable to the maximum value of the inertial force from linear acceleration of the projectile.

In contrast to the first two inertial forces, centrifugal force is active throughout the trajectory of the projectile. The force C decreases in proportion to movement of the projectile in air, since the value of the angular velocity of the projectile decreases. However, as already mentioned, the drop in the angular velocity of the projectile in the trajectory is slight. Therefore, the decrease in the value of centrifugal force is also slight. Having designated $\frac{1}{g} \left(\frac{2\pi}{\eta d} \right)^2 v_0^2 = k_4$, according to formula (8.23), we obtain

$$C_m = k_4 qr. \quad (8.24)$$

The coefficient k_4 , which is numerically equal to the centrifugal force acting on a part with a unit of weight located at a distance of a unit of length from the rotation axis of the projectile, is called the centrifugal arming coefficient. Values of k_4 are within limits of 5000-40,000 for aviation artillery systems.

The parts of missile fuses undergo the effect of centrifugal

forces in turbojet and turning missiles. Rotation is imparted to the former for stabilization in flight and is achieved by an incline of the jet engine nozzles. Finned missiled sometimes are put into "rolling" for improving accuracy - reducing the technical dispersion. Rolling of missiles is normally achieved by installing a fin assembly at a small angle to the axis of the missile. The values of angular velocities of turbojet missiles are of approximately the same order as the angular velocities of artillery shells. The angular velocity of a missile at different points of the active section of the trajectory can be calculated according to an approximate formula:

$$\omega = \frac{I_1 q_3(t) / \sin \gamma}{B} \quad (8.25)$$

where I_1 is a single impulse of the jet thrust; $q_3(t)$ is the weight of the part of the solid-propellant charge which has undergone combustion at the moment t ; l is the arm of the jet power which rotates the missile; γ is the incline angle of the nozzle axis in relation to a plane passing through the missile axis and the center of the nozzle; B is the average value of the polar moment of inertia of the missile.

The angular velocity of turning missiles is relatively low, of the order of 1000-1500 r/min. However, its value does prove sufficient for moving fuse parts. In addition to rotation of the projectiles, gyroscopic precession and nutation of projectiles in flight in air can serve as a source of centrifugal forces acting on fuse parts. The centrifugal forces C_u from oscillations of the projectile (Fig. 8.6) are directed along the projectile axis. They have the same effect on fuse parts as drag forces, tending to move the parts away from the center of mass of the projectile.

The value of the force C_u is as follows:

$$C_u = \frac{q}{g} \Omega^2 l, \quad (8.26)$$

where Ω is the angular velocity of gyroscopic nutation and precession of the projectile; l is the distance from the center of mass of the projectile to the part in question.



Fig. 8.6.

The maximum angular velocity of oscillations of artillery shells is determined by the following formula:

$$\Omega_m = \delta_m \frac{\pi v_0}{\frac{A}{B} \eta d}, \quad (8.27)$$

where δ_m is the maximum value of the angle of gyroscopic nutation of the projectile; A/B is the ratio of the equatorial movement of inertia of the projectile to the polar moment of inertia.

Substituting the value of Ω_m into formula (8.26), we obtain an expression for the maximum value of the force C_{\max} :

$$C_{\max} = \frac{q}{g} \left(\frac{\pi v_0}{\frac{A}{B} \eta d} \right)^2 \delta_m^2 l.$$

Designating $\frac{1}{g} \left(\frac{\pi v_0}{\frac{A}{B} \eta d} \right)^2 \delta_m^2 = k_5$, we find

$$C_{\max} = k_5 g l. \quad (8.28)$$

Values of the coefficient k_5 are within limits of 0.5-10 l/cm for artillery systems. Formulas (8.27) and (8.28) are also valid for turbojet projectiles. In the use of formula (8.27) for turbojet projectiles, it follows from expression (8.18) that the value for $\pi v_0 / \eta d$ in the formula should be replaced with the value of the angular velocity of the projectile.

The Coriolis Force

Coriolis forces act on fuse parts moving in a direction which forms some angle α with the rotation axis of the projectile (Fig. 8.7). These forces are conditioned by the effect of Coriolis acceleration:

$$\bar{J}_k = 2(\bar{\omega} \times \bar{v}), \quad (8.29)$$

where \bar{v} is the vector of the velocity of the mobile part; $\bar{\omega}$ is the vector of the angular velocity of the projectile.

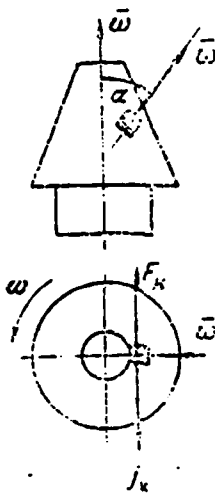


Fig. 8.7.

The Coriolis force is an inertial force and, according to expression (8.29), is determined by the vector product

$$\bar{F}_k = 2 \frac{g}{\omega} (\bar{v} \times \bar{\omega}). \quad (8.30)$$

The direction of the effect of the force \bar{F}_k is determined according to the following rule. From the end of the vector \bar{F}_k , the transition from the vector \bar{v} to the vector $\bar{\omega}$ by the shortest path should be accomplished clockwise. The magnitude of the Coriolis force, as follows from formula (8.30), is as follows:

408

$$F_x = 2 \frac{q}{g} \omega w \sin \alpha. \quad (8.31)$$

Substituting the value of ω from formula (8.18) into expression (8.31), we obtain

$$F_x = \frac{q}{g} \frac{4\pi}{\eta d} w \sin \alpha. \quad (8.32)$$

The force F_x reaches the maximum value at $v=v_0$ and $\sin \alpha=1$, i.e., in a case where the part is moving in a direction perpendicular to the rotation axis of the projectile:

$$F_{x_m} = \frac{4\pi v_0}{g \eta d} q \omega = k_6 q \omega, \quad (8.33)$$

Where

$$k_6 = \frac{4\pi v_0}{g \eta d}.$$

The coefficient k_6 is the maximum value of the Coriolis force acting on a part whose weight is equal to a unit and which is moving in a direction perpendicular to the rotation axis of the projectile with a unit velocity. For aviation artillery systems, $k_6=(5-20)$ s/cm.

The Coriolis force is not used for moving fuse parts. It must be taken into consideration in determining the friction forces acting on moving parts of the fuse.

The Force of Air Resistance

The force of air resistance has a direct effect only on projecting parts of fuses. In nose fuses, such parts normally include membranes (Fig. 8.8) folded into the nose section, which protect the striker or prong against movements in service handling and flight in air. The air pressure on the fuse membrane at subsonic velocities of the projectiles is calculated according to the Bernoulli equation

$$\Delta p = \frac{\rho_0 v^2}{2} \left[1 + \frac{1}{4} \left(\frac{v}{c_n} \right)^2 \right], \quad (8.34)$$

where ρ_0 is the density of the air; c_0 is the velocity of sound in air; v is the velocity of the projectile.

Fig. 8.8.

At supersonic velocities, the pressure on the membrane is calculated by the Rayleigh formula

$$P = P_0 \frac{165.7 \left(\frac{v}{c_0} \right)^7}{\left[7 \left(\frac{v}{c_0} \right)^2 - 1 \right]^{2.5}} \quad (8.35)$$

§ 2. BASIC MECHANISMS OF FUSES

Mechanical impact fuses are made up of the following basic units:

- the striker mechanism;
- the powder delay train;
- safety devices;
- the remote arming mechanism;
- a self-destruction device.

Striker Mechanisms

Striker mechanisms of impact fuses are transmitters which form a command for functioning in impact on an obstacle. Depending on the character of the external forces which put the striker mechanisms into operation, they are divided into reaction, inertial and reaction-inertial mechanisms.

A reaction striker mechanism (Fig. 8.9) is made up of a striker with a prong 1, a safety spring 2 and a set cap 3. Splitting of the cap by the prong occurs due to a direct effect of the obstacle on the head of the striker at the moment of impact on the obstacle. During flight of the projectile or bomb in air, the striker is kept from moving toward the set cap by the safety spring. The cavity of the fuse in which the striker is located is normally covered by a membrane which protects the striker against external effects in service handling and during flight of the projectile in air. Reaction striker mechanisms can be used only in nose fuses situated in the nose section of the projectile.

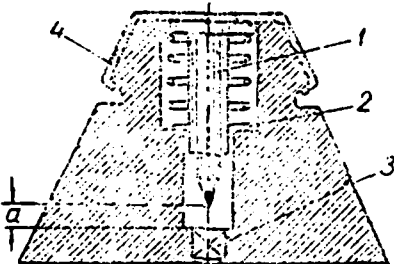


Fig. 8.9.

The operation of inertial striker mechanisms is based on the use of inertial forces which develop in slowing down of projectiles in the process of penetration of obstacles. Depending on the range of impact angles of the projectile with the obstacle at

which reliable functioning of inertial striker mechanisms occurs, the mechanisms are divided into axial action, lateral percussion and general percussion mechanisms.

Axial inertial striker mechanisms (Fig. 8.10) are normally used in base fuses. They are made up of an inertial striker 1 which has the capability of moving only along the axis of the projectile, a set cap 3 and a safety spring 2. Axial inertial striker mechanisms are used comparatively rarely, since they function reliably only at angles of impact with the obstacle of the order of 30° or more.

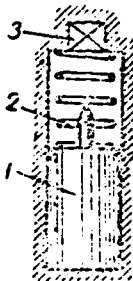


Fig. 8.10.

Lateral percussion inertial mechanisms (Fig. 8.11) are supplemented with an inertial collar 2 capable of moving in a lateral direction, in addition to the inertial striker 1. In the travelling position (in storage or transport), the striker rests by its bottom section, which has a conical shape, on the conical surface of the inertial collar, which is kept from moving by lugs of a rigid safety device 3. At large angles of impact with the obstacle, the component of the inertial force in a lateral direction is insufficient for bending the lugs of the safety device. In this case, the inertial collar remains stationary in impact, and splitting of the set cap occurs due to axial movement of the striker. With low impact angles and in lateral impact of the projectile, the lateral component of the inertial force moves the collar 2, bending

the lugs of the safety device in the process. During lateral movement, the collar forces the striker upward, and the prong splits the set cap. Lateral percussion inertial mechanisms function reliably at angles of impact with the obstacle of 0 to 90° and are normally used in missile fuses.

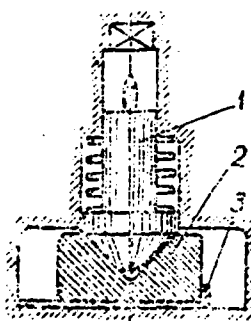


Fig. 8.11.

General percussion striker mechanisms (Fig. 8.12) are used in general-purpose fuses. They function reliably at any impact angle with the obstacle. A typical general percussion mechanism is made up of two inertial strikers 1 and 2 which slide on conical support surfaces. A prong is connected to one of the strikers, while the set cap is connected to the other. An inertial force directed along the axis of the mechanism causes movement of one of the strikers. With a lateral direction of the force, both strikers are put into motion; sliding on the conical surfaces, they come together.

Reaction-inertial striker mechanisms (Fig. 8.13) are made up of two strikers: a reaction striker 1 and an inertial striker 2. They are used only in nose fuses and are distinguished from reaction mechanisms by improved operating reliability.

In addition to striker mechanisms with a splitting action, so-called pneumatic striker mechanisms are also finding use in

practical work; these mechanisms function in heating of the air in a closed space. The pneumatic striker mechanism (Fig. 8.14) is made up of a striker 1, a set cap 2, a plunger 3 and a safety spring 4. The plunger with the set cap fits into a cavity of the striker. In impact of the projectile on an obstacle, rapid movement of the striker occurs, as a result of which the air in the cavity in front of the set cap is rapidly compressed. The compressed air heats up and puts the set cap into operation. Fuses with pneumatic striker mechanisms do not possess sufficient safety in handling if they are not equipped with special safety devices. However, including additional safety devices in them eliminates the main advantage of pneumatic fuses - design simplicity. For this reason, pneumatic striker mechanisms are not used in modern fuses.

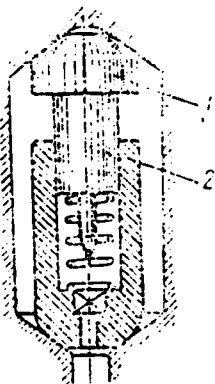


Fig. 8.12.

The basic characteristics of striker mechanisms are as follows: operating speed, sensitivity and reliability. The operating speed of a striker mechanism means the time interval from the moment of impact of the projectile on the obstacle to the moment of explosion of the set cap. The operating speed depends mainly on the distance between the prong and the set cap, the resistance of the safety

spring, the weight of the striker, the type of the striker mechanism and the conditions of impact of the projectile on the obstacle (the velocity and angle of impact and the type of obstacle). Reaction striker mechanisms have the greatest operating speed. The time for operation of the striker mechanism t_y is made up of two components:

$$t_y = t_1 + t_2.$$

where t_1 is the time for movement of the striker for the distance a (Fig. 8.9) between the prong and the set cap and the depth of piercing Δ ; t_2 is the time for excitation of the set cap and formation of a sufficiently powerful flow of explosion products.

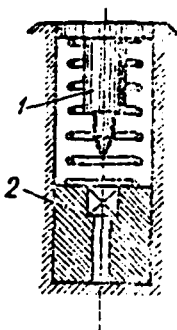


Fig. 8.13.

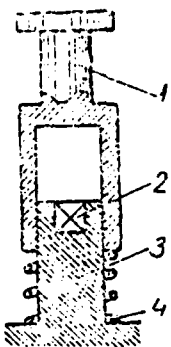


Fig. 8.14.

The time t_1 is determined mainly by the strength of the obstacle and the velocity of the projectile at the moment of impact v_c . It can be established most simply for reaction striker mechanisms. One can assume that with sufficient strength of the obstacle, a reaction striker stops instantaneously at the moment of impact, while the projectile continues to move at the velocity v_c . If the striker is sufficiently strong in this case and does not undergo deformation from impact, assuming that the velocity of penetration of the prong into the set cap is constant and equal to v_c , we obtain

$$t_1 = \frac{a + \Delta}{v_c}.$$

The minimum depth Δ sufficient for reliable functioning of the set cap depends on its sensitivity, the splitting velocity, the shape of the prong and other factors. Experience indicates that the value of Δ for set caps lies within limits of 0.8-1.5 mm. For inertial striker mechanisms, the time for movement of the striker by a distance $a + \Delta$ is determined in a more complex manner, as will be demonstrated below.

The time t_2 for functioning of igniter set caps and igniters can be estimated at a value of the order of 20 μ s.

The sensitivity of striker mechanisms refers to their capacity for reacting to external effects. Sensitivity is characterized quantitatively by the value of the kinetic energy of the striker necessary for functioning of the cap. It is customary to determine the sensitivity of fuses in practice by firing on weak obstacles with the least possible velocity of impact on the obstacle. Requirements of reliable operation in firing on 3-5-mm plywood panels or dense cardboard with a thickness of 1-2 mm with a velocity of impact on the targets of the order of 200 m/s are normally placed on fuses of high sensitivity. The sensitivity of striker mechanisms depends on such design parameters as the resistance of the membrane and the safety spring, the

diameter and weight of the striker, the distance between the prong and the set cap, the sharpening angle of the prong, the sensitivity of the set cap, etc. The sensitivity of reaction mechanisms increases with an increase in the diameter and a decrease in the weight of the striker. The sensitivity of inertial mechanisms, on the other hand, increases with an increase in the striker weight.

It is customary to characterize the reliability of striker mechanisms and of fuses as a whole by the probability of reliable functioning or the percentage of malfunctions. Modern tactical-technical requirements for mechanical impact fuses permit no more than 2% malfunctions of the fuses. The angle of impact of the projectile on the obstacle has the greatest effect on the reliability of axial reaction and inertial striker mechanisms. The greater the impact angle, the more reliably these mechanisms work. The reliability drops with a decrease in the impact angle. The minimum impact angle at which practically trouble-free functioning of a striker mechanism occurs depends on the strength of the obstacle. For example, this angle is of the order of 45° in impact of a projectile on a strong obstacle and $1-2^\circ$ in impact on soft ground for reaction membrane striker mechanisms.

The Powder Delay Train

The combination of ignition and detonation components serving for providing the required operation of a fuse after functioning of the striker mechanism is called the powder delay train. Depending on the type of target being fired on or bombed, the fuse is required to provide either instantaneous explosion of the warhead or explosion with some time lag - with a delay. Depending on the time of operation, impact fuses are divided into instant fuses and fuses of delayed action. Instantaneous explosion is used, for example, in firing on targets located on the ground surface, while explosion of a delay is used on targets situated under cover. The term "instantaneous operation" is provisional, since the time for

operation of a real fuse cannot be equal to zero. It is determined by the time for functioning of the striker mechanism. It is customary to classify fuses whose operating time is less than 1000 μ s as instant fuses. Instantaneous operation can be provided only by nose fuses with a reaction striker mechanism.

The simplest powder delay train for instant fuses is made up of two elements: an igniter of the penetration type and a detonator. The igniter responds in splitting by a prong by exciting explosion of the detonator; a block of a high VV [explosive] - tetryl, pentrite or hexogen - plays the role of detonator. The detonator block amplifies the explosive impulse of the cap, which is passed on to the charge of the warhead.

In fuses which impart a thermal impulse to the charge, an igniter set cap is used instead of an igniter, and a powder magazine is used instead of a detonator block. The more complex powder delay train of instant fuses includes three elements: the igniter set cap, a radiation igniter and a detonator. The first cap responds in splitting by the prong and excites explosion of the igniter with a beam of fire, while the igniter excites explosion of the detonator. Such a powder delay train is used in cases where the striker mechanism and the detonator are located a comparatively great distance apart because of design considerations. The powder delay train of delayed action fuses consists of an igniter set cap, a delay element, an igniter and a detonator. The delay element serves for transmitting a beam of fire from the first cap to the igniter. Depending on the purpose of the fuse, the magnitude of the delay can have a value from hundredths of a second to several hours or even days. A short delay (from fractions of a second to a few minutes) is provided by burning of appropriate fuse compositions either of ordinary time fuse powder or of low-gas compositions. A delay element for fractions of a second normally consists of an igniter powder peg 2, the delay element proper 1 and a reinforcing peg 2 (Fig. 8.15). The pegs are pressed under a low pressure and serve for intensifying the beam of fire: the former, for the

igniter set cap, and the latter, for the time fuse composition. Delay elements for several seconds or minutes consist of one or several discs 1 with annular and radial grooves, into which a time fuse composition 2 is pressed (Fig. 8.16). The shortcoming of pyrotechnic delay devices is the dependence of the size of the delay on external conditions (atmospheric pressure and the temperature).

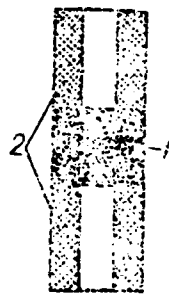


Fig. 8.15.

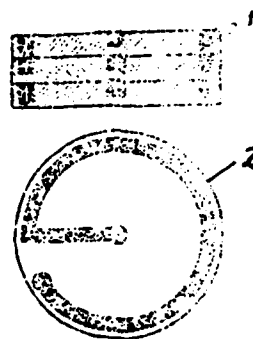


Fig. 8.16.

For obtaining extremely short delays (fractions of a millisecond), so-called gas dynamic delay elements are often used. The principle of operation of such delay elements is based on

movement of gases of the igniter set cap toward the igniter through a labyrinth of openings with a small cross section. The gas dynamic delay element structurally is manufactured in the form of a sleeve with calibrated apertures, which is situated between the set cap and the igniter.

Fuses can have several settings for different operating times. The operating time is normally set in the process of use in accordance with the character of the target which is to be fired on or bombed. Figure 8.17 presents a schematic diagram of a pyrotechnic delay device with three operating time settings.

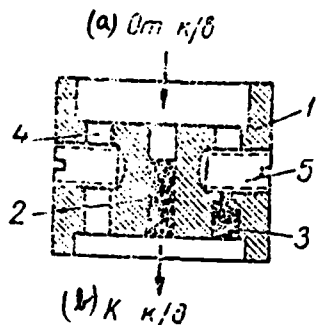


Fig. 8.17.
Key: (a) from k/v [igniter set cap];
(b) to k/d [igniter].

The delay device is made up of a sleeve 1 in which there are three channels 2, 3 and 4 for passage of a beam of fire from the igniter set cap (k/v) toward the igniter (k/d). The delay element which provides the greatest delay is located in the central channel 2. A delay element with the shortest burning time is located in another channel 3. The third channel serves for direct passage of the beam of fire, with by-passing of the delay elements, and provides instantaneous action of the fuse. The channels for the shorter delay and for instantaneous action are covered by set screws 5. If the set screws are screwed in, the fuse functions with the greatest delay. For setting the fuse for instantaneous action or a shorter delay, it is necessary to unscrew the appropriate

screw.

Delay devices which provide a delay time of several hours to several days are used in fuses for aerial bombs in mining of a locality or of individual objects - industrial enterprises, airstrips, railroad junctions, etc. - from the air. The structure of such delay elements can be based on various principles: mechanical, chemical, electrochemical and electrical principles. A mechanism for a long delay constructed based on a mechanical principle is an ordinary clock mechanism. The VVS [air forces] of the German Army of the time were equipped with a long-term fuse with a clock mechanism during the Second World War. The clock mechanism of the fuse provided a delay of 1.5 to 76 hours. The clock mechanism was triggered after impact of the bomb on an obstacle. The possibility of smooth regulation of the delay time in the process of use of the fuse should be considered an advantage of the mechanical principle for construction of delay elements. The complexity of the design, conditioned by increased requirements for strength of the clock mechanism, and the comparative simplicity of determination of the type of fuse with which an unexploded bomb is equipped by listening to the sound in operation of the clock mechanism must be classified as shortcomings of such fuses. After determination of the type of fuse, its operation can be stopped without removing the fuse from the bomb by creation of a strong magnetic field or by freezing. Figure 8.18 shows a schematic diagram of a delay device which operates based on a chemical principle. In the ordinary position, the striker 1 is situated under the effect of a compressed spring 2. This position is fixed by means of a screw 4 resting on a celluloid plate 3. A tube 5 with a solvent is located above the plate. Organic solvents - acetone, etc. - are normally used as the solvent. Before combat use of the fuse, the solvent is isolated from the celluloid plate, which is ensured by airtightness of the tube. The tube can be broken either in impact of the bomb on an obstacle or on the

trajectory of the bomb in the air. In opening of the tube, the solvent comes into contact with the celluloid plate and, going into a chemical reaction with it, dissolves it. As soon as the strength of the celluloid plate is rendered inadequate for holding the striker with the spring, the striker pierces the set cap 6, and the fuse functions. The fuse delay time, other conditions being equal, depends on the composition and quantity of the solvent in the tube and on the composition of the plastic from which the plate is made and the number of plates. The possibility of obtaining any delay comparatively simply should be considered an advantage of the chemical principle. Disadvantages of the principle are a strong dependence of the delay time on the temperature of the environment and the impossibility of adjusting the size of the delay in the process of use. The delay time for each fuse model is set at the factory in manufacturing. Therefore, the desire to have available fuses with different delay times results in an abundance of models, which creates familiar difficulties in use of the fuses and in equipping units with fuses. Electrochemical and electrical delay devices will be considered in the next chapter, which is devoted to electrical fuses.

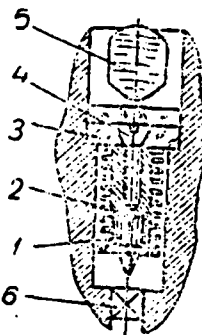


Fig. 8.18.

Safety Devices

The safety of modern fuses is normally provided by a break in their operational chain. The operational chain of a fuse generally consists of the following elements (Fig. 8.19): the striker 1, the igniter set cap 2, a delay element 3, the igniter 4, a magazing detonator 5 and the detonator 6. For operation of the fuse to become impossible, it is sufficient to disengage any element from this chain. The caps and magazine detonators are most often disengaged by shifting them to the side, while disengagement of the striker is accomplished by the use of special parts (stoppers 7) which prevent its movement. The operational chain can also be disengaged by introducing additional partitions and screens 8 between its individual elements; these partitions and screens are removed in arming of the fuse. Fuses are divided

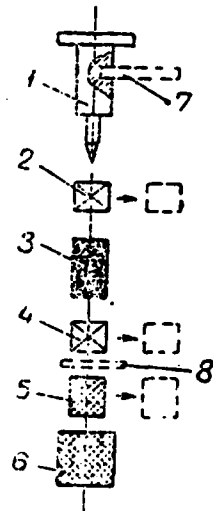


Fig. 8.19.

into non-boresafe, semi-boresafe and bore-safe fuses in regard to the degree of safety in service handling. In non-boresafe fuses, the igniter set cap and the igniter are not insulated from the

detonator; therefore, in accidental response of one of them, explosion of the detonator will occur. In semi-boresafe fuses, the igniter set cap is insulated from the igniter up to the moment of arming. In bore-safe fuses, both the igniter set cap and the igniter are insulated from the detonator; therefore, accidental response of either does not result in explosion of the detonator. The number of elements in the operational chain of a fuse can be different depending on its purpose and the complexity of the functions which it performs. For example, the operational chain is made up of only two elements - the striker and the cap - in the simplest fuses.

Arming Mechanisms

Two types of remote arming mechanisms (MDV) find use in aviation fuses. Mechanisms of the first type perform arming a definite time after firing or dropping of the bomb. The arming range of such mechanisms depends on the velocity of the projectile and the altitude at which firing is performed. With a predetermined arming time, the arming range increases with an increase in the velocity and the altitude. This is one of the shortcomings of time MDV. The main advantage of time MDV is the comparative simplicity of the structure, due to which they have been most widely used in modern fuses. Arming mechanisms of the second type perform arming after the projectile has travelled a definite distance from the firing point or after the projectile has reached a definite velocity or acceleration. Remote arming mechanisms, as a rule, are made up of three basic parts:

- an actuating device, functioning of which determines the moment of the beginning of operation of the MDV;
- a delay device, which determines the size of the time for transfer of the fuse parts into the operational position;

- a device which drives the fuse parts into the operational position.

Depending on the principle of construction of the delay device, MDV are divided into pyrotechnic, mechanical and electrical MDV.

The arming time in pyrotechnical MDV is determined by the time for burning of the pyrotechnic fuse composition, which holds the stopper which prevents either movement of the striker or movement of the set cap, which is offset in relation to the prong. Figure 8.20 shows a schematic diagram of a pyrotechnic MDV with an offset set cap. The cap is situated in a slide 1 which is shifted in a direction away from the prong up to the moment of arming. In such a position, the slide is held by a stopper 3 resting in a fuse composition 4 of a pyrotechnic compound. This compound is ignited by a trigger device (PU) at the moment of firing (dropping of the bomb). After burning of the compound, the spring forces the stopper downward. The freed slide takes the operating position under the action of its spring 2. Piercing mechanisms and electrical devices are used for triggering pyrotechnic MDV.

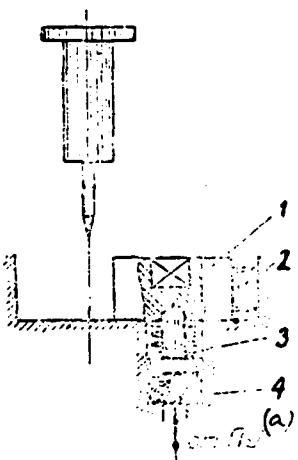


Fig. 8.20.
Key: (a) from PU.

Figure 8.21 presents three characteristic diagrams of piercing mechanisms of MDV. The first system is used in artillery fuses. In firing, the striker 1 sinks down under the action of an axial force, compresses the safety spring 2 and pierces the igniter set cap 3, which ignites the delay device of the MDV. The resistance of the safety spring and the weight of the striker should be selected so that the piercing mechanism, while functioning reliably in firing, does not function in service handling. Functioning of the mechanism in service handling can occur under the effect of forces which emerge in accidental dropping of a projectile with a fuse on hard obstacles, in shaking of fuses during transport on bad roads, in vibration of the projectiles on an airplane, etc. Inertial forces caused by falling of a projectile with the bottom down on rigid and elastic obstacles represent the greatest danger. Therefore, the maximum height H from which falling does not cause functioning of the piercing device of the MDV is accepted as a measure of the safety of fuses with an inertial trigger device. This height is called the safe falling height of the projectile. It is obvious that in falling of a projectile from the height H , the kinetic energy of the striker at the moment of impact on an obstacle is equal to the energy E necessary for overcoming the resistance of the spring in the way of arming:

$$\frac{q}{2g} v^2 = E, \quad (8.36)$$

where q is the weight of the striker; v is the velocity of the striker in relation to the set cap after impact on the obstacle.

Since a rebound of the projectile from the obstacle occurs after impact, one must assume that

$$v = v_1 + v_2,$$

where v_1 is the velocity of the projectile at the moment of impact; v_2 is the velocity of the projectile at the moment of rebounding.

Substituting the expression for the velocity of the striker

into equation (8.36), we obtain

$$\frac{qv_1}{2g} (1 + \beta)^2 = E, \quad (8.37)$$

where $\beta = v_2/v_1$ is a coefficient for reestablishing the velocity at impact.

The value of the coefficient β depends on the elastic properties of the obstacle and the projectile material. If the projectile and the obstacle are absolutely rigid, the kinetic energy of the projectile is expended totally on plastic deformation of the projectile and the obstacle. The projectile does not rebound from the obstacle in this case, and $\beta=0$. However, in falling of an absolutely elastic projectile on an absolutely elastic obstacle, the entire kinetic energy is spent on rebounding of the projectile from the obstacle, and $\beta=1$. In intermediate collision cases, $0 < \beta < 1$. It is customary to assume that $\beta=0.4$ in calculations of fuses.

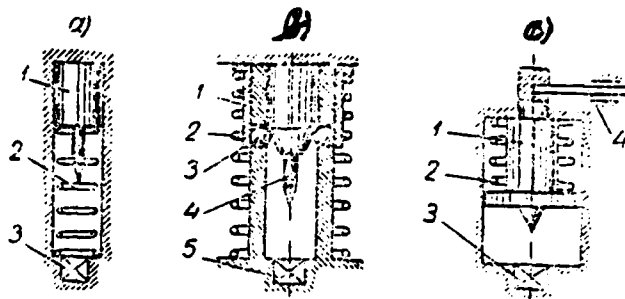


Fig. 8.21.

In falling of a projectile from a height H ,

$$v_1 = \sqrt{2gH}. \quad (8.38)$$

We establish from expressions (8.37) and (8.38) that

$$H = \frac{E}{(1 + \beta)^2 q} \quad (8.39)$$

The value of the energy E is equal to the product of the average resistance of the spring R_{cp} and the length of the course of the striker a :

$$E = R_{cp} a.$$

The condition necessary to reliable functioning of a fuse can be written in the form of an inequality:

$$nqa > E + E_0, \quad (8.40)$$

where n is the average value of the acceleration factor along the axis of the projectile; E_0 is the magnitude of the kinetic energy of the striker at the moment of piercing necessary for response of the set cap.

The inequality (8.40) means that the work of the inertial force on the path of movement of the striker should exceed the total energy of resistance of the spring and of piercing of the cap. Substituting the value of E from (8.39) into expression (8.40), we obtain an expression for determining the minimum value of the average acceleration factor of the projectile at which reliable operation of the piercing mechanism is ensured:

$$n > \frac{E_0}{ma} + \frac{(1+3)^2 H}{a}. \quad (8.41)$$

In firing of artillery guns, the axial overload of the shell at the beginning of its movement along the bore is quite great. Therefore, there is no difficulty in selecting parameters of the piercing mechanism of the artillery fuse in such a way as to satisfy the condition (8.41). In firing of missiles, on the other hand, it is practically impossible to fulfill this condition, since the acceleration factors are relatively low in this case. Therefore, piercing mechanisms of a different type are used in missile fuses. One such mechanism is shown in Fig. 8.21, b. A collapsing sleeve 1 compressed by a spring 2 serves as the safety part of the mechanism. The sleeve holds balls 3 on which the inertial striker 4 rests. After firing, the sleeve collapses under the effect of the inertial force, compresses the spring and frees the balls. The inertial

force acting on the striker moves it toward the set cap. If the inertial force is insufficient for imparting the necessary piercing energy E_0 to the striker, a compressed firing spring is used and imparts additional velocity to the striker.

In contrast to the piercing mechanism of the first type, there is no need for placing a safety spring between the striker and the cap of the second mechanism, due to which the required piercing energy can be achieved in the action of a smaller inertial force on the striker, i.e., with a lower overload of the projectile. In cases where the force of the safety spring holding the sleeve is low, a zigzag groove is made on the sleeve surface for improving safety in handling the fuse, due to which the safe falling height is increased.

Inertial piercing mechanisms cannot be used in fuses for aerial bombs, since overloads caused by slowing down on the bomb in free fall are extremely slight.

Firing mechanisms (Fig. 8.21, c) are used as mechanical trigger devices in bomb fuses. The striker 1 of the firing mechanism is situated under the influence of a compressed spring 2. It is held back from movement toward the set cap 3 by a stopper 4, which is connected to the snap hook of a device for controlling the fuses on the airplane. After departure of the bomb from the aircraft, the snap hook removes the stopper under the effect of the weight of the bomb. In this case, the compressed spring pushes the striker toward the set cap and causes its ignition. For providing reliable operation of the firing mechanism, the resistance of the spring is selected in such a way that the energy of the striker at the moment of piercing is not less than the required value E_0 . The possibility of premature breaking away of the stopper under the influence of aerodynamic forces acting on parts of the locking device in outer suspension of the bombs and a high flight speed of the airplane is a substantial shortcoming of MDV of bomb fuses with firing mechanisms.

It seems impossible to increase the resistance of the stopper to breaking away significantly, especially due to an increase in thrust at the moment of dropping of the bomb, which has a negative effect on the stability of the bomb on the trajectory. Therefore, the firing mechanisms have been replaced in modern bomb fuses with electrical trigger devices consisting of an electric igniter and a current conducting cord. In departure of the bomb from the airplane, a current pulse is fed to the electric igniter through the conducting cord, which is connected to the bombing gear, from a power source of the aircraft; the pulse results in functioning of the electric igniter and triggering of the MDV. The main shortcoming of pyrotechnic MDV lies in the fact that the reliability and the accuracy of their operation depend heavily on the temperature and meteorological conditions. In addition, in the use of pyrotechnic delay devices in MDV, it is difficult to provide a long arming time.

Remote arming mechanisms constructed based on a mechanical principle are superior. Of the mechanical MDV, clock mechanisms have found the most extensive use.

Clock mechanisms used in fuses have the design of ordinary clocks and include:

- a motor (an energy source);
- a gear system (a device which sequentially increases the angular velocity of rotation of the gears);
- a verge wheel (an intermediate part between the gear system and the regulator);
- a regulator (an element which slows down and disengages the gear system at uniform time intervals).

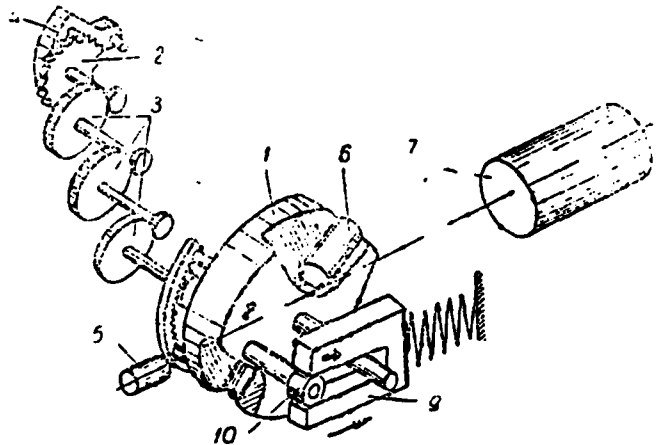


Fig. 8.22.

Coil springs, as in ordinary clocks, or inertial forces can serve as the motor for clock mechanisms of fuses. Inertial forces from linear acceleration and centrifugal forces are used in the latter case. Inertial forces from linear acceleration can be used for driving clock mechanisms only in missile fuses, because the positive acceleration is active for a comparatively long time only in the flight of missiles. Figure 8.22 presents a schematic diagram of an MDV of the clock type used in missile fuses. A rotary disc 1 serves as the motor of the clock mechanism in the diagram; the disc is connected to the regulator 4 through the gear system 3 and the verge wheel 2 by means of a toothed section. An igniter 6 is situated in a channel of the rotary disc and absorbs a fire impulse from the igniter set cap 5 and transmits it to the detonator block 7. In the initial position, the disc 1 is turned so that the channel with the igniter is offset in relation to a line connecting the igniter set cap with the detonator block. In such a position, the disc is held in place by an inertial safety device 9 with a spring. A roller 10 attached to the disc

fits into a slot of the safety device. In launching of the missile, the safety device 9 under the influence of an inertial force compresses the spring and moves aside, thus freeing the roller 10. Since the center of gravity of the rotary disc is offset in relation to its axis, it will begin to speed up under the action of the inertial force, thus driving the gear system of the clock mechanism into motion. Their verge wheel drives the regulator into oscillation motion through pins, and the regulator converts the continuous rotation of the disc into intermittent rotation and thereby slows its turning. The powder delay train of the fuse is completed at the moment when the disc channel takes a position opposite the detonator block. At this moment, the gear rack is disengaged from the gear system, and the disc is locked by special fixers.

Arming clock mechanisms in which a spring serves as the motor are similar to remote mechanisms of time fuses. These mechanisms will be considered below, in the chapter "Time Fuses." Electrical MDV will be considered in the chapter "Electrical Fuses."

Self-Destruction Devices

Self-destruction devices are used in fuses of aviation artillery shells and missiles of the "air-to-air" class. They are intended for putting the fuse into operation on the trajectory a definite time after firing. Due to the self-destruction device, bursting of the projectile in firing on aerial targets occurs in the air in case of a miss, which ensures safety of ground forces in firing above friendly territory. Self-destruction devices of pyrotechnic and clock types find use in mechanical fuses. They do not differ in any way from remote arming mechanisms in regard to their principle of construction and operation. Devices called destruction devices or antiremoval devices, which are used in bomb fuses with long delays, are similar in purpose to self-destruction devices. Their purpose is to ensure instant explosion of the bomb in an attempt to remove

the fuse from it. As a rule, destruction devices based on a mechanical operating principle are used in chemical and mechanical fuses for prolonged operation. They are combined structurally with the striker mechanism of the fuse. Figure 8.23 presents a schematic diagram of a destruction device of a fuse with a chemical delay mechanism. In the striker mechanism of the fuse, the prong 8 is restrained from moving toward the cap by safety balls 5. The balls 5 rest in the inner walls of a plastic cylinder 4 and are not capable of moving out to the sides. The striker mechanism is mounted in a sleeve 2 which is situated under the influence of a compressed main spring 3. The sleeve is restrained from moving by retaining balls 9 pressed against the fuse housing by a rib of the cap tube. Under normal conditions, operation of the fuse proceeds as follows.

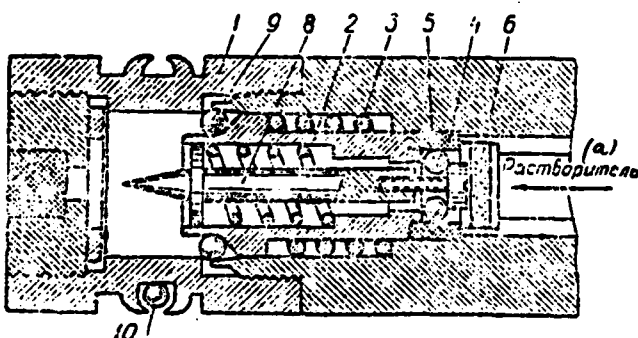


Fig. 8.23.
Key: (a) solvent.

After opening of the tube, the solvent, soaking through delaying wadding 6, begins to dissolve the plastic cylinder 4. After a definite time interval, the plastic cylinder dissolves to the extent that the balls 5 which hold in place the prong 8 move apart and are pressed into the cylinder. As a result, the prong under the influence of the spring pierces the cap, and the fuse functions. The sleeve 2 with the spring 3 and the balls 9 play the part of the destruction device. Just before placing of the fuse in the bomb, a retaining ball pin is inserted in a special groove on the

burster tube. The groove has a variable depth. In placing of the fuse in the fuse hole of the bomb, the retaining ball 10 moves along the groove, occupying a position in which it does not prevent screwing in of the fuse until it rests at the bottom of the burster tube of the bomb. In an attempt to unscrew the fuse from the bomb by rotation in the opposite direction, the ball 10, in moving along the same groove, jams the cap sleeve 1 in the burster tube, while all the rest of the fuse is unscrewed. In rotation of the fuse housing by a certain angle, the ball bearings 9 are released. The sleeve 2 under the action of the spring 3 moves along with the prong in the direction of the cap, causing explosion of the bomb.

§ 3. CALCULATION OF THE RELIABILITY AND RESPONSE SPEED OF IMPACT FUSES

For calculating the reliability and speed of response of a fuse, it is necessary to compose an equation of motion of the striker in relation to the set cap. By solving this equation, one can obtain the velocity of the striker at the moment of piercing of the cap and the time of movement of the striker toward the cap. The kinetic energy of the striker at the moment of piercing of the cap E_H is calculated according to the velocity of the striker and is then compared to the energy necessary for reliable functioning of the cap E_0 .

The condition for reliable functioning of the fuse has the following form:

$$E_H > E_0.$$

As the first example, we shall solve the problem which has been stated for the simplest case, in application to an inertial axial striker mechanism. We shall assume that in penetration of the obstacle by the projectile, the inertial force $q_n(t)$ acting on the inertial striker (Fig. 8.24) forms an angle ϕ with its axis.

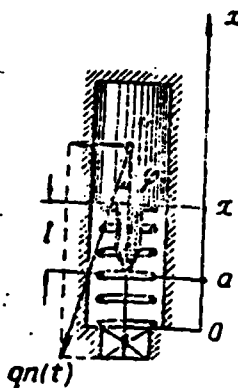


Fig. 8.24.

The equation of motion of the striker in relation to the set cap along the x axis is written in the following form:

$$\frac{q}{g} \frac{d^2x}{dt^2} = -qn(t)\cos\varphi + q'n(t)\sin\varphi + R(x), \quad (8.42)$$

where q is the weight of the striker; $n(t)$ is the acceleration factor of the projectile, which is a function of the time; f is the coefficient of friction of the striker against the housing; $R(x)$ is the force of resistance of the spring.

The acceleration factor is determined by the following expression:

$$n(t) = \frac{F(t)}{G}, \quad (8.43)$$

where $F(t)$ is the force of resistance of the obstacle to penetration by the projectile; G is the weight of the projectile.

The force of resistance of the spring, as follows from Fig. 8.25, is expressed by the following formula:

$$R(x) = R_0 + (1+a-x)\tan\alpha, \quad (8.44)$$

where R_0 is the force of preliminary tension of the spring; l is the length of the prong; a is the distance between the prong and the cap in the initial position; $\tan \alpha = k$, the rigidity of the spring.

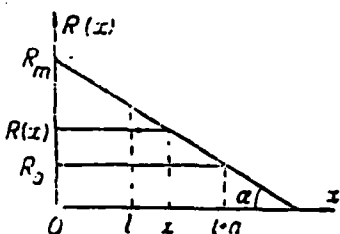


Fig. 8.25.

We shall rewrite formula (8.44) in the form

$$R(x) = R_m - Rx$$

or

$$R(x) = k(x_0 - x), \quad (8.45)$$

where $R_m = R_0 + (l+a)k$ is the resistance of the spring under full tension; x_0 is the length of the spring in a free state.

Substituting values of $n(t)$ and $R(x)$ from (8.43) and (8.45) into equation (8.42), and performing elementary transformations, we obtain:

$$\frac{d^2x}{dt^2} + p^2 x = - \frac{F(t)g}{m} (\cos \varphi - f \sin \varphi) + p^2 x_0. \quad (8.46)$$

where $p = \sqrt{\frac{kg}{m}}$ is the frequency of free oscillations of the striker-spring system.

Introducing a new variable $y = x_0 - x$, we shall rewrite equation (8.46) in the following form:

$$\frac{d^2y}{dt^2} + p^2y = \frac{F(t)}{G} g(\cos\varphi - f\sin\varphi). \quad (8.47)$$

The initial conditions for integration of equation (8.47) are as follows:

$$t = 0, \quad y = x_0 - (l + a), \quad \frac{dy}{dt} = - \frac{dx}{dt} = 0.$$

The problem which was stated thus has been reduced to solving a linear differential equation with a right member. The solution of this equation is established by the method of variation of arbitrary constants. In an expression for the common integral of equation (8.47) without a right member,

$$y = C_1 \cos pt + C_2 \sin pt \quad (8.48)$$

the arbitrary constants C_1 and C_2 are considered to be unknown functions of the time, which are selected in such a way that the expression (8.48) satisfies the full equation (8.47). Applying this method to solving equation (8.47), we find

$$y = [x_0 - (l + a)] \cos pt + \int_0^t \frac{A(\tau)}{p} \sin p(t - \tau) d\tau, \quad (8.49)$$

where

$$A(\tau) = \frac{F(\tau)}{G} g(\cos\varphi - f\sin\varphi).$$

For computing the integral in expression (8.49), the force of resistance of the obstacle can be adopted, for example, in the following form [see formula (4.8)]:

$$F(t) = F_0(1 + bv^3), \quad (8.50)$$

where v is the velocity of the projectile in penetration into the obstacle; F_0 is the static component of the force of resistance.

The velocity of the projectile is related to the penetration time by a well-known formula [Translator's note: the abbreviations "arctg" and "tg" in mathematical expressions should be read as "arc tan" and "tan," respectively]:

$$t = 2\sqrt{b}L_0(\operatorname{arctg} \sqrt{b}v_c - \operatorname{arctg} \sqrt{b}v). \quad (8.51)$$

From (8.51) we find the penetration velocity:

$$v = \frac{1}{\sqrt{b}} \operatorname{tg} \left(\operatorname{arctg} \sqrt{b}v_c - \frac{t}{2\sqrt{b}L_0} \right).$$

Since the total time for penetration of the projectile t_{np} is as follows,

$$t_{np} = 2\sqrt{b}L_0 \operatorname{arctg} \sqrt{b}v_c,$$

then

$$v = \frac{1}{\sqrt{b}} \operatorname{tg} \left(\frac{t_{np} - t}{2\sqrt{b}L_0} \right). \quad (8.52)$$

Substituting the value of the projectile velocity from (8.52) into expression (8.50), we obtain

$$F(t) = F_0 \left[1 + \operatorname{tg}^2 \left(\frac{t_{np} - t}{2\sqrt{b}L_0} \right) \right]. \quad (8.53)$$

With the use of the law of variation of the force of resistance of the obstacle in the form of (8.53), the integral in expression (8.49) can be computed only by a numerical method. Having computed this integral, we shall find the dependences $y(t)$ and, consequently, $x(t) = x_0 - y(t)$. According to a graph of the family of curves of $x(t)$ (Fig. 8.26) calculated for different angles ϕ , assuming $x=1$, we find the response time of the striker mechanism t_1 . The response time of the fuse t_c , without consideration for the magnitude of the delay, will be as follows:

$$t_c = t_1 + t_2,$$

where t_2 is the response time of the cap.

For determining the velocity of the striker, we shall differentiate expression (8.49):

$$\frac{dy}{dt} = -p[x_0 - (l + a)] \sin pt + \int A(\tau) \cos p(t - \tau) d\tau. \quad (8.54)$$

Since $dx/dt = -dy/dt$, the velocity of the striker will be determined by the following formula:

$$\frac{dx}{dt} = p[x_0 - (l + a)] \sin \rho t - \int A(\tau) \cos \rho(t - \tau) d\tau. \quad (8.55)$$

We shall find the velocity of the striker at the moment of piercing of the set cap v_H from (8.55), assuming that $t=t_1$:

$$v_H = p[x_0 - (l + a)] \sin \rho t_1 - \int A(\tau) \cos \rho(t_1 - \tau) d\tau.$$

Having calculated the value of v_H for different angles ϕ by formula (8.56), and having computed the kinetic energy of the striker E_H , one can plot a graph of $E_H(\phi)$ (Fig. 8.27). With a knowledge of the value of the energy E_0 necessary for reliable functioning of the set cap, one can easily find the range of angles of impact of the projectile on the obstacle in which the fuse will function reliably according to the graph of $E_H(\phi)$. The limit impact angle at which operation of the fuse will be reliable is as follows:

$$\theta_{cnp} = \frac{\pi}{2} - \varphi_{np}$$

where φ_{np} is the limit angle between the axis of the striker and the direction of the inertial force (Fig. 8.27).

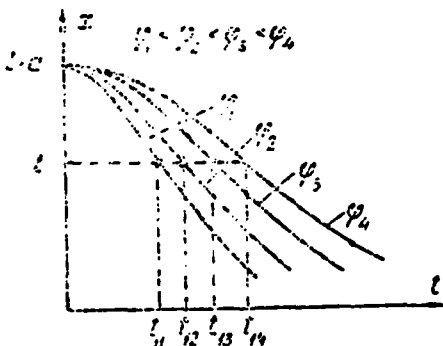


Fig. 8.26.

With a given angle ϕ , the formula (8.56) makes it possible to determine the minimum value of the velocity of impact of the projectile on the obstacle necessary for reliable functioning of

the fuse, i.e., the sensitivity of the fuse, by a similar method.

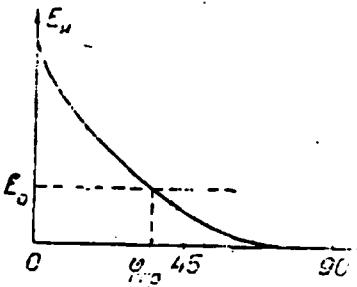


Fig. 8.27.

As a second example of solution of the problem of evaluating the reliability and operating speed of a fuse, we shall compose an equation of motion of the striker of a lateral striker mechanism (Fig. 8.28). We shall consider the most unfavorable case for operation of a lateral mechanism, where the inertial forces act in a direction perpendicular to the striker axis. Using the diagram of forces shown in Fig. 8.28, we shall compose equations of motion of the lateral percussion collar and the striker. The equation of motion of the collar is written in the following form:

$$\frac{q_2}{g} \frac{d^2x}{dt^2} = nq_2 - Q - F_2 - N \cos(\alpha - \delta), \quad (8.57)$$

where n is the coefficient of the overload acting on the projectile in penetration of the obstacle; q_2 is the weight of the lateral percussion collar; Q is the resistance of lugs of the safety washer; F_2 is the force of friction of the washer against the housing; N is the reaction force at the point of contact of the collar with the striker; α is the angle between the striker axis and the generatrix of the contact surfaces; δ is the friction angle.

It follows from Fig. 8.28 that

and

$$F_2 = fN \sin(\alpha - \delta),$$

$$\operatorname{tg} \delta = \frac{F}{P} = \frac{fP}{P} = f. \quad (8.58)$$

where f is the friction coefficient; P is the force of pressure of the striker on the collar; F is the force of friction of the collar on the striker.

The value of the friction coefficient will be assumed to be the same for all friction surfaces. Substituting the value of the friction force F_2 into equation (8.57), we obtain

$$\frac{q_2}{g} \frac{d^2 x}{dt^2} = nq_2 - Q - N[\cos(\alpha - \delta) + f \sin(\alpha - \delta)]. \quad (8.59)$$

Since $f = \tan \delta$,

$$\cos(\alpha - \delta) + f \sin(\alpha - \delta) = \frac{\cos(\alpha - 2\delta)}{\cos \delta}. \quad (8.60)$$

With consideration for equation (8.60), equation (8.59) will take on the following form:

$$\frac{q_2}{g} \frac{d^2 x}{dt^2} = nq_2 - Q - N \frac{\cos(\alpha - 2\delta)}{\cos \delta}. \quad (8.61)$$

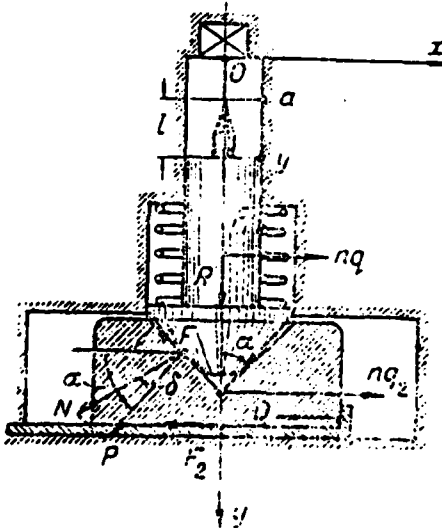


Fig. 8.28.

We shall write the equation of motion of the striker, having noted the fact that the reaction force of the collar N in this case acts on the striker in a direction opposite to what is shown in Fig. 8.28:

$$\frac{q_1}{g} \frac{d^2 y}{dt^2} = R + F_1 - N \sin(\alpha - \delta), \quad (8.62)$$

where q_1 is the weight of the striker; R is the force of resistance of the safety spring; F_1 is the force of friction of the striker against the housing.

The force F_1 is conditioned by the effect of the inertial force nq_1 and the lateral component of the reaction force of the collar N:

$$F_1 = f[nq_1 + N \cos(\alpha - \delta)]. \quad (8.63)$$

Having replaced the force F_1 in equation (8.62), with its expression from (8.63), we obtain

$$\frac{q_1}{g} \frac{d^2 y}{dt^2} = R + f n q_1 + N \frac{\sin(\alpha - 2\delta)}{\cos \delta}, \quad (8.64)$$

where

$$\frac{\sin(\alpha - 2\delta)}{\cos \delta} = \sin(\alpha - \delta) - f \cos(\alpha - \delta).$$

Using equation (8.61), we exclude the unknown reaction force N from equation (8.64).

We find from (8.61) that

$$N = \frac{\cos \delta}{\cos(\alpha - 2\delta)} \left[n q_2 - Q - \frac{q_2}{g} \frac{d^2 x}{dt^2} \right]. \quad (8.65)$$

It follows from Fig. 8.28 that in joint movement of the collar and the striker,

$$dy = - dx \operatorname{tg} \alpha.$$

Consequently,

$$\frac{d^2 x}{dt^2} = - \frac{d^2 y}{dt^2} \operatorname{tg} \alpha.$$

Therefore,

$$N = \frac{\cos \delta}{\cos(\alpha - 2\delta)} \left[nq_2 - Q + \frac{q_2}{g} \frac{d^2 y}{dt^2} \operatorname{tg} \alpha \right]. \quad (8.66)$$

Having substituted the value of N from (8.66) into equation (8.64) and having reduced similar members, we obtain

$$\begin{aligned} \frac{q_1}{g} \left[1 + \frac{q_2}{q_1} \operatorname{tg} \alpha \operatorname{tg} (\alpha - 2\delta) \right] \frac{d^2 y}{dt^2} &= \\ = R + n_f q_1 - (nq_2 - Q) \operatorname{tg} (\alpha - 2\delta). \end{aligned} \quad (8.67)$$

The force of resistance of the spring in equation (8.67) is expressed for a formula similar to (8.45):

$$R = k(y_0 - y).$$

Taking into consideration the expression for the force of resistance R , we shall rewrite equation (8.67) in the following form:

$$\frac{q_1}{g} \beta \frac{d^2 y}{dt^2} + k y = k y_0 + n_f q_1 - (nq_2 - Q) \operatorname{tg} (\alpha - 2\delta), \quad (8.68)$$

where

$$\beta = 1 + \frac{q_2}{q_1} \operatorname{tg} \alpha \operatorname{tg} (\alpha - 2\delta).$$

With a knowledge of the dependence $n(t)$, one can integrate equation (8.68) and find the values of t_1 and E_H .

CHAPTER 9

ELECTRICAL IMPACT FUSES

§ 1. FEATURES OF THE STRUCTURE OF ELECTRICAL FUSES

Electrical impact fuses differ from mechanical fuses in the structure of the command transmitter. The command for functioning in electrical fuses is formed as a result of passage of electric current through an electric igniter or an electric detonator. A schematic diagram of the command transmitter of electrical fuses is shown in Fig. 9.1. An electrical circuit consisting of a contact target sensor (DTs), a power source and an electric igniter (EV) plays the role of command transmitter. This circuit is otherwise known as the ignition or operational circuit of the fuse. The contact target sensor performs the function of the striker in mechanical fuses. In impact on an obstacle, it closes the circuit, connecting the power source to the electric igniter.

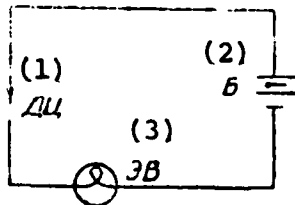


Fig. 9.1.
Key: (1) DTs; (2) B; (3) EV.

Depending on the character of the forces used for closing the operational circuit, contact target sensors are divided into reactive and inertial sensors. The former close the circuit under the effect of reaction forces of the obstacle, while the latter close the circuit under the effect of inertial forces.



Fig. 9.2.

A reactive sensor is made up of two electrodes, to which the ends of the ignition circuit are connected. In the initial position, the electrodes are situated at some distance apart, thus they break the ignition circuit of the fuse. The electrodes can have different structures. Figure 9.2 shows a schematic diagram of a reactive sensor with a cap serving as the outer electrode and a rod insulated from it serving as the inner electrode. Figure 9.3 shows a diagram of a sensor whose outer electrode has the shape of a tube. The nose cone of a missile (Fig. 9.4) can be used as a reactive sensor; it is insulated from the inner electrode - a cone-shaped cap. Reactive sensors possess a short response time. This time is within limits of tens to thousands of microseconds, depending on the impact velocity, the strength of the obstacle and the structure of the sensor. The reliability of the response of reactive sensors depends on their point of installation on the missile and the direction of the effect of reactive forces.

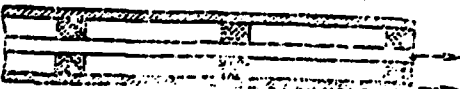


Fig. 9.3.

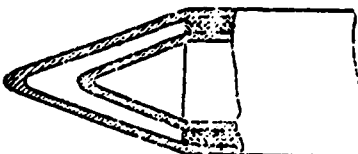


Fig. 9.4.

Inertial sensors are made up of stationary and mobile electrodes. The mobile electrode closes the circuit of the fuse in its movement under the effect of inertial forces. Figure 9.5 shows the structure of a vibration inertial sensor. A ball soldered to an elastic rod of steel wire serves as the mobile electrode of the sensor, while a hollow cylinder serves as the stationary electrode. The sensitivity of the sensor depends on the direction of the effect of the inertial force. The sensor possesses maximum sensitivity in a direction perpendicular to the axis of the rod. In deviation of the inertial force from this direction by an angle α , the sensitivity changes approximately in proportion to the sine of angle α . Two such sensors situated perpendicular to each other will provide approximately the same sensitivity in all directions. In selecting the parameters of inertial sensors, one must take into consideration the possibility of their premature response due to resonance phenomena. Premature response of a sensor before impact on the obstacle is possible when the frequencies of natural oscillations of the sensor coincide with the frequency of

vibration oscillations of the missile. For reducing the probability of resonance phenomena, the frequency of natural oscillations of the sensor should be outside the band of vibration frequencies.

The possibility of installing them at any point of a missile is an advantage of inertial sensors.

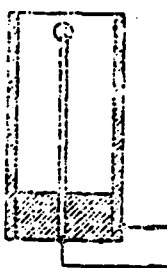


Fig. 9.5.

Electric igniters (EV) of the bridge type (incandescent igniters) find the greatest use in electrical fuses; the structure and characteristics of such igniters were considered in § 10 of Chapter 1. Contact-incandescent and spark electric igniters, in addition to bridge EV, can be used in electrical fuses. The heating bridge is replaced in a contact-incandescent electric igniter (Fig. 9.6) by a conductive igniting composition surrounding the ends of the wires. The conductivity of the ignition composition is provided by metallic powder contained in it. In passage of current through the EV, heat is released at the points of contact of the conducting particles, as a result of which a reaction of decomposition of the ignition composition is excited.

A diagram of the layout of a spark EV is shown in Fig. 9.7. The explosive in which the wires of the spark EV are situated does not contain conductive impurities. The gap between wires is of the order of 0.1 mm. In the action of a sufficiently high voltage

(1000-2000 V) on the EV, a discharge develops between the wires, causing ignition of the initiating VV [explosive]. The distinguishing feature of spark electric igniters is their high sensitivity to induced static charges, which can cause spontaneous functioning of the EV if safety measures are not taken.

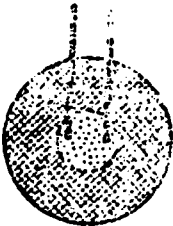


Fig. 9.6.



Fig. 9.7.

The operation of ignition and other circuits of electrical fuses can occur due to the energy of the fuse's own current source or an external source located on the airplane or the missile. Electrochemical current sources, pulse generators, piezogenerators, etc., can be used as independent power packs in fuses.

In fuses which use the energy of the on-board electrical supply system of an aircraft, capacitors which have the ability to store energy obtained during charging for a long time carry out the functions of power sources. Such capacitors are charged at the

moment of firing (dropping of the bomb) from a special charging device of the airplane. Electrical fuses in which capacitors accomplish the functions of power sources are called capacitor fuses. In addition to command transmitters, electrical fuses include powder delay trains, remote arming mechanisms, and safety devices, which normally do not differ from corresponding units of mechanical fuses in their principle of operation for structure. Only electrical fuses of the capacitor type, in which the operation of remote arming mechanisms can be based on an electrical principle, are an exception in this regard.

Electrical impact fuses can be used in aerial bombs and in free-flight and guided missiles and firing at ground targets. The main advantages of electrical fuses as compared to mechanical fuses are enhanced instantaneousness and reliability of their operation. High reliability in the operation of electrical fuses can be achieved by connecting several target sensors which back each other up in operation to the ignition circuit.

§ 2. ELECTRICAL FUSES OF THE CAPACITOR TYPE

The simplest design of an impact capacitor fuse is shown in Fig. 9.8. The design includes a capacitor C, a target sensor DTs, an electric igniter EV and a contact device, closing of which is controlled by a remote arming mechanism (MDV). In firing (dropping of a bomb), the capacitor C is charged from the on-board power supply system of the aircraft. The charging current does not pass through the electric igniter in this process, since the ignition circuit is broken by the target sensor and the MDV contact. The system is prepared for operation at the moment of completion of operation of the MDV, which closes the open contact in the ignition circuit. Operation of the remote arming mechanism can be based on either a pyrotechnic or a mechanical principle. In impact on an obstacle, the target sensor closes the ignition circuit, and the capacitor C, in discharging rapidly through the EV, causes functioning

of the fuse.

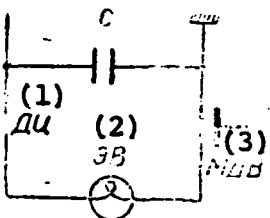


Fig. 9.8.

Key: (1) DTs; (2) EV; (3) MDV.

Figure 9.9 presents a diagram of a fuse in which remote arming is provided by an electrical method. The design includes: a storage capacitor C_1 , an ignition capacitor C_2 , a high resistance R , an electric igniter EV, and a target sensor DTs. Operation of the system proceeds as follows. In firing (release of the bomb), the storage capacitor is charged from a charging device of the airplane up to a voltage u_{10} . After charging of the storage capacitor, the fuse loses its connection to the aircraft, and the charge capacitor is connected to the rest of the fuse circuit by the contact K.

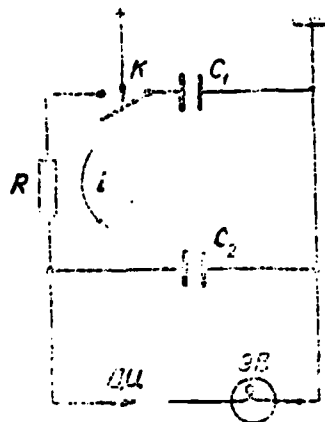


Fig. 9.9.

Key: (1) DTs; (2) EV.

Beginning from this moment, the capacitor C_1 will begin to discharge through the resistance R to the capacitor C_2 , which will charge. Due to the resistance R , the discharge of capacitor C_1 and charging of C_2 will occur not instantaneously but gradually. The laws of changing of the voltages u_1 and u_2 on the capacitors C_1 and C_2 in time are shown in Fig. 9.10. If the process in question could

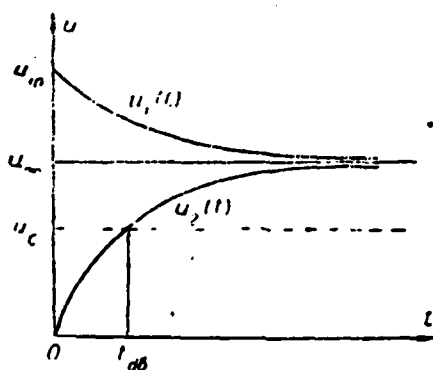


Fig. 9.10.

continue for an infinitely long time without being accompanied by losses of energy, the voltages u_1 and u_2 at the end would become equal, having taken on some value u_∞ . One can find the value of u_∞ by applying the law of the conservation of the charge of electricity. According to this law, the total charge of capacitors C_1 and C_2 at any moment in time should be equal to the charge which the storage capacitor received from the airdraft source; i.e.,

$$u_{10}C_1 = u_1 C_1 + u_2 C_2.$$

With $t=\infty$, $u_1=u_2=u_\infty$ and, consequently,

$$u_{10}C_1 = (C_1 + C_2)u_\infty.$$

From this we find that

$$u_\infty = u_{10} \frac{C_1}{C_1 + C_2}.$$

The voltage on the ignition capacitor u_2 in increasing reaches a value u_c necessary for functioning of the electric igniter at some moment in time $t_{\Delta B}$. Beginning from this moment, the fuse is ready for operation. Remote arming of the fuse is provided by the

for instantaneous action and a short delay. The fuse is set for instantaneous action "M" or a short delay "MZ" on the ground just before takeoff of the airplane. With any of these settings, in a case of release of a bomb from a low altitude, the fuse automatically functions with a long delay "BZ," which provides safety for the aircraft itself. The fuse has two ignition circuits: an assault action circuit (C_2 , DTs_1 and EV_1) and a circuit for the set time of operation - instantaneous or a short delay (C_3 , DTs_2 , EV_2 and EV_3). Setting for instantaneous operation or a short delay is performed by screwing in the appropriate screw ("M" or "MZ"). The delay values are provided by pyrotechnic compositions, which transmit the fire beam of electric igniters EV_1 and EV_3 to the igniter. Automatic operation of the fuse depending on the bombing altitude is achieved due to the fact that the ignition circuit for assault action is armed earlier than the circuit for instantaneous action or a short delay. In discharging of the storage capacitor, simultaneous charging of two ignition capacitors C_2 and C_3 occurs. Since charging of capacitor C_2 occurs through a smaller resistance than charging of capacitor C_3 , the voltage on it increases more rapidly (Fig. 9.12); therefore, the assault action circuit is armed first. If the time of fall of the bomb is less than the time for arming the second circuit $t_{\text{дв}2}$, the fuse functions with the assault delay. On the other hand, if this time exceeds the value of $t_{\text{дв}2}$, both ignition circuits function in impact on the obstacle. However, the fire beam from the electric igniter EV_2 or EV_3 reaches the igniter before that of EV_1 , and the fuse responds after the set time - instantly or with a short delay.

For selecting parameters of the design of capacitor fuses, one must know the laws of variation of the voltage on the capacitors - the recharging curves. The recharging curves are established by well-known methods of the theory of circuits. As an example, we shall consider solution of this problem for the simplest fuse design (Fig. 9.9).

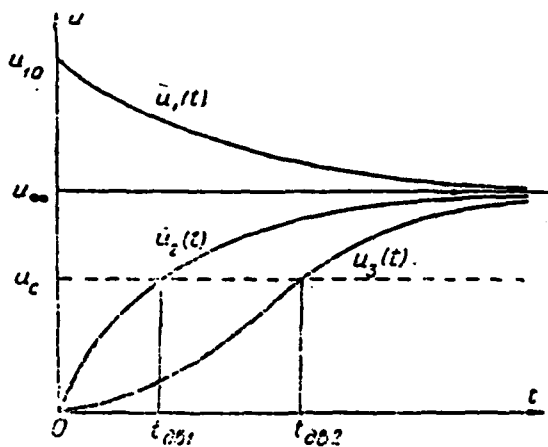


Fig. 9.12.

One can write the following obvious formulas for determining the dependences $u_1(t)$ and $u_2(t)$:

$$u_1 = iR + u_2; \quad (9.1)$$

$$i = -C_1 \frac{du}{dt}; \quad (9.2)$$

$$i = C_2 \frac{du_2}{dt}. \quad (9.3)$$

The three equations which have been written are quite sufficient for determining the three unknowns: u_1 , u_2 and i .

Substituting the value of i from (9.3) into equation (9.1), we obtain

$$u_1 = C_2 R \frac{du_2}{dt} + u_2. \quad (9.4)$$

We shall find the relationship between the voltages u_1 and u_2 . Setting the right members of expressions (9.2) and (9.3) equal, we have

$$C_2 du_2 = -C_1 du_1 \quad (9.5)$$

Integrating equation (9.5) under the initial conditions $u_1=u_{10}$ and $u_2=0$, we obtain

$$u_1 = u_{10} - \frac{C_2}{C_1} u_2. \quad (9.6)$$

We shall substitute the value of u_1 from (9.6) into equation (9.4):

$$u_{10} - \frac{C_2}{C_1} u_2 = C_1 R \frac{du_2}{dt} + u_2.$$

Performing elementary transformations, we reduce this equation to the following form:

$$\frac{du_2}{dt} + \frac{1}{\tau} u_2 = \frac{u_{10}}{C_1 R}. \quad (9.7)$$

where

$$\tau = \frac{C_1 C_2}{C_1 + C_2} R.$$

The general integral of equation (9.7) is written in the following form:

$$u_2 = A e^{-\frac{t}{\tau}} + \frac{u_{10} \tau}{C_1 R}. \quad (9.8)$$

where A is the integration constant.

The first addend in expression (9.8) is the general integral of equation (9.7) without the right member, while the second addend is a special integral of the equation with a right member.

We shall find the constant value of A using the initial condition: at $t=0$, $u_2=0$.

Assuming that $t=0$ and $u_2=0$ in expression (9.8), we find

$$A = \frac{u_{10} \tau}{C_1 R} = u_{10} \frac{C_1}{C_1 + C_2} = u_{10}. \quad (9.9)$$

Consequently,

$$u_2 = u_{10} \left(1 - e^{-\frac{t}{\tau}}\right). \quad (9.10)$$

Substituting expression u_2 from (9.10) into (9.6), after transformations, we find

$$u_1 = u_{\infty} \left(1 + \frac{C_2}{C_1} e^{-\frac{t}{T}} \right). \quad (9.11)$$

Expression (9.10) is used for selecting the parameters of the circuit C_1 , C_2 and R . The predetermined values in selection of the parameters of the circuit are as follows:

- the voltage necessary for response of the electric igniter u_c ;
- the energy which should be imparted to the bridge of the EV for its reliable operation E_0 ;
- the remote arming time $t_{\text{дз}}$;
- the voltage u_{10} of the charging device of the airplane.

The capacitance of the ignition capacitor C_2 is determined from the condition of reliable operation of the EV.

This condition can be written in the form

$$\frac{C_2 u_c^2}{2} \geq E_0. \quad (9.12)$$

where $Cu^2/2$ is the energy stored by the capacitor.

It follows from inequality (9.12) that

$$C_2 = \frac{2nE_0}{u_c^2}, \quad (9.13)$$

where n is a storage coefficient greater than 1.

For bridge electric igniters, $E_0 = 2 \cdot 10^{-4}$ joule. The capacitance of the storage capacitor is selected from design considerations so

that

$$u_e > u_c \quad (9.14)$$

For selecting the value of the resistance R , one should assume in expression (9.10) that $t=t_{\text{дв}}$ and $u_2=u_c$.

The problem is solved in a similar way in the case of more complex designs. The shortcoming of capacitor fuses is the necessity of equipping the airplane with an additional charging device.

§ 3. ELECTRICAL FUSES WITH THEIR OWN POWER PACK

Fuses with an Electrochemical Power Source

The operation of electrochemical power sources is based on the emergence of a contact e.d.s. [electromotive force] at the point of contact with a metal with an electrolyte in which the metal can dissolve. Sources of this kind are otherwise known as galvanic elements. The simplest galvanic element is made up of two electrodes immersed in an electrolyte. Galvanic elements have a number of shortcomings as current sources. These shortcomings condition a number of features in their use for supplying power to a fuse design. The main shortcoming of galvanic elements is poor preservation. In storage of an element, gradual drying up of the electrolyte and spontaneous discharging occur in it. This shortcoming is eliminated by insulating the electrolyte from the electrodes and storing it in airtight tubes up to the moment of operational use of the fuses. The tube with electrolyte can be opened either at the moment of preparation of the fuse for combat use or in the process of combat use. In cases where the electrolyte has not been separated from the electrodes, the fuse design should include the possibility of replacing the power pack after passage of established storage periods. The value of the electromotive force of galvanic elements depends on the material of the electrodes and the electrolyte composition and is within limits of 1.0-1.6 V.

Batteries of series connected elements for transformers of low voltage of an element to high voltages (150-200 v) are used in cases where high voltages are required for operation of the fuse system.

As an example of the use of electrochemical current sources in fuses, Fig. 9.13 presents a diagram of the delaying unit of a bomb fuse for prolonged operation. The delaying unit of the fuse includes a battery B_1 of galvanic elements, a resistance R , a contact target sensor DTs_1 and an elastic box with the electrolyte E . The housing of this box forms one half of the contact K which is connected to the operational circuit of the fuse. In the initial

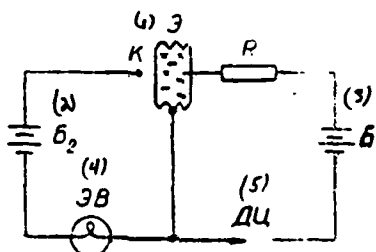


Fig. 9.13.
Key: (1) E; (2) B_2 ; (3) B_1 ; (4) EV;
(5) DTs .

position, there is a gap between the box housing and the other half of the contact K , due to which the operational circuit of the fuse proves to be broken. In impact on an obstacle, the target sensor closes the circuit of the delay device. Current of battery B_1 begins to flow through the resistance R and the electrolyte E . During passage of the current through the electrolyte, release of gases - hydrogen and oxygen - occurs due to electrochemical processes; the gases increase the pressure inside the box. Under the influence of this pressure, the box undergoes deformation and closes contact K after a definite time. After closing of contact K , the current from battery B_2 causes response of the electric igniter. The

magnitude of the delay of the fuse depends on the value of the resistance R , the electromotive force of the battery, the electrolyte composition and the size of the gap between the box and contact K . A delay of several hours to several days can be set.

Fuses with Pulsed Current Generators

A schematic diagram of a fuse with a pulsed current generator is shown in Fig. 9.14. It includes a pulsed current generator, an electric igniter and a contact which is closed by the remote arming mechanism (MDV). The main parts of the generator are a permanent magnet in the shape of a cylinder, and a winding. In movement of the magnet, the magnetic flux intersects coils of the winding and causes the formation of an impulse of an electromotive force in the winding. Forces acting on fuse parts in impact on the obstacle are used for moving the magnet.

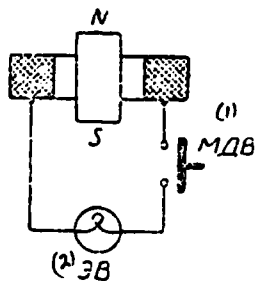


Fig. 9.14.
Key: (1) MDV; (2) EV.

Figure 9.15 shows a schematic diagram of a pulse generator with a stationary magnet. Such a generator creates an electromotive force impulse due to a change in the magnetic flux in the magnetic circuit in movement of the armature. In impact on an obstacle, movement of the armature in the direction toward the magnet (or away from the magnet) occurs, and the distance δ between the armature and the magnet changes. A change in the magnetic conductivity between poles of the magnet leads to a change in the magnetic flux

intersecting loops of the coil and to formation of a pulsed electromotive force. The advantage of pulse generators is the possibility of providing enhanced instantaneousness in response of the fuse.

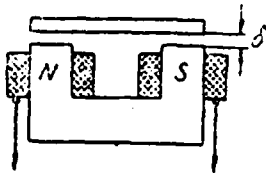


Fig. 9.15.

Piezoelectric Fuses

In piezoelectric fuses, the energy of piezoelectric current generators is used for functioning of the operational circuit. Operation of the piezoelectric generator is based on the piezoelectric effect, which consists of the emergence of electrical charges on the surfaces of certain dielectric materials under the influence of mechanical strains. Crystals of quartz, tourmaline, Seignette salt and a number of ceramic dielectrics, such as bariuus titanate, for example, possess piezoelectric properties.

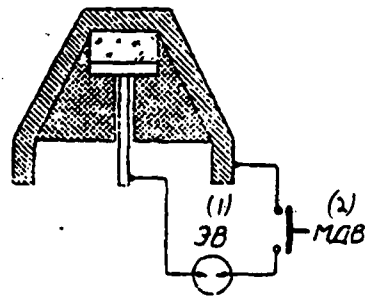


Fig. 9.16.
Key: (1) EV; (2) MDV.

A schematic diagram of a fuse with a piezoelectric generator is shown in Fig. 9.16. The generator is made up of a plate of barium titanate (the piezoelement) held between the fuse housing and a steel plate which plays the part of an electrode. The steel plate is insulated from the housing by an insulation sleeve. The generator is connected through contacts of the MDV to the spark electric igniter EV. In impact on an obstacle, deformation of the piezoelement occurs, and electrical charges develop on its faces. The potential difference between faces of the piezo element can be calculated by the formula

$$u = \frac{q}{C_0}$$

where C_0 is the capacitance between faces of the piezoelement; q is the magnitude of the charge on the faces of the piezoelement.

The value of u can reach several thousand volts. The voltage is fed from the piezogenerator directly to the spark EV and causes functioning of the EV.

Fuses with a piezoelectric generator are distinguished by increased instantaneousness of their operation. The increased instantaneousness of the fuses is explained by the lack of moving parts in them and by the use of high-speed spark electric igniters in the operational circuit.

CHAPTER 10

TIME FUSES

§ 1. PRINCIPLES OF CONSTRUCTION OF TIME FUSES

Time (remote) mechanisms which measure the time from the moment of the beginning of their operation to the moment of functioning of the fuse serve as the transmitters of the command for functioning in time fuses. The time mechanisms initiate action of the filling of the ammunition according to the passage of this time. The time mechanism of a fuse is put into operation either at the moment of firing (release of the bomb) or at a predetermined point of the trajectory (at the moment of arming, at the moment of disengagement of the guidance system of a missile, etc.). The time in which response of time fuses occurs, called the delay time, can be set on the ground just before the operational flight, from the cockpit of the aircraft immediately before firing, or after firing at a definite point of the trajectory of the projectile. The basic characteristic of time fuses determining the possibility of their use in certain firing situations is the accuracy of working out of the set delay time by the time mechanism. The value of the probable or mean square deviation of the actual operating time from the set time serves as a measure of the accuracy of time fuses. Time fuses are divided into pyrotechnic, mechanical (clock) and electrical fuses depending on the principle

of operation of the time mechanisms.

Pyrotechnic Fuses

The time mechanism of pyrotechnic fuses is made up of two or more metal rings, with a pyrotechnic composition pressed into their annular grooves. The mechanism is installed in the powder delay chain of the fuse (Fig. 10.1) between the igniter set cap 2 and the igniter 6. In fuses intended for igniting bursting charges or the filling of ammunition, either powder magazines or igniter set caps are used instead of the igniter.

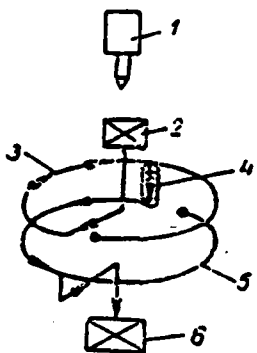


Fig. 10.1.

After firing (release of the bomb), the striker 1 pierces the cap. The fire beam of the cap is transmitted to the pyrotechnic composition 3 of the top ring, which begins to burn at a rate of the order of 0.3-1 cm/s. Reaching a transition aperture 4 which connects the rings, the fire is transmitted to the composition 5 of the bottom ring. After burning out of the composition of the bottom ring, the fire beam passes to the igniter, and the fuse functions. The time which passes from the moment of ignition of the first cap to the moment of functioning of the fuse is determined by the length of the burning composition. The length of the composition participating in transfer of fire from one cap to another

can be regulated by turning the bottom ring in relation to the top ring, and the magnitude of the delay time is changed in this way. Pyrotechnic fuses were the first examples of time fuses and were widely used up to the Second World War in antiaircraft artillery and in aviation (in illumination bombs, photographic flash bombs and smoke bombs and in free-flight rockets).

Pyrotechnic fuses with devices for setting different operating times are hardly used at present. Only fuses with a constant operating time find use, in drill rounds for an automatic aircraft weapon system, for example. The basic shortcoming of pyrotechnic fuses is the large spread in operating times, which depend on the meteorological conditions (mainly on the temperature and pressure of the environment), the procedures for manufacture of the pyrotechnic composition, the time and conditions of storage of the fuse and a number of other factors.

Mechanical Fuses

Clock mechanisms are used for measuring the time in mechanical time fuses. Figure 10.2 shows a kinematic diagram of a typical clock mechanism used in aviation fuses. The clock mechanism of the fuse consists of a drum 1 with a spring 2, a system of gears and a regulator. The spring is the motor of the clock mechanism. One end of the spring is rigidly attached to a central axle 3, while the other is attached to the drum. The spring is wound by rotation of the drum, which is locked with a special catch preventing reverse rotation of the drum after winding. The central axle 3 is restrained from rotation by an arrow 4 resting on the trigger detainer 5. The arrow is rigidly connected to a prong 6, which is linked by two slots to the central axle and rotates together with it in operation of the clock mechanism. A retainer 8 with a contoured slot 10 according to the shape of the arrow is situated between the arrow and the cap 7. The retainer prevents downward movement of the arrow with the prong under the action of the compressed spring 9. The

regulator of the clock mechanism consists of a verge wheel 11, a balance 12 with weights, a hair spring 13 and an anchor 14.

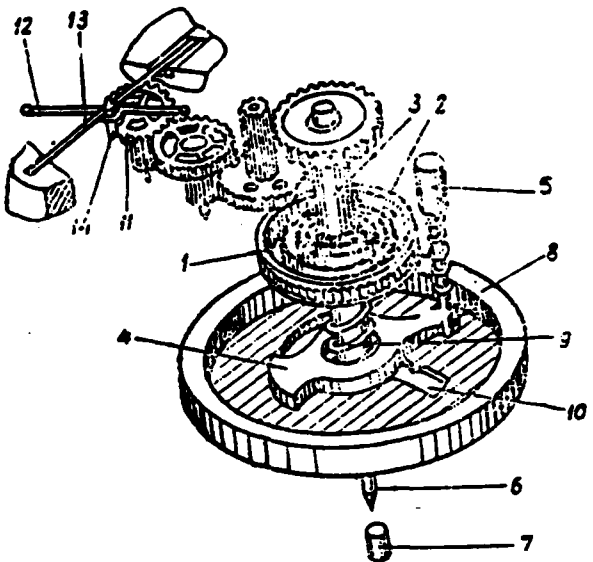


Fig. 10.2.

After firing or release of the bomb, the detainer 5 of the clock mechanism is released; the detainer moves upward under the effect of the spring and does not prevent rotation of the arrow. From this moment, the arrow begins to rotate regularly together with the central axle, sliding over the retainer. The fuse functions when the arrow coincides with the contoured slot of the retainer. Under the influence of the compressed spring 9, the arrow slips into the slot of the retainer, and the prong pierces the cap. The fuse is set for the appropriate operating time by turning the retainer in relation to the arrow. The greater the angle formed by the arrow with the slot of the retainer, the greater the time after which the fuse functions.

Mechanical time fuses are distinguished from pyrotechnic fuses

by higher operating precision. The probable deviation of their operating time is 0.5-1% of the set time. The time of operation of mechanical fuses practically does not depend on atmospheric conditions. For setting of the operating time from the cockpit of the aircraft, the fuse should have an electrical drive, which turns the arrow in relation to the retainer on a command from control instruments of the aircraft.

Mechanical time fuses are used at present in aviation for equipping bomb clusters for one-time use and aerial bombs for special and auxiliary purposes (illumination bombs, photographic flash bombs, position-finding signal bombs, etc.). Delay mechanisms of the clock type also find use as mechanisms for remote arming of missile fuses and self-destruction devices of missile proximity fuses.

Electrical Fuses

The simplest design of an electrical time fuse is shown in Fig. 10.3. It differs from the impact fuse design considered previously (Fig. 9.9) only in that a spark discharger L is connected to its ignition circuit together with a contact sensor. The fuse functions on the trajectory of the missile (bomb) when the voltage u_2 on the ignition capacitor C_2 reaches a value u_{11} sufficient for sparkover of the spark gap. In sparkover of the spark gap, the ignition circuit is completed, and the capacitor C_2 discharges through the electric igniter. The time interval from the moment of charging of the accumulating capacitor (the moment of firing) to the moment of functioning of the fuse is equal to the time for build-up of the voltage on the ignition capacitor to the sparkover voltage of the spark gap. The operating time of the fuse can be changed either by changing the resistance R or by changing the voltage u_{10} to which the accumulating capacitor is charged. The former method for setting the operating time is more complicated

than the latter method; therefore, it has not found practical use.

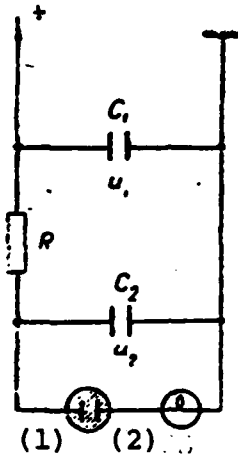


Fig. 10.3.

Key: (1) L; (2) EV [electric igniter].

The effect of the magnitude of the charging voltage u_{10} on the delay time of the fuse t_d can be seen in graphs (Fig. 10.4).

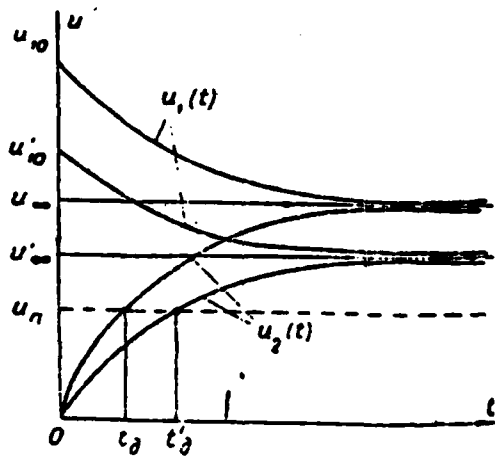


Fig. 10.4.

The second method has found limited use in pure form, since it is necessary to charge the storage capacitor to extremely high voltages for setting a short operating time. With setting of a long operating time, this method does not ensure high operating precision. The indicated shortcomings are easily eliminated by preliminary recharging of the ignition capacitor to a voltage $u_{20} < u_n$. A system with preliminary recharging is shown in Fig. 10.5. In contrast to the previous design, both capacitors - storage and ignition - are connected to the charging device in this design. In firing or release of the bomb, the charging voltages are fed to both capacitors.

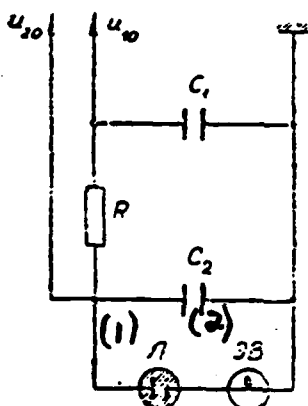


Fig. 10.5.
Key: (1) L; (2) EV.

Curves characterizing the law of the variation of voltages on capacitors of a system with recharging are shown in Fig. 10.6. In addition to designs with direct recharging of the ignition capacitor, we know of designs for time fuses with automatic recharging. An impact-time fuse design (Fig. 10.7) which has been used in firing of free-flight missiles at aerial targets can serve as an example of such designs. The design makes it possible to set a fuse operating time of 1 to 5 s by changing the charging voltage within limits of 233 to 394 V. The distinguishing feature of the fuse design is automatic recharging of the ignition capacitor

C_3 , due to which it has been possible to reduce the values of charging voltages of the storage capacitor C_1 . In addition to the normal components, the design includes an automatic recharging

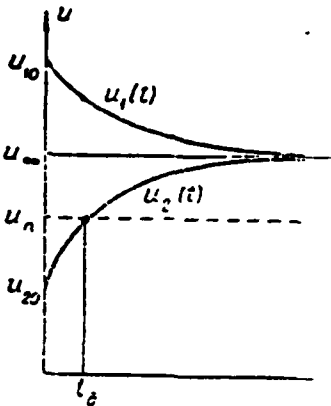


Fig. 10.6.

circuit C_2R_2 . This circuit provides an increased rate of voltage build-up on the ignition capacitor during the initial period of the charging process as compared to the normal design. Operation of the system proceeds as follows. Both capacitors C_2 and C_3 are charged from the storage capacitor C_1 during the first period of operation. In this process, charging of the capacitor C_3 occurs through two resistances R_1 and R_2 connected parallel to each other; their resultant resistance is less than resistance R_1 . Therefore, the voltage on capacitor C_3 increases more rapidly during this period than in a design without the R_2C_2 circuit.

The second period of operation of the system begins at the moment when the voltage u_1 on capacitor C_1 becomes equal to the total voltage u_2+u_3 on capacitors C_2 and C_3 . During this period, capacitor C_2 discharges through resistance R_2 , while ignition capacitor C_3 continues charging as before from the storage capacitor C_1 , but now only through one resistance R_1 . During this period, the rate of build-up of the voltage u_3 will be the same as in the

normal design. Recharging curves for the fuse design are shown in Fig. 10.8, where similar curves for a design without the R_2C_2 circuit are shown with dotted lines for comparison. It is easy to see by comparing the curves that a design without an automatic recharging circuit requires a larger charging voltage u_{10} for setting of a given operating time t_0 .

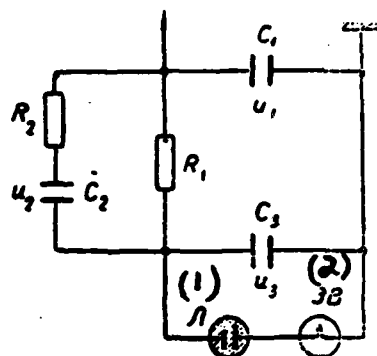


Fig. 10.7.
Key: (1) L; (2) EV.

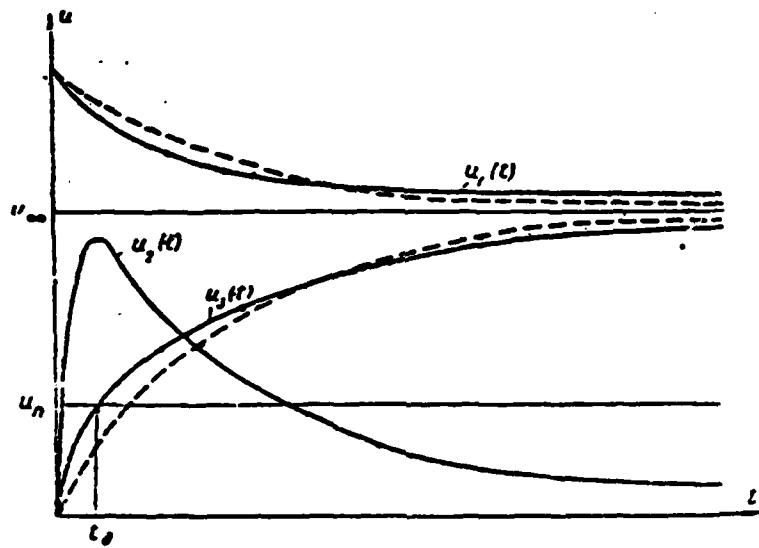


Fig. 10.8.

The precision of operation of electrical fuses is determined by the working spread of parameters of the design and the precision of computation and setting of the charging voltage level. The probable deviation of the delay time of the fuse which has been used in free-flight missiles was 3% of the set time.

§ 2. THE ACCURACY OF TIME FUSES

We shall evaluate the accuracy of time fuses for the most general case, where setting of their operating time is controlled by instruments located either aboard the aircraft or on the missile.

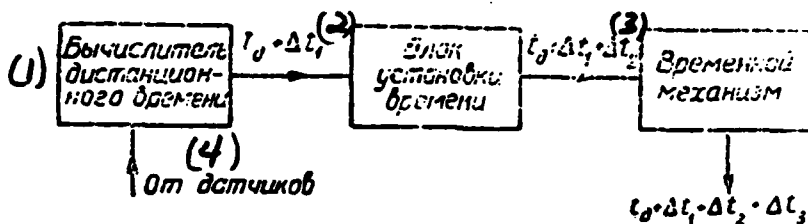


Fig. 10.9.

Key: (1) delay time computer; (2) time setting unit; (3) time mechanism; (4) from sensors.

A functional diagram of control of setting of the delay time of a fuse t_0 is shown in Fig. 10.9. In addition to the time mechanism of the fuse, the system includes a delay time computer and a delay time setting unit. In the use of fuses in antiaircraft missiles, data on the flight altitude, the target range, the velocity of the carrier aircraft and the velocity of the target, the ballistic characteristics of the missile, etc., are fed from the appropriate sensors to the computer, which is located aboard the aircraft. The computer solves the problem of the point where the missile engages the target and determines the flight time of the missile to the point of impact - the lead time T_y - according to these data. When one wishes to provide bursting of the warhead of the missile at the moment when it comes up to the target, a

delay time t_y , equal to the lead time T_y is selected. The time t_y calculated in this way is transmitted in the form of an electrical signal to the delay time setting unit, which sets the operating time of the time mechanism of the fuse according to the signal level. In mechanical fuses, the setting unit is a part of the fuse and has the form of an electric motor which controls the rotation of the arrow in relation to the retainer. The setting unit of electrical fuses is located on the aircraft. It controls the charging of storage capacitors of the fuses.

The delay time can be set aboard the missile at a definite point of the trajectory - at the moment of disengagement of the guidance system, for example. In this case, all the instruments for control of the fuse are situated aboard the missile, and the guidance system serves as the source of information on the conditions of approach to the target. For setting the delay time, the on-board computer should solve the problem of the flight time of the missile from the moment of disengagement of the guidance system to the point of explosion of the warhead.

Control of time fuses of aerial bombs is accomplished in a similar way. In this case, the computer must solve the problem of the time of fall of the bomb for a given altitude.

As a result of inevitable errors in determining, setting and executing the delay time, the actual point of functioning of a fuse will not coincide with the calculated point.

The total error in regard to the operating time of a fuse Δt is made up of the following:

- the computer error Δt_1 ;
- the error in setting of the time mechanism Δt_2 ;

- the error in execution of the set time by the time mechanism of the fuse Δt_3 :

$$\Delta t = \Delta t_1 + \Delta t_2 + \Delta t_3. \quad (10.1)$$

Individual components of the error Δt are independent random variables distributed according to a normal law. Therefore, the total error will also be distributed according to a normal law. The standard deviation of the total error, according to (10.1), is as follows:

$$\sigma_t = \sqrt{\sigma_1^2 + \sigma_2^2 + \sigma_3^2}, \quad (10.2)$$

where σ_1 , σ_2 and σ_3 are standard deviations of errors Δt_1 , Δt_2 and Δt_3 , respectively.

With a knowledge of the time error, one can easily find the error in regard to the range.

For a case of firing at aerial targets (Fig. 10.10), we shall characterize the range error with the value Δz of the deviation of the point of functioning of the fuse from a plane $z=0$ passing through the center of the target perpendicular to the vector of the relative velocity of the missile \bar{v}_{lu} .

The range of flight of the missile from the firing point to the point of functioning of the fuse is as follows:

$$D = \int_0^{t_f + \Delta t} v_{lu}(t) dt = \int_0^{t_f} v_{lu}(t) dt + \int_{t_f}^{t_f + \Delta t} v_{lu}(t) dt. \quad (10.3)$$

Since $t_f = T_y$,

$$\int_0^{T_y} v_{lu}(t) dt = D_y \quad (10.4)$$

where D_y is the future range.

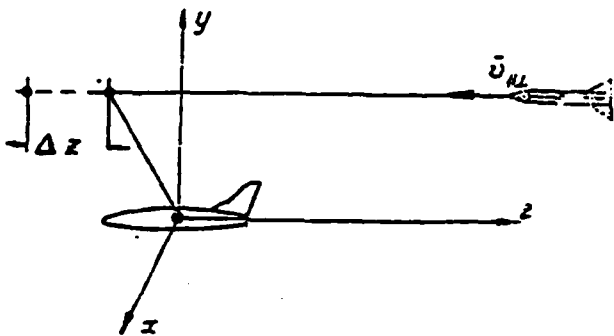


Fig. 10.10.

It follows from (10.3) and (10.4) that

$$\Delta z = D - D_y = \int_{t_0}^{t_0 + \Delta t} v_{1u}(t) dt. \quad (10.5)$$

For actual firing conditions, the time Δt is relatively small. Therefore, in computing of the integral of (10.5), the relative velocity of the missile can be considered constant, corresponding to the moment of passage of the missile near the target. Consequently,

$$\Delta z = v_{1u} \Delta t$$

and

$$c_z = v_{1u} s_z. \quad (10.6)$$

We shall establish the values of individual components of the total error Δt .

The computer error is conditioned by error of input data and the instrument error of the computer itself; i.e.,

$$\Delta t_i = \Delta t_{1B} + \Delta t_{1W}, \quad (10.7)$$

where Δt_{1B} and Δt_{1W} are the input and instrument errors of the computer.

As the simplest example illustrating the procedure for calculating input and instrument errors of the computer, we shall

consider a case of firing of antiaircraft missiles at a high altitude, where one can ignore the effect of drag on the missile. For determining the lead time, we shall write the laws of motion of the missile and the target.

The law of motion of the missile will be written in the following form, without consideration for the operating time of the engine:

$$D_p = v_1 t. \quad (10.8)$$

where v_1 is the velocity of the missile in relation to the air; D_p is the path of the missile from the firing point in the time t .

The value of the velocity v_1 is as follows:

$$v_1 = v_c + v_m.$$

where v_c is the velocity of the firing aircraft; v_m is the additional velocity of the missile.

The law of motion of the target in firing to overtake has the following form:

$$D = D_0 + v_u t, \quad (10.9)$$

where D_0 is the range at the moment of firing; v_u is the target velocity.

At the future position, $D = D_u$.

Setting equal the right members of expressions (10.8) and (10.9), and assuming that $t=t_d$ in them, we obtain an equation for determining the delay time:

$$v_1 t_d = D_0 + v_u t_d,$$

from which we find that

$$t_d = \frac{D_0}{v_1 - v_u} = \frac{D_0}{v_{1u}}. \quad (10.10)$$

Formula (10.10) is the working formula of the computer, by which it calculates the value of the delay time. As one can see, data on

the range at the moment of firing, the target velocity and the missile velocity must go to the computer for calculating the time t_d . Errors with which these data are introduced are the source of the error Δt_{1B} . The standard deviation of the error Δt_{1B} is determined by the well-known method of linearization of a function from random arguments.

Using the linearization method, we find that

$$\sigma_{t_B}^2 = \left(\frac{\partial t_B}{\partial D} \right)^2 \sigma_D^2 + \left(\frac{\partial t_B}{\partial v_1} \right)^2 \sigma_{v_1}^2 + \left(\frac{\partial t_B}{\partial v_n} \right)^2 \sigma_{v_n}^2, \quad (10.11)$$

where σ_D , σ_{v_1} and σ_{v_n} are the standard deviations of errors of input data D , v_1 and v_n , respectively. Having computed values of partial derivatives by formula (10.10) and inserted them expression (10.11), we obtain

$$\sigma_{t_B}^2 = \frac{\sigma_D^2}{v_{1n}^2} + \frac{D_0^2}{v_{1n}^4} \sigma_{v_1}^2 + \frac{D_0^2}{v_{1n}^4} \sigma_{v_n}^2 = \frac{D_0^2}{v_{1n}^2} \left(\frac{\sigma_D^2}{D_0^2} + \frac{\sigma_{v_1}^2 + \sigma_{v_n}^2}{v_{1n}^2} \right)$$

or

$$\sigma_{t_B}^2 = t_B^2 \left(\frac{\sigma_D^2}{D_0^2} + \frac{\sigma_{v_1}^2 + \sigma_{v_n}^2}{v_{1n}^2} \right). \quad (10.12)$$

For determining the instrument error, one must consider the functional diagram of the computer (Fig. 10.11). It follows from the diagram that

$$t_B + \Delta t_{1B} = \frac{D_0}{v_1 - v_n + \Delta_1} + \Delta_2, \quad (10.13)$$

where Δ_1 is the adder error; Δ_2 is the divider error.

Using the method of linearization, we find that

$$\sigma_{t_B}^2 = \left(\frac{\partial \Delta t_{1B}}{\partial \Delta_1} \right)^2 \sigma_{\Delta_1}^2 + \left(\frac{\partial \Delta t_{1B}}{\partial \Delta_2} \right)^2 \sigma_{\Delta_2}^2, \quad (10.14)$$

where σ_{Δ_1} and σ_{Δ_2} are the standard deviations of errors of the adder and the divider, respectively.

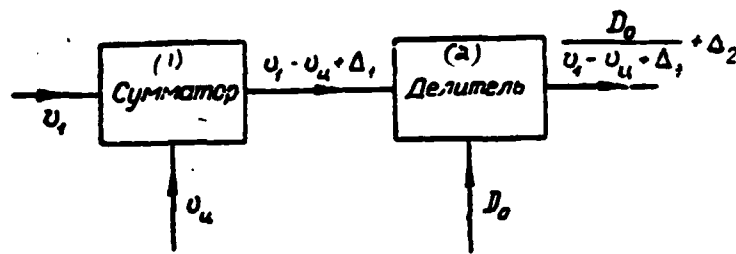


Fig. 10.11.
Key: (1) adder; (2) divider.

Having computed the values of partial derivatives, we find by formula (10.14):

$$\sigma_{\text{in}}^2 = \varepsilon_1^2 + \frac{D_o^2}{u_{\text{in}}^2} \varepsilon_2^2. \quad (10.15)$$

Since the precision of computing units normally is specified in the form of maximum relative errors of input variables, it is advisable to express the standard deviations of absolute errors in formula (10.15) in terms of standard deviations of relative errors.

It is obvious that

$$\varepsilon_1 = t_\delta \varepsilon_1^\circ;$$

$$\varepsilon_2 = v_{1\Delta} \varepsilon_2^\circ,$$

where ε° is the standard deviation of the relative error.

Inserting values of ε_Δ and ε_Σ into formula (10.15), we obtain

$$\sigma_{\text{in}}^2 = t_\delta^2 [(\varepsilon_1^\circ)^2 + (\varepsilon_2^\circ)^2]. \quad (10.16)$$

The values of ε° are assumed to be equal to $\frac{1}{3}\delta$, where δ is the relative error.

For existing computing units, $\delta_\Sigma = (0.1-1)\%$; $\delta_\Delta = 3\%$.

It follows from expression (10.7) that

$$\sigma_1^2 = \sigma_{1u}^2 + \sigma_{1n}^2 . \quad (10.17)$$

Taking into account expressions (10.12) and (10.16), we find by formula (10.17):

$$\sigma_1^2 = t_0^2 \left[(\sigma_D^c)^2 + (\sigma_s^c)^2 + (\sigma_a^c)^2 + \frac{\sigma_{z1}^2 + \sigma_{v_n}^2}{v_{1u}^2} \right], \quad (10.18)$$

where $\sigma_D^c = \sigma_D / D_0$ is the standard deviation of the relative error in the range.

The computer error normally includes a systematic component in addition to a random component. The systematic error of the computer is conditioned by approximation of the working formulas and by assumptions made in solving the problem.

We shall find the value of the systematic error for the example under consideration.

It was assumed in writing the law of motion of the missile (10.8) that the missile takes on an additional velocity v_m at the moment of firing. In reality the missile achieves this velocity at the end of the active section of the trajectory, after conclusion of operation of the engine. The acceleration of the missile in the active section of the trajectory can be assumed, with adequate precision, to be constant. Then the additional velocity of the missile can be assumed to vary according to a linear law from 0 to v_m . Consequently, the velocity of the missile in the active section of the trajectory will increase according to the following law:

$$v_t = v_0 + \frac{t}{\tau} v_m \quad \text{with } t < \tau,$$

where τ is the time of operation of the engine.

The length of the active section of the trajectory is defined by the expression

or

$$D_0 = v_0 \tau + \frac{v_m}{\tau} \int_0^\tau t dt = v_0 \tau + \frac{1}{2} \tau v_m$$

$$D_0 = \left(v_0 - \frac{v_m}{2} \right) \tau.$$

The law of motion of the missile is written in the following form with consideration for the active section of the trajectory:

$$D_0 = \left(v_0 - \frac{v_m}{2} \right) \tau + v_1 (\tau - \tau). \quad (10.19)$$

Setting equal the right members of expressions (10.9) and (10.19) with $\tau = t_d$, we obtain

$$\left(v_0 - \frac{v_m}{2} \right) \tau + v_1 (t_d - \tau) = D_0 + v_{1u} t_d.$$

from which we find that

$$t_d = \frac{D_0 + \frac{1}{2} v_m \tau}{v_{1u}}. \quad (10.20)$$

Comparing the formula obtained to formula (10.10), we find the value of the systematic error of the computer:

$$\Delta t_d = \frac{1}{2} \frac{v_m}{v_{1u}} \tau. \quad (10.21)$$

The systematic error in regard to the range will be as follows:

$$\Delta z = \frac{1}{2} v_m \tau. \quad (10.22)$$

One must keep in mind that formulas (10.21) and (10.22) pertain only to the special case under consideration. The expression for the systematic error must be determined in each individual case depending on the assumptions and simplifications which have been made in computing the delay time.

The value of the standard deviation σ_2 of the error in setting of the time mechanism of the fuse is determined by the accuracy of operation of the delay time setting unit.

The value of δ_3 , as already mentioned in § 1 of this chapter,

can be considered to be proportionate to the value of the delay time. For mechanical fuses, $\sigma_3 \approx (0.007-0.015) t_d$; for electrical fuses, $\sigma_3 \approx (0.03-0.045) t_d$. The value of σ_3 for electrical fuses can be computed when necessary according to known tolerances of the components included in the fuse design (resistances, capacitors, spark gaps).

As an example, we shall consider the order for computation of σ_3 for the simplest fuse design (10.3).

The law of variation of the voltage on the ignition capacitor is expressed by the following formula:

$$u_1 = u_\infty (1 - e^{-\frac{t}{\tau}}), \quad (10.23)$$

where $\tau = \frac{C_1 C_2 R}{C_1 + C_2}$ is the time constant of the system;

$$u_\infty = \frac{C_1}{C_1 + C_2} u_{10}.$$

At the moment of functioning of the fuse, $u_2 = u_\Pi$, where u_Π is the sparkover voltage of the spark gap.

Assuming that $u_2 = u_\Pi$ in formula (10.23), we find

$$t_d = -\tau \ln \left(1 - \frac{u_\Pi}{u_\infty} \right). \quad (10.24)$$

For determining σ_3 , it is necessary to compute partial derivatives from t_d in regard to all the parameters of the system C_1 , C_2 , R and u_Π . The value of σ_3 is found by the following formula:

$$\sigma_3^2 = \left(\frac{\partial t_d}{\partial C_1} \right)^2 \sigma_{C_1}^2 + \left(\frac{\partial t_d}{\partial C_2} \right)^2 \sigma_{C_2}^2 + \left(\frac{\partial t_d}{\partial R} \right)^2 \sigma_R^2 + \left(\frac{\partial t_d}{\partial u_\Pi} \right)^2 \sigma_{u_\Pi}^2.$$

One can find σ_3 for any design by a similar method. In cases where it is impossible to obtain dependences of t_d on parameters of the system in explicit form, the partial derivatives are determined for different values of t_d according to an implicit function.

In conclusion, we shall evaluate the minimum possible value of the variable $(\sigma_z)_{\min}$ for electrical fuses. In evaluation of the minimum possible value of $(\sigma_z)_{\min}$, we shall assume that $\sigma_1 = \sigma_2 = 0$, i.e., that the delay time is computed and introduced to the fuse with absolute precision. With such an assumption, it follows from formulas (10.2) and (10.6) that

$$(\sigma_z)_{\min} = v_{\text{in}} \sigma_3.$$

Assuming that $\sigma_3 = 0.03 t_d$, we find that $(\sigma_z)_{\min} = 0.03 v_{\text{in}} t_d$. If we assume that $v_{\text{in}} = 1000 \text{ m/s}$ and $t_d = 2 \text{ s}$, we obtain $(\sigma_z)_{\min} = 60 \text{ m}$. As one can see, the value of $(\sigma_z)_{\min}$ for real firing conditions has an order of several tens of meters. Such a large dispersion of time fuses does not permit using them in firing at aerial targets in a case where setting of the operating time is performed from the firing aircraft. In setting of the fuse from the aircraft, the required operating time proves relatively large, which is one of the reasons for large fuse errors in regard to range. The fuse errors can be reduced substantially if the delay time is set aboard the missile at a distance from the target significantly less than the initial range at the moment of firing. The greatest precision of remote detonation can be provided with setting and triggering of the time mechanism of the fuse at the moment of disengagement of the guidance system of the missile, i.e., at the minimum range at which the guidance system still records parameters characterizing the conditions of approach to the target (range, velocity of the target, etc.). For example, if the range for disengagement of the system is assumed to be 100 m, the required value of t_d at a relative velocity of 1000 m/s will be 0.1 s, and $(\sigma_z)_{\min} = 3 \text{ m}$.

CHAPTER 11

GENERAL INFORMATION ON PROXIMITY FUSES. ELECTROSTATIC, MAGNETIC AND ACOUSTIC PROXIMITY FUSES.

§ 1. THE PURPOSE AND A CLASSIFICATION OF PROXIMITY FUSES

Proximity fuses (NV) are finding the most extensive use in guided missiles intended for hitting aerial targets. They are also used for explosion of aerial bombs, naval mines and torpedos, artillery shells and free-flight and guided missiles in firing at ground targets. The use of NV instead of impact and time fuses is dictated in all cases by the attempt to improve the efficiency of tactical use of ammunition.

For example, the use of NV in antisubmarine bombs results in an increase in the probability of damage to the submarine due to enlargement of the area which must be hit to put the vessel out of action. The area which the bomb must hit is bounded by a curve (Fig. 11.1) equidistant from the outline of the vessel and at a distance from it equal to the effective radius of the fuse.

In cases of firing of missiles at ground targets and bombing with high-explosive fragmentation bombs, NV promote more rational utilization of the fragments and an increase in the area of destruction as compared to impact fuses. With contact detonation (Fig. 11.2), part of the fragments are wasted by going into the ground at the point where the bomb or projectile falls. In an

explosion near the surface of the ground, these fragments together with the other fragments strike the obstacle from above, thereby destroying targets in the area located under the explosion point. With an increase in the explosion altitude, the total area on which the flow of fragments falls is enlarged. However, this does not mean that the area of destruction also grows larger without limits, because the density of the flow of fragments at the obstacle decreases with an increase in the explosion altitude. Therefore, there is some optimum explosion altitude at which the area of destruction is maximal.

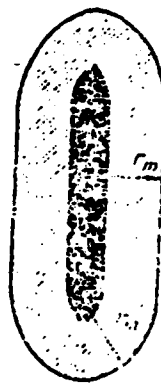


Fig. 11.1.

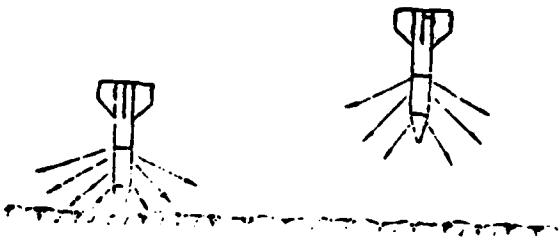


Fig. 11.2.

The effect of NV on firing efficiency is manifested to a greater degree in firing of missiles at aerial targets. It is well known that even in firing guided missiles at aerial targets, the probability of a direct hit is relatively low. In connection with this, remote-action warheads capable of destroying a target both in a direct hit and in explosion at some distance are used in missiles of the "air-to'air" class. Fragmentation warheads with directed scattering of the fragments serve as a characteristic example of such warheads. The three-dimensional region of scattering of the fragments (Fig. 11.3) is normally bounded by two conical surfaces with the peak at the center of the warhead. It is represented by an angle sector with a width of 10-20° in any plane containing the axis of the missile. This feature of fragmentation

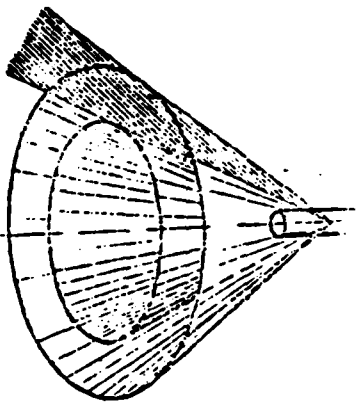


Fig. 11.3.

warheads conditions extremely rigid requirements for accuracy in determining the moment of functioning by the fuses. For the directed flow of fragments to hit the target, it is necessary that explosion of the warhead be effected by the fuse with definite mutual positions of the target and the missile. For illustration of the latter arrangement, Fig. 11.4 shows a diagram of the approach of a missile to a target is a special case where the missile

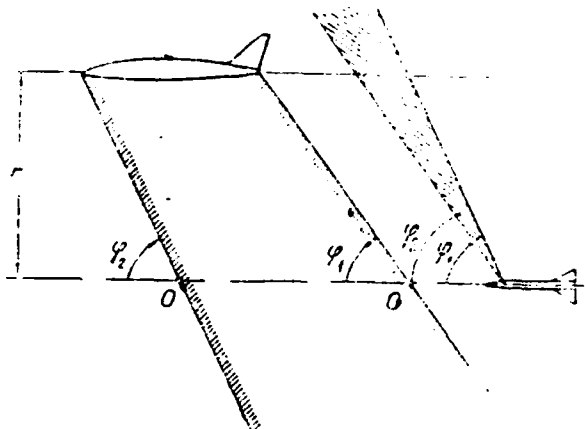


Fig. 11.4.

overtakes the target on a pursuit course. Due to the error of the guidance system, the trajectory of the missile passes at a distance r from the target. Considering the relative movement of the missile, one can easily conclude that hitting of the target by fragments and, consequently, destruction of the target are possible only in a case where the point of functioning of the fuse lies in trajectory section $O-O'$, between two lines drawn from the end points of the target at angles ϕ_1 and ϕ_2 , which define the positions of front and rear boundaries of the fragment scattering sector. The length of segment $O-O'$ determines the acceptable range of response points of the fuse along the relative trajectory of the missile. For a narrow fragment scattering sector and real misses of the missile, segment $O-O'$ is approximately equal to the length of the target. If we take into account the fact that the average length of fighter aircraft is of the order of 12 m and that of bombers is 30-40 m, the acceptable probable deviations of response points can be assumed to be 1.5-2 m in firing at fighters and 3-5 m in firing at bombers. Such high accuracy in determination of the moment of explosion of the warhead cannot be ensured by time fuses, whose errors are significantly

higher than the acceptable values. Only proximity fuses, which are capable of determining the relative positions of the missile and the target, possess the accuracy required for the conditions in question.

Proximity fuses function under the influence of either the very target being fired on or the medium surrounding the target. The effect of the target on the fuse is related to the ability of certain targets to emit or reflect energy of one kind or another. Aircraft, cruise missiles, warheads of ballistic missiles, artificial satellites, etc., can serve as examples of targets which emit energy. An aircraft in flight is a source of emissions of sonic vibrations and electromagnetic energy from infrared rays to ultra-violet rays. It also has the property of reflecting radio waves well. The energy level at each point in space around the target depends on its location in relation to the target. With a knowledge of this dependence, one can judge the relative positions of the target and the projectile according to the energy level. This pattern forms the basis for operation of most NV.

Depending on the origin of the energy used by the NV for determining the moment of response, they are divided into passive, active and semi-active fuses. The former use energy emitted by the target itself, while active proximity fuses emit energy themselves and use only the part of the energy reflected from the target for determining the moment of response. Fuses of the semi-active type, like active fuses, react to reflected energy, but in contrast to active fuses, they do not have their own energy source. A source located either on the ground or on the aircraft accomplishes irradiation of the target in this case. Different types of energy can be used for operation of NV: the energy of an electrical field, a magnetic field, an electromagnetic field, sonic vibrations, radioactive decay of nuclei, etc. The type of energy used determines the type of the fuse and forms the basis for classification of NV.

Proximity fuses are divided into the following:

- electrostatic NV (use the energy of an electrical field for operation);
- magnetic NV (use the energy of a magnetic field);
- radio fuses (use the electromagnetic energy in the range of radio waves);
- optical NV (use electromagnetic energy in the range from infrared to ultraviolet rays);
- acoustic NV (use the energy of sonic vibrations);
- hydrodynamic NV (use the energy of vibrations of the water medium in movement of a ship);
- vibration NV (use the energy of vibrations of the ground in movement of tanks, trains and other items of war equipment), etc.

The operation of NV which respond under the influence of the medium surrounding the target is based on regular variation of the pressure of the medium in the direction of a vertical to the ground surface. Such fuses include barometric and hydrostatic fuses. Barometric NV determine the moment of response in regard to the dependence of atmospheric pressure on the altitude above the target (the ground surface). They function at a predetermined altitude, where atmospheric pressure reaches the appropriate value. Hydrostatic fuses are used for explosion of depth charges at a predetermined depth below the water surface. Their operation is based on the dependence of the water pressure on the depth of immersion. Of all the types of NV, radio fuses and optical fuses are finding most extensive use at present in aviation ammunition.

5 2. FEATURES OF THE CONSTRUCTION OF PROXIMITY FUSES AND THEIR BASIC CHARACTERISTICS

Proximity fuses differ from other types of fuses in the structure of the target sensor. The target sensor of NV forms a command for explosion as a result of contactless interaction with the target. A receiver-transmitter, which performs irradiation of the target with some kind of energy, reception of reflected energy and formation of a command for explosion, serves as the sensor of an NV of the active type. Receivers which receive radiation of the target itself act as sensors of passive and semi-active NV.

In addition to target sensors, NV also include powder delay chains, remote arming mechanisms, safety devices and self-destruction devices, which do not differ in regard to the principle of construction from corresponding units of mechanical and electrical impact and time fuses. These assemblies of NV are often joined structurally into a unit called the safety and operations mechanism (PIM). According to its structure and the character of problems which it solves, the PIM can be considered an electromechanical fuse which functions on a command from the target sensor.

The basic characteristics of NV which influence the efficiency of tactical use of ammunition are as follows: the response surface, accuracy, resistance to noise and functional reliability.

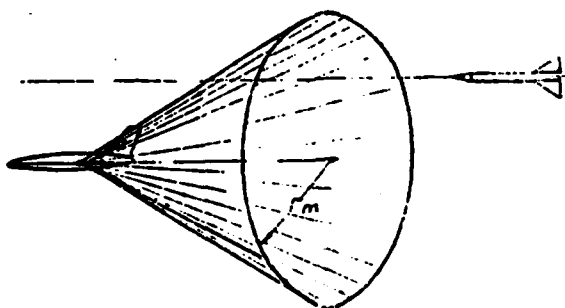


Fig. 11.5.

The response surface of an NV is the geometric location of positions of the target in relation to the projectile* or of the projectile in relation to the target at the moment of functioning of the fuse. For each relative trajectory of the projectile (Fig. 11.5), the response surface defines the average location of a point characterizing the position of the projectile in relation to the target at the moment of response of the NV. For the sake of brevity, this point hereinafter will be referred to as the response point of the fuse. The shape of the response surface depends on the type of NV, its characteristics and other factors, and the location of the response surface in relation to the target depends on the conditions of approach of the projectile to the target (the direction of approach, the value of the relative velocity of the projectile, etc.). In a case where the sensor of the NV interacts with a target of limited dimensions, such as an aircraft, the dimensions of the response surface are limited to some maximum miss of the projectile r_m called the radius of action of the NV. With misses exceeding the value of r_m , the fuse fails to operate, since the signal from the target is below the level of sensitivity of the sensor receiver.

In a case of firing at ground targets, when the fuse interacts with the ground surface, the position of the projectile in relation to the target at the moment of explosion is determined by the response altitude of the fuse. The response altitude is the measure of NV used in firing at ground targets.

The accuracy of a fuse is a characteristic determining the magnitude of possible deviations of actual response points from the response surface. The following can be causes of deviation of

*The term "projectile" is taken in a general sense here as before.

response points: the working spread of parameters of different components of the NV target sensor, instability of operation of the sensor, the random character of the process of interaction of the sensor with the target, and a number of other factors. The magnitude of the standard deviation of response points from the response surface is a numerical measure of the accuracy of NV.

The ability of fuses not to function under the influence of false signals - noise - is called their noise resistance. The susceptibility of NV to the influence of different kinds of noise is their basic shortcoming as compared to impact and time fuses. Interference for operation of NV can develop in the sensor itself during its functioning and can be created specially by the enemy. Interference of the former type is called natural interference, while interference of the latter type is called artificial interference, or jamming. Natural interference includes interference conditioned by noise of tubes and other components of the target sensor system, vibrations of parts in flight of the projectile and the presence of fog, clouds, rain, snow and other local irregularities in the atmosphere, for example. Artificial interference for radio fuses can be created by special jamming transmitters or by clouds of false reflectors of metallic tape, for example. Under the influence of interference, the fuse can function prematurely far from the target, where the effect of the ammunition represents no danger to the target; therefore, the extreme sensitivity of NV to noise makes them unsuitable for practical use.

The reliability of proximity fuses is evaluated by the probability of reliable operation. The NV possess lower reliability than mechanical fuses, which is explained by the presence of a large number of electronic instruments in their structure differing from mechanical devices in their significantly lower reliability.

§ 3. ELECTROSTATIC PROXIMITY FUSES

Electrostatic proximity fuses (ENV) determine the moment of response according to the intensity of the electrical field created by the target itself. For example, they can be used in firing at aircraft and other aerial targets which during flight take on electrostatic charges with a potential of several thousand volts. An electrical field is created due to the charge around the aircraft.

The action of ENV is based on the phenomenon of electrostatic induction, consisting of redistribution of electrical charges of current-conducting bodies under the influence of an external electrical field. In this case, the electrical field of the target is such a field, and the fuse is the current-conducting body. A schematic diagram of the simplest ENV is shown in Fig. 11.6. The diagram includes a spark gap L, an electric igniter EV, a power source - the battery B - and an electrode insulated from the fuse housing. The EDS [electromotive force, cmf] of the battery E is selected as somewhat less than the sparkover voltage of the spark gap; therefore, no current passes through the electric igniter before approach to the target. In flight of the projectile near

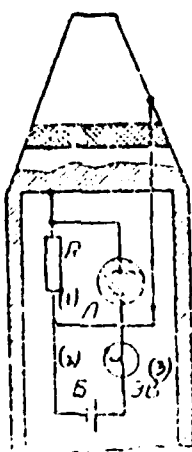


Fig. 11.6
Key: (1) L; (2) B; (3) EV [electric igniter].

the target, a potential difference Δu develops between the electrode and the housing and is fed to the resistance R . Due to the potential difference Δu , the voltage applied to leads of the spark gap increases to a value $E + \Delta u$. The value of Δu increases in proportion to approach to the target. At some distance, the total voltage $E + \Delta u$ acting on the spark gap reaches a value sufficient for sparkover of the gap. After sparkover of the spark gap, the current passes from the battery through the electric igniter, and the fuse functions. The advantage of electrostatic NV is structural simplicity. The basic shortcomings of ENV are susceptibility to natural interference in the form of charged clouds, and a small radius of action. One fuse of this type, developed during the Second World War in Germany, had a radius of action of 3-5 m. Attempts to increase its radius of action resulted in an increase in the percentage of premature responses due to electrical heterogeneity of the atmosphere.

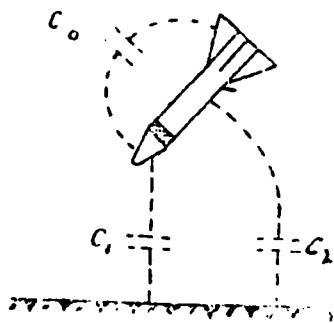


Fig. 11.7.

So-called capacitive fuses are a variety of ENV. In contrast to the fuses which have been considered, their operation is based on the use of an electrical field created in the space between the fuse housing and the shell of the projectile. The fuse and the projectile shell which is insulated from it (Fig. 11.7) form an electrical capacitance C_0 . In approach to the target, this capacitance changes, which leads to a redistribution of the electrical

field around the projectile. In the vicinity of the target, the projectile and the fuse form additional capacitances C_1 and C_2 with the target; these capacitances are connected parallel in relation to the capacitance C_0 . The total capacitance therefore will be as follows:

$$C_t = C_0 + \frac{C_1 C_2}{C_1 + C_2}.$$

The values of capacitances C_1 and C_2 depend on the distance to the obstacle. With a knowledge of this dependence, one can judge the distance to the target according to the magnitude of the capacitance C_{Σ} . A block diagram of an NV using the effect described is shown in Fig. 11.8.

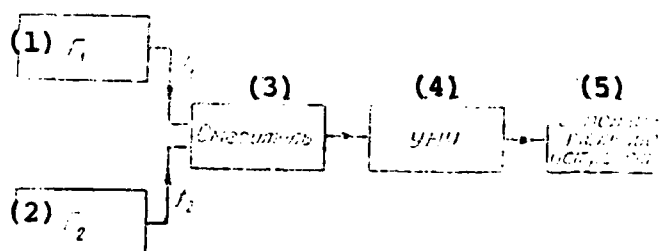


Fig. 11.8.
Key: (1) G_1 [oscillator]; (2) G_2 ; (3) mixer;
(4) UNCh [low-frequency amplifier]; (5) actuator.

The design includes two high-frequency oscillators, a mixer, a low-frequency amplifier (UNCh) and an actuator. The oscillation frequency f_1 of oscillator G_1 is stabilized, while the frequency f_2 of the other oscillator is determined by the parameters of the oscillatory circuit which includes the capacitance C_{Σ} . Oscillations pass from the oscillators to the mixer, which extracts oscillations of a difference frequency $F=f_1-f_2$. These oscillations are amplified, after which they act on the actuator. The actuator responds at the moment when the voltage at the amplifier output reaches a definite value. The amplifier possesses a narrow transmission band;

therefore, it is capable of amplifying only oscillations whose frequencies are near the frequency F_0 to which it is adjusted. In regulation of the fuse system, oscillator frequencies f_1 and f_2 are selected such that their difference does not fall within the transmission band of the UNCh. An increase in the capacitance C_{Σ} occurs in the process of approach to the target, leading to a decrease in the frequency f_2 of oscillator G_2 and, consequently, to a change in the difference frequency F . The moment its value comes close to F_0 , the amplified oscillations cause functioning of the fuse. The basic shortcoming of capacitive NV is the small radius of action.

§ 4. MAGNETIC PROXIMITY FUSES

The operation of magnetic proximity fuses (MNV) is based on the ability of targets possessing ferromagnetic properties to distort the magnetic field of the Earth in the area of their location. The magnetic field of the Earth can be considered homogeneous within the area in which flight of aviation ammunition (bombs, missiles, shells) occurs; i.e., the force lines of the field can be assumed to be parallel. In the vicinity of ferromagnetic targets (ships, aircraft, tanks, etc.), the homogeneity of the magnetic field of the Earth breaks down. The force lines of the field (Fig. 11.9) become concentrated in the vicinity of a target, since the permeance of ferromagnetic bodies is much higher than that of the air. One can assume provisionally that the target's own magnetic field develops around the target under the influence of the geomagnetic field. The intensity of this field is the geometric difference of intensities of the geomagnetic field in the presence and in the absence of the target.

One can use either the intensity of the magnetic field of the target or the speed of changing of the field in relative movement of the projectile for determining the moment of response of an MNV. Magnetic proximity fuses accordingly are divided into magnetostatic and magnetodynamic fuses. The former are normally called simply

magnetic proximity fuses, while the latter, in contrast, are referred to as induction proximity fuses. Magnetic NV, which react to the intensity of the magnetic field, first came into use as early as the First World War for contactless explosion of naval mines. A magnetic needle which closed the operational circuit in passage of a ship near the mine served as the target sensor of such fuses.

Design complexity and low noise resistance are serious shortcomings of magnetostatic NV. The design complexity is conditioned by the necessity of having a device for compensating for the geomagnetic field at the point where the mine is placed. Magnetic storms have a great influence on the operation of the fuses and are capable of causing their premature functioning. The only way of combatting the influence of magnetic storms is to reduce the sensitivity of the sensor, which results in a decrease in the range of action of the NV.

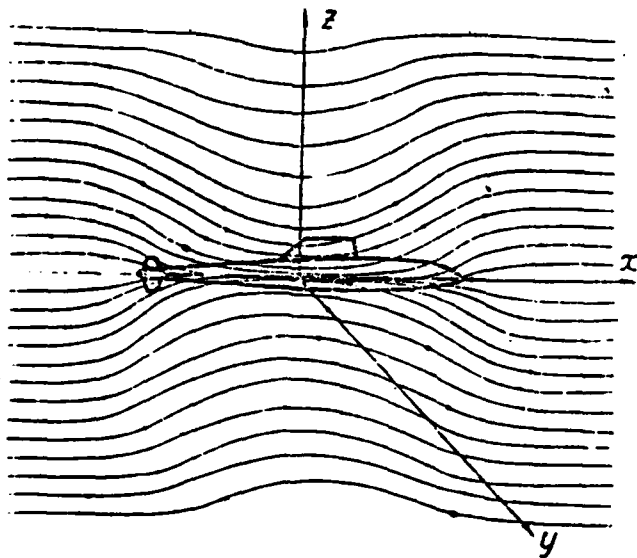


Fig. 11.9.

Magnetodynamic or induction proximity fuses function under the influence of a change in the magnetic field. An inductance coil serves as their target sensor. In movement of a projectile in relation to the target, a magnetic flux which varies in time intersect the coil and induces an e. d. s. [electromotive force, emf] in it. The magnitude of the emf induced in the coil is as follows:

$$e = -n \frac{d\Phi}{dt}, \quad (11.1)$$

where n is the number of turns of the coil; Φ is the magnetic flux permeating a turn.

The flux Φ , as we know, is calculated by the formula

$$\Phi = \mu H S \cos \alpha, \quad (11.2)$$

where μ is the permeability of the coil core material; H is the intensity of the magnetic field of the target; S is the area of a turn of the coil; α is the angle between a normal to a turn and the orientation of the field intensity vector.

The intensity vector of the magnetic field of the target is normally specified in the form of three components (H_x , H_y and H_z) in the direction of coordinate axes of a rectangular system of coordinates Oxyz (Fig. 11.9). If we assume that the coil axis remains parallel to the z axis in movement of the projectile, only the vertical component of the magnetic field H_z will be used for creating the emf in the coil. Such a special case corresponds to vertical movement of an antisubmarine bomb in the vicinity of a stationary submarine, for example, if the coil axis is parallel to the bomb axis in this case.

All three components of the magnetic field of the target generally participate in creation of the induction emf. In the use of only the vertical component of the field, the formula (11.2) will take on the following form:

$$\Phi = \mu H_z S. \quad (11.3)$$

Inserting the value of ϕ from (11.3) into expression (11.1), we obtain

$$e = -k \frac{dH_z}{dt}, \quad (11.4)$$

where $k=n\mu S$.

Having designated the velocity of movement of the bomb in the water as v , we shall reduce formula (11.4) to the following form:

$$e = -k \frac{dH_z}{dz} \cdot \frac{dz}{dt} = -kv \frac{dH_z}{dz}. \quad (11.5)$$

It follows from formula (11.5) that the magnitude of the emf induced in the coil in vertical movement of the bomb in the vicinity of a submarine is proportionate to the velocity of the bomb and the rate of change of the field intensity along the z axis.

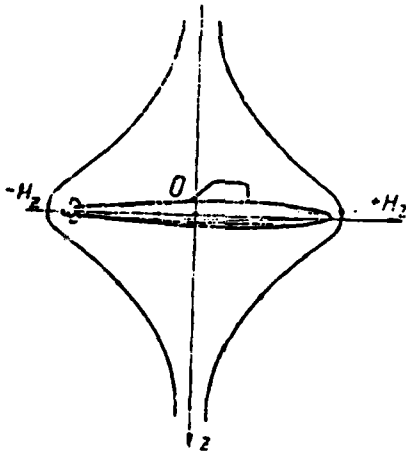


Fig. 11.10.

The curve of variation of the intensity of the vertical component of the magnetic field of the vessel has the form of a bell-shaped signal (Fig. 11.10). With such a character of variation of H_z , as follows from formula (11.5), a dual-impulse signal similar in form to a sinusoidal signal will be induced in

the coil. The sign of the first impulse of the signal depends on the sign of the field intensity and can be both positive and negative. The signal duration depends on the value of the distance at which the bomb passes the vessel and its velocity. For real conditions, it varies from fractions of a second to several seconds. A dual-impulse signal with such a duration corresponds to a sinusoidal emf with a frequency of fractions of a cycle per second to several cycles per second. A block diagram of the simplest induction NV

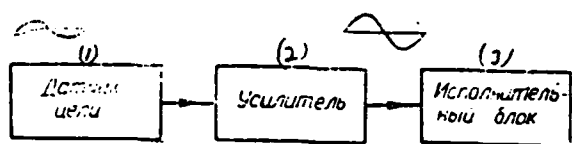


Fig. 11.11.

Key: (1) target sensor; (2) amplifier;
(3) actuating unit.

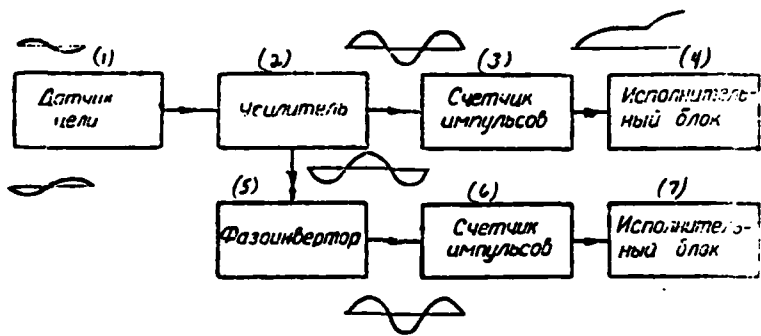


Fig. 11.12.

Key: (1) target sensor; (2) amplifier;
(3) pulse counter; (4) actuating unit;
(5) phase inverter; (6) pulse counter;
(7) actuating unit.

capable of detonating an antisubmarine bomb in the vicinity of the vessel is shown in Fig. 11.11. In addition to the target sensor, the design includes a low-frequency amplifier and an

actuator. Functioning of the actuator causes a positive pulse of the amplified signal. A design of an NV which functions under the action of a single pulse does not possess high noise protection. One can improve the noise protection of the design, for example, if one transforms the dual-impulse signal into a triple-impulse signal and introduces an additional unit - a pulse counter - into the design. A block diagram of an NV with pulse counters is shown in Fig. 11.12. Transformation of the dual-impulse signal into a triple-impulse signal is performed by the amplifier due to the appropriately selected time lag. The signal passes from the amplifier output to a dual-channel actuator. Pulse counters connected just before the actuating units are adjusted so that these units respond if at least two positive pulses are active at the amplifier output. The first actuating unit operates when the signal at the amplifier output has two positive pulses. The second unit operates if this signal has one positive and two negative pulses. A phase inverter which shifts the signal phase by 180° and thereby transforms the signal with two negative pulses into a signal with two positive pulses is connected between the amplifier and the second actuating unit.

Induction NV can be used in aviation for explosion of anti-submarine bombs and torpedos.

A common shortcoming of MNV is the possibility of combatting them. For combatting magnetic proximity fuses, ship designs include special demagnetizing devices which compensate for the field of the ship and thereby render operation of the fuses difficult.

§ 5. ACOUSTIC PROXIMITY FUSES

Acoustic proximity fuses of the passive type were one of the first examples of NV tried for use for detonating aviation and antiaircraft projectiles in firing at aerial targets. Elastic diaphragms and crystal microphones were used as target sensors

in them. Figure 11.13 presents a schematic diagram of a fuse with a diaphragm sensor. Such a design was used in the German "Kranich" fuse, which was intended for small-caliber rocket missiles. The diaphragm M was located in the nose of the projectile. A contact prong which completed the operational circuit in vibrations of the membrane caused by sonic vibrations of the target aircraft was attached at the center of the diaphragm. The fuse functioned at a range of up to 7 m.

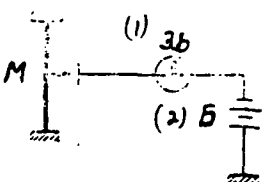


Fig. 11.13.
Key: (1) EV; (2) B.

A schematic diagram of a microphone sensor is shown in Fig. 11.14. A plate of a material possessing piezoelectric properties (quartz, barium titanate, etc.) serves as the basic part of the sensor. The plate absorbs sonic pressure and transforms it into a sinusoidal electrical signal, which is fed through a capacitor C to a resistance R at the input of an amplifier. Due to the capacitor, the direct current voltage which can develop on the plate due to the effect of the impact air pressure on it is not delivered to the amplifier. The German "Meise" fuse with a microphone sensor provided a range of action of up to 15 m in firing at aircraft.

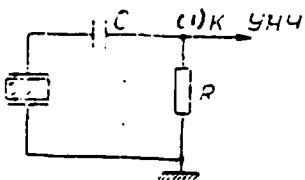


Fig. 11.14.
Key: (1) to UNCh.

Despite the simplicity of their construction, acoustic NV of the passive type have not found use in aviation. The basic shortcoming of acoustic NV is their low noise resistance. Their premature response can occur from bursting of shells, due to oscillations and vibration of the projectiles on the trajectory, etc. The use of acoustic proximity fuses essentially becomes impossible when the target has a supersonic velocity.

Acoustic proximity fuses of the active type can be used only in water, where the velocity of propagation of sound ($c=1500$ m/s) is significantly greater than the velocity of movement of the ammunition (bombs, torpedos). The velocity of sound in air ($c=340$ m/s) is significantly less than in water and does not exceed the velocities of most modern ammunition.

Acoustic NV of the active type with an ultrasonic emitter can be used in antisubmarine aviation ammunition (bombs and torpedos). The use of the range of ultrasonic oscillations (an oscillation frequency above 20 kHz) provides the possibility of achieving high directivity of emissions with small dimensions of the emitter. We know that the directivity of emissions depends on the ratio between the wavelength of the oscillations being emitted and the dimensions of the emitter. The smaller the wavelength as compared to the dimensions of the emitter, the higher the directivity of the emissions. In the use of ultrasound, it is possible to obtain extremely short sonic waves. For example, ultrasound with a frequency of 20,000 Hz has a wavelength of 7.5 cm in water, while at a frequency of 150,000 Hz, the wavelength is only 0.01 cm. Ultrasonic NV can use the sonar method for detecting submarines for determining the moment of response. A block diagram of an NV which operates according to the sonar method is shown in 11.15. The diagram includes a high-frequency oscillator, a modulator, a hydrophone, an amplifier, a detector and an actuating unit.

The high-frequency oscillator generates electrical oscillations

of ultrasonic frequency with a constant amplitude. The operation of the oscillator is controlled by a modulator, which accomplishes pulsed modulation of the oscillations generated. Pulses of electrical oscillations pass from the oscillator to the hydrophone, which transforms them into ultrasonic oscillations and emits them into the surrounding space (the water medium). The hydrophone is manufactured from a material possessing piezoelectric properties. Its shape and dimensions determine the beam pattern of the emissions. Proximity fuses of antisubmarine ammunition should possess a beam pattern which provides a circular scan of the space around the bomb or torpedo. A pattern (Fig. 11.16) bounded by two conical surfaces with the center of the emitter serving as their peak, while a continuation of the bomb axis is the axis, satisfies this requirement. If the submarine comes into the emission zone of the

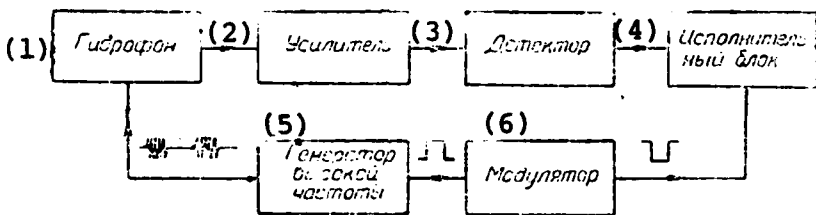


Fig. 11.15.

Key: (1) hydrophone; (2) amplifier; (3) detector; (4) actuating unit; (5) high-frequency oscillator; (6) modulator.

hydrophone, reflection of ultrasonic impulses occurs. Within the limits of working distances from the bomb to the vessel, reflected impulses reach the hydrophone during a pause between two adjacent pulses of the oscillator. The reflected ultrasonic impulses in acting on the hydrophone are transformed by it into electrical pulses, which are then amplified by the amplifier and rectified by a video detector. The pulses pass from the output of the detector to an actuator. For improving the noise protection of the NV, a pulse counter can be installed just before the actuating unit; the

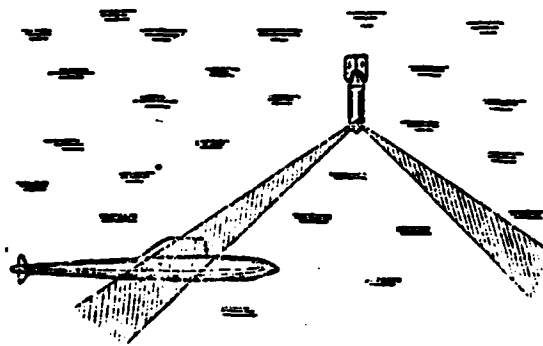


Fig. 11.16.

counter permits functioning of the NV only under the action of a definite number of pulses. Negative pulses are fed to the input of the actuator from the modulator during emission of sounding impulses and protect it against functioning under the influence of oscillator pulses penetrating through the amplifier.

CHAPTER 12

RADIO FUSES

§ 1. THE PRINCIPLE OF OPERATION OF RADIO FUSES OF THE ACTIVE TYPE WITH CONTINUOUS EMISSIONS

Radio proximity fuses (RV) with continuous emission of radio waves are divided into two groups - heterodyne and autodyne - according to the method of reception and transformation of the reflected signal.

The target sensor in heterodyne RV has separate channels for transmission and reception of reflected radio waves. The antenna system of such fuses consists of two or more antennas. One antenna (or group of antennas) is used for transmission, while the other is used for reception. Transformation of the reflected signal occurs in a mixer, to which a small part of the power of the transmitter is fed as the heterodyne voltage.

A single unit called the transponder performs functions of transmitting and receiving in autodyne fuses. Autodyne RV use the same antenna simultaneously for transmitting and receiving. We shall consider the operation of the target sensor of a heterodyne fuse according to a block diagram (Fig. 12.1). A high-frequency oscillator generates high-frequency oscillations with a constant amplitude. These oscillations are fed to a transmitting antenna A_1 and are emitted into the surrounding space. Having reached the

target, the radio waves are reflected from it and, travelling a reverse path, act on the receiving antenna A_2 . The reflected waves induce a high-frequency e. d. s. [electromotive force, emf] in the receiving antenna; the emf passes to the mixer, to which an insignificant part of the power is also fed directly from the oscillator. Thus two signals will be active in the mixer when a target enters the radiation zone of the transmitting antenna: a signal u_1 from the oscillator and a signal u_2 reflected from the target.

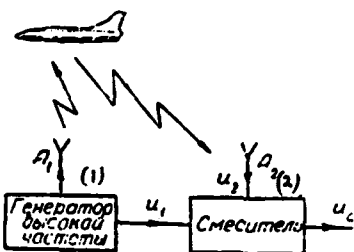


Fig. 12.1.
Key: (1) high-frequency oscillator;
(2) mixer.

The signal from the oscillator can be written in the following form:

$$u_1 = U_{1m} \cos \phi(t), \quad (12.1)$$

where U_{1m} is the signal amplitude; $\phi(t)$ is the phase, which is a function of the time t .

The reflected signal differs in amplitude and phase from the oscillator signal. Due to scattering of the radio waves, the reflected signal possesses a significantly smaller amplitude, the value of which depends on the distance to the target. The reflected signal lags in phase in relation to the emitted signal by a time τ necessary for propagation of radio waves to the target and back. Consequently, the reflected signal can be written in the following form:

$$u_2 = U_{2m} \cos \varphi(t - \tau), \quad (12.2)$$

where

$$\tau = \frac{2D}{c};$$

D is the distance to the target; c is the velocity of propagation of radio waves, which amounts to ~300,000 km/s.

Addition of signals u_1 and u_2 occurs in the mixer. We shall find the law of variation of the resulting signal:

$$u = u_1 + u_2.$$

Using expressions (12.1) and (12.2), we can write

$$u = U_{1m} \cos \varphi(t) + U_{2m} \cos \varphi(t - \tau). \quad (12.3)$$

We shall represent the phase of the reflected signal in the following form:

$$\varphi(t - \tau) = \varphi(t) + \Delta\varphi(t - \tau),$$

where $\Delta\varphi(t - \tau) = \varphi(t - \tau) - \varphi(t).$

We shall rewrite expression (12.3) with consideration for the designation which has been introduced:

$$u = U_{1m} \cos \varphi + U_{2m} \cos(\varphi + \Delta\varphi). \quad (12.4)$$

An indication of the functional dependence $\varphi(t)$ and $\Delta\varphi(t - \tau)$ has been omitted in expression (12.4) for simplifying writing the expression. We shall assume this dependence.

We shall transform expression (12.4) to the following form:

$$\begin{aligned} u &= (U_{1m} + U_{2m} \cos \Delta\varphi) \cos \varphi - (U_{2m} \sin \Delta\varphi) \sin \varphi = \\ &= A \cos \varphi - B \sin \varphi. \end{aligned} \quad (12.5)$$

We shall designate the following:

$$\frac{A}{\sqrt{A^2 + B^2}} = \cos \psi, \quad \frac{B}{\sqrt{A^2 + B^2}} = \sin \psi. \quad (12.6)$$

Then we can write

$$u = \sqrt{A^2 + B^2} \cos(\varphi + \psi). \quad (12.7)$$

It follows from expressions (12.5) and (12.6) that

$$\begin{aligned} \sqrt{A^2 + B^2} &= \sqrt{(U_{1m} + U_{2m} \cos \Delta\varphi)^2 + U_{2m}^2 \sin^2 \Delta\varphi} = \\ &= U_{1m} \sqrt{1 + 2 \frac{U_{2m}}{U_{1m}} \cos \Delta\varphi + \left(\frac{U_{2m}}{U_{1m}}\right)^2}; \\ \psi &= \arctg \frac{B}{A} = \arctg \frac{U_{2m} \sin \Delta\varphi}{U_{1m} + U_{2m} \cos \Delta\varphi}. \end{aligned}$$

Inserting the value of the square root into expression (12.7), we obtain

$$u = U_{1m} \sqrt{1 + 2 \frac{U_{2m}}{U_{1m}} \cos \Delta\varphi + \left(\frac{U_{2m}}{U_{1m}}\right)^2} \cos(\varphi + \psi). \quad (12.8)$$

Keeping in mind that $U_{2m}/U_{1m} \ll 1$, one can simplify expression (12.8) by replacing the root with the first two members of its expansion to an exponential series in regard to the parameter U_{2m}/U_{1m} ; i.e., one can assume that

$$u = U_{1m} \left(1 + \frac{U_{2m}}{U_{1m}} \cos \Delta\varphi\right) \cos(\varphi + \psi). \quad (12.9)$$

It follows from the latter expression that the resulting signal in the mixer has the form of a high-frequency voltage (Fig. 12.2) modulated in regard to the amplitude by a harmonic function $\cos \Delta\varphi$. The envelope of this voltage is extracted at the mixer output and acts as the working signal for the fuse:

$$u_c = U_{mc} \cos \Delta\varphi, \quad (12.10)$$

where $U_{mc} = kU_{2m}$ is the amplitude of the working signal; k is the mixer voltage transmission coefficient.



Fig. 12.2.

Extraction of the working signal in autodyne fuses occurs due to changing of the operating mode of the transmitter under the influence of the reflected signal. The reflected signal causes amplitude modulation of oscillations of the transmitter according to a law of $\cos \Delta \phi$.

In firing at ground targets, when reflection of radio waves normally occurs from the ground surface, the effect of the working signal begins to appear as soon as its value exceeds the level of characteristic noise of the fuse receiver. The amplitude of the working signal in this case depends only on the altitude at which the missile or bomb with the RV is located, increasing in proportion to approach to the ground surface. In firing at aerial targets, there is no working signal ($U_{2m} = 0$) up to the moment when the target enters the emission zone of the RV. It appears only at the moment when the target enters the emission zone and disappears as it goes out of the zone. The maximum amplitude of the working signal in this case depends on the miss of the missile. With an increase in the miss, the amplitude decreases, which serves as the cause of limitation of the radius of action of the fuse.

The frequency of the working signal $\Delta \phi$, as follows from determination of the function $\Delta \phi(t-\tau)$, is equal to the difference between frequencies of the reflected and emitted signals:

$$\Omega = \Delta \dot{\phi}(t-\tau) = \dot{\phi}(t-\tau) - \dot{\phi}(t).$$

where $\dot{\phi}(t-\tau)$ is the circular frequency of the reflected signal; $\dot{\phi}(t)$ is the circular frequency of the emitted signal.

The value of the frequency Ω depends primarily on the law of variation of the frequency of the emitted signal $\dot{\phi}(t)=\omega(t)$.

We shall consider two possible cases:

- the frequency ω is constant;

- the frequency ω varies according to a periodic law.

1) The case with $\omega = \omega_0 = \text{const.}$

Since $\phi(t) = \omega_0 t$, $\phi(t-\tau) = \omega_0 t - \omega_0 \tau$ and $\phi(t-\tau) = \omega_0(t-\tau)$. Consequently, $\Delta\phi(t-\tau) = \phi(t-\tau) - \phi(t) = -\omega_0 \tau$.

The frequency of the working signal in this case will be as follows:

$$\Omega = \Delta\dot{\phi}(t-\tau) = -\omega_0 \frac{d\tau}{dt}.$$

Taking into consideration the expression $\tau = 2D/c$, we obtain

$$\Omega = -\frac{2\omega_0}{c} \frac{dD}{dt}, \quad (12.11)$$

where dD/dt is the velocity of approach to the target.

It follows from formula (12.11) that the difference between frequencies of reflected and emitted signals and, consequently, the appearance of a working signal with the frequency Ω are conditioned by the relative movement of the target and the fuse. In the absence of relative movement, $dD/dt=0$, and $\Omega=0$. In a case of approach to the target $dD/dt < 0$ and, as follows from formula (12.11), $\Omega > 0$. On the other hand, with movement away from the target, $dD/dt > 0$ and $\Omega < 0$. Thus, in approach to the target, the frequency of the reflected signal exceeds the frequency of the emitted signal by the value Ω , while in movement away from the target, it is less than the frequency of the emitted signal by the same amount. The phenomenon of variation of the frequency of reflected oscillations due to relative movement of the target and the fuse is familiar under the name of the Doppler effect. The value Ω by which the frequency of the reflected signal is changed is called the Doppler frequency.

We shall reduce expression (12.11) for the Doppler frequency to a different form.

Since

$$\frac{2\omega_0}{c} = \frac{4\pi f_0}{c} = \frac{4\pi}{\lambda},$$

then

$$\Omega = -\frac{4\pi}{\lambda} \frac{dD}{dt}; \quad (12.12)$$

$$F = -\frac{2}{\lambda} \frac{dD}{dt}, \quad (12.13)$$

where λ is the wavelength of the emitted oscillations; f_0 is the frequency of the emitted oscillations in Hz; F is the Doppler frequency in Hz.

One must keep in mind that the Doppler frequency is a low frequency as compared to the frequency of the emitted signal. For example, with a frequency of the emitted signal $f_0 = 300$ MHz, which corresponds to a wavelength $\lambda = 1$ m, and an approach velocity $dD/dt = 1000$ m/s, the Doppler frequency is only 2000 Hz. Therefore, in a case where the frequency of the signal emitted by the fuse is constant, extraction of the working signal occurs due to the Doppler effect. The working signal in this case is a low-frequency voltage which varies at the Doppler frequency. Radio fuses with continuous emission of radio waves whose frequency is constant have been given the name Doppler fuses.

2) A case where $\omega(t)$ varies according to a periodic law.

We shall assume that the frequency of the emitted signal varies according to a sinusoidal law (Fig. 12.3); i.e., the emitted signal is modulated in regard to frequency.

We shall write the law of variation of the frequency in the following form:

$$\dot{\omega}(t) = \omega_0 + \Delta\omega_m \sin \Omega_m t, \quad (12.14)$$

where ω_0 is the average value of the frequency; $\Delta\omega_m$ is the amplitude of frequency variation; Ω_m is the modulation frequency.

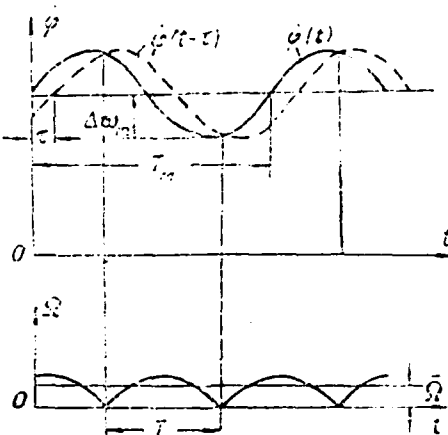


Fig. 12.3.

We shall assume that the relationship $\omega_0 \gg \Delta\omega_m$ which is normal for frequency modulation occurs between ω_0 and $\Delta\omega_m$. By integrating expression (12.14), we obtain

$$\phi(t) = \omega_0 t - \frac{\Delta\omega_m}{\Omega_m} \cos \Omega_m t.$$

It follows from this that

$$\phi(t-\tau) = \omega_0(t-\tau) - \frac{\Delta\omega_m}{\Omega_m} \cos \Omega_m(t-\tau);$$

and

$$\Delta\phi(t-\tau) = -\omega_0\tau - \frac{\Delta\omega_m}{\Omega_m} \cos \Omega_m(t-\tau) + \frac{\Delta\omega_m}{\Omega_m} \cos \Omega_m t.$$

The frequency of the working signal will be as follows:

$$\begin{aligned} \Omega &= \Delta\phi(t-\tau) = -[\omega_0 + \Delta\omega_m \sin \Omega_m(t-\tau)] \frac{dt}{d\tau} + \\ &\quad + \Delta\omega_m [\sin \Omega_m(t-\tau) - \sin \Omega_m t]. \end{aligned} \quad (12.15)$$

It follows from formula (12.15) that the frequency of the working signal is made up of two components, the first of which is conditioned by the Doppler effect (relative movement of the target and the fuse), while the second is conditioned by the lagging of the reflected signal by the time τ . The ratio between these components depends mainly on the parameters of the law of modulation $\Delta\omega_m$ and Ω_m . We shall assume that $\Delta\omega_m$ and Ω_m satisfy the condition under which the Doppler component of the frequency Ω can be

neglected; i.e., we shall assume that

$$\Omega = \Delta\omega_m [\sin \Omega_m(t - \tau) - \sin \Omega_m \tau] \quad (12.16)$$

The conditions under which this assumption is valid will be considered below.

We shall replace the difference of sines in expression (12.16) with a product of trigonometric functions:

$$\Omega = -2\Delta\omega_m \cos \Omega_m \left(t - \frac{\tau}{2}\right) \sin \frac{\Omega_m \tau}{2} \quad (12.17)$$

Since the frequency is an essential positive variable, the right member of formula (12.17) should be taken as an absolute value.

Figure 12.3 presents graphs illustrating the extraction of the working signal. The solid curve in the top graph shows the law of variation of the oscillator frequency, while the dotted line shows the law of variation of the frequency of reflected oscillations without consideration for the Doppler effect. The dotted curve is shifted by the time τ of lagging of reflected oscillations in relation to the solid curve. The bottom graph shows the law of variation of the frequency of the working signal Ω . For any moment in time t , the frequency can be established with the top graph as the absolute value of the difference between ordinates of curves of $\phi(t)$ and $\phi(t-\tau)$. As one can see, the frequency Ω varies periodically in time according to the law of the cosine modulus. The period T of variation of the frequency Ω is equal to half the modulation period of the oscillator frequency $T_M = 2\pi/\Omega_M$.

The working signal amplifier reacts to the average frequency value rather than the momentary frequency Ω . The average value of the frequency for a time segment significantly exceeding the period of its variation can be established as the average value for the period:

$$\bar{\Omega} = 2\Delta\omega_m \sin \frac{\Omega_u \tau}{2} \cdot \frac{1}{T} \int_{t_1}^{t_1+T} \left| \cos \Omega_u \left(t - \frac{\tau}{2} \right) \right| dt. \quad (12.18)$$

Since the moment in time t_1 from which the segment T is measured is arbitrary, it is convenient to adopt a time equal to $\tau/2$. Then expression (12.18) can be rewritten in the following form:

$$\bar{\Omega} = \frac{2\Delta\omega_m}{T} \sin \frac{\Omega_u \tau}{2} \int_0^T |\cos \Omega_u x| dx. \quad (12.19)$$

Substituting the values $T=T_M/2$ and $\Omega_u=2\pi/T_M$ into (12.19), we obtain

$$\begin{aligned} \bar{\Omega} &= \frac{4\Delta\omega_m}{T_u} \sin \pi \frac{\tau}{T_u} \int_0^{\frac{1}{2}T_u} \left| \cos \frac{2\pi}{T_u} x \right| dx = \\ &= \frac{8\Delta\omega_m}{T_u} \sin \pi \frac{\tau}{T_u} \int_0^{\frac{1}{2}T_u} \cos \frac{2\pi}{T_u} x dx. \end{aligned}$$

Having performed the integration, we find

$$\bar{\Omega} = \frac{4\Delta\omega_m}{\pi} \sin \pi \frac{\tau}{T_u}. \quad (12.20)$$

A modulation period is selected such that with any range to the target, the inequality $\tau \ll T_M$ is fulfilled when the signal exceeds the level of characteristic noise of the system. With such an inequality, the sine argument in expression (12.20) is a low value. Replacing the sine with its argument, we obtain an expression for the frequency $\bar{\Omega}$ in a simpler form:

$$\bar{\Omega} \approx \frac{4\Delta\omega_m \tau}{T_u}.$$

Inserting the value of τ into the formula obtained, we find

$$\bar{\Omega} \approx \frac{8\Delta\omega_m F_u D}{c} \quad (12.21)$$

$$F_u = \frac{8\Delta f_m F_u D}{c} \quad (12.22)$$

where $F_u = 1/T_M$ is the modulation frequency in Hz.

It follows from expression (12.22) that the frequency of the working signal is proportionate to the range to the target. It decreases in approach to the target.

We shall evaluate the influence of the Doppler effect on the frequency Ω . The Doppler component of the frequency Ω , as follows from expression (12.15) is as follows:

$$\Omega_d = -[\omega_0 + \Delta\omega_m \sin \Omega_x(t - \tau)] \frac{d\tau}{dt}$$

Since $\Delta\omega_m \ll \omega_0$, one can assume with adequate precision that

$$\Omega_d = -\omega_0 \frac{d\tau}{dt}.$$

It was established previously [(12.11) and (12.12)] that

$$\Omega_d = -\frac{4\pi}{\lambda} \frac{dD}{dt}.$$

The Doppler frequency appears graphically in the shifting of the curve showing the frequency of the reflected signal along the ordinate axis. In approach to the target ($\Omega_d > 0$), the curve shifts upward (Fig. 12.4); in movement away from the target ($\Omega_d < 0$), it shifts downward. Such shifting of the curve results in distortion of the cosine law of variation of the frequency of the working signal and disruption of the proportional relationship between the frequency and the range to the target.

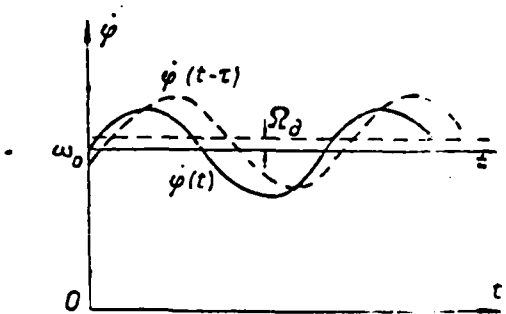


Fig. 12.4.

If the frequency $\bar{\Omega}$ dominates over the Doppler frequency Ω_0 , the Doppler effect results in an increase in the frequency $\bar{\Omega}$ for a modulation period and practically the same decrease in the frequency $\bar{\Omega}$ for another period. As a result, the average frequency $\bar{\Omega}$ for a modulation period remains unchanged; consequently, one can ignore the Doppler effect in this case.

We shall find the condition under which the relationship $\bar{\Omega} \gg \Omega_0$ is valid. Using the expression for the Doppler frequency and formula (12.21), we shall write the following inequality:

$$\frac{8\Delta\omega_m F_M}{c} D \gg \frac{4\pi}{\lambda} \left| \frac{dD}{dt} \right|.$$

It follows from this that:

$$\frac{4\Delta f_m F_M}{c} D \gg \frac{1}{\lambda} \left| \frac{dD}{dt} \right|$$

and

$$\Delta f_m F_M \gg \frac{1}{4} f_0 \frac{1}{D} \left| \frac{dD}{dt} \right|. \quad (12.23)$$

The latter inequality should be provided for the maximum possible approach velocity and the minimum range. It is used for selecting parameters of the law of modulation Δf_m and F_M when it is necessary to exclude the Doppler effect. If the inequality (12.23) is not fulfilled, the frequency of the working signal must be assumed to be as follows:

$$\Omega = \bar{\Omega} + \Omega_0.$$

Thus, in emission of frequency-modulated oscillations by RV, extraction of the working signal occurs due to lagging of the reflected signal and the Doppler effect. With fulfillment of certain conditions, the frequency of the working signal can be assumed to be proportionate to the range to the target.

Radio fuses with continuous emission of radio waves modulated in regard to frequency have been given the name of fuses with frequency modulation. Radio fuses with frequency modulation are

more complex than Doppler RV. A special modulator unit is necessary for modulation of the oscillator frequency.

The basic advantage of RV with frequency modulation is their enhanced noise protection in relation to jamming. Their specific shortcoming is the parasitic amplitude modulation of the emitted signal, which is inevitable in frequency modulation. A false working signal will be extracted at the mixer output due to parasitic modulation of the signal u_1 and can cause premature functioning of the fuse far from the target. Balanced circuits of the mixers are used for eliminating the false signal.

Doppler and frequency-modulated RV can be constructed in both heterodyne and autodyne versions. Autodyne RV are distinguished by structural simplicity and small dimensions and are being used at present in artillery shells, aerial bombs and small-caliber missiles. The shortcoming of autodyne fuses is the limited range of action. The maximum radius of action of such fuses in firing at aerial targets, for example, is 30-40 m. The advantage of heterodyne RV is the possibility of significant weakening of the level of internal noise at the mixer input due to isolation of the mixer from the transmitter along the heterodyne channel. This possibility can be used either for improving the reliability of the RV or for increasing the radius of action. The range of action of heterodyne fuses is determined by the power of the transmitter.

§ 2. METHODS FOR USE OF THE WORKING SIGNAL FOR DETERMINING THE MOMENT OF RESPONSE OF RADIO PROXIMITY FUSES

The very fact of the appearance of a working signal and information contained in the signal concerning the position of the target can be used for determining the moment of response of RV. It was demonstrated in the previous section that the amplitude of the working signal with any principle of operation of RV and the

frequency of the signal in frequency-modulated RV contain information on the range to the target, while the frequency of the signal of Doppler RV contains information concerning the velocity of approach to the target.

We shall consider cases of the use of RV in firing at aerial and ground targets separately.

A Case of Firing at Aerial Targets

The moment of response of RV in firing at aerial targets is normally determined according to the moment of appearance of the working signal. Information contained in this signal is used for target selection, which makes it possible to distinguish the working signal from noise.

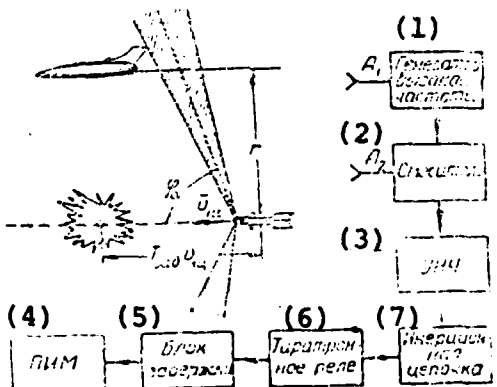


Fig. 12.5.

Key: (1) high-frequency oscillator; (2) mixer; (3) UNCh [low-frequency amplifier]; (4) PIM [safety and operations mechanism]; (5) delay unit; (6) thyratron relay; (7) inertial circuit.

We shall consider the operation of an RV according to the block diagram shown in Fig. 12.5. We shall assume that in the case of a heterodyne RV version, the beam pattern shown in Fig. 12.5

is the beam pattern of transmitting and receiving antennas at the same time. This assumption is valid because identical characteristics are selected for the transmitting and receiving antennas, and the distance between them is significantly less than the target ranges of interest to us. The RV antenna possesses circular emission, providing target selection in flight of the missile along any relative trajectory, and directed action in a plane passing through the longitudinal axis of the missile. The three-dimensional beam pattern of the antenna has a funnel shape. Its cross section in any plane passing through the missile axis is bounded by two petals, while its cross section in a plane perpendicular to the axis is bounded by a circle. The high directivity of the antennas with their limited dimensions is achieved by the use of a range of meter, decimeter and centimeter waves for RV operation.

The working signal emerges in the RV system at the moment the target comes within the beam pattern. The working signal is fed from the mixer output to the low-frequency amplifier (UNCh) and after amplification passes through an inertial circuit, which performs time selection of signals. The inertial circuit accomplishes transformation of a sinusoidal working signal into a gradually increasing positive voltage, resulting in functioning of a thyratron relay (ignition of the thyratron). The time for build-up of this voltage to the value at which the thyratron relay responds, called the time lag of the RV, depends on the value of the time constant of the inertial circuit and the amplitude and frequency of the working signal. So that the time lag of the RV will not depend on the miss of the missile, the output cascade of the low-frequency amplifier is constructed according to an amplitude limiter design, so that the amplitude of the working signal delivered to the inertial circuit is constant within the limits of misses from zero to the radius of action of the RV.

The time constant of the inertial circuit is selected based on the intention that a definite number of oscillations of the working signal be required for ignition of the thyratron. It is obvious that

the inertial circuit will protect the fuse against the effect of individual brief pulsed interference with a time of action less than the value of the time lag of the RV. Under the condition of limitation of the amplitude of the pulses, their magnitude will have no significance.

In functioning of the thyratron relay, a voltage pulse develops in the anode circuit of the thyratron and acts as the command for functioning of the operational circuit of the safety and operations mechanism (PIM). This command is transmitted to the PIM through a delay unit with some time delay t_K , which can vary in general depending on the conditions of approach of the missile to the target. The delay in transmission of the command is used for shifting of response points of the RV in relation to the target to a position at which explosion of the warhead is most dangerous for the target. During the time from the moment of emergence of the command for functioning to the moment of explosion of the warhead, the missile moves by an amount $v_{lu} t_K$ in relation to the target. The delay is often measured from the moment of appearance of the working signal. In this case, it has the following value:

$$T_3 = t_n + t_K,$$

where t_n is the value of the RV time lag.

The required delay time T_3 is provided fully in certain cases by the time lag of the system t_n , and there is no need for an additional delay unit.

We shall discuss the requirements for frequency characteristics of the low-frequency amplifier. The frequency of the working signal of Doppler RV is proportionate to the approach velocity dD/dt .

In approach to a point target (Fig. 12.6),

$$\frac{dD}{dt} = v_{lu} \cos \phi,$$

where v_{lu} is the relative velocity of the missile; ϕ is the angle

between the vector \bar{v}_{1u} and the direction to the target.

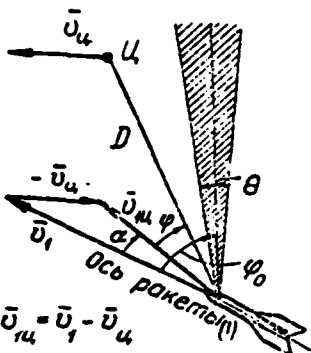


Fig. 12.6.
Key: (1) missile axis.

In this case, the frequency of the working signal will be as follows:

$$f = \frac{2v_{1u}}{\lambda} \cos\phi. \quad (12.24)$$

The angle ϕ in formula (12.24) should be assumed to vary in the process of approach within the following limits:

$$\phi_0 - \frac{\theta}{2} \pm \alpha \leq \phi \leq \phi_0 + \frac{\theta}{2} \pm \alpha,$$

where ϕ_0 is the angle between the missile axis and the orientation of the main maximum of radiation of the antenna; θ is the angular width of the beam pattern; α is the angle between the missile axis and the direction of the vector \bar{v}_{1u} .

The angle α is selected with a "plus" sign when the vector \bar{v}_{1u} deviates from the missile axis in a direction opposite to the target direction and with a "minus" sign in deviation in the direction of the target. In approach on a parallel course, $\alpha=0$. In cases where the angle ϕ does not satisfy the condition presented, the target is located outside the emission zone. In approach to a real target, the reflection of radio waves occurs from part or all of the target surface coming into the emission zone rather than from a single

point. Due to this fact, the working signal of the RV is formed as a result of addition of a large number of elementary signals conditioned by reflection from individual points of the target. Since the velocities of approach to these points are different, the Doppler frequencies of the elementary signals will also be different. Therefore, the working signal should be considered as a spectrum of oscillations of Doppler frequencies whose width depends on the width of the beam pattern of the antennas, the dimensions of the target and the miss of the missile.

The pass band of the amplifier is normally selected on the assumption that reflection occurs from a point target. In this case, the pass band according to formula (12.24) is determined by the range of Doppler frequencies:

$$F_{\max} = \frac{2v_{lu}}{\lambda} \cos \left(\varphi_0 - \frac{\theta}{2} \pm \alpha \right);$$

$$F_{\min} = \frac{2v_{lu}}{\lambda} \cos \left(\varphi_0 + \frac{\theta}{2} \pm \alpha \right).$$

The frequency range $F_{\max} - F_{\min}$ defines the minimum acceptable pass band of the amplifier for providing reliable functioning of RV with a given relative velocity of the missile v_{lu} . Since the value of v_{lu} can vary within limits from $v_{lu\max}$ to $v_{lu\min}$, the pass band should be increased based on the calculation that

$$F_{\max} = \frac{2v_{lu\max}}{\lambda} \cos \left(\varphi_0 - \frac{\theta}{2} \pm \alpha \right);$$

$$F_{\min} = \frac{2v_{lu\min}}{\lambda} \cos \left(\varphi_0 + \frac{\theta}{2} \pm \alpha \right).$$

The required frequency characteristics of the amplifier of a Doppler RV are shown by the dotted line in Fig. 12.7, a. The solid curve in the same figure shows the actually achievable characteristics closest to the required characteristics. As one can see, an amplifier possessing a definite pass band accomplishes selection of signals according to frequency, in addition to amplification of the working signal. The smaller the pass band of the amplifier, the higher its

selective capability. Therefore, the minimum acceptable pass band should be selected from the point of view of improving the noise protection of RV.

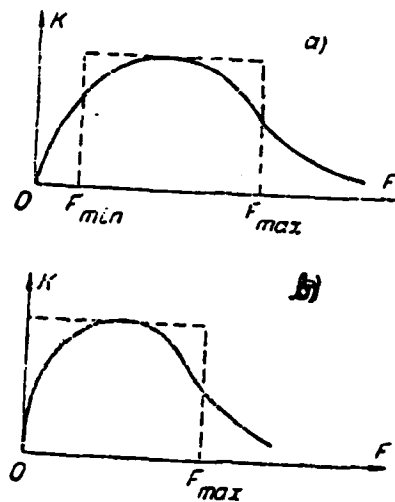


Fig. 12.7.

The frequency of the working signal of frequency-modulated RV is proportionate to the range. Since the range in the case in question can vary within limits from 0 to some maximum value D_m , the pass band of the amplifier should be limited to frequencies

$$F_{\min} \approx 0;$$

$$F_{\max} = \frac{8\Delta f_m F_v D_{\max}}{c}$$

The required and actually achievable frequency characteristics of the UNCh of a frequency-modulated RV are shown in Fig. 12.7, b. In this case, the selection accomplished by the amplifier in regard to frequency is equivalent to selection in regard to range. At target ranges greater than D_{\max} , the frequency of the working signal does not fall within the pass band.

A Case of Firing at Ground Targets

In firing at ground targets, the moment of response of RV is determined according to the dependence of the amplitude and frequency of the working signal on the altitude above the ground surface. The antenna beam pattern which is the optimum for the given conditions is shown in Fig. 12.8. The antenna emission maximum coincides with the axis of the missile (bomb). In the process of approach to the ground, the amplitude of the working signal increases continuously, and the moment it reaches a certain value, functioning of the thyratron relay occurs. It is advisable to use amplifiers with selective frequency characteristics for signal selection in regard to frequency (Fig. 12.9).

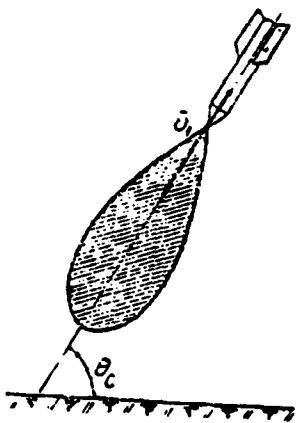


Fig. 12.8.

In frequency-modulated RV, the resonance frequency of the amplifier F_0 should be selected from the following condition:

$$F_0 = \frac{8\pi f_m F_u}{c \sin \theta_c} H_0,$$

where θ_c is the angle of impact of the missile on the ground surface; H_0 is the fuse response altitude.

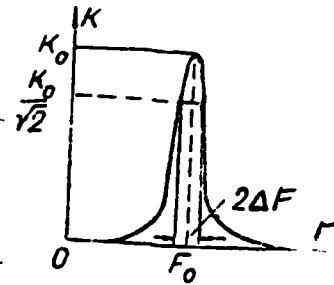


Fig. 12.9.

The resonance frequency in Doppler fuses should be as follows:

$$F_0 = \frac{2v_c}{\lambda} \cos \theta_c,$$

where v_c is the velocity of impact of the missile on the ground surface.

The pass band of the amplifier $2\Delta F$ should envisage the possible spread of impact angles θ_c and of the velocity v_c .

The method which has been considered for determining the moment of response can also be used in firing at aerial targets. In the latter case, the working signal at a given distance from the target D_0 (Fig. 12.10) creates a command for functioning, which is transmitted to the PIM with a definite delay. The size of the delay is selected based on the condition that the missile occupy a certain position in relation to the target, at which the probability of destruction of the target is at a maximum, in the time from the moment of appearance of the command to the moment of functioning of the RV.

We shall assume, for example, that the maximum probability of destruction of the target is achieved in explosion of the warhead at points with $z=0$, i.e., when the missile comes up to the target. Then the necessary delay time should be as follows:

$$t_k = \frac{z_0}{v_{lu}},$$

where

$$z_0 = \sqrt{D_0^2 - r^2}.$$

With $D_0 > r$, one can assume that

$$t_s = \frac{D_0}{v_{ts}}.$$

The basic shortcoming of RV which determine the moment of response in regard to the amplitude and frequency of the working signal is their low noise protection in relation to jamming as compared to RV which react to the moment of appearance of the working signal. They are capable of providing target selection only in regard to the range and the approach velocity, while fuses which react to the moment of appearance of the signal, with a narrow beam pattern, also provide selection in regard to the direction to the target.

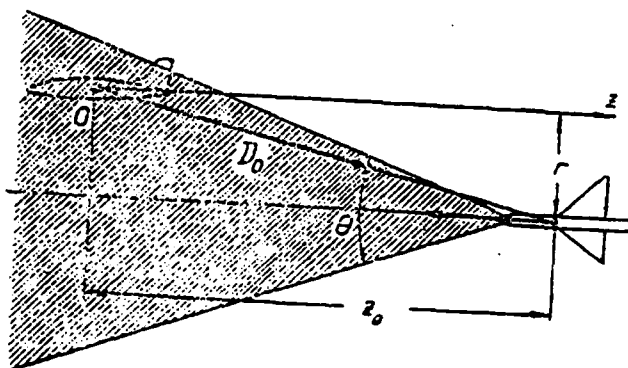


Fig. 12.10.

§ 3. PULSE RADIO PROXIMITY FUSES

Pulse RV are similar to pulse radar stations used for determining the distance to various objects in regard to the principle of operation.

The transmitter of pulse RV emits high-frequency oscillations

in the form of a series of rectangular pulses (Fig. 12.11) of a definite duration τ_u , which succeed each other with a repetition period T . Pulses reflected by the target reach the receiver with a time lag τ proportionate to the distance to the target. The fuse can be adjusted for functioning either when the missile reaches a definite distance from the target or when this distance is within predetermined limits.

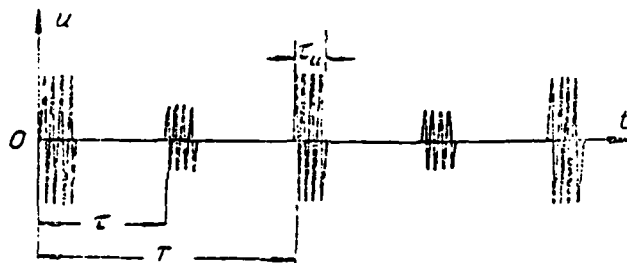


Fig. 12.11.

A typical block diagram of a pulse RV is shown in Fig. 12.12. The RV transmitter consists of a modulator, a high-frequency oscillator, an antenna A_1 and a strobing pulse generator. The modulator shapes rectangular pulses of an assigned duration τ_u and repetition frequency F (Fig. 12.13, a), which are used for modulation of high-frequency oscillations and control of the operation of the strobing pulse generator.

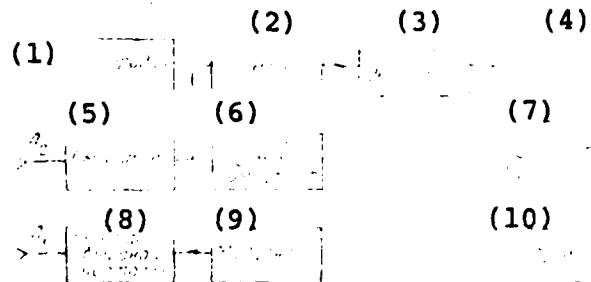


Fig. 12.12.

Key: (1) heterodyne; (2) UPCh; (3) video detector; (4) video amplifier; (5) mixer;

(6) strobe pulse generator; (7) pulse counter; (8) high-frequency oscillator; (9) modulator; (10) PIM.

The strob ing pulse generator also shapes rectangular pulses of a definite duration and, in addition, accomplishes delay of the pulses by a definite time Δt in relation to the leading edge of the modulating pulses. The strobe pulses are fed to one grid of an electronic tube (a pentode) of an intermediate-frequency amplifier (UPCh). A reflected pulse, after frequency transformation in the mixer, passes to the other grid of the amplifier tube. During the pause between strobe pulses, the amplifier is blocked; it opens only for the time of action of the strobe. A modulation frequency such that the reflected pulse passes to the UPCh during pauses between two adjacent strobe pulses at great distances from the target is selected. In this case, the UPCh will be blocked during action of the reflected pulses, and there will be no signal at the amplifier output. The time lag of a reflected pulse in relation to the strobe will decrease in proportion to approach to the target. At some distance from the target, the reflected pulse will arrive during action of the strobe (Fig. 12.13, d); consequently, it will be amplified by the UPCh. The pulse which has developed at the output of the intermediate-frequency amplifier will act as the working signal, which acts on the actuator of the RV after rectification by a video detector and amplification.

The range of response of RV D_0 can be established from the following condition:

$$t = \Delta t + \tau_c - \tau_m,$$

where τ_c is the strobe duration; Δt is the strobe delay time.

It follows from the condition which has been written that

$$D_0 = \frac{(\Delta t + \tau_c - \tau_m)c}{2}. \quad (12.25)$$

For ensuring reliable functioning of the RV, the strobe pulse duration τ_c should be selected based on the condition $\tau_c \geq \tau_m$.

From the point of view of noise protection, it is desirable to select the minimum acceptable value of τ_c , since the RV receiver (the UPCh) is blocked during pauses between strobe pulses and, consequently, it is not subject to the effect of interference.

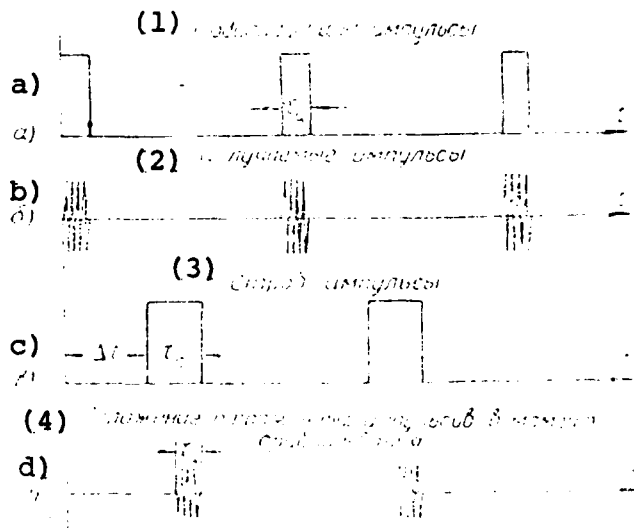


Fig. 12.13.

Key: (1) modulating pulses; (2) emitted pulses; (3) strobe pulses; (4) location of reflected pulses at the moment of response.

At $\tau_c = \tau_H$, it follows from formula (12.25) that

$$D_s = \frac{c \Delta t}{2}.$$

As one can see, setting the RV for a given response range is accomplished by appropriate selection of the strobe delay time Δt .

For improving the noise protection of RV, it is advisable to connect a pulse counter between the video amplifier and the actuator; the counter forms a voltage proportionate to the number of pulses which reach it. In the presence of such a counter, functioning of the RV becomes possible only when at least a certain number of

reflected pulses reach the receiver. We shall designate the number of pulses necessary for functioning of the actuator as n . It is obvious that the distance to the target changes during the time for counting of n pulses by the following amount:

$$\Delta D = (n - 1) T v_{ta} = \frac{(n - 1) v_{ta}}{F},$$

where T is the repetition period of sounding pulses.

Therefore, the range of response of RV with consideration for the counter time lag will be as follows:

$$D_0' = D_0 - \Delta D = D_0 - \frac{(n - 1) v_{ta}}{F}.$$

The moment of response of pulse RV in firing at aerial targets, in the case of a circular field for scattering of fragments of the warhead, is determined according to the moment when the target enters the beam pattern of the antenna (Fig. 12.14). The reflected pulse which has passed through the UPCh is the working signal which develops at this moment. The time lag of this pulse depends on the miss of the missile, varying from 0 at $r=0$ to τ_m at $r=r_m$:

$$\tau_m = \frac{2D_m}{c} = \frac{2r_m}{c \sin\left(\varphi_0 - \frac{\theta}{2}\right)}.$$

In order to ensure functioning of RV in a range of misses from 0 to r_m , it is necessary for the beginning of a strob ing pulse to be made coincident with the beginning of a sounding pulse, and for a duration equal to the value of the time lag of the reflected pulse τ_m in a miss of the missile r equal to the radius of action of the fuse r_m to be selected for it.

In the presence of a pulse counter, functioning of the RV occurs with the following delay:

$$T_s = (n - 1) T = \frac{n - 1}{F}.$$

The value of n should be selected based on the intention that the

delay time (the pulse calculation) be less than the time t_u during which the target is located within the beam pattern of the antenna. The time t_u is minimal for a miss $r=0$:

$$t_u = \frac{l}{v_{lu}}$$

where l is the target length in the direction of the vector \bar{v}_{lu} .

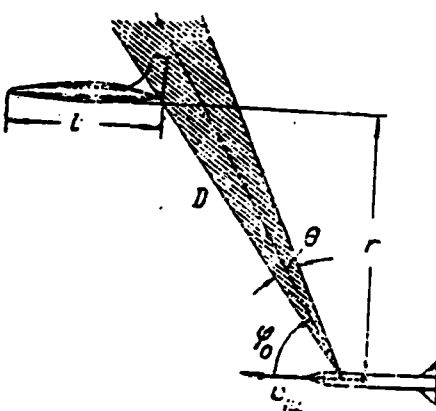


Fig. 12.14.

Solving the inequality $\frac{n-1}{F} < \frac{l}{v_{lu}}$ in relation to n , we obtain a formula for the maximum acceptable value n_m :

$$n_m < 1 + \frac{lF}{v_{lu}}$$

One of the shortcomings of pulse RV is the possibility of "leaking" of sounding pulses into the receiver; these pulses when they coincide with strobes can cause premature functioning of the fuse. Such a possibility exists, for example, with inadequate separation of the receiving and transmitting antennas. The effect of "leaking" sounding pulses with a duration τ_u is avoided with a delay of the strobe pulses by a time Δt greater than or equal to τ_u . However, a fuse with strobe pulses delayed by such a time in firing at aerial targets will possess a so-called "dead zone" in which functioning is impossible. The "dead zone" lies in a range of misses from 0 to r_{min} . The radius of the "dead zone" with

$\Delta t = \tau_H$ is as follows:

$$r_{\min} = \frac{c\tau_H}{2} \sin \varphi_0.$$

It is desirable to select the smallest possible duration of the sounding pulses τ_H for reducing the value of r_{\min} . In evaluating the size of the "dead zone" one must keep in mind that reflection of radio waves occurs from points located at different distances from the fuse as a result of finite dimensions of the targets. This leads to an increase in the duration of a reflected pulse as compared to the sounding pulse and to contraction of the "dead zone." A decrease in the duration of sounding pulses is also desirable from the point of view of improving noise protection of RV. With a decrease in τ_H , there is a possibility of boosting the power in a pulse $P_{\Sigma H}$ without changing the average power of the transmitter P_{cp} , which is limited to the acceptable power of the oscillator tube, in the process.

As we know,

$$P_{cp} = \frac{P_{\Sigma H} \tau_H}{T}.$$

An increase in $P_{\Sigma H}$ makes it possible to reduce the sensitivity of the RV receiver and thereby increase its noise protection.

Improved noise protection in relation to jamming, which is explained, first, by the possibility of boosting the transmitter power in a pulse and, second, by selection of signals in regard to the range to the target, should be considered an advantage of pulse RV. Selection in regard to range is provided by strobing of the receiver, which limits the reflected signal reception time to an interval corresponding to the maximum range of action of the RV. The limit range from which interference similar in form to a reflected signal can cause premature response of a pulse RV is determined by the location of the trailing edge of the strobe pulse.

It is as follows:

$$D_{np} = \frac{c(\tau_c + \Delta t)}{2}.$$

At distances exceeding D_{np} , interference will be active during pauses between strobe pulses; therefore, it will not be able to cause functioning of the fuse.

Programmed control of amplification (PRU), consisting of changing of the amplification factor of the UPCh depending on the time of action of the strobe, can be performed for improving noise protection in pulse RV. In the initial section of a strobe (Fig. 12.15) corresponding to a short range to the target, a small amplification factor is provided. With the passage of time, the amplification factor gradually increases, reaching a maximum value corresponding to the greatest range at the moment of response at the end of action of the strobe. The PRU is accomplished by feeding of pulses of a definite shape to one of the grids of the UPCh tube. The PRU pulses are shaped by a special generator, whose operation is controlled by the strob ing pulse generator. They are fed to the UPCh simultaneously with the strob ing pulses.

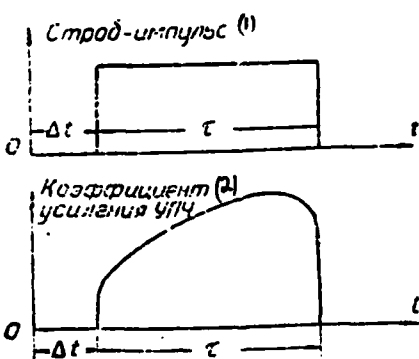


Fig. 12.15.
Key: (1) strobe pulse; (2) UPCh
amplification coefficient.

Pulse RV provide the possibility of measuring target dimensions, the value of which is necessary in automatic control of the location of response points depending on the type of target, by varying the delay, for example. Measurement of target dimensions is based on

the dependence of the reflected pulse duration on these dimensions. The basic shortcoming of pulse RV as compared to RV with continuous emission is their complexity, conditioned by the necessity of shaping and reception of extremely short pulses.

Pulse-Doppler fuses are a variety of pulse RV. The coherent pulse method for selection of moving targets which is well known in radar is used in these fuses for extracting the working signal. A block diagram of the simplest pulse-Doppler RV is shown in Fig. 12.16. The fuse transmitter consists of a driving oscillator which generates continuous oscillations (Fig. 12.17, a); these oscillations are fed to the input of a power booster. The power booster is controlled by a modulator, which transforms the continuous oscillations of the oscillator into sounding radio pulses emitted by antenna A_1 . The pulses reflected from the target are combined in a mixer with the voltage of the driving oscillator.

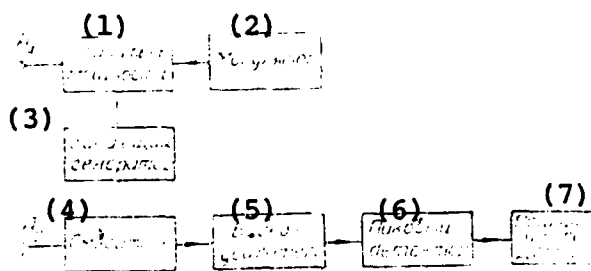


Fig. 12.16.

Key: (1) power booster; (2) modulator;
(3) driving oscillator; (4) mixer; (5)
video amplifier; (6) peak detector;
(7) Doppler frequency amplifier.

The amplitude of the resulting oscillations acting in the mixer during reception of reflected pulses (Fig. 12.17, e) is determined by an expression obtained previously (12.9):

$$U_m = U_{im} \left(1 + \frac{U_{im}}{U_{im}} \cos \Delta\phi \right).$$

In approach to the target, the phase shift angle $\Delta\phi$ between the voltage of the driving oscillator and the reflected oscillations will vary with the Doppler frequency, which results in a change in the amplitude of resulting oscillations during periods of action of reflected pulses.

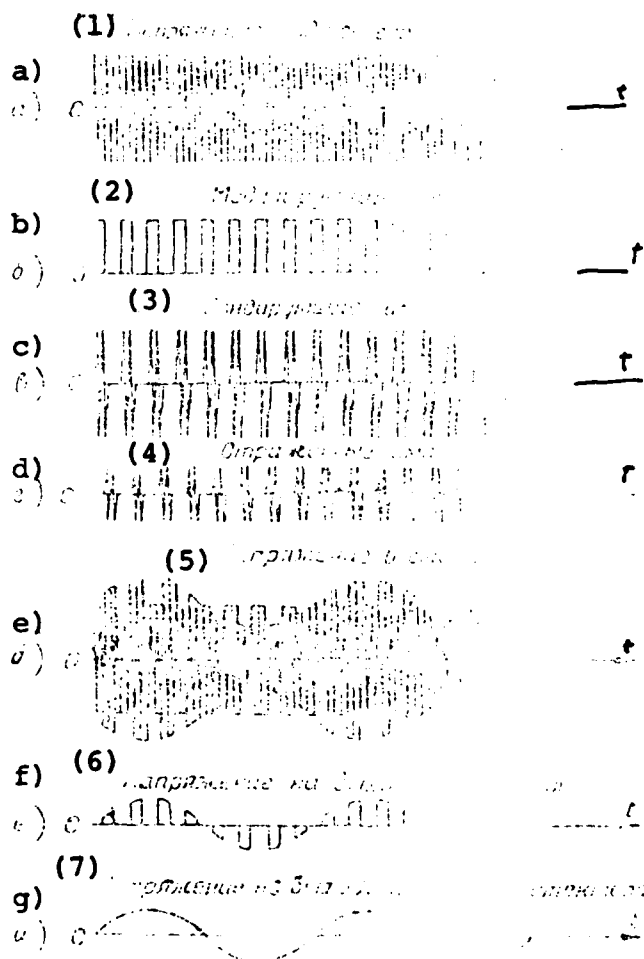


Fig. 12.17.

Key: (1) driving oscillator voltage; (2) modulating pulses; (3) sounding pulses; (4) reflected pulses; (5) voltage in mixer; (6) voltage at mixer output; (7) voltage at output of peak detector.

Video pulses extracted at the input of the mixer after amplification are transformed by the peak detector into a sinusoidal voltage of the Doppler frequency, which is used for functioning of the actuator. The distinguishing feature of pulse-Doppler RV lies in the fact that they have no "dead zone;" therefore, they do not require shaping of extremely short pulses. Pulse-Doppler RV can be constructed in autodyne as well as heterodyne versions. In the case of an autodyne version, it is necessary for normal operation of the RV that the sounding pulse duration somewhat exceed the maximum possible reflected pulse time lag.

§ 4. SEMI-ACTIVE RADIO PROXIMITY FUSES

Semi-active RV can be used in missiles with semi-active radar homing systems. As we know, with a semi-active homing method, the target is irradiated by an "illumination" radar station situated on the ground or aboard the aircraft. "Illumination" from ground stations is performed for guidance of antiaircraft missiles, while it is performed from the aircraft for guidance of "air-to-air" missiles.

Radio waves reflected from the target are received by a receiver of the homing head and used for determining the current coordinates of the target, according to which appropriate commands for control of the position of the missile are generated. These radio waves are also used by semi-active RV for determining the moment of explosion of the warhead. The principle of operation of semi-active RV is determined by the mode of operation of the "illumination" station. In operation of the station in a continuous emission mode, either the Doppler effect, if the emission frequency is constant, or the difference between times for signals to reach the missile from the target and directly from the "illumination" station, if the emissions of the station are modulated in regard to frequency, is used for extracting the working signal of the RV. In operation of the station in a pulsed mode, the moment of

response is determined in regard to the size of the time lag of a reflected pulse in relation to a pulse passing to the missile from the "illumination" station. We shall consider the principle of operation of semi-active RV in operation of the "illumination" station in a mode of continuous emission. Figure 12.18 presents a diagram of the convergence of a target, an attacking aircraft and a missile, while Fig. 12.19 presents a block diagram of a semi-active RV of the Doppler type. In the process of guidance of the missile, the "illumination" station tracks the target continuously by rotation of the antenna system and keeps it within the beam pattern. Reflected waves begin arriving at the fuse from the moment the target enters the beam pattern of the receiving antenna A. A high-frequency signal is sent from the antenna to the mixer, where it is combined with the signal arriving from the receiver of the rear station of the missile. The rear station receives radio waves emitted by the "illumination" station.

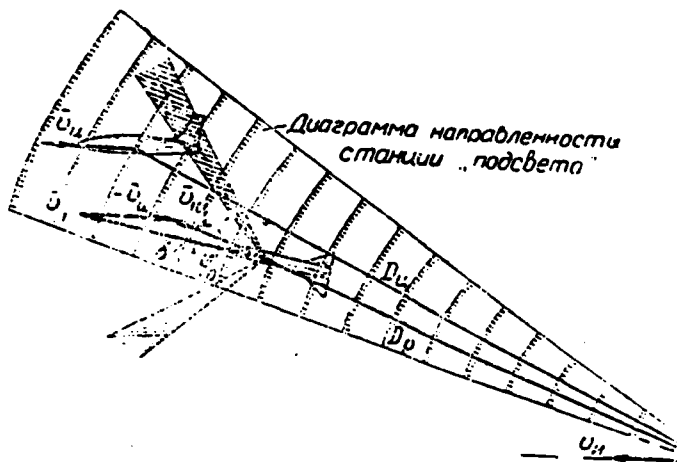


Fig. 12.18.

Key: Beam pattern of "illumination" station.

As a result of the Doppler effect, the resulting signal in the mixer will be modulated in regard to amplitude. Therefore, a low-frequency voltage proportionate to the envelope of the resulting signal will be extracted at the mixer output. This

voltage is the working signal for the fuse and after amplification in the UNCh is used for creating a command for functioning. The amplification factor of the UNCh can be regulated by a system for automatic control of amplification (ARU) depending on the level of the reflected signal arriving at the receiver of the homing head. Automatic control of amplification provides a weak dependence of the level of the working signal at the UNCh output on the distance $D_{\text{ц}}$ between the target and the "illumination" station. With an increase in $D_{\text{ц}}$, the power of the reflected signal drops, and the amplification factor of the UNCh increases due to the ARU system. In the absence of a rear station on the missile, a local heterodyne adjusted to the frequency of the "illumination" station can be used for extracting the working signal. We shall find an expression for the frequency of the working signal of an RV. The frequency of radio waves reflected by the target is as follows:

$$f_u = f_0 + \frac{v_{\text{ци}}}{\lambda} \cos \phi_u. \quad (12.26)$$

where f_0 is the frequency of the transmitter of the "illumination" station; λ is the wavelength of the "illumination" station; $v_{\text{ци}}$ is the target velocity in relation to the attacking aircraft; ϕ_u is the angle between vectors $\bar{D}_{\text{ц}}$ and $\bar{v}_{\text{ци}}$.

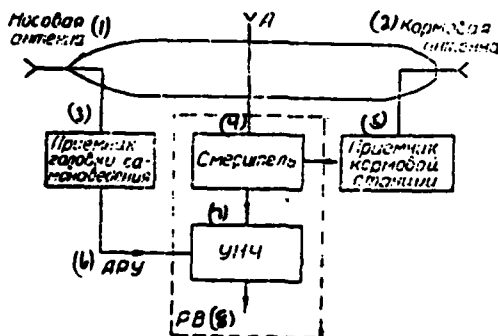


Fig. 12.19.

Key: (1) nose antenna; (2) rear antenna; (3) receiver of homing head; (4) mixer; (5) receiver of rear station; (6) ARU [automatic amplification control]; (7) UNCh; (8) RV.

The second component in formula (12.26) is the Doppler frequency conditioned by convergence or divergence of the target and the attacking aircraft.

The frequency of the signal induced in the RV antenna, with consideration for the Doppler effect, is as follows:

$$f_1 = f_u + \frac{v_{1u}}{\lambda} \cos(\varphi_0 - \delta), \quad (12.27)$$

where v_{1u} is the velocity of the missile in relation to the target; φ_0 is the angle between the missile axis and the direction of the main maximum of the beam pattern of the RV receiving antenna; δ is the angle between the missile axis and the vector \bar{v}_{1u} .

The Doppler component of the frequency f_1 in formula (12.27) is conditioned by approach of the missile to the target. Inserting the value of f_u from (12.26) into formula (12.27), we obtain

$$f_1 = f_0 + \frac{1}{\lambda} [v_{1u} \cos \varphi_u + v_{1a} \cos(\varphi_0 - \delta)]. \quad (12.28)$$

The frequency of the signal received by the rear station of the missile from the "illumination" station is as follows:

$$f_2 = f_u + \frac{v_{1u}}{\lambda} \cos \varphi_p, \quad (12.29)$$

where v_{1u} is the velocity of the missile in relation to the attacking aircraft; φ_p is the angle between vectors \bar{D}_p and \bar{v}_{1u} .

The Doppler component of the frequency in formula (12.29) is conditioned by movement of the missile away from the attacking aircraft.

The frequency of the working signal F is equal to the difference between frequencies f_1 and f_2 . Using formulas (12.28) and (12.29), we obtain:

$$F = \frac{1}{\lambda} [v_{1u} \cos \varphi_u + v_{1a} \cos(\varphi_0 - \delta) - v_{1u} \cos \varphi_p]. \quad (12.30)$$

In a case where the rear station is replaced with a local heterodyne, the frequency $f_2 = f_0$, and

$$F = \frac{1}{\lambda} [v_{u\pi} \cos \varphi_u + v_{lu} \cos(\varphi_0 - \delta)].$$

As one can see, the difference between oscillation frequencies combined in the mixer of semi-active RV, as in RV of the active type, is conditioned by the Doppler effect. However, in contrast to active RV, the Doppler frequency of semi-active fuses is determined by a more complex expression.

Semi-active RV are finding extensive use at present in anti-aircraft and aviation missiles of the USA and England. "Hawk," "Falcon" and "Sparrow" missiles, etc., are being equipped with them. The basic advantages of semi-active RV as compared to active RV are smaller weight and dimensions and greater operational reliability. Semi-active RV do not have transmitter parts; therefore, their weight can be reduced substantially. The lack of transmitting antennas in a fuse simplifies the missile configuration. Lower operating accuracy and lower noise protection are shortcomings of semi-active RV.

§ 5. THE RESPONSE SURFACE OF RADIO PROXIMITY FUSES

We shall consider a case of approach of a missile to a target on a parallel course (Fig. 12.20). We shall combine the origin of a rectangular system of coordinates Oxyz with the target center. We shall stipulate that the z axis is oriented in a direction opposite to the vector of the relative velocity of the missile \bar{v}_{lu} , and the plane Oxy is perpendicular to the z axis. We shall assume that the moment of response of the RV is determined in regard to the moment of the appearance of a working signal.

In calculations involved with evaluating the firing efficiency, the response surface of RV can be considered approximately as the surface of rotation of a plane curve $z_0(r)$ around the z axis. The equation of this curve in the most general case can be represented in the form of an n-degree polynomial:

$$z_0(r) = a + br + cr^2 + \dots, \text{ with } r \leq r_m, \quad (12.31)$$

where a , b and c are constant coefficients; r is the magnitude of the miss of the missile; r_m is the radius of action of the RV.

Experience indicates that it is sufficient to limit ourselves to consideration of the first three members in equation (12.31) and even two members in some cases. We shall assume, therefore, that

$$z_0(r) = a + br + cr^2 \text{ with } r \leq r_m. \quad (12.32)$$

We shall find the values of the coefficients a , b and c .

Assuming that $r=0$ in equation (12.32), we obtain $a=z_0(0)$. It follows from this that the coefficient a is the z coordinate of the response point of the RV with a miss of the missile equal to zero.

With small misses, the working signal develops due to the presence of practically unavoidable radiation of the antenna in the direction of the missile axis. The level of these emissions is determined by leading (secondary) lobes of the beam pattern. Since the possibility of emissions in the direction of leading lobes is low, one can assume with a level of accuracy sufficient for practical work that the working signal with r near zero develops when the missile comes up to the extreme point of the target nearest to it.

Consequently, with consideration for the time lag of the RV system T_u and the additional delay t_k which is introduced,

$$\text{and } z_0(0) = \frac{1}{2} l - v_{lu}(T_u + t_k)$$

$$a = \frac{1}{2} l - v_{lu} T_3, \quad (12.33)$$

where l is the geometric length of the target; $v_{lu} T_3$ is the path travelled by the missile in relation to the target during the delay

time T_3 .

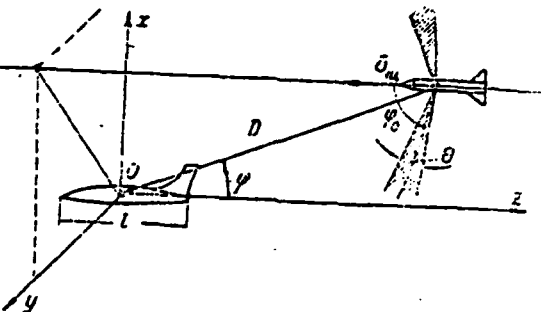


Fig. 12.20.

As one can see, the coefficient a takes into account the dimensions of the target and the delay in response of the RV.

For a point target with $T_3=0$, the coefficient $a=0$. Therefore, if we assume that $a=0$ in equation (12.32), it will determine the locations of response points of RV without a time lag in approach to a point target.

Functioning of RV without a time lag occurs at the moment the target touches a surface on which the power of the reflected signal is equal to the level of sensitivity of the receiver. This surface is defined by an equation of the range of action of the radar station. In polar coordinates (D, ϕ) , the equation for the range of action is written in the following form:

$$D(\phi) = \sqrt{\frac{P_{\Sigma} \lambda^2 S_u G^2(\phi)}{(4\pi)^3 P_{\text{min}}}}, \quad (12.34)$$

where P_{Σ} is the total power emitted by the RV transmitter; λ is the transmitter wavelength; $G(\phi)$ is the coefficient of directional action of the antenna (k. n. d.); P_{min} is the sensitivity of the receiver (the minimum reflected signal power necessary for response of the RV); S_u is the effective reflecting surface area of the

target.

The value of P_{min} in general depends on the frequency of the working signal and, consequently, on the angle ϕ . However, assuming the pass band of the amplifier to be matched to the possible spread of relative velocities of the missile and the amplification factor of the UNCh to be constant within the pass band, one can ignore this dependence. In using formula (12.34), one must keep in mind that the value of the effective reflecting surface area of the target S_{II} included in it differs from a similar value used in long-range radar. This difference is conditioned by the following features of operation of RV.

In the time for interception of the target by beam patterns of RV antennas, the angle of view ϕ varies within the limits of the width of the patterns, due to which the working signal is the result of the effect of reflecting surfaces of different sizes. With a narrow beam pattern, the target may not be completely irradiated.

In cases where the distance to the target is comparable to the wavelength, the finite dimensions of the antennas begin to be manifested. Different parts of the target prove to be at different distances from the emission source (the antennas). For example, the section irradiated by the major lobe of the beam pattern of the transmitting antenna may not be located in the direction of the maximum of the pattern of the receiving antenna.

For RV with a time lag, the surface $D(\phi)$ determines the moment of the appearance of a working signal rather than the point of response and, for this reason, is often called the reaction surface. The response surface is offset in relation to the reaction surface (Fig. 12.21) in the direction of relative movement of the missile by an amount $v_{II} T_3$. With a narrow beam pattern, one can assume that the interaction ("reaction") of the fuse in all misses of the missile occurs with the same point O_1 at the greatest distance

from the target center in the direction of the z axis.

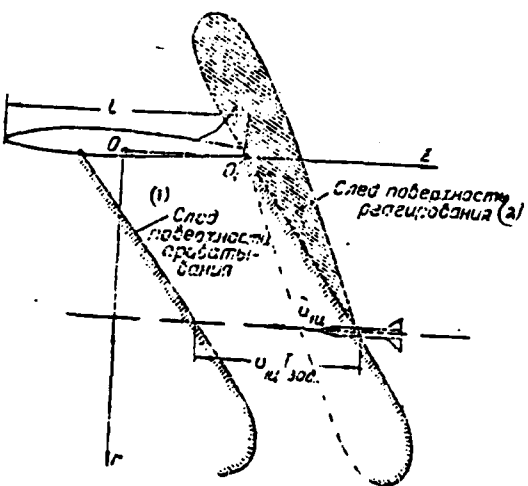


Fig. 12.21.

Key: (1) trail of response surface;
(2) trail of reaction surface.

We shall represent the function $G(\phi)$ in equation (12.34) in the following form:

$$G(\varphi) = G_m G_1(\varphi),$$

where G_m is the maximum value of the k. n. d.; $G_1(\varphi)$ is the normed k. n. d. of the antenna (it varies within limits from 0 to 1).

We shall write the range equation as follows:

$$D(\varphi) = D_m \sqrt{G_1(\varphi)}. \quad (12.35)$$

where D_m is the maximum range of action of the RV.

According to (12.34),

$$D_m = \sqrt[4]{\frac{P_s \lambda^2 G_m^2 S_4}{(4\pi)^3 P_{4m}}}. \quad (12.36)$$

with a knowledge of D_m and the angle ϕ_0 at which the k. n. d. reaches the maximum value $G_1=1$, one can establish the radius of action of the RV:

$$r_m = D_m \sin \phi_0.$$

Formula (12.36) pertains to heterodyne RV. For autodyne fuses,

$$D_m = \sqrt{\frac{S \cdot G_m \cdot V S_n}{4\pi \sqrt{\pi} U_0}}, \quad (12.37)$$

where S is the radio frequency sensitivity of the RV transponder; U_0 is the sensitivity of the low-frequency unit (the minimum voltage at the UNCh input necessary for functioning of the RV).

The value of the radio frequency sensitivity characterizes the ability of the transponder of an autodyne RV to react to the action of a reflected signal (to change its operating mode). The numerical value of S is determined by the value of the amplitude of the working signal which develops with a relative change in the resistance of emissions of the antenna equal to 1.

One can see from a comparison of formulas (12.36) and (12.37) that in contrast to heterodyne RV, the range of action of autodyne fuses does not depend on the transmitter power. This fact serves as the cause of limitation of the range of action of autodyne RV.

We shall use equation (12.35) for finding coefficient b and c which define the response surface in a rectangular system of coordinates in the case of a point target.

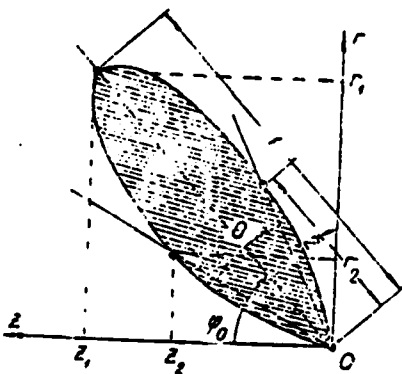


Fig. 12.22.

Since equation (12.35) cannot be replaced precisely by the equation $z_0 = br + cr^2$, we shall find coefficients b and c from the condition that these equations coincide in at least three or more characteristic points of the beam pattern (Fig. 12.22): in the direction of emissions of maximum power ($\phi = \phi_0$), half power ($\phi = \phi_0 - \theta/2$) and zero power ($\phi = 0$). At these points, as follows from equation (12.35) and Fig. 12.22,

$$\begin{aligned} z_1 &= D_m \cos \varphi_0; \\ r_1 &= D_m \sin \varphi_0; \\ z_2 &= \frac{D_m}{\sqrt{2}} \cos \left(\varphi_0 - \frac{\theta}{2} \right); \\ r_2 &= \frac{D_m}{\sqrt{2}} \sin \left(\varphi_0 - \frac{\theta}{2} \right); \\ z_3 &= 0; \\ r_3 &= 0. \end{aligned}$$

Substituting pairs of values (z_i, r_i) into the equation $z_0 = br + cr^2$, we obtain a system of two equations which makes it possible to find the values of b and c :

$$\begin{aligned} D_m \cos \varphi_0 &= b D_m \sin \varphi_0 + c D_m^2 \sin^2 \varphi_0 \\ \frac{D_m}{\sqrt{2}} \cos \left(\varphi_0 - \frac{\theta}{2} \right) &= b \frac{D_m}{\sqrt{2}} \sin \left(\varphi_0 - \frac{\theta}{2} \right) + c \frac{D_m}{2} \sin^2 \left(\varphi_0 - \frac{\theta}{2} \right). \end{aligned}$$

Performing elementary transformations, we shall rewrite the equations in the following form:

$$\left. \begin{aligned} \operatorname{ctg} \varphi_0 &= b + c D_m \sin \varphi_0 \\ \operatorname{ctg} \left(\varphi_0 - \frac{\theta}{2} \right) &= b + \frac{c D_m}{\sqrt{2}} \sin \left(\varphi_0 - \frac{\theta}{2} \right) \end{aligned} \right\}. \quad (12.38)$$

By solving the system (12.38) with respect to b and c , we obtain

$$\begin{aligned} b &= \frac{\operatorname{ctg} \left(\varphi_0 - \frac{\theta}{2} \right) \sin \varphi_0 - \frac{1}{\sqrt{2}} \operatorname{ctg} \varphi_0 \sin \left(\varphi_0 - \frac{\theta}{2} \right)}{\sin \varphi_0 - \frac{1}{\sqrt{2}} \sin \left(\varphi_0 - \frac{\theta}{2} \right)} \\ c &= \frac{\operatorname{ctg} \left(\varphi_0 - \frac{\theta}{2} \right) - \operatorname{ctg} \varphi_0}{D_m \left[\frac{1}{\sqrt{2}} \sin \left(\varphi_0 - \frac{\theta}{2} \right) - \sin \varphi_0 \right]} \end{aligned} \quad (12.39)$$

For RV with a narrow beam pattern, one can simplify the formulas of (12.39) by replacing their right members with the first two members of an expansion to an exponential series in regard to the small parameter θ .

Approximate formulas for b and c with a small θ have the following form:

$$b = c_1 g \varphi_0 + \frac{\theta}{2 \left(1 - \frac{1}{\sqrt{2}}\right) \sin^2 \varphi_0}; \quad (12.40)$$

$$c = - \frac{\theta}{2 \left(1 - \frac{1}{\sqrt{2}}\right) r_n \sin^2 \varphi_0} \quad (12.41)$$

It follows from the formulas obtained that the coefficient b depends on the location of the main maximum of emissions of the antenna and the width of the beam pattern θ . The coefficient c depends, in addition, on the radius of action of the RV. With an increase in the directivity of the emissions, $\theta \rightarrow 0$, $b \rightarrow \cot \varphi_0$, $c \rightarrow 0$ and, consequently, the response surface approaches the surface of a circular cone whose angle of taper is equal to $2 \varphi_0$.

The location of the response surface in relation to the center of the target, as follows from formula (12.33), depends on the velocity v_{lu} . With an increase in v_{lu} , the response surface shifts in the direction of relative movement of the missile. The larger the time lag of the fuse t_u and the delay time t_k , the greater the size of this shift.

§ 6. CONTROLLING THE LOCATION OF THE RESPONSE SURFACE OF RADIO PROXIMITY FUSES

By changing the parameters of RV by one method or another just before firing or in the process of approach of the missile to the target, one can control the location of the response surface. The necessity of controlling the response surface arises in firing

missiles with warheads with a directional effect at aerial targets.

Considering a case of approach of a missile to a target on a parallel course (Fig. 12.23) as before, we shall establish the requirements placed on the location of the response surface. We shall assume that the region of scattering of the fragments of the warhead in relation to the target is defined by angles $\bar{\phi}'$ and ϕ' , of which the former characterizes the location of the fragment scattering sector, while the latter characterizes the width of the sector.

As we know,

$$\bar{\phi}' = \operatorname{arctg} \frac{\sin \phi'}{\cos \bar{\phi}' + \frac{v_{1u}}{v_0}}, \quad (12.42)$$

where $\bar{\phi}'$ is the average direction of scattering of fragments under static explosion conditions; v_0 is the initial velocity of the fragments.

We shall draw straight lines parallel to the front and rear boundaries of the fragment scattering sector from the end points of the target O_1 and O_2 at angles $\bar{\phi}' - \frac{1}{2}\phi'$ and $\bar{\phi}' + \frac{1}{2}\phi'$ to the z axis. These lines distinguish a region on the plane (r, z) for which explosion in the region results in the fragments hitting the target. If the explosion occurs outside this region, the fragments miss the target. The region which has been established is called the dangerous burst zone. The location of the dangerous burst zone in relation to the z axis is determined by the angle ϕ_M' formed by its middle line (median) with the z axis. With a narrow fragment scattering sector, one can assume with sufficient accuracy that $\bar{\phi}_M' = \bar{\phi}'$.

It follows from formula (12.42) that the size of the angle $\bar{\phi}'$ and, consequently, ϕ_M' depends on the parameters of the warhead $(\bar{\phi}, v_0)$ and the relative velocity of the missile. The angle $\bar{\phi}'$ decreases with an increase in the relative velocity. It is obvious

that for the missile to be able to destroy the target, the response surface of the fuse should be located within the dangerous burst zone. In this event, in an ideal case, when the fuse operates without errors, a location of the response surface within the dangerous burst zone has practically no influence on the degree of damage to the target. For example, if the response surface is a circular cone, the manner in which the generatrix of this cone is arranged in the dangerous burst zone is of no importance from the point of view of firing efficiency. The response points of real RV are not located on any surface; rather, they occupy some region determined by the law of their distribution along the z axis. The response surface of real fuses is the mathematical expectation of the z coordinate of the response point. It determines only the average rather than the actual location of response points, which is random. Therefore, a location of the response surface of real RV within the dangerous burst zone can have a substantial effect on firing efficiency. A special characteristic called the function of matching of the fuse to the dangerous burst zone is introduced for evaluating this effect.

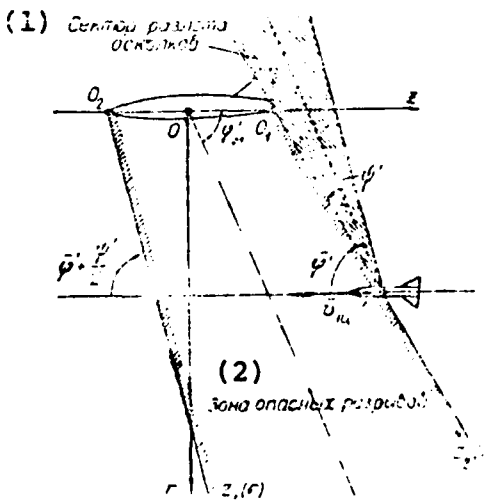


Fig. 12.23.

Key: (1) fragment scattering sector;
 (2) dangerous burst zone.

The matching function $S(r)$ is defined as the probability of response of RV within the dangerous burst zone with a given miss of the missile r :

$$S(r) = \int_{z_1(r)}^{z_2(r)} p(z|r) dr. \quad (12.43)$$

where $p(z|r)$ is the law of distribution of response points of the RV along the z axis with a miss r ; $z_1(r)$ and $z_2(r)$ are equations of boundaries of the dangerous burst zone.

We shall assume that the distribution of response points is subject to a normal distribution law:

$$p(z|r) = \frac{1}{\sqrt{2\pi\sigma_z^2}} e^{-\frac{(z-z_0(r))^2}{2\sigma_z^2}} \quad (12.44)$$

where $z_0(r)$ is the response surface of the RV; σ_z is the standard deviation of response points from the surface $z_0(r)$.

With a normal distribution law, the integral of (12.43) will be written in the following form:

$$S(r) = \frac{1}{2} \left[\Phi\left(\frac{z_1 - z_0}{\sqrt{2\sigma_z^2}}\right) - \Phi\left(\frac{z_2 - z_0}{\sqrt{2\sigma_z^2}}\right) \right] \quad (12.45)$$

where $\Phi(x)$ is a Laplace function.

The character of variation of the function $S(r)$ for different positions of the generatrix of a conical response surface is shown qualitatively in Fig. 12.24. Depending on the angle of inclination of the generatrix, its position in relation to the center of the target, and the relationship between the width of the dangerous burst zone and the standard deviation σ_z , the function $S(r)$ may practically not change, can increase or decrease monotonously and can have a maximum.

It is easy to see that a circular cone whose generatrix coincides with the median of the dangerous burst zone will be the optimum response surface for providing the best matching. The optimum surface is defined by the following coefficients: $a=0$,

$b = c \operatorname{tg} \bar{\phi}$, $c = 0$. In connection with the fact that the angle of inclination of the median of the dangerous burst zone $\bar{\phi}$ and the position of the response surface in relation to the target center depend on the value of the relative velocity of the missile, the best matching with constant parameters of the RV can be provided only for a single value $v_{lu} = v_{lu0}$. With an increase in the relative velocity, the angle $\bar{\phi}$ decreases, and the peak of the response surface ($z=a$) shifts away from the target center in the direction of the vector \bar{v}_{lu} . With a decrease in the velocity, a reverse phenomenon occurs - the angle $\bar{\phi}$ increases, and the peak of the response surface shifts away from the target center in a direction opposite to the vector \bar{v}_{lu} . Therefore, in deviation of the relative velocity Δv_{lu} from the value v_{lu0} at which an optimum position of the response surface was provided, the generatrix of the surface moves away from the median of the dangerous burst zone, and matching deteriorates - the values of the function $S(r)$ for all misses r decrease. At values of Δv_{lu} exceeding a definite limit, part of the response surface or even all of the surface go out of the dangerous burst zone, which normally results in a sharp decrease in firing efficiency. The range of relative velocities at which a given degree of matching occurs decreases with a decrease in the target dimensions, the width of the scattering sector and the initial velocity of the fragments.

Matching of a fuse to a dangerous burst zone under any approach conditions can be ensured only by including an additional device which makes it possible to control the location of the response surface in the fuse design. Two methods for controlling the response surface are possible. The first method (Fig. 12.25) is based on changing the direction of the main maximum of the beam pattern of the RV antenna system. We shall find the value of the angle ϕ_0 determines the direction of the main maximum of the pattern at which a location of the response point which is the optimum for given conditions of approach of the missile to the target (r, v_{lu}). It is obvious that the angle ϕ_0 will satisfy the condition cited if

the path of the missile Δz from the moment of the appearance of a working signal to the median of the dangerous burst zone is equal to the distance covered by the missile in relation to the target in the delay time T_3 .

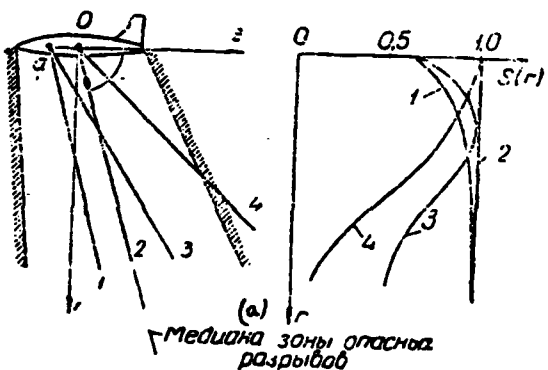


Fig. 12.24.
Key: (a) median of dangerous burst zone.

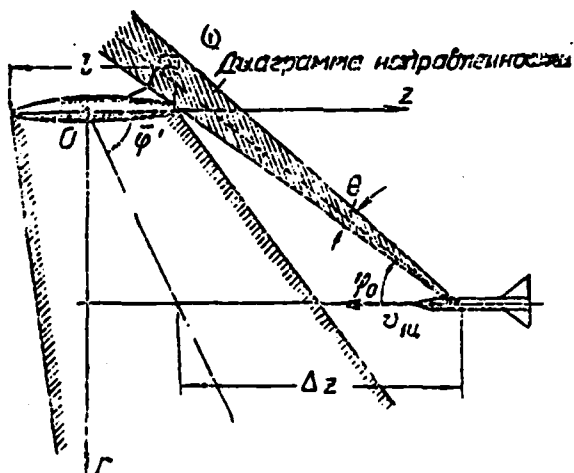


Fig. 12.25.
Key: (1) beam pattern.

Consequently, for determining the angle ϕ_0 , one can write the following equation:

$$\Delta z = T_s v_{lu} - r \operatorname{ctg} \left(\varphi_0 - \frac{\theta}{2} \right) + \frac{1}{2} l - r \operatorname{ctg} \bar{\varphi}'.$$

Inserting the value of the angle $\bar{\varphi}'$ from formula (12.42) into the latter equation, we obtain:

$$T_s v_{lu} - r \left[\operatorname{ctg} \left(\varphi_0 - \frac{\theta}{2} \right) - \operatorname{ctg} \bar{\varphi} - \frac{v_{lu}}{v_0 \sin \bar{\varphi}} \right] + \frac{l}{2}. \quad (12.46)$$

from which we find:

$$\varphi_0 = \operatorname{arcctg} \left| \operatorname{ctg} \bar{\varphi} + \frac{v_{lu}}{v_0 \sin \bar{\varphi}} + \frac{T_s v_{lu} - \frac{l}{2}}{r} \right| + \frac{\theta}{2}. \quad (12.47)$$

It follows from formula (12.47) that for determining the angle φ_0 , it is necessary to have information on the miss of the missile and the value of the relative velocity. One must keep in mind that this amount of information is sufficient for solving the problem only in a special case, where approach of the missile to the target occurs on a parallel course. In approach at an arbitrary angle of approach, one must know not only the value but also the direction of the vector v_{lu} .

For controlling the angle φ_0 , the fuse must have a special computer of the angle φ_0 and a unit for controlling the position of the beam pattern. Information on the conditions of approach goes to the computer; using this information, it computes the necessary value of the angle φ_0 according to formula (12.47). In accordance with the value of the angle φ_0 , a definite command emerges at the computer output and is realized by the control unit, which provides variation of the angle φ_0 . The angle φ_0 can be changed by electrical and mechanical methods. The electrical method boils down to appropriate changing of the transmitter wavelength, on which the position of the beam pattern depends, while the mechanical method amounts to rotation of the antenna system in relation to the missile axis.

The control method which has been considered envisages continuous changing of the angle φ_0 and provides optimum matching

under any approach conditions.

Fuses with discrete variation of the angle ϕ_0 are simpler from a structural point of view. Such RV have several antennas with beam patterns similar in shape but with different directions of the main radiation maximum. Each of the antennas provides the required degree of matching in a certain range of relative velocities of the missile. Connecting the transmitter to one antenna or another can be accomplished from the cockpit of the aircraft just before firing, depending on the firing direction, the type of target and other factors. The simplest fuse of this type can have two antennas, one of which is used in firing on head-on courses, while the other is used in firing for overtaking.

Another method for control of the response surface is based on variation of the delay in transmission of the command for functioning. The size of the delay which provides the optimum location of the RV response point will be found from equation (12.46) if we assume that $\phi_0 = \text{const}$ in the equation. By solving this equation with respect to t_k , we obtain

$$t_k = r \left[\frac{\operatorname{ctg} \left(\varphi_0 - \frac{\theta}{2} \right) - \operatorname{ctg} \bar{\varphi}}{v_{1u}} - \frac{1}{v_0 \sin \bar{\varphi}} \right] + \frac{l}{2v_{1u}} - t_m. \quad (12.48)$$

As one can see, for determining the required delay, it is necessary to have the same information which was necessary for calculating the angle ϕ_0 .

For the required delay t_k to be a positive value, it is necessary to ensure the inequality

$$r \left[\frac{\operatorname{ctg} \left(\varphi_0 - \frac{\theta}{2} \right) - \operatorname{ctg} \bar{\varphi}}{v_{1u}} - \frac{1}{v_0 \sin \bar{\varphi}} \right] + \frac{l}{2v_{1u}} > t_m. \quad (12.49)$$

where v_{1u} is the maximum relative velocity of the missile for which the fuse is intended.

The inequality (12.49) should be fulfilled for all possible values of r . Otherwise the flight time of the missile from the moment of action of the working signal to the median of the dangerous burst zone will be less than the time lag of the system. Requirements for the value of the time lag of the system and for the angle ϕ_0 follow from the inequality (12.49). For a miss $r=0$, inequality (12.49) takes on the following form:

$$\frac{l}{2v_{\text{lim}}} > t_{\text{..}}$$

This inequality imposes a limitation on the maximum acceptable value of the RV time lag. For misses $r>0$, inequality (12.49) will be written in the following form, with consideration for the latter inequality:

$$\frac{\operatorname{ctg}\left(\varphi_0 - \frac{\theta}{2}\right) - \operatorname{ctg}\bar{\varphi}}{v_{\text{lim}}} - \frac{1}{v_0 \sin \bar{\varphi}} > 0,$$

from which follows a requirement for the angle of inclination of the beam pattern of an RV with a variable delay:

$$\varphi_0 < \frac{\theta}{2} + \operatorname{arcctg}\left(\frac{v_{\text{lim}}}{v_0 \sin \bar{\varphi}} + \operatorname{ctg}\bar{\varphi}\right). \quad (12.50)$$

For control of the delay, the fuse should have a computer which forms a voltage proportionate to the value of t_k , by means of which variation of the mode of operation of the variable delay unit is accomplished. Discrete control of the delay is also possible by analogy with the discrete method for variation of the angle ϕ_0 . In this case, the fuse design envisages the possibility of setting of several delay values, each of which provides matching in a definite range of relative velocities.

We shall discuss briefly the sources of the information necessary for controlling the response surface. For obtaining information, the fuses either should have their own sensors or should use information which can be obtained by instruments of the carrier aircraft or the missile. The use of sensors of the

fuses themselves results in significant complication of the RV design, which can prove inefficient in practice in a number of cases. It is possible aboard the carrier aircraft to obtain only extremely approximate information concerning the value of the relative velocity of the missile, which can be used for setting the delay immediately before firing.

A fuse design using information obtained by the homing system of the missile will be the most rational. For example, in guiding of the missile by the parallel approach method, the homing radar provides the possibility of obtaining data on values of the relative velocity, the miss of the missile and the direction of approach to the target - the angle of approach. The parallel approach method is illustrated by a diagram in Fig. 12.26. The artillery target plotter of the homing system is situated on a platform which is mobile in relation to the missile and is stabilized in space by means of a free gyroscope. Before launching of the missile, the axis of the plotter is made to coincide with the missile-target line P_{II_0} , forming an angle ϵ with the missile axis equal to the calculated lead. The value of the lead is calculated by the aircraft sight based on the condition that the missile axis be directed at the point of impact on the target U_y . It is obvious that the vector of the relative velocity of the missile \bar{v}_{II_0} in this case will be directed along the range vector. It follows from the triangle of velocities based on the sine theorem that

$$\text{and } \frac{\sin \epsilon}{v_u} = \frac{\sin q}{v_1}$$

$$\sin \epsilon = \frac{v_u}{v_1} \sin q, \quad (12.51)$$

where q is the target angle; v_1 is the velocity of the missile, which is equal to the velocity of the attacking aircraft before firing; v_u is the target velocity.

Formula (12.51) determines the momentary lead corresponding to given values of v_1 , v_u and q . With a change in these parameters,

the angle ϵ must change. Just before launching of the missile from the launcher, the gyroscope is released. The axis of the artillery plotter, preserving an unchanged orientation in space, will move parallel to itself. With a change in the missile velocity or a maneuver of the target (a change in $v_{1\mu}$ and q), the plotter axis will be deflected from the missile-target line at some angular velocity $\dot{\epsilon}$. According to the value of the angular velocity $\dot{\epsilon}$, the homing system generates a signal which passes to the vanes, and the missile turns in relation to the plotter axis at the same angular velocity. As a result, the plotter axis will always track the target in the process of guidance, remaining parallel to its initial orientation, while the missile axis will be aimed at the momentary point of impact. The lead will vary in this process.

Therefore, the homing system in parallel approach fixes the following:

- the angular velocity of the artillery plotter in relation to the missile $\dot{\epsilon}$, which is equal to the relative angular velocity of the target;
- the angle ϵ between axes of the plotter and the missile, which is equal to the angle between the vectors $\bar{v}_{1\mu}$ and \bar{v}_1 .

In addition, a radar artillery plotter makes it possible to obtain data on the current range D and approach velocity \dot{D} .

In a parallel approach, as follows from Fig. 12.26, the value of $\dot{D} = v_{1\mu}$. The miss of the missile can be computed according to values of $\dot{\epsilon}$, D and \dot{D} .

The presence of a miss is conditioned mainly by limitation of the maneuverability of the missile or "blindness" of the homing head at short distances from the target. As a result of the effect of these causes, the homing system is disengaged at some

range D_0 . Free flight of the missile begins at this moment. We shall find the value of the miss r , assuming that the time of approach of the missile to the target t_0 from the moment of disengagement of the homing system is small; therefore, the vector \bar{v}_{III} does not change its orientation in space during this time.

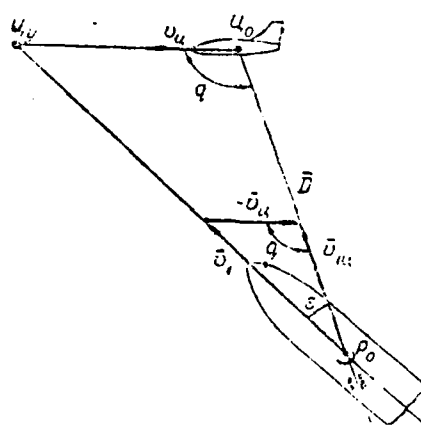


Fig. 12.26.

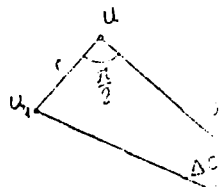


Fig. 12.27.

It follows from Fig. 12.27 that the time of approach t_0 is as follows:

$$t_0 = \frac{D_0}{\dot{D}_0} = \frac{D_0}{v_{\text{III}}}, \quad (12.52)$$

where \dot{D}_0 is the approach velocity at the moment of disengagement of the homing system.

During the time t_0 , the rocket-target line $P\Gamma_1$ will depart

from the direction of the vector \dot{D}_0 by an angle $\Delta\epsilon$ with the following value:

$$\Delta\epsilon = \dot{\epsilon}_0 t_0,$$

where $\dot{\epsilon}_0$ is the relative angular velocity of the target at the moment of disengagement of the guidance system; the target will shift from the relative trajectory of the missile by an amount

$$r = D_0 \Delta\epsilon = D_0 \dot{\epsilon}_0 t_0.$$

Substituting the value of t_0 from (12.52) into the latter formula, we obtain

$$r = \frac{D_0^2 \dot{\epsilon}_0}{\dot{D}_0} = \frac{D_0^2 \dot{\epsilon}_0}{v_{1u}}.$$

This formula makes it possible to compute the magnitude of the miss of the missile according to data of the homing system (D_0 , $\dot{\epsilon}_0$, v_{1u}) pertaining to the moment of its disengagement. We shall find an expression for calculating the target angle (the angle of approach).

It follows from the triangle of velocities (Fig. 12.26) that

$$\frac{\sin q}{v_1} = \frac{\sin(\pi - q - \epsilon)}{v_{1u}} = \frac{\sin(q + \epsilon)}{v_{1u}},$$

from which we obtain

$$\operatorname{ctg} q = \frac{1}{\sin \epsilon} \left(\frac{v_{1u}}{v_1} - \cos \epsilon \right).$$

The value of the missile velocity at the target can be introduced into the guidance unit depending on the altitude and range of firing or as a constant average value. We shall note in conclusion that the use of auxiliary devices making it possible to control the region of response in RV results in an increase in the dimensions and weight of the fuse. In cases where the dimensions specified for the fuse do not permit their use, the RV parameters are selected for any average approach conditions. Analysis of the effect of the approach conditions on the firing efficiency should precede solution of the problem of the advisability of control of the response surface. If it turns out that the firing efficiency does not vary substantially due to the effect of the fuse in a given range of conditions for

tactical use of the missile, the use of devices for controlling the response region can be considered inefficient.

§ 7. THE DISPERSION OF RESPONSE POINTS OF RADIO PROXIMITY FUSES

The dispersion of response points of RV is conditioned mainly by two causes: fluctuations of the effective reflecting surface area of the target S_u and instability of the fuse parameters which influence the location of response points. Such parameters include the sensitivity of the RV, the delay time, the width and position of the main maximum of the beam patterns of the antennas, the wavelength, etc. Instability of each of these parameters is conditioned, in turn, by the operating spread of parameters of the fuse system (resistances, capacitors, radio tubes, etc.) and by instability of the feeding voltages.

Fluctuations of the effective reflecting surface area are explained by the fact that it is actually composed of individual elements of the target surface, whose orientations in space are random and depend on slight fluctuations of the roll, pitch and yaw angles of both the target itself and the missile. Vibrations of the target surface during flight also serve as causes of fluctuation of S_u .

Experimental research indicates that the diagram of reflection of radio waves from aerial targets has a complex, multiple-lobe configuration. Sharp changes in the value of S_u lead to significant dispersion of response points of RV without a time lag. However, the effect of fluctuations of S_u decreases sharply when an amplitude limiter and an inertial circuit which performs averaging of the working signal are included in the fuse. In the presence of a limiter and an inertial circuit, the fuse is not capable of responding to the effect of brief signals, even when they significantly exceed the sensitivity of the receiver.

The dispersion of RV response points can be considered as the sum of a large number of independent or slightly dependent deviations generated by various causes. Since the effect of each of these elementary deviations on their sum is approximately the same, there is every reason to consider the law of the distribution of response points of RV as similar to a normal law. As we know, a normal law of the distribution of a single random variable (12.44) (the z coordinate of the response point, in this case) is defined by the mathematical expectation z_0 and the mean square deviation of the random variable σ_z .

The response surface serves as the mathematical expectation of the z coordinate of the RV response point:

$$z_0(r) = a + br + cr^2. \quad (12.53)$$

The coefficients a, b and c included in the equation of the response surface are calculated for average values of the RV parameters and an average effective reflecting surface area of the target. We shall find the value of the standard deviation of response points σ_z along the z axis assuming that coefficients a, b and c in equation (12.53) are random variables.

Equation (12.53) is linear in relation to the random coefficients a, b and c.

Using the well-known theorem of the dispersion of a linear function of uncorrelated random arguments, we find that

$$\sigma_z = \sqrt{\sigma_a^2 + \sigma_b^2 + \sigma_c^2}. \quad (12.54)$$

where σ_a , σ_b and σ_c represent the standard deviation for coefficients a, b and c.

We shall write the formulas (12.33), (12.40) and (12.41) obtained previously for coefficients of the response surface:

$$\left. \begin{aligned} a &= \frac{1}{2} l - v_{tu} (t_s + t_u) \\ b &= \operatorname{ctg} \varphi_0 + \frac{\theta}{0.6 \sin^2 \varphi_0} \\ c &= -\frac{\theta}{0.6 r_m \sin^2 \varphi_0} = -\frac{\theta}{0.6 D_m \sin^3 \varphi_0} \end{aligned} \right\} \quad (12.55)$$

where

$$0.6 \approx 2 \left(1 - \frac{1}{\sqrt{2}} \right).$$

It follows from the first formula that

$$\sigma_a = v_{tu} \sqrt{\sigma_u^2 + \sigma_k^2},$$

where σ_u and σ_k represent standard deviations of the time lag of the RV and the delay in transmission of the command.

In general, when the delay is controlled, the value of σ_k is calculated by the following formula:

$$\sigma_k = \sqrt{\sigma_1^2 + \sigma_2^2 + \sigma_3^2}.$$

where σ_1 is the standard deviation of the delay time conditioned by errors of information on the approach conditions; σ_2 is the standard deviation of the delay time conditioned by errors of the computer of the size of the delay; σ_3 is the standard deviation of the delay time conditioned by errors of the delay unit.

For determining σ_b and σ_c , it is necessary to use the method of linearization of a function of random arguments. Using the linearization method, we can write the following:

$$\left. \begin{aligned} \sigma_b &= \sqrt{\left(\frac{\partial b}{\partial \theta} \right)^2 \sigma_\theta^2 + \left(\frac{\partial b}{\partial \varphi_0} \right)^2 \sigma_\varphi^2} \\ \sigma_c &= \sqrt{\left(\frac{\partial c}{\partial \theta} \right)^2 \sigma_\theta^2 + \left(\frac{\partial c}{\partial \varphi_0} \right)^2 \sigma_\varphi^2 + \left(\frac{\partial c}{\partial D_m} \right)^2 \sigma_{D_m}^2} \end{aligned} \right\} \quad (12.56)$$

where σ_θ , σ_φ and σ_{D_m} are the standard deviations of values of θ , φ_0 and D_m , respectively.

The values of partial derivatives included in the formulas of

(12.56) can easily be computed by the expressions of (12.55) for b and c. The value of σ_{Dm} is calculated by a similar method with formulas (12.36) or (12.37).

It follows from the expressions obtained for σ that the RV dispersion depends on the value of the relative velocity of the missile v_{lk} , the miss of the missile r, the width of the radiation pattern θ , the location of the main radiation maximum ϕ_0 and other parameters of the fuse. The value of σ_z increases with an increase in v_{lk} , θ and r and with a decrease in the angle ϕ_0 . The value of σ_z has an order of several meters for RV.

For improving the reliability for noise protection, the RV design can be made up of several independent channels (Fig. 12.28). The individual channels perform functions of independent fuses in which commands for functioning are formed. These commands pass from each channel to a common actuator. The law of the dispersion of response points of multichannel RV can differ substantially from the laws of dispersion of individual channels. We shall consider the problem of determining the law of dispersion of a multichannel RV with known dispersion laws of the channels.

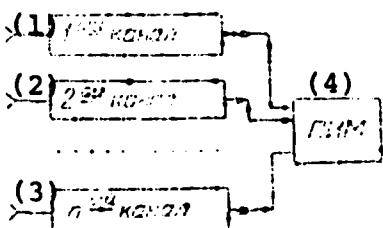


Fig. 12.28.
Key: (1) first channel; (2) second
channel; (3) n channel; (4) PIM.

Two types of connection of the channels to the RV actuator are possible: parallel and series. The connection of the channels is called parallel if arrival of a command from at least one channel is

sufficient for functioning of the actuator. Connection of the channels is called series if functioning of the actuator can occur only in arrival of commands from all the channels. It is obvious that parallel connection of the channels improves reliability while series connection improves noise protection of the RV. In parallel connection, each of the channels backs up all the other channels, which are spare channels. We shall find the dispersion law $\phi(z)$ of a two-channel RV with parallel connection of the channels. We shall designate the dispersion laws of the channels as $\phi_1(z)$ and $\phi_2(z)$. The probability of response of the RV $\phi(z)dz$ in a segment dz of the z axis is equal to the sum of probability of two events, each of which consists of a command for functioning developing in the given segment dz in one of the channels and later in the other.

Therefore, one can write that

$$\phi(z)dz = \phi_1(z)dz \int_{-\infty}^z \phi_2(x)dx + \phi_2(z)dz \int_{-\infty}^z \phi_1(x)dx,$$

where $\phi_i(z)dz$ is the probability of arrival of a command from the i channel in segment dz ;

$\int_{-\infty}^z \phi_i(x)dx$ is the probability of arrival of a command from the i channel after segment dz .

Consequently,

$$\phi(z) = \phi_1(z) \int_{-\infty}^z \phi_2(x)dx + \phi_2(z) \int_{-\infty}^z \phi_1(x)dx. \quad (12.57)$$

Assuming the dispersion laws of the channels to be identical,

$$\phi_1(z) = \phi_2(z) = \phi(z),$$

we have

$$\phi(z) = 2\phi(z) \int_{-\infty}^z \phi(x)dx. \quad (12.58)$$

It follows from expressions (12.57) and (12.58) that the dispersion law of a two-channel RV differs from the dispersion laws of the individual channels.

Assuming the dispersion law $\phi(z)$ to be normal (12.44),

according to formula (12.58) we obtain

$$\psi(z) = \frac{1}{\sqrt{2\pi}\sigma_z} e^{-\frac{(z-z_0)^2}{2\sigma_z^2}} \left[1 + \Phi\left(\frac{z-z_0}{\sqrt{2}\sigma_z}\right) \right], \quad (12.59)$$

where $\Phi(x)$ is a Laplace function.

We shall find the mathematical expectation \bar{z} and the dispersion σ^2 of response points of the two-channel RV:

$$\begin{aligned} \bar{z} &= \int_{-\infty}^{\infty} z \psi(z) dz = \frac{1}{\sqrt{2\pi}\sigma_z} \cdot \int_{-\infty}^{\infty} z e^{-\frac{(z-z_0)^2}{2\sigma_z^2}} dz + \\ &+ \frac{1}{\sqrt{2\pi}\sigma_z} \int_{-\infty}^{\infty} z e^{-\frac{(z-z_0)^2}{2\sigma_z^2}} \Phi\left(\frac{z-z_0}{\sqrt{2}\sigma_z}\right) dz. \end{aligned} \quad (12.60)$$

The first integral in formula (12.60) is the mathematical expectation of the random variable z with a normal distribution and, consequently, is equal to z_0 .

For computing the second integral, we shall perform substitution of the variable

$$\begin{aligned} \frac{z-z_0}{\sqrt{2}\sigma_z} &= t; \\ \bar{z} &= z_0 + \frac{1}{\sqrt{2\pi}\sigma_z} \int_{-\infty}^{\infty} z e^{-\frac{(z-z_0)^2}{2\sigma_z^2}} \Phi\left(\frac{z-z_0}{\sqrt{2}\sigma_z}\right) dz = \\ &= z_0 + \frac{1}{\sqrt{\pi}} \int_{-\infty}^{\infty} (z_0 + \sqrt{\frac{2}{\pi}}\sigma_z t) e^{-t^2} \Phi(t) dt = \\ &= z_0 + \frac{z_0}{\pi} \int_{-\infty}^{\infty} e^{-t^2} \Phi(t) dt + \frac{\sigma_z \sqrt{2}}{\sqrt{\pi}} \int_{-\infty}^{\infty} t e^{-t^2} \Phi(t) dt. \end{aligned} \quad (12.61)$$

Since the Laplace function $\Phi(x) = \frac{2}{\sqrt{\pi}} \int_0^x e^{-t^2} dt$ is an uneven function $\Phi(-x) = -\Phi(x)$, the first integral in formula (12.61) is equal to zero.

The second integral is computed by partial integration:

$$\begin{aligned} \int_{-\infty}^{\infty} \Phi(t) t e^{-t^2} dt &= \left[-\frac{1}{2} e^{-t^2} \Phi(t) \right]_{-\infty}^{\infty} + \frac{1}{\sqrt{\pi}} \int_{-\infty}^{\infty} e^{-2t^2} dt = \\ &= \frac{1}{\sqrt{2\pi}} \int_{-\infty}^{\infty} e^{-t^2} dt = \frac{1}{\sqrt{2}}. \end{aligned} \quad (12.62)$$

where $\int_{-\infty}^{\infty} e^{-t^2} dt = \sqrt{\pi}$ is an Euler-Poisson integral.

Inserting the value of the integral of (12.62) into formula (12.61), we find

$$\bar{z} = z_0 + \frac{\sigma_z}{\sqrt{\pi}}. \quad (12.63)$$

It follows from this that the response surface of a two-channel RV with parallel connection of the channels is shifted in the direction of larger values of z in relation to the response surface of the individual channels. This fact must be taken into consideration in selecting z_0 in a case where the value of σ_z is comparable to the target dimensions.

We shall compute the dispersion of response points:

$$\begin{aligned} \sigma^2 &= \int_{-\infty}^{\infty} \left(z - z_0 - \frac{\sigma_z}{\sqrt{\pi}} \right)^2 \varphi(z) dz = \\ &= \frac{1}{\sqrt{2\pi}\sigma_z} \int_{-\infty}^{\infty} \left(z - z_0 - \frac{\sigma_z}{\sqrt{\pi}} \right)^2 e^{-\frac{(z-z_0)^2}{2\sigma_z^2}} \left[1 + \Phi\left(\frac{z-z_0}{\sqrt{2}\sigma_z}\right) \right] dz. \end{aligned}$$

Using replacement of the variable $\frac{z-z_0}{\sqrt{2}\sigma_z} = t$, again, we obtain:

$$\begin{aligned}
\sigma^2 &= \frac{1}{V\pi} \int_{-\infty}^{\infty} \left(V\sqrt{\frac{2}{\pi}} \sigma_z t - \frac{\sigma_z}{V\pi} \right)^2 e^{-r} [1 + \Phi(t)] dt = \\
&= \frac{1}{V\pi} \left\{ 2 \int_{-\infty}^{\infty} \sigma_z^2 t^2 e^{-r} - \frac{2V\sqrt{\frac{2}{\pi}}}{V\pi} \sigma_z^2 \int_{-\infty}^{\infty} t e^{-r} dt + \right. \\
&\quad + \frac{\sigma_z^2}{\pi} \int_{-\infty}^{\infty} e^{-r} dt + 2\sigma_z^2 \int_{-\infty}^{\infty} t^2 \Phi(t) e^{-r} dt - \\
&\quad \left. - \frac{2V\sqrt{\frac{2}{\pi}}}{V\pi} \sigma_z^2 \int_{-\infty}^{\infty} t \Phi(t) e^{-r} dt + \frac{\sigma_z^2}{\pi} \int_{-\infty}^{\infty} \Phi(t) e^{-r} dt \right\}. \tag{12.64}
\end{aligned}$$

The second, fourth and sixth integrals in expression (12.64) are equal to zero, since their integrands are uneven. The first integral is equal to the dispersion of a normal distribution law σ_z^2 . The third and fifth integrals were computed previously - the first of them is the Euler-Poisson integral, while the second is determined by formula (12.62).

Therefore, one can write that

$$\sigma^2 = \sigma_z^2 + \frac{\sigma_z^2}{\pi} - \frac{2\sigma_z^2}{\pi} \tag{12.65}$$

or

$$\sigma = \sigma_z \sqrt{1 - \frac{1}{\pi}} \approx 0.83 \sigma_z. \tag{12.66}$$

It follows from formula (12.66) that parallel connection of the channels results in a decrease in the dispersion of the RV.

Now we shall consider an RV made up of two series connected channels. The law of the dispersion of such an RV is established in the same way as in the case just examined with parallel connection of the channels. The only difference will lie in the fact that in determining the probability of response $\psi(z)dz$ in the interval dz , the probability of the appearance of a command in one of the channels in this interval must be multiplied by the probability that

a command will appear earlier in the other channel. Consequently, the law of dispersion in series connection of the channels can be obtained from expressions (12.57) or (12.58) by replacing the bottom limits of the integrals with z and the top limits with $+\infty$. With identical laws of dispersion of the individual channels, we have

$$\psi(z) = 2\phi(z) \int_z^{+\infty} \phi(z) dz. \quad (12.67)$$

For a normal law $\phi(z)$, from formula (12.67) we obtain

$$\psi(z) = \frac{1}{\sqrt{2\pi}\sigma_z} e^{-\frac{(z-z_0)^2}{2\sigma_z^2}} \left[1 - \Phi\left(\frac{z-z_0}{\sqrt{2}\sigma_z}\right) \right]. \quad (12.68)$$

It follows from formulas (12.59) and (12.68) that the laws of dispersion of RV differ in parallel and series connection of the channels only in the law of the Laplace function. This fact makes it possible to use formulas (12.63) and (12.65) obtained for a case of parallel connection for determining the mathematical expectation and the dispersion of response points in series connection of the channels.

Changing the signs just before the last members in formulas (12.63) and (12.65), we obtain

$$\bar{z} = z_0 + \frac{\sigma_z}{\sqrt{\pi}} \quad (12.69)$$

and

$$\sigma^2 = \sigma_z^2 + \frac{z_0^2}{\pi} + \frac{2z_0^2}{\pi}$$

or

$$\sigma = \sigma_z \sqrt{1 + \frac{3}{\pi}} \approx 1.4\sigma_z. \quad (12.70)$$

The response surface of a two-channel RV with series connected channels is shifted in the direction of lower values of z in relation to the response surface of the individual channels. One can see from formula (12.70) that series connection of the channels leads to noticeable increase in the dispersion of response points. The standard deviation of the response points of a two-channel RV is

40% higher than for an individual channel.

§ 8. THE RELIABILITY OF RADIO PROXIMITY FUSES

The reliability of RV refers to their capacity for normal functioning, avoiding premature response on the trajectory (before engaging the target) and providing reliability of operation in interaction with the target. The value of the probability P of reliable functioning in interaction with the target, which will be referred to in abbreviated form hereinafter as the probability of response to the target, is accepted as a quantitative measure of the reliability of RV. We shall find an expression for the probability P in application to a case of firing of missiles at aerial targets.

The following events can be the result of functioning of the RV after firing:

A_1 - failure in operation or premature response on the trajectory due to malfunctioning of certain components of the system. Malfunctions of tubes, breaks of filaments of electric igniters, burning out of resistances, breakdown of capacitors, etc., for example, can serve as causes of failures. Premature responses are caused by voltage jumps, which can develop at the input of the actuator either at the moment of engagement of a faulty system or in sudden malfunctioning of certain components of the system. Malfunctions in the RV system can appear in the process of storage, during flight of an aircraft with the missiles or after firing.

A_2 - premature response on the trajectory under the influence of fluctuation (thermal) and vibration noise. Resistances and electronic tubes are sources of fluctuation noise. Vibration noise emerges under the influence of vibration overloads on parts of the system in movement of the missile in air, in operation of the

missile engine and in movements of parts of adjacent units with the RV during their operation (wing actuator assemblies, generators, etc.). One can ignore the effect of fluctuation noise for the conditions of operation of RV, since the level of the noise normally is lower than the level of vibration noise.

A_3 - failure in operation due to a low level of the reflected signal. Fluctuations of the working signal, the operating spread of parameters of the RV system and deviations of the parameters from their nominal values in storage can serve as causes of failures of serviceable fuses.

A_4 - response to the target.

Event A_4 - response of the fuse to the target - can be represented as the product of events \bar{A}_1 , \bar{A}_2 and \bar{A}_3 , the opposite events to A_1 , A_2 and A_3 :

$$A_4 = \bar{A}_1 \bar{A}_2 \bar{A}_3.$$

Using the theorem of multiplication of probabilities for computing the probability of event A_4 , we obtain:

or $P(A_4) = P(\bar{A}_1)P(\bar{A}_2|A_1)P(\bar{A}_3)$

$$P = P_1 P_2 P_3, \quad (12.71)$$

where $P_1 = P(\bar{A}_1)$ is the probability that the RV system is efficient; $P_2 = P(\bar{A}_2|\bar{A}_1)$ is the probability that a serviceable fuse will not respond prematurely; $P_3 = P(A_3)$ is the probability that the reflected signal will exceed the level necessary for response.

The Probability P_1

For determining the probability P_1 , it is necessary to distinguish the components in the RV system whose malfunctioning results in failure or premature response of the fuse on the trajectory. Assume that there are n such components in the system, the probabilities of faulty operation of which are known and are

equal to p_i , where $i=1, 2, \dots, n$. We shall assume that malfunctioning of at least one of the n components is sufficient for failure (premature response) of the RV, and that the probabilities of simultaneous malfunctioning of two or more components are values an order less than the corresponding probabilities for a single component. Under the assumptions which have been made, the probability that the RV system is efficient is defined as the probability of a combination of n events consisting of accuracy of each of the n components:

$$P_1 = \prod_{i=1}^n p_i. \quad (12.72)$$

We shall note that formula (12.72) is applicable in a case where malfunctioning of the RV can be conditioned by malfunctioning of two or more components. Such a case can occur, for example, in duplication of the operation of certain components by backup components which accomplish the functions of the main components when they malfunction. With duplication, one must insert the probabilities of accurate operation of at least one of the components - the main and reserve components - into formula (12.72) in place of the probabilities p_i of the components which are subject to redundancy.

We shall assume, for example, that the i component of the RV system has m backup components similar to it. The probability of failure of all the components is equal to $(1-p_i)^m$; consequently, the probability of accurate operation of at least one of them will be expressed by the following formula:

$$p_{i,0} = 1 - (1 - p_i)^m. \quad (12.73)$$

All the components included in the functional system of the RV can be divided into two types. The components of the first type include electrical and electronic parts and instruments (resistances, capacitors, tubes, etc.), the probability of failure of which is determined mainly by the duration of service of the fuse: the storage time and the time during which the components have been in a working state. Malfunctions of these components

develop as a result of gradual, comparatively slow changing of their basic properties. A decrease in the emission of tubes, a change in the capacitance of capacitors, a change in values of the resistances, etc., can serve as examples of such malfunctions. The probability of accurate operation of the indicated components depends on their storage time and their time in the working state. The numerical value of this probability is determined according to a well-known formula of the theory of reliability:

$$P_i = e^{-\lambda_i t_i}, \quad (12.74)$$

where λ_i is the intensity (or frequency) of failures of the i component; t_i is the time which has passed from the last check of the working order of the i component to the moment of interaction of the RV with the target in tactical use.

The intensity of failures λ is determined experimentally as the ratio of the number of failures which occur per unit of time to the original number of components tested. In the theory of reliability, the intensity of failures is called the lambda characteristic of the component. The value of the intensity of failures depends strongly on the conditions for service of the apparatus in which the corresponding components are used.

Three characteristic service periods can be pointed out with respect to RV of air launched missiles: storage, operational and plant checks of working order, and operation in tactical use. Taking into account the dependence of λ on the service conditions, we shall rewrite expression (12.74) in the following form:

$$P_i = e^{-(\lambda_{xp} t_{xp} + \lambda_n t_n + \lambda_p t_p)}, \quad (12.75)$$

where t_{xp} is the storage time of the fuse; t_n is the time for which the fuse is in the working state in plant and operational checks; t_p is the time for operation of the RV system under combat conditions; λ_{xp} is the intensity of failures during storage; λ_n is the intensity of failures in operation under laboratory conditions; λ_p is the intensity of failures for missile flight conditions.

The values of λ_{xp} , λ_{π} and λ_p are determined experimentally.

Components of the second type include electric igniters, magazine detonators, detonators, inertial contacts and a number of other mechanical parts which operate only in tactical use of the RV during arming and at the moment of development of a command for explosion of the warhead. The probability of accurate operation of these components, in contrast to components of the first type, practically does not depend on the storage time but is determined mainly by the efficiency of the design and the quality of production.

Substituting values of p_i from formula (12.75) into expression (12.72) we obtain:

$$P_1 = e^{-\sum_{i=1}^k (\lambda_{xp} t_{xp} + \lambda_{\pi} t_{\pi} + \lambda_p t_p)} \prod_{j=1}^{n-k} p_j, \quad (12.76)$$

where k is the total number of electrical and electronic components whose malfunctioning results in failure or premature response of the RV; $n-k$ is the number of components, the probability of accurate operation of which can be assumed not to depend on the storage time or the time spent in a working state.

Since the storage time of the RV $t_{xp} \gg t_{\pi} + t_p$, the probability of failure of an RV which was serviceable before firing is quite low. For reducing the probability of failure of an RV due to failure of components during storage, periodic operational checks of the RV system can be specified. Operational checks result in a decrease in the time t_{xp} to a value $t_{xp} = T_{\pi}/2$, where T_{π} is the time between two checks.

Another means for reducing the probability of failure of RV is duplication of components of the system and the use of multichannel systems with parallel connected channels. However, one must keep in mind in this case that multichannel systems with parallel channels possess lower noise protection and lower resistance to premature

responses on the trajectory.

The Probability P_2

Premature response of RV under the influence of vibration noise can occur on a section of the missile trajectory from the moment of arming of the fuse to the moment the target enters the radiation zone of the transmitting antennas. Response of the RV occurs at the moment when the noise voltage $u_m(t)$ at the input of the thyratron relay, which is a random function of the time, takes on a value exceeding the level U_{20} at which the thyratron is ignited. We shall designate the average number of swings of the random voltage $u_m(t)$ beyond the level U_{20} per unit of time as $\gamma(t)$, and we shall establish the conditional probability of response of the RV in the interval $t, t+\Delta t$, assuming that the fuse has not responded before the moment t . It is obvious that this probability is equal to the probability that at least a single swing of the voltage $u_m(t)$ beyond the level U_{20} will occur in the given time interval Δt . With a sufficiently short interval Δt , the probabilities of two or more swings will be small values of a higher order in relation to Δt . Therefore, one can assume that the desired probability will be equal to the probability of a single swing, which, in turn, can be assumed to be equal to the product $\gamma(t)\Delta t$. With a knowledge of the conditional probability of response of the RV in the interval Δt , we shall find the probability that the fuse will not respond during flight of the missile from the moment of arming ($t=0$) to the moment of contact with the target (t_u). For this purpose, we shall divide the given time interval t_u into n small intervals Δt .

The probability that the fuse will not respond in the i interval Δt under the condition that it has not responded in any of the previous intervals is as follows

$$1 - \gamma(t_i) \Delta t.$$

We shall find the probability that the fuse will not respond in the time t_u using the theorem of multiplication of probabilities:

$$P_2 = \lim_{\Delta t \rightarrow 0} \prod_{i=1}^n [1 - \gamma(t_i) \Delta t]. \quad (12.77)$$

Taking the logarithms of both members of equation (12.77), we obtain the following:

$$\ln P_2 = \lim_{\Delta t \rightarrow 0} \ln \left\{ \prod_{i=1}^n [1 - \gamma(t_i) \Delta t] \right\} = \lim_{\Delta t \rightarrow 0} \sum_{i=1}^n \ln [1 - \gamma(t_i) \Delta t].$$

Since the value of $\gamma(t_i) \Delta t \ll 1$, we shall replace the function $\ln[1 - \ln[1 - \gamma(t_i) \Delta t]]$ with the first member of its expansion to a series.

Then we have

$$\ln P_2 = - \lim_{\Delta t \rightarrow 0} \sum_{i=1}^n \gamma(t_i) \Delta t = - \int_0^u \gamma(t) dt. \quad (12.78)$$

It follows from formula (12.78) that

$$P_2 = e^{- \int_0^u \gamma(t) dt}. \quad (12.79)$$

The probability that the fuse will not respond P_2 is determined by a formula similar to the formula for computing the probability of reliable operation of a component for a given time segment t , when the intensity of failures depends on the operating time:

$$P = e^{- \int_0^u \gamma(t) dt}$$

Formula (12.79) includes the function $\gamma(t)$ equal to the average number of swings of the noise voltage beyond a definite level U_{20} per unit of time, instead of the intensity of failures. By analogy with the intensity of failures, the function $\gamma(t)$ can be called the intensity of noise voltage swings resulting in response of the RV. The function $\gamma(t)$ is determined by methods of the theory of random processes. Analysis of formula (12.79) indicates that the probability of premature response of the RV depends on the average power of the vibration noise, the width of the vibration frequency band, the sensitivity of the low-frequency unit of the fuse (the voltage U_{20}), the flight time of the missile from the moment of arming of the RV to contact with the target, and the characteristics of individual units of the fuse system. The basic means for reducing the intensity of vibration noise are as follows:

the use of vibration-resistant parts in the fuses, cushioning of the parts and units, and installation of the fuse in sections of the missile which are least vulnerable to the effect of vibration, as far as possible from mechanisms with moving parts.

The Probability P_3

For determination of the probability P_3 , we shall consider the working signal of the RV in the form of a spectrum of oscillations similar in character to the noise voltage. As already noted, the working signal of the RV is formed as a result of combining of a large number of elementary sinusoidal signals of different amplitudes conditioned by reflection from individual points of the target. Since the velocities of approach to these points are different, the signals which are combined differ in phase.

According to the limit theorem of the theory of probabilities, the total signal formed in this way can be considered a stationary normal noise with a zero mathematical expectation randomly modulated in regard to amplitude and phase. In connection with the fact that functioning of the thyratron relay of the RV occurs under the influence of the amplitude (envelope) of the working signal, we shall be interested hereinafter only in the statistical characteristics of the envelope U_{cm} . For a stationary signal, its envelope will also be a stationary process. With a normal law of the distribution of the working signal, it will be distributed according to Rayleigh's law:

$$f(U_{cm}) = \frac{U_{cm}}{\sigma_c^2} e^{-\frac{U_{cm}^2}{\sigma_c^2}}, \quad (12.80)$$

where σ_c is the standard deviation of the working signal.

As we know, the dispersion of a stationary signal is equal to its average power detected on a load resistance of 1 ohm. Consequently,

$$a_e^2 = \frac{U_{cm}^2}{2} . \quad (12.81)$$

The value of U_{cm} is determined by the signal power at the mixer input,

$$U_{cm} = \kappa \sqrt{P_{np}} , \quad (12.82)$$

where κ is the transformation coefficient of the mixer; P_{np} is the power of the reflected signal at the mixer input.

The power of the reflected signal can be established according to a well-known radar formula:

$$P_{np} = \frac{P_t \lambda^2 S_n G^2(\phi)}{(4\pi)^3 D^4} , \quad (12.83)$$

this formula was used previously for writing equation (12.34). With a narrow radiation pattern of the antennas, the distance D varies only slightly in the process of irradiation of the target.

Therefore, one can assume approximately that

$$D = \frac{r}{\sin \varphi_0} ,$$

where φ_0 is the angle between the missile axis and the direction of the main maximum of the radiation pattern; r is the magnitude of the miss of the missile.

With consideration for the latter assumption, formula (12.83) will take on the following form:

$$P_{np} = \frac{P_t \lambda^2 S_n G^2(\varphi_0)}{(4\pi)^3 r^4} \sin^4 \varphi_0 . \quad (12.84)$$

Substituting formula (12.84) into (12.82), we obtain

$$U_{cm} = \kappa \frac{\lambda G(\varphi_0) \sin^2 \varphi_0}{4\pi r^2} \sqrt{\frac{P_t S_n}{4\pi}} . \quad (12.85)$$

We shall designate the amplitude of the signal voltage at the amplifier input necessary for response of the thyratron relay of an RV without a time lag as U_{10} . The miss r at which this amplitude is still achieved is called the radius of action of the fuse r_m .

It follows from expression (12.85) that

$$U_{10} = \frac{\pi \lambda G(\varphi_0) \sin^2 \varphi_0}{4\pi r_m^2} \sqrt{\frac{P_t S_u}{4\pi}}. \quad (12.86)$$

Having divided both members of expression (12.85) by (12.86), we find

$$U_{cm} = U_{10} \left(\frac{r_m}{r} \right)^2. \quad (12.87)$$

Consequently, the dispersion of the working signal (12.81) can be written in the following form:

$$\sigma_c^2 = \frac{U_{10}^2}{2} \left(\frac{r_m}{r} \right)^4. \quad (12.88)$$

One must keep in mind that the dispersion σ_c^2 characterizes fluctuations of the level of the working signal only due to fluctuation of the effective reflecting surface area of the target and instability of the operation of the transponder. It does not take into consideration the spread of the signal amplitude due to the operational spread of parameters of the RV system.

We shall assume that the working signal after the mixer passes through a typical RV circuit including a low-frequency amplifier, an amplitude limiter, a peak detector and an inertial circuit. In a case where the pass band of the UNCh [low-frequency amplifier] completely covers the spectrum of the working signal, the standard deviation of the signal at the amplifier output will be as follows:

$$\sigma_A = k_0 \sigma_c, \quad (12.89)$$

where k_0 is the amplification factor of the UNCh.

A diagram of a limiter which performs nonlinear transformation of the amplitude A of the amplified signal is shown in Fig. 12.29.

It is approximated by a piecewise-linear function

$$B(A) = \begin{cases} \mu A & \text{if } A < a \\ 0 & \text{if } A = a \\ B_0 & \text{if } A > a, \end{cases} \quad (12.90)$$

Key: (1) with.

where a is the limitation threshold; B is the voltage at the limiter output.

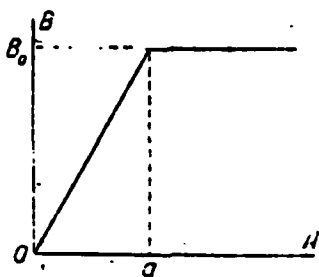


Fig. 12.29.

The transformation $B(A)$ is linear in the interval from $A=0$ to $A=a$. Therefore, the law of the distribution of the amplitude B within this interval can be found according to a well-known rule, like the law of the distribution of a monotonously increasing function from a random argument A . We know that for such a case,

$$f(B) = f_A(A(B)) \frac{dA}{dB}, \quad (12.91)$$

where $A(B)$ is a function which is the inverse of the given $B(A)$.

Applying formula (12.91) to the transformation $B=\mu A$, we find

$$f(B) = \frac{1}{\mu} f_A\left(\frac{B}{\mu}\right). \quad (12.92)$$

According to (12.80) and (12.89), we have

$$f_A(A) = \frac{A}{\sigma_A^2} e^{-\frac{A^2}{2\sigma_A^2}}. \quad (12.93)$$

It follows from formulas (12.92) and (12.93) that

$$f(B) = \frac{B}{\sigma_B^2} e^{-\frac{B^2}{2\sigma_B^2}} \quad \text{with } 0 < B < B_0, \quad (12.94)$$

where $\sigma_B = \mu k_0 \sigma_c$.

All the values of A greater than the limitation threshold a

are transformed by the limiter into the single value B_0 .

It is obvious that the probability of a value $B=B_0$ is as follows:

$$P(B = B_0) = \int_a^{\infty} f_A(A) dA. \quad (12.95)$$

Inserting the distribution law $f_A(A)$ in the form of (12.93) into formula (12.95) and performing integration, we obtain

$$P(B = B_0) = e^{-\frac{B_0^2}{2\sigma_A^2}}. \quad (12.96)$$

Since $B_0 = u_a$, the latter formula can be written in the following form:

$$P(B = B_0) = e^{-\frac{B_0^2}{2\sigma_B^2}}. \quad (12.97)$$

Using the delta function, the law of the distribution of the voltage B can be written in the following form:

$$f(B) = \begin{cases} \frac{B}{\sigma_B^2} e^{-\frac{B^2}{2\sigma_B^2}} + e^{-\frac{B_0^2}{2\sigma_B^2}} \delta(B - B_0) & \text{with } 0 < B < B_0; \\ 0 & \text{with } B > B_0. \end{cases} \quad (12.98)$$

As we know, the delta function $\delta(B - B_0)$ is determined so that it is equal to zero everywhere with the exception of the special point B_0 at which it reverts to infinity. The integral from the delta function distributed to as small a segment as desired including the special point is equal to one.

The voltage at the output of the inertial circuit, consisting of a resistance R and a capacitor with a capacitance C , is determined by the well-known expression

$$v_2 = B(1 - e^{-at}), \quad (12.99)$$

where $a=1/RC$ represents a value which is the inverse of the time constant of the circuit.

We shall find the time segment from the moment of appearance

of the working signal to the moment of creation of the command for functioning - the value of the time lag of the fuse t_H - by formula (12.99):

$$t_H = -\frac{1}{\alpha} \ln \left(1 - \frac{U_{20}}{B} \right). \quad (12.100)$$

where U_{20} is the voltage at the output of the inertial circuit at which the thyratron relay functions.

The value of U_{20} is related to the value of U_{10} by the following relationship:

$$U_{20} = k_0 \mu U_{10}. \quad (12.101)$$

Formula (12.100) is valid at $U_{20}/B < 1$. With $U_{20}/B \geq 1$, functioning of the thyratron relay is impossible, no matter how great the signal duration. The dependence $t_H(B)$ is shown qualitatively in Fig. 12.30. For each value of B in the interval from U_{20} to B_0 , it determines the time segment in the course of which the voltage at the output of the inertial circuit reaches the value U_{20} . The value of t_H is limited at the bottom by the value t_{H0} conditioned by the threshold of limitation of the signal passing to the input of the inertial circuit. We find from formula (12.100) that

$$t_{H0} = -\frac{1}{\alpha} \ln \left(1 - \frac{U_{20}}{B_0} \right). \quad (12.102)$$

The top limit of t_H is determined by the boundedness of the time of action of the signal, equal to t_c . The value of t_c determines the minimum signal B_1 at the input of the inertial circuit at which the fuse is still capable of response. According to formula (12.100),

$$B_1 = \frac{U_{20}}{1 - e^{-\alpha t_c}}. \quad (12.103)$$

Since the fuse is capable of responding only with a voltage $B > B_1$, the probability of response of the RV will be as follows:

$$P_3 = P(B > B_1) = \int_{B_1}^{\infty} f(B) dB.$$

With consideration for expression (12.98), the latter formula will take on the following form:

$$P_3 = \int_{B_1}^{B_0} \frac{B}{\sigma_B^2} e^{-\frac{B^2}{\sigma_B^2}} dB + e^{-\frac{B_0^2}{\sigma_B^2}} \int_{B_0-\Delta}^{B_0+\Delta} \delta(B - B_0) dB, \quad (12.104)$$

where Δ is as small a positive value as desired.

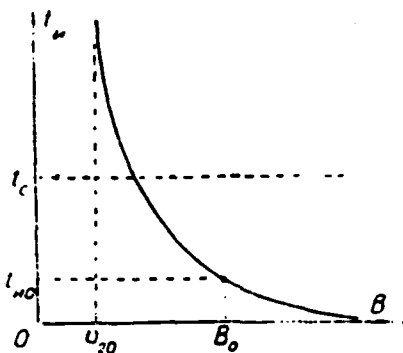


Fig. 12.30.

After integration, we obtain the following from formula (12.104):

$$P_3 = e^{-\frac{B_0^2}{\sigma_B^2}}. \quad (12.105)$$

Substituting values of B_1 and σ_B from formulas (12.88), (12.101) and (12.103) into (12.105), we find

$$P_3 = e^{-\frac{1}{(1-e^{-\alpha t_c})^2} \left(\frac{r}{r_m}\right)^4}. \quad (12.106)$$

With a narrow radiation pattern of the RV antenna, the value of t_c is as follows:

$$t_c = \frac{l}{v_{lu}},$$

where l is the length of the target in the direction of the vector \vec{v}_{lu} .

Having specified $\alpha l/v_{lu} = q$, we shall rewrite formula (12.106) in the following form:

$$P_3 = e^{-\frac{1}{(1-e^{-q})^2} \left(\frac{r}{r_m}\right)^4} = e^{-m \left(\frac{r}{r_m}\right)^4}, \quad (12.107)$$

where

$$m = \frac{1}{(1 - e^{-q})^2}.$$

The dependence of the probability of response of the RV on the relative miss r/r_m for different values of q is shown in Fig. 12.31. The graphs were plotted according to formula (12.107). The curve for $q=\infty$ corresponds to a case of a fuse without a time lag ($RC=0$). As one can see, introducing an inertial circuit results in a decrease in the probability P_3 with all misses differing from $r=0$. The greater the time lag of the system, the lower the probability of response with any miss $r>0$. With a given value of the time lag, the probability P_3 decreases with an increase in the relative velocity of the missile v_{lm} or with a decrease in the dimensions of the target. For accounting for the operational spread of parameters of the RV system, the value of the probability P_3 should be averaged with consideration for the law of the distribution of these parameters.

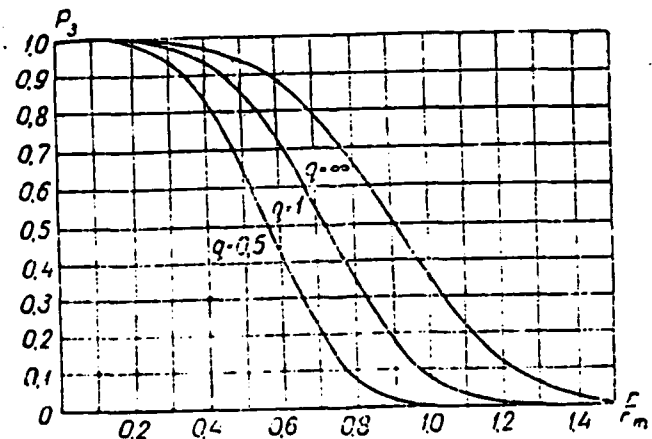


Fig. 12.31.

Having the dependence $P_3(r)$, one can establish the average radius in the probability sense for action of the RV.

It is obvious that

$$\bar{r}_m = \int_0^{\infty} P_3(r) dr = \int_0^{\infty} e^{-m} \left(\frac{r}{r_m}\right)^q dr. \quad (12.108)$$

By replacing the variable r with $x = \frac{\sqrt{m}r}{r_m}$, we reduce the integral

of (12.108) to the following form:

$$\bar{r}_m = \frac{r_m}{\sqrt{m}} \int_0^{\infty} e^{-x^2} dx = \frac{r_m}{4\sqrt{m}} \Gamma\left(\frac{1}{4}\right),$$

where $\Gamma(z)$ is the gamma function. Since

$$z\Gamma(z) = \Gamma(z+1).$$

then

$$\frac{1}{4} \Gamma\left(\frac{1}{4}\right) = \Gamma(1.25) = 0.906.$$

Consequently,

$$\bar{r}_m = 0.906 \sqrt{(1 - e^{-q}) r_m}. \quad (12.109)$$

It follows from the latter formula that for an RV without a time lag ($q=\infty$), the average radius of action \bar{r}_m is approximately 10% less than the conditional radius of action r_m at which the voltage amplitude at the input of the thyratron relay is equal to the thyratron ignition voltage. With $q=1$, $\bar{r}_m = 0.72 r_m$, and with $q=0.5$, $\bar{r}_m = 0.564 r_m$.

§ 9. THE NOISE RESISTANCE OF RADIO PROXIMITY FUSES IN RELATION TO JAMMING

The problem of improving the noise protection of RV [radio proximity fuses] is of primary importance, since low resistance RV to interference can be the cause of low efficiency of an entire missile weapons system.

At the current level of development of means for electronic countermeasures, combatting RV by using organized interference does not present great difficulties, if all the possibilities available to the enemy in regard to creating interference have not been taken into consideration in development of the fuses.

All combat aircraft can have available the minimum necessary means for electronic countermeasures. Group protection of airplanes flying in close formation can be provided by special aircraft - suppliers of interference - which are equipped with apparatus for electronic countermeasures instead of weapons (such as bombing weapons).

Organized interference is divided into active interference, created by special jamming stations, and passive (reflecting) interference. The basic types of active jamming are retransmitting (answering) interference and noise interference.

Interference created by reception of a signal emitted by an RV and its subsequent retransmission is called retransmitting jamming. In the process of retransmission, the signal is amplified, so that the answering interference proves similar to the signal from a target with a large reflecting surface.

Noise interference is similar in character to the thermal noise of resistances. It is made up of sinusoidal oscillations which occupy a continuous spectrum of a definite width. The necessary condition for response of an RV to noise interference is that the pass band of the amplifier fall within the noise spectrum. Noise interference, in contrast to retransmitting interference, is emitted regardless of the presence of a signal attesting to operation of an RV. A noise jamming station can operate throughout the flight time of the target.

Passive interference is created in the form of clouds of metallic tape and adjusted reflectors, which serve as the cause of the appearance of a false reflected signal capable of causing premature response of the RV. The tape and reflectors are manufactured from thin aluminum foil or fiberglass and are placed in individual packs. The reflector packs are released from the aircraft by special automatic devices. Passive interference can

also be organized by firing of special artillery shells for rocket missiles which scatter reflectors.

Most of the methods for protecting RV against jamming are based on the use of physical features of interference which distinguish it from a useful signal and are normally realized by increased complication of the fuse design. We shall consider some methods for improving the noise protection of RV.

Improving the Directivity of Antenna Operation

The smaller the width of the radiation pattern of antennas, the higher the noise protection of the RV against active and passive interference. With a decrease in the width of the radiation pattern of receiving antennas, the power of the working signal increases, in connection with which the possibility of reducing the sensitivity of the RV receiver emerges. Decreasing the sensitivity of the receiver results in an increase in the power of the active jamming necessary for response of the RV at a given distance, i.e., a decrease in the radius of action of the jamming station.

The resistance of RV to passive interference is enhanced as a result of a decrease in the number of reflectors which get into the radiation patterns. For response of an RV to a cloud of reflectors with a small width of the radiation pattern, a high density of reflectors in the cloud is required; this can be achieved only by increasing the number of reflectors released from the aircraft.

With limited dimensions of the RV, increasing the directivity of the operation of the antennas is achieved by reducing the working wavelength of the transmitter. In addition to the width of the radiation pattern, the level of leading (secondary) lobes of the beam pattern of the receiving antennas has a great influence on the

noise protection of RV. The presence of such lobes (Fig. 12.32) expands the region of space from which the jamming station can act on the fuse.

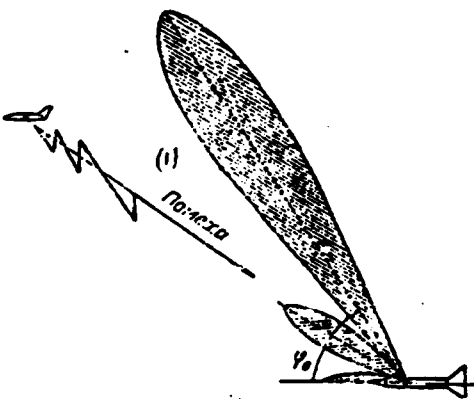


Fig. 12.32.
Key: (1) interference.

Selection in Regard to Characteristics of the Working Signal

This method for noise protection is based on the difference of characteristics of a working signal (amplitude, frequency, time of action, etc.) from interference.

Three types of selection can be used in RV systems: frequency, amplitude and time. Frequency selection consists of limiting the pass band of the UNCh [low-frequency amplifier] to the range of possible frequencies of a working signal; amplitude selection consists of limiting the signal amplitude; time selection consists of giving the RV system a definite time lag, which makes possible response only to a signal of a predetermined duration.

Signal Selection in Regard to Range

Selection in regard to range can provide protection of RV against retransmitting (answering) jamming, which differs from a

signal reflected by the target in a large propagation time. This form of selection can be used in pulse and frequency-modulated RV. In pulse RV, as demonstrated previously, selection in regard to range is provided by strobing of the receiver, while in frequency-modulated RV, selection is provided by appropriate selection of the frequency characteristics of the UNCh. Strobing of pulse RV limits the signal reception time to an interval corresponding to a maximum range of action of the fuse. Therefore, in cases where the distance to the answering jamming station exceeds this range, the interference will pass to the receiver during pauses between strobe pulses, when the receiver amplifier is blocked.

The Use of Multichannel Systems

Designs of RV with several transceiving channels operating on a common actuating circuit possess enhanced noise protection. Individual channels of such RV can possess different characteristics; for example, they can operate at different wavelengths; thus they can complicate setting up interference. One should keep in mind that enhanced noise protection of multichannel systems is provided only with series connection of the channels, in which the functioning of the actuator of the RV is possible only with arrival of commands from each channel. In parallel connection of the channels, the noise protection of a multichannel RV is lower than that of a single-channel fuse.

It must be mentioned in conclusion that the methods described naturally do not exhaust all the possible ways of improving RV noise protection. Questions involved with improving noise protection are among the most important problems of RV engineering and have not found sufficient explanation in the open press for quite understandable reasons.

CHAPTER 13

OPTICAL FUSES

§ 1. THE PRINCIPLE OF OPERATION OF OPTICAL FUSES OF THE PASSIVE TYPE

Optical proximity fuses (ONV) of the passive type find use in missiles in firing at aerial targets. Their operation is based on the use of infrared (thermal) radiation of the targets.

Heated engine parts (nozzles, exhaust tubes, etc.), the flare of hot gases and the aircraft fuselage itself, heated up in the flow of air around it, are sources of infrared radiation of aerial targets (airplanes, missiles, etc.). With low flight speeds, the radiation of the fuselage is low as compared to radiation of the engines and their gas jets. However, this radiation increases sharply with an increase in the flight speed. For example, the temperature of the skin of an aircraft flying at an altitude of 10 km at a velocity corresponding to a Mach number $M=0.8$ is 250° K. With an increase in the velocity of the airplane to $M=2.4$, the skin temperature approximately doubles, and the output of infrared radiation increases by a factor of 16.

Radiation of the engines of aircraft possesses a sharply pronounced directivity of its effect. The basic portion of the radiation of the engines falls within the region to the rear of the aircraft, where the jets of exhausted gases of the engines are

directed. Such a character of the radiation energy distribution limits the range of use of optical fuses, which react to the radiation of the engines, making firing possible only from the direction of the rear hemisphere of the target. The distinguishing feature of radiation of the skin of aircraft is the practically uniform distribution of the output in all directions. In the use of radiation of the skin, the use of ONV is possible in firing from any direction. The range of wavelengths in which the maximum of the intensity of infrared radiation of aerial targets falls is determined by the temperature of the radiation source. With an increase in the temperature, the radiation maximum shifts into a region of shorter waves. For example, a source with a temperature or the order of 300°C has a maximum of intensity of infrared rays on a wave of about $5 \mu\text{m}$. With a source temperature of 100°C , the radiation maximum falls on a wave of $7.8 \mu\text{m}$. The heated metal parts of jet engines have a radiation maximum on a wave of the order of $3.5 \mu\text{m}$. The spectral characteristics of radiation of jet engines corresponds quite well to the spectral characteristics of the sensitivity of lead sulfide photoresistors. A PbS photoresistor possesses maximum sensitivity in the wavelength range of $3-3.5 \mu\text{m}$; therefore, it can be used in sensors of ONV which react to the radiation of engines of aerial targets. The sensitivity of lead sulfide resistors depends on their temperature. With a decrease in the temperature, the region of maximum sensitivity shifts in the direction of longer waves. A lead sulfide photoresistor cooled to the appropriate temperature can be used in fuses which react to low-temperature radiation - radiation of the skin of an aircraft, for example.

New types of photoresistors (germanium, indium antimonide, etc.) developed in recent years, whose range of sensitivity reaches up to $10 \mu\text{m}$, can be used for the same purpose. Special devices using liquid nitrogen, liquid hydrogen, dry ice, etc., are used for cooling the photoresistors.

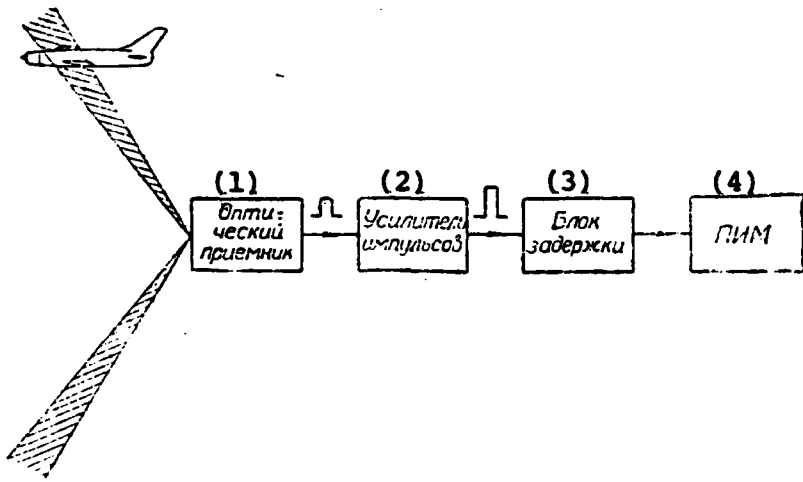


Fig. 13.1.

Key: (1) optical receiver; (2) pulse amplifier;
 (3) delay unit; (4) PIM [safety and operations
 mechanism].

A block diagram of an optical fuse which reacts to infrared radiation of aerial targets is shown in Fig. 13.1. An optical receiver which receives radiation of the target and transforms it into an electrical signal - the command for functioning of the ONV - serves as the target sensor of the fuse. The receiver possesses an extremely narrow sensitivity zone bounded by two conical surfaces, the angle between the generatrices of which has an order of 1.5-2°. Such a shape of the sensitivity zone provides a circular survey of the space around the missile and matching of the fuse to a warhead with a directed action. The sensitivity zone determines the geometric location of positions of the radiation source in relation to the missile in which radiation reaches the receiver. If the source is located outside the sensitivity zone, its radiation does not reach the receiver. A small width of the sensitivity zone limits the possibility for emissions from interfering sources to reach the receiver and reduces the effect of the surrounding background on operation of the fuse. The fuse

functions in flight of the missile in relation to the target. At the moment of passage through the sensitivity zone by a radiating part of the target, such as the engine nozzle face, infrared radiation acts on the photoresistor of the receiver, changing its conductivity for electric current. A voltage pulse is formed in the receiver circuit in this process, and the leading edge of the pulse coincides with the moment of entry of the emitter into the sensitivity zone, while the trailing edge coincides with the moment it passes out of this zone. This pulse, which is the command for functioning of the ONV, is amplified by an amplifier and passed to an actuator (the PIM [safety and operations mechanism]) with a definite delay. The delay in transmission of the command, as in RV [radio proximity fuse] systems, makes it possible to shift the fuse response surface to the location needed.

The optical receiver of the fuse is made up of an optical system and a photoresistor connected in an electrical circuit. The optical system serves for collecting energy emitted by the target and focusing it on the sensitive surface of the photoresistor.

The electrical circuit transforms the change in conductivity of the photoresistor which occurs under the influence of radiation of the target to a voltage pulse - the working signal. Two types of optical systems - lens and mirror - can be used in fuses.

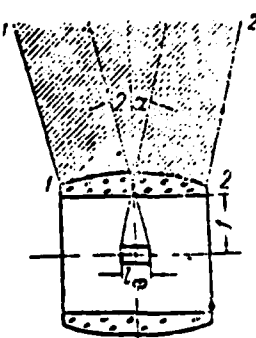


Fig. 13.2.

A lens optical system is made up of one or several circular scanning lenses. Figure 13.2 shows a lens optical system made up of a single converging lens of a cylindric shape. The lens axis coincides with the axis of the missile. Its inner radius is equal to the focal length f . A photoresistor in the form of a cylinder is placed along the lens axis. The photosensitive layer of the photoresistor is applied to the lateral surface of the cylinder. The field of vision of the lens, which is the sensitivity zone of the receiver, is bounded by two conical surfaces, which are formed by rotation of lines 1-1 and 2-2 around the lens axis. The width of the field of vision of the lens in a meridian plane is defined by an angle 2α , as follows:

$$2\alpha = 2 \arctg \frac{l_0}{2f},$$

where l_0 is the length of the photoresistor.

Inclination of the field of vision of the lens by a predetermined angle in relation to a normal to its axis is accomplished by shifting the photoresistor along the lens axis.

For weakening the effect of visible rays and infrared rays in a nonworking section of the spectrum on the operation of the ONV, special light filters which absorb energy in a range of wavelengths which do not fall within their pass band can be placed in front of the photoresistor. Solid light filters for infrared rays can be manufactured from gelatin, tinted glass or plastic, and other substances.

A mirror optical system is made up of one (Fig. 13.3) or several parabolic mirrors 1, which collect the flow of infrared rays hitting them and direct it to a photoresistor 2 situated at their focus. The mirror surface after careful processing is covered with a thin layer of a material which reflects infrared rays well - normally aluminum.

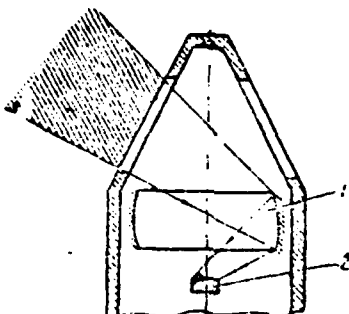


Fig. 13.3.

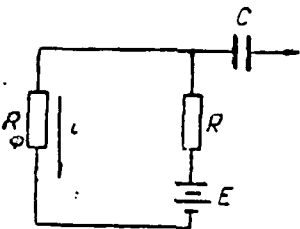


Fig. 13.4.

The mirror is situated inside the housing of the fuse or the missile. For passage of infrared rays to the mirror, there are special windows in the fuse housing. An electrical diagram of an optical receiver is shown in Fig. 13.4. Direct current flows through the photoresistor R_ϕ and the load resistance R in the circuit until the missile approaches a target; the value of the current is as follows:

$$i = \frac{E}{R + R_\phi}, \quad (13.1)$$

where E is the e. d. s. [electromotive force, emf] of the power source.

The value of the current pulse Δ_i developing in the circuit

in flight of the target through the sensitivity zone of the fuse can be established as

$$\Delta i = \left| \frac{\partial i}{\partial R_\phi} \right| \Delta R_\phi. \quad (13.2)$$

where ΔR_ϕ is the change in the photoresistor value caused by radiation of the target.

It follows from expression (13.1) that

$$\frac{\partial i}{\partial R_\phi} = - \frac{E}{(R + R_\phi)^2}. \quad (13.3)$$

Substituting the value of the derivative $\partial i / \partial R_\phi$ into formula (13.2), we obtain

$$\Delta i = \frac{E \Delta R_\phi}{(R + R_\phi)^2}. \quad (13.4)$$

The working signal voltage pulse transmitted from the load resistance to the amplifier input is as follows:

$$\Delta u = \Delta i R = \frac{ER \Delta R_\phi}{(R + R_\phi)^2}$$

or

$$\Delta u = \frac{E p \Phi}{(1 + p)^2} S_\phi. \quad (13.5)$$

where $p = R / R_\phi$; Φ is the level of the radiation flux irradiating the photoresistor; $S_\phi = \Delta R_\phi / \Phi R_\phi$ is the sensitivity of the photoresistor.

The sensitivity of the photoresistor in formula (13.5) is defined as the magnitude of the relative change of the photoresistor under its irradiation by a radiation flux of 1 W or 1 lm. It follows from formula (13.5) that the level of the signal formed by the optical receiver of the OVN depends on the value of the radiation flux Φ irradiating the photoresistor, the sensitivity of the photoresistor S_ϕ , the voltage of the power source and the relationship between the load resistance and the photoresistor. With given target radiation characteristics and optical receiver parameters and a given miss of the missile, the value of Δu is determined by well-known methods of infrared technology.

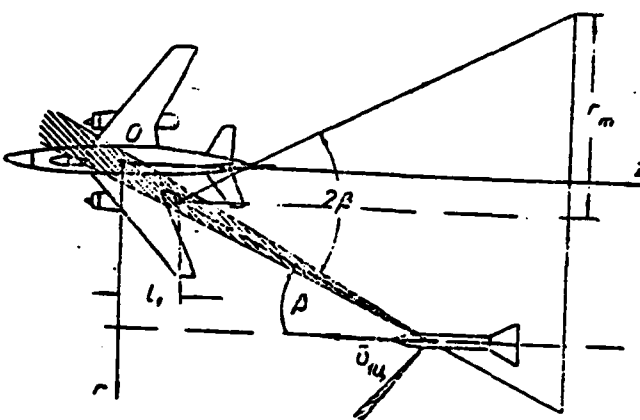


Fig. 13.5.

In approach of a missile to a target on a pursuit course, the response surface of an ONU without a time lag reacting to radiation of the engine is a cone (Fig. 13.5) whose peak is located at the center of the engine nozzle face, while its axis is a continuation of the axis of symmetry of the nozzle. The angle between the cone axis and its generatrix is equal to the angle formed by the field of vision of the optical receiver of the fuse with the missile axis. The length of the generatrix of the cone is limited to the radius of action of the fuse r_m . At the moment the missile reaches any point of the cone, the radiation of the engine nozzle will be directed at the optical receiver.

Consequently, the equation of the response surface of the ONU can be written in the following form:

$$z_0 = a + br, \quad (13.6)$$

where $b = \operatorname{ctg} \beta$; β is the angle between the missile axis and the field of vision of the receiver.

For a fuse without a time lag, $a = l_1$, where l_1 is the distance from the center of the aircraft to the engine nozzle face. In the presence of a delay unit in the ONU design, $a = l_1 - v_{lu} t_k$. The

dispersion of response points of the ONV is conditioned mainly by fluctuations of the gas jet of the engine and the spread of the delay time t_k .

Direct solar radiation and clouds illuminated by the sun are natural interference for passive ONV. When the sun and clouds get into the field of vision of the optical receiver, a sharp change occurs in the illumination of the photoresistor, as a result of which a voltage pulse capable of causing premature response of the fuse is formed in the sensor circuit.

The effect of scattered solar radiation on the ONV is manifested in the form of background (sky) radiation, which creates an illumination of the photoresistor which is constant in intensity and thereby reduces its sensitivity. For reducing the effect of solar radiation, light filters which absorb a significant part of the interfering radiation are installed in ONV receivers.

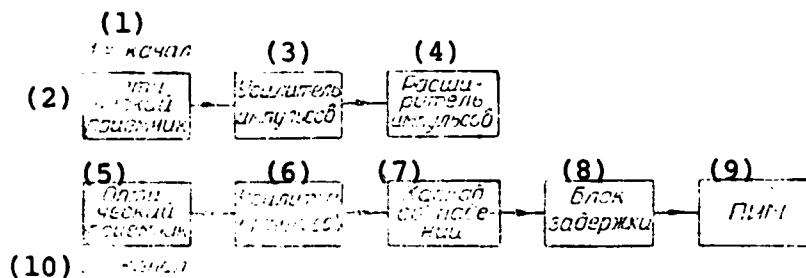


Fig. 13.6.

Key: (1) first channel; (2) optical receiver; (3) pulse amplifier; (4) pulse widener; (5) optical receiver; (6) pulse amplifier; (7) coincidence cascade; (8) delay unit; (9) PIM [safety and operations mechanism]; (10) second channel.

Dual-channel ONV (Fig. 13.6) with receiving channels connected in series to the actuating unit are distinguished by improved noise protection in relation to natural interference. The field of

vision of the receiver of the first channel forms an angle β_1 with the missile axis smaller than the angle β_2 formed by the field of vision of the second channel. In flight of the missile in relation to the target, the field of vision of the receiver of the first channel intercepts the emitting part of the target first, after which the field of vision of the second channel intercepts it. At the moments of intercepting of the fields of vision, voltage pulses develop in the optical receivers and are used for forming a command for functioning of the ONV. The pulse which has developed in the first channel, after amplification and limiting in regard to amplitude, is widened in regard to the time of action to the value of τ . The widened pulse passes into a coincidence cascade, to which the pulse which has developed in the second channel is also delivered. If these pulses coincide in regard to the time of action, the coincidence cascade functions, and a new pulse, which is the command for functioning, is shaped at the cascade output. This command is transmitted through a delay unit to the actuator of the fuse. As one can see, response of the ONV can occur only in a case where the moment of the appearance of a pulse in the second channel lags behind the moment of the appearance of a pulse in the first channel by a time Δt which does not exceed the value of τ . Neglecting the width of the field of vision of the optical receivers, we find (Fig. 13.7) that

$$\Delta t = \frac{\Delta z}{v_{\text{ts}}},$$

where Δz is the path covered by the missile in relation to the target in the time Δt .

The value of Δz depends on the miss of the missile and the direction of approach to the target. For a case of approach on a parallel course,

$$\Delta z = r(\operatorname{ctg} \beta_1 - \operatorname{ctg} \beta_2)$$

and

$$\Delta t = \frac{r(\operatorname{ctg} \beta_1 - \operatorname{ctg} \beta_2)}{v_{\text{ts}}} \quad (13.7)$$

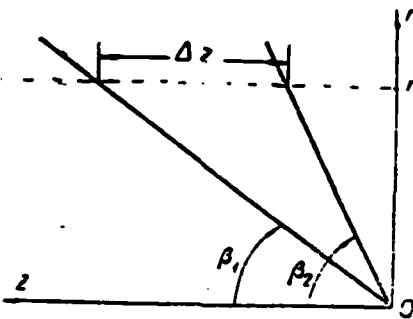


Fig. 13.7.

The magnitude of the time lag of the pulse of the second channel Δt increases with an increase in the miss of the missile. Such a dependence leads to limitation of the radius of action of the fuse. The radius of action of the ONV r_0 , which is limited by the time selection of the system, is established from the following condition:

$$\Delta t = \tau.$$

Using this condition and formula (13.7), we find that

$$r_0 = \frac{v_{ls}}{\text{ctg } \beta_1 - \text{ctg } \beta_2}. \quad (13.8)$$

Since the radius of action of the ONV is also limited by the definite sensitivity of the optical receivers, one should consider it as equal to the following:

$$R_m = \begin{cases} r_m & \text{with } r_0 > r_m \\ r_0 & \text{with } r_0 < r_m. \end{cases} \quad (13.9)$$

where r_m is the radius of sensitivity of the optical receivers.

The improved noise protection of a two-channel system with time selection is explained by the fact that if a missile flies past a cloud at a distance $r > r_0$, for example, the fuse will not be able to respond, no matter what the intensity of pulses at the coincidence cascade input in this case.

The fuse is not capable of responding directly to the solar disc, which is located at infinity in relation to the missile, therefore

cannot be intercepted by sensitivity zones of the two receivers, which form different angles with the missile axis.

Pyrotechnic emitters released from an aircraft or fired from aviation guns can serve as active jamming for passive ONV.

§ 2. THE PRINCIPLE OF OPERATION OF OPTICAL FUSES OF THE ACTIVE TYPE

Active optical fuses can be used in aerial bombs and in missiles in firing at ground and air targets.

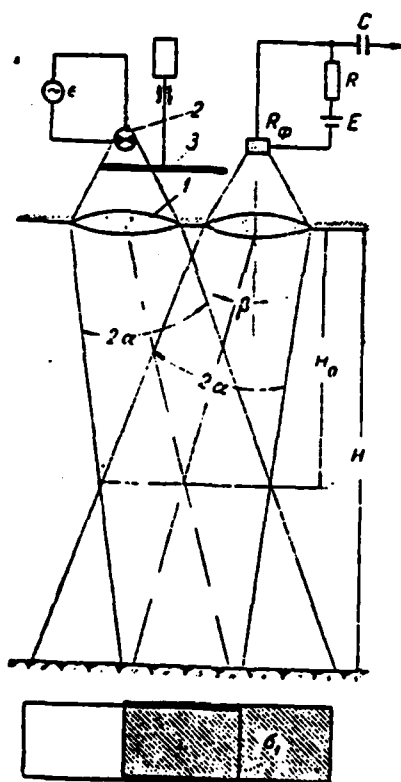


Fig. 13.8.

We shall consider the principle of operation of an active ONV intended for detonating ammunition in the vicinity of the ground surface. A schematic diagram of the fuse sensor is shown in Fig. 13.8. The ONV sensor is made up of a transmitter and a

receiver of radiation energy. The basic components of the transmitter are as follows: an optical system 1, a source of radiation energy 2 and a modulator 3. An incandescent bulb situated in the focal plane of a lens plays the role of radiation energy source. The bulb is fed from a source of a constant or variable e. d. s. [electromotive force, emf] e. The radiation energy of the bulb is focused by the lens into a narrow beam, which is aimed toward the obstacle, "illuminating" some area σ_1 on it. Scattered (diffuse) reflection of the radiation flux from this area occurs. The modulator has the form of a disc with slots (Fig. 13.9) driven into rotation by a special drive. The rotating disc is placed between the incandescent bulb and the objective in such a way that the disc slots are located opposite the bulb. Due to the disc, the radiation energy will fall on the objective only at moments in time when one of the disc slots is located opposite the bulb. As a result, the transmitter will emit energy in pulses rather than continuously. The shape of the pulses depends on the contour of the slots, while the frequency for sending the pulses depends on the number of slots and the rate of rotation of the disc. Modulation of the radiation flux is used so that the ONV receiver has the capability of separating the transmitter flux reflected by the obstacle from the flux of solar rays which is constant in intensity.

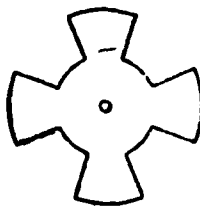


Fig. 13.9.

Basic components of the receiver are an optical system, a photoresistor and a transforming network. The photoresistor is situated in the focal plane of a lens, which is similar to the transmitter lens in regard to its shape and geometric dimensions.

The width of the field of vision of the receiver is defined by an angle 2α and is equal to the width of the beam into which the radiation flux has been focused by the transmitter lens.

The transforming network of the receiver includes a source of a constant emf E , a photoresistor R_ϕ and a load resistance, which is connected through a separating capacitor to the input of an amplifier. When a radiation flux which is variable in time is not acting on the photoresistor, direct current will flow in the receiver circuit from the emf source E through the resistors R_ϕ and R . The direct current voltage distinguished on resistance R in this case will not be transmitted through the capacitor C to the amplifier input.

In approach to the obstacle, part of the "illuminated" area of the obstacle will be located in the field of vision of the receiver. The radiation flux reflected from this part of the illuminated area hits the receiver lens and is aimed by it at the photoresistor. Under the influence of a radiation flux which varies in time, periodic variation in the value of the photoresistor occurs, which results in periodic variation of the current in the receiver circuit. The variable component of the voltage created by the current on the resistance R is transmitted through the separating capacitor to the amplifier input and serves as the working signal for the fuse. The amplified working signal causes response of the fuse at a predetermined altitude. With other conditions equal, the response altitude depends on the type of the obstacle, which determines the value of the radiation flux reflection coefficient.

Under real conditions of the tactical use of ONV, the reflection coefficient can vary from 0.03 (asphalt, chernozem soil) to 0.9 (snow). For simplifying adjustment of the fuse system for response to an obstacle with a minimum reflection coefficient, inclination of the field of vision of the optical systems of the transmitter and the receiver in relation to the fuse axis by some angle β is effected. Such an inclination is achieved by shifting the

incandescent bulb and the photoresistor in the focal planes of the lenses. In the case of inclination of the field of vision of the lenses, at some altitude H_0 , the entire area "illuminated" by the transmitter comes within the field of vision of the receiver. At this altitude, the working signal of the ONV reaches a maximum value. The altitude H_0 is called the fuse setting altitude. The fuse system is adjusted in such a way that it responds to an obstacle with the minimum possible reflection coefficient at the altitude H_0 . It is obvious that response of an ONV to all other obstacles will occur at altitudes greater than H_0 . In addition to the type of the obstacle, the structural parameters of the ONV design (the power of the incandescent bulb, the sensitivity of the photoreceiver, the width of the field of vision, the amplification factor of the amplifier, etc.), the angle of impact of the bomb or missile with the obstacle, the state of the atmosphere, the illumination of the obstacle by solar rays and other factors influence the response altitude of the ONV.

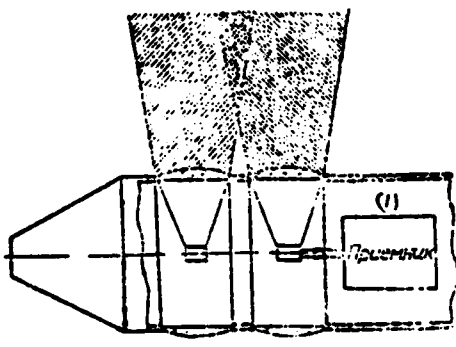


Fig. 13.10.
Key: (1) receiver.

Figure 13.10 presents a schematic diagram of the sensor of an ONV intended for use in missiles in firing at aerial targets. The optical systems of the transmitter and the receiver of the sensor include cylindric lenses, which provide circular scanning of the space around the missile. Since the transmitter should emit energy

within a space bounded by a circular field of vision, the required fuse radiation power is many times greater than the ONV radiation power in firing at ground targets. The high power of the transmitter can be provided with the use of gas discharge flash lamps filled with gases - hydrogen, xenon, argon, etc. The radiation of such lamps develops when capacitors of a high capacitance charged to a high voltage of the order of 1000-1500 V are discharged through them. A flash of the lamp characterized by a short duration (1-1500 μ s) and great brightness occurs in a discharge. A special unit which determines a definite flash frequency should control the lamp operation.

A device similar to a passive ONV serves as the fuse receiver.

Operation of the fuse proceeds as follows. During flight of the target through the radiation zone of the transmitter, reflection of radiation flux pulses occurs, and the pulses, in returning to the receiver, are focused by a lens on the sensitive surface of a photoelectric cell. Voltage pulses which emerge in the receiver circuit in this process after amplification cause response of the fuse. For the system to respond reliably, the duration of the pause between pulses should be less than the time for the projectile to fly a distance equal to the length of the target.